MATERIALS TECHNOLOGY FOR ELECTRON TUBES

by

WALTER H. KOHL

Consultant to the Director of Research,
Collins Radio Company,
Cedar Rapids, Iowa

BOOK DIVISION
REINHOLD PUBLISHING CORPORATION
330 West Forty-second St., New York, U.S.A.
1951

TO

WINFIELD W. SALISBURY

PREFACE

It is the purpose of this book to present the physical characteristics of the solids used in the fabrication of vacuum tubes and to describe some of the processes for the application of these materials. It had often occurred to me, during my prolonged activity in this field, that such a text should be useful to the tube designer, development engineer and technician alike, especially since no English text is available, so far, to take the place of the now classic treatise by Espe and Knoll.*

The contents will give a fair idea of the scope of the book. The selection of the subjects was naturally dictated by my personal experience but as broad a base as possible was attempted. This turned out to be a rather formidable task since so many disciplines of science enter into Vacuum Tube Technology that no one person can claim to be competent in all of them. For this reason, all of the chapters have been submitted for review to a number of experts in the various fields who generously supplied additional data and helped to make the text more concise. A number of subjects, which might be expected in a book of this kind, have been omitted, especially those on which specialized treatises have become available recently. This refers to luminescence of solids, the treatment of gases and vapors, electron emission and high vacuum technique. A summary and guide to the literature of High Vacuum Technique and Electron Emission as well as several tables, are given in the last two chapters.

Extensive references are listed at the end of each chapter and the index of authors and subjects has been prepared with some care in order to permit the reader to extend his studies in the literature.

Beyond the field of electronics, the book should be of some value to materials engineers in related fields where glass, ceramics and metals are used. The chapter on Solders and Brazes will of course be of general interest to experimenters in all fields. The book is essentially nonmathematical although there are a few pages where equations do occur.

I would be grateful if the readers would point out mistakes and omissions of which there must be many in spite of a sincere effort to avoid them.

It is my pleasant duty to thank the management of the Collins Radio Company for their generous support of this work. Their help made this

* "Werkstoffkunde der Hochvakuumtechnik," Verlag Julius Springer, Berlin, 1936.

book a practical reality. At the same time, it must be said that the content of the book has in no way been restricted by this support and that anything stated in it does not commit the Collins Radio Company but is entirely my own responsibility. I am deeply indebted to Dr. Winfield W. Salisbury, Director of Research of the Collins Research Division,* for his continued interest, friendly encouragement and trust in seeing this job through to the end. It is, therefore, a great pleasure to dedicate this book to him who had the vision and confidence that something worthwhile might be achieved by writing it.

I tender my sincere thanks to the many reviewers and their companies or institutions who have so generously cooperated in this venture. The names and affiliations of these reviewers are listed below together with the numbers of the chapters on which they cooperated. This acknowledgement does not imply that the reviewers in question are in any way committed by the text or that they agree with all details. Many others have read the manuscript and either simply voiced their approval or, in spite of substantial contributions, have preferred not to be mentioned. The selection of reviewers has been quite arbitrary and was mostly dictated by my personal or indirect contact with them and their further suggestion of other names.

Also listed are the publishing houses, institutions, and companies who have kindly given permission to use text excerpts, graphs, tables, and illustrations from their publications as acknowledged in the text.

This venture was begun, on the constant urging of my publisher, during the summer of 1948 and the manuscript was completed at the end of 1950. The various chapters were written in the sequence in which they are presented in this book. The following members of the staff of Collins Radio Company had a large share in processing the book. Mrs. Betty Krejci typed and retyped the manuscript and took care of its extensive distribution. Mrs. Jean Van Cura handled the voluminous correspondence connected with these activities. Bernard Erlacher and Charles Kurka prepared most of the line drawings and John Ridge and Don Hanson the photographs.

The relations with the publisher have been very pleasant indeed. Messrs. F. M. Turner, F. P. Peters and G. G. Hawley of the Reinhold Publishing Corporation supported the venture most generously and left me a completely free hand in carrying it out. The care which they, on their part, applied to all details, should be reflected in the book's final appearance. To all these I am most grateful.

* Now Professor of Electrical Engineering, University of California, Berkeley, California.

Last, but not least I am indebted to my wife who not only endured my prolonged preoccupation with this venture but was a continuous source of encouragement and helped by reading the proofs and preparing part of the index.

Walter H. Kohl

Cedar Rapids, Iowa
January 2, 1951.

LIST OF REVIEWERS

		Chapter No.
Acheson Colloids Corp. Research Laboratory Newark 2, N.J.	R. Szymanowitz Vice President in Charge of Research	13
Air Reduction Sales Co. 60 East 42nd Street New York 17, N.Y.	A. N. Kugler Chairman, A.W.S. Committee on Brazing & Soldering	14
Allegheny Ludlum Steel Corp. Brackenridge, Pa.	L. C. Hicks Director of Research	4
American Lava Corp. Chattanooga 5, Tenn.	H. Thurnauer Director of Research	15, 16
The American Metal Co., Ltd. 61 Broadway New York 6, N.Y.	D. L. Ogden Metall. Consult.	12
American Platinum Works Newark 5, N.J.	J. F. Thompson, Jr. A. S. Cross, Jr.	14
Bartol Research Foundation Whittier Place Swarthmore, Pa.	W. E. Danforth Assistant Director	19
Bell Telephone Laboratories Murray Hill Laboratory Murray Hill, N.J.	F. J. Biondi	14
British Thomson-Houston Co. Ltd. Research Laboratory Sheffield Road, Chesterfield Derbyshire, England	J. E. Stanworth G. D. Redston	4, 6
Burroughs Adding Machine Co. Research Division 511 Broad Street Philadelphia 23, Pa.	T. H. Briggs (formerly Superior Tube Company)	11
The Carpenter Steel Company Reading, Pa.	G. V. Luerssen Chief Metallurgist	4
Cerro De Pasco Copper Corp. 40 Wall St. New York 5, N.Y.	O. J. Seeds	14

		Chapter No.
Chase Brass and Copper Co., Inc. Waterbury 2, Conn.	D. K. Crampton Director of Research W. E. Johnston Research Engineer	12
Commonwealth Engineering Company of Ohio 1771 Springfield Street Dayton 3, Ohio	Engineering & Research Staff	8
Copper and Brass Research Association 420 Lexington Avenue New York 17, N.Y.	T. E. Veltfort, Mgr.	12
Distillation Products Industries Rochester 3, N.Y.	B. B. Dayton	18
Division Lead Company 836 W. Kinzie Street Chicago 22, Ill.	W. E. Karry Technical Director	14
Driver Harris Company Harrison, N.J.	F. E. Bash (deceased) Vice President S. Poch, Metallurgist	4
Duplate of Canada, Ltd. Oshawa, Ontario, Canada	S. Bateson Director of Research	1–6
Fansteel Metallurgical Corp. North Chicago, Ill.	L. R. Scribner Chief Engineer—Tantalum J. Chelius	8–10 9
Federal Telecommunications Laboratories, Inc. 500 Washington Avenue Nutley 10, N.J.	A. K. Wing, Jr. Vacuum Tube Dept.	8
Ferranti Ltd. Manchester 10, England	W. G. F. Roberts	15
General Ceramics & Steatite Corp. Keasbey, N.J.	E. Albers-Schoenberg Director of Research	15, 16
General Electric Co. Research Laboratory Schenectady, N.Y.	Katherine B. Blodgett	5
General Electric Co. Spec. & Tech. Data Section Schenectady Works Lab Schenectady, N.Y.	J. E. McGraw	14
General Plate Division Metals & Controls Corporation Attleboro, Mass.	J. E. Woodward	14
Globe-Union, Inc. 900 East Keefe Avenue Milwaukee 1, Wis.	R. R. Roup Chief Ceramic Engineer	15

		Chapter No.
The International Nickel Company, Inc. Development & Research Division 67 Wall Street New York 5, N.Y.	E. M. Wise Platinum Metals & Electronics Section J. Shaw	11
Machlett Laboratories, Inc. Springdale, Conn.	H. D. Doolittle Engineering Dept.	1–6 15–19
National Bureau of Standards Electronics Division Washington, D.C.	C. P. Marsden Electronic Scientist	8, 9, 10
National Carbon Division Union Carbide & Carbon Corp. 30 East 42nd Street New York 17, N.Y.	Research Laboratory Staff	13
National Lead Co. 111 Broadway New York 6, N.Y.	Alex. Stewart Director of Research	14
National Research Corp. 70 Memorial Drive Cambridge 42, Mass.	R. A. Stauffer Vice President, Director of Research	12, 18
North American Aviation, Inc. Box 309 Downey, Calif.	C. R. Malmstrom Atomic Energy Res. Dept. Group Leader	13
Office of Naval Research Department of the Navy Washington 25, D.C.	J. J. Harwood Acting Head, Metallurgy Branch	9
Ontario Research Foundation Queens Park, Toronto, Ontario, Canada	O. W. Ellis Director, Department of Engineering & Metallurgy	12
Pittsburgh Plate Glass Company Research Laboratories Creighton, Pa.	J. V. Fitzgerald	6
Revere Copper and Brass Inc. Rome, N.Y.	R. C. Dalzell Chief Technical Advisor	12
Speer Carbon Company Saint Marys, Pa.	H. W. Abbott Director of Research C. P. McKnight Development Engineer	13
Stackpole Carbon Company Saint Marys, Pa.		13
Stupakoff Ceramic & Manufacturing Co. Latrobe, Pa.	E. J. Straus Assistant Vice President	4
Superior Tube Company Norristown, Pa.	A. M. Bounds	11
Sylvania Electric Products, Inc. Bayside, N.Y.	W. E. Kingston, Manager Metallurgical Laboratories	4, 7, 8–11

		Chapter No.
Tin Research Institute 492 West Sixth Avenue Columbus 1, Ohio	R. M. MacIntosh Supervisor, Chemical Development	14
University of Missouri Department of Physics Columbia, Mo.	A. S. Eisenstein Professor of Physics	19
Western Electric Company Allentown, Pa.	J. T. Acker	11
Westinghouse Electric Corporation Research Laboratories Electronics & Nuclear Physics Dept. East Pittsburgh, Pa. also:	R. O. McIntosh	8–16
Metallurgical Development Section Materials Engineering Department East Pittsburgh, Pa.	E. F. Losco	4
Wilbur B. Driver Company 150 Riverside Avenue Newark 4, N.J.	R. W. Judkins Director of Research	4

LIST OF PUBLISHERS AND INSTITUTIONS

Allegheny Ludlum Steel Corporation
American Ceramic Society
American Chemical Society
American Institute of Electrical Engineers
American Institute of Physics
American Institute of Mining and Metallurgical Engineers
American Metal Company, Ltd.
American Society of Metals
American Society for Testing Materials
American Standards Association
American Welding Society
British Institution of Radio Engineers
British Non-Ferrous Metals Research Association
British Society of Glass Technology
Bryan Davis Publishing Company
Butterworth Science Publishers, London
Chapman & Hall, Ltd., London
Collins Radio Company
Cornell University Press
Corning Glass Works
Electrochemical Society
Fansteel Metallurgical Corporation
Franklin Institute
Gage Publishing Company
General Electric Company
Handy and Harman
Imperial Chemical Industries, London
Institute of Metals, London
Institute of Physics, London
Institute of Radio Engineers
International Graphite and Electrode Corporation
Interscience Publishers
Johann Ambrosius Barth, Leipzig
John Wiley and Sons, Inc.
Julius Springer, Berlin
Longmans Green & Company, London
Machlett Laboratories, Inc.
McGraw-Hill Book Company
McGraw-Hill Publishing Company
McMillan & Company Ltd., London
Mica Fabricators Associates
North American Aviation, Inc.
Ogden Publishing Company
Philips Gloeilampenfabrieken, Eindhoven, Holland
Pittman Publishing Company
Radio Corporation of America, R.C.A. Victor Division
Reinhold Publishing Corporation
Stupakoff Ceramic and Manufacturing Company
Superior Tube Company
U. S. Bureau of Standards
U. S. Department of Labor
Washington Academy of Science
Westinghouse Electric Corporation

CONTENTS

CHAPTER 1
PHYSICS OF GLASS

Introduction

The age-old spell which glass in its many compositions and shapes has cast upon the human race presents a temptation to relate the role which glass has played in the growth of civilization. This would indeed make a fascinating story, but several books are available which tell it well.[1,2] The technology of glass has likewise been treated extensively,[3–6] and professional journals continuously cover the advances in this field.[7–12] For these reasons we will confine ourselves mainly to the discussion of the properties of glass which concern the electronic-tube industry, with enough background for an appreciation of the many intricacies which often make a concise appraisal of these properties so difficult.

Glass is ideally suited to many applications in the tube industry, particularly for tube envelopes. The introduction of metal-envelope receiving tubes in 1935 changed this picture for a time, but the very general use of miniature and subminiature tubes in recent years has again brought glass to the fore as the preferred material. For television tube envelopes a similar transition has taken place with the introduction of metal envelopes, which led in turn to glass bulbs of special shape and competitive cost. Glass is easily blown into a variety of shapes by high-speed machines, which make small tube envelopes available at a very nominal cost. The transparency to radiation permits ready dissipation of power from the internal structure. Electrical leads to these elements can be sealed through the glass without difficulty, and its mechanical rigidity is satisfactory in most cases. Glass will break, however, when abused mechanically or when subject to excessive internal strains. It softens at a relatively low temperature, which limits the temperature of out-gassing on the pump and also its power-dissipating ability. Air-cooling then becomes necessary, with corresponding expense for equipment. In addition, dielectric losses may become objectionable at high frequencies. Thus, both limitations and advantages have to be weighed when a particular design is chosen.

In addition to the possible sealing of metal wires through glass the advantage of glass-to-metal seals, where metal disks, rings, or cylinders can be joined to glass members, should be mentioned (Chapter 4). Thus,

it is possible to put power-dissipating elements within metal envelopes which can be cooled externally and to use glass for insulation and support of the remaining structure at a place where the temperature is lower. This is the familiar structure used for conventional power tubes.

It is of interest to note that the value of glass blanks consumed by the electronic-tube industry in the United States during 1947 amounted to $14,000,000.* The main suppliers of such semifinished glass as bulbs, rods, and tubing are the Corning Glass Works, Corning, New York and Kimble Glass Co., Toledo, Ohio. The various shapes and sizes are specified by number codes, and tolerance ranges have been established. These data are available from the manufacturers. Dimensions of bulb shapes are also listed in the handbook of the Joint Electron Tube Engineering Council (J.E.T.E.C.) of the Radio-Television Manufacturers Association (R.T.M.A.)[13] and in the "Tube Handbook" of the Radio Corporation of America (R.C.A.).

It goes without saying that, wherever possible, existing sizes and shapes of bulbs should be chosen for design as otherwise special moulds have to be made which will increase cost and delay delivery. The university laboratories and self-styled experimenters should establish connections with a commercial tube company where small quantities of glass parts are quickly available from stock. A number of scientific apparatus companies will supply glass rod and tubing as well as stopcocks, bell jars, and many specialized components. Manufacturers of flowmeters, pressure gauges, and similar equipment, which contain glass components, usually have specialized glass stock on hand; otherwise, it is manufactured. Precision-bore tubing is naturally required for flowmeters and heavy wall cylinders for pressure gauges. Experimental quantities of glass can thus be often procured more quickly from glass fabricators rather than prime manufacturers.

An enormous amount of effort still seems to be unjustifiably spent in colleges doing things the hard way where simpler methods are available. Often the reasoning behind this is that the student's time does not cost anything in the first place and that, furthermore, experimental difficulty is good training. The latter point cannot be refuted, but the struggle should take place on the highest possible plane after all available techniques are utilized. There is no justification for mounting electrodes for a vacuum tube on rubber stoppers and for sealing the latter with beeswax when a multi-electrode glass press can be obtained. The direct sealing of glass headers to bulbs is best done in a vertical sealing lathe, with proper attention being given to preheating and cooling. When skill and

* Tentative information received from the U.S. Department of Labor, Bureau of Labor Statistics, Division of Interindustry Economics.

equipment for this technique are lacking, a satisfactory seal can often be obtained with the aid of Para Rubber Tape.*

Thousands of different kinds of glasses have been developed, and new compositions are continuously being added to meet the varying demands for special applications. The optical industry is especially concerned with such properties as refractivity, dispersion, and absorption, and requires glass of a high degree of uniformity. Chemical stability and resistance to thermal shock are essential for chemical glassware and cooking utensils. Glass electrodes for pH meters must have a constant resistivity, and in recent years special lithium glasses have been developed for this application. High-voltage glass insulators should have high breakdown values, a low dielectric constant, and a low power factor in the presence of high frequencies. On the other hand, high dielectric glasses are needed for glass used in capacitors. In electronic tubes the designer will aim at a minimum of electrolysis at elevated temperature in the presence of D.C. potentials. He will prefer a high softening point within practical limits of sealing techniques, but will have to match expansion coefficients of metals sealed through or to the glass unless special techniques are resorted to which obviate this need (Chapter 4). Glass used for fluorescent lamps should not give up components that are harmful to the life of the fluorescent coating nor should mercury-vapor lamp bulbs be liable to blackening because of excessive solarization. These are only a few of the many requirements which have to be met by glass under varying conditions of use.

Glass Types

Fortunately, the number of glass types used in the electronic industry is quite limited. The two main types are soft glasses and hard glasses. The latter soften at a higher temperature than the former. Two representative glasses frequently used are Corning 0010 and 0120, soft glasses, and "Nonex 7720," a hard glass; their compositions, together with a number of other glasses, are given in Table 1.1.[3,14] The broad range of physical characteristics for commercial glasses and silica is indicated in Table 1.2, and specific data for Corning glasses are given in Table 1.3.[15] Table 1.4 gives the composition of a number of English glasses.[18]

Widespread use of Corning glasses makes it desirable to clarify the code numbers by which they are specified and to clear up some misconceptions which prevail in regard to the Corning trade mark, "Pyrex." This word is applied to glassware and certain other products of Corning and does not identify the glass composition from which the article is made. Nearly 150 different glass compositions are used in glassware marketed under this trade mark. Various authors use it to refer to

* Available from Central Scientific Company.

chemically resistant glass 7740, but this is not justified. The only clear-cut designation of Corning glasses is the four-number code, which has been in use for some time. Application of a laboratory code, together with a number code, has been discontinued, and only the four-number code will be used in this book, even when references are quoted which use

TABLE 1.1. CHEMICAL COMPOSITIONS OF SOME GLASSES USED IN HIGH VACUUM DEVICES*

Classification		Constituent Oxides (Wt %)										Uses
		SiO_2	B_2O_3	Al_2O_3	PbO	CaO	Na_2O	K_2O	MgO	BaO	Mn_2O_3	
Soft Soda	1	70.5		1.8		6.7	16.7	0.8	3.4			Lamps and tubing for neon signs
	2	69		4		5.8	17.5	1.9	1.6			
	3	69.3	1.2	3.1		5.6	16.8	0.6	3.4			
	4	73.6				5.37	17.23		3.67			
Lead	5	56.5		1.5	29	0.2	5.6	6.6	0.6			Stems for lamps and radio tubes
	6	57		1.5	29.4	0.2	4.1	7.3	0.4			
	7	63.10		0.28	20.22	0.94	7.60	5.54			0.88	
Hard Borosilicate	8	80.1	12	3		0.2	3.9	0.3				High wattage lamp and tube bulbs, diffusion pumps, chemical apparatus
	9	71	13.7	7.4		0.3	5.3	2.4				
	10	80.5	12.9	2.2			3.8	0.4				
	11	73	16.5		6		4.5					
	12	67	22	2			6.5					
Extra Hard	13	54.5	7.4	21.1		13.5				3.5		Mercury vapor discharge tubes
	14	58.7	3	22.4		5.9	1.1	0.2	8.4			
Special	15	22.6	37	23.7		10	6.5	0.2				Sodium vapor lamps

7: Corning 0010 10: Corning 7740 11: Corning 7720 12: Corning 7050

* Compiled from Ref. 3 and 14.

the old designations in the original. However, to tie in the old code with the new, Table 1.5 is given as a cross-reference.

Mechanical Strength

While some data on mechanical strength have been included in Table 1.2, it must be emphasized that they can only indicate what might be observed under certain conditions. The intrinsic strength of glass is extremely high, and may reach 3×10^6 psi. Glass fibers have supported tensile stresses of over 10^6 psi, and it has been shown that the stress-strain

curve for glasses is a straight line up to the breaking point. Glass fractures only from tensile stresses, never from shear or compression. Unfortunately, the high values of strength are rarely reached by glass bodies in bulk sizes other than freshly drawn fibers. Strength then becomes an

TABLE 1.2. RANGE OF PHYSICAL CONSTANTS OF GLASSES (INCLUDING SILICA)

Item	Range	Units	Ref.
Density	2.1–8.1	g/cc	1, 3, 15, 16
Mohs Hardness	4–8		
Young's Modulus	6.5–12.7	10^6 psi	16
	450–825	Kilobar	
Poisson's Ratio	0.14–0.3		
Tensile strength			
(a) Tension	0.4–100	10^4 psi	16
	0.3–7	Kilobars	
(b) Compression	9–18	10^4 psi	16
	6.2–12.4	Kilobars	
(c) Bending	1.5–3.6	10^4 psi	
	1–2.5	Kilobars	
(d) Torsion	~ 1.3	10^4 psi	
	~ 0.9	Kilobars	
		Values vary with conditions of test and specimen	
Thermal expansion	8–140	$10^{-7}\ \frac{\text{cm}}{\text{cm}}/°\text{C}$	16
Specific heat	0.1–0.2	$\frac{\text{g-cal}}{\text{gr}}/°\text{C}$	
Thermal conductivity	0.16–0.3	$10^{-2}\ \frac{\text{g-cal}}{\text{cm}^2}/\text{cm}/°\text{C}/\text{sec}$	
Softening point	440–1510	°C	
Annealing point	350–910	°C	
Strain point	320–820	°C	15
Normal service	110–800	°C	
		for commercial glasses	
Volume resistivity (20°C)	10^8–10^{18}	ohm cm^{-1}	16
Surface resistivity (20°C)	10^{11}–10^{13}	ohm/square	
Electrical strength	16–40	Kv/mm	
		varies tremendously with conditions of tests	
Dielectric constant	3.7–16.5		16
Power factor	0.0117–0.664	† (tan δ) (%)	16
Loss factor	0.07–6.5	† (tan δ) (%)	
Refractive index	1.46–1.96		16
Total thermal emissivity	0.6–0.9		17

† Power factor of 0.02 p.c. means that tan δ = 0.0002. The same reasoning applies to the loss factor.

elusive quantity which depends on the surface texture of the glass, the surrounding atmosphere, the amount of moisture present, and the test conditions in general. The habit of an experienced glass worker of holding a piece of glass tubing to his mouth and exhaling onto a freshly

TABLE 1.3.* PHYSICAL CHARAC

1	2	3	4	5	6	7				8		
						Upper Working Temperatures (Mechanical Considerations Only)				Thermal Shock Res. Plates 6″ × 6″		
						Annealed		Tempered		Annealed		
Glass Code	Type	Color	Principal Use	Forms Usually Available	Thermal Expansion Coeff.	Normal Service (°C)	Extreme Limit (°C)	Normal Service (°C)	Extreme Limit (°C)	⅛″ Thk. (°C)	¼″ Thk. (°C)	½″ Thk. (°C)
0010	Potash soda lead	Clear	Lamp tubing	T	91×10^{-7}	110	380			65	50	35
0041	Potash soda lead	Clear	Thermometers	T	84×10^{-7}	110	400			70	60	40
0080	Soda lime	Clear	Lamp bulbs	BMT	92×10^{-7}	110	460	220	250	65	50	35
0120	Potash soda lead	Clear	Lamp tubing	TM	89×10^{-7}	110	380			65	50	35
1710	Hard lime	Clear	Cooking utensils	BP	42×10^{-7}	200	650	400	450	135	115	75
1770	Soda lime	Clear	General	BP	82×10^{-7}	110	450	220	250	70	60	40
2405	Hard red	Red	General	BPU	43×10^{-7}	200	480			135	115	75
2475	Soft red	Red	Neon signs	T	91×10^{-7}	110	440			65	50	35
3321	Hard green sealing	Green	Sealing	T	40×10^{-7}	200	470			135	115	75
4407	Soft green	Green	Signal ware	BPU	90×10^{-7}	110	460			65	50	35
6720	Opal	White Opaque	General	P	80×10^{-7}	110	480	220	275	70	60	40
6750	Opal	White Opaque	Lighting ware	BPR	87×10^{-7}	110	420	220	220	65	50	35
6810	Opal	White Opaque	Lighting ware	BPR	69×10^{-7}	120	470	240	270	85	70	45
7050	Borosilicate	Clear	Series sealing	T	46×10^{-7}	200	440	235	235	125	100	70
7052	Borosilicate	Clear	Kovar sealing	BMPT	46×10^{-7}	200	420	210	210	125	100	70
7070	Borosilicate	Clear	Low loss electrical	BMPT	32×10^{-7}	230	430	230	230	180	150	100
7250	Borosilicate	Clear	Baking ware	P	36×10^{-7}	230	460	260	260	160	130	90
7340	Borosilicate	Clear	Gauge glass	T	67×10^{-7}	120	510	240	310	85	70	45
7720	Borosilicate	Clear	Electrical	BPT	36×10^{-7}	230	460	260	260	160	130	90
7740	Borosilicate	Clear	General	BPSTU	32×10^{-7}	230	490	260	290	180	150	100
7760	Borosilicate	Clear	Electrical	BP	34×10^{-7}	230	450	250	250	160	130	90
7900	96% Silica	Clear	High temp.	BPTU	8×10^{-7}	800	1090			1250	1000	750
7900	96% Silica (multiform)	White Opaque	High temp.	M	8×10^{-7}	800	1090			1250	1000	750
7910	96% Silica	Clear	Ultraviolet transmission	BTU	8×10^{-7}	800	1090			1250	1000	750
7911	96% Silica	Clear	Ultraviolet transmission	T	8×10^{-7}	800	1090			1250	1000	750
8870	High lead	Clear	Sealing or electrical	MTU	91×10^{-7}	110	380	180	180	65	50	35
9700		Clear	Ultraviolet transmission	TU	37×10^{-7}	220	500			150	120	80
9741		Clear	Ultraviolet transmission	BUT	39×10^{-7}	200	390			150	120	80

COLUMN 5

B—Blown Ware
M—Multiform Ware
P—Pressed Ware
R—Rolled Sheet
S—Plate Glass
T—Tubing and Rod
U—Panels

COLUMN 6

From 0° to 300°C in/m/°C or cm/cm/°C

COLUMN 7

These data approximate only. Freedom from excessive thermal shock is assumed. See Column 8.
At extreme limits annealed glass will be very vulnerable to thermal shock. Recommendations in this range are based on mechanical considerations only. Tests should be made before adapting final designs.

COLUMN 8

These data approximate only.
Based on plunging sample into cold water after oven heating. Resistance of 100°C means no breakage if heated to 110°C and plunged into water at 10°C. Tempered samples have over twice the resistance of annealed glass. Gasses 7900, 791 0 7911 cannot be tempered.

TERISTICS OF CORNING GLASSES

9	10				11	12	13	14			15			16
	Viscosity Data							Log_{10} of Volume Resistivity			Dielectric Properties of 1 Mc and 20°C			
Thermal Stress Resistance (°C)	Strain Point (°C)	Annealing Point (°C)	Softening Point (°C)	Working Point (°C)	Impact Abrasion Resistance	Density (Sp. gr.)	Modulus of Elasticity psi	25°C	250°C	350°C	Power Factor %	Dielectric Const.	Loss Factor %	Refractive Index Sod. D Line (.5893 Microns)
19	397	428	626	970		2.85	9.0×10^6	17+	8.9	7	0.16	6.6	1.1	1.539
19	426	460	648			2.89								1.545
17	478	510	696	1000	1.2	2.47	9.8×10^6	12.4	6.4	5.1	.9	7.2	6.5	1.512
17	400	433	630	975		3.05		17+	10.1	8	.16	6.6	1.1	1.560
29	672	712	915	1200	2	2.53	12.7×10^6	17+	11.4	9.4	.37	6.3	2.3	1.534
19	470	503	710			2.40								1.496
36	506	537	802			2.50								1.508
17	466	501	693			2.56								1.511
39	497	535	780			2.27								
17	485	518	695			2.53								1.525
19	499	531	775			2.58								1.507
18	445	475	672			2.63								1.513
23	496	529	768			2.65								1.508
34	461	496	703			2.25		16	8.8	7.2	.33	4.9	1.6	1.479
34	438	475	708	1115		2.28		17	9.2	7.4	.26	5.1	1.3	1.484
70	455	490		1100	4.1	2.13	6.8×10^6	17+	11.2	9.1	.06	4.0	0.24	1.469
43	486	524	775		3.2	2.24		15	8.2	6.7	.28	4.7	1.3	1.475
20	538	575	785			2.43	11.5×10^6	16	8.5	6.9				1.506
45	484	518	755	1110	3.2	2.35	9.5×10^6	16	8.8	7.2	.27	4.7	1.3	1.487
48	515	555	820	1220	3.1	2.23	9.8×10^6	15	8.1	6.6	.46	4.6	2.1	1.474
51	475	515	780	1210		2.23	9.1×10^6	17	9.4	7.7	.18	4.5	0.79	1.473
200	820	910	1500		3.5	2.18	9.7×10^6	17	9.7	8.1	.05	3.8	.19	1.458
200	820	910	1500		3.5	2.18	9.7×10^6	17	9.7	8.1	.05	3.8	.19	1.458
200	820	910	1500		3.5	2.18	9.7×10^6	17+	11.2	9.2	.024	3.8	.091	1.458
200	820	910	1500		3.5	2.18	9.7×10^6	17+	11.7	9.6	.019	3.8	.072	1.458
22	398	429	580		0.6	4.28	7.6×10^6	17+	11.8	9.7	.09	9.5	.85	1.693
42	517	558	804	1195		2.26		15	8	6.5				1.478
40	407	442	705			2.16		17+	9.4	7.6				

COLUMN 9

Resistance in °C is the temperature differential between the two surfaces of a tube or a constrained plate that will cause a tensile stress of 1000 p.s.i. on the cooler surface.

COLUMN 10

See Fig. 1.1b. These data subject to normal manufacturing variations.

COLUMN 11

Data show relative resistance to sandblasting.

COLUMN 12

Units are g/cc.

COLUMN 14

Data at 25° extrapolated from high temp. readings and are approximate only.

GLASSES 7910 AND 7911

Electrical properties measured on lamp worked specimens.
All data subject to normal manufacturing variations.

* Corning Glass Works. Bull. B-83 (1949).

drawn file mark before exerting pressure to break it, is an example of the influence of surface moisture on strength. This factor has been investigated quantitatively by Preston and Baker[19,20] and others.

Weyl[21] has developed new ideas on the chemical aspects of some mechanical properties of glass. Microscopic fissures and cracks, present in a glass surface from the necessary handling during manufacture, always act as stress-raisers, limiting its ultimate strength to about 10^4 psi for practical purposes. It is possible to increase the strength of glass by treating the surface with diluted hydrofluoric acid, thus removing the

TABLE 1.4. CLASSIFICATION OF SEALING GLASSES INTO GROUPS ACCORDING TO CONTENT OF GLASS-FORMING OXIDES*

Group number	Group I 100% glass-forming oxides	Group II Between 80 and 100% glass-forming oxides						Group III Between 60 and 80% glass-forming oxides		Group IV Between 40 and 60% glass-forming oxides			
Glass Type	Fused silica	"Borosilicate" glasses						"Soda" glasses		"Lead" glasses. New iron sealing glasses			Special lamp glass
Glass number		R.48	R.49	R.50	C.38	C.9	C.11	C.19	C.22	C.12	C.31	C.76	C.14
Silica SiO_2	100	83.5	78.5	74.5	68.5	74.6	73	72	67.5	57	52	48.2	58.5
Boric oxide B_2O_3		12.5	17.5	17.5	30	18	14		0.7				3
Alumina Al_2O_3		4	4	4		1	2.3	1	3.9	1	1		22.5
Lead oxide PbO										30	30		
Oxides of the divalent metals MgO, CaO, BaO				4		0.3	3	9.4	6.7		2.5	30	15.2
Calcium fluoride CaF_2												5	
Oxides of alkali metals					1.5	5.9	7.5	17.3	20.7	12	14.5	16.8	0.8
Average thermal expansion coefficient between 0° and 400° × 10^7	5.5	13	18	23	30	36	45	94	105	90	100	116	37

* Ref. 18.

thin layer containing microscopic cracks or rounding off their profiles. This treatment increases the tensile or bending strength of glass specimens by as much as 10 times, provided that care is taken not to touch the surface after treatment.[22] The polishing action of flames playing on the outer surface of a glass bulb during manufacturing and later the stem-sealing process has a similar effect. When an adequate safety factor is provided, the maximum working stress for annealed glass is taken as 1000 psi and for tempered or heat-treated glass as 2000 to 4000 psi, depending on the size and shape of the piece in question. It should be noted that the composition of glass has no practical effect on its strength although most borosilicate glasses resist scratching and therefore give better mechanical service.[15]

Composition of Glass

The constituents of glass have been classified by Kuan Han Sun under the headings glass-formers, modifiers, intermediates, and impurities.[23]

Glass-formers are the most important as each individually forms a glass within practical temperature ranges. They are: B_2O_3, SiO_2, GeO_2, P_2O_5, As_2O_5, Sb_2O_5, V_2O_5, ZrO_2, P_2O_3, SbO_3, B_2O_3, etc.

TABLE 1.5. CORNING GLASS CODES

Present Code No.	Old Lab. Code No.	Old Code No.
0010	G-1	001
0050	G-5	005
0080	G-8	008
0110	G-164-HC	011
0120	G-12	012
	G-6 (obsolete)	013
0240	G-125-BB	024
1990	G-189-IY	1990
1991	G-184-ET	1991
3320	G-371-BN	332
7040	G-705-BA	704
7050	G-705-AJ	705
7052	G-705-FN	7052
7060	G-705-AO	706
7070	G-707-DG	707
7520	G-750-AJ	752
7530	G-805-F	753
7550	G-805-G	755
7560	G-705-AL	756
	G-71 (obsolete)	771
7720	G-702-P ("Nonex")	772
7740	G-726-MX	774
7750	G-705-R	775
7780	GT-70	778
7991	G-704-EO	7991
8160	G-814-KW	816
8870	G-858-V	887

Modifiers, by themselves, do not form a glass under ordinary conditions, but are introduced into glass to modify its properties. They usually weaken the glass structure; but this is not always the case. Some of them are listed as follows: Na_2O, K_2O, CaO, SrO, BaO, etc.

Intermediates occupy a position somewhere between glass formers and modifiers. They do not form glasses themselves, but enhance glass formation. They are: Al_2O_3, BeO, ZnO, CdO, PbO, TiO_2, etc.

Impurities are present as contaminants in the original batch com-

ponents and from chemical or physical interaction with the tank walls and handling tools at elevated temperatures. Some of these are: Mn_2O_3, Fe_2O_3, As_2O_3, SO_3, etc.

To arrive at a final product which satisfies his requirements the glassmaker is confronted with the problem of choosing the proper components from this list. Nature has given him a lead in this respect as there are *natural glasses* occurring in massive deposits (i.e., the Obsidian Ranges in Yellowstone Park) or in the form of isolated pieces, known as "fulgurites" and "tektites." The Obsidian Ranges are a mass of black glass, about 9 miles long and 5 miles wide, which rise about 250 feet above the level of the surrounding country. They are of igneous origin and represent essentially a granite which has been cooled from its liquid state quickly enough to prevent crystallization. The three components of granite are feldspar, quartz, and mica, which contain the following chemicals, shown by their respective formulas: $[Na, K]\ AlSi_3O_8$; SiO_2; and $[K, Na, Li]\ H\ [Mg, Fe, Ca, Mn]_2\ [Al, Fe]_2\ (SiO_4)_3$.

Fulgurites are formed when lightning strikes sand or other loose or porous material. A sample found in a sandpit near South Amboy, N.J. measured 9 feet in length, decreasing from a maximum diameter of 3 inches to a point $^3/_{16}$ inch in diameter.

Tektites range in size from tiny bubbles to 10-pound pieces. Scattered over areas as much as 50 miles in extent, they may have been formed by the impact of meteors on sand dunes. Like fulgurites, they contain mostly SiO_2 and are formed by rapid cooling of the molten sand.

This brief excursion into the field of geology shows the scope of forces and energies at work in this enormous glass shop, where gigantic pressures and temperatures were available. During the course of the past 5000 years man has endeavored to simulate these conditions on a small scale, and has succeeded in producing glasses to satisfy his needs. If quartz were not so difficult to melt, to free from bubbles, and to work, pure silica glass would be the most suitable material for most applications. It is strong mechanically, resistant to severe heat shock and chemical attack, and transparent to ultraviolet, visible, and infrared radiation. However, the melting point of cristobalite, the most stable form of crystalline silica, is 1713°C—a temperature quite beyond the range of commercial furnaces. Furthermore, the viscosity of this form of silica, when molten, is so high that it would be impossible to remove bubbles occluded in the melt because of previous volume expansion, or to work it into desirable shapes by mass-production machines.[24]

Viscosity is the reciprocal of fluidity, thus indicating resistance to flow. According to Maxwell's definition "the viscosity of a substance is measured by the tangential force on unit area of either of two horizontal planes of indefinite extent at unit distance apart, one of which is fixed

while the other moves with unit velocity, the space between being filled with a viscous substance." The coefficient of viscosity is usually denoted by the symbol η, and Maxwell's definition may be expressed by the formula:

$$\eta = \frac{F \times s}{A \times v} \tag{1.1}$$

F is the force, s the distance by which the two parallel planes are separated, v the relative velocity of one plane with respect to the other, and A the area over which the planes are in contact. The unit of viscosity is one poise, and its dimension is $ML^{-1}T^{-1}$. In the c.g.s. system of units it is thus measured in dynes per sec per cm^2.[1] Golden syrup has a viscosity of 350 poises at 25°C, pitch 10^8 poises at 25°C, water 0.015 poise at 20°C, and air 0.183×10^{-3} poise at 18°C.

Viscosities of glasses include a range of 12 orders of magnitude from room temperature to melting temperatures. Consequently, it is often convenient to express them logarithmically. In its molten state in the glass tank the viscosity is of the order of 10 ($\log \eta = 1$) or less. Pouring into molds takes place at about $\eta = 100$ and blowing shapes from the mold at η from 10^3 to 10^7. The values of η for bench work range from 10^3 to 10^8. At the Transformation Point, T_g, all glasses attain a viscosity $\eta = 10^{13}$–10^{14}, and the viscosity and many other physical parameters of glass undergo a discontinuous change as a function of temperature unless sufficient time is taken to establish equilibrium (page 33). Fig. 1.1a shows the change of viscosity with temperature for a number of the glasses listed in Table 1.1 and silica (after Douglas[14]). Fig. 1.1b gives similar data for a number of Corning glasses.[15] For limited temperature ranges, the relationship between viscosity and temperature can be expressed by a formula of the general type:

$$\eta = Ae^{b/T} = Ae^{B/RT} \tag{1.2}$$

where B is the activation energy, R the gas constant, and T the absolute temperature. Plots of $\log \eta$ vs $1/T$ thus give straight lines.

Fig. 1.2 reproduces measurements by Preston[25] of the effect of different Na_2O contents on the viscosity of soda-silica glasses at high temperatures. Although the viscosity is reduced by increasing contents of Na_2O, it is by no means a linear function of the Na_2O content. More generally, it may be said that the properties of the glass components or their effects on the glass properties are not additive.

A study of these effects is of course of prime interest, and in the absence of a reliable theory of the state of glass systematic investigations of a large variety of compositions have been undertaken by many workers in the field. Conditions of controlled experimentation are difficult to maintain on account of the high temperatures at which the melt is made,

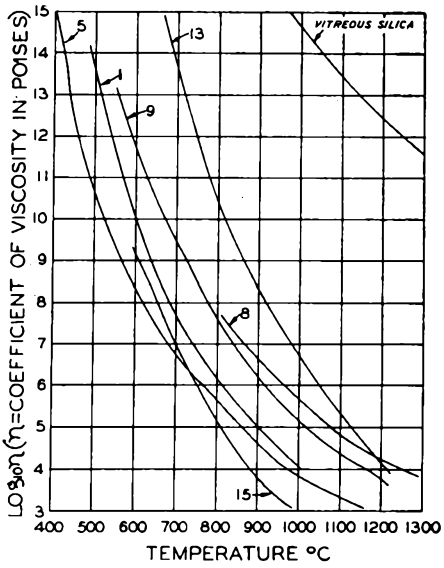

Fig. 1.1(a). Viscosity-temperature relation for some glasses listed in Table 1.1. After R. W. Douglas.[14] (*Courtesy Institute of Physics, London.*)

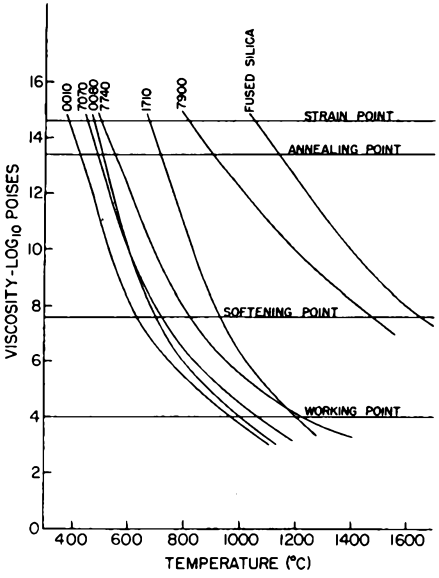

Fig. 1.1(b). Viscosity-temperature curves for various Corning glasses. (*Courtesy Corning Glass Company Corning, N.Y., Bulletin B-83.*)

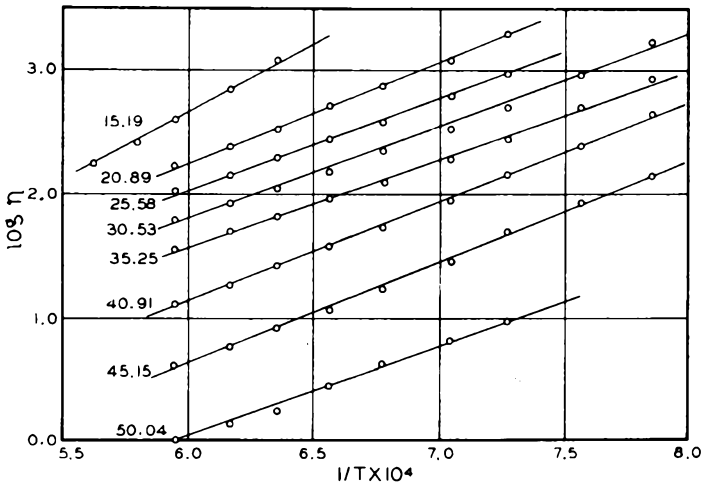

Fig. 1.2. Relationship between viscosity and absolute temperature for soda-silica glasses at high temperatures. The varying Na_2O content in per cent is the parameter shown on the curves. After E. Preston.[25] (*Courtesy Cambridge University Press, London.*)

whereas reactions of the glass tank walls with the melt may alter the composition of the batch. With the reservation that results from any source need verification, it may be interesting to note those obtained by G. Gehlhoff and M. Thomas:[26]

(1) Alkalies decrease viscosity more than any other oxide, especially at high temperatures, and Na_2O more than K_2O.
(2) Na_2O-K_2O glasses have a minimum viscosity in certain proportions, which is particularly noticeable at lower temperatures.
(3) MgO and SnO increase the viscosity, especially at lower temperatures.
(4) CaO raises viscosity more than any other oxide at low temperatures, but at higher temperatures it first decreases, then increases viscosity.
(5) BaO and PbO decrease the viscosity at all temperatures.
(6) Addition of B_2O_3 up to 15 per cent increases viscosity, but further addition diminishes it, the effect being much greater at low temperatures.
(7) Al_2O_3 increases and Fe_2O_3 decreases viscosity.

The intricacy of the "behavior pattern" of multicomponent glass systems is indicated by the various effects which different admixtures to the batch have on the viscosity. Another striking example is the lowering of the melting point by addition of suitable oxides. Since the high M.P. of silica, to which reference was made above, drops by nearly 1000°C when 25 per cent of soda (Na_2O) is added, it comes well within the working range of practical furnaces. Unfortunately, such a binary glass is soluble in water, and other compounds must be added to counteract this property. Lime (CaO) is generally chosen, resulting in the basic soda-lime-silica glass, which, in its essential composition, dates back to the time of the Egyptians, and has been used with little modification ever since.

The modern glassmaker must be in a position to analyze in advance the system as a whole and to direct his processes so that desired results prevail. Thus, a graphical representation of the "behavior pattern" is of great help, and some space is devoted to the description of phase diagrams in Chapter 17, which might be read to advantage at this point. It must be remembered, however, that the data presented by phase-equilibrium diagrams can be applied only to conditions of equilibrium and that such conditions are not the most important, technically, in the production of glasses. Valuable as these diagrams are in showing precisely the crystalline phases (if any) which are present under given conditions of composition and temperature, even more essential to the technologist, and of equal interest scientifically, are the kinetics of the

crystallization process.[27] This will become evident from a study of the "glassy state" in the following.

The Glassy State

The properties which we associate with glass are such that it might be called a solid. However, the fact that glass is rigid does not make it a solid in the physical sense of the word. Lengthy discussions on the definitions of terms for the "glassy state" have been published from time to time, and it is becoming apparent that this study will materially contribute to the understanding of the "liquid state," for which no satisfactory theory yet exists.[25] When an ordinary melt is cooled below the liquidus temperature, the solid phase will crystallize out and result in a regular crystal lattice extending throughout the volume of the solid. The temperature will remain constant until all the liquid phase has solidified, and then drop to room temperature during the cooling cycle. Solids, then, have a sharply defined melting point and are crystalline in nature.

In the case of a glass-forming compound the transition from the liquid to the solid phase is not sharply defined, and one cannot speak of a M.P. in the same sense. While there is a narrow range of temperature where a tendency towards crystallization (devitrification) exists, this range is passed quickly enough during the cooling of the glass melt so that the rapidly increasing viscosity of the melt freezes the molecular aggregates as they exist in the liquid state and maintains the disorderly array at room temperature where glass is a rigid body. Glass is thus "a vitreous substance which is called a frozen or rigid liquid." It is thermodynamically unstable and tends to crystallize when held long enough at the proper temperature. The slow rate of crystallization thus has a chance to act on the whole body of the melt. Ordinarily, however, the critical temperature range is passed quickly, so that crystallization does not occur to any noticeable extent.

The difference between a crystalline solid and a vitreous body, such as glass, is then a matter of the size of the domains through which molecular aggregates of definite structure extend. With the aid of x-ray analysis, applied first by Wykoff and Morey,[28] then by J. T. Randall, H. P. Rooksby, and B. S. Cooper,[29] and later by B. E. Warren and A. D. Loring[30] and others, the concept gradually evolved that SiO_4 groups exist in all glasses as well as in crystalline silica. This idea was first proposed by Zachariasen.[31] Each silicon atom is surrounded by four oxygen atoms spaced tetrahedrally at a distance of 1.62 A.U. from the silicon atom, and each oxygen atom is generally shared by two tetrahedral groups. The building blocks of vitreous and crystalline silica are thus the same. In glass the tetrahedra may form a regular lattice over a distance of a few or

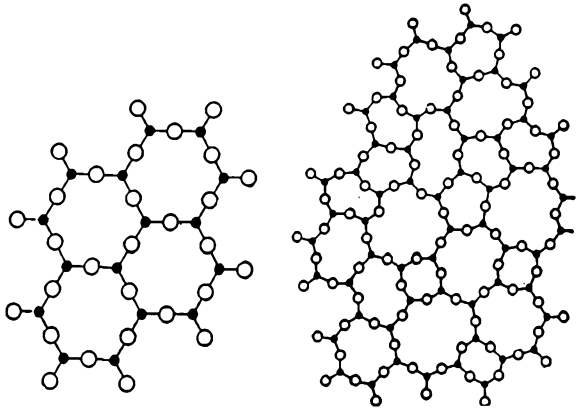

Fig. 1.3. Schematic representation in two dimensions of the difference between the structure of a crystal (left) and a glass (right). After W. H. Zachariasen.[31] (*Courtesy Journal of the American Chemical Society.*)

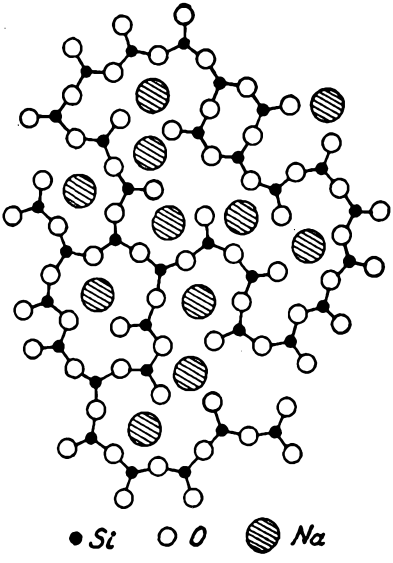

Fig. 1.4. Schematic representation in two dimensions of the difference between the structure of a crystal (left) and a glass (right). After B. E. Warren and J. Biscoe.[32] (*Courtesy Journal of the American Ceramic Society.*)

a few thousand Angstrom units, but not more. In a crystal the regular lattice extends to visible dimensions. The ability of glass to maintain the random network against the tendency toward crystal formation is due to the existence of networks of strong chemical bonds which resist re-orientation on cooling. Fig. 1.3 illustrates schematically in two dimensions the irregular structure of a glass as distinguished from the regularly repeating structure of a crystal (after Zachariasen). Fig. 1.4

similarly gives the structure of a soda-silica glass after Warren and Biscoe,[32] who comment as follows:

"Since the real structure exists in three dimensions, it is necessary to take certain liberties in making a schematic two-dimensional representation. In three dimensions each silicon is tetrahedrally surrounded by four oxygens, and in the two-dimensional representation each silicon is shown surrounded by only three oxygens. The oxygens are correctly represented, some of them bonded between two silicons, and others bonded to only one silicon. The sodium ions (Na^+) are shown in various holes in the irregular silicon-oxygen network. This figure represents very well the essential scheme of structure in a soda-silica glass. There is a definite scheme of coordination; each silicon tetrahedrally surrounded by four oxygens, and part of the oxygens bonded between two silicons and part to only one silicon. The sodium ions are held rather loosely in the various holes in the silicon-oxygen network, and surrounded on the average by about 6 oxygens. Although it is a perfectly definite scheme of structure, there is no regular repetition in the pattern, and hence the structure is noncrystalline."

Furthermore Morey[1] remarks:

"There is no regular repetition, and soda-silica glass has no definite chemical composition. As the soda content is increased and the proportion of oxygen atoms to silicon atoms increases more and more of the oxygens are bonded to only one silicon, and more and more sodium atoms find places in the irregular openings in the three-dimensional silicon-oxygen network. The atoms of that network oscillate about average positions as the result of temperature motion, and under the influence of an electric field the sodium ions readily migrate from one hole to another, and the electrical conductivity is due to this stepwise migration.

"The lowering of the softening point of silica glass on addition of soda is the result of breaks in the silicon-oxygen framework resulting from an increasing number of oxygens being bonded to only one silicon. As more and more of these bonds are broken, the structure becomes less rigidly braced in three dimensions. 'Since there is no scheme of repetition in the glass, no two points are exactly identical. There are points with widely varying degrees of weakness, at which flow or breakage can occur at a continuous variety of temperatures. Hence it is readily understood why glass gradually softens, rather than having a definite melting point like a crystal.

"The picture of the structure of glass worked out on the basis of x-ray studies by Warren, which is in agreement with the theoretical deductions of Zachariasen, is one of a random nonrepeating and nonsymmetrical network. It is in complete agreement with the concept of the constitution of glass as that of a typical liquid, in which the atomic configurations characteristic of some high temperature have become fixed by reason of the great viscosity of glass at ordinary temperatures. It is in accord with the definition: A glass is an inorganic substance in a condition which is continuous with, and analogous to, the liquid state of that substance, but which, as the result of having been cooled from a fused condition, has attained so high a degree of viscosity as to be for all practical purposes rigid."

Much is being done to clarify these concepts further, and work is in progress at the Department of Ceramic Engineering, Ohio State University, Columbus, Ohio, to apply the use of radioactive tracers to the elucidation of the glassy state.[33,34] From their report[34] Fig. 1.5 is reproduced, giving a graphic illustration of the crystal lattice of solid silica,

silica glass, and soda-lime glass. By measuring the rate of diffusion of radioactive Na^{24} conclusions can be drawn on the energy required to move the ion from one equilibrium position to another. For a more compre-

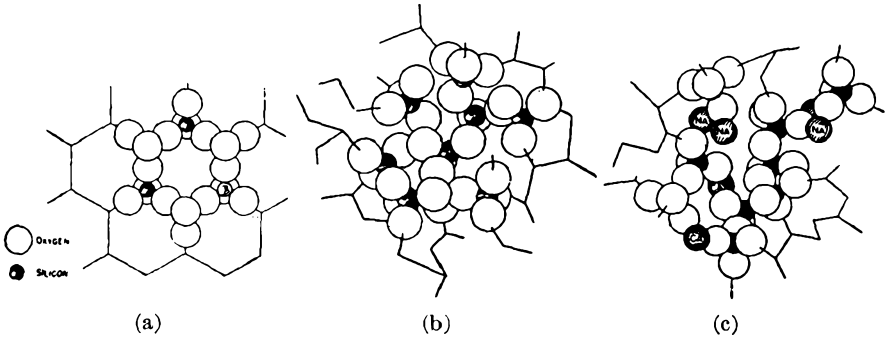

Fig. 1.5. Schematic arrangement of SiO_4 tetrahedra (a) in a crystalline form of silica; (b) in silica glass; (c) in a soda-lime glass together with Na and Ca cations. Radii in all three figures not proportional to actual ionic radii. After H. H. Blau and J. R. Johnson.[34] (*Courtesy Ogden Publishing Company.*)

hensive review of the progress in the theory of the physical properties of glass, see Stevels.[35]

REFERENCES

1. Morey, G. W., "The Properties of Glass," New York, Reinhold Publishing Corp., 1938.
2. Phillips, C. J., "Glass, the Miracle Maker," 2d Ed. New York, Pitman Publishing Corp., 1948.
3. Espe, W. and Knoll, M., "Werkstoffkunde der Hochvakuumtechnik," Berlin, J. Springer, 1936. (Obtainable from Edward Bros., Ann Arbor, Mich.)
4. Hodkin, F. W., and Cousen, A., "A Textbook of Glass Technology," London, Constable, 1929.
5. Scholes, S. R., "Modern Glass Practice," Chicago, Industrial Publications, Inc., 1935.
6. Scoville, W. C., "Revolution in Glassmaking," Harvard Univ. Press, 1948.
7. *Glass Ind.*, Ogden Publishing Co., 55 West 42nd St., New York 18, N.Y.
8. *Am. Ceram. Soc. Bull.*, 20th and Northampton Streets, Easton, Pa.
9. *J. Am. Ceram. Soc.*, 20th and Northampton Streets, Easton, Pa.
10. Handbooks and Bulletins, American Society for Testing Materials (ASTM), 1916 Race St., Philadelphia, Pa.
11. *J. Soc. of Glass Tech.*, "Elmfield" Northumberland Rd., Sheffield 10, England.
12. *Transact Brit. Ceram. Soc.*, North Staffs Technical College, Stoke on Trent, England.
13. Radio-Television Manufacturers Association Data Bureau, 90 West St., New York, N.Y.
14. Douglas, R. W., "The Use of Glass in High-Vacuum Apparatus," *J. Sci. Inst.*, **22**, 81–87 (1945).
15. "Properties of Selected Commercial Glasses," *Bull. B-83*, Corning, N.Y., Corning Glass Works (1949).

16. Phillips, C. J., "Glass as an Electrical Insulator," *J. Appl. Phys.*, **11**, 173–181 (1940).
17. Barnes, B. T., Forsythe, W. E., and Adams, E. Q., "The Total Emissivity of Various Materials at 100 to 500°C," *J. Opt. Soc. Am.*, **37**, 804–807 (1947).
18. Dale, A. E., and Stanworth, J. E., "Sealing Glasses," *J. Soc. Glass Tech.*, **29**, 77–91 (1948).
19. Preston, F. W., "The Mechanical Properties of Glass," *J. Appl. Phys.*, **13**, 623–634 (1942).
20. Baker, T. C., and Preston, F. W., "The Effect of Water on the Strength of Glass," *J. Appl. Phys.*, **17**, 179–188 (1946).
21. Weyl, W. A., "Chemical Aspects of Some Mechanical Properties of Glass," *Research*, **2**, 50–61 (1948).
22. Long, B., "Recent Progress in the Uses of Glass as a Structural Material" (In French), *Bull. Tech. de Bur. Veritas*, **28**, 127–133 (1946). Also, *Eng. Dig.*, 173–175 (Apr., 1947).
23. Sun, Kuan Han, "Fundamental Conditions for Glass Formation," *J. Soc. Glass Tech.*, **31**, 143, 245–253 (1947).
24. Day, A. L., "Developing American Glass" (Edgar Marburg Lecture), *Proc. ASTM*, **36**, Pt. 2, 1–16 (1936).
25. Preston, E., "Supercooled Silicates and their Importance in Considerations of the Liquid State," *Proc. Phys. Soc. London*, **53**, 568–584 (1941).
26. Gehlhoff, G., and Thomas, M., "The Physical Properties of Glasses and their Dependence on Composition" (In German), *Z. Tech. Phys.*, **7**, 260–278 (1926).
27. Stanworth, J. E., "Physical Properties of Glass," Oxford, Clarendon Press, 1950.
28. Wyckoff, R. W. G., and Morey, G. W., "X-ray Diffraction Measurements on some Soda-Lime-Silica Glasses," *J. Soc. Glass Tech.*, **9**, 265–267 (1925).
29. Randall, J. T., Rooksby, H. P., and Cooper, B. S., "The Diffraction of X-rays by Vitreous Solids and its Bearing on their Constitution," *Nature*, **125**, 458 (Supplement 3151) (1930).
30. Warren, B. E., and Loring, A. D., "X-ray Diffraction Study of the Structure of Soda-Silica Glass," *J. Am. Ceram. Soc.*, **18**, 269–276 (1935).
31. Zachariasen, W. H., "The Atomic Arrangement in Glass," *J. Am. Chem. Soc.*, **54**, 3841–3851 (1932).
32. Warren, B. E., and Biscoe, J., "Fourier Analysis of X-ray Patterns of Soda-Silica Glass," *J. Am. Ceram. Soc.*, **21**, 259–265 (1938).
33. Johnson, J. R., "Radioactive Tracer Methods Applicable to Ceramic Research," *Ceram. Bull.*, **29**, 16–19 (1950).
34. Blau, H. H., and Johnson, J. R., "Investigation of the Glass Structure using Radioactive Tracers," Ohio State University Engineering Experiment Station News (Dec. 1948); also: *Glass Ind.*, **30**, 393–394 (1949).
34*a*. Johnson, J. R., Bristow, R., and Blau, H. H., "The Study of simple Soda Lime Glass Structures using Radioactive Isotopes." *J. Am. Cer. Soc.* (July, 1951).
35. Stevels, J. M., "Progress in the Theory of the Physical Properties of Glass," New York, Elsevier Publishing Co., Inc., 1948.

CHAPTER 2

THE ANNEALING OF GLASS

The very low thermal conductivity of glasses and their greatly varying unit-expansion with temperature makes them liable to mechanical stresses when heated or cooled. The elimination of these stresses or their confinement to safe values is of vital concern to the glassmaker. Electron-tube designers and manufacturers know how important it is to pay the greatest attention to the thermal resistance of glass in order to safeguard their product. A discussion of the underlying factors will thus be worth while.

When a glass body is cooled from the molten state, it is initially in thermal equilibrium. On entering a mould or being drawn from the tank the surface will cool more rapidly than the body, and the contraction of the surface will exert a force on the interior. This interplay of forces sets up a hydrostatic pressure exerted by the interior on the surface layer, which must flow to relieve the pressure. As long as such flow is possible, no stresses will result.* On further cooling, the interior body will become rigid, but remain hotter than the surface throughout the cooling cycle and maintain its stress-free condition as long as the temperature gradient is constant.

The temperature distribution through the cross-section of a slab will be parabolic, as shown in Fig. 2.1(a). When the temperature throughout the body is equalized at room temperature, the vanishing of the temperature gradient will introduce a *permanent strain*, shown in the lower part of Fig. 2.1(b). Fig. 2.1(a) and 2.1(b) are separated in time. The upper part of each diagram represents the temperature distribution through the cross section of a slab of glass and the lower part the strain distribution through the slab, where compression is plotted upwards and tension downwards. The strain distribution caused by heating or cooling at a constant rate is a parabola crossing the horizontal axis of zero strain at a distance from the center of the slab equal to 0.578 of the semithickness.[1] From the temperature of solidification to room temperature the interior contracted by a greater amount than the surface. The interior is, therefore, in tension and the surface in compression by induction. This is the opposite distribution of strain to that removed at elevated tempera-

* The writer is indebted to Dr. H. R. Lillie for this concept.

ture by viscous flow when the surface began to contract. The permanent strain is equal to and opposite in sign to that removed on cooling from the viscous state. The magnitude will be proportional to the temperature gradient carried down from the viscous state, and it will therefore depend on the rate of cooling.

It may be useful to point out that the application of a force in one direction always produces a force in the system which is equal to and opposite that applied. This is known as Hooke's Law: "*Ut tensio, sic vis.*" In evaluating strain patterns it is best to visualize the effect of the primary cause, such as the contraction of the hot interior of the slab

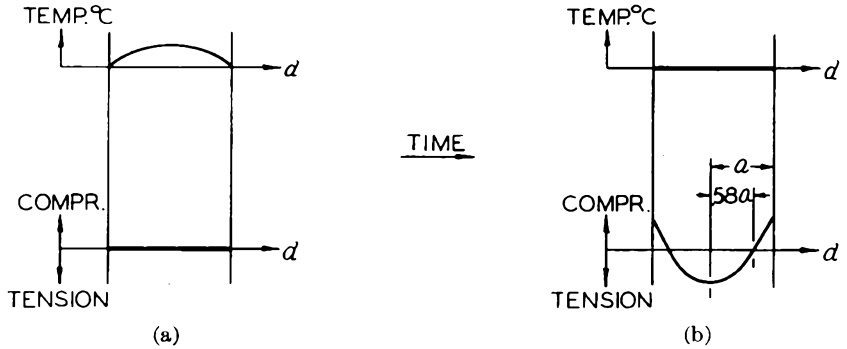

Fig. 2.1. Temperature and stress distribution in a glass slab. (a) During cooling from viscous state as long as temperature gradient between surface and interior is constant. (b) After equalization of temperature throughout the slab.

above, which is opposed by the colder outer layers. The contraction in the interior is thus not able to work itself out, leaving a state of tension.

Let us now consider a slab of glass which has already set. However, because of extremely slow cooling from the molten state it has no temperature gradient and no strain at 200°C. On cooling at a uniform rate to room temperature the outer surface of the slab will cool first, the interior remaining hotter. The tendency of the surface to contract will be resisted by the interior, which now cannot yield; this leads to compression in the interior and tension at the surface as long as the temperature gradient exists (Fig. 2.2[a]). When uniform temperature throughout the slab is reached at room temperature, the strain will disappear (Fig. 2.2[b]). It is thus a *temporary strain.* If the same slab is now heated from its stress-free condition at room temperature, the surface will be hotter than the interior and a temperature and stress distribution results, as shown in Fig. 2.3 (a,b). There is tension at the center and compression at the surface. Both will disappear when the temperature gradient ΔT disappears. They are temporary stresses co-existent with ΔT as long as heating is not carried into the viscous range. If, on the other hand,

heating is continued into the annealing range and maintained long enough for the stress pattern (Fig. 2.3[b]) to equalize itself by viscous flow, the sequence of Fig. 2.1 and a permanent strain will be obtained on subsequent cooling, as shown in Fig. 2.1 (b).

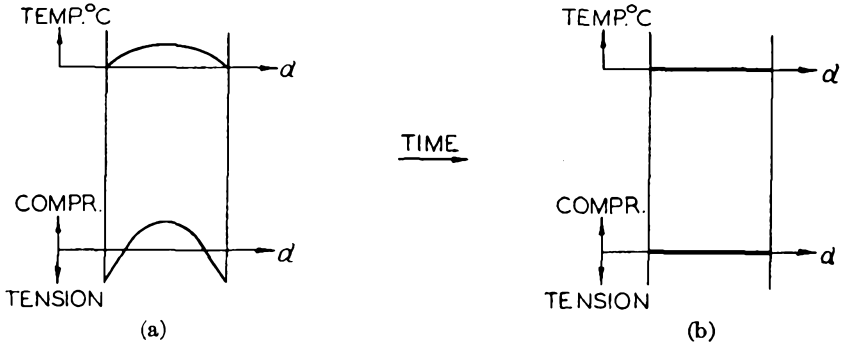

Fig. 2.2. Temperature and stress distribution in a glass slab. (a) A temperature gradient is produced in a strain-free slab below the annealing range; a temporary strain results. (b) After equalization of the temperature, the strain disappears.

This last example shows that it is possible to produce surface compression by annealing originally strain-free glass. A glass article is particularly strong in surface compression. By increasing the cooling rate in the annealing range the amount of surface compression in the final product can be increased. This technique is applied to a variety of commercial products, such as motorcar window panes.

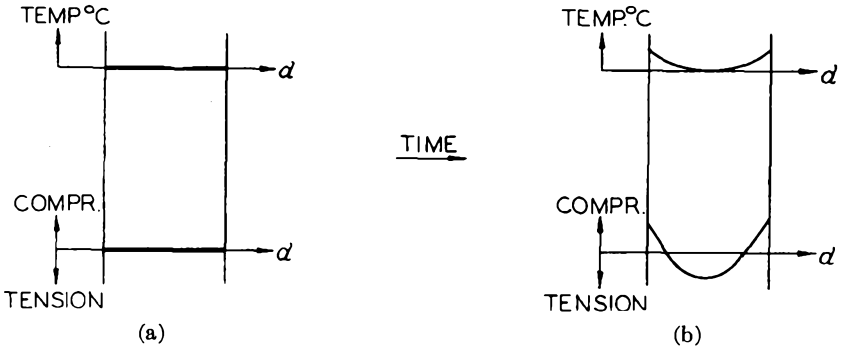

Fig. 2.3. Temperature and stress distribution in a glass slab. (a) A strain-free slab at room temperature throughout; (b) After heating the surfaces.

If, on cooling the glass from the annealing range, the temperature gradient is stabilized at such a point that the strains resulting from the establishment of the gradient are only partly equalized by viscous flow, a certain amount of surface tension and body compression will be carried

down to low temperatures. When the glass slab then attains room temperature throughout, the permanent strain, which appears because of the vanishing of the temperature gradient (surface compression), will in part be neutralized by the strain carried down from high temperature (surface tension) and will result in a smaller compression at the surface. If no strain was lost on establishing the temperature gradient at elevated temperature, no permanent strain will result.

Definition of Terms

Certain conventions have been established to define the critical temperature ranges for annealing. Thus, on a joint recommendation of the British and German Glass Technological Societies in 1930,

> "It is agreed that the symbol *Tg* shall replace all other conventions to denote the *Transformation Temperature* of a glass. The maximum point reached on the complete thermal expansion curve for the glass, namely the point normally corresponding with its *Softening Temperature*, shall be denoted by the symbol *Mg*, and that this symbol shall replace any other convention in use."

While Transformation Temperature, *Tg*, is still used in European literature, it is now generally realized that it is not a critical temperature for a given glass composition and that it is better to speak of a Transformation Range. The "Glass Glossary," compiled by the Glass Division Committee on Classification, Nomenclature, and Glossary of the American Ceramic Society,[2] does not list either term. There is no entry under "transformation." The following definitions are taken from this "Glossary":

(1) **Annealing Point:** The temperature at which the internal stress is substantially relieved in 15 minutes. It corresponds to the equilibrium temperature at which the glass has a viscosity of $10^{13.4}$ poises, as measured by the loaded fiber method, using the equation:

$$\eta = \frac{m \times gl}{3\pi r^2 \frac{dl}{dt}} \tag{2.1}$$

where η = viscosity in poises
m = load in grams
g = acceleration due to gravity = 980 cm/sec/sec
l = heated or effective length of fiber in cm
r = fiber radius in cm
$\frac{dl}{dt}$ = elongation rate in cm/sec

The annealing point corresponds generally to the upper end of the annealing range.

(2) **Softening Point:** The temperature at which a uniform fiber, 0.5 to 1.0 mm in diameter and 22.9 cm long, elongates under its own weight at a

rate of 1 mm per min when the upper 10 cm of its length is heated in a prescribed furnace[3] at the rate of approximately 5°C per min. For a glass of density near 2.5 this temperature corresponds to a viscosity of $10^{7.6}$ poises.

(3) **Melting Temperature:** The range of furnace temperatures within which melting takes place at a commercially desirable rate and at which the resulting glass generally has a viscosity of $10^{1.5}$ to $10^{2.5}$ poises. For purposes of comparing glasses it is assumed that the glass at melting temperature has a viscosity of 10^2 poises.

(4) **Working Range:** The range of surface temperature in which glass is formed into ware in a specific process. The "upper end" refers to the temperature at which the glass is ready for working (generally corresponding to a viscosity of 10^3 to 10^4 poises), the "lower end" to the temperature at which it is sufficiently viscous to hold its formed shape (generally corresponding to a viscosity greater than 10^6 poises). For comparative purposes, when no specific process is considered, the working range of glass is assumed to correspond to a viscosity range from 10^4 to $10^{7.6}$ poises.

(5) **Deformation Point:** The temperature observed during the measurement of expansivity by the interferometer method, at which viscous flow exactly counteracts thermal expansion. The deformation point generally corresponds to a viscosity in the range from 10^{11} to 10^{12} poises.[2]

This definition makes the deformation point equal to the former Softening Temperature, *Mg*, defined above, while the Softening Point corresponds to a much higher temperature. How soon this suggested terminology will be generally adopted remains to be seen. In any case the reader should be on his guard when meeting these terms. In addition, at the lower end of the annealing range there is the Strain Point, which is generally taken to be the temperature at which glass can be annealed commercially in 16 hours. The viscosity at that temperature is of the order of $10^{14.6}$ poises.

These various reference temperatures and temperature ranges are tabulated in Table 2.1, which is an extension of a table by Phillips.[4] Table 1.3 (pp. 6,7) contains the reference temperatures for a number of Corning Glasses.

Fundamental investigations on the theory of annealing were undertaken in 1917 at the Carnegie Institution of Washington by Adams and Williamson and co-workers[1,5] when sudden demands by the armed forces for large quantities of optical glass found the United States with little experience in its manufacture. During the few ensuing years until the end of World War I over 600,000 pounds of optical glass were made under the scientists' close supervision. The working theory of annealing, which they derived, was applied to industrial problems for the next 20 years.

This was indeed a remarkable achievement. At the same time their theory of strain release by thermal treatment was restricted in its application to the range of temperatures, known as the "annealing range." Clerk Maxwell had derived a theory of elasticity for viscous bodies in 1890, according to which the rate of strain release was proportional to the amount of strain present. Adams and Williamson found, however, from

TABLE 2.1. REFERENCE TEMPERATURES AND TEMPERATURE RANGES WITH CORRESPONDING VISCOSITIES FOR REPRESENTATIVE GLASS TYPES

Ref. Temp.	Max. Range	Borosilicates	Lime Glasses	Lead Glasses	Viscosity in Poises	log η	Ref.
Melting temp. (°C)					10^2	2	2
Working range		−1220	−1200	−1000	10^4–$10^{7.6}$	4.0–7.6	2
Softening point (°C)	440–1510	690–1510	670–750	580–660	4.5×10^7	7.6	2, 4
Deformation point (°C) (softening temp. Mg)					10^{11}–10^{12}	11–12	2
Annealing point	350–890	480–890	500–570	425–460	2.5×10^{13}	13.4	2, 4
Strain point	300–790	445–790	470–530	380–430	4.0×10^{14}	14.6	2, 4

experimental measurements that the rate of strain release was proportional to the square of the strain present and not to the first power. They expressed their findings by the following equation:

$$-\frac{dF}{dt} = ABF^2 \tag{2.2}$$

F is the stress which produces the strain (stress and strain are equivalent) and dF/dt is its time rate of change. A, the "annealing constant," determines the time necessary to anneal the glass at constant temperature. It is determined experimentally for a large number of glasses, and found to be an exponential function of temperature, θ, according to

$$\log A = M_1\theta - M_2 \tag{2.3}$$

M_1 and M_2 are experimental constants. The integration of Equation 2.2 leads to

$$\frac{1}{F} - \frac{1}{F_0} = ABt \tag{2.4}$$

F_0 is the stress at time $t = 0$, and F is the stress at time t. B is the stress-optical coefficient which is discussed further in Chapter 3. It relates the measured birefringence δ, observed in the length of path l, to the stress F, which produces it, by

$$\delta = BFl \tag{2.5}$$

Noting the proportionality of δ with F and introducing a constant $A' = A$, one may write Equation 2.4 by substitution as follows:

$$\frac{1}{\delta} - \frac{1}{\delta_0} = A't \tag{2.6}$$

δ_0 is the observed birefringence, a measured indication of strain, at time $t = 0$ and δ the birefringence remaining after annealing for a period of time t. The remaining strain is thus reduced proportionally with time as actually observed.

Efforts have been made from time to time to relate these experimental equations with viscosity and put them on a sound theoretical basis. Lillie[6] first established a relation between stress and viscosity, and showed that viscosity is changing at such a rate during annealing that strain release is following the time-law discovered by Adams and Williamson. By this added consideration Maxwell's model of stress release can be reinstated. Redston and Stanworth[7] have followed this course and derived annealing schedules which can be set up without the use of the "annealing constant A", referred to above, but are based on the usually more readily available data of "annealing point" and "strain point." For the glass in question the annealing schedule can then be easily set up from charts. This work was done for the specific applications encountered in the tube industry, and might be of sufficient interest to be incorporated in this text.*

Maxwell's relation for the release of strain in a viscous body can be expressed by

$$F = F_0 e^{-t/T} \tag{2.7}$$

F and F_0 have the meaning defined above, and T is the relaxation time which is large in a highly viscous medium and small in a more fluid medium. It can thus be tied to a coefficient of viscosity η by the relation

$$\eta = RT \tag{2.8}$$

R is the modulus of rigidity. By differentiating Equation 2.7 and introducing Equation 2.8, one obtains

$$\frac{d(ln\, F)}{dt} = \frac{1}{T} = \frac{R}{\eta} \tag{2.9}$$

On the basis of his measurements of viscosity and stress on identical samples under the same conditions of test Lillie[6] has shown that

$$\frac{d(ln\, F)}{dt} = \frac{M}{\eta} \tag{2.10}$$

* By permission of the editor, the Society of Glass Technology, Sheffield 10, England.

M is a constant which has the value "one-fourth that of the shear modulus at room temperature." According to Lillie M was found to have the value 5.5×10^{10} dynes per cm^2 for a soda-lime-silica glass. By comparing Equation 2.9 and 2.10 Redstone and Stanworth suggested that M is "very nearly equal to R in the annealing range of the glass," and they proceeded on that basis. One may then write after integration of Eq. 2.10

$$t = \frac{\eta}{R} \times ln \frac{F_0}{F} \tag{2.11}$$

For a stress release of $F_0/F = 1000$ the following is obtained:

$$t = \frac{\eta}{5.5 \times 10^{10}} \times \frac{2.3 \times 3}{60} \text{ minutes} \tag{2.12}$$

This gives the time for which the glass must be held at the annealing temperature θ_0. Assuming that η is invariant with time and equal to 10^{13} poises at θ_0, the annealing time becomes $t_0 = 21$ minutes.

"The values used for θ_0 were based on measurements of the viscosity of samples held for 30 minutes at the temperature of observation. For shorter times than this the viscosity of the chilled glass will be somewhat lower, so that the stress release will be faster for these shorter times. This means that the method of calculation gives a margin of safety, that is, somewhat longer times than are actually required. More precise calculation would have to take into account the marked differences between glasses of various types in the rate at which the viscosity changes with time.[8] Such calculations would needlessly complicate the present schedules. Again, for simplicity, we assume that the glass viscosity decreases by half for every 10° rise of temperature, a value sufficiently correct for most glasses. The time of holding will also become halved, as shown in Fig. 2.4."

After stresses have been released at the annealing temperature θ_0 to a sufficient extent, the ware must be cooled to room temperature at such a rate as to strike a compromise between economical factors (time costs money) and the introduction of permanent strains. Adams and Williams derived the following expression for the cooling rate h

$$h = \frac{s}{ca^2} \text{ °C/min} \tag{2.13}$$

where s is the strain introduced during cooling, measured as birefringence in mμ/cm, a the half thickness of the sample in cm, and c the constant depending on the shape and composition of the glass. For a slab or disk of soda-lime-silica glass, $c \sim 13$; for "Pyrex" glass, $c \sim 3$.

Redston and Stanworth[7] made the simplifying assumption that "the cooling rate is independent of holding time and temperature.

Actually, for a given stress introduction the glass may be cooled more quickly with decrease in the holding temperature, particularly as the temperature drops markedly below θ_0. This fact again provides a margin of safety in the annealing schedule adopted. The full expression for c is given by

$$c = \frac{\alpha E \beta}{\sigma K(1 - \sigma)} \tag{2.14}$$

α is the linear thermal expansion coefficient per °C, E is Young's Modulus in kg/cm^2, β is the stress optical coefficient in mμ/cm per kg/cm^2, σ is

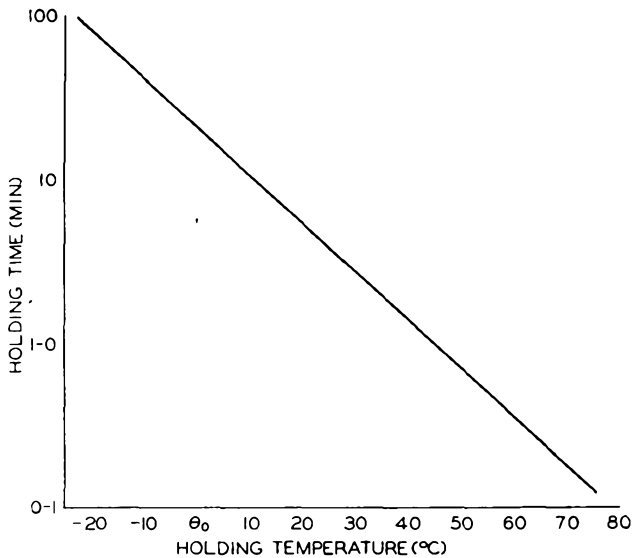

Fig. 2.4. Relation between time and temperature of holding for 1000-fold stress reduction in glass. (θ_0 is the temperature at which the glass viscosity is 10^{13} poises.) After G. D. Redston and J. E. Stanworth.[7] (*Courtesy British Society of Glass Technology.*)

Poisson's Ratio, and K is the thermal diffusivity (equal to the thermal conductivity divided by the product of specific heat and density) in cm^2/min. If typical values for $\frac{1 - \sigma}{E}$ and for K are used and it is assumed that these are practically the same for all glasses, the cooling rates which leave a final strain of 2.5 mμ/cm at the center are plotted in Fig. 2.5 for slabs of various thicknesses." Taking the thermal expansion coefficient of the glass as a parameter, a family of parallel lines is obtained from which it is apparent that a low expansion glass of a given thickness can be cooled at a much faster rate than a high expansion glass of the same thickness.

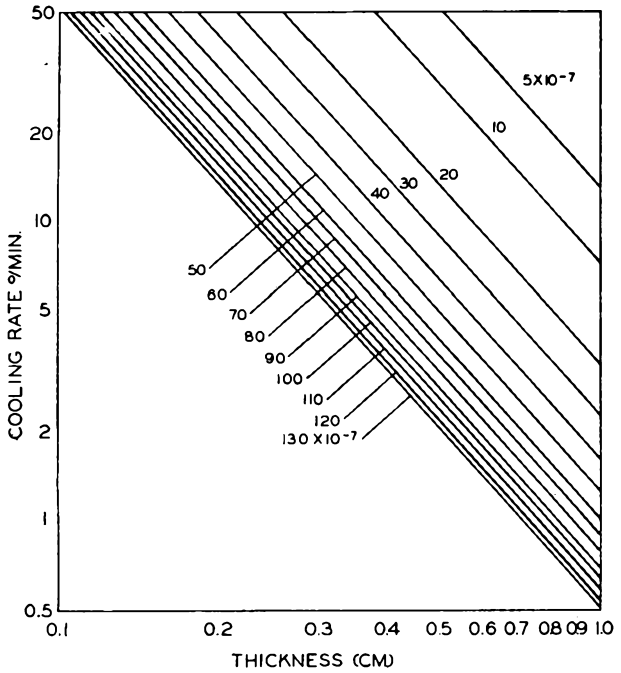

Fig. 2.5. Effect of thickness and linear expansion coefficient on cooling rate necessary to produce 2.5 mμ/cm retardation at the center of a glass slab. After G. D. Redston and J. E. Stanworth.[7] (*Courtesy British Society of Glass Technology.*)

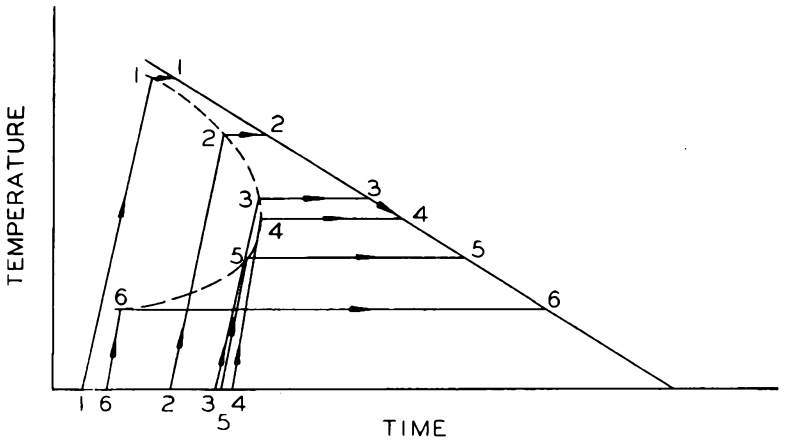

Fig. 2.6. Six possible annealing schedules which produce the same degree of annealing. Schedule No. 4 occupies the least time. After G. D. Redston and J. E. Stanworth.[7] (*Courtesy British Society of Glass Technology.*)

It is apparent from Fig. 2.4 that a wide choice of annealing schedules is available. In Fig. 2.6 six possible schedules are shown, all of which would anneal the sample to about the same extent. It is evident that Schedule 4 requires the least amount of time, and is thus the most economical, provided that the loss incurred from breakage is the same as in the others. The optimum holding temperature for various cooling rates is plotted in Fig. 2.7.

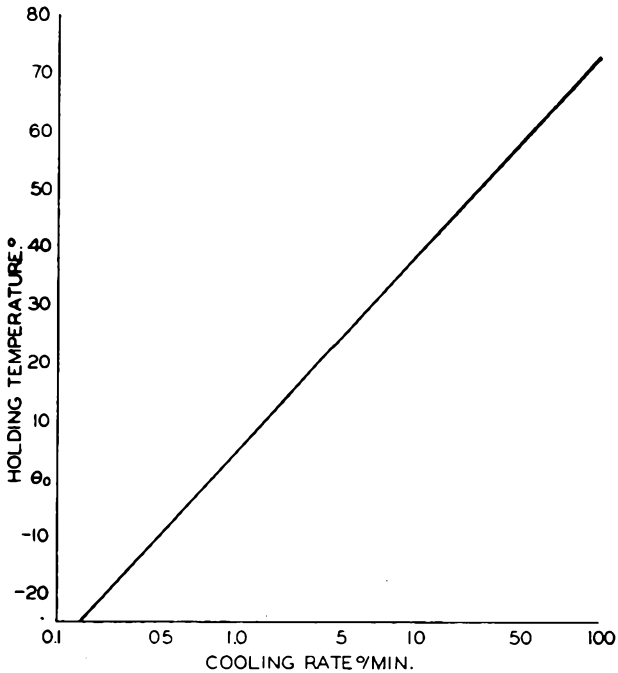

Fig. 2.7. Dependence of optimum holding temperature for glass annealing on cooling rate. After C. D. Redston and J. E. Stanworth.[7] (*Courtesy British Society of Glass Technology.*)

According to these data of Redston and Stanworth[7] a practical annealing schedule can be set up from the graphs in Figs. 2.4 to 2.7, provided the following data are known:

Thermal expansion coefficient (α)
Annealing Point (T_A) (for $\eta = 10^{13}$)
Strain Point (T_s)
Thickness of the glass article (d)

First the cooling rate (h) is obtained from Fig. 2.5, then the optimum holding temperature (T_{opt}) from Fig. 2.7, and finally the holding time

(t_0) from Fig. 2.4. Following these steps for Corning 7720 "Nonex" glass and assuming a thickness of 0.3 cm the following data are obtained:

$$\alpha = 36 \times 10^{-7} \qquad T_s = 484°C$$
$$T_A = 518°C \qquad d = 0.3 \text{ cm}$$

From the graphs it follows that:

$$h = 20°C/\text{min}$$
$$T_{opt} = \theta_0 + 49° = 567°C$$
$$t_0 = 0.7 \text{ min}$$

Schedule A would thus be:

(1) heat to 567°C (at 400°C/min)
(2) hold at 567°C for 42 sec
(3) cool to 484°C at 20°C/min
(4) cool to room temperature (100°C/min)

The data given in Table 2.3 would suggest the following (Schedule B):

(1) heat at 523°C (at 400°C/min)
(2) hold at 523°C for 5 min
(3) cool to 479°C at 39°C/min
(4) cool to 429°C at 78°C/min
(5) cool to 25°C at 400°C/min

Depending somewhat on the cooling rate adopted in Schedule A, both schedules take about 10 minutes. In practice, compromises are necessary, depending on available facilities and temperature control gear. A uniform rate of cooling from the holding temperature all the way to near room temperature is generally advantageous. On the other hand, too short holding times may be difficult to control, and nothing is gained by aiming at optimum holding time when it turns out to be less than a minute. The analysis of the remaining strain will in the end determine the feasibility of any chosen schedule.

Ideal schedules for commercial annealing of ordinary ware, as prepared by Corning Glass Works, are given in Table 2.2 and annealing data for Corning glasses at various thicknesses in Table 2.3.

These general principles on annealing seem to be quite straightforward, and may raise the question in the reader's mind as to why so much mystery is often attached to the working out of successful annealing schedules for given ware with given equipment. There are indeed many complicating factors entering into this art which cannot be treated here in detail. They are of two categories: One group comprises the specific features of the ware (its shape, thickness, and initial stress distribution) and the properties of the annealing furnace (its size, temperature distribution within the chamber, and heat control). The other group is con-

TABLE 2.2. SCHEDULES (IDEAL) FOR COMMERCIAL ANNEALING—ORDINARY WARE*

Annealing Periods

A—Heating to 5°C above annealing point
B—Hold temperature for time—t
C—Initial cooling to a °C below strain point
D—Cooling—next 50°C
E—Final cooling

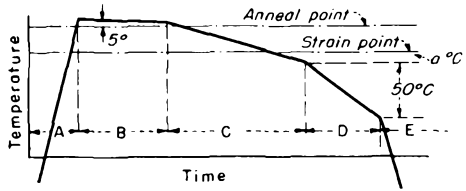

Expansion Coeff. of Glass per °C	Thick. of Glass		Cooling on One Side						Cooling on Two Sides					
			A	B	C		D	E	A	B	C		D	E
	In.	mm.	Heat Rate °C/Min	Time t—Min	Temp. a—°C	Cool Rate °C/min	Cool Rate °C/min	Cool Rate °C/min	Heat Rate °C/min	Time t—min	Temp. a—°C	Cool Rate °C/min	Cool Rate °C/min	Cool Rate °C/min
	⅛	3.2	130	5	5	12	24	130	400	5	5	39	78	400
33×10^{-7}	¼	6.3	30	15	10	3	6	30	130	15	10	12	24	130
	½	12.7	8	30	20	0.8	1.6	8	30	30	20	3	6	30
	⅛	3.2	85	5	5	8	16	85	260	5	5	26	52	260
50×10^{-7}	¼	6.3	21	15	10	2	4	21	85	15	10	8	16	85
	½	12.7	5	30	20	0.5	1.0	5	21	30	20	2	4	21
	⅛	3.2	50	5	5	4	8	50	140	5	5	14	28	140
90×10^{-7}	¼	6.3	11	15	10	1	2	11	50	15	10	4	8	50
	½	12.7	3	30	20	0.3	0.6	3	11	30	20	1	2	11

* Courtesy Corning Glass Works, Corning, New York.

cerned with the physical mechanism of annealing within the glass. From both categories arise factors which cannot be taken into account by an idealized theory. The contribution from the first group is fairly obvious. Large differences in thickness of the ware, in any one piece or, variations from piece to piece necessitate an approximation of the value d to be entered into the equations given above. If the furnace or lehr is not long enough or of sufficient volume, temperature gradients may exist in the ware while it is supposed to be soaking at a uniform temperature and additional permanent strains may thus be introduced on cooling. Lillie has evaluated these factors in a recent publication.[9]*

TABLE 2.3. ANNEALING DATA FOR CORNING GLASSES OF VARIOUS THICKNESSES*

Glass Thicknesses		Annealing Time		Annealing Temp (°C)							
In.	mm	Min	Sec	0010	0080	0120	7040	7050	7070	7720	7740
1.00	25.40	240	0	389	475	395	450	461	455	486	510
0.50	12.70	60	0	407	493	413	467	479	473	504	532
.25	6.35	15	0	425	510	431	484	496	490	521	553
.125	3.18	3	45	443	528	449	501	514	508	539	575
.062	1.59	0	56	461	545	467	518	531	525	556	596
.031	0.79	0	14	479	563	485	535	549	543	574	618
.015	.39	0	3.5	497	580	503	552	566	560	591	639
2+ temp. interval to half viscosity				18	17.5	18	17	17.5	17.5	17.5	21.5
Strain point				397	478	400	450	461	455	484	515
Annealing point				428	510	433		496	490	518	555
Softening point				626	696	630		703		755	820

* Courtesy Corning Glass Works, Corning, New York.

The events taking place in the glass itself during ideal annealing conditions are so complex that they cannot yet be described mathematically. The empirical relations established by Adams and Williamson must serve, therefore, as a satisfactory approach to analysis until the theory has advanced farther. Information on these problems may be found in Refs. 10 to 21.

While the main purpose of annealing, in the generally accepted sense, is the reduction of existing stresses to a sufficiently low value as to make the ware resistant to temperature shock and surface abrasion in use, there are other effects of heat treatment that should be mentioned in passing. The properties of glass can be stabilized by prolonged heat treatment in the lower reaches of the annealing range, whereupon they are less likely to change during subsequent service at somewhat elevated

* The author is indebted to Dr. H. R. Lillie for the opportunity of seeing the manuscript prior to publication.

temperatures.[9,15–18] Glass thus treated is called "stabilized glass." Some stabilizing effect can occur even well below the annealing range.

Ghering and Preston[22] recently reported on experiments performed with Standard Strain Disks. After a set of such disks were heated in an oven at 200°C for 30 days, an average reduction of strain (birefringence) by 8 per cent was observed although the normal annealing temperature of this particular glass is 500°C. "When these same disks were reheated at the same temperature (200°C) for another 30 days, no further change occurred."[22] This emphasizes the important effect of the thermal history of glass articles in general when statements about its physical properties are to be valid.

The following, taken from a paper by A. Q. Tool,[23] shows the fallacy of referring to a critical Transformation Point, *Tg*, where expansion and other properties were thought to undergo a discontinuous change. (Such discontinuities are observed only when the rate of heating or cooling is too rapid to permit the establishment of equilibrium.)

"When almost any glass is cooled and heated through its annealing range at a low enough rate, it is always practically in equilibrium on reaching any temperature in that range. By determining the changes in various properties as these treatments proceed, equilibrium curves can be established. A rapid heating or cooling from any temperature at which a glass is in equilibrium causes departures from such curves."

REFERENCES

1. Adams, L. H., and Williamson, E. D., "The Annealing of Glass," *J. Franklin Inst.*, **190**, 597–631; 835–870 (1920).
2. *Am. Ceram. Soc. Bull.*, **27**, 353–362 (1948).
3. *J. Am. Ceram. Soc.*, **10**, 259 (1927).
4. Phillips, C. J., "Glass, The Miracle Maker," 2d Ed. New York, Pitman Publishing Corp., 1948.
5. Adams, L. H., "The Annealing of Glass as a Physical Problem," *J. Franklin Inst.*, **216**, 39–71 (1933).
6. Lillie, H. R., "Stress Release in Glass, A Phenomenon involving Viscosity as a Variable with Time," *J. Am. Ceram. Soc.*, **19**, 45–54 (1936).
7. Redston, G. D., and Stanworth, J. E., "The Theoretical Development of Simplified Annealing Schedules," *J. Soc. Glass Tech.*, **32**, 32–39 (1948).
8. Dale, A. E., and Stanworth, J. E., "On the Viscosity of Some Glasses in the Annealing Range," *J. Soc. Glass Tech.*, **29**, 414–427 (1945).
9. Lillie, H. R., "Basic Principles of Glass Annealing," *Glass Ind.*, **31**, 355–358; 382, (1950).
10. Morey, G. W., "The Properties of Glass," New York, Reinhold Publishing Corp., 1938.
11. Stanworth, J. E., "Physical Properties of Glass," Oxford, Clarendon Press, 1950.
12. Littleton, J. T., "A Method for Measuring the Softening Temperature of Glasses," *J. Am. Ceram. Soc.*, **10**, 259–263 (1927).
13. Littleton, J. T., and Roberts, E. H., "A Method for Determining the Annealing Temperature of Glass," *J. Opt. Soc. Am.*, **4**, 224–299 (1920).

14. Lillie, H. R., "Viscosity of Glass Between the Strain Point and Melting Temperature," *J. Am. Ceram. Soc.*, **14**, 502–511 (1931).
15. Littleton, J. T., "The Effect of Heat Treatment on the Physical Properties of Glass," *Bull. Am. Ceram. Soc.*, **15**, 306 (1936).
16. Lillie, H. R., "Viscosity-Time-Temperature Relations in Glass at Annealing Temperatures," *J. Am. Ceram. Soc.*, **16**, 619 (1933).
17. Winter, A., "Transformation Region of Glass," *J. Am. Ceram. Soc.*, **26**, 189 (1943).
18. Tool, A. Q., "Relation between Inelastic Deformability and Thermal Expansion of Glass in its Annealing Range," *J. Am. Ceram. Soc.*, **29**, 240 (1946).
19. Tilton, L. W., Finn, A. N., and Tool, A. Q., "Some Effects of Carefully Annealing Optical Glass," *J. Am. Ceram. Soc.*, **11**, 292 (1928).
20. Winter, A., "Structural Homogeneity of Glass," *J. Am. Ceram. Soc.*, **26**, 277 (1943).
21. Littleton, J. T., "The Physical Processes Occurring in the Melting and Cooling of Glass," *J. Am. Ceram. Soc.*, **11**, 292 (1928).
22. Ghering, L. G., and Preston, F. W., "Stability of Birefringence in Glass Articles," *J. Am. Ceram. Soc.*, **33**, 321–322 (1950).
23. Tool, A. Q., "Viscosity and the Extraordinary Heat Effects in Glass," *J. Res. Nat. Bur. Stand.*, **37**, 73–90 (1946).

CHAPTER 3

STRAIN ANALYSIS OF GLASS

The annealing of glass, as described in the previous chapter, would be subject to a large amount of guesswork were it not possible to measure accurately at any stage of the schedule the actual amount and type of strain present. In the present chapter these methods and the theory on which they are based will be described. There will again be occasion to refer frequently to the original investigations by Adams and Williamson.[1-3] Annealing and strain analysis are of necessity two aspects of one subject—the strength of glass.

It is not by any means a simple matter to obtain a clear concept of the interplay of forces acting in a glass body of intricate shape. This is especially true when metallic members are sealed into the glass and the whole body has various temperature gradients throughout its volume. Since time and skill are seldom available, full advantage cannot be taken of the analytical approach offered by methods of photoelasticity[4] and simple operational tests in the form of heat-shock tests and life tests under extreme conditions must suffice. Failures during such tests can at best give a clue of the trouble, and many costly experiments on a trial-and-error basis will be necessary before a satisfactory solution is found. For this reason, and because much time and effort will be saved in the end, it is urgently recommended that a quantitative strain analysis be made at the very beginning of a new glass project.

It was first observed by D. Brewster in 1813[5] that strained glass displays the properties of a birefringent crystal and that the birefringence is proportional to the intensity of the stress. When viewed in polarized light between crossed nicols or sheets of "Polaroid," interference patterns become visible from which the directions and amounts of strain may be deduced.

Ordinary light, when it enters a birefringent crystal or strained glass, is split into two components known as the "ordinary ray" and the "extraordinary ray." These two rays have their electrical vibrations at right angle to each other and travel through the specimen at different velocities. The orientation of the planes of vibration in space depends on the orientation of the optical axis of the crystal. The *optical axis* of the crystal is defined as the direction in which light is transmitted without birefringence (i.e., the ordinary and extra-ordinary rays coincide along the optical axis

and travel with the same velocity). In the case of calcite ($CaCO_3$) the optical axis coincides with the axis of trigonal symmetry. In certain other crystals the ordinary and extra-ordinary rays can coincide and travel with equal velocities in two mutually perpendicular directions in the crystal. Crystals of the first type, like calcite, are called "uni-axial"; crystals of the second type, for which mica is an example, are called "bi-axial".

When light is incident on a crystal at an angle to the optical axis, the direction of vibration at any point in the ordinary wave front is perpendicular to the plane containing the ray in question and the optic axis, and the direction of vibration at any point in the extra-ordinary wave front lies within the plane containing the extra-ordinary ray and the optic axis. The relative intensities of the two beams depend on the direction of vibration in the incident beam with respect to the optical axis. If this direction of vibration in the incident beam is 45° to the optical axis, the intensities of the ordinary and extra-ordinary ray are equal. The refractive index (n_ϵ) for the extra-ordinary ray may be greater or smaller than that for the ordinary ray (n_ω) and, therefore, its velocity less or more ($v = c/n$) than that of the ordinary ray in different crystals. If the ordinary ray travels faster than the extra-ordinary ray, one speaks of a positive crystal, in the reverse case of negative crystals. Quartz, according to this definition, is a positive uni-axial crystal and calcite a negative uni-axial crystal. Glass in tension is a positive uni-axial crystal and in compression a negative uni-axial crystal.

Unfortunate terminology was established for polarized light before the directions of vibration in a polarized beam were determined. The plane of polarization is the plane normal to the plane in which the electrical vibrations of a plane-polarized light beam take place. A light beam is said to be "polarized" in the plane of incidence when the vibrations of the electrical vector take place at right angles to the plane of incidence. As the electrical and magnetic vector, representing light in the electromagnetic theory, are mutually perpendicular to each other and intensity is associated with the electrical vector, one may say that the plane of polarization, as defined above, is understood to be the plane containing the magnetic vector.[6] Whenever possible the use of these terms will be avoided; but they are firmly established in the literature.

If we visualize a block of glass (Fig. 3.1), which is strained in the vertical direction by the action of a thrust, P, parallel to OY, and uniformly distributed over the area, A, an equal and opposite reactive force, P', will result which, together with P, tends to compress the block in the vertical direction. Correspondingly, the block will be expanded in the horizontal mid-plane parallel to XZ. On removal of thrust P the block will regain its original shape.

Glass is thus an elastic body at ordinary temperatures, and is characterized by the validity of Hooke's Law, which states that strain is proportional to stress. The stress-strain diagram for glass is a straight line and the constant of proportionality for each type of stress is a characteristic property of the glass composition and its thermal history. The various elastic moduli are ratios of stress to strain and, together with Poisson's Ratio, are denoted by the following symbols:

E = modulus of extension in tension or Young's Modulus
R = modulus of rigidity or shear modulus
K = modulus of compressibility or bulk modulus
σ = Poisson's Ratio, the ratio of lateral to longitudinal strain under unidirectional stress

The strains resulting from a system of stresses applied to an isotropic substance, such as glass, are described by any two of the above four moduli; the other moduli may be calculated from them according to the relations established by P. G. Tait.[7] As shown in Fig. 3.1 the edges of the cube parallel to thrust P will be shortened by an amount, q, and the edges normal to P will be elongated by p. These are the directions of principal stress. When equal and opposing stresses, P, are applied parallel to two opposite sides of the cube, the resulting strain is a shear expressed by the modulus of rigidity R. If a compressive force, P, is applied uniformly to all sides of the cube, the compression is expressed by the bulk modulus, K or by the compressibility β, which is defined as $1/K$. The following relations apply with respect to the various moduli in terms of the observed displacements:

$$E = \frac{P}{p}; \qquad \sigma = \frac{p}{q} \tag{3.1}$$

$$R = \frac{P}{2(p - q)} \tag{3.2}$$

$$K = \frac{P}{3(p - 2q)} = \frac{1}{\beta} \tag{3.3}$$

$$E = \frac{qKR}{3K + R} \tag{3.4a}$$

$$= 3K(1 - 2\sigma) \tag{3.4b}$$

$$= 2R(1 + \sigma) \tag{3.4c}$$

Each modulus of elasticity is the ratio of a stress intensity to a percentage strain. The intensity of a stress is the force acting per unit area over which the stress is distributed, or the ratio of total force to total area. Its dimension is thus $ML^{-1}T^{-2}$. If weight is used to express a force, the necessary conversion into force units must be made. Table 3.1 gives a tabulation of conversion factors which has been extended to include additional terms not given in its original version.[8]

The experimental fact that glass becomes birefringent under the action

TABLE 3.1. CONVERSION FACTORS FOR PRESSURE AND STRESS UNITS*

Microbar (dyne/cm²)	Micron (μ)	Millibar	Tor (mm Hg)	Poundal psi	In. of Hg	Psi	Newton per cm²	Kg. wt/cm²	Bar	Normal Atm.	Kg wt/mm²	Kilobar
1.0	0.750062	1.0×10^{-3}	7.50062×10^{-4}	4.66650×10^{-4}	2.9530×10^{-5}	1.45038×10^{-5}	1.0×10^{-5}	1.01972×10^{-6}	1.0×10^{-6}	9.86923×10^{-7}	1.01972×10^{-8}	1.0×10^{-9}
1.33322	1.0	1.33322×10^{-3}	1.0×10^{-3}	6.22147×10^{-4}	3.27056×10^{-5}	1.93370×10^{-5}	1.33322×10^{-5}	1.35951×10^{-6}	1.33322×10^{-6}	1.31579×10^{-6}	1.35951×10^{-8}	1.33322×10^{-9}
1.0×10^{3}	7.50062×10^{2}	1.0	7.50062×10^{-1}	4.66650×10^{-1}	2.9530×10^{-2}	1.45038×10^{-2}	1.0×10^{-2}	1.01972×10^{-3}	1.0×10^{-3}	9.86923×10^{-4}	1.01972×10^{-5}	1.0×10^{-6}
1.33322×10^{3}	1.0×10^{3}	1.33322	1.0	6.22147×10^{-1}	3.27056×10^{-2}	1.93370×10^{-2}	1.33322×10^{-2}	1.35951×10^{-3}	1.33322×10^{-3}	1.31579×10^{-3}	1.35951×10^{-5}	1.33322×10^{-6}
2.14295×10^{3}	1.60735×10^{3}	2.14295	1.60735	1.0	6.32813×10^{-2}	3.10808×10^{-2}	2.14295×10^{-2}	2.18520×10^{-3}	2.14295×10^{-3}	2.11493×10^{-3}	2.18520×10^{-5}	2.14295×10^{-6}
3.38645×10^{4}	2.54005×10^{4}	3.38645×10	2.54005×10	1.54571×10	1.0	4.9115×10^{-1}	3.38645×10^{-1}	3.4532×10^{-2}	3.38645×10^{-2}	3.3421×10^{-2}	3.45315×10^{-4}	3.38645×10^{-5}
6.89471×10^{4}	5.17148×10^{4}	6.89471×10	5.17148×10	3.21739×10	2.0360	1.0	6.89471×10^{-1}	7.03070×10^{-2}	6.89471×10^{-2}	6.80455×10^{-2}	7.03070×10^{-4}	6.89471×10^{-5}
1.0×10^{5}	7.50062×10^{4}	1.0×10^{2}	7.50062×10	4.66649×10	2.9530	1.45038	1.0	1.01972×10^{-1}	1.0×10^{-1}	9.86923×10^{-2}	1.01972×10^{-3}	1.0×10^{-4}
9.80665×10^{5}	7.35557×10^{5}	9.80665×10^{2}	7.35557×10^{2}	4.57619×10^{2}	2.8959×10	1.42233×10	9.80665	1.0	9.80665×10^{-1}	9.67841×10^{-1}	1.0×10^{-2}	9.80665×10^{-4}
1.0×10^{6}	7.50062×10^{5}	1.0×10^{3}	7.50062×10^{2}	4.66650×10^{2}	2.9530×10	1.45038×10	1.0×10	1.01972	1.0	9.86923×10^{-1}	1.01972×10^{-2}	1.0×10^{-3}
1.01325×10^{6}	7.600×10^{5}	1.01325×10^{3}	7.600×10^{2}	4.72838×10^{2}	2.9921×10	1.46960×10	1.01325×10	1.03323	1.01325	1.0	1.03323×10^{-2}	1.01325×10^{-3}
9.80665×10^{7}	7.35557×10^{7}	9.80665×10^{4}	7.35557×10^{4}	4.57619×10^{4}	2.8959×10^{3}	1.42233×10^{3}	9.80665×10^{2}	1.0×10^{2}	9.80665×10	9.67841×10	1.0	9.80665×10^{-2}
1.0×10^{9}	7.50062×10^{8}	1.0×10^{6}	7.50062×10^{5}	4.66650×10^{5}	2.9530×10^{4}	1.45038×10^{4}	1.0×10^{4}	1.01972×10^{3}	1.0×10^{3}	9.86923×10^{2}	1.01972×10	1.0

Note: All units containing weights used as forces are at standard temperature, pressure and gravity.

* Adapted from G. W. Morey: Properties of Glass, 1938, Reinhold Publishing Corporation, New York, N.Y.

of stresses indicates a change of the refractive index, n, of glass due to stress. As the strains are different in different directions, the velocity of propagation of light in different directions will also change. A ray of white light entering the cube in the direction XO (Fig. 3.1) will be split into two wave fronts proceeding with different velocities and each polarized in a direction at right angles to the other.

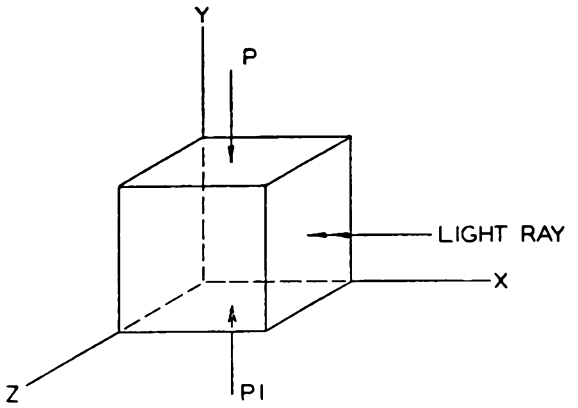

Fig. 3.1. The effect of strain in glass on a beam of polarized light. After Adams and Williamson.[3] (*Courtesy Washington Academy of Sciences.*)

F. Neumann[9] has analyzed the influence of elastic deformation on the propagation of light, and derived the following equations:

$$v_x = v + qx_x + py_y + pz_z \tag{3.5a}$$
$$v_y = v + px_x + qy_y + pz_z \tag{3.5b}$$
$$v_z = v + px_x + py_y + qz_z \tag{3.5c}$$

in which x_x, y_y, and z_z are dilations in the three directions parallel to the three principal axes; v is the velocity of light in the unstressed material; v_x, v_y, and v_z are the velocities of light waves whose vibrations are parallel to the three axes respectively; and p and q are the observed displacements or strains.

If n is the refractive index of the unstressed medium and n_x, n_y, and n_z the refractive indices for light vibrating in the three principal directions, the following relations apply:

$$nv = n_x v_x = n_y v_y = n_z v_z \tag{3.6}$$

From Eq. (3.5a) follows,

$$\frac{v_x - v}{v} = \frac{n - n_x}{n_x} = \frac{q}{v} x_x + \frac{p}{v}(y_y + z_z) \tag{3.7}$$

where for the condition shown in Fig. 3.1, with P acting in the direction OY, the three principal dilations are:

$$x_x = \frac{\sigma P}{E} \tag{3.8a}$$

$$y_y = -\frac{P}{E} \tag{3.8b}$$

$$z_z = \frac{\sigma P}{E} \tag{3.8c}$$

Substituting these values in equation 3.7,

$$\frac{n_x - n}{n_x} = \frac{P}{E}(1 - \sigma)\frac{p}{v} - \left(\frac{P\sigma}{E}\right)\frac{q}{v} = \frac{P}{E}\left[(1 - \sigma)\frac{p}{v} - \sigma\frac{q}{v}\right] \tag{3.9}$$

and similar expressions are obtained for the other directions so that the following set results are:

$$\frac{n_x - n}{n_x} = \frac{P}{E}\left[(1 - \sigma)\frac{p}{v} - \sigma\frac{q}{v}\right] \tag{3.10a}$$

$$\frac{n_y - n}{n_y} = \frac{P}{E}\left(-2\sigma\frac{p}{v} + \frac{q}{v}\right) \tag{3.10b}$$

$$\frac{n_z - n}{n_z} = \frac{P}{E}\left[(1 - \sigma)\frac{p}{v} - \sigma\frac{q}{v}\right] \tag{3.10c}$$

It is seen that the relative change in refractive index in the OX and OZ direction are the same for a thrust in the OY direction. Therefore, a ray of light entering the cube in the OY direction will not show any birefringence. The ray shown as entering the cube in the OX direction in Fig. 3.1 will, however, display birefringence which is defined by $n_y - n_z$ for this direction, and can be determined from equation 3.10 (b and c) when the coefficients p and q have been found by experiment. An error of a small fraction of 1 per cent results when the following relation is adopted:

$$\frac{n_y - n}{n_y} - \frac{n_z - n}{n_z} = \frac{n_y - n_z}{n} \tag{3.11}$$

This simplifies to

$$\frac{n_y - n_z}{n} = \frac{P}{2R}\left(\frac{q}{v} - \frac{p}{v}\right) \tag{3.12}$$

where R is the modulus of rigidity defined above.

In most substances the ray vibrating in a plane parallel to the direction of the compressive stress (p) travels faster than the ray vibrating in the direction of the tensile stress (q). A beam of natural light entering the strained block of glass (Fig. 3.1), as shown from the right along the X-axis, will have its transverse vibrations in the YZ plane. It will then be split up into two plane-polarized components vibrating in the directions Y and Z, respectively. In a unit of time these two components travel different distances, and these will develop between them a *path-difference* δ which will be expressed by

$$\delta = C(p - q)l \tag{3.13}$$

where l is the thickness of the specimen through which the light travels and C a quantity which is proportional to the difference $(n_\epsilon - n_\omega)$ between the refractive indices of the two components. This difference may be designated as Δn. From Equ. (3.12) it is evident that $(p - q)$ is inversely proportional to the applied stress P.

Introducing $F = P/A$ as unit stress measured in kg/cm^2, Equ. (3.13) may be written as follows:

$$\delta = \Delta n \times l = F \times B \tag{3.14}$$

B is the stress-optical coefficient or the birefringence-stress ratio and δ is the optical path difference defined by the product of the birefringence Δn times the length of the light path l. For most common glasses the value of B is about 3×10^{-7} if F is measured in kg/cm^2. A stress of 1 kg/cm^2, applied to a block of glass, then causes an optical path difference of about 3 mμ (millimicrons*) per centimeter length. It is this value δ which is usually measured. The sign of the birefringence may be determined from the fact that under tension an ordinary block of glass behaves as a uni-axial, optically positive, crystal (i.e., the greater index is in the direction of tensile stress). B is measured in "Brewsters" when δ is expressed in mμ, l in cm, and F in bars.† A convenient form of the above equation is the following:

$$\text{Stress (kg/cm}^2) = \frac{\text{Retardation (m}\mu)}{0.981 \times B \text{ (Brewsters)} \times l \text{ (cm)}}$$

Methods of Measurement

There are several experimental procedures available for the observation and measurement of birefringence in glass. The choice of any one of these will depend on the accuracy required. Common methods used in the electronic industry permit the measurement of δ to ± 5 mμ. Refined methods will allow the measurement of ± 0.05 mμ.[10] For optical glass an optical path difference per cm equal to 5 mμ is considered satisfactory. For electronic glassware a strain equal to $1/20$ of the breaking strength is acceptable after annealing. Taking the safe loading as 1 kg/mm^2 or 100 kg/cm^2, gives $\delta = 300$ mμ as an upper limit (1 kg/cm^2 $\sim 3 \times 10^{-7}$ cm). Therefore, the range of accuracy required for routine strain determinations is not excessive. The apparatus described in the following is commonly used for strain analysis by visual observation, and easily extended for quantitative measurements. The polariscope then becomes a polarimeter.

* mμ = 10^{-7} cm.

† For numerical values of B for various glasses and details of application see Ref. 21.

As illustrated in Fig. 3.2, a light source, L, sends a collimated beam through a polarizer, P, usually consisting of a sheet of "Polaroid."* The linearly polarized light emerging from the polarizer passes through the specimen, S, and the components of this beam are observed through the analyzer, A, which also consists of a sheet of "Polaroid." The "preferred directions" of polarizer and analyzer (i.e., the directions of light vibrations which each by itself would pass) are arranged in opposite directions at 45° to the vertical, so that P and A are "crossed" and their preferred directions are at 90° to each other. The field of view will then be dark. When the glass sample is strained, however, either by applying a stress mechanically or, because of the presence of a permanent strain, carried down during the annealing cycle, the glass behaves like a uniaxial crystal.

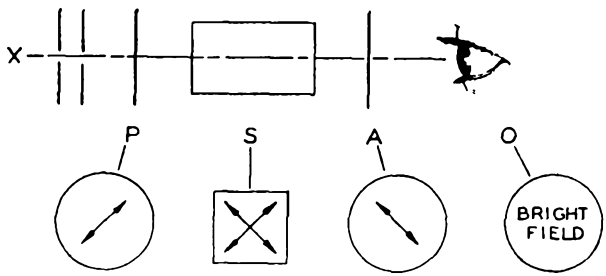

Fig. 3.2. Strain analysis of glass with the aid of polarized light. Light Source X, Polarizer P, Glass Sample S, Analyzer A, Observer O. In the lower part of the figure views of P, S, A, O are given in the direction of the axis of the array. See text for details.

Let us assume that the optical axis lies in such a direction as to split the incident polarized beam into directions of vibration coinciding with the preferred directions of the crossed polarizer and analyzer. Obviously then, one of the two will be suppressed and the other be passed freely by the analyzer. The observer will see a brightened field. Fig. 3.2 illustrates this situation, where each sketch in the lower half of the figure presents the view in the direction of the observer as it would appear in succession from left to right, P, S, A, O. This particular orientation of the planes of vibration is a very special case, not likely to be found when the specimen is placed in a random position. By suitable rotation of the specimen it could, however, always be brought about. One would need only turn it until the field brightens to the fullest extent. This manipulation may not always be practical; furthermore, it permits no conclusion as to the type of strain present.

* Thin transparent sheet containing small crystals of herapathite in parallel orientation, embedded in a plastic binder and available in large sheet several square feet in area.

Fig. 3.3 shows a strained body of glass placed in such a position between P and A that its optical axis 0-0′ is horizontal and parallel to the plane of the "Polaroid" sheets P and A. The plane of vibration, in which light passes polarizer P, is indicated by the double arrow at P. When the polarized beam enters the strained glass, its preferred plane of vibration is resolved into two directions at right angles to each other, one of which coincides with that of the optical axis 0-0′. These components are indicated by R_1 and R_2 in Fig. 3.3b and signify planes of vibration normal to the plane of the paper on which they are drawn. When these

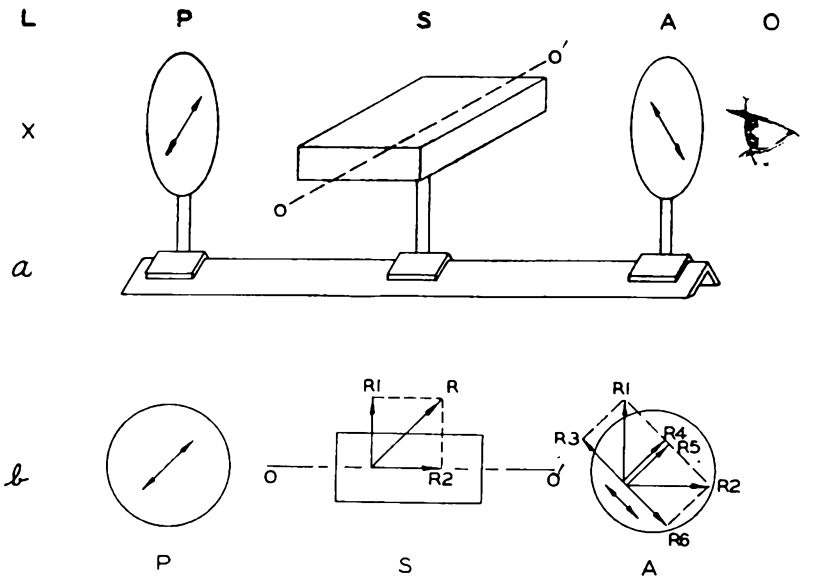

Fig. 3.3. Strain analysis of glass with the aid of polarized light. The optical axis of the birefringent glass is horizontal and in the plane of polarizer and analyzer.

two components, R_1 and R_2, enter the analyzer, A, each is in turn split into two components so that R_1 resolves into R_3 and R_4, and R_2 into R_5 and R_6, where one component of R_1 and R_2 is in the preferred direction of the analyzer. (Double arrow at A is at 90° to double arrow at P.) Thus, the subcomponents R_4 and R_5 cannot pass, but R_3 and R_6 do.

Since the light beams which vibrate in planes R_3 and R_6 are coplanar and of common origin (coherent), they interfere with each other. Because of the different velocities of the beams in planes R_1 and R_2 they travel different optical distances, and their respective retardation is $\delta = \Delta n \times l$. This is the optical path difference measured in millimicrons. The two interfering rays R_3 and R_6 also have a phase difference φ, which is given by

$$\varphi = \frac{l(n_2 - n_1)}{\lambda} = \frac{l\Delta n}{\lambda} = \frac{\delta}{\lambda} \tag{3.15}$$

where λ is the wave length of the light for which n_1 and n_2 are the refractive indices of the ordinary and extra-ordinary ray. In addition a phase shift of 180°, or $\lambda/2$, is introduced between R_3 and R_6 for the special case of crossed P and A.

If $\left(\varphi + \frac{\lambda}{2}\right)$ is an even number of half wave lengths, the two beams will amplify each other, resulting in a bright field. If $\left(\varphi + \frac{\lambda}{2}\right)$ is an odd number of half wave lengths, the beams will attenuate each other; this results in a dark field provided that a monochromatic light source is used.* For white light as a source the relation for extinction will apply to one particular color so that the complementary color appears in the field of the analyzer. The color of the field will depend on the thickness of the specimen and the intensity of the strain. Thus, the whole gamut of colors of the spectrum can be produced by either gradually increasing the thickness or gradually increasing the strain. This is readily demonstrated by moving a quartz wedge in the field or by increasing the strain through increased mechanical loading of the glass or the application of heat. The analysis of stress distribution in structural members by models made of plastics is an important field of civil engineering, and it utilizes these same principles of photoelasticity.

When the optical axis of the specimen lies in an arbitrary direction, the same resolution of the incident plane-polarized light, as described above, takes place; but the patterns of interference in the field of the analyzer may be less distinct for certain positions. As the maximum intensity is obtained for a position of the optical axis at 45° to the preferred direction of P and A, the glass specimen is placed in such a position that optimum brightness of the strain pattern results.

To increase the contrast for the observation of weak strains many polariscopes have a tint plate, made of a sheet of doubly refracting material, such as selenite or quartz, inserted between P and A. The latter introduces a constant retardation for a given wave length, and consequently colors the field in a hue complementary to that extinguished if the plate is an even number of half wave lengths thick. Thus, a "red plate" is often employed which consists of a plate of quartz of such thickness as to produce a retardation of 530 mμ between the ordinary and extra-ordinary ray. This results in a purple color in the field of the analyzer when a white source is used. It is easier to observe additional

* See J. H. Partridge's "Glass-to-Metal Seals," p. 122, for a detailed explanation of this unusual state of affairs.

color changes produced by strained objects, especially when the strains are weak.

Let us assume that a specimen under investigation, placed between P and A, retards 100 mμ. When the plane of vibration of the faster ray in the glass coincides with the plane of vibration of the faster ray in the tint plate, the values of retardation add up, giving $\delta = 630$ mμ, a yellowish-red, which is suppressed by interference. The strain pattern then shows in blue, the complementary color, against the purple background. Complementary colors side by side give the greatest contrast and make observation easy. If, on the other hand, the faster ray in the glass has the same direction of vibration as the slower ray in the "red plate," the light having a wave length of 430 mμ is extinguished (violet) and a yellow interference color is observed.[10] If a glass rod is bent at the location of the specimen, one can easily determine which color corresponds to tension and which to compression and thus obtain a qualitative picture of the strains present. Further details on the operation and construction of polariscopes are found in Refs. 11–13.

The qualitative determination of strains in glass, which we have discussed so far, is sufficient for many applications in the tube shop, especially if supplemented with standard strain disks which are commercially available. These permit rejection of excessively strained articles on the basis of color match. In many cases, however, particularly when new designs are tested, a quantitative evaluation of the strains present is essential. This requires additional refinements in instrumentation, which resolve from the following alternatives.[14]*

(a) It is evident from the definitions stated above that strain implies a physical displacement of the material under test. It should then be possible to measure these displacements point by point along the surface and to arrive at the strain pattern. The magnitude of these displacements is of the order of 10^{-6} inches, but they can be measured with interferometers to a high degree of accuracy (± 0.0001 mm). For routine investigations this is evidently impractical.

(b) As it has been shown that birefringence is directly proportional to the strains, it is possible to measure either the optical path ($l \times n$) directly with an interferometer or the refractive index and length of path separately by established methods. These are useful but limited in accuracy. An optical path difference of 10 mμ, or about $1/50$ of an interference fringe is the limit of precision of the usual interferometer methods. For $l = 10$ cm, this corresponds to $\Delta n \sim 10^{-7}$, which is about ten times the accuracy obtainable by direct refractive index determinations.

(c) As the light emerging from the specimen in a polariscope is ellip-

* The following, a–c, has been taken over almost verbatim from Goranson and Adams.

tically polarized, the phase lag and path difference can be obtained by measuring the ellipticity and the azimuth of the elliptically polarized light. This is done by restoring the elliptical vibration to a plane polarization with the aid of a properly oriented quarter-wave plate, which is called a "compensator." The orientation of the compensator and the azimuth of the resultant plane-polarized light determine the constants of the elliptical vibration. These methods are capable of high precision since the angular displacements can be accurately measured on a graduated circle. This becomes rather complicated, however, when applied to strain in glass because adjustments and measurements on three graduated circles are necessary.

(d) Methods have been devised by which the birefracting specimen under investigation is combined with other birefracting plates in such a way that a beam of plane-polarized light initially entering the assembly is still plane polarized after passing through the combination. The plane of polarization is rotated by an amount which is proportional to the birefringence δ of the specimen to be analyzed. This rotation is easily measured with high accuracy to ± 0.04 mμ or less with suitable equipment.

(e) The most common methods used in the electronic industry are based on the observation of interference phenomena between crossed polaroids, as outlined above. A graduated quartz wedge or a Babinet Compensator are used to measure the spacing of the fringes. With either one the observer must estimate the position of a relatively wide band which becomes fuzzy at its outer edges. In the case of the graduated wedge there is usually an uncertainty of 10 mμ in the path difference, and it is difficult to make measurements better than 5 mμ. The Babinet Compensator allows somewhat greater accuracy at the expense of a diminished range.

The operation of the *quartz wedge* as a quantitative refinement of the polariscope will now be described in some detail.[15,16] Its use for measuring stress in rectangular glass plates was first described by C. V. Boys,[17] and H. Poritsky[18] showed that it can be applied to cylindrical rods and seals.

A wedge of quartz cut from a crystal in such a way that its optical axis is perpendicular to the thin edge of the wedge shall be placed in the field between P and A, (Fig. 3.4) so that the thin edge is vertical and one plane of the wedge parallel to P and A. The incident plane-polarized light will again be split into two components vibrating at right angles to each other (i.e., one vibrates in a vertical and the other in a horizontal plane). As the light passes the analyzer the conditions are the same as described above, with the result that interference fringes appear parallel to the edge of the wedge. If the position of the wedge remains fixed, the difference

$(n_2 - n_1)$ for the ordinary and extra-ordinary ray of any given wave length remains constant and equals 0.009 for quartz. The retardation is then a linear function of the thickness l of the wedge traversed by light rays according to $\delta = \Delta n \times l$. Dark bands appear where δ/λ is an integral number of half wave lengths and bright bands where δ/λ is an odd number of half wave lengths. This is illustrated in Fig. 3.4b for monochromatic light. When a strained glass object is placed in front of the

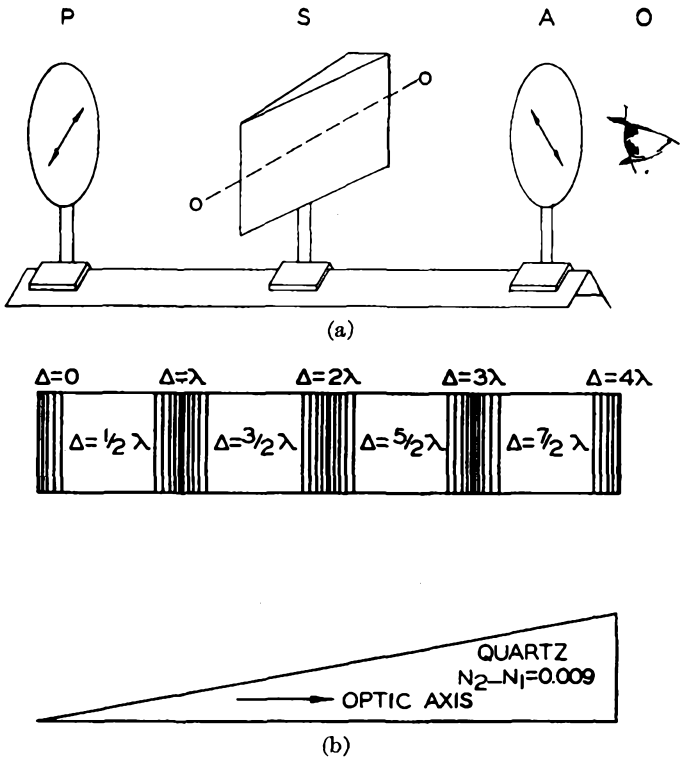

Fig. 3.4(a and b). Strain analysis of glass with the aid of polarized light and a quartz wedge.

quartz wedge, the dark lines will be displaced to the right or left, depending on the type of strain present. The maximum displacement of the line can be measured by moving the cross hairs in the microscope or telescope used for the observation of the pattern. A calibration of the displacement in terms of actual strains can be obtained by loading a plate of the same kind of glass as that to be analyzed with appropriate weights. Fig. 3.5 shows the layout of components for this technique, according to Hull and Burger,[16] and Fig. 3.6 illustrates the type of pattern obtained on a bead seal.

A Babinet Compensator consists of two quartz wedges, one of which may be moved with a micrometer. They are arranged with their optical axes at a right angle to each other. The ordinary ray, which has passed the first wedge oscillating normal to the optical axis, passes the second wedge as the extra-ordinary ray; and *vice versa*. As the extra-ordinary

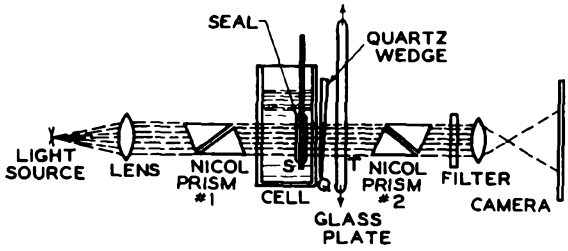

Fig. 3.5. Arrangement for photoelastic measurement of stresses in seals. T and Q are used alternatively. When the glass plate T is used, it is stretched with a known tension until it just neutralizes the effect of stress in S. When the quartz wedge Q is inserted, photographs are obtained like Fig. 3.6 in which the displacement of the horizontal dark lines is proportional to the stress. After A. W. Hull and E. E. Burger.[16] (*Courtesy American Institute of Physics.*)

ray travels more slowly in quartz than the ordinary ray, the resulting phase difference is changed by moving the second wedge with respect to the first. If the light ray passes equal thicknesses of the two wedges, the effects cancel. The phase difference introduced by the second wedge is proportional to its translation. A phase difference originally present in a glass specimen in line with the compensator can thus be eliminated by

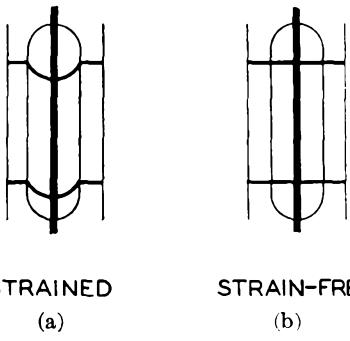

Fig. 3.6. Schematic diagram of photographs obtained with arrangement shown in Fig. 3.5 when quartz wedge is used. (a) Strained Bead-Seal; (b) Strain-Free Bead-Seal. After A. W. Hull and E. E. Burger.[16] (*Courtesy American Institute of Physics.*)

the translation of the second wedge and measured on the micrometer head controlling the movement.

"The study of odd-shaped glass articles, such as bead seals, presses, etc., is best performed in an immersion cell filled with a liquid of the same refractive index as that of the glass under investigation. Suitable mixtures of benzol and alcohol serve this purpose. This eliminates distortion of the fringe pattern by reflection and refrac-

tion at the glass surfaces which would introduce additional polarization in the light beam."[19]

The effect of a quartz wedge on white plane-polarized light is illustrated in Fig. 3.7.[15] As many different wave lengths are now present, each will be subject to retardation and cause a phase difference at any given thickness of the wedge. Even multiples of $\lambda/2$ will be extinguished

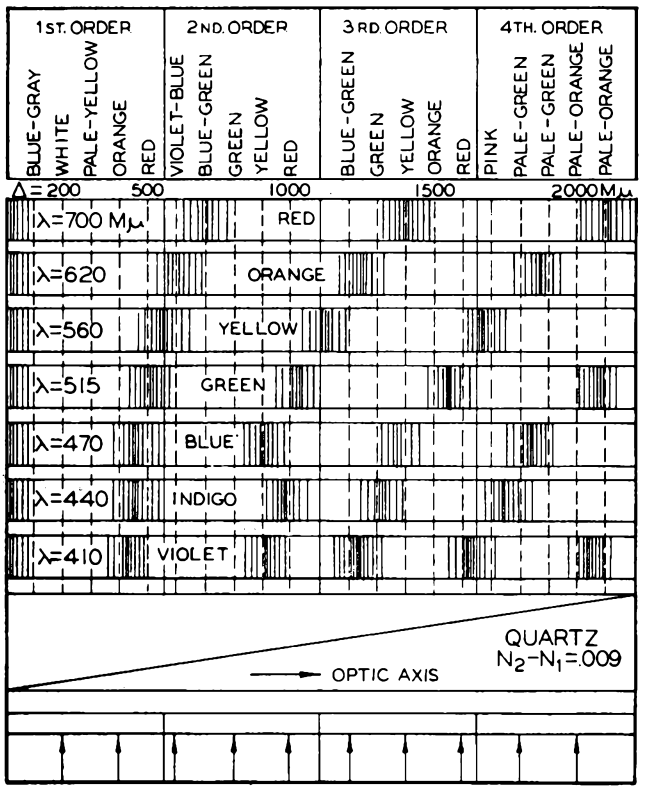

Fig. 3.7. The effect of a quartz wedge on white plane polarized light. (*By permission from "Optical Mineralogy" by A. F. Rogers and F. P. Kerr. Copyright, 1942. McGraw-Hill Book Company, Inc.*)

by the analyzer, and will give rise to the complementary color; however, odd multiples of $\lambda/2$ will be passed. If all the suppressed components are subtracted from white, the final hue of the resulting interference color is obtained. As the wedge increases in thickness, the color patterns repeat each other with diminishing intensity and different hues.

Bands of the 1st, 2nd, 3rd, and 4th order can be distinguished. Above the 4th order, colors are not easily separated. When the retardation δ is less than 550 mμ interference colors of the first order are obtained.

Sensitive violet (δ = 550 mμ) is at the boundary of the 1st and 2nd order, and a small change in δ produces a marked change in color. Second-order colors correspond to δ = 550 to 1128 mμ. Third-order colors extend from δ = 1128 to 1652 mμ. These bands are shown at the top of Fig. 3.7.

The corresponding values of retardation are entered below the color bands. The seven rows of interference patterns show the distribution of fringes obtained with any one monochromatic component of white light. If a vertical line in this diagram is followed, the top color is obtained by subtracting all the black monochromatic bands from white in the proper percentages. The quartz wedge and the direction of the incident plane-polarized white light is shown at the bottom of Fig. 3.7.

Standard color charts are available for a given quartz wedge where the retardation is entered at each color. The color of the specimen under investigation can then be compared with the color of the wedge in the field and the strain obtained in this manner.

Read[20] has recently described an optical bench setup for factory inspection of electron-tube bulbs, where the interpretation of the strain patterns obtained with a quartz wedge has been simplified by the assignment of experimentally determined factors.

The evaluation of stresses is further complicated in the case of odd-shaped glass articles and glass-to-metal seals by the co-existence of different stresses in different directions. Thus, in a symmetrical rod-type seal axial, radial, and tangential stresses, which assume different magnitude as a function of the ratio of glass-to-metal diameter, are encountered. Only the axial stress is observed in the polariscope when the axis of the rod is held at right angles to the light path. Other stresses can be derived from it according to relations established by Hull, Burger, and Poritsky[16,18] and elaborated on in the treatise by Partridge,[21] to which the reader is referred for details. Two series of articles, which deal extensively with the problem of stress analysis as applied to glass-to-metal seals, are now in the process of publication.[22,23]

REFERENCES

1. Adams, L. H., and Williamson, E. D., "The Annealing of Glass," *J. Franklin Inst.*, **190**, 597–631, 835–870 (1920).
2. Adams, L. H., "The Annealing of Glass as a Physical Problem," *J. Franklin Inst.*, **216**, 39–71 (1933).
3. Adams, L. H., and Williamson, E. D., "The Relation Between Birefringence and Stress in Various Types of Glass," *J. Washington Acad. Sci.*, **9**, 609–625 (1919).
4. Coker, E. G., and Filon, L. N. G., "A Treatise on Photoelasticity," Cambridge, Univ. Press, 1931.
5. Brewster, Sir David, "Results of Some Recent Experiments on the Properties Impressed upon Light by the Action of Glass Raised to Different Temperatures

and Cooled under Different Circumstances," *Philos. Transact. Royal Soc. of London*, 436–439 (1814). *Ibid.*, Numerous other papers by same author, 1814–1816.

6. Hardy, A. C., and Perrin, F. H., "The Principles of Optics," New York, McGraw-Hill Book Co., Inc., 1932.
7. Tait, P. G., "Properties of Matter," 4th ed., London, Adam and Charles Black, 1899.
8. Morey, G. W., "The Properties of Glass," New York, Reinhold Publishing Corp., 1938.
9. Neumann, F., "The laws of Birefringence in compressed or non-uniformly heated non-crystalline bodies," (In German), *Ann. Phys. Chem.*, **54**, 449–476 (1841).
10. Padmos, A. A., and de Vries, J., "Stresses in Glass and Their Measurement," *Philips Tech. Rev.*, **9**, 277–284 (1947/48).
11. Spencer, C. D., and Jones, S., "Design and Construction of Polariscopes for Use in Glass Factories," *J. Am. Ceram. Soc.*, **14**, 512 (1931).
12. Fortey, J., "A Projection Type of Strain-Viewer," *J. Soc. Glass Tech.*, **29**, 124–127 (1945).
13. Mylonas, C., and Greek, M., "The Optical System of Polariscopes as Used in Photoelasticity," *J. Sci. Inst.*, **25**, 77–81 (1948).
14. Goranson, R. W., and Adams, L. H., "A Method for the Precise Measurement of Optical Path-Difference, Especially in Stressed Glass," *J. Franklin Inst.*, **216**, 475–504 (1933).
15. Rogers, A. F., and Kerr, F. P., "Optical Mineralogy," New York, McGraw-Hill Book Co., Inc., 1942.
16. Hull, A. W., and Burger, E. E., "Glass-to-Metal Seals," *Physics*, **5**, 384–405 (1934).
17. Boys, C. V., "Annealing Glass," *Nature*, **98**, 150–151 (1916).
18. Poritsky, H., "Analysis of Thermal Stresses in Sealed Cylinders and the Effect of Viscous Flow During Annealing," *Physics*, **5**, 406–411 (1934).
19. Beeton, E. E., "An Immersion Cell for Polariscope Use," *Glass Ind.*, **19**, 51–53 (1938).
20. Read, W. T., "Optical Measurements of Residual Stresses in Glass Bulbs," *Bell Lab. Rec.*, **28**, 62–65 (1950); *J. Appl. Phys.*, **21**, 250–257 (1950).
21. Partridge, J. H., "Glass-to-Metal Seals," *Soc. Glass Tech.*, Sheffield 10, England 1949.
22. Trébuchon, G., and Kieffer, J., "Physical Aspects of Glass to Metal Seals used in the Electron Tube Industry," (In French), *Annales de Radioélectr.*, **5**, 125–149 (1950); **5**, 243–258 (1950).
23. Martin, F. W., "Stresses in Glass-Metal Seals: I, The Cylindrical Seal," *J. Am. Ceram. Soc.*, **33**, 224–229 (1950).
24. Stanworth, J. E., "Physical Properties of Glass," London, Oxford University Press, 1950.

CHAPTER 4

GLASS-TO-METAL SEALS

Introduction

The need for joining metals to glass is so fundamental to scientific experimentation and industrial production in the electronic field that these activities could not exist without this important technique. Any advance made in the art of sealing metals to glass must, of necessity, have a profound influence on the design of electronic devices. During recent years glass has been replaced by ceramic for some special applications. Metal-to-ceramic seals thus assume an increasing importance. This subject will be treated in Chapter 16.

If two metals of dissimilar expansion coefficients are joined in strip form, a well-known bimetallic strip results, which is widely used for temperature compensation or translation of motion by the application of heat in thermostats. As the temperature of the strip is raised, one strip becomes longer than the other and a curvature of the biform results. Assuming that the strips are brazed uniformly along their common interface, a considerable force acts on this interface at elevated temperature and permanent deformation will result if the elastic limit of shear is exceeded. Similarly, we may visualize two coaxial cylinders of dissimilar metals brazed together along their common cylindrical interface. If the inner cylinder has the larger expansion coefficient, a considerable radial tension inward will be exerted on the interface after cooling; this may cause the brazed joint to separate.

These examples serve to illustrate the basic problem that applies to glass to metal joints in a more pronounced degree. The specific thermal expansion of pure metals is a constant which, for practical considerations, is independent of temperature as long as no phase changes take place. A bar of pure metal will thus increase in length linearly with temperature. Glasses, on the other hand, will grow in length at an increasing rate since their specific thermal expansion usually increases with temperature. This behavior is illustrated in Fig. 4.1 (a, b). The expansion coefficient of glasses depends much on the glass composition and to a lesser extent on thermal history and the condition of strain. It is fairly constant over the temperature range up to the vicinity of the annealing point, but then rises rapidly and sometimes goes through a maximum.

Ideally, one would wish glass and metal to have identical values of

elongation over the entire range of temperature to which they are exposed during sealing, annealing, and operation. This is rarely realized in practice. Fig. 4.1 (b) assumes a metal and a glass rod of equal length and diameter at room temperature. With increasing temperature the metal rod grows in length at a constant rate, and is longer than the glass rod until at point P the glass rod catches up and finally overtakes the metal rod, becoming longer than the latter. It is evident that the joint between the two materials will be free of strain at temperature T_1, where

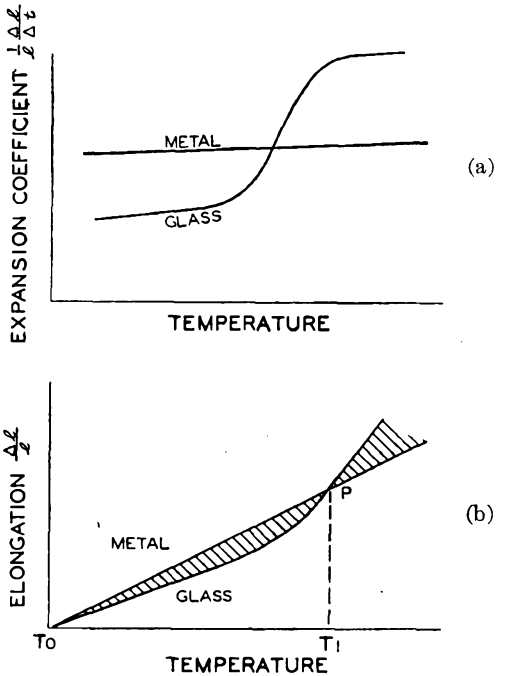

Fig. 4.1. Thermal expansion characteristics for metals and glasses. (a) Expansion coefficient vs. temperature; (b) elongation vs. temperature.

both have increased in length (and volume) by the same amount. During further heating above T_1 and cooling below T_1 strains will be introduced which are proportional to the differential expansion shown by the shaded area between the two curves (Fig. 4.1[b]). If point P should be in the annealing range, as is often the case, and the strains introduced during cooling do not exceed the breaking strength of the glass in question, a sound joint will result at room temperature T_0. These conditions are not always attainable and compromises become necessary.

Table 4.1* gives the tangential stresses in kg/mm^2, which result in

* Courtesy Machlett Laboratories, Springdale, Conn.

TABLE 4.1. STRESSES IN GLASS TO GLASS AND GLASS TO METAL SEALS*

So. Pt.	Ann. Tp.	St. Pt.		7050	7052	7070	7040	3320	7720	7740	7750	7760	1720	L650	W	"Kovar"
1297	925	862	7050		1.1	1.4	0.6	1.2	**1.7**	**2.6**	0.3	**2.5**	1	0.7	0.4	0.8 to **1.2**
1306	896	828	7052	1.1		**2.7**	0.6	**2.1**	**2.7**	**3.4**	1.2	**3.3**	1.3	0.2	**1.3**	0.1 to 0.5
	914	851	7070	1.4	**2.7**		**2.1**	0.2	0.1	1.1	1.3	0.9	0.6	**2.2**	**1.1**	**2.1** to **2.7**
1299	903	842	7040	0.6	0.6	**2.1**		**1.7**	**2.2**	**2.9**	0.8	**2.7**	1.4	0.2	0.8	0.1 to 0.7
1436	995	927	3320	1.2	**2.1**	0.2	**1.7**		0.1	**1.7**	0.7	1.2	0.1	**1.9**	0.4	**2.6** to **3.4**
1381	964	903	7720	**1.7**	**2.7**	0.1	**2.2**	0.1		**1.6**	1.3	1.2	0.1	**2.2**	0.6	**2.5** to **3.4**
1508	1027	950	7740	**2.6**	**3.4**	1.1	**2.9**	**1.7**	**1.6**		**1.9**	0.4	1.5	**3.4**	**2**	**4.6** to **5.5**
1299	873	808	7750	0.3	1.2	1.3	0.8	0.7	1.3	**1.9**		**1.9**	0.4	1.3	0.2	0.8 to **1.4**
1436	968	896	7760	**2.5**	**3.3**	0.9	**2.7**	1.2	1.2	0.4	**1.9**		1.3	**3.1**	**1.8**	**4** to **4.5**
1679	1314	1242	1720	1	1.5	0.6	1.4	0.1	0.1	1.5	0.4	1.3		**1.8**	0.5	
1312	941	887	L650	0.7	0.2	**2.2**	0.2	**1.9**	**2.2**	**3.4**	1.3	**3.1**	**1.8**		**1.2**	0.3 to 0.7
			W	0.4	**1.3**	**1.1**	0.8	0.4	0.6	**2**	0.2	**1.8**	0.5	**1.2**		
			"Kovar"	0.8 to **1.2**	0.1 to 0.5	**2.1** to **2.7**	0.1 to 0.7	**2.6** to **3.4**	**2.5** to **3.4**	**4.6** to **5.5**	0.8 to **1.4**	**4** to **4.5**		0.3 to 0.7		

Revised in accordance with latest expansion curves.
Note: Stress figures in bold face are beyond safe limits.
Safe limits glass to glass—1.5 kg/mm² glass to metal—0.9 kg/mm².
* Courtesy Machlett Laboratories, Inc., Springdale, Conn.

annealed tubular butt joints between common glasses and between glasses and common sealing metals, according to H. R. Lillie's simplified formula for tangential stresses, S, at the seal interface:

$$S = \frac{\bar{E}D}{2} \tag{4.1}$$

where S = stress in kg/mm^2
$\bar{E}$ = the average of the values of Young's Modulus for the two glasses
D = the differential contraction $\Delta L/L$ between the two materials at the lower setting point if two glasses are joined, or at the setting point of the glass if glass and metal are joined.

While a minimum value of stress will result when the two glasses have the same elastic modulus, it can be shown that the two moduli can differ greatly from each other without introducing much change in the resulting

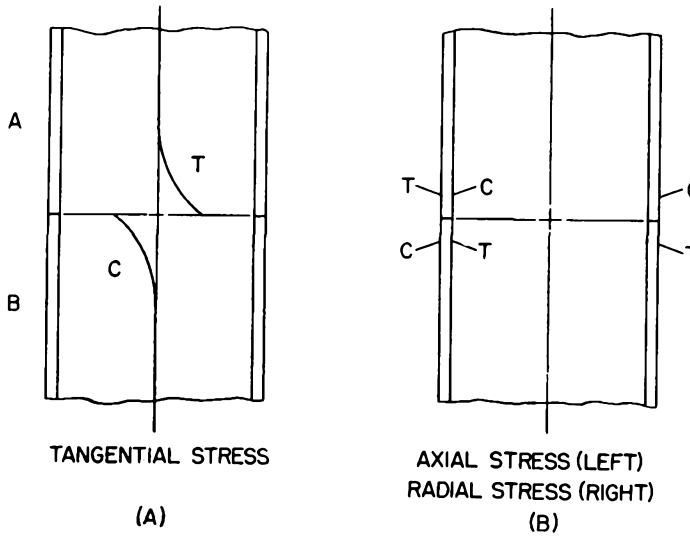

Fig. 4.2. Stress distribution in a tubular butt seal. (a) Tangential stresses. (b) Axial and radial stresses. After H. R. Lillie.

stress value. The accuracy is thus impaired only slightly by introducing the average $\bar{E}$ = 7000 kg/mm² for glasses commonly used for seals, as listed in Table 4.1.

Stresses from 0.5 to 1.5 kg/mm² can be tolerated in tubular butt seals of glasses, depending on size and perfection of fusing. The lower figure is safe under quite unfavorable conditions. Values in excess of 1.5 are printed in bold face type in the table. For glass to metal tubular butt seals, a stress of 0.9 kg/mm² has been taken as the upper safe limit, and higher values are printed in bold face type accordingly.

It has been established by mathematical treatment and actual experience that tangential stresses are large in comparison to stresses in the axial and radial direction as far as tubular butt seals are concerned. At the seal boundary the two glasses assume opposite kinds of stress. This is shown for the tangential stresses in a tubular butt seal in Fig. 4.2a and for axial and radial stresses in Fig. 4.2b. In Glass A, which has the higher expansion coefficient, the tangential stress at the interface is in the direction of tension, and it diminishes rather rapidly at short distances away from the interface. Glass B shows the corresponding tangential compression at the interface.

The differential contraction, D, which enters into Equ. 4.1 is illustrated in Fig. 4.3, where the expansion curves for two glasses are shown.

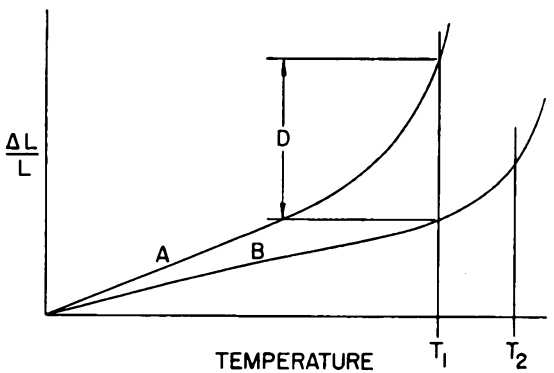

Fig. 4.3. Elongation vs temperature for two glasses A and B. The glasses set on cooling at the respective temperatures T_1 and T_2. D indicates the differential contraction. After H. R. Lillie.

Glass A has a setting point at T_1, Glass B at T_2. Setting points may be taken at 20°C below the annealing point; they indicate the temperature at which viscous yield to stresses ceases for practical rates of cooling. As the seal between the two glasses cools, Glass B sets first and any differential contraction which takes place above temperature T_1 will be absorbed by the flow of Glass A. Below temperature T_1 differential contraction of the two glasses will give rise to stresses. At room temperature the geometrical dimensions at the interface are necessarily identical for both glasses. The distance D, given in Fig. 4.3, thus marks the circumferential length which must be taken up by the two glasses during cooling. Each unit length on the circumference of Glass A at the interface must accordingly be stretched an amount equal to the remaining fraction of D. For glass-to-metal seals the stress to be expected at room temperature is proportional to the difference between the two elongation curves at the effective setting temperature of the glass.

Stresses at intermediate temperatures may be derived from the plot shown in Fig. 4.4. If D_T is the differential contraction at a temperature T and D the value at T_1 as previously specified, D' is defined as

$$D' = D - D_T \tag{4.2}$$

and plotted in Fig. 4.4 against temperature. The tangential stress appearing at any temperature, T, during cooling or during service at other than room temperature will then be given by

$$S' = 3{,}500 \times D' \text{ (kg/mm}^2\text{)} \tag{4.3}$$

At room temperature $D' = D$, but at higher temperatures D' gradually decreases.

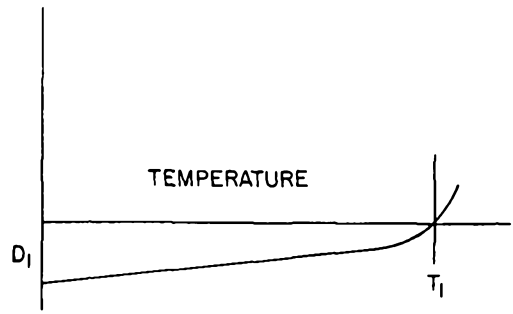

Fig. 4.4. Differential contraction D' for the two glasses in Fig. 4.3 as a function of temperature. After H. R. Lillie.

The elongation of a number of pure metals as a function of temperature is shown graphically in Fig. 4.5. Fig. 4.6 gives the corresponding plots for various Corning glasses, and a shaded zone indicates the annealing range. The expansion coefficients, $\frac{1}{l}\frac{\Delta l}{\Delta t}$ (cm/cm/°C), will be expressed by a number times 10^{-7}. It is evident that among the common sealing metals copper has the highest expansion ($\alpha = 165 \times 10^{-7}$) and tungsten the lowest ($\alpha = 46 \times 10^{-7}$). In turn the highest expansion glasses are the soft soda-lime and lead glasses with $\alpha = 90 \times 10^{-7}$, and borosilicate glasses represent low-expansion glass with $\alpha = 32 \times 10^{-7}$ (Table 1.3). High silica "Vycor" glasses bridge the gap to silica glass for which $\alpha = 5.5 \times 10^{-7}$ applies. Expansion coefficients are represented by the slopes of the curves in Figs. 4.5 and 4.6. In the literature the expansion coefficients given for glasses are generally averages for the low temperature range, 0 to 300°C. The average coefficient to the setting point is several points higher. As an approximate working rule it may be said that glasses and metals which are to be joined should not differ in their expansion coefficients by much more than 10×10^{-7}. From this state-

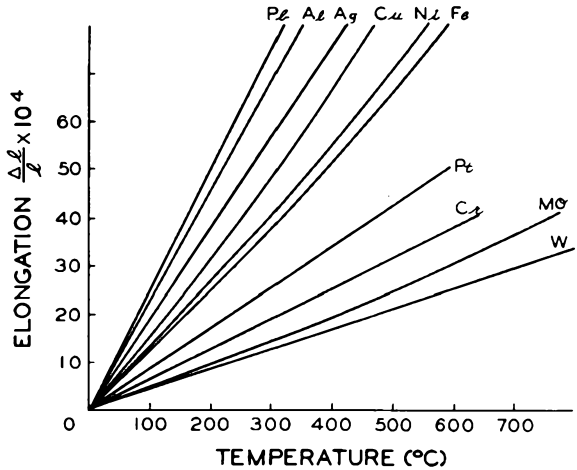

Fig. 4.5. Relative thermal expansion of various metals as a function of temperature.

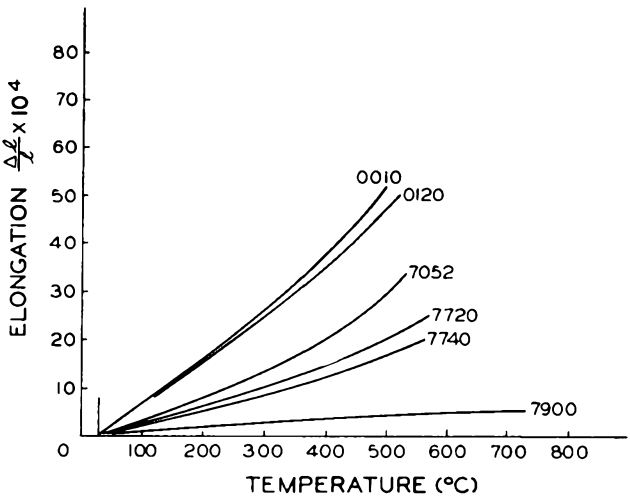

Fig. 4.6. Relative thermal expansion of various Corning glasses as a function of temperature. (*Courtesy Corning Glass Works, Corning, N.Y.*)

ment it is obvious that tungsten cannot be joined to Corning glass 7740, except in the form of fine wire in the 10 mil* size range, as their expansion coefficients are 14×10^{-7} apart; but tungsten to uranium glass 3320 or glass 7780 gives a reliable seal ($\Delta\alpha \sim 6$). It is also evident that platinum ($\alpha = 90.7 \times 10^{-7}$) well matches the soft glasses, 0010, 0080, 0120 ($\alpha = 89$

* 1 mil = 0.001 inch
1 mm = 0.1 cm = 40 mils
100 microns (μ) = 4 mils = 0.1 mm

to 91×10^{-7}). Platinum was used as early as 1821 by Davy, and it served in Edison's incandescent lamp in 1879, in the early x-ray tubes, and later in electron tubes and lamps until more economical substitutes were developed. A special technique for sealing platinum to "Pyrex" was described by Wichers and Saylor[1] and Kraus[2]. The strains are minimized by sealing seamless platinum tubing into "Pyrex" glass over part of its length, and such seals stand up satisfactorily " . . . if the outside diameter of the platinum tube is at least 12 times its wall thickness and not much more than twice the wall thickness of the glass." The platinum tubes were 2 mm in diameter and had a wall thickness from 0.003 to 0.006 inch. Cost and size limit this technique to very special applications.

The use of platinum for lead seals in lamps and receiving tubes has become obsolete by the introduction in 1911 of "Dumet" wire by Fink and Eldred.[3] This wire consists of a copper-coated nickel-iron alloy, containing about 42 per cent nickel. It is made by fusing or welding a nickel-iron core into a copper tube with an intermediate sheath of brass. This billet is swaged and drawn to the wire which is passed through a solution of sodium borate. The final thickness of copper is about ½ mil, depending on the diameter, comprising 25 per cent of the total weight of the wire. "Dumet" wire seals are practical up to 40-mil diameter, but are rarely used above 20 mils in the tube industry for soft-glass seals, 0010, 0080, 0120. A 32-mil diameter wire will pass currents up to 20 amps. The "sandwich-structure" of the wire results in quite unusual expansion characteristics. There is a difference of 41.5 per cent between the longitudinal and radial expansion coefficients of the wire, which are 65×10^{-7} and 92×10^{-7}, respectively.[4] The large stresses encountered in the seals made with "Dumet" are taken up by the thin copper-sheath so that a serviceable joint results. The seals are usually not fully annealed so that the glass is left in longitudinal compression, whereas longitudinal tension would result in a fully annealed seal.[5]

These techniques were established before the beginning of World War I, and contained the basic concepts which, at a later date, led to major advances in the art of sealing glass to metals. The platinum-tube seal as well as the copper-sheath on "Dumet" point to the possibility of taking up large strains by elastic yield of very thin metal members, and the composition of the "Dumet" core suggests the usefulness of nickel steels as sealing metals. The "Housekeeper Seal," introduced in 1923, carried the idea of elastic coupling between metal and glass to its logical conclusion on a larger scale, and the matching of nonlinear glass expansion by special chrome-iron and nickel-iron-cobalt alloys opened a field of application hitherto closed to the tube engineer.

To a certain extent the designer of large power tubes owes to the

"Housekeeper Seal" what the designer of small tubes owes to the iron-alloy seals. This statement is not to be interpreted as an effort to limit one or the other technique to small and large tubes; they do apply interchangeably. From a historical viewpoint the broadcast industry, at its very beginning in the '20's, was supplied with large water-cooled power tubes through the advent of the "Housekeeper Seal," and the all-metal receiving tubes in the '30's were possible through the introduction of nickel-iron and nickel-iron-chrome alloys. In recent years Fe-Cr alloys have been used for very large diameter seals on metal cone television tubes. Let us view these developments now in more detail.

"Housekeeper Seal"

The art of sealing copper to glass of all types was described in its many modifications by Housekeeper,[6] who introduced the "Feather-Edge Seal." Since this technique has also been dealt with in other texts,[4,7–11] we shall limit ourselves to some general remarks. While these seals are not too easily made without proper precautions and a fair amount of experience, they have lost the mystery in which they were shrouded in the earlier days. As a young man, the author nearly lost his job one day after passing on some taper dimensions to a university laboratory. During World War II such seals were made by the thousands on specialized machinery run by girl operators who turned out good seals after about two weeks' training.

To start with, only high-grade OFHC copper should be used; the letters stand for "oxygen-free-high-conductivity." This material is made to order in quantity by several copper mills, and is difficult to get in small lots. It can be fabricated into any desired shape, such as wire, rod, tubing, and blocks, from which special forms can be turned on the lathe. ASTM* Spec. B170-47 covers the characteristics for this material, which has a minimum copper content of 99.92 per cent. A "certified" grade of OFHC is available, which is preferred over the regular grade. Its minimum copper content is 99.96 per cent. Other high-purity copper is obtained by vacuum casting, and is especially gas free and superior to the ordinary OFHC grade. For acceptance tests and general metallurgy of copper the reader is referred to Chapter 12.

The taper of the feather edge is very critical if it is to perform satisfactorily. The thickness at the edge is to be 1.5 ± 0.5 mils, and a taper of about 5 degrees should extend back from the edge until the wall is 40 mils thick (Fig. 4.7). Depending on the size of the seal the taper must be chosen so as to form a practical compromise between strength and elastic yield. A good test for the edge thickness is to press it lightly

* American Society for Testing Materials, 1916 Race Street, Philadelphia 3, Pennsylvania.

on the thumb nail, the edge should perceptibly yield to this pressure.[11] The surface of the feather edge should be smooth and polished. Outside tapers may be rolled or machined against a steel arbor and the excess material cut off with a sharp steel roller. Inside tapers may be ground; they are less common.

After degreasing and cleaning, the part is frequently borated by heating to redness and immersing in a concentrated solution of sodium borate.

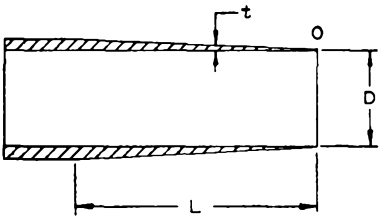

Fig. 4.7. Schematic outline of a tapered copper tube for a housekeeper seal.

This is a sensitive test for the surface condition of the copper. Any impurities or contaminations will show up as dark spots. A properly treated part will have a uniform deep red to purple sheen of cuprous oxide. Glassing can now proceed by heating to a bare orange heat and laying down the glass either on the inside, outside, or both, depending on the size of the work. In the case of inside-outside seals the inner glass ring is made twice as wide as the outer one.[4,8]

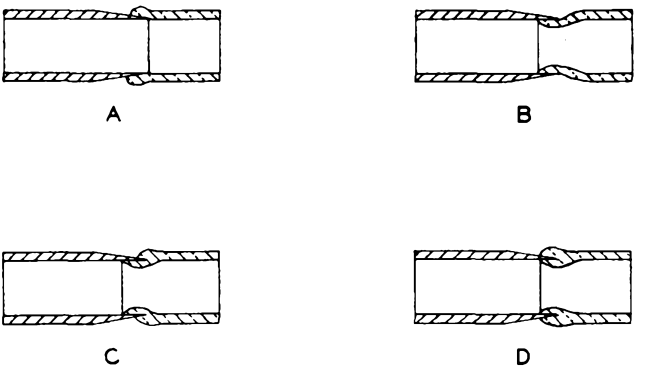

Fig. 4.8. Various types of housekeeper seals for tubular members. (a) Inside seal; (b) Outside seal; (c) Inside-outside seal; (d) Push-in or edge seal.

This beading operation can be performed in different ways: The copper tube, with its taper on one end, is held in the headstock of a horizontal sealing-lathe and the glass tubing of proper diameter in the tailstock. The edge of the glass tubing may be sealed to the outside of the taper and then cut off a few millimeter beyond the taper. This excess of glass is then rolled over to the inside of the taper; thus a bead

is formed to which the final glass member can be joined (Fig. 4.9). Or, the glass may be shaped to fit the inside of the tapered tube and thrown against the inner wall by speeding up the lathe enough to enable the centrifugal forces acting on the molten glass to be used as an internal paddle.

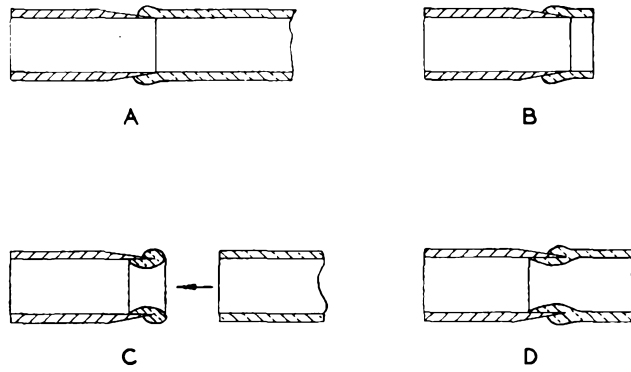

Fig. 4.9. Schematic outline of one of the possible techniques for the production of an inside-outside tubular housekeeper seal.

When this inner seal is made, the lathe is slowed down again and the glass gathered at the edge of the taper by advancing the tail stock. The rim of glass thus created is then rolled over onto the outside of the taper with a

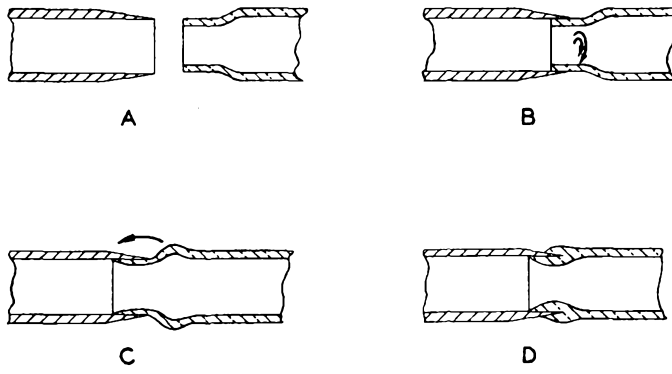

Fig. 4.10. Schematic outline of the production of a tubular inside-outside housekeeper seal by a combination of centrifuging and spading. (*Courtesy General Electric Co., England.*)

spade (Fig. 4.10). Air should be available through the headstock of the lathe to facilitate the shaping of the final seal. A careful annealing cycle in an oven should follow immediately. If inspection of the seal with the polariscope is passed satisfactorily, the seal is ready for chemical cleaning

to remove the oxide from the copper. Subsequent assembly and exhaust of the tube will complete the job.*

Fig. 4.8 (d) suggests a still different procedure of joining the feather edge to the glass member. A heavy bead is "gathered" at the end of the tubing and the copper edge pushed into it. A refinement of this technique has been described recently by Goodale,[12] who pushes the edge into the glass bead by $\frac{3}{32}$ inch and then withdraws it a certain amount, thus forming a concave meniscus. One may say that this bead-pushing technique is, on the whole, rather tricky unless the glass tubing is of a very heavy wall thickness.

The physical nature of the bond between glass and metal, after the seal has been formed, has been the subject of several theories and many discussions. The most generally accepted view is that the formation of an oxide layer on the metal just prior to sealing is necessary to secure a strong bond. This metal oxide must be strongly adherent to the metal and form an intricate part of it. When in contact with the molten glass, some of the metal oxide diffuses into the glass, thus forming a transition layer which, in turn, is an intricate part of the glass. A bridge, which is firmly anchored at each end by atomic forces acting on the constituent elements, is then formed between the metal and the glass. If this bridge has too wide a span (i.e., the oxide layer is too thick), it will collapse in the middle in spite of the firm foundations at its ends. Careful control of temperature and time are thus important to obtain an oxide layer of the right thickness and texture.

The color of the finished seal will be largely determined by the oxide layer, and it serves as a fair criterion for the quality of the seal. Overoxidized seals will assume a dark color and not sufficiently oxidized seals will be correspondingly light in color. Metals which oxidize readily must be protected from overoxidation during the preparation of the seal. In the case of copper this is frequently done by "borating" (see below). Tungsten and molybdenum wires and rods are "prebeaded" in a reducing flame where the tight-fitting glass sleeve prevents access of oxygen to the metal surface being coated with glass. The nature of the oxide formed depends to a large extent on the composition of metal and glass and the presence of impurities and admixtures. The presence of carbon dioxide, water vapor, and sulfur compounds in the gas flame also has an effect.

Bearing in mind that the composite oxide layer is only a few thousand Angstrom Units thick and may often consist of several layers of different oxides which should have the optimum relative proportions, it is indeed surprising that uniform seals can be produced by manual operation.

* Ref. 8 gives an exhaustive description of glass working which is highly recommended to the reader interested in this subject.

These hazards are reduced considerably by pre-oxidizing the metal under controlled conditions in a furnace and then coating it with a suspension of glass powder in a suitable liquid carrier (Pask[13]). The powder-glass coating is then dried and fused onto the metal in a furnace so that the subsequent sealing operation only consists of sealing glass to glass.

Pask describes in particular the application of this technique to "Kovar" seals, according to the developments carried out at the Research

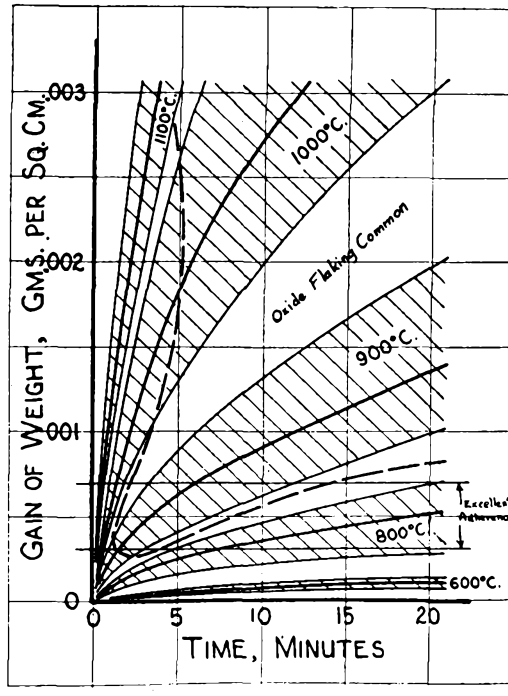

Fig. 4.11. Oxidation of "Kovar." Time-rate curves are shown. Area inside V-shaped dotted curve indicates conditions under which greatest tendency for oxide flaking exists. After Pask.[13] (*Courtesy the Institute of Radio Engineers.*)

Department of the Westinghouse Lamp Division at Bloomfield, N.J. "Kovar" is dealt with at some length below. It may nevertheless be referred to here as an example of seal processing.

"Prior to oxidation the 'Kovar' is baked in a wet hydrogen atmosphere at 1100°C for 15 to 30 minutes, in order to eliminate possible bubbling at the glass-metal interface during sealing.

"Experiments on oxidation were carried out in an electrically heated oven at controlled temperatures and varying times. Curves for weight gain per unit area versus time were thus obtained for a number of constant temperatures, as shown in Fig. 4.11. A range of values is indicated, since such variations occurred with changes in H_2 baking, cleanliness of pieces, standing prior to oxidation, etc.

"The excellent adherence of the glass to 'Kovar' is obtained with a weight gain of about 0.0003 to 0.0007 grams per square centimeter, regardless of temperature of oxidation, i.e., approximately 17 minutes at 800°C, 3 minutes at 900°C, 1 minute at 1000°C, or ¼ minute at 1100°C.

"If the piece is underoxidized, the strength of the seal is poor but it is still vacuum-tight. If it is overoxidized, the strength is good but the seal may be a leaker because the glass is unable to penetrate the oxide layer completely, thus leaving a continuous porous path through which gases can seep into the tube.

"With the preoxidation of 'Kovar' any tendency for peeling or flaking shows up on cooling to room temperature. Statistical recording has shown that this tendency exists more strongly under certain conditions of temperature and time, as indicated in Fig. 4.11 by the area inside the V-shaped dotted line. Flaking is emphasized by improper or lack of H_2 baking, dirty 'Kovar,' and other factors.

"Pieces with flaking or peeling oxide layers should be eliminated immediately, since poor oxide adherence also results in poor glass adherence. Such a tendency may be missed with the usual glassing technique, wherein the glass is sealed to the oxidized metal while the latter is still hot.

"Wet-hydrogen baking, for instance, in the time allotted should remove any carbon in the surface of the 'Kovar' at either 900 or 1100°C, but the temperature also controls the grain size of the 'Kovar.' Variations in time also alter the grain size, but not as effectively. The whole temperature range is used in baking, but the large grain-size structure is desirable since the oxide, and the glass in turn, then have been found on an average to adhere more firmly to the metal surface.

"Grinding of glass in any form to pass through a 200-mesh sieve constitutes the first step in the preparation of the glass for use in the powder-glassing method of making seals. A porcelain-ball mill is used to avoid contamination by iron. The composition of the ground glass is the same as normally used for sealing to a given metal; for instance, Corning 7052 or 7040 for 'Kovar.'

"The powdered glass is suspended in a suitable liquid, such as water or alcohol. With alcohol, which has been used most extensively at Westinghouse, a few drops of $LiNO_3$ solution or NH_4OH keep the glass particles from settling out into a hard mass, thus enabling the suspension to be easily dispersed after standing. The best ratio of liquid to solid is determined by careful experimentation.

"The powdered-glass suspension is then applied to the oxidized 'Kovar' surface by spraying. The pressure of the spray is controlled by the viscosity of the suspension and the shape of the piece. Pressures ranging from 10 to 40 pounds have been employed.

"If the powdered glass is to be applied by dipping or slushing, the suspension is adjusted to the proper viscosity and mobility to obtain the necessary thickness of coating. In either case the glass is restricted to the desired areas by proper masking prior to application, or by brushing afterwards.

"The dried powdered-glass coating is then fused in an electrically heated oven. 7052 and 7040 glasses produce a smooth coating by firing at 1000°C for 6 minutes. The powdered glass can also be fused by fires or by induction heating of the metal. 'Kovar'-glass seals are fired in air since the rate of oxidation of the 'Kovar' is slow in relation to the rate of fusion of the glass. For seals with copper, however, if oxidation during fusion is undesirable, the firing would have to be carried out in a neutral atmosphere, since the rate of oxidation of the metal is faster than the rate of fusion of the glass. The fired pieces are removed from the heat and allowed to cool in air without any annealing. These powder-glassed parts are now ready for tube assembly and can be stored indefinitely.

"The thickness of the fused-glass coating is not critical, but has ranged mostly from 4 to 6 mils. The thinner coatings are generally preferred since there is less tendency for pulling away from edges. Considerable amounts of bubbles, seen with low-power magnification, are present. However, these can be ignored, since no detrimental effects have been noticed because of their presence.

"Afterwards, the sealing of the tube or bulb to the powder-glassed parts becomes simply a glass-to-glass seal. Nothing is gained in temperature, since just as much heat and "working" are necessary to make the glass-to-glass seal. The advantage lies in the fact that the seals are now protected and extended heating will not affect them, allowing the operator to work on the seals without any time limitations, which is very important in some cases."

Edwards and Garoff[14] report their experience in regard to the application of powdered glass to "Kovar" as follows:

"Spraying the powdered glass takes some practice if an even coating of the desired thickness is to be obtained. A small DeVilbiss gun under 20 lbs pressure of tank nitrogen, with the work 8 to 12 inches from the gun gives the most satisfactory results. The first coat is light and wet and permitted to dry only partially before the next coat is added. The 7052 powdered glass should be used as soon as possible after it is ball-milled and sized, in order to minimize the moisture adsorbed by the glass. The mixture must be stirred after every minute of spraying to maintain a uniform density of the sprayed material. Methyl alcohol was found to be a very poor substitute for ethyl alcohol as a carrier for the powdered glass. However, Sylvania has reported favorably on the use of 'Isco Algin No. 117'* as a binder."

One part of 200-mesh 7052 glass to three-parts ethyl alcohol by volume forms the spray suspension.

Iron-Alloy Seals

The mechanical weakness inherent in feather-edge seals and the limiting current-carrying capacity of "Dumet" seals made it desirable to find metal-to-glass combinations which could be sealed in bulk. Tungsten and molybdenum have been available since 1912 for heavy leads sealed to hard glasses,[15] but only in wire or rod form because of the limitations of fabrication of these refractory materials. The advent of nickel-iron-chrome and nickel-iron-cobalt alloys provided metallic members that could be sealed in substantial thickness to soft and hard glasses, respectively. These alloys have expansion characteristics which closely match those of the glasses with which they are used. They can be produced in quantity at the metallurgical tolerances of the composition required; they form a well-adhering oxide that combines with the glass; and they have such electrical conductivity as to make them useful as current leads without overheating. In addition they are easily machined and obtainable at economical cost. It goes without saying that it required extensive research efforts on the part of many to bring such manifold requirements within practical reach.

* Obtained from Innis Speiden and Co., 121 Liberty St., New York 6, N.Y.

Nickel-Iron Alloys

The use of Ni-Fe alloys for seals with soft glasses was suggested as early as 1897,[16] and their properties were investigated by several workers.[17–21] Fig. 4.12 gives a graph of the mean expansion coefficient (0–100°C) for different weight-percentage compositions as well as the thermal conductivity.[22] It might appear from these curves that almost any glass could be matched by a suitable Ni-Fe composition of the proper expansion coefficient. It must be borne in mind, however, that the Transformation Point or Inflection Point of the alloy, where its elongation

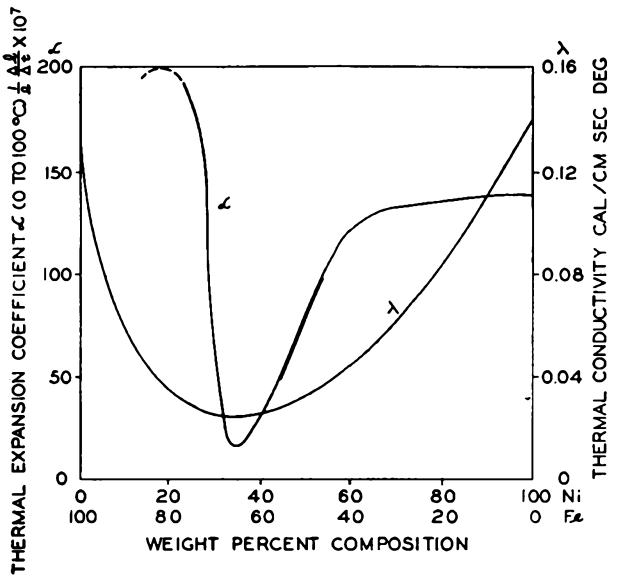

Fig. 4.12. Thermal expansion coefficient (0–100°C) and thermal conductivity for Fe-Ni alloys. After Espe and Knoll.[22] (*Courtesy J. Springer, Berlin.*)

rate with temperature begins to increase, should be as close to the Transformation Point of the glass; otherwise, objectionable strains would arise.

Fig. 4.13 shows a plot of curves, giving elongation versus temperature for Ni-Fe alloys of different Ni contents.[21] Corresponding characteristics for a number of glasses are also given in the same graph. These include a special Corning Glass 7060 (formerly designated 705-AO), which was developed specially to match Ni-Co-Fe alloys. It is seen that "42 Alloy" and 7060 glass match well over the temperature range 0–300°C, but depart markedly at higher temperatures where the sealing operation takes place. To appraise the match at the sealing temperature the latter has been defined as the temperature given by the intersection of a straight line with a slope 15 per cent greater than the average expan-

sion coefficient between 0 and 300°C of the glass with the expansion curve of the glass. This quite accurately represents the "sealing temperature" of borosilicate glasses with Ni-Co-Fe alloys, and is used here to appraise Ni-Fe alloys.

It is seen from Fig. 4.13 that a severe mismatch would occur for glass 7060 and "42 Alloy" at the sealing temperature of about 550°C. Under the Code 1075 the General Electric Company has developed a special glass, which has its sealing point at 450°C, where "42 Alloy" and 1075 glass expansion meet (Fig. 4.14). Seals obtained with this combination are free from stress at all temperatures below 350°C; this is shown by the

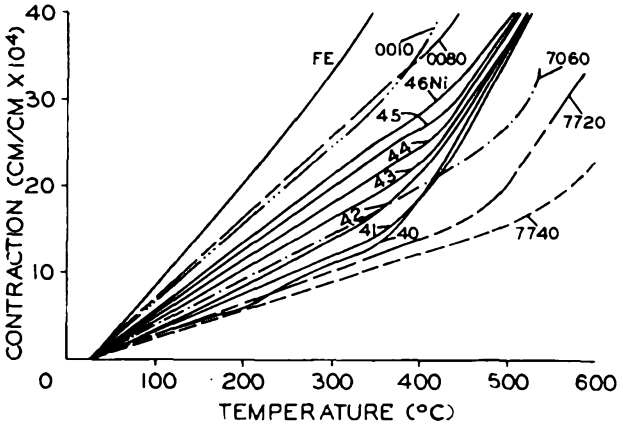

Fig. 4.13. Thermal expansion of Fe-Ni alloys and some Corning glasses. After Hull, Burger and Navias.[21] (*Courtesy American Institute of Physics.*)

stress pattern obtained with a quartz wedge on a bead seal, which is inserted in Fig. 4.14.[21] Stresses introduced by the divergence of the expansion curves between 350 and 450°C are not severe enough to cause breakage during cooling. The composition of 1075 glass is:

	%
SiO_2	34
B_2O_3	28
PbO	29
Al_2O_3	7
Na_2O	2

The composition of "42 Alloy," which matches this glass, is:

	%
Ni	41.5
Mn	0.5
Si	0.2
C	< 0.06
Fe	Bal.

The Transformation Point of Ni-Fe alloys depends on the magnetic properties of the material and occurs near the Curie point, where ferromagnetism is lost. Apart from the proper location of this magnetic inflection it is necessary to make sure that allotropic transformation of the iron component of the alloy from the γ-phase to the α-phase (Ar_3 Point) occurs outside the range of temperatures to which the glass seal is exposed during fabrication or operation, (i.e., $-40°C$ to $600°C$, approximately). If this is not the case, the expansion curve of the alloy is not reversible and will follow a different course on heating than with cooling. Fig. 4.15 gives an illustration of this behavior for the case of Ni-Co-Fe

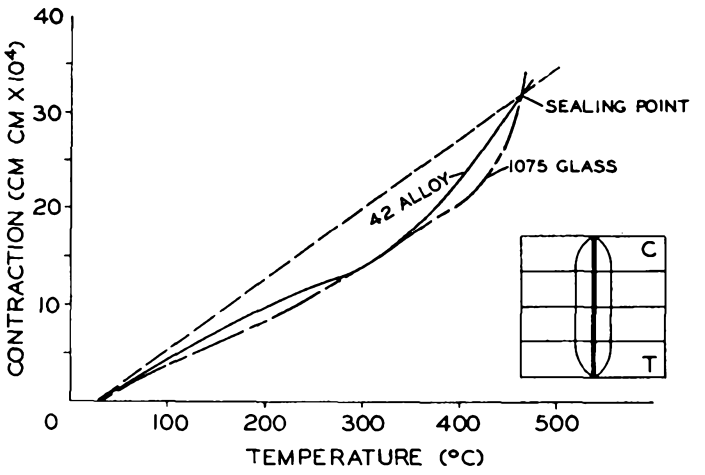

Fig. 4.14. Thermal expansion curves of 42 Alloy and 1075 Glass, and photoelastic stress pattern of a seal between them. Absence of stress in the seal is shown by the straightness of the interference lines crossing it. After Hull, Burger and Navias.[21] (*Courtesy American Institute of Physics.*)

(H. Scott[19]). To insure that the alloy is in the γ-state, it is advisable to subject the parts prior to sealing to an annealing treatment which well exceeds the Ar_3 Point and to follow this by slow cooling.

Extensive investigations on Ni-Fe alloys were carried out by Kingston,[23]* who was concerned with the development of an alloy suitable for pins in their "Loctal" tubes. He found the pure Ni-Fe alloy series unsuitable because their oxides did not adhere well to the metal. The oxide was rich in nickel next to the surface, where it tended to give a loose scaly oxide. Hull, Burger, and Navias[21] were evidently not confronted with this difficulty with their particular "42 Alloy" (Mn, Si, C additions), but were concerned instead with the appearance of lead at the interface between metal and glass 1075 from which PbO was reduced.

* Sylvania Electric Products, Inc.

By precoating the metal with a lead-free glass, such as 7060, or by coating the alloy with copper or platinum, which do not reduce PbO, this difficulty was overcome. Scott[24] had suggested small additions of one or more of the elements Cr, Co, Mn, Si, Al, or B to produce a more fusible oxide coating for seals to soft glass.

"42 Alloy"* is used in the electronic industry for receiving and transmitting tubes, x-ray tubes, cathode ray tubes, mercury arc rectifiers, sealed instruments, and radio components. Sealed headlights for motor

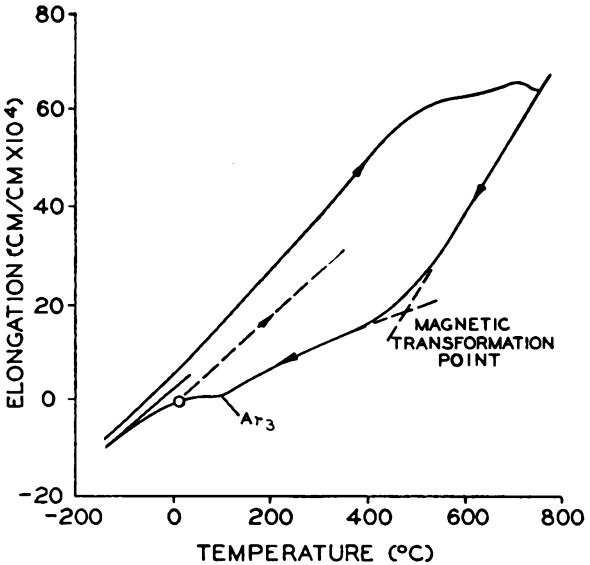

Fig. 4.15. Elongation vs temperature for an Fe-Ni-Co alloy not suitable for sealing purposes. The Ar_3 transformation from α to γ phase lies above room temperature. After Scott.[19] (*Courtesy American Institute for Mining and Metallurgy.*)

cars and sealed refrigeration units are other examples. Hard-glass seals with "42 Alloy" are made by using a feather-edge of about 4 mil thickness. Nickel-iron alloys are preferably heated to 950°C in hydrogen to obtain a clean surface prior to sealing. This treatment also removes the effects of cold work without causing excessive grain growth.[11]

Fine and Ellis[11a] have investigated the temperature dependence of Young's Modulus in Ni-Fe alloys, containing from 36 to 52 per cent Ni.

"There is a temperature at which an increase in Young's Modulus, arising from loss of ferromagnetism, exactly compensates the normal decrease, and a zero thermoelastic coefficient results. The temperature of zero coefficient depends on composition and on straining and annealing history. The temperature range of low coeffi-

* "Carpenter 42" from the Carpenter Steel Co., Reading, Pa.
"Allegheny 42" from Allegheny Ludlum Steel Corp., Pittsburgh, Pa.

TABLE 42. PHYSICAL CHARACTERISTICS OF METALS AND ALLOYS FOR GLASS TO METAL SEALS

Ser. No.	Metal or Alloy	Type Composition	Practical Shape Available W—Wire B—Ribbon R—Rod S—Sheet T—Tubing F—Formed	Thermal Expans. Coefficient $\Delta l/l/\Delta t \times 10^7$ cm/cm/°C	Thermal Conductivity Cal/cm³ sec °C	Electrical Resistivity Ohm. cm $\times 10^6$ (20°C)	Glass Type H—Hard S—Soft	Sealing Glasses* *Commonly Used*	Sealing Glasses* Sometimes Used
1	Platinum	Essentially pure Pt	W-T-B-S-F	91 (25–300)	0.166	10	S (H)	0120, 0010, 0080, 8160 LG-12; LG-12-7; GEC-L1; GEC-X4; BTH-C12; Ch-GWA	
2	"Dumet"	Core: Ni-43; Bal: Fe Sheath: Borated copper	W (0.040" dia. max.)	80–100 (radial) 61–65 (axial)	~ .4	4.6	S	0120, 0010, 0080, 8160 LG-12; LG-12-7; GEC-L1; GEC-X4; BTH-C12; Ch-GWB	
3	Copper	Essentially pure Cu (O.F.H.C.)	W-R-T-B-S-F	164 (25–300)	.92	1.724	S H	Almost any glass for thin copper in form of sheet, ribbon or tubing	
4	Steel (SAE 1010) (plated or bare)	Mn: 0.30 to 0.50; C: 0.08 to 0.13; S: 0.050 max; P: 0.040; Bal: Fe	W-R-T-B-S-F	125 (25–300)	.11	18		1990, 1991 GEC-R16; BTH-C41/76	0080, 0240
	Nickel-Iron G.E. Alloy	Ni: 41.5; Mn: 0.5; C: 0.06; Si: 0.2; Bal: Fe	W-R-T-B-S-F					G.E. 1075	
	Allegheny 42	Ni: 42; Bal: Fe		78 (20–500)	.026	66			
5	4750	Ni: 47–50; Bal: Fe		98 (20–500)	.037	50		0010, 0080, 0120, 8160	
	Driver Harris 142	Ni: 41.5; Bal: Fe	W-R-B-S	78 (20–500)	.026	66			
	52	Ni: 50–51; Bal: Fe	W-R-B-S	95 (20–500)	.0399	43.22	S		
	Carpenter 42	Ni: 42; Bal: Fe		50 (20–350)		71			
	49	Ni: 49; C: 0.10 max; Bal: Fe		90 (20–350)		43			
6	Low Chrome Nickel Iron		W-R-T-B-S-F						
	Sylvania 4	Ni: 42; Cr: 6; Mn: 0.29; C: 0.04; Si: 0.12, Bal. Fe		79 (20–300)	.032	34		0010, 0080, 0120, 8160	

* Four-number code: Corning Glass Works, Corning, N.Y.
LG: Libbey Glass Division, Owens-Illinois Glass Comp. (formerly Kimble glass) Toledo, Ohio.
GEC: General Electric Company, Ltd., Wembley, England.
BTH: British Thomson-Houston Company Limited, London, England.
Ch: Chance Brothers, Limited, Smethwick, England.

TABLE 4.2. PHYSICAL CHARACTERISTICS OF METALS AND ALLOYS FOR GLASS TO METAL SEALS. (*Continued*)

Ser. No.	Metal or Alloy	Type Composition	Practical Shape Available	Thermal Expans. Coefficient	Thermal Conductivity	Electrical Resistivity	Glass Type	Sealing Glasses	
			W—Wire B—Ribbon R—Rod S—Sheet T—Tubing F—Formed	$\Delta l/l/\Delta t \times 10^7$ cm/cm/°C	Cal/cm³ sec °C	Ohm. cm $\times 10^6$ (20°C)	H—Hard S—Soft	Commonly Used	Sometimes Used
	"Sealmet" 4	Ni: 42; Cr: 6; Bal: Fe		111 (20–500)	.029	34	S	LG-12; LG-12-7; BTH-C12; GEC-L1	
6	Driver Harris 14	Ni: 42; Cr: 6; Bal: Fe		92 (25–350)	.032	34			
	Carpenter 426	Ni: 42; Cr: 6; Bal: Fe		93 (20–350)		94			
	(Stanworth)	Ni: 47; Cr: 5; Bal: Fe		99 (20–400)					
	High Chrome Iron		W-R-T-B-S-F					0240	0010
	Sealmet 1	Cr: 28; Bal: Fe		110 (20–500)	.059	72		GEC-L14; Ch-GWA/B	
7	Carpenter 27	Cr: 28; Bal: Fe					S		
	Driver Harris 446	Cr: 28; Bal: Fe							
	Allegheny Telemet	Cr: 16–23; Mn: 2 max. C: 0.25 max; S: 0.030 max; P: 0.040 max; Si: 1 max; Bal: Fe		117 (30–530) (max. value)				Window glass	0120, 0010
	Nickel Cobalt Chrome Iron		W-R-T-B-S-F						
8	Fernichrome	Ni: 30; Co: 25; Cr: 8; Bal: Fe					H	0010, 0120, 0050, 7040, 7052, 7060	7050
	Fernico II	No: 31; Co: 15; Bal: Fe						L-704/705/650; GEC-FCN; BTH-C40; Ch-GSB	
	"Kovar" (Nilo K)	Ni: 29; Co: 17; Bal: Fe		50 (25–300)	.046	49			
9	Molybdenum	Essentially pure Mo	W-R-T-B-S-F	55 (25–300)	.35	5.7	H	GEC-HH/H26; BTH-C11; 11/37/46; Ch-GSC	
10	Tungsten	Essentially pure W	W-R-B	46 (0–500)	.38	5.5	H	7720, 3320, 7991, 7750 L-772; GEC-W1/WQ31; BTH-C9; Ch-GSD	7050, 7740

cient is greatly extended by cold work. For example, alloys near 42.5 per cent Ni when worked cold and then annealed at 400°C or 600°C, have nearly zero mean thermoelastic coefficients between −50 and 100°C.

"The general behavior of the modulus and its temperature dependence is explained on the basis of three ferromagnetic effects: (A) direct effect of the energy of ferromagnetism on the modulus, (B) the stress-produced volume magnetostriction within the domains, and (C) the stress-produced linear magnetostriction."

Table 4.2 gives a tabulation of the physical properties of glass-sealing metals and alloys, and lists the matching glasses.

Ni-Cr-Fe Alloys

The objectionable feature of "42 Alloy" (i.e., the formation of a flaky oxide) was overcome by the addition of 6 per cent chrome. This material is known as "Sylvania 4" alloy or "Sealmet 4," and is manu-

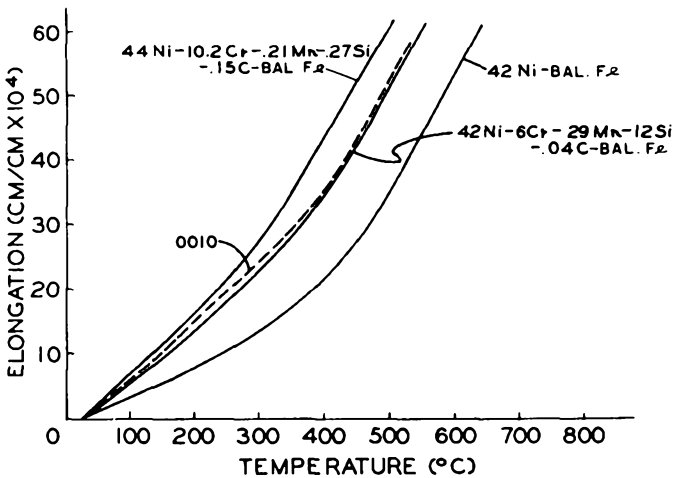

Fig. 4.16. Thermal expansion curves of Ni-Fe and Ni-Cr-Fe alloys. Also shown is the expansion curve of Corning Glass 0010. After W. E. Kingston.[23] (*Courtesy Allegheny Ludlum Steel Corp.*)

factured by the Allegheny Ludlum Steel Corporation. It is also obtainable as "Driver-Harris 14"* and "Carpenter 426."† The addition of Cr to the "42 Alloy" raises its expansion, as shown in Fig. 4.16.[23] The expansion curves for Corning 0010 and 0120 are also shown in this figure and Fig. 4.14.[25] It is evident that a good match is obtained between "Sylvania No. 4" and these glasses, especially through the annealing range, and the conformity of both expansions extends towards low temperatures to −75°C. The alloy has a reversible expansion over the range

* Driver-Harris Co., Harrison, New Jersey.

† Carpenter Steel Co., Reading, Pennsylvania.

of −75 to 1000°C. Its composition is given in Table 4.2. This is chosen so that a well-adhering protective layer of chromic oxide (Cr_2O_3) is formed at the surface. By addition of 0.52 per cent of carbon the hardness of the alloy is improved so that it will withstand the mechanical wear on sealing pins during insertion of tubes in their sockets. These alloys should be oxidized, prior to seal making at 1050–1250°C, in a hydrogen atmosphere which has been saturated with water vapor at 40°C.[11]

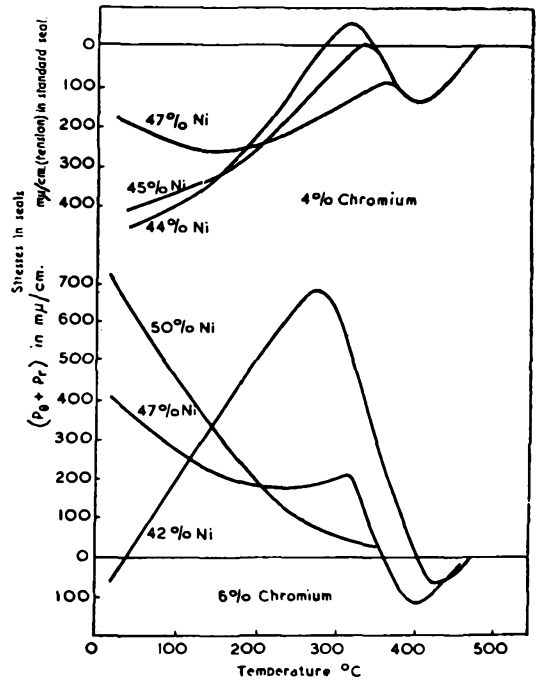

Fig. 4. 17. Stress-temperature curves obtained with alloys containing 4% chromium and 6% chromium. The 42% nickel 6% chromium alloy was available in wire form only so the results for the lower three curves are given for the sum of the circumferential and radial stresses in bead seals. After Stanworth.[26] (*Courtesy Institute of Physics, London.*)

Stanworth[26] has recently shown that the match of this alloy (42 Ni-6 Cr) to lead glass is not as good as might be desired. Fig. 4.17 indicates that the stress in a seal, cooling from the annealing temperature, increases to a peak at about 300°C before decreasing to a very low value at room temperature. In an attempt to find an alloy composition which would show at least as good a match to lead glass as "Kovar" gives to borosilicate glass he arrived at the alloy 47 Ni-5 Cr. Fig. 4.18 gives the stress temperature curves for these two metal-to-glass seals. It is evident that an outstandingly good match to lead glass is obtained with the new

Ni-Cr alloy composition. The interface of the seals is olive green in color, and adhesion of glass to metal is very satisfactory.

During the course of this investigation some interesting curves were obtained, which are reproduced here from Stanworth's paper. Fig. 4.19

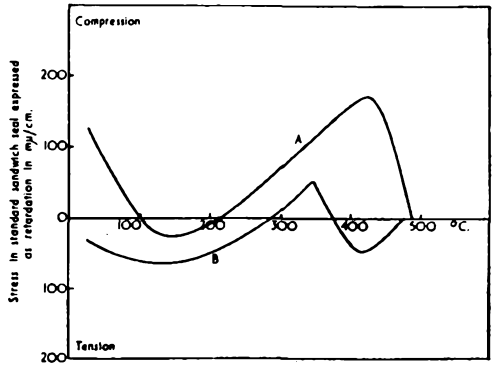

Fig. 4.18. Stress-temperature curves for (a) C40 Borosilicate glass to Kovar-type alloy; (b) C12 lead glass to nickel-chrome-iron (47 Ni – 5 Cr – Bal Fe) alloy. After Stanworth.[26] (*Courtesy Institute of Physics, London.*)

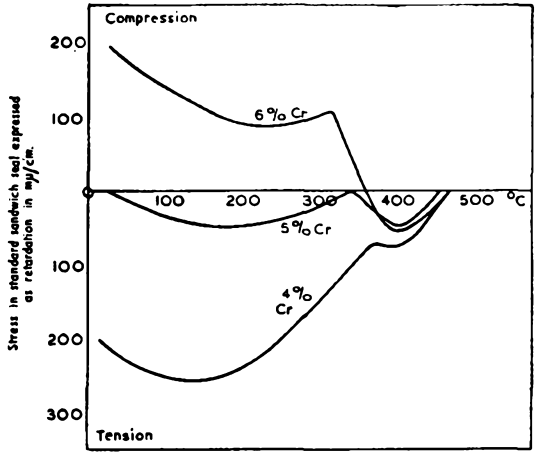

Fig. 4.19. Effect of chromium at 47% nickel. Note that the ordinates in all figures refer to mμ retardation per cm of light path length. After Stanworth.[26] (*Courtesy Institute of Physics, London.*)

shows the effect of varying Cr-additions to a 47 per cent Ni alloy on the stress-temperature curves and Fig. 4.20 the corresponding curves when the same Cr-additions are made to a 49 per cent Ni alloy. The stress is measured in each case by the retardation in mμ/cm as observed from a sandwich seal in a polarimeter. Small amounts of carbon, manganese, and silicon were present in the alloys, the balance being iron.

"It will be noted that the stress developing below about 470°C in all cases passes through a minimum, then through a maximum, and then, in some cases, through a second minimum. The more pronounced minimum and maximum stresses at about 400° and 275–375°C are caused respectively by the transformation in the glass contraction curve and the inflection in the metal contraction curve at its Curie temperature. This is shown diagrammatically for a particular case in Fig. 4.21. The higher rate of contraction of the glass between *H* and *G* gives tension in the glass of the sandwich seal at temperatures immediately below about 470° because the contraction of the glass is in this region greater than that of the alloy. Below *G* the contraction of the glass decreases, and the stress, therefore, goes through a minimum, to become zero at *F*, but then passes through a maximum at *E*, and becomes increasingly more

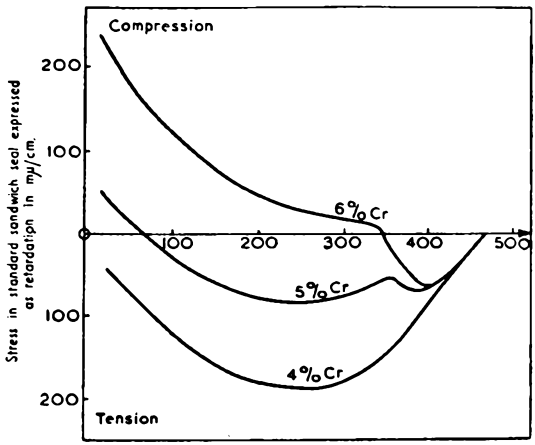

Fig. 4.20. Effect of chromium at 49% nickel. After Stanworth.[26] (*Courtesy Institute of Physics, London.*)

tensile in the region *EC*, because, once again, the glass is contracting at a greater rate than the metal. Below *C* the metal contraction increases so that the increasing tensile nature of the stresses in the glass is arrested; the stresses throughout the whole range down to room temperature remain low."

Cr-Fe Alloys

Prior to the introduction of "Sylvania No. 4" an alloy containing 28 per cent to 30 per cent Cr, balance Fe, was used for sealing to a soft glass, Corning 0240, specially developed to match this alloy. Such alloys were widely used in Europe before World War II, and the manufacture of British tubes* in the United States and Canada during the war made large scale operation with such alloys necessary. They form a very firmly adhering green oxide layer when heated to 950°C in wet hydrogen prior to sealing. Acid-pickling by immersion in 20 per cent hydrochloric acid for about 2 minutes, followed by neutralizing and water rinse, also brings about oxidation;[11] 28 Cr-Fe has a rather high electrical resistivity (Table

* Valve Type VR91, adopted from the Philips Type EF50, is an example.

4.2), and spot welding is very difficult without previous sandblasting to remove the oxide layer. Silver plating overcomes this difficulty and glassing operations can be carried out in the ordinary manner on silver-plated chrome iron.[27,28] Plain chrome iron cannot be brazed to copper in a hydrogen atmosphere unless extreme precautions are taken to remove the last traces of oxygen from the hydrogen. Brazing to nickel is less

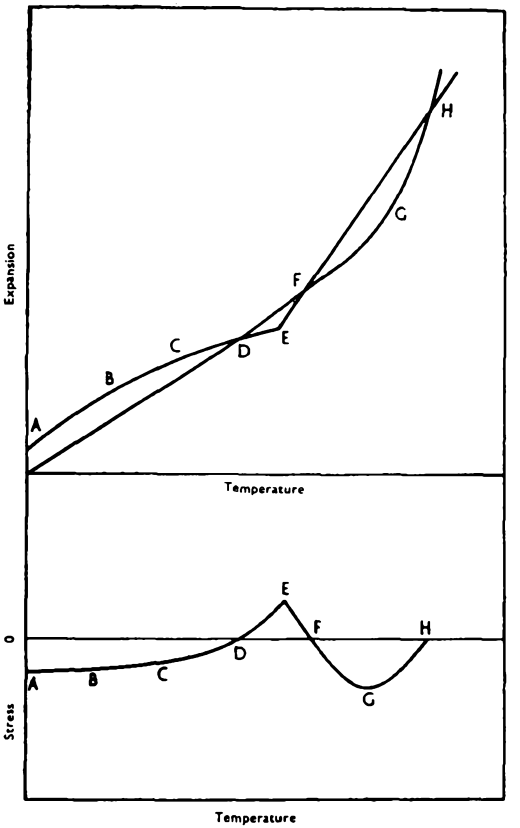

Fig. 4.21. Relation between expansion properties and the stress-temperature curve. After Stanworth.[26] (*Courtesy Institute of Physics, London.*)

difficult. Fig. 4.17 gives expansion curves for this alloy and 024 glass.[25] These high Cr-alloys are also available under the trade designations "Sealmet 1,"* and "Carpenter 27."† "Allegheny 55" and "Ascoloy 446"* are obsolete designations for stainless-steel grades not intended specifically for glass sealing. An alloy known as "Fernichrome" was developed by Hull and Burger[4] to match soft glasses better than chrome-

* Allegheny-Ludlum Steel Corp., Brackenridge, Pa.

† The Carpenter Steel Company, Reading, Pa.

iron. Its composition is Fe-37, Ni-30, Co-25, Cr-8 per cent, and its differential expansion characteristic relative to chrome-iron is shown in Fig. 4.23, together with a number of other sealing alloys and metals.

The high chromium-bearing commercial alloy AISI, Type 446 (modified) (Allegheny Sealmet 1) has recently found application in glass-to-metal sealing for television kinescopes Type 16AP4, introduced by R.C.A. These tubes have a large metal cone, spun from the aforesaid alloy to which the 16-inch diameter screen face of high quality window glass, 3/16 inch thick, is sealed on one end and the neck assembly of 0120

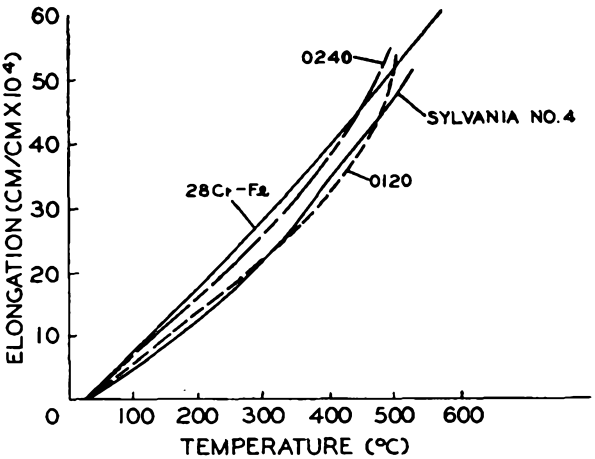

Fig. 4.22. Thermal expansion curves of 28% chrome-iron and Sylvania No. 4 Alloy. Also shown are the expansion curves of the Corning Glasses 0240 and 0120 which match these alloys respectively. After Monack.[25] (*Courtesy The Gauge Publishing Company.*)

glass on the other. These sealing operations are performed on automatic machinery which make possible economic production on a large scale.[29,30]

According to Rose and Turnbull[31] the alloy chosen for the cones contains 28 per cent of chrome. The thermal expansion coefficient extends from 108 to 110 $\times 10^{-7}/°C$ in the range from 25 to 500°C. During the sealing operation the temperature of the rim of the cone to which the glass dish is attached reaches 1200°C. This takes 3 minutes. For annealing, the cone seal is then transferred to an oven and held at 550°C for 8 minutes. It is then removed from the oven and allowed to cool in the air to room temperature. The sheet glass used for the screen face has a thermal expansion coefficient of 91 $\times 10^{-7}/°C$ in the range from 30 to 300°C. It is worthy of note that the difference in thermal expansion coefficients between metal and glass is as high as 19 $\times 10^{-7}$, and may reach 23 $\times 10^{-7}$ before the metal is rejected. Window glass has a rather

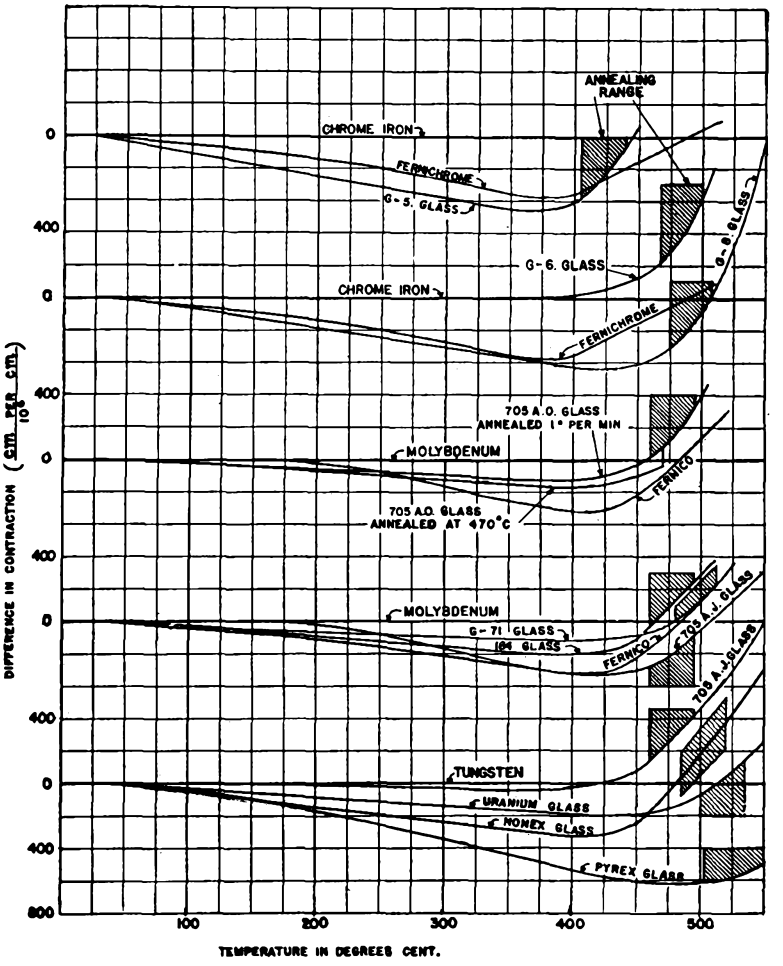

Fig. 4.23. Relative contraction of principal sealing glasses and metals when cooled at rate of 1° per minute. Cross-hatched areas represent annealing range of temperature. Ordinates are the differences in contractions, per unit length of sample, between the metal taken as standard (axis horizontal) and the glasses and other metals nearest to it in expansion. The differences, in conjunction with the annealing conditions, determine the stresses in seals. After Hull and Burger.[4] (*Courtesy American Institute of Physics.*)

sharp and steep inflection, which may bring its average coefficient to the setting point to nearly that of the metal. The fact that it is even lower is important to the strength of metal kinescopes under external pressure.

It is important that this already very large value of $\Delta\alpha$ for the low temperature range is not further increased because of phase changes which the metal might undergo during the heating cycle. These phase

changes, on heating chrome-iron alloys, have been studied by Bain.[32] Twenty-eight per cent chrome-iron will retain without change its predominantly α ferritic crystal structure when heated to 1200°C and higher, and consequently suffer no change of its thermal expansion coefficient. Alloys with a chrome content lower than 26 per cent, on the other hand, change to the austenite structure on heating and retain it partly on cooling. This results in an increase of the thermal coefficient of expansion over a temperature range where the glass has already set and cannot yield, thus causing the seal to fracture. Acceptance tests have been set up by Rose and Turnbull[31] to ensure that the metal is suited for cone sealing. For general glass-sealing applications in electronic devices the ASTM Committee B-4, Section E, Subcommittee 8 is preparing a tentative specification, which requires the following chemical composition of 28-per cent chrome-iron alloy:

Carbon	0.25 per cent max.
Manganese	2.00 " " "
Sulfur	0.030 " " "
Phosphorus	0.040 " " "
Silicon	1.00 " " "
Chromium	23 to 30 " "

Two procedures are recommended for the determination of thermal expansion characteristics as follows:

"Procedure A: The alloy shall be heated in air to 1200° ± 10°C and held for 15 minutes at temperature at the end of which it shall be cooled continuously to a temperature of 530° ± 10°C within a maximum period of 8 minutes. Upon further cooling from 530° ± 10°C to 30°C ± 5°C there shall be no evidence of transformation as manifested by an abrupt discontinuity in the cooling curve. In the latter range the coefficient of thermal contraction shall not exceed 11.4×10^{-6} in./in./deg. C. If x is the thermal expansion at 530° ± 10°C in inches per inch and y is the expansion at 30° ± 5°C, then the coefficient of contraction is calculated as follows:

$$\text{C.C.} = \frac{x - y}{(530 \pm 10) - (30 \pm 5)}$$

Upon still further cooling from 30° ± 5°C to −40°C the cooling curve shall be free of evidence of transformation as indicated by abrupt changes.

"Procedure B: The alloy shall be heated in air to 1200° ± 10°C and held for 15 minutes at the end of which it shall be cooled by quenching in water. Upon subsequent heating to 530° ± 10°C there shall be no evidence of transformation as manifested by an abrupt discontinuity in the heating curve. In the range between 30° ± 5°C and 530°C ± 10°C the coefficient of thermal expansion shall not exceed 11.4×10^{-6} in./in./deg. C. The coefficient shall be computed as described under Procedure A.

"In the temperature range between −40°C and +30°C ± 5°C the heating curve shall be free of evidence of transformation as indicated by abrupt changes.

Test for Thermal Expansion

"The thermal expansion characteristics shall be determined in accordance with Tentative Recommended Practice for Dilatometric Analysis of Metallic Materials, ASTM Designation: E80-49T."

R.C.A.[33] has recently introduced a chrome-iron alloy containing only 17 per cent chromium, for which a tentative specification has likewise been prepared by the ASTM Committee. The chemical composition is specified as follows:

Carbon,	per cent max	0.25
Manganese,	" " "	2.00
Sulfur,	" " "	0.030
Phosphorus,	" " "	0.040
Silicon,	" " "	1.00
Chromium,	" "	16 to 23

Again two procedures for the determination of thermal-expansion characteristics have been suggested as follows:

"Procedure A: The alloy shall be heated in air to 1200° ± 10°C and held for 15 minutes at temperature at the end of which time it shall be cooled continuously to a temperature of 530° ± 10°C within a maximum period of 8 minutes. Upon further cooling from 530° ± 10°C to 30°C ± 5°C there shall be no evidence of transformation, as manifested by an abrupt discontinuity in the cooling curve. In the latter range the coefficient of thermal contraction shall not exceed 11.7×10^{-6} in./in./deg. C. If x is the thermal expansion at 530° ± 10°C in inches per inch and y the expansion at 30°C ± 5°C, then the coefficient of contraction is calculated as follows:

$$\text{C.C.} = \frac{x - y}{(530 \pm 10) - (30 \pm 5)}$$

Upon still further cooling from 30° ± 5°C to −40°C, the cooling curve shall be free of evidence of transformation as indicated by abrupt changes.

"Procedure B: The alloy shall be heated in air to 1200° ± 10°C and held for 15 minutes, at the end of which it shall be cooled by quenching in water. Upon subsequent heating to 530° ± 10°C there shall be no evidence of transformation, as manifested by an abrupt discontinuity in the heating curve. In the range between 30° and 530 ± 10°C the coefficient of thermal expansion shall not exceed 11.7×10^{-6} in./in./ deg. C. The coefficient shall be computed as described under Procedure A.

"In the temperature range between −40° and +30° the heating curve shall be free of evidence of transformation as indicated by abrupt changes."

The 17-per cent chrome alloy has greater ductility than the 28-per cent alloy. This makes for easier spinning. It also holds an optimum position with respect to cost, corrosion resistance, heat resistance, and thermal expansion. The objectionable transformation to the austenitic phase, referred to above, can be suppressed by the addition of varying amounts of aluminum, columbium, molybdenum, titanium, vanadium, tungsten, and tantalum. Typical compositions of three modified alloys, which are commercially available, are the following:

	A (%)	B (%)	C (%)
Chromium	18.5	17.1	18.1
Carbon	0.08	0.06	0.08
Manganese	0.49	0.42	0.51
Phosphorus	0.02	0.02	0.02
Sulfur	0.01	0.006	0.008
Nickel	0.20	0.34	
Titanium	0.62	0.68	0.35
Aluminum	0.11		
Silicon	0.29	0.84	
Molybdenum			0.9

The coefficient of thermal expansion of the stabilized 17-per cent chromium alloy varies between 11.1 and 11.3 $\times 10^{-6}$ in./in./deg. C through the range from 30 to 500°C. While these values for expansion are slightly higher than those normally obtained for the 28-per cent chrome-iron, this increased disparity with the expansion of the glasses used is only a minor consideration in making glass-to-metal seals. The introduction of the new alloy into the production line was accomplished without any serious dislocation.[33]

Ni-Co-Fe Alloys

To provide an alloy that would seal with hard glasses and at the same time lend itself to the fabrication of geometrical shapes, such as cylinders, sheet, and tubing, basic investigations were carried out by H. Scott[19,20] and A. W. Hull, E. E. Burger, and L. Navias.[4,21] As a result an alloy was developed which satisfied the above requirements. These materials are known as "Kovar" and "Fernico," the latter being the name coined by Hull and Burger for their alloy. "Kovar" (Trade mark 337962) is the trade name for an alloy of similar composition; it is melted by the Westinghouse Electric Corporation and distributed in a variety of standard and special shapes by the Stupakoff Ceramic and Manufacturing Company, Latrobe, Pennsylvania.

"Fernico," in its original form, had the following composition: 54 Fe, 28 Ni, 18 Co. It matched Corning Glasses G-71 and 7060 reasonably well. In a later study Hull, Burger, and Navias[21] adjusted the composition to 54 Fe, 31 Ni, 15 Co, which gives a more stable alloy at low temperature and, when free from all impurities, including Mn and Si, also matches 7060. It was found that this pure alloy, made in hydrogen by powder metallurgical techniques, is ductile and free from embrittlement under all conditions of ordinary use, including heating and annealing in air, hydrogen, or gas, and soldering, brazing, and welding. Table 4.3 gives

some of the physical characteristics of "Fernico."[21] Expansion curves for "Fernico" and 7060 glass are given in Fig. 4.24, together with a stress pattern for a wire-bead seal of 7.5 mm diameter glass on a 2.5 mm diameter "Fernico" wire. The lines in the stress pattern are straight within

TABLE 4.3. PHYSICAL CHARACTERISTICS OF FERNICO[21]
(54 Fe-31 Ni-15 Co)

Tensile strength	72,000 to 80,000 psi
Percent elongation	2 to 33%
Percent reduction in area	62 to 63
Elastic modulus	18×10^6
Density	8.24 g/cc
Electrical resistivity	43.8 microhms/cm³
Temperature coefficient of expansion	49.5×10^{-7} (25 to 300°C)
Melting point	1460°C
Hardness	75 "Rockwell B"
Yield point	55,000 psi

1/100 of the distance between two adjacent fringes; this indicates that the remaining stress after cooling at the rate of 1 degree per minute is less than 0.02 kg/mm².

The physical characteristics of "Kovar A"[34] are given in Table 4.4, and expansion curves are shown in Fig. 4.25, together with those of Corn-

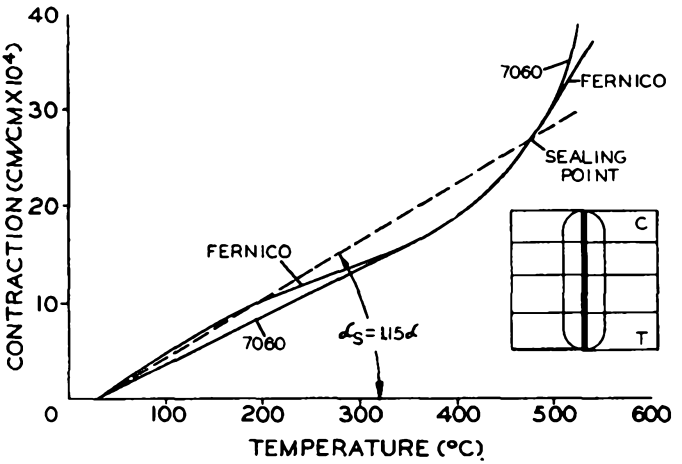

Fig. 4.24. Thermal contraction of Fernico and Corning Glass 7060. The insert shows the stress pattern of a test seal between these materials. After Hull, Burger and Navias.[21] (*Courtesy American Institute of Physics.*)

ing glasses 7052 and 7040. Mechanical characteristics extending to higher temperatures are shown in Figs. 4.26 to 4.28, according to measurements by J. S. Theilacker.[35]

Toward the end of World War II the great demand for hard glass-

TABLE 4.4. PHYSICAL CHARACTERISTICS OF "KOVAR A"[34]

Specific Properties of "Kovar A"

Composition	29% nickel, 17% cobalt, 0.3% manganese, balance iron
Melting point	1450°C (approx)
Density	0.302 lb/cu in.
Hardness—annealed	140–160 B.H.N. 760°C
Hardness—unannealed	200–250 B.H.N. depending on degree of cold work
Specific electrical resistance	49 microhm cm—294 ohms/cir mil ft
Thermal conductivity	0.046 cal/cm/sec/°C (approx. as measured at room temp)
Curie point	435°C (approx.)

Physical Properties of 0.030 Thick Sheet
Tested Parallel to the Direction of Rolling

Yield point	50,500 psi
Proportional limit	32,300 psi
Tensile strength	89,700 psi
Modulus of elasticity	20×10^6 psi

Thermal Expansion—After annealing in hydrogen for 1 hr at 900°C or for 15 min. at 1100°C. The average coefficient of thermal expansion of "Kovar A" falls within the following limits:

30°–200°C	4.33 to 5.30	$\times 10^{-6}$ per °C
30–300	4.41 to 5.17	
30–400	4.54 to 5.08	
30–450	5.03 to 5.37	
30–500	5.71 to 6.21	
30–600*	7.89	
30–700	9.31	
30–800	10.39	
30–900	11.47	

Magnetic Permeability

Magnetic Permeability	Flux Density (Gauss)
1000	500
2000	2,000
3700	7,000 (max. value)
2280	12,000
213	17,000

Magnetic Losses (Watts per lb)

Thickness (inch)	10 Kilogauss 60 cycles sec	10 Kilogauss 840 cycles sec	2 Kilogauss 5000 cycles sec	2 Kilogauss 10,000 cycles sec
0.010	1.05	23.4	16.6	41
.030	1.51			
.050	2.77			

Tensile strength of "KOVAR" Glass Seals is 600 psi. All of the above are typical values.

* These values added from Special Alloy Memo No. 24, Nov. 7, 1947, by J. S. Theilacker of Westinghouse Electric Corp., with the kind permission of this company.[35]

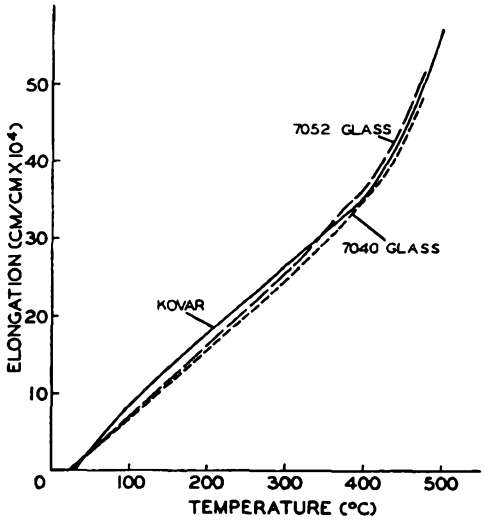

Fig. 4.25. Thermal expansion curves of "Kovar A" and Corning Glasses 7052 and 7040.[34] (*Courtesy Stupakoff Ceramic & Manufacturing Co., Latrobe, Pa.*)

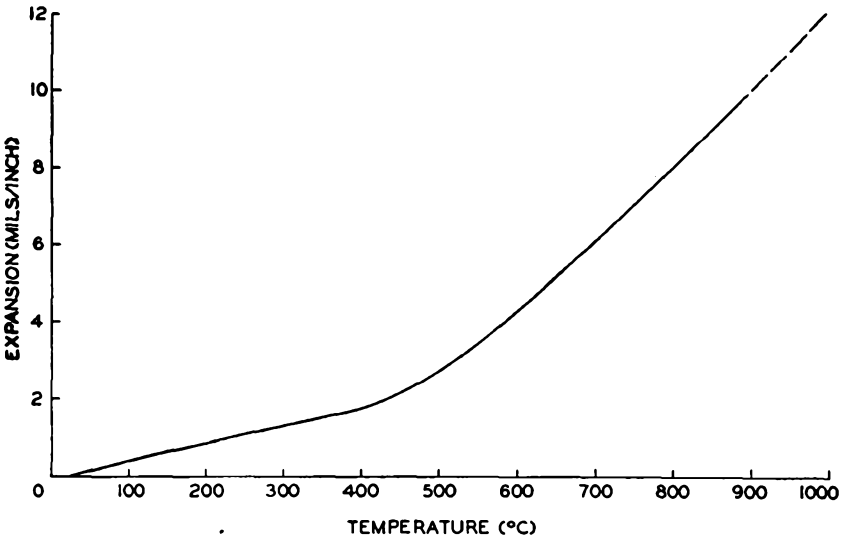

Fig. 4.26. Thermal expansion curve of "Kovar" in the high-temperature range. After J. S. Theilacker.[35] (*Courtesy Westinghouse Electric Corp.*)

sealing alloys brought about the manufacture of these alloys in Great Britain; G. D. Redston[36] reports on the controlled melts produced by the British Metal Industry. As a result of these investigations a proposed alloy specification was issued as follows:

Ni	29 ± 0.5 per cent
Co	17 " "
Mn	0.3 " "
Si	0.15 " "
(Ni + Co)	46 ± 0.5 per cent
Fe	balance

Studies were made on the effects of composition on expansion and transition temperature. It is shown in Figs. 4.29 and 4.30 that transition

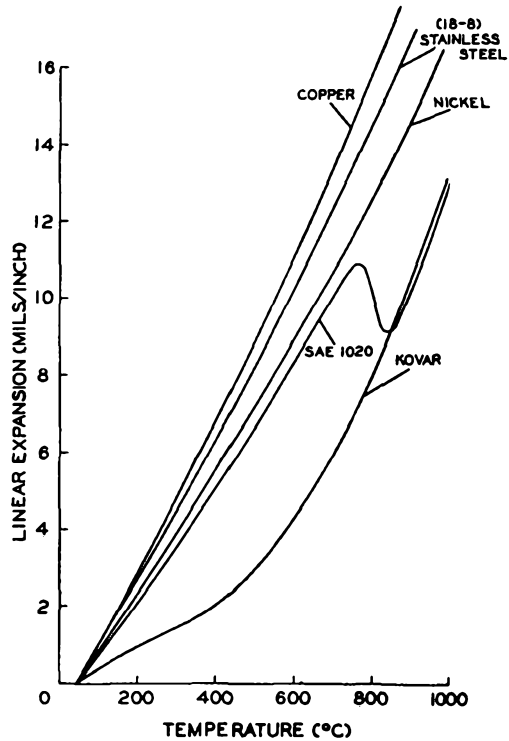

Fig. 4.27. Thermal expansion curve of "Kovar," copper, stainless steel (18–8), nickel and SAE 1020. After J. S. Theilacker.[35] (*Courtesy Westinghouse Electric Corp.*)

temperatures fall within a narrow range if the combined (Co + Ni) content is closely controlled. The curves show relative expansion against molybdenum, which was used as a reference standard in the dilatometer. This type of presentation, also used by Hull and Burger,[4] clearly shows

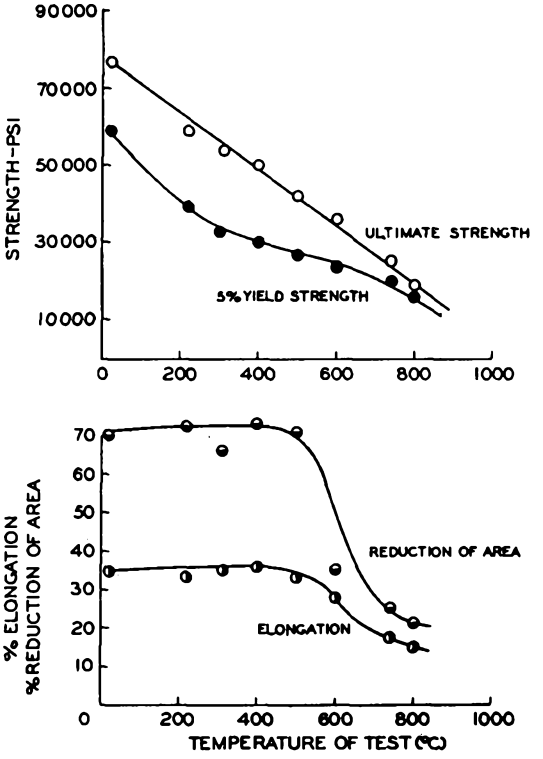

Fig. 4.28. Plot of ultimate strength, yield strength, reduction of area and elongation vs temperature of test for "Kovar." After J. S. Theilacker.[35] (*Courtesy Westinghouse Electric Corp.*)

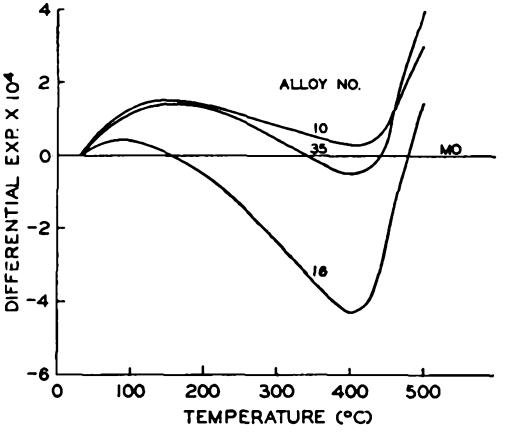

Fig. 4.29. Differential thermal expansion curves of Fe, Ni, Co alloys numbers 10, 16 and 35 against molybdenum. After Redston.[36] (*Courtesy Institute of Physics, London.*)

the differential expansion which, after all, is the main criterion for the quality of a seal. The alloys thus produced were sealed with the British glass C-40, developed by the British Thomson-Houston Company Research Laboratory. Fig. 4.31 gives the retardation in mμ/cm over the

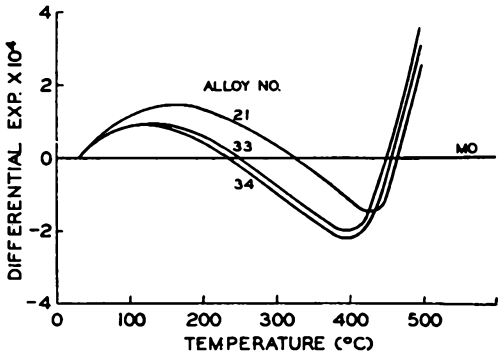

Fig. 4.30. Differential thermal expansion curves of Fe, Ni, Co alloys numbers 21, 33 and 34 within the suggested composition aim against molybdenum. After Redston.[36] (*Courtesy Institute of Physics, London.*)

temperature range 0–500°C for a sandwich seal between alloy 34 (28.6 Ni; 17.7 Co; 0.24 Mn; 0.19 Si; 0.04 C) and C-40 glass. Bearing in mind the discussion in Chapter 3.6, where 300 mμ/cm was given as an upper limit for safe loading, it is evident that these seals are well within this range. In Fig. 4.32 may be found similar stress versus temperature curves for a conventional molybdenum seal, with Mo sealing glass (Curve A), C-40 glass with alloy 34 (Curve B), and C-40 to Mo (Curve C).

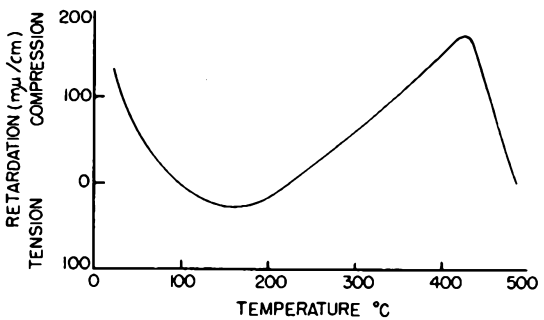

Fig. 4.31. Retardation-temperature curve for a sandwich seal of C40 Glass to Fe, Ni, Co Alloy No. 34. After Redston.[36] (*Courtesy Institute of Physics, London.*)

The electrical resistivity of "Kovar" and "Fernico" is much higher than that of copper; in high-frequency tubes it may cause the seals to become overheated during operation of the tube. By electroplating a film of Cu, Au, Ag or Cr, several mils thick, onto the "Kovar" the resis-

TABLE 4.5. PROPERTIES OF SOME BRITISH SEALING GLASSES[39]

Designation	B.T.H.* C12	B.T.H. C19	B.T.H. C40	G.E.C.† L.1	G.E.C. F.1.N	G.E.C. X.8	Chance§ G.W.A.	Chance G.W.B.	Chance G.S.B.	P. & T.‡ Kodial	P. & T. Normal (2 Blue Lines)
Type	Lead	Soda lime silicate	Boro silicate	Soft lead	Boro silicate	Soda lime silicate	Soda lime silicate	Soft lead	Boro silicate	Boro silicate	Soda zinc silicate
Sealed to	Ni-Fe	Ni-Fe	Nilo-K	Ni-Fe Dumet	Nilo-K	Ni-Fe	Ni-Fe Dumet	Ni-Fe Dumet	Nilo-K	Nilo-K	Ni-Fe
Exp. coeff. $\times 10^{-7}$ (20–350°C)	87.5	92	47.5	91.5	4.75	96.5	91.5	95	54.5	49	83
Temp (°C) corresp. to viscosity = 10^4 poises	960	1025		960		1005	1030				
= $10^{7.6}$	632	700	715	630		700	700	610	710		
= 10^{12}	465	550	535	465	560	555	540	430	500		
= 10^{13}	435	530	505	435	530	540	510	390	450		
Log D.C. resistivity at 150°C	12.3	8.4	11.5	12.4	11.7	7.9					
Log D.C. resistivity at 300°C	8.6	5.7	8.1	8.6	8.3	5.3					

* B.T.H.—British Thomson Houston Company, Limited, London, England.
† G.E.C.—General Electric Comp. Ltd., Wembley, England.
‡ P. & T.—Plowden & Thompson.
§ Chance—Chance Brothers Limited, Smethwick, England.

tivity of the seal can be lowered by a factor of 10 to 20 in comparison to an unplated seal at frequencies in excess of 50 MC.[37,38] Rheaume[38] stated that 1.9 cm diameter "Kovar"-glass seals will pass 30 amps R.F. at 40 MC/sec without excessive heating at the metal-to-glass interface due to circulating currents, and that a 16.4 cm diameter "Kovar" seal should

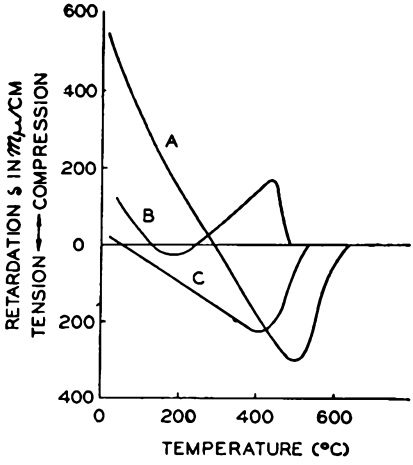

Fig. 4.32. Comparative retardation-temperature curves for combinations of over-all expansion coefficient (0 – 400°C) 50×10^{-7} approximately. (a) Standard molybdenum-sealing glass to molybdenum. (b) C40 to alloy 34. (c) C40 to molybdenum. After Redston.[36] (*Courtesy Institute of Physics, London.*)

be good for 258 amps. R.F. at 40 MC. These values can be raised considerably by gold-plating. According to Doolittle[10] the charging currents in lead seals are proportional to $f^{3/2}$, E^2, and C^2, where f is the frequency in cycles/sec, E is the voltage applied between adjacent electrodes, and C is the interelectrode capacity.

Since readers in the United States and Canada are not usually familiar with British codes for glasses and sealing alloys, but nevertheless

TABLE 4.6. LINEAR COEFFICIENTS OF THERMAL EXPANSION OF NILO SERIES OF ALLOYS*

Per °C	Nilo 42	Nilo 48	Nilo K
0–100	5.2×10^{-6}	8.7×10^{-6}	5.8×10^{-6}
0–200	4.8×10^{-6}	8.3×10^{-6}	5.12×10^{-6}
0–300	4.9×10^{-6}	8.3×10^{-6}	4.71×10^{-6}
0–400	5.6×10^{-6}	8.3×10^{-6}	4.64×10^{-6}
0–500	7.6×10^{-6}	8.8×10^{-6}	6.00×10^{-6}

* Manufactured by Henry Wiggin and Company, Ltd., Birmingham, England,

encounter them in the literature, this may be an appropriate place to insert some information on this subject. Table 4.5 is reproduced from *Metal Industry*,[39]* giving properties of some British glasses and the alloys

* With permission of the publisher of *Metal Industry*. The Louis Cassier Co. Ltd., Dorset House, Stamford St., London, S.E. 1, England.

TABLE 4.7. CHANCE SEALING GLASSES[40]

Type	Composition										Identification		Sp. Gr. gr/cc	Linear Expansion Coefficient (10–100°C)	Softening Temp. Log Viscosity 7.6 (°C)	Upper Annealing Temp. Log Viscosity 12 (°C)	Lower Annealing Temp. Log Viscosity 13 (°C)	Young's Modulus	Stress Optical Coefficient Wavelengths per cm/kg/mm²	Thermal Endurance	
	SiO_2	PbO	Na_2O	Na_2O_3	K_2O	Al_2O_3	B_2O_3	BaO	CaO	Sb_2O_3	Color	Fluorescence Under Black Lamp								Beaker Method (°C)	Rod Method (°C)
Hysil GHA	80.4		4.2			2.7	12.4		0.3	0.014	Pale yellow-green	None	2.24	33.6×10^{-7}	780	610	575	5.95×10^{11}	0.65	320	300
Intasil GSD	78.6		4.9			2.56	12.87	0.03	0.01	0.07	Pale brown	Faint orange	2.30	38.7×10^{-7}	780	605	570	6.3×10^{11}	.65	280	260
GSC	76		6			4	10.5	3	0.5		None	None	2.32	45×10^{-7}	760	620	590	6.3×10^{11}	.6	240	220
GSB	67		3		4.5	4	21			0.02	Pale green	Bright green	2.23	49×10^{-7}	710	500	450	5.4×10^{11}	.72	240	220
GWA	73.8		15.33		0.46	1.62			7	0.42	Pale blue-green	Faint grey	2.49	87×10^{-7}	700	540	510	6.4×10^{11}	.45	125	120
GWB	58.4	29.0	5.8		4.9	0.5			0.5	0.6	Very faint yellow-green	Thin sections, bright blue thick sections, blue-green	2.99	86×10^{-7}	610	430	390	5.9×10^{11}	.5	130	120

with which they are sealed. The latter are essentially represented by the "Nilo" series* of low-expansion alloys, for which characteristic data are given in Table 4.6 with the permission of the manufacturer. It is evident that "Nilo-K" is the equivalent of "Kovar." Further data are tabulated by Partridge,[11] but he does not list sealing glasses made by Chance Brothers, Ltd. Table 4.7 thus gives some data on these glasses from *Mechanical World*.[40]†

Sealing by Induction

Modern sealing techniques of which some were described above, have eliminated much of the guesswork on sealing operations. There are still jobs where the discretion of the craftsman is invaluable and must be relied on to the fullest extent, but there is less room for arguments based on mystery. Reference was made above to the wide use of sealing lathes, but these are, after all, nothing but a "handle" serving to support and rotate the work. Great judgement is required of the operator in choosing the correct degree of oxidation of the metal (unless this has been taken care of by the powder glass technique), the proper flame temperature, the right amount of pressure on the paddle, and the length of time for annealing in the flame. These details are mastered fully only after prolonged experience. The author was intimately concerned with them during World War II, and he developed, quite independently, the technique of sealing by induction,‡ only to realize later that he was antedated by earlier workers in the field. While the principle of this technique is old,[6,41] it was applied on a large scale for tube production only during World War II.[42,43]§

Induction sealing in its application to glass-to-metal seals is an indirect method insofar as the glass is heated by conduction of heat from the hot metal to the glass. The work is surrounded by a coil carrying alternating currents of suitably high frequency, which in turn induce Eddy currents in the metal, thus heating it to a cherry red or orange temperature. The glass is in contact with the hot metal and is thus softened at and near the contact area. It flows under the influence of gravity or the applica-

* Manufactured by Henry Wiggin and Company, Limited, Wiggin Street, Birmingham 16, England.

† With permission of the publisher of *Mechanical World and Engineering Record.* Emmott and Co. Limited, 78 Palatine Road, Manchester 20, England.

‡ Reports of these developments, especially applied to reflex klystrons and T.R. tubes, which were carried out by the writer while he was with Rogers Electronic Tubes, Ltd., Toronto, Canada, were sent to British and U.S. agencies during the early part of World War II, and it is likely that he thus contributed to the wider application of this technique.

§ There is no mention of this technique in Knoll and Espe's extensive treatise on high-vacuum technology.[22]

tion of an external mechanical force to make the bond with the metal. This is the general theme which has an almost unlimited number of variations. The technique is applicable to all sealing metals, and is especially suited to disk seals, cylindrical seals, and terminal seals of not too small diameters.

Disk seals will be discussed first, as they are probably the most common. Fig. 4.33(a) shows the assembly of the components within the coil (1). A metal disk (2), with an aperture or other contour at its central part, rests on a glass cylinder (3), and a similar glass cylinder (4) rests on the metal disk. The three components are kept in alignment by suitable fixtures. The glass faces touching the metal must be cut square and be smooth and clean. They should not be handled after cutting or cleaning,

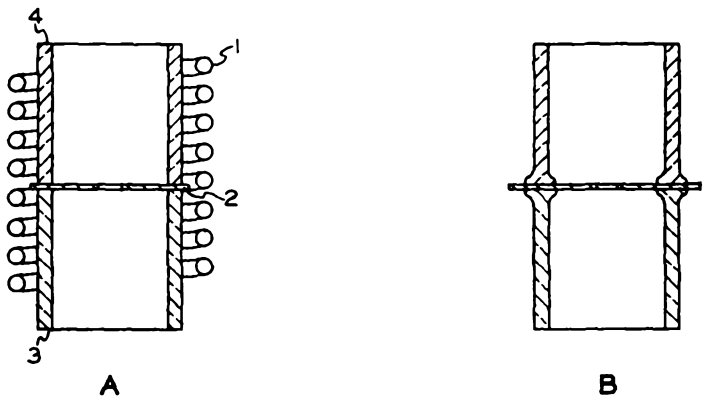

Fig. 4.33. Schematic outline of the production of a tubular disk seal by induction heating. (a) Set-up; (b) Completed seal.

whichever is the last operation; otherwise bubbles will result in the seal. Rough glass surfaces, caused by cutting on an emery wheel, will produce an infinite number of tiny bubbles, which are not necessarily objectionable. A diamond cut, produced by scratching the glass with the point of a diamond and then heating it briefly in a flame, will result in a very smooth surface not requiring additional polishing or cleaning.

The metal disk must be clean and smooth for the same reasons. If copper is used, its thickness should not exceed 12 mil for a disk about 2 inches in diameter. Other metals or alloys used in conjunction with matching glasses may have any thickness desired. The metal may be pre-oxidized and copper may be borated if the sealing operation is carried out in a neutral atmosphere of nitrogen or carbon dioxide. If it is carried out in air the initial heating will oxidize the metal interface; however, the remaining surface will continue to oxidize during the whole sealing cycle.

This may be objectionable as it requires excessive cleaning after the seal is made.

The borating procedure for this type of seal is the subject of a patent by H. J. McCarthy,[44] who prescribes the following steps:

(1) Metal forming

(2) Metal cleaning by immersion in carbon tetrachloride, followed by a hot water rinse

(3) Metal etching by first applying 15 per cent nitric acid for 8 to 15 minutes, followed by a thorough washing in water, a brief application of 50 per cent nitric acid for about 12 seconds, and another washing in water. The nitric acid must be completely removed from the metal to avoid staining through the catalytic action of the acid when the disk is exposed to air.

(4) Further cleaning is carried out by soaking the disk in a 25-per cent solution of ammonium carbonate for about a minute and then rinsing the disk in water.

(5) Drying by bodily removing the liquid from the copper disk in a centrifuge operating at about 3600 rpm. This further helps to avoid staining.

(6) Borating by brushing out the disk with a solution of the order of 25 g of borax in 170 cc of water, to which 12 drops of "Titron"* is added as a wetting agent. The solution is kept at 90°C. The borax is applied while the disk rotates about its vertical axis. It precipitates out almost as fast as it is applied because the concentration of borax in the solution at 90°C is greater than that which will remain dissolved at room temperature. When a dull mat surface appears, the operation is completed.

(7) Oxidation of the metal under the borax layer is readily achieved by heating with R.F. for a few seconds because of the porosity of the coating.

The disk is now mounted between the glass cylinders, as shown in Fig. 4.33 (a), and R.F. is applied through a suitable coil for the correct period of time. The current is then turned off; as soon as the glass has set, the seal is transferred to an annealing oven. It then has the appearance of Fig. 4.33 (b). The glass joints must be made on opposite sides, as shown in the case of copper disks where the mismatch of expansion between metal and glass is taken up by elastic yield of the copper. It might be mentioned here that a substitute for a graded seal is easily obtained by sealing hard glass to one side and soft glass to the other side of the copper, which now takes on the shape of a flat ring to provide as low an impedance as possible to the flow of gas. The writer has used such seals successfully over prolonged periods.

It goes without saying that more than one disk can be sealed at the

* An organic polyether alcohol.

same time, and Fig. 4.34 indicates this procedure schematically for a klystron cavity assembly. The required fixtures now become a little more elaborate, as allowance must be made for the shortening of the glass members during sealing, and as proper gap distance must be assured by a stop between the two copper anodes, either within the gap or at the periphery of the anodes. A further example for the extended use of induction sealing is the high-voltage accelerator tube* (Fig. 4.35), where 175 "Kovar" disks are sealed successively by a traveling H.F. coil to the intermediate glass rings, about 3 inches in diameter.[45] The method adopted in this case and found to give the least number of leaks comprised a combination of flame-sealing and induction-sealing.[46] After the initial

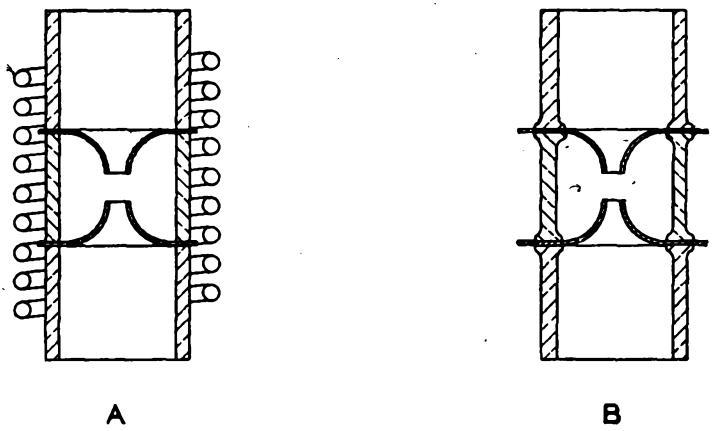

Fig. 4.34. Schematic outline of the production of a tubular multiple disk seal by induction heating. (a) Set-up; (b) Completed seal.

seals are made by conventional flame technique, induction heating is applied to raise the metal under the glass to the proper temperature, and this is followed by a final flame treatment for reshaping the glass by means of paddles. The column passes through an annealing oven as individual sections are completed.

A similar combined flame and induction-sealing technique is often applied to disk seals of the type shown in Fig. 4.33 and others. A glass ring is first cut from glass tubing of the proper size and sealed to the disk with the aid of gas flames rotating around the work.† Essentially, this lays down a bead on both sides of the disk to which the main glass cylinders are sealed by induction.

* Manufactured by Machlett Laboratories, Inc., Springdale, Conn.

† The Litton Type C vertical sealing machine is ideally suited for such work. A full range of glass lathes is produced by Litton Laboratories, Inc., San Carolos, California.

The advantage of these techniques is obvious: it permits the duplication of seals under identical conditions and obviates all operator skill that could not be acquired in a very short time. After establishing the optimum values for timing, current intensity and gas flow, specifications can be established which should give the same product and permit close quality control.

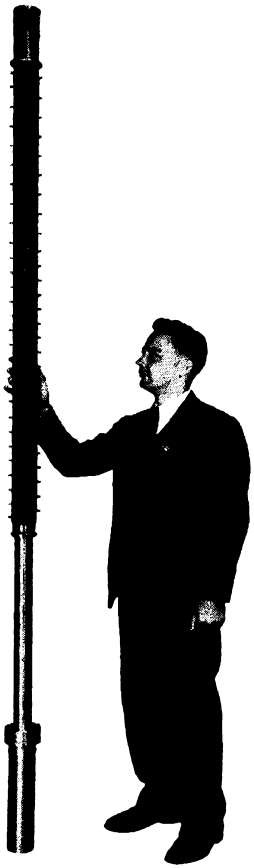

Fig. 4.35. 2-Million-volt precision x-ray tube.[45] (*Courtesy Machlett Laboratories, Inc.*)

A few additional procedures will now be briefly described which will help to illustrate the flexibility of the method and be of interest to workers in the laboratory. Experimental headers and pin seals may be produced by forming a dish from copper sheet, which is about 12 mils thick and has the necessary perforations. Fig. 4.36 (a) shows the copper dish which is formed in a die and punched to provide holes for the pins. A glass ring (1) and a piece of cane glass (2) in the center of the ring are placed into the dish (3) with the pins (4) in place. A ceramic cup, machined from

soapstone or "Alsimag 222,"* serves to support the assembly. After the dish is heated by means of the induction coil (6), the glass in it will melt and flow around the pins to form an intimate seal. After the copper dish has been properly cooled, it may be torn off; this results in a header assembly. Any remaining discoloration of the glass base can be removed by boiling in ammonium-chloride solution. If desired, a tubulation can be sealed to the header at the same time. The dish then has an additional hole in the center, and the central piece of cane is not required. In place of a copper dish a graphite mold may be used. It is also possible

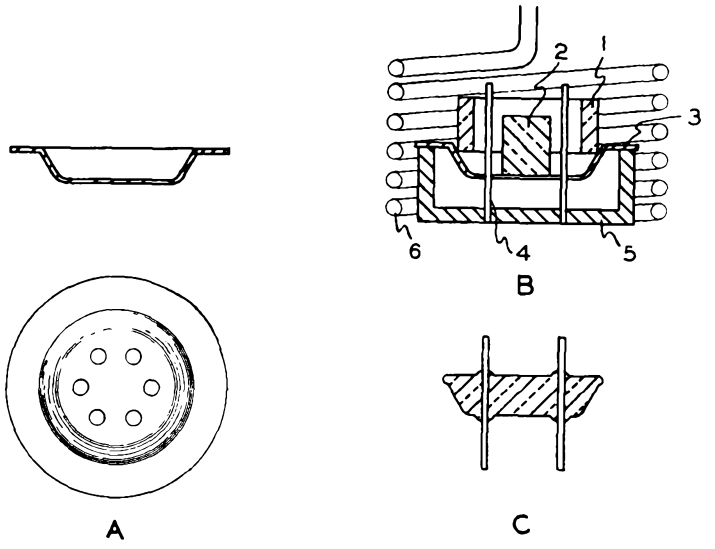

Fig. 4.36. Schematic outline of glass header fabrication by induction sealing.

to make seals between headers and bulbs by permanently sealing a thin copper ring between the two glass members, as shown in Fig. 4.37. Overheating the parts which are mounted on the header can be prevented by suitable Eddy Current Concentrators, discussed by Babat and Losinsky.[47] Their technique has been used to advantage by the present writer on several occasions, and it is surprising that no reference is made to it in any of the later literature on induction heating; however, it was described again recently by Reinartz.[48]

The commercial realization of header manufacture by high production machines using gas flames is described by Monack[49] and others. After having struggled in the laboratory to produce headers one at a time (according to Fig. 4.33), it is a considerable thrill to see machines in operation which have an output of several hundred pieces per hour.

* Obtainable from American Lava Corporation, Chattanooga, Tennessee.

Another quite novel method for glass-to-metal sealing has been described by Kohl.[50] To circumvent the need for hot-working the seal components, both glass and metal, it has been suggested that a satisfactory joint may be produced by metal-spraying methods. A very excellent review of the development of glass-working techniques in France, as applied to the electronic industry, is given by Violet, *et al.*[51] and an extensive treatise on glass-to-metal seals has been contributed by Tre-

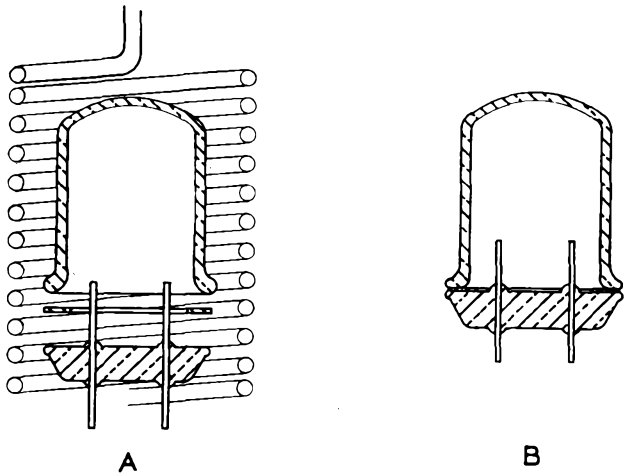

Fig. 4.37. Schematic outline of procedure to seal bulbs to headers by means of induction heating of an auxiliary thin copper washer.

buchon and Kieffer.[52] A series of articles on stresses in glass-metal seals was published by Martin of the Corning Glass Works.[53]*

REFERENCES

1. Wichers, E., and Saylor, C. P., "Sealing Platinum to Pyrex Glass," *Rev. Sci. Inst.*, **10**, 245–250 (1939).
2. Kraus, C. A., *U.S. Patent 1,093,997* (1914).
3. Eldred, D. E., *U.S. Patent 1,140,134/135/136* (1913).
4. Hull, A. W., and Burger, E. E., "Glass-to-Metal Seals," *Physics*, **5**, 384–405 (1934).
5. Guyer, E. M., "Electrical Glass," *Proc. I.R.E.*, **32**, 743–750 (1944).
6. Housekeeper, W. G., "The Art of Sealing Base Metals Through Glass," *J. Am. Inst. El. Eng.*, **42**, 954–960 (1923); *U.S. Patent 1,294,466*.
7. Spangenberg, K. R., "Vacuum Tubes," New York, McGraw-Hill Book Co., Inc., 1948.
8. Barr, W. E., and Anhorn, V. J., "Scientific and Industrial Glass Blowing and Laboratory Techniques," Pittsburgh, Instrument Publishing Co., 1949.

* Since this material was written, an excellent monograph on glass-to-metal seals[11] has become available which is highly recommended to the reader interested in this subject. Some data have been incorporated into the manuscript by permission of the author.

9. Strong, J., "Procedures in Experimental Physics," New York, Prentice-Hall, 1943; 2nd Ed., 1948.
10. Doolittle, H. D., "Glass-to-Metal Seals in High-Voltage, High-Power Tubes, Machlett Laboratories, Inc., Springdale, Conn., Machlett Cathode Press, Spring, 1947.
11. Partridge, J. H., "Glass-to-Metal Seals," Sheffield 10, England, Society of Glass Technology, 1949.
11a. Fine, M. E., and Ellis, W. C., "Young's Modulus and its Temperature Dependence in 36 to 52 Per Cent Nickel-Iron Alloys," *Transact. Am. Inst. Min. Met. Eng. J. of Metals*, **188**, 1120–1125 (Sept., 1950).
12. Goodale, L. C., "Glass-to-Metal Seal," *U.S. Patent 2,457,144*, Fed. Tel. and Radio Corp. (Dec. 28, 1948).
13. Pask, J. A., "New Techniques in Glass-to-Metal Sealing," *Proc. I.R.E.*, **36**, 286–289 (1948).
14. Edwards, E. V., and Garoff, K., "Fabrication of a High-Power Resonant Wave Guide Window," *Rev. Sci. Inst.* **21**, 787–789 (1950).
15. Weintraub, E., *U.S. Patent 1,154,081* (1915).
16. Guillaume, C. E., "On the Expansion of Nickel-Steels" (In French), *C. R. Acad. Sci. Paris*, **124**, 176–179 (1897).
17. Chevenard, P., *Rev. de Met. Mem.*, **11**, 841–862 (1941).
18. Hidnert, P., "Thermal Expansion of Heat-Resisting Alloys: Ni-Cr, Fe-Cr, and Ni-Cr-Fe Alloys," *J. Res. Bur. Stand.*, **7**, 1031–1066 (1931). (RP388).
19. Scott, H., "Expansion Properties of Low-Expansion Fe-Ni-Co Alloys," *Transact. Am. Inst. Min. Met. Eng., Inst. of Metals Div.*, **89**, 506–537 (1930).
20. Scott, H., "Recent Developments in Metals Sealing into Glass, *J. Franklin Inst.*, **220**, 733–753 (1935).
21. Hull, A. W., Burger, E. E., and Navias, L., "Glass-to-Metal Seals II," *J. Appl. Phys.*, **12**, 698–707 (1941).
22. Espe, W., and Knoll, M., "Werkstoffkunde der Hochvakuumtechnik," Berlin, J. Springer, 1936.
23. Kingston, W. E., "Hygrade Sylvania's Low-Expansion Alloy for Glass-to-Metal Seals," *Tech. Horizons*, **3**, 1–12, Allegheny Ludlum Steel Corp., Pittsburgh, Pa. (1942).
24. Scott, H., *U.S. Patent 2,065,404* (1936).
25. Monack, A. J., "Glass-to-Metal Seals in Electronic Components and Applications," *El. Mfg.*, **39**, 96–101, 162, 164, 166, 168, 170, 172, 174, 176, 178, 180 (1947).
26. Stanworth, J. E., "A Nickel-Chromium-Iron Alloy for Sealing to Glass," *J. Sci. Inst.* **27**, 282–284 (1950).
27. Freedman, N. S., "Silver-Plating Facilitates Bonding Glass to Steel," *Steel*, **121**, 92–94, (Aug. 25, 1947).
28. Miller and Spooner, *U.S. Patent 2,334,020* (Nov. 9, 1943). Assignee R.C.A.
29. Steier, H. P., Kelar, J., Lattimer, C. T., and Faulkner, R. D., "Development of a Large Metal Kinescope for Television," *R.C.A. Rev.*, **10**, 43–58 (1949).
30. Steier, H. P., and Faulkner, R. D., "High-Speed Production of Metal Kinescopes," *Electronics*, 81–83, (May 1949).
31. Rose, A. S., and Turnbull, J. C., "The Evaluation of Chromium-Iron Alloys for Metal Kinescope Cones," *R.C.A. Rev.*, **10**, 593–599 (1949).
32. Bain, E. C., "The Nature of the Alloys of Iron and Chromium," *Trans. Am. Soc. Steel Treaters*, **9** (1926).
33. Rose, A. S., "Stainless Steel for Television," *Metal Progress*, **57**, 761–764 (1950).
34. "Sealing Glass to 'Kovar'," *Bull. 145*, Stupakoff Ceramic and Mfg. Co., Latrobe, Pa. (1945).

35. Theilacker, J. S., "Elevated Temperature Properties of Kovar," *Special Alloy Memo No. 24*, Westinghouse Electric Corp., Metallurgical Development Section, Materials Engineering Dept. (Nov. 7, 1947).
36. Redston, G. D., "Iron-Nickel-Cobalt Alloy for Sealing to Glass," *J. Sci. Inst.*, **23**, 53–57 (1946).
37. Smith. P. T., and Hegbar, H. R., "Duplex Tetrode U.H.F. Power Tubes," *Proc. I.R.E.*, **36**, 1348–1353 (1948).
38. Rheaume, R. H., "A Co-axial Power Triode (ML-354) for Higher Power at the Higher Frequencies," Machlett Cathode Press, Winter, 1949–50. Machlett Laboratories, Inc., Springdale, Conn.
39. "Glass-to-Metal Seals—The Application of Iron-Nickel-Cobalt Alloys," *Metal Ind.* (London), **75**, 263–266, 292–293 (Sept., Oct. 1949).
40. "Metal-to-Glass Sealing," *Mech. World*, **116**, 339–341; 346 (1944).
41. Ronci, V. L., *Brit. Patent 474,706* (Stand. Tel. and Cables, Ltd.) London (1936).
42. Holloway, D. L., "The Manufacture of a Reflex Klystron," *J. Brit. I.R.E.*, **8**, 97–109 (1948).
43. Spitzer, E. E., "Induction Heating in Electron-Tube Manufacture," *Proc. I.R.E.*, **34**, 110W–115W (1946).
44. McCarthy, H. J., *U.S. Patent 2,422,628* (1947).
45. "Precision Two Million Volt X-Ray Tube," **3**, 5–7, Machlett Laboratories, Inc., Springdale, Conn., Machlett Cathode Press, Summer, 1946.
46. Machlett, R. R., *et al.*, *U.S. Patent 2,462,205* (1949).
47. Babat, G., and Losinsky, M., "Concentrator of Eddy Currents for Zonal Heating of Steel Parts," *J. Appl. Phys.*, **11**, 816–823 (1940).
48. Reinartz, J. L., "Industrial Brazing by Pulse Techniques," *Electronics* **23**, 78–80 (1950).
49. Monack, A. J., *U.S. Patent 2,345,278* (Mar. 28, 1944). Assignee: R.C.A.
50. Kohl, W. H., *U.S. Patent Application* (Mar. 3, 1949).
51. Violet, F., Danzin, A., and Commin, A., "Glass in the Electron Tube Industry (in French)," *Ann. de Radioel.*, **2**, 24–77 (1947).
52. Trébuchon, G., and Kieffer, J., "The Physical Aspect of Glass-to-Metal Seals in the Electron Tube Industry" (In French), *Ann. de Radioél.* **5**, 20, 125–149 (1950); **5**, 21, 243–258 (1950); **5**, 22, 407–418 (1950).
53. Martin, F. W., "Stresses in Glass-Metal Seals," *J. Am. Ceram. Soc.*, **33**, 224–229 (1950).

CHAPTER 5

ELECTRICAL CONDUCTION IN GLASS

This chapter will discuss the properties of glass which are apparent in the presence of electrical fields when these are applied to the glass body by means of contact electrodes. The fields to be considered will include those of the static and the alternating type and, in the latter case, will cover a wide range of frequencies. Temperature will enter as an important parameter which, together with field strength, severely restricts the possible applications of glass if failure in service is to be avoided. We are used, from every-day experience, to look upon glass as a solid insulator. It will become apparent from the following that this concept must be modified.

Volume Conductivity

Glasses are electrolytic conductors at all temperatures, and the resistivity may range from 10^{19} ohm-cm at room temperature to 1 ohm-cm at 1200°C, depending on the glass composition. This fact was established by the classic work of E. Warburg (1884), who showed that Faraday's Law of electrolytic conduction was satisfied. A distinction must be made between surface and volume conductivity, and precautions should be taken during their measurement unless the presence of one overshadows the other. Fig. 5.1 shows curves for volume resistivity as a function of temperature for Corning Glasses 7740, 0010, and 0080.[1] It is apparent that the ohmic resistance in direct-current fields drops rapidly with increasing temperature. In the range of operating temperatures, encountered in electron-tube applications, lead glass 0010 has a higher electrical resistivity by a considerable margin, than either 7740 "Pyrex" or soda-lime glass 0080. It is, therefore, common practice to make conventional stems for receiving tubes from 0010 or 0120 glass, while bulbs are made from soda-lime glass 0080 or its equivalent. This does not imply, as Stanworth[2] points out, that lime glasses of even higher resistivity than lead glasses cannot be made. On a factory scale, however, lead glasses are produced more easily, without difficulties arising from devitrification and unfavorable viscosity-temperature relationships. It may happen at times that the electrical resistivity of a glass envelope is

so high that electrical charges accumulate and lead to puncture, whereas a more conductive glass would have permitted the charges to leak off.

All measured data indicate that the addition of Na_2O increases the volume conductivity more than any other oxide and that CaO markedly decreases it. It is also commonly accepted that sodium ions are the

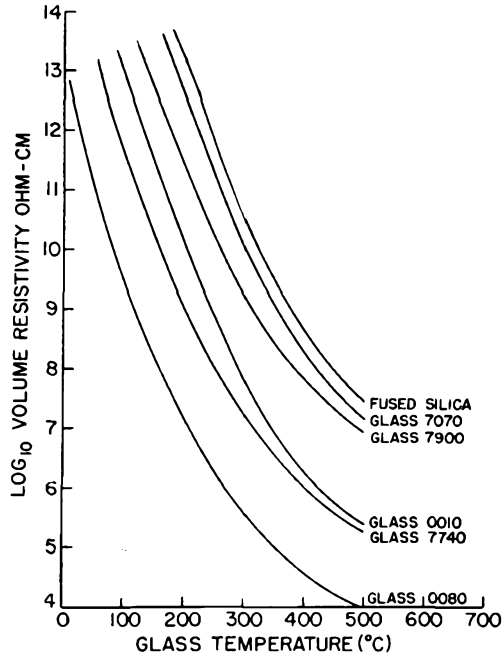

Fig. 5.1. Volume resistivity as a function of temperature for Corning glasses 0010, 0080, 7070, 7900 and fused silica. (*Courtesy Corning Glass Works, Corning, N.Y., Bull. B-83.*)

carriers of conduction in all glasses. This is readily demonstrated by the formation of free-sodium films on the inside glass wall of an evacuated bulb, having an electron source as cathode and a sodium nitrate bath on the outside of the bulb as anode.[3] The amounts of Na deposited agree with Faraday's Law. Electrolytic formation of sodium films on evacuated "Pyrex" tubes immersed in a $NaNO_2$ bath at approximately 500°C has also been reported.[4] The dependence of conductivity on temperature, so characteristic of all glasses, has been expressed in two types of experimental equations:

$$lnx = A + BT \tag{5.1}$$

$$lnx = C - \frac{D}{T} \tag{5.2}$$

where x is the specific conductivity, T is the absolute temperature, and A, B, C, and D are constants. Equation 2 is known as Rasch and Hinrichsen's Law.[5] Glasses seem to fall into two groups which satisfy either one or the other of these relations. Equation 2 has also been derived later from theoretical considerations of the binding forces acting on the Na^+ ions in the glass network.[6]

Kirby[7] gives a review of the phenomena involved in the electrical conduction in glass.

The measurement of the volume resistivity of glass is obscured by the presence of "anomalous charging currents" or "dielectric absorption."[8–11]

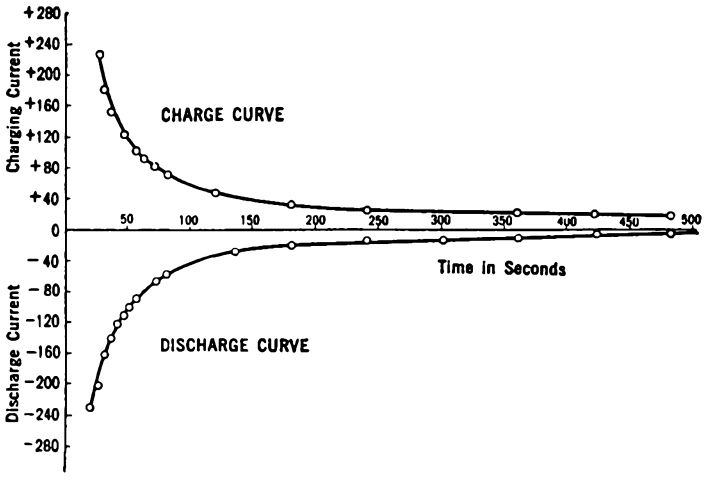

Fig. 5.2. Typical charge and discharge curves of a glass. After E. M. Guyer.[12] (*Courtesy American Ceramic Society.*)

This effect, which is common to dielectrics in general, was first observed on glass by Benjamin Franklin in 1746 during his studies of residual electrical charges on Leyden jars. When a voltage is first applied, the charging current in glass is much larger than the normal conduction current, and only after several hours does it decrease to assume a constant value. Similarly, a discharge current is observed after removal of the applied voltage, which is the reverse of the charging current.

On repetitive application of charging or discharging cycles the principle of superposition, stated by Hopkinson (1876–97), applies, according to which "the variation in charging current resulting from several successive variations in the applied voltage is the summation of the individual variations in charging current which would have taken place if each voltage variation had been separately impressed upon the uncharged condenser."[9] Guyer of the Corning Glass Works has described measurements of these effects on various glasses,[12] and Figs. 5.2–5.4 show his

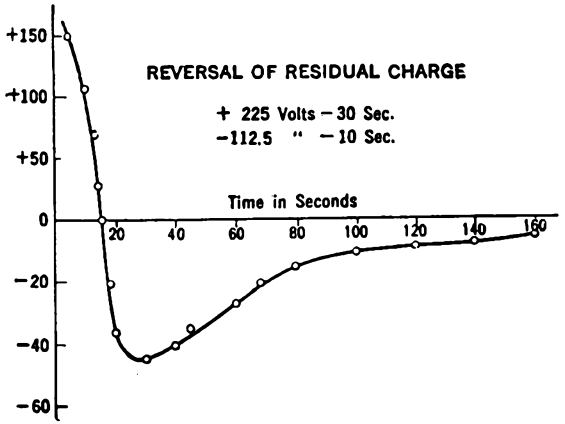

Fig. 5.3. Reversal of residual charge in a borosilicate glass. The charging cycle is given in the figure; readings were taken after disconnecting the charging battery. After E. M. Guyer.[12] (*Courtesy American Ceramic Society.*)

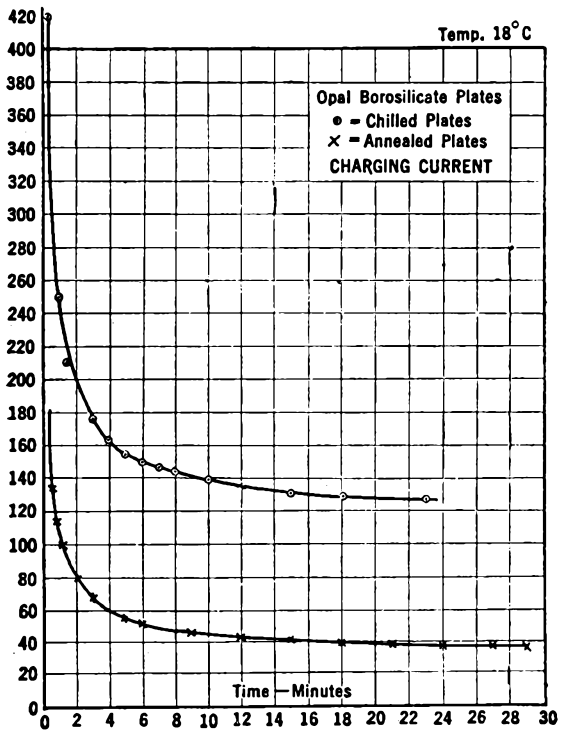

Fig. 5.4. Effect of chilling and subsequent annealing on the charging current in an opal borosilicate glass. After E. M. Guyer.[12] (*Courtesy American Ceramic Society.*)

results. The differences between charge and discharge currents will be constant at different time intervals for completely reversible charging currents, and also represent the true conduction current through the glass. Absorption currents in annealed glass are smaller than those in unannealed glass (Fig. 5.4). An interpretation of anomalous charge and discharge currents in glasses on the basis of their structure has been given by Weyl.[13]

Surface Conductivity

The surface conductivity of glass is partly due to films of water[14] and other contaminations, which are determined by the surrounding

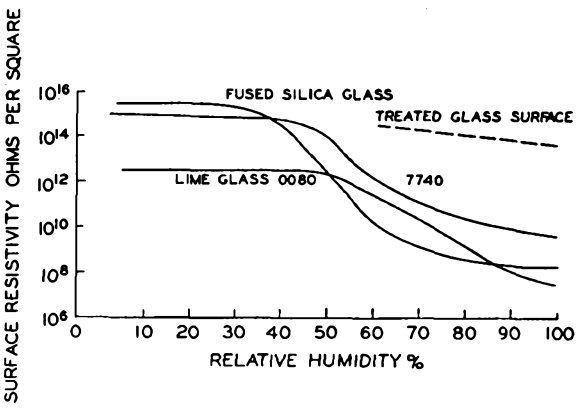

Fig. 5.5. Surface resistivity as a function of relative humidity for fused silica glass, borosilicate electrical glass (Corning No. 7740) and lime glass (Corning No. 0080). After E. M. Guyer.[1] (*Courtesy the Institute of Radio Engineers.*)

atmosphere and the relative humidity prevailing at the time, as well as by temperature and pressure. Different glasses are variously affected by these factors. Fig. 5.5 gives representative plots of surface resistivity for fused silica, "Pyrex" 7740, and soda-lime glass 0080 at different relative humidities at 20°C.[1] The improvement obtainable by surface treatment is also indicated by a dotted line. Such surface treatment may involve outgassing at elevated temperature or the application of nonhygroscopic films, as outlined on p. 110. The effect of glass composition on the resulting surface resistivity is very pronounced, and so far has escaped satisfactory theoretical evaluation. Many attempts have, of course, been made in this direction. Gehlhoff and Thomas[15] were among the first to explore this field systematically. The work of Fulda[16] should also be mentioned. Many other investigators have contributed in this intricate search, and Littleton and Morey's text[11] should be consulted for further data.

The changes in surface conductivity resulting from controlled variations of glass composition are illustrated in Fig. 5.6.[16] Fulda subjected the samples to a heat treatment in the range of 300 to 400°C, cooled them to 25°C in a dry atmosphere, and then took his measurements. The original glass had the composition 0.18 Na_2O, 0.82 SiO_2. The abscissae in Fig. 5.6 indicate how much of the silica in weight per cent was replaced by Na_2O, K_2O, CaO, BaO, PbO, B_2O_3, Al_2O_3, MgO, or ZnO, respectively.

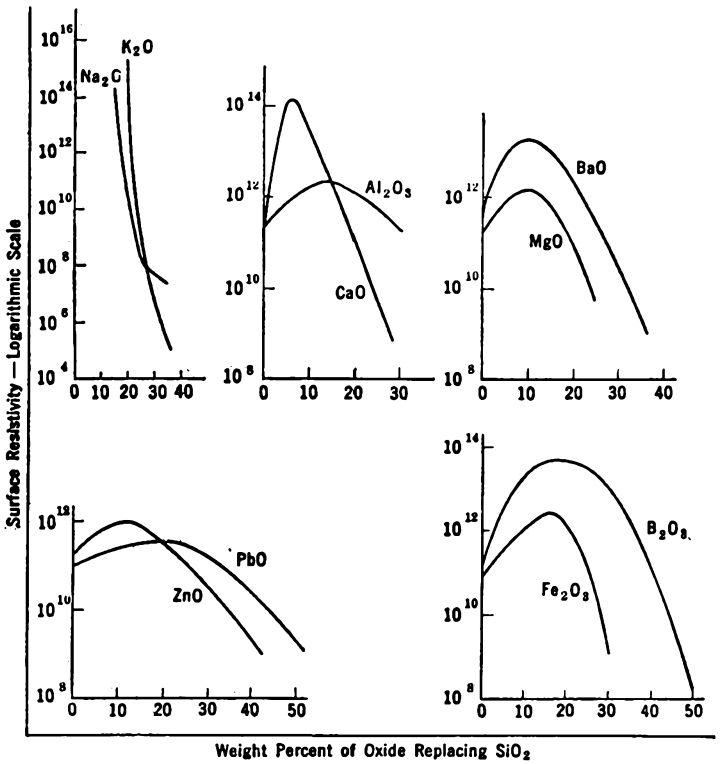

Fig. 5.6. The effect of glass composition on surface resistivity at 25°C and 100% humidity. SiO_2 in the glass of composition 18 Na_2O, 82 SiO_2 is replaced by the indicated weight percentage of other oxides. After M. Fulda.[16]

The same basic glass was investigated by Gehlhoff and Thomas,[15] who plot the temperature at which a reference conductivity, 100×10^{-10} ohm^{-1} cm^{-1}, is reached against the percentage of SiO_2, replaced by the respective oxide MO (Fig. 5.7). Complete plots of conductivity versus temperature are given in Fig. 5.8, according to the same authors. Yager and Morgan[17] have measured the surface leakage of 7740 "Pyrex."

According to an investigation by Green and Blodgett[18] surface conductivity can be imparted to glasses containing sufficiently high contents

of lead, bismuth, or antimony oxides, or combinations of these, by reducing these oxides in hydrogen during heat treatment of several hours' duration. The thickness of the conductive film thus produced on the glass surface is of the order of 0.001 inch, and the color of the treated surface is black. In comparison to conventional metalizing techniques this reduction of oxides mixed into the glass batch permits the production of controlled surface resistivities below those of the bulk metals in question. It is also reported that lead-glass coatings were applied to borosilicate glass as a frit, which was then reduced in hydrogen. Fig. 5.9

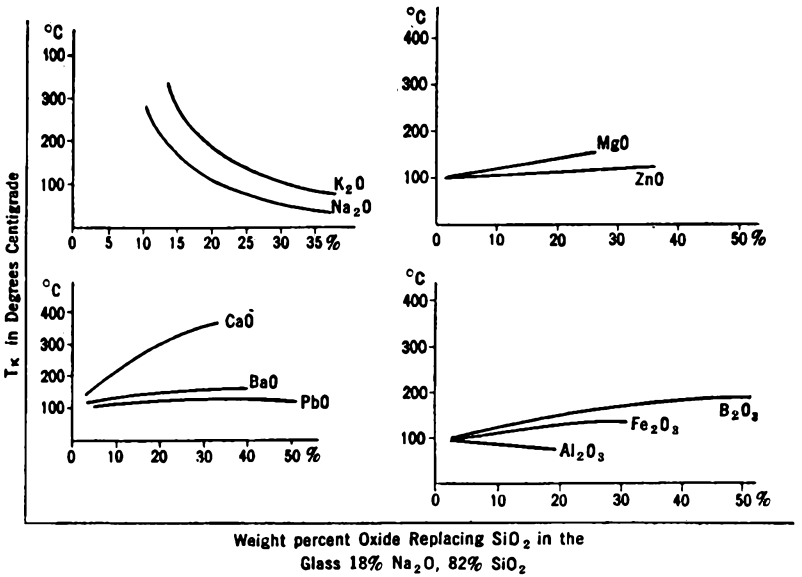

Fig. 5.7. The temperature at which the specific conductivity becomes 10^{-8} mho/cm plotted against the percentage by weight of the indicated oxide replacing SiO_2 in the glass 18 Na_2O, 82 SiO. After G. Gehlhoff and M. Thomas.[15]

gives a representative plot of the minimum surface resistivities (ohms per square) for varying PbO contents.

This research was extended by Dr. Katharine Blodgett during the ensuing years, and her report has just been published.[19]* The investigation was carried out with x-ray shield glass (*XRS*) obtained from the Pittsburgh Plate Glass Company. Its composition is PbO: 0.61; BaO: 0.08; SiO_2: 0.31 per cent by weight. The following conclusions were reached:

* The author is indebted to Dr. H. R. Lillie for bringing this paper to his attention and to Dr. Katharine Blodgett and the General Electric Company for letting him have an advance copy and permitting the summary to be reproduced here.

"The amount of conductivity which can be developed in x-ray shield glass was found to depend on a variety of factors. Samples of this glass were treated in hydrogen at a series of constant temperatures and the resistance measured throughout the run. The resistance was found to diminish with time and approach a limiting low value. At treating temperatures 335°–400°C the limit was at 2000 to 3000 megohms

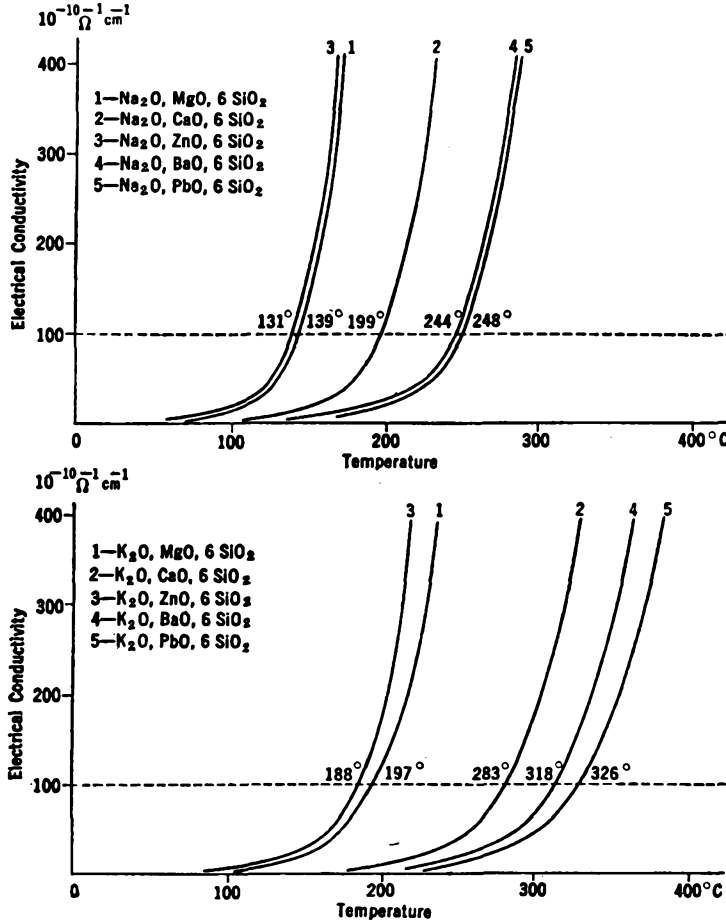

Fig. 5.8. The change in electrical conductivity with temperature of a series of glasses having the general composition Na_2O (or K_2O), MeO, $6SiO_2$. After G. Gehlhoff and M. Thomas.[15]

per square. At higher temperatures the limit increased with temperature until at 520°C the glass had no conductivity after hydrogen treatment, although it was a dense black. It was found that treatment at a low temperature followed by a high temperature developed more conductivity than the low temperature alone. The procedure was worked out of taking a sample from 350° to 520°C at a slow rate, about 2.0°C per minute. This gave a resistance about 1000 megs per square. If the sample was held at 350°C for 16 to 64 hours preceding this procedure, the resistance was somewhat less.

"The conductivity was found to be located in a layer at the surface having a thickness 50 to 100 Å. The specific resistance could then be calculated and was found to be 800 ohm-cm or more. The resistance decreased with increasing temperature, corresponding to bk* = 0.065 ev at 25° to 100°C and bk = 0.11 ev at 335° to 440°C. The ratio of hot to cold resistance was found to be independent of the particular value of cold resistance used for the test. Therefore, it is believed that the conducting substance is a semiconductor in which the centers are reduced lead atoms, presumably atomically dispersed. This substance provides an example of semi-conductivity in an amorphous material. The density of the lead atoms which act as centers can be

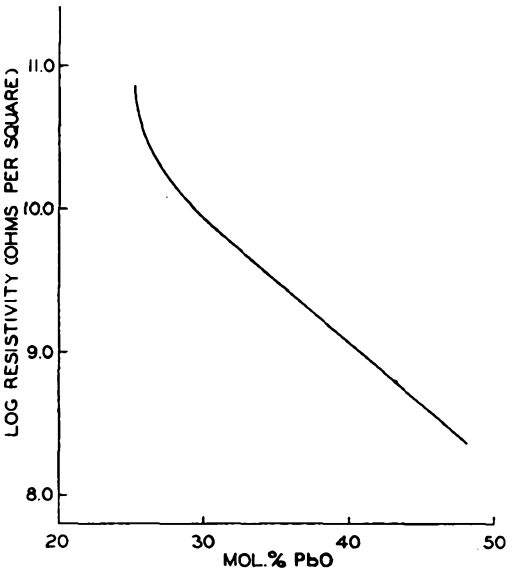

Fig. 5.9. Variation of minimum surface resistivities of reduced lead glasses with varying PbO contents. After R. L. Green and K. B. Blodgett.[18] (*Courtesy the American Ceramic Society.*)

calculated from the specific conductivity, and is of the order of magnitude of one-millionth of all the lead atoms in the glass. The remainder of the lead gathers into aggregates which give the glass a black color but make no contribution to the conductivity. It is believed that the dispersed atoms are those which for some reason become locked in a position in the lead silicate structure from which they are unable to escape.

"The problem of developing a designated value of resistance was investigated. The method that proved the most satisfactory was that of treating the sample in hydrogen till the resistance was considerably less than the desired value, then bringing the resistance up by treatment in hot water or in hot damp air. The increase is attributed to a reoxidation of the lead that was reduced in hydrogen. The resistance increases continuously in hot water vapor at a rate which depends on the type of hydrogen treatment that the sample had been given. The initial increase is rapid until the layer that lies nearest the surface has been oxidized, then slows down as the

* bk is the activation energy required to move an electron from the impurity level to the conduction band.

oxidation proceeds to deeper layers. A study was made of methods that can be employed to make a sample resistant to oxidation in the atmosphere.

"Tests were made at high voltages using a porcelain ring coated with *XRS* glass on the inner wall. The coating did not fail at voltages up to 150 kv across 1.5 inches in a high vacuum. The method of applying a coating of *XRS* glass to porcelain is described."

Surface conductivity on glass can be markedly reduced, particularly in atmospheres of high humidity, by the application of certain organic chlorosilanes (e.g., dimethyldichlorosilane $(CH_3)_2SiCl_2$). Films of these materials, in a thickness of the order of 1000 molecular layers, react very rapidly with the adsorbed water film on the glass. Hydrochloric acid gas is evolved, and a layer of dimethylsiloxane groups is left behind which presents a layer of methyl groups toward the outer free surface.[2]

Electrically conductive glass has been recently introduced by the Libbey-Owens-Ford Glass Company under the trade name "Electrapane," by the Pittsburgh Plate Glass Company under "Nesa", and by Corning under "E-C Glass." At the surface "Electrapane" has a thin coating (0.00002 inch) of stannic oxide, which is applied at elevated temperature near the softening point of the glass. As it withstands weather conditions, it may be used for ice-free windshields on motor cars and in airplane cockpits. The resistivity is of the order of 100 ohms per square, and a current is passed through the film from strip electrodes at opposite edges. Temperatures may rise to about 230°C before the resistivity of the film changes appreciably.[20] "E-C Glass" has a maximum operating temperature of 350°C. Its temperature coefficient of resistivity ranges from +0.05 to −0.05 per cent, and the resistivity is about 20 times that of "Nichrome." SnO is again the main constituent of the coating, which is applied in a very thin film. Radiant-heating panels are in commercial production. It is an interesting fact that most of the heat is radiated from the uncoated side of the panel because the glass body is an excellent absorber at the operating temperature and acts as a black body.*

Glass Electrolysis

The problem of glass electrolysis at elevated temperatures is one of particular concern in tube design. Whenever the operating temperatures of glass parts containing sealed-in current leads are elevated sufficiently to permit migration of sodium ions under the influence of impressed voltages, discoloration of the glass and ultimate fracture will result. This difficulty has been encountered with rectifier tubes in particular, and was studied in detail by J. Gallup[21] and more recently by J. Peysson.[22]

* Data on "E-C Glass" from a lecture by Dr. R. H. Dalton of Corning Glass Works at Iowa City (5/17/50).

The general mechanism of glass electrolysis with glass-embedded current leads has been known for a considerable time, and was studied by Becquerel and Thomson as early as 1854 and 1875.[23,24] It may be summarized as follows:

(1) Positive sodium ions migrate toward the electrode which is at the most negative potential (i.e., the "effective cathode"); they migrate through the glass under the influence of the electrical field impressed by the sealed-in electrodes.

(2) At the "effective cathode" metallic sodium will be released and accumulated, whereas the glass layers near the "effective anode" will be depleted in sodium, resulting in a poorly conducting silica-rich glass.

(3) Oxygen is released at the "effective anode" and hydrogen at the "effective cathode." It is known that all commercial glasses contain minor amounts of CO_2, SO_3, and H_2O, which, as the anions CO_3^{--}, SO_4^{--} and OH^-, participate in the glass structure. These gases can be reduced electrolytically to CO, SO_2, and H_2, reactions which are more likely to occur than the reduction of Na^+ or Ca^{++}. Passing a current through a soda-lime glass, therefore, reduces its gas content.[25] The same authors point out that molybdenum or tungsten-lead seals may become overoxidized by virtue of the water content of the glass, and porous and leaky seals thus result.

These primary effects may lead to the following observations:

(1) The vicinity of the "effective cathode" lead will develop a dark discoloration because of the reduction of lead oxide to lead by the released sodium. In the absence of PbO the colloidal dispersion of Na in itself will give a brown or blue appearance. "Dumet" leads are likely to become light-colored because of the reduction of cuprous oxide.

(2) The "Dumet" lead representing the "effective anode" will, by the same token, take on a darker color because of the formation of higher copper oxide.

(3) Gas bubbles will appear at the electrodes and be released into the tube, spoiling the vacuum. Spectrometric analysis of the gas content by Gallup, using 814 KW glass stems, disclosed the presence of the following gases in order of decreasing amounts: H_2, H_2O, O_2, CO, CO_2, and N_2.

(4) The change in composition of the glass near the electrodes will set up considerable strains leading to fracture.

It is important to realize that the anode lead of a rectifier tube will act as the effective cathode during the inverse voltage cycle, and that the magnitude of the inverse voltage frequently exceeds the operating forward anode voltage by a large factor. Electrolysis effects can also be present when symmetrical A.C. voltages are applied since surface effects at the leads often cause a preferred conduction in one direction. Gallup[21] also describes in particular an effect which shows that electrolysis of stems

can occur between a current lead and the surface of the glass stem when the latter is exposed to bombardment by stray electrons, thus leading to the creation of a virtual cathode. This condition was found responsible for the appearance of longitudinal cracks along the filament leads of the rectifier tube.

Dielectric Properties

Like most of the common insulators, glass is a dielectric, which passes a displacement current on application of intermittent or alternating electrical fields. In an ideal dielectric the displacement current I_c is exactly 90 electrical degrees out of phase with the applied voltage, and thus does not lead to a consumption of power. Physical dielectrics never fulfill this condition, and the amount of power dissipated is given by the expression:

$$W = E \times I \times \cos \theta \text{ (watts)} \tag{5.3}$$

E is the effective value of the alternating voltage $E = E_o \cos wt$ and I the resulting current leading the voltage vector by the phase angle θ. Equation 3 can be written in terms of capacity C (in farads), dielectric constant K, and power factor $\tan \delta$ to read

$$W = \omega C E^2 \times \tan \delta \text{ (watts)} \tag{5.4}$$

or

$$W' = \omega F^2 \times K \times \tan \delta \times 0.088442 \times 10^{-12} \frac{\text{watts}}{\text{cm}^3} \tag{5.5}$$

$$W'' = 0.555 \times (\text{LF}) \times f(\text{MC}) \times F^2 \left(\frac{\text{kv}}{\text{cm}}\right) \frac{\text{watts}}{\text{cm}^3} \tag{5.6}$$

which gives the energy dissipated per unit volume when the field $F = E/d$ is applied across the dielectric of thickness d and cross-section A.* The loss in the dielectric is proportional to frequency, field strength, dielectric constant, and power factor. The product $K \times \tan \delta$ is referred to as the loss-factor of the dielectric, and it determines the quality of a dielectric for most applications. As the energy loss appears in the dielectric in the form of heat, the loss factor should be as low as possible. In cases where a high capacity is not the primary objective—and this is rarely the case in tube engineering—a low K and low $\tan \delta$ should be sought.

The "dielectric strength" is the voltage at which the dielectric is punctured, and it is, therefore, identical with "breakdown voltage." This quantity is usually given in kv/cm or kv/mil, representing, in most cases, an extrapolation from the measured value. Because of the difficulties encountered in measuring technique and the many variables that occur, it is very hazardous to compare the test results obtained by different investigators. In general, it is found that the measured dielectric strength in kv/mil decreases with increased thickness of the test specimen.

* For a detailed analysis of the loss in dielectrics see Refs. 10, 11, 26, and 27.

These general remarks on dielectrics apply particularly to glass, for which specific data will now be given. By changing the composition of glass the dielectric constant K and the power factor tan δ can be separately altered. This is apparent from Tables 1.2 and 1.3. Corning Glass 7070 is the lowest-loss glass reported as it is a low-alkali, borosilicate glass which combines low expansion and high surface stability with low K and low tan δ. A high content of heavy metals in conjunction with low alkali content gives glasses with high K and low tan δ. The dielectric strength of glass is so much higher than that of other substances, including air and oils, that in measuring breakdown on glass samples one is likely to measure the breakdown of the surrounding medium, or the corona resistance of glass in the presence of bombardment with ions from localized discharges taking place in the weaker gaseous or liquid medium.[1] Moon and Norcross[28] measured breakdown on glass samples, 8 mils thick, at room temperature and at 300°C, and found the values tabulated in Table 5.1 for D.C. tests. These data are indicative of the two types of breakdown, distinguished as "disruptive breakdown" and "thermal breakdown."

TABLE 5.1. ELECTRIC BREAKDOWN ON GLASS SAMPLES 8 MILS THICK OBSERVED BY MOON AND NORCROSS[28]

Glass Type	Dielectric Strength (Kv/cm)	
	At 20°C	At 300°C
Fused silica glass	5,000	560
Borosilicate glass	4,800	200
Lead glass	3,100	102
Lime glass	4,500	32

According to the theory of von Hippel,[29] disruptive breakdown results directly from an electrical overstress of the dielectric material, without perceptible temperature rise, and is caused by electronic ionization by collision within the molecular structure of the material. Disruptive breakdown is roughly proportional to the thickness of the sample under test. Thermal breakdown is caused by the accumulative overheating of the test specimen, and is largely determined by the electrical and thermal conductivities of the material and the variation of these properties with temperature. There is no sharp transition from disruptive breakdown to thermal breakdown. For increasing thickness a limiting condition is reached where a further increase in thickness will not result in higher thermal breakdown. Duration of application of voltage, wave form, and field distribution (edge effects) all have an important bearing on the test results obtained.[30]

Fig. 5.10 shows breakdown voltage for lime glass as a function of temperature for D.C. voltage application and 435 KC A.C.[1] The same reference gives the variation of power factor (P.F.), loss factor (L.F.), and dielectric constant K as a function of frequency, (Fig. 5.11) and the variation of P.F. and L.F. as a function of temperature for a number of Corning glasses (Fig. 5.12). Fig. 5.13 shows variation of P.F. with

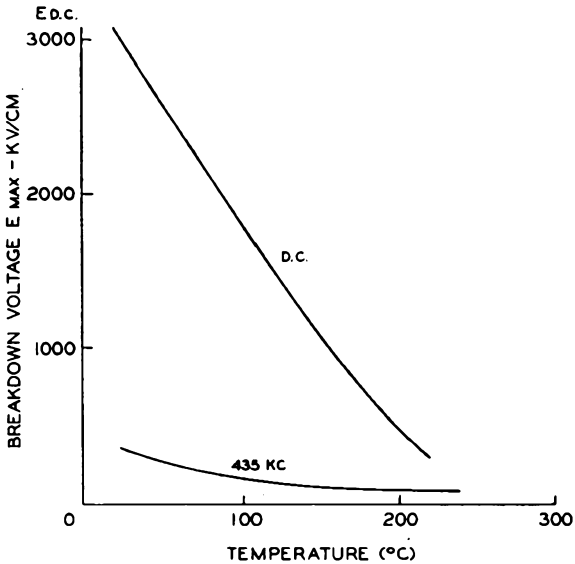

Fig. 5.10. Breakdown voltage as a function of temperature for direct current and for 435 KC alternating current. After E. M. Guyer.[1] (*Courtesy the Institute of Radio Engineers.*)

temperature and Fig. 5.14 variation of K with temperature for various frequencies, according to Strutt.[31] His glasses are numbered 1–5:

1	Borosilicate, similar to "Pyrex" 7740
2, 3, 4	Soda silicate, 70 per cent SiO_2, 16 per cent Na_2O
5	Heavy lead glass

Like other investigators, he finds that

$$\tan \delta = Ae^{\alpha T}$$

in the temperature range (30–300°C) and frequency range (50–10^5 cycles/sec), where α decreases with increasing temperature. Stevels[32] investigates the power factor of glasses as a function of their composition, and Meunier[33] reports on the electrical properties of glass used for the construction of electron tubes in France.

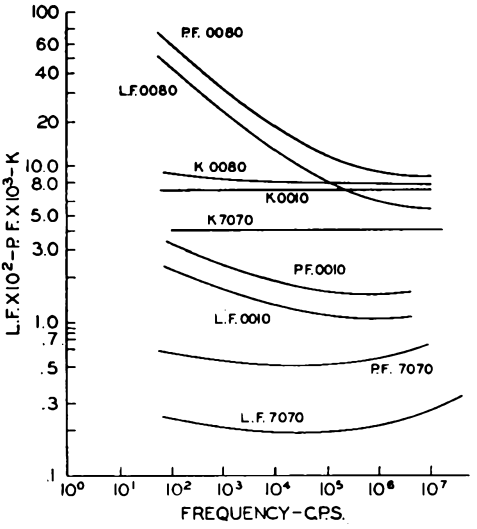

Fig. 5.11. Variation of power factor (P.F.), loss factor (L.F.) and dielectric constant (K) with frequency for borosilicate glass (Corning No. 7070), lead glass (Corning No. 0010), and lime glass (Corning No. 0080). After E. M. Guyer.[1] (*Courtesy the Institute of Radio Engineers.*)

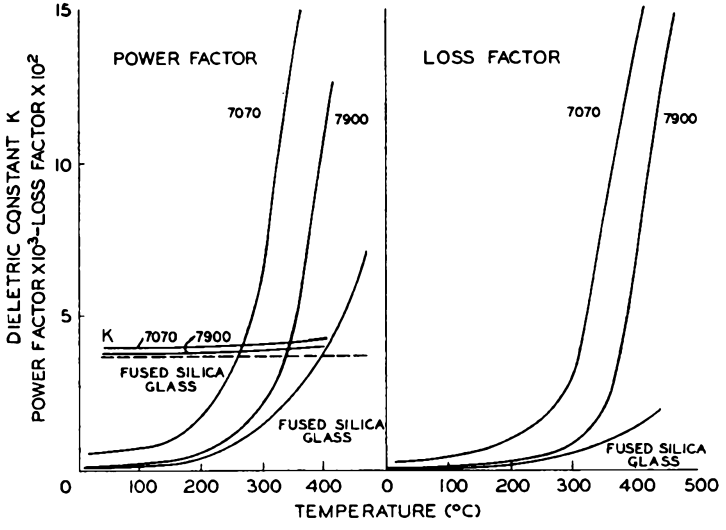

Fig. 5.12. Power factor and loss factor as functions of temperature for fused silica glass, borosilicate glass (Corning No. 7070), and 96% silica glass (Corning No. 7900). After E. M. Guyer.[1] (*Courtesy the Institute of Radio Engineers.*)

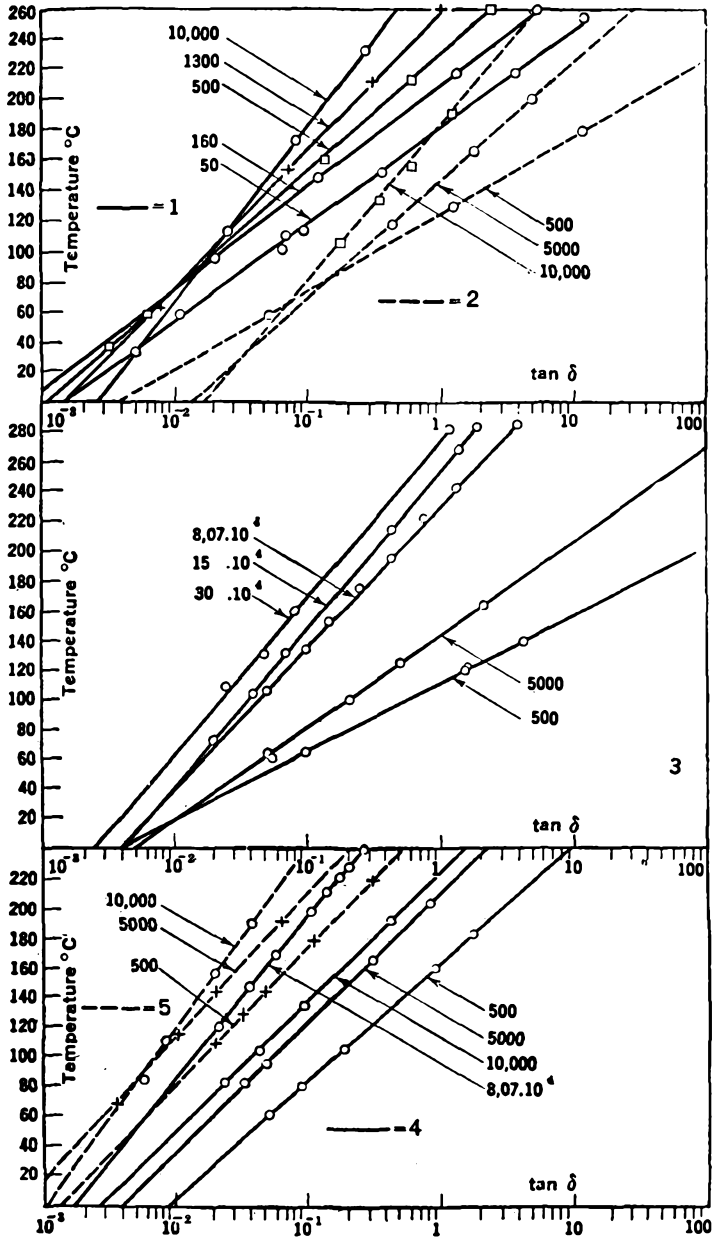

Fig. 5.13. Relation between temperature and power factor at various frequencies. After M. J. O. Strutt.[31]

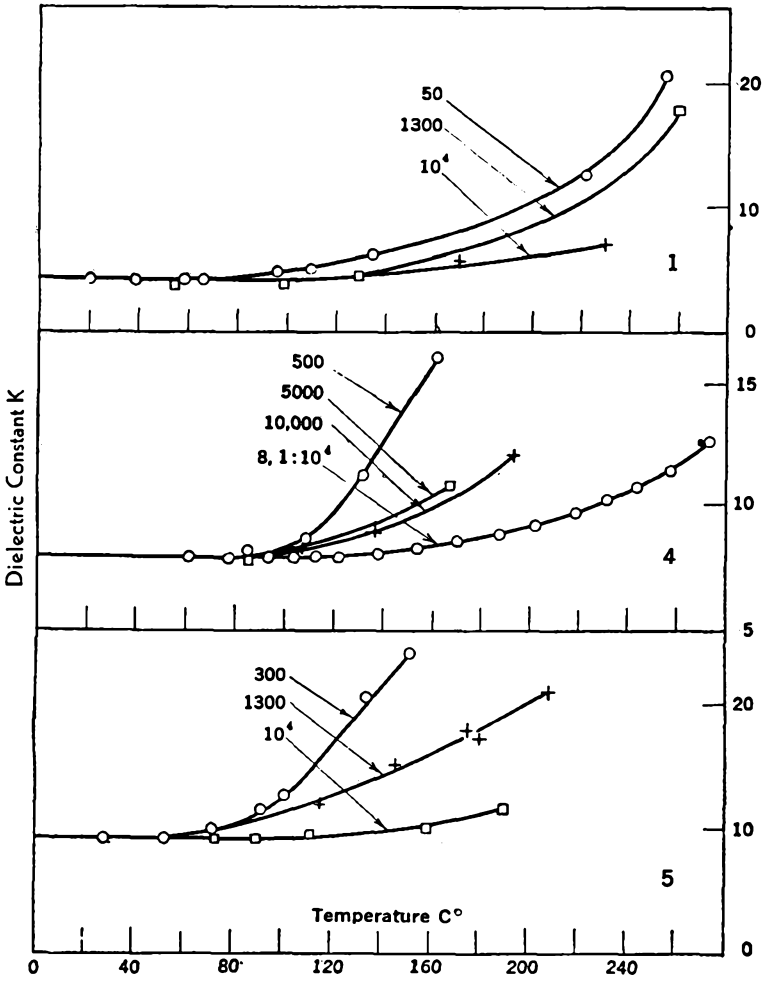

Fig. 5.14. Dependence of dielectric constant, K, on temperature at various frequencies. After M. J. O. Strutt.[31]

REFERENCES

1. Guyer, E. M., "Electrical Glass," *Proc. I.R.E.*, **32**, 743–750 (1944).
2. Stanworth, J. E., "Physical Properties of Glass," Oxford, Clarendon Press, 1950.
3. Burt, R. C., "Sodium by Electrolysis through Glass," *J. Opt. Soc. Am.*, **11**, 87–91 (1925).
4. Pike, E. W., "The Electrolysis of Sodium through 'Pyrex' Glass," *Rev. Sci. Inst.*, **4**, 687 (1933).
5. Rasch, E., and Hinrichsen, F. W., "On a Relation Between Electrical Conductivity and Temperature" (In German), *Z. Elektrochemie*, **14**, 41–46 (1908).
6. Stevels, J. M., "Progress in the Theory of the Physical Properties of Glass," New York, Elsevier Publishing Co., Inc., 1948.
7. Kirby, P. L., "Electrical Conduction in Glass," *Brit. J. Appl. Phys.*, **1**, 193–202 (1950).

8. Whitehead, J. B., "Lectures on Dielectric Theory and Insulation," New York, McGraw-Hill Book Co., Inc., 1927.
9. Morey, G. W., "The Properties of Glass," New York, Reinhold Publishing Corp., 1938.
10. Murphy, E. J., and Morgan, S. O., "The Dielectric Properties of Insulating Materials," Pt. 1. *Bell Syst. Tech. J.*, **16**, 493–512 (1937); *Ibid.*, Pt. 2, **17**, 640–669 (1938).
11. Littleton, J. T., and Morey, G. W., "The Electrical Properties of Glass," New York, John Wiley and Sons, Inc., 1933.
12. Guyer, E. M., "Electrical Behavior of Glass at Room Temperature," *J. Am. Ceram. Soc.*, **16**, 607–618 (1933).
13. Weyl, W. A., "The Dielectric Properties of Glass and Their Structural Interpretation," *J. Soc. Glass Tech.*, **33**, 153, 220–238 (1949).
14. Veith, H., "Simple Method for the Determination of the Water Film Adhering to Glass" (In German), *Z. Phys. Chem.*, **193**, 378–385 (1944).
15. Gehlhoff, G., and Thomas, M., "The Physical Properties of Glasses as a Function of their Composition" (In German), *Z. Tech. Phys.*, **6**, 544–554 (1925).
16. Fulda, M., *Sprechsaal*, **60**, 769, 789, 810, 831 (1927).
17. Yager, W. A., and Morgan, S. O., "Surface Leakage of 'Pyrex' Glass," *J. Phys. Chem.* **35**, 2026–2042 (1931).
18. Green, R. L., and Blodgett, K. B., "Electrically Conducting Glasses," *J. Am. Ceram. Soc.*, **31**, 89–100 (1948).
19. Blodgett, K. B., "Surface Conductivity of Lead-Silicate Glass After Hydrogen Treatment," *J. Am. Ceram. Soc.* 34, 14–27 (1951).
20. "Electrically Conducting Glass," *Mater. and Meth.*, 70–71 (Aug., 1949).
21. Gallup, J., "Electrolysis Phenomena in Soft-Glass Stems of Rectifier Tubes," *J. Am. Ceram. Soc.*, **29**, 277–281 (1946).
22. Peysson, J., "Electrolysis Phenomena in Glass" (In French), *Annales Radioél.*, **3**, 107–114 (1948).
23. Becquerel, A. C., "Note on Production of Thermal Electricity" (In French), *Compt. Rend.*, **38**, 905 (1854).
24. Thomson, W., "Electrolytic Conduction in Solids. First Example, Hot Glass," *Proc. Roy. Soc.*, **23**, 468 (1875).
25. Rindone, G. E., Marboe, E. C., and Weyl, W. A., "Oxidation and Reduction of Glasses by Electrolysis," *J. Am. Ceram. Soc.*, **30**, 314–319 (1947).
26. Hoch, E. T., "Power Losses in Insulating Materials," *Bell Syst. Tech. J.*, **1**, 110 (1922).
27. "Methods of Test for Power Factor and Dielectric Constant of Electrical Insulating Materials," ASTM Standards, Pt. 3-B, D150-47T.
28. Moon, P. H., and Norcross, A. S., "Three Regions of Dielectric Breakdown," *El. Eng.*, **49**, 755–762 (1930).
29. Von Hippel, A., "Electric Breakdown of Solid and Liquid Insulators," *J. Appl. Phys.*, 815 (1937).
30. Shand, E. B., "The Dielectric Strength of Glass—An Engineering Viewpoint," *El. Eng. Transact.* **60**, 814–818 (1941).
31. Strutt, M. J. O., "Dielectric Properties of Various Glasses as a Function of Frequency and Temperature" (*In German*), *Arch. Elektro tech.*, **25**, 715–722 (1931).
32. Stevels, J. M., "Some Experiments and Theories on the Power Factor of Glasses as a Function of Their Composition," *Philips Res. Rep.*, **5**, 1 (Feb. 1950).
33. Meunier, P., "Contribution to the Study of Electrical Properties of Glass Used for the Construction of Electron Tubes" (In French), *Annales Radioel*, **4**, 54–67 (1949).

CHAPTER 6

GLASS IN RADIATION FIELDS

Transmission of radiations of various frequencies by glass is of practical importance in many electronic applications. This statement hardly needs elaboration when we remind ourselves that cm-wave radiation, heat, visible and ultraviolet light, and x-rays are forms of energy which are commonly generated in tubes where at least part of the envelope is made of glass. The amount of "useful energy" absorbed by the envelope of a generator will be lost for external use, and thus detracts from the efficiency of the device. On the other hand, where "useless energy" is to be dissipated through the glass envelope, the amount absorbed will limit the operating level because of the temperature rise of the envelope. Some discretion is necessary, therefore, in choosing the type of glass for a particular application. The effect of glass composition on transmittance in the U.V. visible and infrared region of the spectrum has been studied by many investigators. One of the first systematic researches covering this whole range is that by Fritz-Schmidt, Gehlhoff, and Thomas,[1] where, apart from original contributions, a summary of their work published prior to 1930 can be found.

Let us turn first to the study of heat absorption by various glasses, as this is probably of prime interest in conventional tube design. The part of the spectrum of electromagnetic radiation with which the term "heat" is associated is known as the infrared region. It begins at a wave length of 0.75 μ, where the visible spectrum ends, and extends to 350 μ; this is the long wave limit up to which conventional heat-radiation methods have been applied for detecting the radiation. This extended range of the infrared spectrum is subdivided into three regions:

very near infrared:	0.75 to 2.5 μ
near infrared:	2.5 to 25 μ
far infrared:	25 to 300 μ

The microwave region at 1 cm (10,000 μ) is also considered as part of the infrared although a different instrumentation is here required.[2]

While radiation throughout the electromagnetic spectrum is inherently of the same physical nature, as the name of the spectrum implies, the mechanism by which emission and absorption of the radiant energy take place is different for different regions. It is concerned with molecular

and atomic vibrations in the infrared and with electronic oscillations in the visible range and adjacent regions toward a shorter and shorter wave length (i.e., the ultraviolet, x-rays, γ-rays and cosmic rays), where, in that order, electrons of different levels in the atomic structure and finally nuclear reactions are involved. Different materials show distinct bands of selective absorption in the infrared region, and their behavior can be quantitatively correlated with specific molecular species of which

TABLE 6.1. COEFFICIENTS OF TRANSPARENCY IN THE INFRARED REGION FOR VARIOUS GLASSES*

Wavelength (μ)	0.7	1.1	1.7	2.3	2.7	3.1
Crown, borate	1	0.55	0.21	0.025	0.04	
Boro-silicate		.74	.61	.33	.034	0.021
Flint, light	1	.91	.82	.45	.083	.019
Flint, heavy	1	1	1	1	.45	.019

* Handbook of Chemistry and Physics, 1949, p 2288.

the material is composed. The technique of infrared spectrometry has become of great importance in industry.

Table 6.1 gives coefficients of transparency in the infrared for various types of glasses at normal incidence for 1 mm thickness of the glass plate. From this it is apparent that glasses in general do not transmit radiation to any degree beyond 2.5 μ. For specially prepared glasses, transmission can be extended to 5 μ. The relative emission of a black body in the infrared at 2000°K is shown in Table 6.2,[2,3] which indicates the intensity distribution of heat radiation at that temperature. Fig. 6.1 gives a

TABLE 6.2. THE RELATIVE EMISSION IN THE INFRARED BY A BLACK BODY AT 2000°K*

Wavelength in Microns	Relative Emission of Black Body at 2000°K
1.44	1
2	8×10^{-1}
5	9×10^{-2}
10	9×10^{-3}
50	2×10^{-5}
100	1×10^{-6}
200	8×10^{-8}

* After Eucken-Wolf (Ref. 3).

typical black-body radiation curve for $T = 5000°K$, according to Planck's radiation law:

$$E_\lambda = \frac{C_1 \lambda^{-5}}{\epsilon^{C_2/\lambda T} - 1} \tag{6.1}$$

where E_λ = total radiation in ergs per second per cm^2 per mμ
λ = wave length in mμ
T = temperature in degrees K
$C_1 = 3.703 \times 10^{23}$; $C_2 = 1.433 \times 10^7$
$\epsilon = 2.71828$

Fig. 6.2 gives black-body radiation curves for various absolute temperatures on a logarithmic scale, with units chosen according to Equ. 6.1.[4] With the aid of these data the temperature rise of a glass envelope due to the absorption of heat from a radiating hot anode or filament within could be calculated, provided that its thermal emissivity and temperature were known. The accurate determination of these quantities is often difficult and available data unreliable. A safe working range is a dissipation of 2.5 watt/cm^2 for a glass thickness of $\frac{1}{16}$ inch in quiet air, or about 15 watts/in^2.*

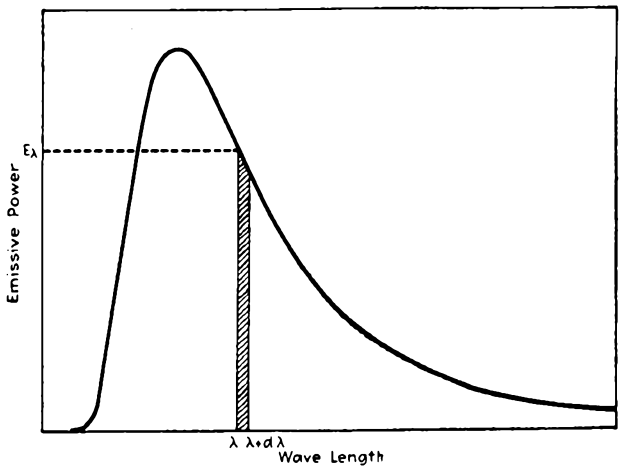

Fig. 6.1. A typical black-body radiation curve. (*By permission from "Principles of Optics" by A. C. Hardy and F. H. Perrin. Copyright, 1932. McGraw-Hill Book Company, Inc.*)

The transmittance of near-infrared energy by binary glasses was studied by Florence *et al.*,[7–8] and their results may be found in Fig. 6.3 (a-c), where no corrections have been made for reflectance. The composition of their experimentally prepared glasses is given in Table 6.3. It is evident that lithium-silicate glass has a higher transmittance for infrared energy than any of the sodium-silicate glasses. From earlier investigations by the Russian scientist, Gerlovin, glasses with a high lead oxide (PbO) content have been known for their great transmission of infrared. Florence shows that increasing the percentage of PbO in lead-silicate glass does not increase the transmittance of infrared for all

* A. H. Canada[5] has described a radiation slide rule, which permits conversion of energy units at different temperatures, location of the wave length at which a black body radiates the maximum of energy, the percentage of the total energy radiated below λ_m, and other calculations. It is available on varnished card stock under Code GEN-15 for 75 cents from General Electric Co., 1 River Road, Schenectady, N.Y. A more elaborate radiation slide rule has been described by Makowski.[6]

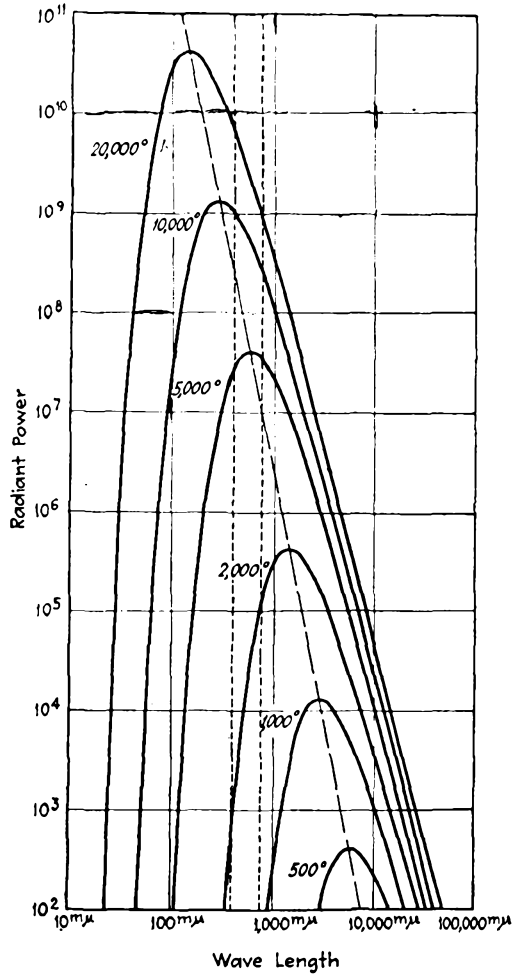

Fig. 6.2. Black-body radiation curves for various absolute temperatures plotted on a logarithmic scale. The power is expressed in ergs per second per square centimeter per millimicron. The dotted lines define the visible region; the broken line is the locus of the maximum of the radiation curves. These curves are similar in their dimensions and orientation and differ only in their positions along the locus of the maximum. The curve for 5000°K is plotted on a natural scale in Fig. 6.1. (*By permission from "Principles of Optics" by A. C. Hardy and F. H. Perrin. Copyright 1932. McGraw-Hill Book Company, Inc.*)

wave lengths. A glass containing 71 per cent PbO and 29 per cent SiO_2 gives the maximum transmittance in the wave-length range of 0.8 to about 2.7 μ. Increasing the quantity of PbO above 71 per cent increases the transmittance from 3.25 to about 5 microns, but lowers it from 0.8 to 2.7 μ. Their greater transmittance for heat radiation coupled with

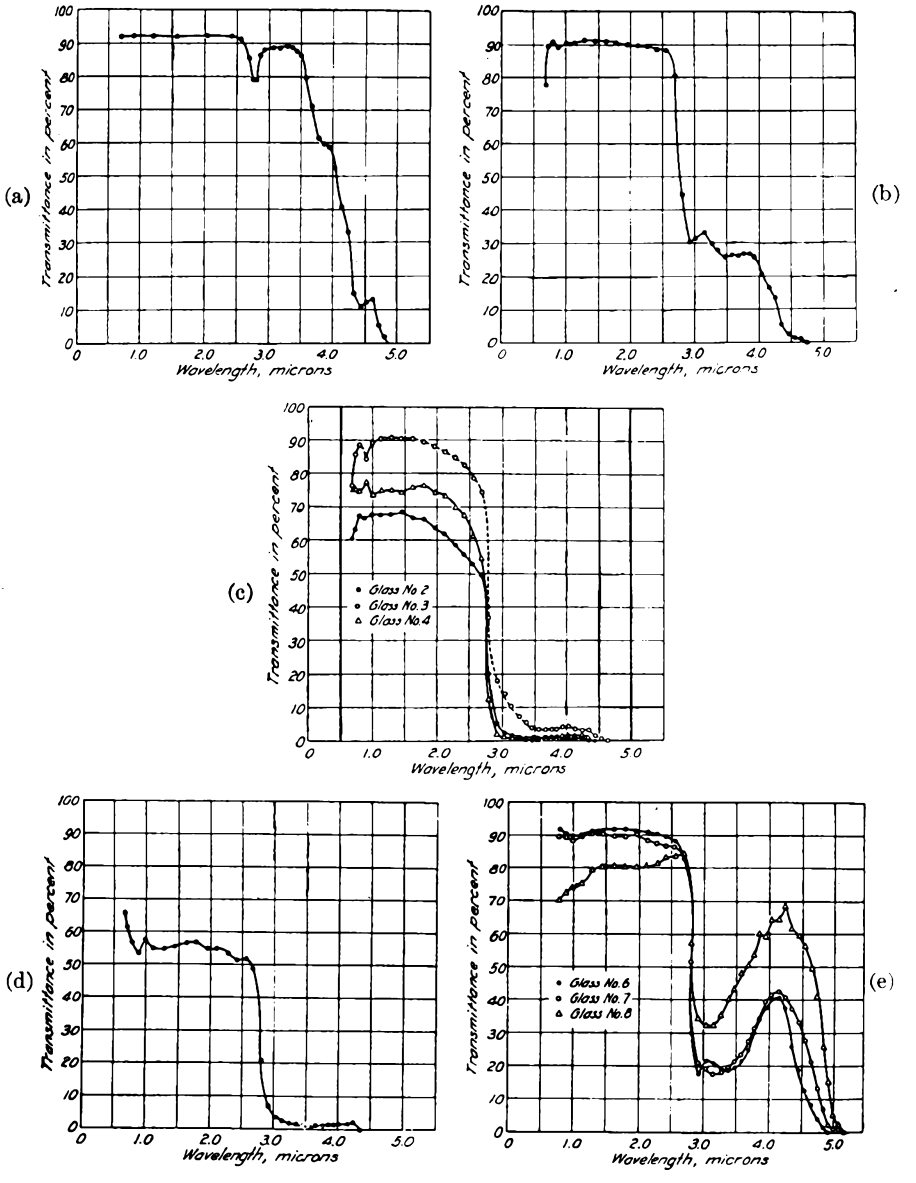

Fig. 6.3. Transmittance of near Infra-red energy by binary glasses. (a) By fused silica sample (2.85 mm thick); (b) by lithium-silicate glass No. 1 (5.74 mm thick); (c) By sodium silicate glasses Nos. 2, 3 and 4 (6.21, 4.84 and 4.67 mm thick respectively); (d) By potassium silicate glass No. 5 (4.45 mm thick); (e) by lead silicate glasses Nos. 6, 7 and 8 (3.00, 3.21 and 2.81 mm thick respectively). After J. M. Florence, F. W. Glaze, G. H. Hahner and R. Stair,[7] (*Courtesy the American Ceramic Society.*)

TABLE 6.3. GLASS COMPOSITIONS*

Glass No.	SiO_2		Li_2O		Na_2O		K_2O		PbO		Fe_2O_3	
	Wt. (%)	Mol. (%)	Wt. (%)	Mol. (%)	Wt. (%)	Mol. (%)	Wt. (%)	Mol. (%)	Wt. (%)	Mol. (%)	Wt. (%)	Mol. (%)
1	80.72	67.58	19.26	32.41							0.017	0.005
2	78.01	78.71			21.97	21.28					.015	.006
3	74.60	75.21			25.38	24.79					.015	.006
4	68.29	68.97			31.70	31.02					.014	.006
5	71.37	79.64					28.61	20.35			.016	.007
6	29.13	60.44							70.86	39.55	.009	.01
7	20.08	48.28							79.91	51.70	.008	.01
8	11.91	33.44							88.08	66.54	.007	.02

* Studied by Florence, *et al.*, Ref. 7.

their absorption for x-rays make high lead-oxide glasses (30 per cent) particularly suitable for envelopes of power tubes as pointed out by Bell, Davies, and Gossling of the G.E.C. Research Laboratories at Wembley.[9] To obviate the danger of electrolysis half of the Na_2O content was replaced by K_2O and glass-to-metal seals up to 5 inches in diameter were used on a production basis with good results.

The limit of transmission in the infrared is largely determined by the presence of FeO, which shows strong absorption at about 1 μ. "Aklo" heat-absorbing glass, manufactured by Corning Glass Works, contains a substantial amount of FeO (Fig. 6.4). According to Zsigmondy[11] most common glasses of various compositions, but free of FeO, have a trans-

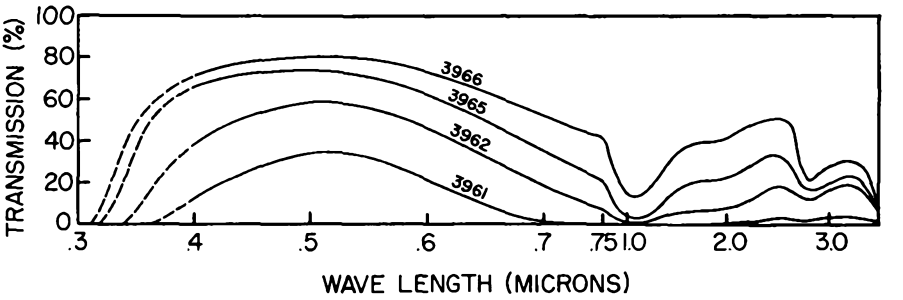

Fig. 6.4. "Aklo" heat-absorbing glasses.[10] The three-digit code numbers shown in earlier publications, such as Ref. 10, are obsolete. They were 395 to 398 and the last digit indicated the shade or darkness. When the codes were changed to four-digit numbers, the Aklo-glasses were all designated by 396 with the following fourth digit signifying the approximate thickness ratios required to give the same absorption. Thus, 6 units of thickness of the light shade 3966 will absorb about like one unit of thickness of the dark shade 3961. (*Courtesy Corning Glass Works, Corning, N.Y.*)

mittance for heat radiation equal to 60 per cent for 7 mm thickness; however, this value is reduced to 0.75 per cent when as little as 1 per cent of FeO is present. Fig. 6.5 shows the transmission of 7740 "Pyrex" glass through the useful range of the spectrum from U.V. to infrared, and Fig. 6.6 gives infrared transmission for a variety of Corning glasses.

A recent investigation by Frerichs[13] has led to the discovery of new optical glasses, which are transparent in the near infrared up to 12 μ. They are binary sulfide glasses, represented by arsenic trisulfide (As_2S_3), which forms a perfectly clear, stable red glass of remarkable optical properties. The glass softens at 300°C, distills without decomposition at 500°C, and is nonhygroscopic.

The selective reflection of infrared radiation by glasses also has been the subject of extensive investigations.[14–17] It is of practical interest in the field of spectroscopy and for the construction of photoelectric detectors and image tubes for military applications. Anderson[18] has recently

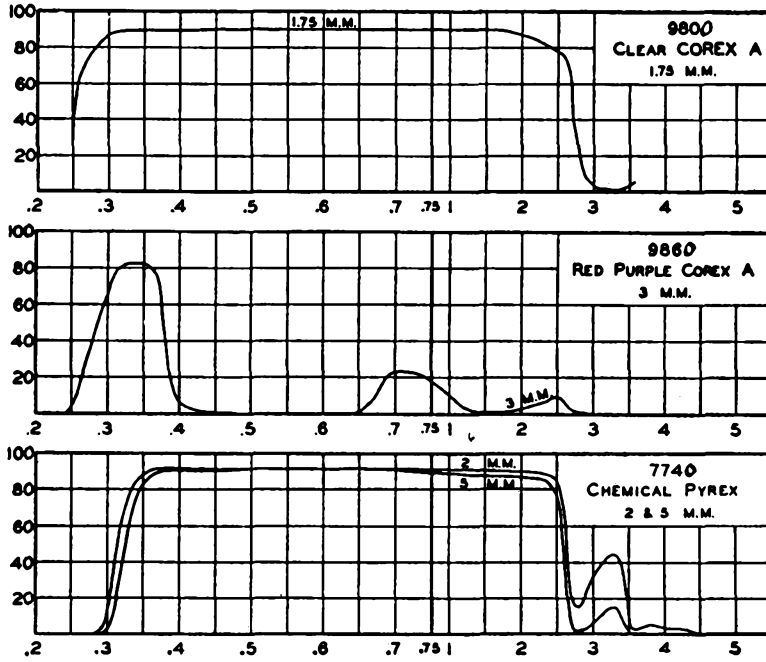

Fig. 6.5. Transmission curves of Corex A glass and of Pyrex brand chemical resistant glass. (*Courtesy Corning Glass Works.*)

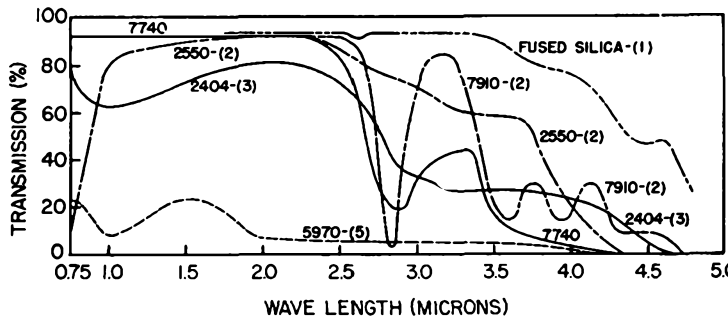

Fig. 6.6. Spectrophotometric curves for the optical transmission of certain Corning glasses. The number in parentheses is the glass thickness in millimeters. After C. J. Phillips.[10] (*Courtesy Pittman Publishing Company.*)

reported on the interpretation of infrared reflection spectra of various glasses in terms of their composition and structure. Fig. 6.7 is reproduced from his paper giving reflection and absorption spectra of pure B_2O_3 glass and Corning 7740 glass. It turns out that some of the absorption peaks of B_2O_3 glass nearly coincide with similar peaks obtained from BF_3 glass and, furthermore, that the curve for 7740 is quite similar to

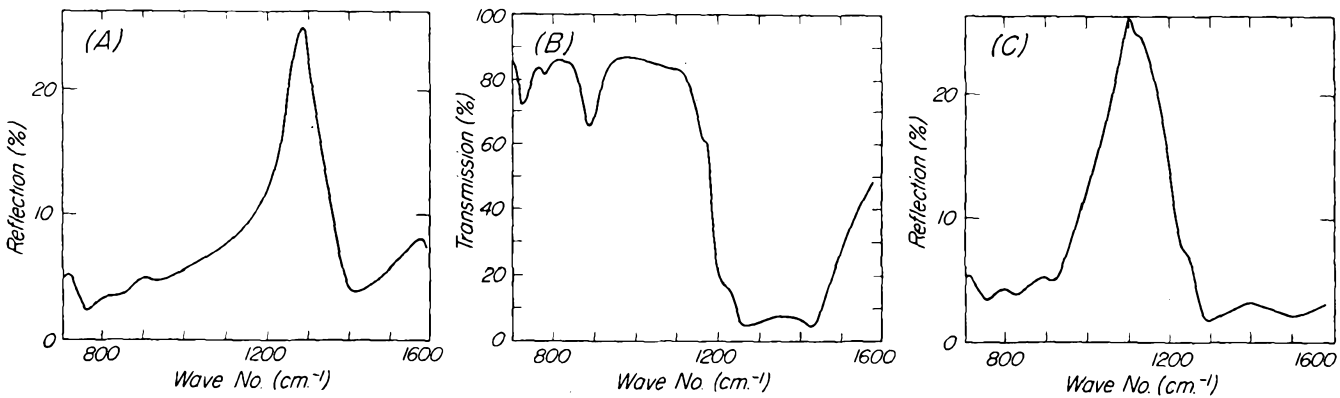

Fig. 6.7. (A) Reflection spectrum of B_2O_3 glass. (B) Absorption spectrum of thin film of B_2O_3 glass. (C) Reflection spectrum of Corning 7740 chemical glass. After S. Anderson.[18] (*Courtesy the American Ceramic Society.*)

the sum of the curve for the B_2O_3 glass and for fused silica. This suggests, according to Anderson, that the silicon-oxygen and boron-oxygen groups in "Pyrex" glass are similar to their arrangement in the respective pure glasses.

The transmission in the ultraviolet region of the spectrum is largely determined by the content of Fe_2O_3. Cerium oxide also has a pronounced effect, as first established by W. Crookes (1914). Vitreous silica trans-

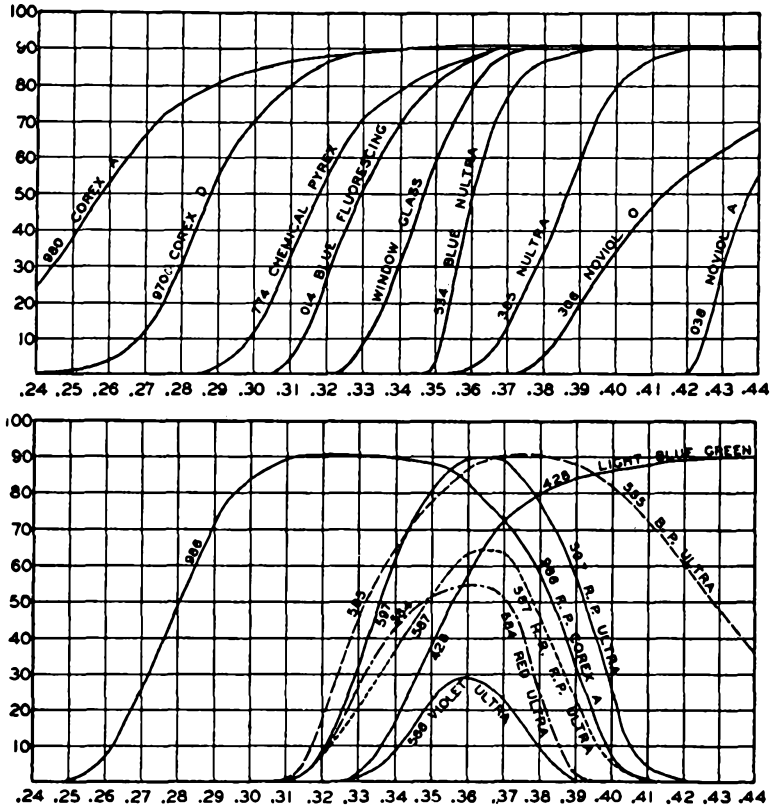

Fig. 6.8. Transmission curves of glasses for controlling the ultra-violet portion of the spectrum. (*Courtesy Corning Glass Works.*)

mits well below 0.2 microns. When sufficiently pure, silica and silicate glasses are thus well suited for U. V. transmission in the short-wave regions. It has been claimed that phosphate glasses are more transparent than any of the silica glasses in the U.V. spectrum.[24] "Corex A," Corning phosphate glass 9800, is a representative for which transmission curves are shown in Fig. 6.5, together with "Pyrex" 7740. Fig. 6.8 gives curves for the U.V. transmission of a number of other Corning glasses specially prepared for controlled transmission in the U.V. region.

Ordinary window glass is of the soda-lime-silica type; in single strength it is from 0.087 to 0.100 inch thick, while double strength ranges in thickness from 0.118 to 0.133 inch. Since single-strength window glass is opaque to U.V. radiation below 0.310 micron, it thus largely absorbs the component of solar radiation in the U.V. (0.28–0.32 μ) which is beneficial to biological processes (sun tan effect). Special window glass, which transmits 12 per cent at 0.310 μ and 2 per cent at 0.302 μ, has been developed for use in poultry houses, green houses, and hospital solaria.[10]

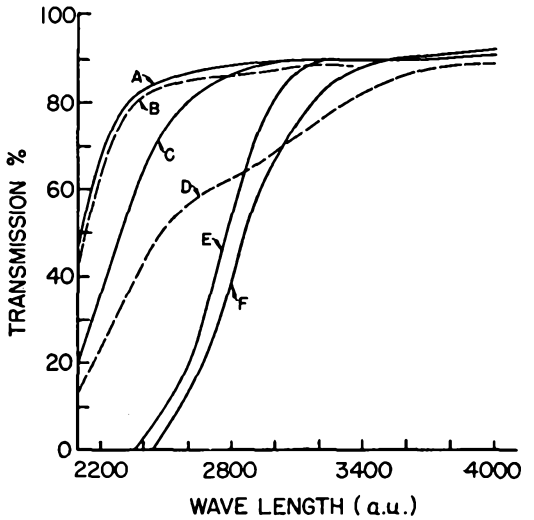

Fig. 6.9. Ultra-violet transmission of Pyrex and Vycor brands of glasses and Vitaglass. Curve (A) Vycor brand No. 7910; (B) Vycor brand No. 7910, solarized; (C) Pyrex brand No. 9741; (D) Pyrex brand No. 9741, solarized; (E) Pyrex brand No. 9700; (F) Vitaglass; transmission through 1 MM thickness. After M. E. Nordberg.[19] (*Courtesy the American Ceramic Society.*)

Mercury-vapor lamps, as sources of U.V. radiation for sun lamps and bactericidal lamps, have found widespread use and present special problems to the glass technologist. This subject has been discussed by Nordberg[19] on the basis of comparative measurements for "Vycor" 7910 and 7911, "Pyrex" 9741 and 9700, "Vitaglass,"* and fused silica. Fig. 6.9 gives the results of measurements made with a Beckman quartz spectrophotometer, calculated to a sample thickness of 1 mm by using Lambert's Law. Curve F for "Vitaglass" is taken over from Coblentz and Stair.[20]

It has always been assumed that U.V. transmitting glasses had to be hard glasses. Stanworth[21] has hown, however, that soft-soda glass, containing about 15 per cent of alkali oxides and 0.01 per cent of iron oxide,

* Introduced by Chance Bros. & Co. (Birmingham).

can be made with excellent transmission at 2537 A.U. This glass has an expansion coefficient of about 95×10^{-7} cm/cm/deg. C, and is thus readily sealed to other soft glasses and sealing alloys described in Chapter 4. The following is quoted from Stanworth.[21]

"It is generally very difficult in large-scale melting to keep the iron oxide very much below 0.01 per cent. The failure of previous workers is probably to be attributed either to incomplete reduction to the ferrous condition of the small percentage of iron still remaining in the glass or to the presence of other impurities also harmful to ultra-violet transmission. In connection with the latter we have found that small amounts of sulfur, iodine or titanium are important. Thus, the presence of sulfur as an impurity in commercial barium carbonate markedly reduces the ultraviolet transmission of the soft-soda glasses when melted under the conditions referred to above, and in fact, also promotes a yellowish color. This effect of sulfur may explain some of the difficulties of previous workers. For example, although it has been suggested that simple borate glasses containing high proportions of Na_2O necessarily have poor ultra-violet transmission and a yellow color because the absorption band in the ultra-violet of such glass compositions spreads into the visible region, we have been able to make colorless sodium-borate glasses containing 25 per cent Na_2O and with $\sim$ 75 per cent transmission at 2537 A through a thickness of 3 mm.

"Another harmful impurity in simple sodium-borate melts is iodine. Thus, in a sodium-borate glass containing 12.4 per cent Na_2O, the addition to the melt of 0.15 per cent iodine in the form of potassium iodide (not all of which would be retained in the finished glass) reduces the transmission at 2537 A through a thickness of 4 mm from 82 per cent to 35 per cent without producing any visible color in the glass.

"We have found that a most important impurity in silicate glasses melted under the reducing conditions already described is titanium, which produces a marked effect on 2537 A transmission when present in quantities even as low as 0.002 and 0.005 per cent, as shown by the results in the accompanying graph. It has not been realized before how harmful such small percentages of titanium can be. It is unfortunate that sands available in Great Britain contain titanium; there are American sands which are not only lower in iron content than British sands, but are also free from titanium."

The useful life of U.V. lamps is often limited by two effects, known as "solarization" and "mercury blackening." The term "solarization" was originally applied to the decrease in transmission in the U.V. region and at times also to the visible range of the spectrum when glass is exposed to sunlight; but common usage has extended its meaning to cover the same effect when caused by radiation from artificial sources. The loss in U.V. transmission is usually attributed to the oxidation of ferrous iron to ferric iron which, as mentioned above, is the determining factor for U.V. transmission. The ease with which this oxidation occurs is a function of the glass composition. Often the original transmission of the glass can be restored by heating. The solarization effect is illustrated in Fig. 6.10, according to Nordberg.[19] Mercury blackening is caused by the formation of a dark layer on the inner tube wall; this results from adsorption of or reaction with the mercury in the arc. "Vycor 7910,"

when exposed for 2000 hours in a low-pressure cold cathode lamp, showed a 13-per cent loss in transmission of 2537 A.U. radiation due to blackening alone; this is lower than usually encountered with glasses.

The subject of solarization has been treated at length by Weyl,[22] who describes the colors produced by exposure of various glasses to radiation and reviews critically the physical mechanism responsible for the changes. White and Silverman[23] have carried out quantitative measurements, both by the mercury arc and by sunlight, on the influence of glass constituents on solarization. It is of interest to note that the mercury arc produces color changes in glass only in a thin surface layer, while solar radiation changes the color continuously through the whole volume of the glass.

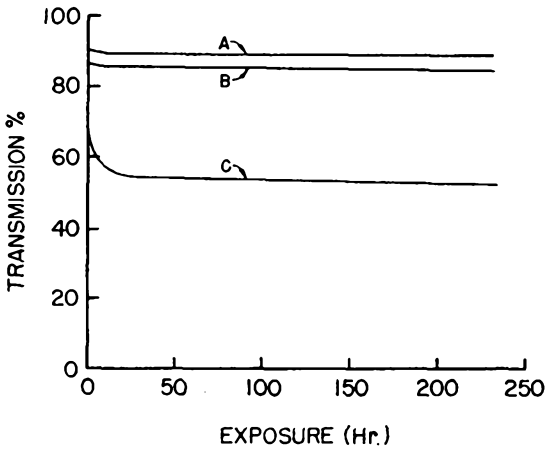

Fig. 6.10. Effect of exposure to ultra-violet radiation (2537 A.U.) from a Hanovia Arc on 2537 A. U. Transmission; specimens approximately 6 in. from arc; Curve (A) fused silica; (B) Vycor brand No. 7910; (C) Pyrex brand No. 9741. After M. E. Nordberg.[19] (*Courtesy the American Ceramic Society.*)

Spectral-transmissive characteristics of some German glasses,[24] covering the U.V. visible and infrared range, were recently described. Special U.V. absorbing glasses, which are transparent to visible radiation were studied by Ctyroky.[25] Photosensitive glass, responding to irradiation in the near U.V. and permitting development of the image by heat treatment at 600°C and fixation by cooling, contains colloidal gold and cerium. Exposure times range from 5 to 10 minutes, and colors obtained are a result of the colloidal gold. White opal pictures can be obtained by precipitating other materials on the gold. This development, according to work by Stookey,[26–28] is being carried out by Corning Glass Works, and photosensitive glass plates are in commercial production.

The behavior of glass toward x-rays is important in two respects: First, its absorption will detract from the output of the tube if the window

of an x-ray tube is made of glass; on the other hand, desirable absorption of the remaining envelope will protect the operator. This naturally calls for special glasses.[29a] More suitable materials perform the functions of transmission and absorption much better, to mention only in passing the use of beryllium windows[29] and lead shields; a brief discussion of glass is nevertheless desirable. Fig. 6.11 gives a graphic illustration of the relative transmittance of beryllium, aluminum, and "Pyrex" glass in terms of calculated intensity based on ionizing power of x-rays produced at 50 kv and transmitted through a window 1 mm thick.[30] By

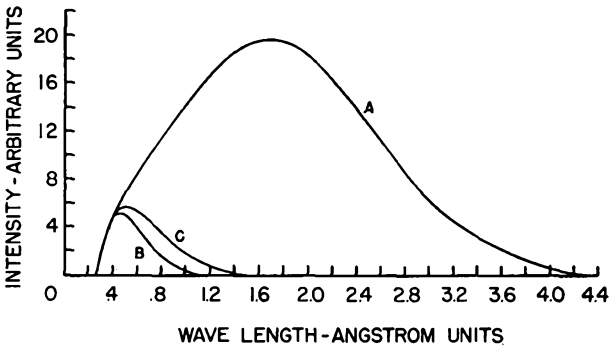

Fig. 6.11. Calculated intensity vs. wavelength distribution of X-radiation at 50 kilovolts, intensity expressed in terms of ionizing power: (A) Filtered by 1 millimeter beryllium; (B) Filtered by 1 millimeter aluminum; (C) Filtered by 1 millimeter Pyrex brand glass (Corning 7740). After T. H. Rogers.[30] (*Courtesy the Institute of Radio Engineers.*)

integrating the area under each curve the total transmitted energy for each material and the following percentages are obtained:

	%
beryllium	100
"Pyrex" glass	7.9
aluminum	4.9

It is quite evident that ordinary glass is a poor transmitter. Lindemann glass has been used since 1911 for x-ray tube windows.[31] It consists of 2.5 BeO, 83.5 LiB_4O_7, and 14 B_2O_3. By replacing Ca ($Z = 20$) by Be ($Z = 4$), K($Z = 19$) by Li ($Z = 3$), Si ($Z = 14$) by B ($Z = 5$), the remaining absorption is mainly due to oxygen ($Z = 8$). The effective absorption, which is proportional to Z^4, is thus greatly reduced.[32] Care must be taken that the constituent materials are free of water of crystallization. This glass will seal to soft glass, but cannot be shaped by blowing and is rapidly attacked in air. It transmits well in the long-wave range above 200 mμ.[11] Glasses containing PbO are natural absorbers of x-rays. Fig. 6.12 gives an illustration of this effect for increasing PbO

content in terms of weight per cent for a sample 1 cm thick passing radiation from a tungsten anode x-ray tube operated at 100 kv.[12] According to Ungelenk[11] lead glasses with 40, 51, and 65 per cent by weight PbO content have densities of 3.35, 3.81, and 4.56, respectively, and their

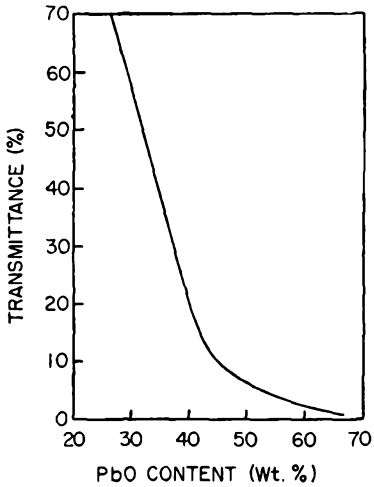

Fig. 6.12. Transmittance of 1 cm thick protective glasses of different PbO-contents to x-rays (W-anode, 100 KV). After W. Espe and M. Knoll.[11] (*Courtesy Julius Springer, Berlin.*)

absorbing action is equivalent to a sheet of lead having 12, 18, and 23 to 30 per cent thickness of that of the lead glass respectively.

"The 'protection coefficient' of a protective material is the ratio of the thickness of lead to the thickness of material which absorbs a given X-ray beam to the same extent."* In the case of glasses, only lead and barium contribute appreciably to x-ray absorption. This has led to the development of two kinds of x-ray shield glasses, i.e., dense flint glasses (high PbO-content) which owe their protective action to their lead content alone and barium-flint glasses where both Ba and Pb contribute to the protective action.[34] Correlations exist between the protection coefficient of a glass and its chemical composition, density and refractivity. Protective coefficients are determined experimentally for a given type of X-radiation and do not necessarily apply to harder or softer x-rays than those specified. It turns out that the protection coefficient for flint glass is in general independent of the radiation quality but this does not apply to barium-flint glass which shows a maximum protection coefficient near 105 KV. For a given radiation the protection coefficient is a linear function of the glass density and refractive index within specified ranges. These matters have been discussed in detail by Singer[34] and others.

* Definition by the American Advisory Committee on X-ray and Radium Protection.

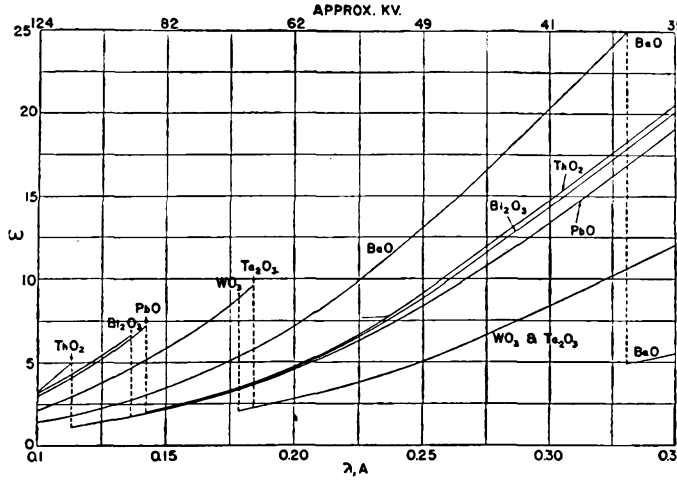

Fig. 6.13. Mass absorption coefficients of oxides M_mO_n, vs. wavelengths. After L. L. Sun and Kuan Han Sun.[33] (*Courtesy Ogden Publishing Company, New York.*)

An extensive study of "x-ray absorbing and transmitting glasses" has recently been published by L. L. Sun and Kuan-Han-Sun,[33] to which the reader is referred for tables on mass-absorption coefficients of oxygen and various oxides encountered in glass making. Fig. 6.13 is taken from this paper and shows the mass-absorption coefficient $\omega = \mu/\rho$, where μ is the absorption coefficient and ρ the density of the absorbing material according to the universal equation which applies to the absorption of all types of electromagnetic radiation, from γ-rays to infrared, by absorbing substances of thickness t:

$$I = I_0 e^{-\mu t} \tag{6.2}$$

I_0 is the initial intensity of the radiation and I the intensity after passing through the substance. By writing $\mu = \frac{\mu}{\rho} \times \rho = \omega\rho$, one obtains $\omega = \mu/\rho$. This indicates that x-ray absorption is caused by two effects: Compton scattering and the Einstein photoelectric effect. The mass-absorption coefficient ω is independent of physical state, and thus applies to liquids, gases, and solids. It is independent of temperature and pressure and dependent only on the wave length of the x-rays, the atomic number, and the atomic mass or weight of the elements in the absorbing material.

It has been demonstrated that the mass-absorption coefficients of compounds are correctly represented by adding the coefficients of the constituent elements. It is of course essential that the x-ray energy be specified before the lead equivalent of a glass with respect to x-ray stopping power is mentioned. Thus, a binary x-ray shielding glass containing barium and lead has an enhanced barium K absorption band, and in the

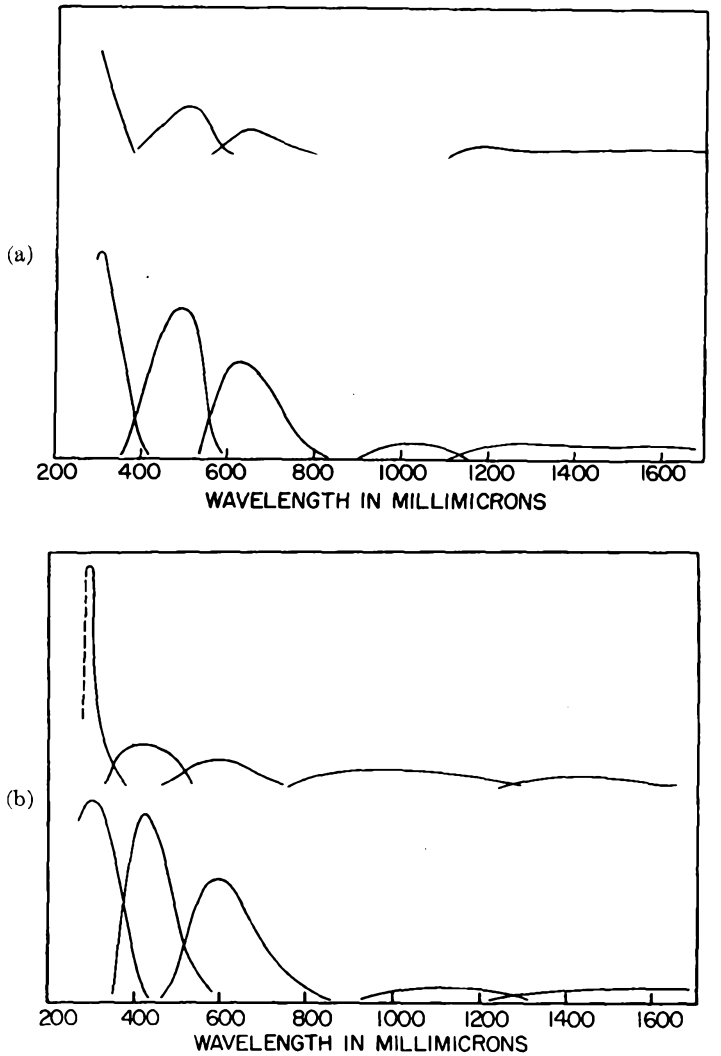

Fig. 6.14. Color centers induced in (a) Potassium silicate glass; (b) Sodium silicate glass by 10^5 roentgens of x-rays. The upper part of each graph shows the same color centers after exposure to the bleaching action of U.V. light. After J. V. Fitzgerald. (*Courtesy Pittsburgh Plate Glass Co.*)

region of higher energy x-rays and α-rays the lead is the more effective absorbing constituent. Victoreen[35] has recently shown how mass-absorption coefficients can be calculated for all elements from atomic data, and he published tables of these coefficients for wave lengths less than the K critical absorption wave length.

TABLE 6.4. DATA ON GROUP (A) AND GROUP (B) GLASSES*

Glass No.	SiO_2	B_2O_3	Al_2O_3	Li_2O	Na_2O	Wave length (10 cm)		Wave length (3 cm)	
						K	*PF*	*K*	*PF*
Group (A) with glass-forming oxides only									
1	100					3.78	0.00025	3.81	0.0005
2	50	50						3.55	.0014
Group (B) with more than 90% of glass-forming oxides									
3	96	3			Low			3.85	0.0016
4	96	3			Low	3.77	0.0023		
5	69	28	1	2		4.07	.0022	4.20	.0028
6	92				4	4.50	.0034	4.41	.0053

* Studied by Navias and Green Ref. 43.

Glasses with a high absorption for x-rays, γ-rays, and neutrons help to prevent cataracts from accidental exposure to radiation,[36] and are, therefore, critically important to workers in the field of nuclear physics. J. Rothermel and Kuan Han Sun have developed a new glass containing tungsten phosphate which absorbs 50 per cent more high energy x-rays or γ-rays than shielding glass previously available. A slow neutron-absorbing glass containing cadmium borosilicates with fluorides was developed by L. Melnik, H. W. Safford, and Kuan Han Sun. Its slow-neutron absorption is one-third that of pure cadmium sheet, which is opaque. The theory and practical aspects behind this development, which is being carried out at the University of Pittsburgh, have been described by Sun and Sun.[37]

Similar to the effects of solarization, which influence the U. V. transmission of glasses, as described above, there are discolorations following exposure to x-rays, γ-rays, and particle radiation. This type of discoloration of glass is naturally objectionable in many applications, and steps have been taken to overcome it. Special nondarkening glasses for use in television tubes and for shields against γ-radiation have been developed.* Nuclear physicists use such shields in thicknesses of several feet.[36]

The usual type of discoloration induced in many common glasses by radiation of this kind is very similar to that produced in single crystals.[38] The color centers found in simple binary glasses decay with time and are bleached by mild heat and U.V. light. Fig. 6.14 gives an example of this

* Pittsburgh Plate Glass Company, Creighton, Pa.

TABLE 6.5. DIELECTRIC CHARACTERISTICS OF VARIOUS GLASSES AND CRYSTALLINE SILICA (QUARTZ)[44]

Material	Temp. (°C)		Frequency in Cycles/sec								
			10^2	10^3	10^4	10^5	10^6	10^7	10^8	3×10^9	10^{10}
Corning #0010	24	ϵ'/ϵ_0	6.68	6.63	6.57	6.50	6.43	6.39	6.33	6.1	5.96
		tan δ	77.5	53.5	35	23	16.5	15	23	60	90
Corning #0080	23	ϵ'/ϵ_0	8.30	7.70	7.35	7.08	6.90	6.82	6.75	6.71	6.71
		tan δ	780	400	220	140	100	85	90	126	170
Corning #0090	20	ϵ'/ϵ_0	9.15	9.15	9.15	9.14	9.12	9.10	9.02	8.67	8.45
		tan δ	12	8	7	7	8	12	18	54	103
Corning #0100	25	ϵ'/ϵ_0	7.18	7.17	7.16	7.14	7.10	7.10	7.07	7.00	6.95
		tan δ	24	16	13.5	13	14	17	24	44	63
Corning #0120	23	ϵ'/ϵ_0	6.75	6.70	6.66	6.65	6.65	6.65	6.65	6.64	6.60
		tan δ	46	30	20	14	12	13	18	41	63
Corning #1710	25	ϵ'/ϵ_0	6.25	6.16	6.10	6.03	6.00	6.00	6.00	5.95	5.83
		tan δ	49.5	42	33	26	27	34	38	56	84
Corning #1991	24	ϵ'/ϵ_0	8.10	8.10	8.08	8.08	8.08	8.06	8.00	7.92	7.83
		tan δ	12	9	6	5	5	7	12	38	51
Corning #7040	25	ϵ'/ϵ_0	4.84	4.82	4.79	4.77	4.73	4.70	4.68	4.67	4.64
		tan δ	50	34	25.5	20.5	19	22	27	44	57
Corning #7050	25	ϵ'/ϵ_0	4.90	4.84	4.82	4.80	4.78	4.76	4.75	4.74	4.71
		tan δ	93	56	43	33	27	28	35	52	61
Corning #7060	25	ϵ'/ϵ_0	5.02	4.97	4.92	4.86	4.84	4.84	4.84	4.82	4.80
		tan δ	89	55	42	40	36	30	30	54	98
Corning #7070	23	ϵ'/ϵ_0	4.00	4.00	4.00	4.00	4.00	4.00	4.00	4.00	4.00
		tan δ	6	5	5	6	8	11	12	12	21
	100	ϵ'/ϵ_0	4.17	4.16	4.15	4.14	4.13	4.10		4.00	4.00
		tan δ	50	22	13	10	9	11		19	21

TABLE 6.5. DIELECTRIC CHARACTERISTICS OF VARIOUS GLASSES AND CRYSTALLINE SILICA (QUARTZ)[44]. (*Continued*)

Material	Temp. (°C)		Frequency in Cycles/sec								
			10^2	10^3	10^4	10^5	10^6	10^7	10^8	3×10^9	10^{10}
Corning #7230	25	ϵ'/ϵ_0	3.88	3.86	3.85	3.85	3.85	3.85		3.76	
		tan δ	33	23	16	13	11	12		22	
Corning #7720	24	ϵ'/ϵ_0	4.74	4.70	4.67	4.64	4.62	4.61			4.59
		tan δ	78	42	29	22	20	23			43
Corning #7740	25	ϵ'/ϵ_0	4.80	4.73	4.70	4.60	4.55	4.52	4.52		4.52
		tan δ	128	86	65	54	49	45	45		85
Corning #7750	25	ϵ'/ϵ_0	4.45	4.42	4.39	4.38	4.38	4.38		4.38	4.38
		tan δ	45	33	24	20	18	19		43	54
Corning #7900	20	ϵ'/ϵ_0	3.85	3.85	3.85	3.85	3.85	3.85		3.84	3.82
		tan δ	6	6	6	6	6	6		6.8	9.4
	100	ϵ'/ϵ_0	3.85	3.85	3.85	3.85	3.85	3.85		3.84	3.82
		tan δ	37	17	12	10	8.5	7.5		10	13
Corning #1990	24	ϵ'/ϵ_0	8.40	8.38	8.35	8.32	8.30	8.25	8.20	7.99	7.94
		tan δ	4	4	3	4	5	7	9	19.9	42
Corning #3320	24	ϵ'/ϵ_0	5.00	4.93	4.88	4.82	4.79	4.78	4.77	4.74	4.72
		tan δ	80	58	43	34	30	30	32	55	73
Corning #7052	23	ϵ'/ϵ_0	5.20	5.18	5.14	5.12	5.10	5.10	5.09	5.04	4.93
		tan δ	68	49	34	26	24	28	34	58	81
Corning #8460	24	ϵ'/ϵ_0	8.35	8.30	8.30	8.30	8.30	8.30	8.30	8.10	8.06
		tan δ	11	9	7.5	7	8	10	16	40	57
Corning #8871	25	ϵ'/ϵ_0	8.45	8.45	8.45	8.45	8.45	8.43		8.34	8.05
		tan δ	18	13	9	7	6	7		26	49
Owens-Corning "E" Glass	23	ϵ'/ϵ_0									6.11
		tan δ									60
Pittsburgh-Corning Foamglas (Soda Lime)	23	ϵ'/ϵ_0	90.0	82.5	68.0	44.0	17.5	9.0			5.49
		tan δ	1500	1600	2380	3200	3180	1960			455
Fused Quartz (SiO_2)	25	ϵ'/ϵ_0	3.78	3.78	3.78	3.78	3.78	3.78	3.78	3.78	3.78
		tan δ	8.5	7.5	6	4	2	1	1	0.6	1

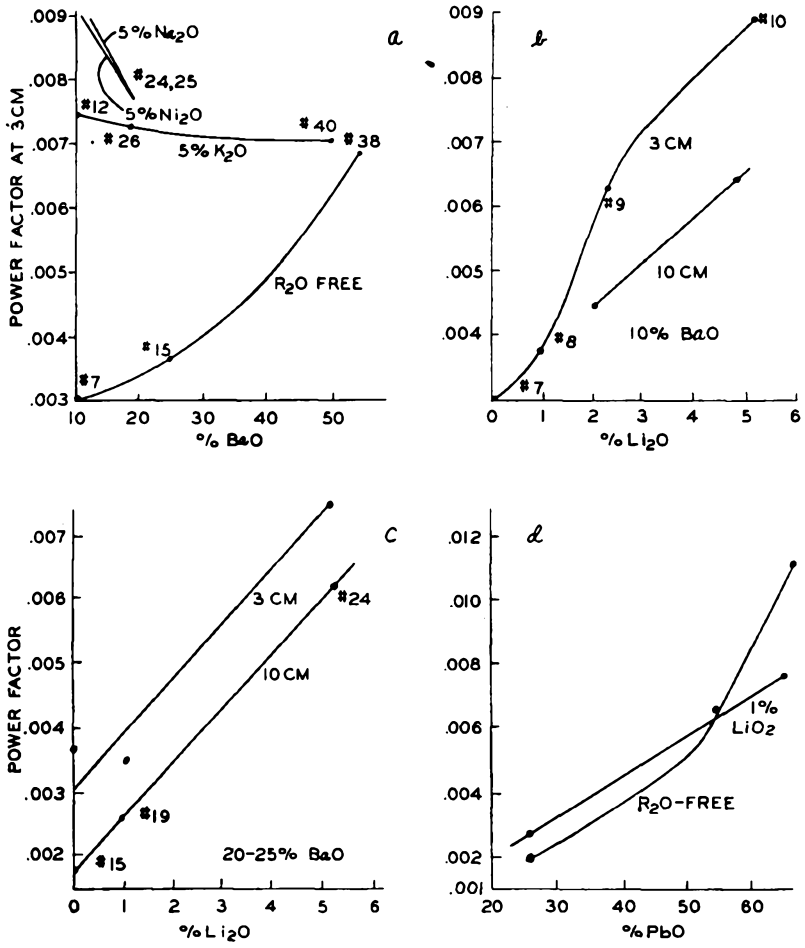

Fig. 6.15. Effect of glass composition on power factor at ultra-high frequencies. (a) Effect of BaO Content on 3 cm power factors of glasses containing 0 to 5% R_2O, (b) Effect of Li_2O content on power factors of glasses with low BaO content (10%) (c) Effect of Li_2O content on power factors of glasses with medium BaO content (20 to 25%); (d) Effect of PbO content on 3-cm power factors of glasses containing 0 to 1% Li_2O. After L. Navias and R. L. Green.[43] (*Courtesy The American Ceramic Society.*)

TABLE 6.6. APPROXIMATE GLASS COMPOSITIONS Studied by Stockdale and Tooley[46]

Glass	SiO_2	Na_2O	K_2O	CaO	MgO	B_2O_3	PbO	Al_2O_3
A	72	13.5		7	5	1.5		1
B	73	17		5	4			1
C	56	4	8				30	2
D	68	7				23		2
E	81	4				13		2

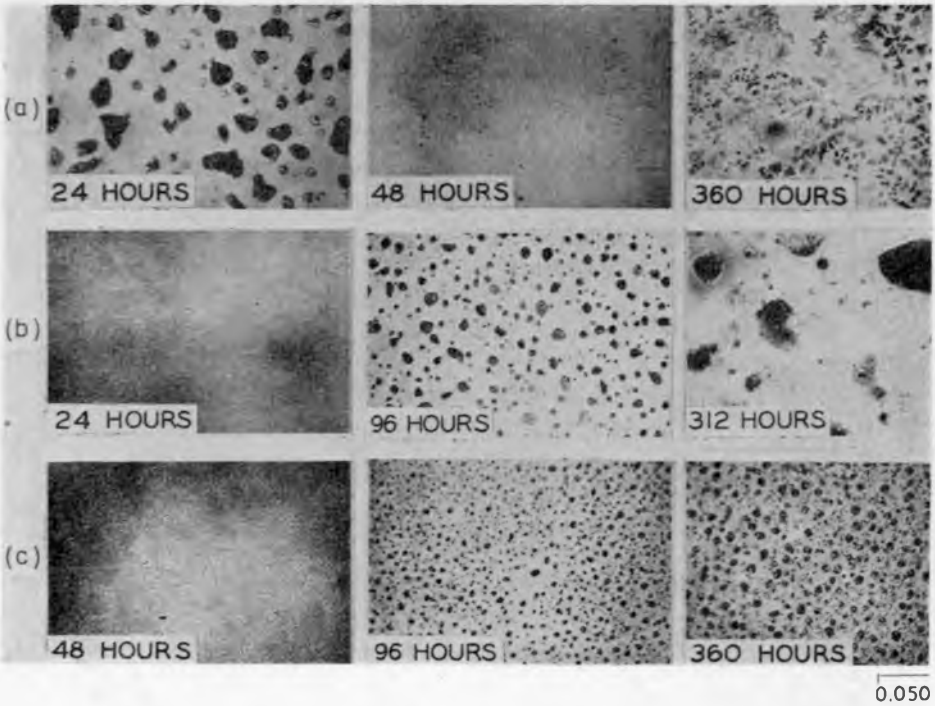

Fig. 6.16. Photomicrographs of Glass B (soda-lime) weathered at (a) 95% relative
Stockdale and F. V. Tooley.[46] (*Courtesy*

bleaching effect according to hitherto unpublished observations made by the Pittsburgh Plate Glass Company.* Refs. 39 to 41 describe in more detail coloring effects in glass by x-rays. Glass which has been in a radiation field emits light when heated. This phenomenon is called "thermoluminescence."[42]

The absorption of radiation in the cm-wave length range is of interest to the designer of microwave tubes, such as klystrons and magnetrons. For klystrons, in particular, a glass member is often located within the oscillating cavity, and its dielectric properties will determine its effect on the efficiency of operation of the tube. A detailed study has been made by Navias and Green of the General Electric Research Laboratories,[43] who measured the dielectric constants and dielectric losses of 104 glasses of widely varying compositions at 3 cm and 10 cm wave lengths by the resonating cavity method. It is best to quote from the abstract of their paper as follows:

* The author is much indebted to J. V. Fitzgerald for kindly submitting these data and other valuable comments.

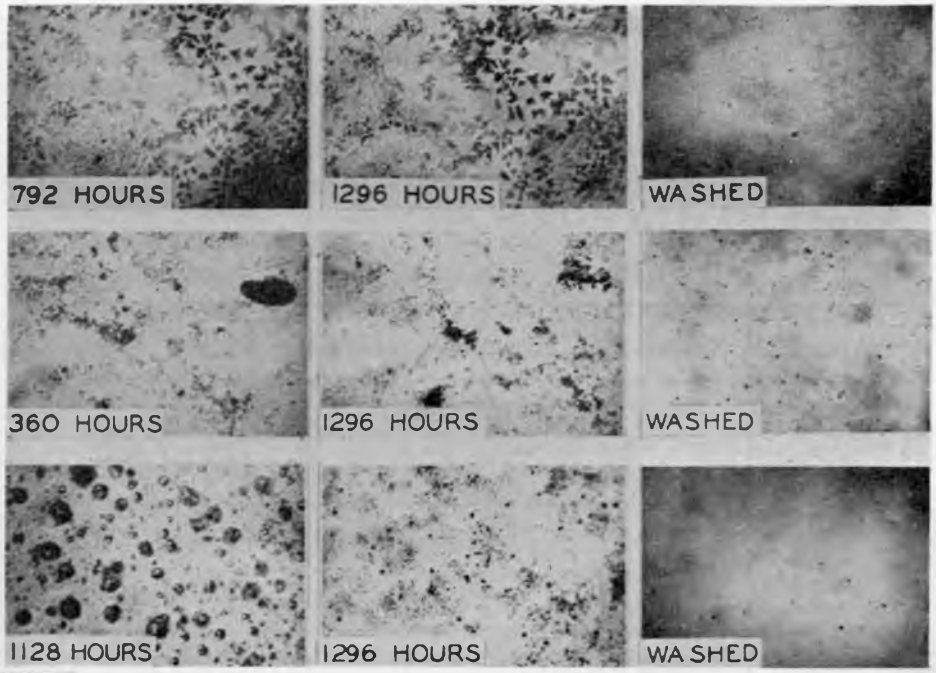

humidity; (b) 73% relative humidity; (c) 57% relative humidity. After G. F. *Journal of the American Ceramic Society.*)

"By correlating the power-factor data with the compositions of these glasses, the authors propose a qualitative explanation of the mechanisms producing energy absorption and dielectric losses in the microwave range. These mechanisms are determined by the nature of the bonds joining atoms and ions in the randomly oriented atomic networks of glasses.

"The rigid and continuous networks of SiO_2 and B_2O_3 glasses are relatively transparent to centimeter wave lengths. Energy absorption and dielectric losses are low. Addition of network-modifying oxides yields glasses of greater energy absorption owing to the oscillation of the interstitial ions thus introduced. Increasing the content of any one of these ions in a glass results in higher losses while the coexistence of a variety of these ions generally results in lower losses.

"Alkali ions in glasses give rise to high losses, which increase as the number of ions present increases. Glasses containing a combination of alkalies show lower losses than the equivalent compositions with only one alkali. Divalent ions do not contribute as much to losses as alkalies, but high-power factors are shown by glasses with high BaO or PbO contents. Using combinations of these oxides instead of only one, slight reductions in power factor are effected. Dissimilar interstitial ions interact in ultra high-frequency fields with the result that energy absorption is reduced. The losses of high-lead glasses are thus reduced by alkalies and, on the other hand, the presence of RO lowers the losses of glasses in much the same manner as other network modifiers."

Pure silica glass, consisting of the glass-forming oxide SiO_2, exclusively, forms a tightly bonded network of SiO_4 tetrahedra, through which high-frequency energy is transmitted without setting the atoms in motion. It has thus been found that silica glass has the lowest power factor of all glasses in the cm-wave length range, and the dielectric constant is also unusually low. A similar reasoning applies to SiO_2-B_2O_3 glasses, where SiO_4 tetrahedra and triangular BO_3 configurations are tightly bonded. Table 6.4 gives values of K and PF for these two types of glasses.[43]

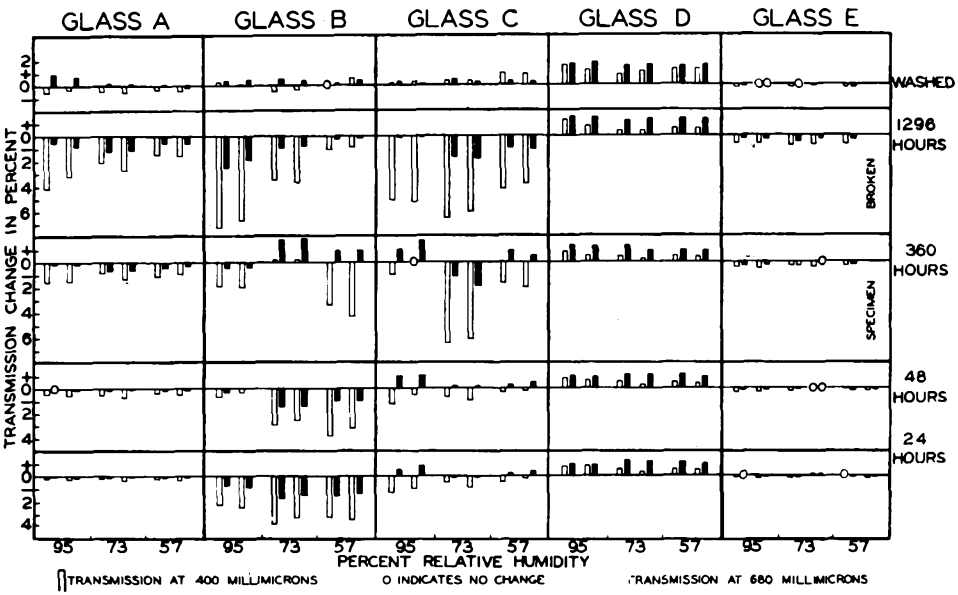

Fig. 6.17. Bar graph showing transmission changes occurring during the progressive weathering of five commercial glasses. After G. F. Stockdale and F. V. Tooley.[46] (*Courtesy Journal of the American Ceramic Society.*)

When the close networks of the primary glass formers are interspersed with network modifiers, such as alkalies and earth alkalies, these ions are bound relatively loosely and are easily set in motion under the influence of ultra high-frequency fields, thus leading to dielectric losses. The dielectric constant is increased directly in proportion to the number of alkali ions present. Other constituent compounds, such as Al_2O_3, PbO, and BaO, and the other alkaline earth oxides, increase the dielectric constant proportional to the percentages of these oxides present. Fig. 6.15 (a-d) give results obtained by Navias and Green for various glass compositions at 3 cm and 10 cm. Table 6.5[44] gives a tabulation of the specific dielectric constant ϵ'/ϵ and the loss tangent tan δ ($X10^4$) for a number of glasses over a wide frequency range, all measured at room temperature. The loss tangent is identical with the power factor cos θ

for low-loss samples.* The relation between the dielectric losses and the composition of glass has been treated by Stevels.[45]

The weathering of glass under carefully controlled conditions of humidity has recently been studied by Stockdale and Tooley[46] for a number of glass compositions. They find that weathering sets in at distinct local spots on the surface; these eventually spread to form larger patches of reaction products (Fig. 6.16). Table 6.6 shows the composition of the glasses studied, and Fig. 6.17 includes a bar graph indicating the gain or loss in transmission at 400 mμ and 680 mμ, respectively, at different per cent relative humidity after test periods extending to nearly 1300 hours. It is of interest to note that one type (D) of borosilicate glasses showed a uniform gain in transmission after weathering. Transmission was measured with a reproducible accuracy of better than 0.25 per cent.

* The author is indebted to Professor A. von Hippel, Director of the Laboratory for Insulation Research at M.I.T. for making these data available.

REFERENCES

1. Fritz-Schmidt, M., Gehlhoff, G., and Thomas, M., "The Transmittance of Glasses in the Ultraviolet, Visible and Infrared Regions of the Spectrum" (In German), *Z. Tech. Phys.*, **11**, 289–235 (1930).
2. Williams, Van Zandt, "Infrared Instrumentation and Techniques," *Rev. Sci. Inst.*, **19**, 135–178 (1948).
3. Eucken-Wolf, "Hand u. Jahrbuch der Chemischen Physik," Vol. 9–2, Leipzig, 1934.
4. Hardy, A. C., and Perrin, F. H., "The Principles of Optics," New York, McGraw-Hill Book Co., Inc., 1932.
5. Canada, A. H., "Simplified Calculation of Black Body Radiation," *G. E. Rev.*, **51**, 50–54 (1948).
6. Makowski, M. W., "A Slide Rule for Radiation Calculations," *Rev. Sci. Inst.*, **20**, 876–884 (1949).
7. Florence, J. M., Glaze, F. W., Hahner, G. H., and Stair, R., "Transmittance of Near-Infrared Energy by Binary Glasses," *J. Am. Ceram. Soc.*, **31**, 328–331 (1948).
8. Florence, J. M., Allshouse, C. C., Glaze, F. W., and Hahner, C. H., Absorption of Near-Infrared Energy by Certain Glasses," *J. Res. Nat. Bur. Stand.*, **45**, 121–128, 1950. (RP2118.)
9. Bell, J., Davies, J. W., and Gossling, B. S., "High-Power Valves: Construction, Testing, and Operation," *J. Inst. El. Eng.*, **83**, 176–198, D.198–207 (1938).
10. Phillips, C. J., "Glass, the Miracle Maker," 2nd Ed., New York, Pitman Publishing Corp., 1948.
11. Espe, W., and Knoll, M., "Werkstoffkunde der Hockvakuumtechnik," Berlin, J. Springer, 1936.
12. Morey, G. W., "The Properties of Glass," New York, Reinhold Publishing Corp., 1938.
13. Frerichs, R., "New Optical Glasses Transparent in the Infrared up to 12 μ," *Bull. Am. Phys. Soc.*, **25**, 11 (E9) (1950).
14. Coblentz, W. W., "Radiation from Selectively Reflecting Bodies," *Phys. Rev.*, **24**, 307–320 (1907).

15. Schaefer, C., Matossi, F., and Wirtz, K., "Infrared Reflection Spectrum of Silicates" (In German), *Z. Phys.*, **89**, 210–233 (1934).
16. Matossi, F., and Kruger, H., Same subject, Ibid., **99**, 1–23 (1936).
17. Matossi, F., and Bluschke, H., "Infrared Reflection Spectrum of Glasses," (In German) Ibid., **108**, 295–313 (1938).
18. Anderson, S., "Investigation of Structure of Glasses by Their Infrared Reflection Spectra," *J. Am. Ceram. Soc.*, **33**, 45–51 (1950).
19. Nordberg, M. E., "U.V. Transmitting Glasses for Mercury-Vapor Lamps," *J. Am. Ceram. Soc.* **30**, 174–179 (1947).
20. Coblentz, W. W., and Stair, R., "Effect of Solarization on U.V. Transmission of Window Materials," *Trans. Illum. Eng. Soc.*, **23**, 1121–52 (1928).
21. Stanworth, J. E., "Transmission of Bactericidal Radiation through Glass," *Nature*, **161**, No. 4100, 856 (1948); **165**, No. 4201, 724–725 (1950); also: *J. Soc. Glass Technol.*, **34**, 153–172 (1950).
22. Weyl, W. A., "Colored Glasses: V. Fluorescence and Solarization of Glass," *J. Soc. Glass Tech.*, **30** (138) 90–172T (1946).
23. White, J. F., and Silverman, W. B., "Some Studies on the Solarization of Glass," *J. Am. Ceram. Soc.*, **38**, 252–257 (1950).
24. Stair, R., Glaze, F. W., and Ball, J. J., "Spectral-Transmissive Characteristics of Some German Glasses," *Glass Ind.*, **30**, 331–335 (1949).
25. Ctyroky, V., "A Study of Some Special U.V. Absorbing Glasses which are Transparent to Visible Radiation," *J. Soc. Glass Tech.*, **32**, 40–45 (1948).
26. Stookey, S. D., "Photosensitive Glass," *Ind. Eng. Chem.*, **41**, 856–861 (1949).
27. Stookey, S. D., "Coloration of Glass by Gold, Silver, and Copper," *J. Am. Ceram. Soc.*, **32**, 246–249 (1949).
28. Stookey, S. D., *U.S. Patent 2,515,949; 2,515,938; 2,515,275; 2,515,943; 2,515,942; 2,515,937; 2,515,940; 2,515,941; Can. Patent 466,318; 466,319.*
29. Machlett, R. R., "An Improved X-Ray Tube for Diffraction Analysis," *J. Appl. Phys.*, **13**, 398–401 (1942).
29a. Zunick, M. J., and Gosling, J. B., "Glass Selection and Production Techniques for X-Ray and other Tubes." Glass Ind., 32, 117–120 (1951).
30. Rogers, T. H., "A High-Intensity Source of Long Wave Length X-Rays," *Proc. I.R.E.*, **35**, 236–241 (1947).
31. Lindemann, C. L., and F. A., "Z. Roentgenkunde," **13**, 141 (1911).
32. Zwicker, C., "Technische Physik der Werkstoffe," Berlin, J. Springer, 1942.
33. Sun, L. L., and Kuan Han Sun, "X-Ray Absorbing and Transmitting Glasses," *Glass Ind.*, **29**, 686–691 (1948).
34. Singer, G., "Absorption of X-Rays by Lead Glasses and Lead-Barium Glasses," *J. Res. Nat. Bur. Stand.*, **16**, 233 (1936) (RP870).
35. Victoreen, J. A., "The Calculation of X-Ray Mass-Absorption Coefficients," *J. Appl. Phys.*, **20**, 1141–1147 (1949).
36. "Control of Radiation Hazards in the Atomic Energy Program," Washington, D.C., U. S. Government Printing Office, 1950.
37. Kuan-Han Sun and Sun, L. L., "Neutron-Absorbing and Transmitting Glasses," *Glass Ind.*, **31**, 507–515 (1950).
38. Seitz, F., "Color Centers in Alkali Halide Crystals," *Rev. Mod. Phys.*, **18**, 384–408 (1946).
39. Nurnberger, C. E., and Livingston, R., "Kinetics of Recoloring of Glass by X-Rays," *J. Phys. Chem.*, **41**, 691–697 (1939).
40. Kerten, H., and Dwight, C. H., "Colorization of Glass by Soft X-Rays," *J. Phys. Chem.*, **1**, 627–629 (1933).

41. Reinhard, M. C., and Schreiner, B. F., "Some Experiments on Reproduction of Color in Glass by X-Rays," *J. Phys. Chem.*, **32**, 1886–1887 (1928).
42. Nyswander, R. E., and Cohn, B. E., "Measurement of Thermoluminescence of Glass Exposed to Light," *J. Opt. Soc. Am.*, **20**, 131–136 (1930).
43. Navias, L., and Green, R. L., "Dielectric Properties of Glasses at Ultra High Frequencies and Their Relation to Composition," *J. Am. Ceram. Soc.*, **29**, 267–276 (1946).
44. Laboratory for Insulation Research, Massachusetts Institute for Technology, Cambridge, Mass. Technical Report No. 10 (June 1948). "Table of Dielectric Materials."
45. Stevels, J. M., "The Relation between the Dielectric Losses and the Composition of Glass," *J. Soc. Glass Tech.*, **34**, 158, 80–100 (1950).
46. Stockdale, G. F., and Tooley, F. V., "Effect of Humid Conditions on Glass Surfaces Studied by Photographic and Transmission Techniques," *J. Am. Ceram. Soc.*, **33**, 11–16 (1950).

CHAPTER 7

ELECTRONS, ATOMS, CRYSTALS, AND SOLIDS

Before turning our attention to the specific properties of metals and alloys employed in the construction of vacuum tubes it may be well to review the concepts of metallurgy which are important to their study. Many competent textbooks on metallurgy are available, and this chapter can only be a brief skirmish into this very interesting field. However, even a condensed treatment of metallurgy will bring into focus the great need for some familiarity with this subject and make it easier to follow the subsequent chapters.

All metals are characterized by a crystal structure which is readily disclosed in suitably prepared sections when observed under the microscope. For more detailed analysis x-ray diffraction and electron diffraction micrographs are now in common use. These techniques can save much time in solving problems that would otherwise be left to mere speculation. For material analysis proper, spectroscopic techniques are most reliable. Commercial instruments are available for all these investigations and are a good investment. In addition to chemical analysis as an indispensable technique there should also be mentioned the great value of the polarizing microscope in the investigation of crystal agglomerates, the phase microscope, and the electron microscope. Fractography is a relatively new technique, developed by Zapffe.[1] By the microscopic study of metal-fractures it reveals valuable information on the structure of individual grains of a crystal.

The many forms of ordered arrangement of atoms and molecules encountered in nature can be described by suitably chosen coordinate systems in which the axes coincide with the axes of the unit cells of which the crystal is composed. Fig. 7.1 shows an arbitrary space lattice, which results when parallel planes are drawn to the three coordinate planes XY, YZ, and ZX in such a manner that they are equidistant from each other. We then obtain a group of symmetrical prisms, each fitting close to the other, and atoms may be visualized as occupying points of intersection or other positions definitely related to the coordinate lattice. They will then form a crystal lattice of their own. Only 14 different space lattices are geometrically possible, and they form the basis of six crystal systems, as shown in Fig. 7.2 and Table 7.1.

The rhombohedral or trigonal system ($a = b = c$; $\alpha = \beta = \gamma \neq 90°$) is counted as a seventh system by some authors. The distances a, b, and c along the axes (Fig. 7.1) represent the spacing between adjacent atoms, and are units of length describing the unit cell. Various planes of the crystal will necessarily intercept the axes in multiples of a, b, and c. A reference or unit plane is chosen, somewhat arbitrarily, for any given crystal; it intersects all three axes, forming intercepts a, b, and c.

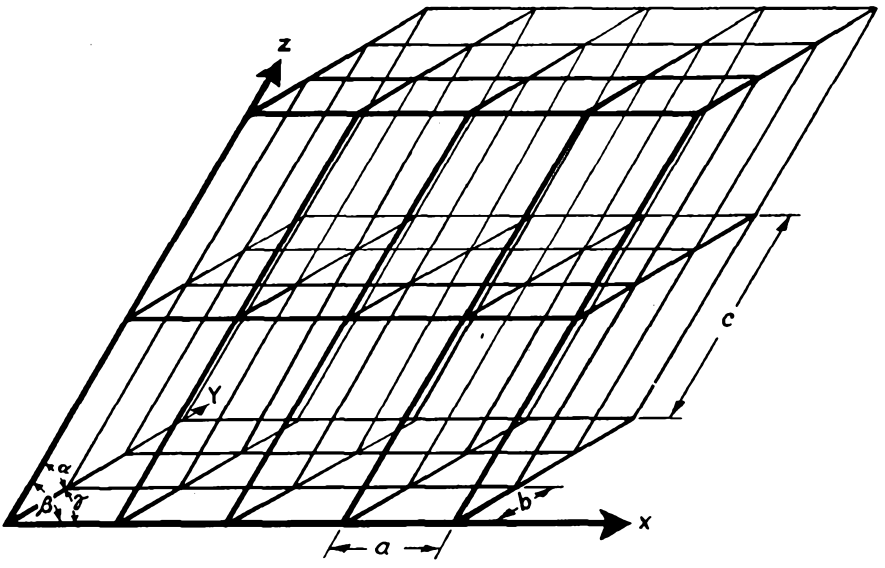

Fig. 7.1. Schematic space lattice. (*By permission from "Study of Crystal Structure" by W. P. Davey. Copyright 1934. McGraw-Hill Book Company, Inc.*)

The ratios of the intercepts are called "axial" ratios, and b is referred to as "unity." The axes are generally so chosen that the b axis lies horizontal from left to right, the a axis horizontal pointing toward the observer, and the c axis vertical in the direction of the most highly developed morphological zone. All faces of the same "form" of a crystal have the same axial ratios. The angles between the axes XYZ are designated by convention so that

a and b form γ
b and c form α
c and a form β

These angles, together with the axial ratios, are known as the elements of the crystal. The general coordinates along the XYZ axes are termed h, k, and l, where h/a, k/b, and l/c are small integers. This basic fact was established by R. J. Haüy in 1784, and is referred to as the "law of rational indices." C. E. Weiss proposed determination of crystal planes

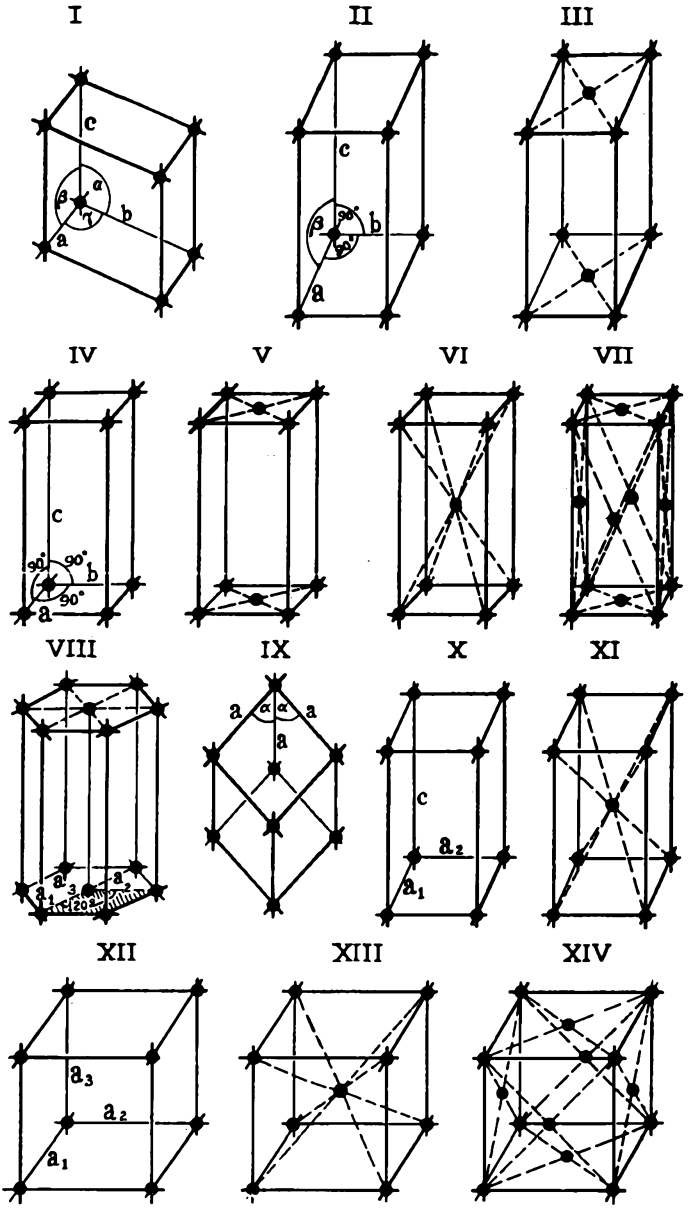

Fig. 7.2. Space lattices: I. Triclinic; II. Simple monoclinic; III. End-face centered monoclinic; IV. Simple rhombic; V. End face centered rhombic; VI. Body centered rhombic; VII. Face centered rhombic; VIII. Hexagonal; IX. Rhombohedral; X. Simple tetragonal; XI. Body-centered tetragonal; XII. Simple cubic; XIII. Body-centered cubic; XIV. Face-centered cubic. *(By permission from "Applied X-Rays" by G. L. Clark. Copyright 1940. McGraw-Hill Book Company, Inc.)*

by their intercepts x, y, and z with the axes where X, Y, and Z are measured in cm. There is nothing wrong with this procedure and it uniquely defines the planes. Calculations of interplanar distances, however, require the use of numbers which are proportional to the reciprocals of the Weiss intercepts.

This led to the universal adoption among crystallographers of indices proportional to $1/x$, $1/y$, and $1/z$, introduced by Grassman and later W. H. Miller (1839), whose name they bear. The "Miller Indices," h, k, and l, are the three smallest integers proportional to a/x, b/y, and c/z,

TABLE 7.1. SPACE LATTICES AND CRYSTAL SYSTEMS

Crystal System	Space Lattice	Coordinate Data
I. Triclinic (anorthic)	1. Simple	$a \neq b \neq c$; $\alpha \neq \beta \neq \gamma \neq 90°$
II. Monoclinic	2. Simple 3. End face-centered	$a \neq b \neq c$; $\alpha = \gamma = 90°$; $\beta \neq 90°$
III. Rhombic (orthorhombic)	4. Simple 5. End face-centered 6. Body-centered 7. Face-centered	$a \neq b \neq c$; $\alpha = \beta = \gamma = 90°$
IV. Hexagonal	8. Simple 9. Rhombohedral	$a = b \neq c$; $\alpha = \beta = 90°$; $\gamma = 120°$
V. Tetragonal	10. Simple 11. Body-centered	$a = b \neq c$; $\alpha = \beta = \gamma = 90°$
VI. Cubic (isometric)	12. Simple 13. Body-centered 14. Face-centered	$a = b = c$; $\alpha = \beta = \gamma = 90°$

respectively. When an index is taken in a negative direction along an axis, a minus sign is placed over it, i.e., $(\bar{1}00)$. Fig. 7.3 shows typical sets of parallel planes in a cubic lattice identified by their "Miller Indices."[3] Thus, a plane intersecting the X-axis at unit distance from the origin and parallel to the Y and Z axes has intercepts 1, ∞, and ∞, and the indices are then 1, 0, 0, usually written as (100). The planes that diagonally bisect the cube faces are (110), (101), and (011). A single specific plane or crystal face is usually designated by parentheses, thus (100); a family of equivalent planes, also called "form," by $\langle 100 \rangle$ or 100. If the faces of a crystal are completely developed, then the "form" is designated $\{100\}$. A crystal in the cubic system will have the form $\{100\}$, cubic shape, where $\{100\} = (100) + (010) + (001) + (\bar{1}00) + (0\bar{1}0) + (00\bar{1})$, or $\{111\}$, an octahedron.

The indices of a direction are defined in a different way and are written in square brackets, thus $[uvw]$; u, v, and w are the smallest integers of

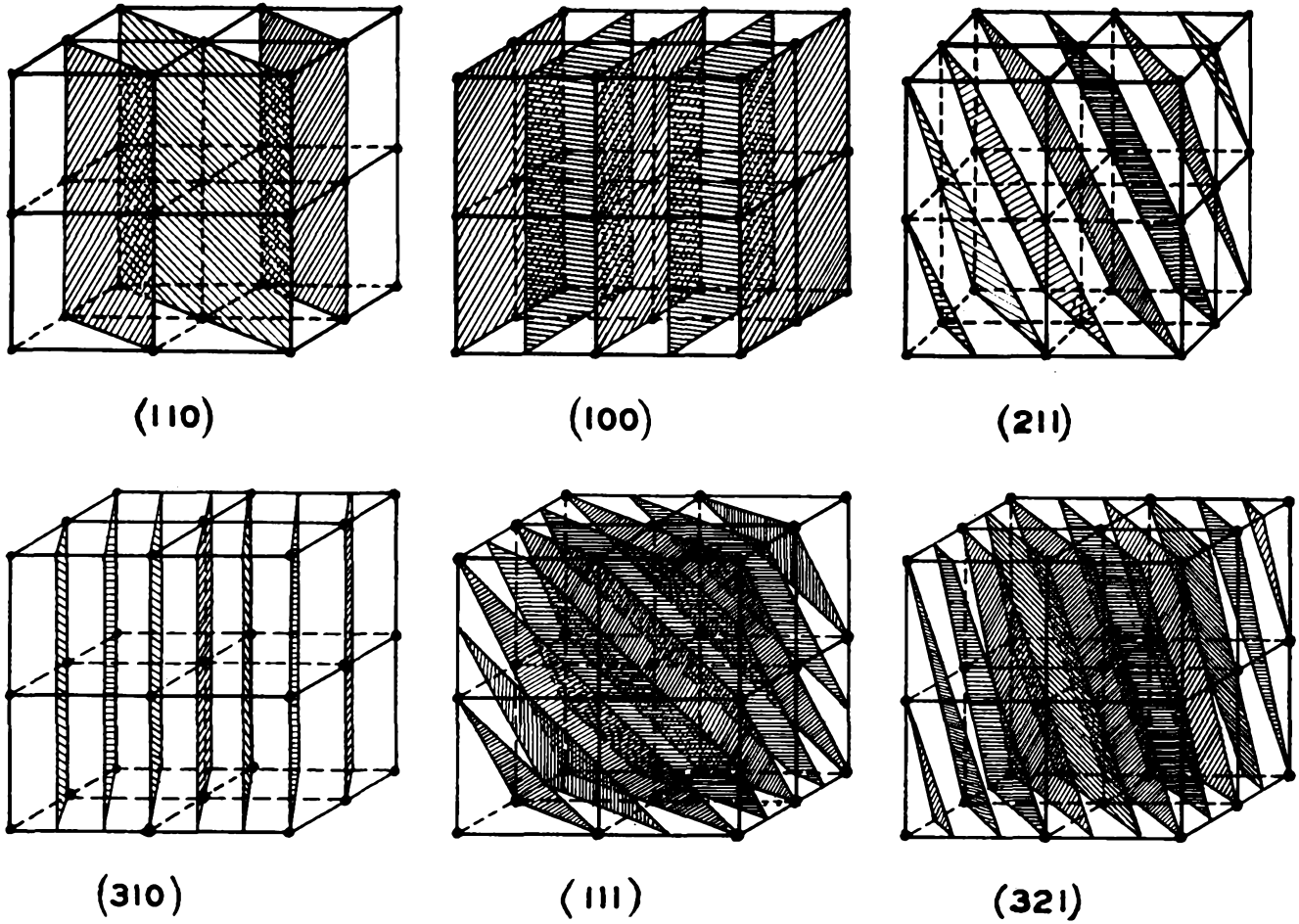

Fig. 7.3. Typical sets of parallel planes in a cubic lattice. *(By permission from "Applied X-Rays" by G. L. Clark. Copyright 1940 McGraw-Hill Book Company, Inc.*

multiple displacement along the axis in terms of the unit-cell distances a, b, and c. They define a desired point in the lattice and, together with the origin, define the direction. The X-axis has indices [100], the Y-axis [010], and the Z-axis [001]. Reciprocals are thus not used in defining indices of a direction. It so happens that for all planes in the cubic system and a few planes in the tetragonal system the direction indices coincide with the normal to the plane with the same indices. This is not true of other systems.[4] Fig. 7.4 shows examples of planes and directions in a cubic lattice.[3]

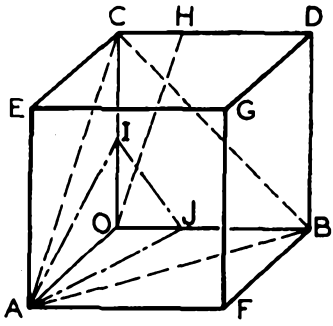

Fig. 7.4. Directions and planes in cubic lattice. Direction OA, (100); Direction OD, (011); Direction OG, (111); Direction OH, (013); Plane AEGF, (100); Plane ABDE, (110); Plane ABC, (111); Plane AIJ, (132). *(By permission from "Applied X-Rays" by G. L. Clark. Copyright 1940. McGraw-Hill Book Company, Inc.)*

For specifying planes and directions in the hexagonal system the Miller-Bravais four-number indices rather than the three-number "Miller Indices" are used by some authors. Their derivation and meaning are the same as those used for "Miller Indices," but they refer to the four axes a_1 a_2 a_3 c (Fig. 7.2). A plane in the hexagonal system will be represented by $(hkil)$, where the first three indices will always be related by the equation

$$i = -(h + k) \tag{7.1}$$

Sometimes the third index is replaced by a dot, thus $(hk \cdot l)$. The "Miller-Bravais Indices" are illustrated in Fig. 7.5.[4]

The classification of crystals, according to their geometry, is not sufficient to distinguish between apparently identical structures. These structures, however, show differences in regard to such properties as velocity of solution of different crystal faces; appearance of etch-figures; values of birefringence, optical activity, and piezo- and pyroelectric properties; formation of adsorption centers; electronic work function, etc. This behavior is caused by different symmetries, 32 classes of which were established in 1830 by J. F. C. Hessel. These are described by a code and, together with the crystal indices h, k, and l, permit the positive identification of a given space lattice with the aid of x-ray analysis. It would lead us too far afield here, to go into the details of this technique.

Altogether, there are 230 possible space groups which are classified by their symmetry characteristics.

Why a particular space lattice is chosen by a given element or compound in preference to any other is, of course, an intriguing question. The theory of solids is concerned with this problem. The size of the atom and the electronic configuration in its outer shells, more than anything else, seem to determine the final architecture of the solid. The realization of this factor led to a revision of the concept of the molecule as a structural entity in the solid state. For a long time this was overemphasized by chemists. The space lattice, through which atoms are regularly dis-

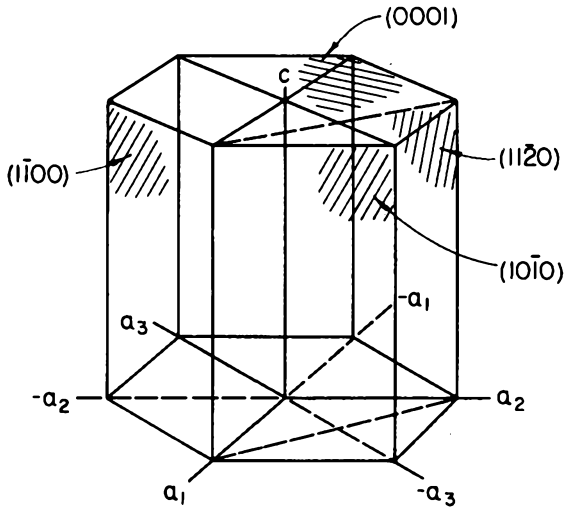

Fig. 7.5. Miller-Bravais indices of some planes in a hexagonal crystal. (*By permission from Structure of Metals by C. S. Barrett.*[4] *Copyright 1943. McGraw-Hill Book Company, Inc.*)

tributed, represents a continuously varying periodic force field to which the valence electrons are subjected. The evaluation of this interplay of forces by the methods of wave mechanics resulted in some valuable correlation of theory and fact, but much remains to be done.

The "model" introduced by Bohr for the structure of the atom was characterized by the then arbitrary assumption of discrete orbits in which electrons could revolve about the central nucleus of positive charge Ze, where Z is the atomic number and e the charge of the electron. To balance the nuclear charge the number of orbital electrons is Z, thus giving a neutral atom. In "assembling" an atom and bringing in an electron from an infinite distance energy is gained on approach of the positive core so that the electron has a negative potential energy within

the confines of the atom. This is a matter of terminology since positive potential is defined as the work done in bringing a positive unit charge from an infinite distance to the proximity of a positive charge. Orbital electrons are thus most stable in the ground state (i.e., closest to the nucleus), and the energy in the stable state is minimum. Therefore, negative potential energy of the electron in the atom signifies attraction to the nucleus due to coulomb forces. On still further approach to the nucleus other forces come into play which make for repulsion. A positive

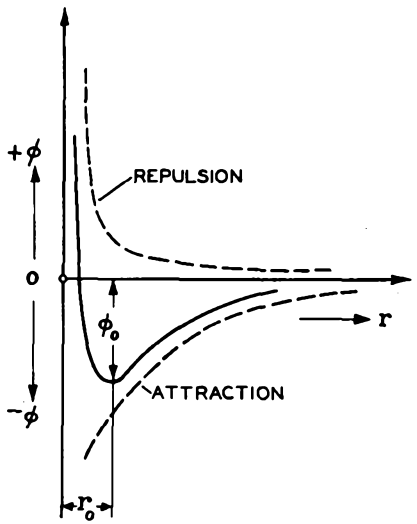

Fig. 7.6. Schematic representation of potential function between electron and nucleus.

component of potential energy thus appears so that the total potential field is given by the sum

$$\varphi(r) = -\frac{a}{r^m} + \frac{b}{r^n}$$

where a, b, m, and n are constants and r signifies the distance from the nucleus. Fig. 7.6 gives a representation of the two components and the resultant potential as a function of the distance r from the nucleus. The potential minimum is located at a critical distance r_0, where the electron will reside in its stable ground state and revolve about the nucleus. As there is more than one electron associated with the atom, Bohr's model distributed the electrons in a number of approximately concentric orbits of increasing radii and it was found necessary to limit the permissible population density in any one orbit. This is expressed by Pauli's Exclusion Principle. In the modern theory of wave mechanics these and other rules, which regulate the behavior of the electrons in the free atom, are

a natural consequence of basic assumptions and their former arbitrariness disappears. The reader is referred to the excellent treatise by Hume-Rothery[5] for further study.

The possible energy states of the electrons in the atom are expressed by the four quantum numbers n, l, n_l, and m_s. Of these, n is the principal quantum number which may assume values $n = 1, 2, 3$, etc.; it signifies the energy of the electron in the particular state in question. It turns out that the energy of a state given by n is proportional to $1/n^2$. The second quantum number l is a measure of the angular momentum $r \times m \times v$ of the electron, and it may assume values from 0 to $(n - 1)$ in whole integers. The case corresponding to $l = 0$ is not to be regarded as one where the electron is at rest, but rather as one for which motion in one direction is as likely as motion in the other direction along the orbit. The letters s, p, d, f, g, and h have been introduced to signify $l = 0, 1, 2, 3, 4, 5$. These letters are preceded by a figure indicating the value of n, and a small superscript outside of parentheses indicates the number of electrons occupying this state. Thus $(1s)^2$ describes two electrons for which $n = 1$, $l = 0$, and refers to the helium atom. This description is incomplete, however, since four quantum numbers are required for a complete specification of the orbital state, as pointed out above. To assume that more than one electron can have the same energy state in an atom would also contradict Pauli's Exclusion Principle. The quantum numbers n_l and m_s provide this differentiation. The quantum number n_l is a measure of the component of the angular momentum in a particular direction, which may be taken to be that of an externally applied magnetic field. The value of n_l may be from $+l$ to $-l$, including zero, and it is referred to as the magnetic quantum number.

The fourth quantum number m_s is also called the "spin quantum number," and may have the value $\pm\frac{1}{2}$, expressed in units of $h/2\pi$.* The word "spin" implies that the electron is assumed to rotate about its own center, and it may do so in either direction thus forming a magnetic pole. Table 7.2 gives a listing of the first two quantum numbers n, l for all elements. These two characterize the energy states in a first approximation. Chlorine would thus be described by $(1s)^2$, $(2s)^2$, $(2p)^6$, $(3s)^2$, and $(3p)^5$. The first orbit ($n = 1$) is fully occupied when two electrons (with opposite spins) are present. The second orbit ($n = 2$) cannot contain more than 8 electrons, the third orbit ($n = 3$) not more than 18, and, in general terms, for any energy state n not more than $2n^2$. For any value of l associated with a state n the maximum population is $2(2l + 1)$ so that s^2, p^6, d^{10}, and f^{14} are obtained. While it is the general tendency of the atoms to fill their shells in sequence, there are a few cases where d or f electrons are captured before p shells are completed (Table

* $h/2\pi = \hbar$.

TABLE 7.2. ATOMIC STRUCTURES

Element and Atomic Number	Principal and Secondary Quantum Numbers									
$n =$	1	2		3			4			
$l =$	0	0	1	0	1	2	0	1	2	3
1 H	1									
2 He	2									
3 Li	2	1								
4 Be	2	2								
5 B	2	2	1							
6 C	2	2	2							
7 N	2	2	3							
8 O	2	2	4							
9 F	2	2	5							
10 Ne	2	2	6							
11 Na	2	2	6	1						
12 Mg	2	2	6	2						
13 Al	2	2	6	2	1					
14 Si	2	2	6	2	2					
15 P	2	2	6	2	3					
16 S	2	2	6	2	4					
17 Cl	2	2	6	2	5					
18 A	2	2	6	2	6					
19 K	2	2	6	2	6		1			
20 Ca	2	2	6	2	6		2			
21 Sc	2	2	6	2	6	1	2			
22 Ti	2	2	6	2	6	2	2			
23 V	2	2	6	2	6	3	2			
24 Cr	2	2	6	2	6	5	1			
25 Mn	2	2	6	2	6	5	2			
26 Fe	2	2	6	2	6	6	2			
27 Co	2	2	6	2	6	7	2			
28 Ni	2	2	6	2	6	8	2			
29 Cu	2	2	6	2	6	10	1			
30 Zn	2	2	6	2	6	10	2			
31 Ga	2	2	6	2	6	10	2	1		
32 Ge	2	2	6	2	6	10	2	2		
33 As	2	2	6	2	6	10	2	3		
34 Se	2	2	6	2	6	10	2	4		
35 Br	2	2	6	2	6	10	2	5		
36 Kr	2	2	6	2	6	10	2	6		

TABLE 7.2. ATOMIC STRUCTURES. (*Continued*)

Element and Atomic Number	Principal and Secondary Quantum Numbers										
$n =$	1	2	3	4				5			6
$l =$				0	1	2	3	0	1	2	0
37 Rb	2	8	18	2	6			1			
38 Sr	2	8	18	2	6			2			
39 Y	2	8	18	2	6	1		2			
40 Zr	2	8	18	2	6	2		2			
41 Cb	2	8	18	2	6	4		1			
42 Mo	2	8	18	2	6	5		1			
43 Tc	2	8	18	2	6	6		1			
44 Ru	2	8	18	2	6	7		1			
45 Rh	2	8	18	2	6	8		1			
46 Pd	2	8	18	2	6	10					
47 Ag	2	8	18	2	6	10		1			
48 Cd	2	8	18	2	6	10		2			
49 In	2	8	18	2	6	10		2	1		
50 Sn	2	8	18	2	6	10		2	2		
51 Sb	2	8	18	2	6	10		2	3		
52 Te	2	8	18	2	6	10		2	4		
53 I	2	8	18	2	6	10		2	5		
54 Xe	2	8	18	2	6	10		2	6		
55 Cs	2	8	18	2	6	10		2	6		1
56 Ba	2	8	18	2	6	10		2	6		2
57 La	2	8	18	2	6	10		2	6	1	2
58 Ce	2	8	18	2	6	10	1	2	6	1	2
59 Pr	2	8	18	2	6	10	2	2	6	1	2
60 Nd	2	8	18	2	6	10	3	2	6	1	2
61 Pm	2	8	18	2	6	10	4	2	6	1	2
62 Sm	2	8	18	2	6	10	5	2	6	1	2
63 Eu	2	8	18	2	6	10	6	2	6	1	2
64 Gd	2	8	18	2	6	10	7	2	6	1	2
65 Tb	2	8	18	2	6	10	8	2	6	1	2
66 Dy	2	8	18	2	6	10	9	2	6	1	2
67 Ho	2	8	18	2	6	10	10	2	6	1	2
68 Er	2	8	18	2	6	10	11	2	6	1	2
69 Tm	2	8	18	2	6	10	12	2	6	1	2
70 Yb	2	8	18	2	6	10	13	2	6	1	2
71 Lu	2	8	18	2	6	10	14	2	6	1	2
72 Hf	2	8	18	2	6	10	14	2	6	2	2

TABLE 7.2. ATOMIC STRUCTURES. (*Continued*)

Element and Atomic Number	Principal and Secondary Quantum Numbers										
$n =$ $l =$	1	2	3	4	5 0	1	2	6 0	1	2	7 0
73 Ta	2	8	18	32	2	6	3	2			
74 W	2	8	18	32	2	6	4	2			
75 Re	2	8	18	32	2	6	5	2			
76 Os	2	8	18	32	2	6	6	2			
77 Ir	2	8	18	32	2	6	7	2			
78 Pt	2	8	18	32	2	6	8	2			
79 Au	2	8	18	32	2	6	10	1			
80 Hg	2	8	18	32	2	6	10	2			
81 Tl	2	8	18	32	2	6	10	2	1		
82 Pb	2	8	18	32	2	6	10	2	2		
83 Bi	2	8	18	32	2	6	10	2	3		
84 Po	2	8	18	32	2	6	10	2	4		
85 At	2	8	18	32	2	6	10	2	5		
86 Em	2	8	18	32	2	6	10	2	6		
87 Fr	2	8	18	32	2	6	10	2	6		1
88 Ra	2	8	18	32	2	6	10	2	6		2
89 Ac	2	8	18	32	2	6	10	2	6	1	2
90 Th	2	8	18	32	2	6	10	2	6	2	2
91 Pa	2	8	18	32	2	6	10	2	6	3	2
92 U	2	8	18	32	2	6	10	2	6	4	2
93 Np	2	8	18	32	2	6	10	2	6	5	2
94 Pu	2	8	18	32	2	6	10	2	6	6	2
95 Am	2	8	18	32	2	6	10	2	6	7	2
96 Cm	2	8	18	32	2	6	10	2	6	8	2
97 Bk	2	8	18	32	2	6	10	2	6	9	2
98 Cf	2	8	18	32	2	6	10	2	6	10	2

7.2). Elements which follow this pattern are called "transition elements." They include scandium (21) to nickel (28) in the first long period, yttrium (39) to palladium (46) in the second, and lanthanum (57) through the rare earths to platinum (78) in the third. The completed shells are of great stability and the chemical behavior of the elements is largely determined by the valence electrons in the uncompleted shells. For the chlorine atom cited above the valence electrons are $(3s)^2(3p)^5$, or seven in all, in addition to the 10 electrons in completed shells. A schematic representation of orbital energy levels of an atom is shown in Fig. 7.7a and, in a similar manner, that for the valence electrons of the Na-atom in Fig. 7.7b.[6]

In spectroscopy the various electron shells of an atom are designated by the letters K, L, M, N, O, P, and Q, corresponding to values $n = 1$,

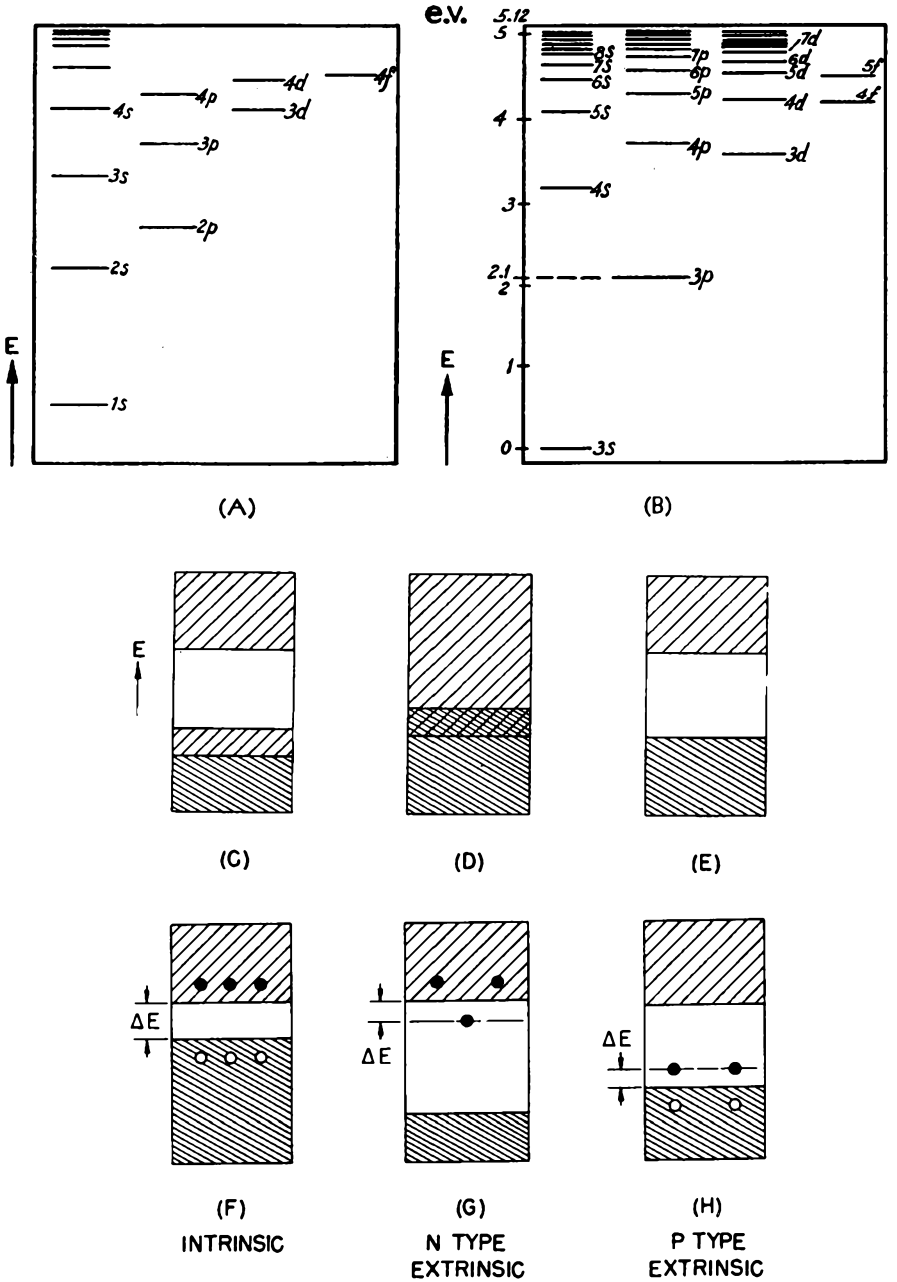

Fig. 7.7. Energy levels of electrons in an atom. (A) Schematic; (B) Sodium atom. After Wagener.[7] (*Courtesy Verlag Johann Ambrosius Barth, Leipzig*). (C–H) The Band Theory of solids.[6b] (*Courtesy National Bureau of Standards.*)

2, 3, 4, 5, 6, 7. The electronic structure of copper, for example, may be expressed in this terminology as (2), (8), (18), and (1), which means that there are 2 electrons in the K-shell, 8 electrons in the L-shell, and so on. The resultant total angular momentum of all electrons in an atom is assigned a quantum number $L = 0, 1, 2, 3, 4, 5$ which is denoted by S, P, D, F, G, H.

It should be emphasized at this point that the seemingly clear-cut arrangement of electrons into orbits applies to the free atom only. When atoms are "condensed" to liquids and solids, conditions become more complicated and interpenetration of orbits takes place which causes the sharply defined energy states of the free atoms, as described in line spectra, to broaden into band spectra characteristic of molecular compounds. Correspondingly, the energy level diagrams depicted in Figures 7a, b for the free atom, where distinct lines were drawn for the energy states of the electrons in the atom, now give place to energy bands for condensed atoms or solids. A word of caution is necessary so that too definite a picture of the electron orbits will not be associated with the free atom. The whole success of wave mechanics is based on the realization that electron orbits can only be described in terms of the probabilities of finding an electron at a given place at a given time. This probability is expressed by the square of the wave function ψ. The volume of space where the probability function is at its maximum is called the "orbital." Electron clouds surrounding the nucleus are a fair representation. These may have a mean average structure with a cloud density which varies throughout its volume and reaches a maximum where the orbits may then be visualized. The quantum numbers impose the condition that the energies in these idealized orbits are multiples of $h/2\pi$, where h is Planck's constant.

When energy is imparted to an atom by absorption of radiation or impact excitation, the energy state of the electrons will be raised and an equivalent amount of energy radiated when the electrons return to the ground state according to the relation

$$E = h\nu = E_2 - E_1 = \frac{hc}{\lambda} \tag{7.2}$$

Where E = energy absorbed and radiated
h = Planck's constant
ν = frequency
E_2 = energy of excited state
E_1 = energy of stable state
c = speed of light
λ = wave length of emitted radiation

The energy radiated may be expressed in a variety of ways: in ergs, electron volts, calories, or wave numbers. The wave number $1/\lambda$ gives

the number of waves per cm and equals ν/c, which results from the relation $c = \lambda\nu$. Table 7.3 gives a tabulation of the energy values per gram-molecule in terms of electron volt and Kg cal as a function of wave length λ, wave number $1/\lambda$, and frequency ν for the range of wave lengths from

TABLE 7.3. TABULATION OF ENERGY VALUES PER GRAM-MOLE IN TERMS OF ELECTRON-VOLTS AND KG-CALORIES AS A FUNCTION OF WAVELENGTH λ WAVE-NUMBER $1/\lambda$ AND FREQUENCY FOR VALUES OF λ FROM 0.1 μ TO 1.0 μ

Wave Number cm^{-1}	Wavelength $m\mu$	Frequency cycles/sec	Energy	
			kcal/g mole	e.V.
10,000	1,000	3.00×10^{14}	28.6	1.240
12,000	833.3	3.60×10^{14}	34.3	1.488
14,000	714.3	4.20×10^{14}	40	1.736
16,000	625	4.80×10^{14}	45.7	1.984
18,000	555.6	5.39×10^{14}	51.5	2.232
20,000	500	6.00×10^{14}	55.4	2.400
22,000	454.6	6.61×10^{14}	62.9	2.728
24,000	416.7	7.20×10^{14}	68.5	2.976
26,000	384.6	7.80×10^{14}	74.7	3.224
28,000	357.1	8.40×10^{14}	80	3.472
30,000	333.3	9.00×10^{14}	85.8	3.720
35,000	285.7	1.05×10^{15}	100	4.340
40,000	250	1.20×10^{15}	114.4	4.960
45,000	222.2	1.35×10^{15}	128.7	5.580
50,000	200	1.50×10^{15}	143	6.200
55,000	181.8	1.65×10^{15}	157	6.820
60,000	166.7	1.80×10^{15}	171.4	7.440
65,000	153.8	1.95×10^{15}	186	8.060
70,000	142.9	2.10×10^{12}	200	8.680
75,000	133.3	2.25×10^{15}	214	9.300
80,000	125	2.40×10^{15}	228.6	9.920
85,000	117.6	2.55×10^{15}	243.4	10.540
90,000	111.1	2.70×10^{15}	257.1	11.160
95,000	105.3	2.84×10^{15}	271.5	11.780
100,000	100	3.00×10^{15}	286	12.400

0.1μ to 1.0μ. In terms of the level from which the electron has been excited one also speaks of K, L, M radiation respectively.

The Band Theory of Solids

The band theory has proven to be a very powerful tool in the understanding of the behavior of solids. It was developed by a number of investigators, most notably Bloch, Peierls, Bethe, Wilson, Wigner, Slater, Mott, Jones and Seitz.*

* The following summary of the band theory has been composed from References 6a and 6b.

"Each band contains as many states as there are unit cells in the crystal and is usually several electron volts in width. In a sense there is a close correspondence between the individual bands, regarded as units, and the atomic or molecular levels. The bands can be regarded as if derived from the atomic levels by the spreading of the latter as the atoms overlap to form a solid. The bands of levels may be separated from one another, in which case the total spectrum consists of quasi-continuous regions separated by gaps, or forbidden regions as shown in Figure 7.7.c.* Here the lower allowed band of energies is only partly filled, and there are allowed states available to an electron, differing only slightly in energy from those already occupied. If an electric field is applied to a solid with this band structure, an electron at the top of the filled states may acquire enough energy from the electrical field to enter one of the empty, allowed states above it and become free to move under the influence of the field. This is the mechanism of electrical conduction in a crystal which applies to alkali metals where only one valence electron exists in an outer s state. As two electrons may be in the same s state, the band is just half full. Figure 7.7.d illustrates the condition where the bands may overlap one another, to a greater or lesser extent, in which case the spectrum is quasi-continuous, starting with the bottom of the lowest band and continuing upward. Such a condition is believed to be typical of the alkaline earth metals. The s band is completely filled, as there are two s electrons, but the p band of next higher energy overlaps the s band so that an electron may be accelerated by an external field as before. The alkaline earth metals are thus electrically conductive. On the other hand, the case in which the bands are separated by gaps (Figure 7.7.e) and in which the electrons occupy a set of bands completely in such a way that the top of the occupied region coincides with the top of one of the bands, which is separated by a forbidden region from the next band, corresponds to an insulator. In this case, a strong field is required to excite any of the electrons and make the system conducting, much as in the case of a dense gas. The behavior of semi-conductors may be explained with the aid of the band concept as suggested by A. H. Wilson. Three possible cases are represented in Figures 7.7.f, g, h. An intrinsic semi-conductor, one that behaves as a semi-conductor even when no impurities are present (Figure 7.7.f) has an energy gap ΔE comparable to kT between the completely filled band and an empty allowed band, so that electrons may be thermally excited from the filled to the empty band. When this happens, not only are the excited electrons accelerated by the field, but, since there are now a few empty allowed states in the normally filled band, the remaining electrons may be accelerated as well. The situation is analogous to a filled checkerboard on which no moves are possible until a piece is removed. This mechanism, in which the electron vacancy behaves like an electron with an effective positive charge, is known as "hole" conduction. Such intrinsic semi-conduction is usually only found at rather elevated temperatures.

"Most semi-conductors depend for their conductivity on impurities within the crystal lattice; these are called extrinsic semi-conductors. Figure 7.7.g indicates a possible effect of adding an impurity to a crystal that would normally be an insulator. The foreign atoms introduce new isolated energy levels into the band diagram. In Figure 7.7.g, these levels are at a small distance ΔE below the empty band. If ΔE is comparable to kT, the foreign atoms may ionize and provide electrons in the conduction band. Impurities of this sort are called *donors*. This material is thus an n-type semi-conductor, which indicates that the sign of the charge carriers is negative. The third type of semi-conductor, illustrated in Figure 7.7.h, is the converse of that just described. The impurity levels are close to the filled band, and may be ionized by accepting an electron from the filled band leaving a hole in that band. Conduction is then by holes, and the name p-type indicates the positive sign of the charge carriers.

*p. 158.

Impurities of this sort are known as *acceptors*. New levels or irregularities may be introduced into the characteristic bands of the perfectly regular, ideal crystal, not only by foreign impurities or excess atoms of one constituent of the crystal, but also by the presence of free surfaces and lattice defects. Such disturbances may be effective as electron traps and have a great influence on conductivity.

"The band theory thus explains the fact that many materials have properties intermediate between those of ideal insulators and ideal metals.. Solids of this kind, such as bismuth, graphite, silicon and germanium, correspond to cases in which the bands either overlap by a very small amount, so that the materials are metals with poor conducting properties (bismuth and graphite), or are insulators with poor insulating properties (silicon and germanium)."

The Classification of Crystals According to the Prevailing Bond

Depending on the type of force field active in the crystal lattice solids are classified into the following four groups which overlap in many cases but nevertheless serve as a guide for discussion.[7]

(1) Metals
(2) Ionic or heteropolar crystals
(3) Valence or homopolar crystals
(4) Molecular crystals

To these are added the three intermediate types suggested by Bernal:

(1) Silicates
(2) Layer lattices
(3) Metalloids

A classification of the crystals according to Bernal[8] is given in Table 7.4. If only one type of bond is present or clearly predominates in a crystal, the latter is said to have a homodesmic structure; if several bond types prevail, a heterodesmic structure. When several bond types are present, the weakest determines the crystalline character. According to Pauling,[9] there is a bond between two or more atoms when forces exist which tend to form an aggregate that is sufficiently stable to be identified experimentally as a molecule.

The metallic bond, which is responsible for the cohesion of metals and gives rise to the crystal structures associated with metals, is characterized by considerable flexibility. It is nondirectional, and disturbances set up in the lattice are readily healed. This results in malleability and an ability to anneal or stress-relieve. The high coordination number of close-packed structures, eight and twelve for B.C.C. and C.P.H., respectively, precludes the assumption of a covalent bond (see below), and a bond type specially suited to metals had to be introduced. According to the model suggested by H. A. Lorentz in 1916 and quantitatively refined by modern concepts of quantum mechanics the metal lattice consists of close-packed positive metal ions with free electrons moving in the interstices of the lattice. These valence electrons cause high electrical conductivity in the presence of an externally applied electric

TABLE 7.4. CLASSIFICATION OF CRYSTALS*

Crystal Type	Crystal Units	Type of Binding	Characteristic Properties				Typical Crystals
			Optical	Electrical	Thermal	Mechanical	
Ionic	Simple and complex ions	Electrical attraction between ions of opposite signs (e/r^2) balanced by repulsion of negative outer shells	Transparent; absorption in visible (color) if present, is due to atoms; in short infrared due to complex ions; in long infrared due to crystal lattice	Moderate insulators; in high fields conduct by transfer of ions. When polarization is slight they dissolve with ionization in ionizing solvents (water); when stronger they are insoluble	Fairly high melting point; ionization occurs in liquid and vapor	Hardness increasing with high ionization. Tendency to fracture by cleavage	NaCl CaF_2 $CaCO_3$ K_2SO_4 $(NH_4)_2PtCl_6$
Silicate	O^{2-} or F^- ions Sc^{4+} or Be^{2+} or Al^{3+} and other positive ions	$\left(\frac{-e}{r^9}\right)$ Weak to moderate polarization	Refractivity due to positive ions		Very high melting points, glasses formed on cooling of melt	Very hard with tendency to cleave or fracture conchoidally	Olivine, Mg_2SiO_4 Cyanite, Al_2SiO_5 Garnet, $RII_3RIII_2Si_3O_{12}$ Spinel, Al_2MgO_4 Corundum, Al_2O_3
Homopolar (covalent)	Atoms of the fourth group and groups on either side of it	Homopolar bonds throughout or strongly polarized ionic binding	Transparent with high refractivity or opaque metalloidal	Diamond is a perfect insulator. The others conduct metalloidally. Very insoluble	Very high melting points with tendency to vaporize except in more metalloidal types	Very hard, hardness less for metalloidal types	Diamond, C Zinc Blende, ZnS Wurtzite, ZnS Carborundum, CSi
Molecular van der Waals	Inert gas atoms. Non-polar and polar molecules	van der Waal's forces or residual electric fields between molecular poles	Transparent optical properties due to molecules and similar to gas and liquid phases	Insulators except when very polar; soluble in non-ionizing (molecular) solvents except when polar	Melting point very low with neutral atoms, rises with heavier molecules and polar molecules	Very soft, hardness increasing with polarity of molecules. Deformation plastic	Argon, A CO_2 Ice H_2O Paraffins, C_nH_{2n+2} Calomel, Hg_2Cl_2
Layer	Strongly polarizing and easily polarized ions	In layers, homopolar or polarized ionic. Between layers, molecular	As homopolar	Various, similar to both molecular and homopolar	Various, similar to both molecular and homopolar	Cleaving readily in layers which are soft and flexible	Graphite, C CdI_2
Metallic	Positive ions and electron gas	Electrical attraction between positive ions and electron gas	Opaque (due to free electrons) with selective reflection in infrared	Conductors, conductivity inversely proportional to number of free electrons. Soluble in acids where H^+ ions absorb free electrons	Moderate to very high melting points. Long liquid interval	Moderate hardness increased by alloying. Elastic but yield by glide plane slipping when overstressed	Copper, iron Iron, Sodium Zinc
Metalloidal	Metal atoms and atoms of the sulfur and arsenic type	Mixture of homopolar ionic and metallic binding	Opaque metallic or transparent with high refractivity and color	Medium to bad conductors. Soluble only with decomposition	Tendency to vaporize or decompose at high temperatures	Moderately hard to soft. Properties a mixture of those of other types	Nickel arsenide NiAs Fahlertz, RII_2SbS_3 Pyrites, FeS_2

* After J. D. Bernal,[8] X-Rays and Crystal Structure, Encyclopedia Brittannica and G. L. Clark.[3] (*By permission of the editor, Encyclopedia Brittannica, Inc.*)

field, and also account for thermal conductivity, low *para*-magnetic properties, high values of heat capacities, and the optical properties of metals. It is noteworthy, as shown in Table 7.5,[9] that metals prefer one of three crystal structures, making for more or less dense packing of the atoms. These are:

A1 Face-centered cubic (F.C.C.)
(Cubic closest packed)
A2 Body-centered cubic (B.C.C.)
A3 Hexagonal close packed (H.C.P.)
A4 Diamond cubic (D.C.)

Below the symbols A1, A2, and A3 in Table 7.5 is given the smallest interatomic distance in Angstrom units, followed by the coordination number, in parenthesis, which indicates the number of equidistant neighboring atoms. Some metals may crystallize in more than one form, and are called "polymorphic." The interatomic distance indicates when two atom centers are closest, and the atomic radius is half this value. This closest possible approach is dictated by the forces at play between the atoms, and the atomic radii given for a crystal lattice are not identical with those applying to free atoms although the difference is small. In an accumulation of free atoms, such as encountered in a gas, the approach of two atoms may be depicted as in Fig. 7.8. where the electron cloud densities associated with the orbits are plotted against the distance of approach between two neighboring atoms. In a crystal lattice, such as a metal, this approach is much closer so that the two curves representing cloud densities overlap to a greater extent (Fig. 7.8).[20] This leads to a continuous re-assignment or exchange of the valence electrons between adjacent ions so that the so-called covalent bond* is established which is responsible for the cohesion of the lattice. One might look upon the ion lattice as being held together by attractions to the common system of negatively charged electrons. The theory of the metallic bond is by far the most difficult of the various bond types, and no satisfactory treatment of all its aspects has so far been evolved.

The cohesion of monatomic metals finds an expression in the heat of sublimation L, which is the energy required to dissociate one mole of a substance into free atoms. Table 7.6 gives values compiled by Bichowsky and Rossini,[10] where L is expressed in kg cal/mole at room temperature. Values set in parenthesis have been estimated by Seitz with the aid of Trouton's Rule, which gives a relation between L and the boiling temperature T_b in K°.

$$L = 0.0235T_b \tag{7.3}$$

It is apparent from Table 7.6 that the "transition elements" (i.e., those with d-shells only partly filled) have higher cohesion, on the whole, than

* This term is used here in a broader sense according to Pauling.

TABLE 7.5. THE STRUCTURE OF CRYSTALS OF METALLIC ELEMENTS*

Li 3 A2 3.04(8)	Be 4 A3 2.224(6) 2.268(6)												
Na 11 A2 3.72(8)	Mg 12 A3 3.190(6) 3.202(6)	Al 13 A1 2.858(12)											
K 19 A2 4.618(8)	Ca 20 A1 3.932(12) A3 3.940(6) 3.955(6)	Sc 21	Ti 22 A3 2.915(6) 2.953(6)	V 23 A2 2.627(8)	Cr 24 A2 2.493(3) A3 2.709(6) 2.717(6) A12	Mn 25 A6 2.582(8) 2.669(4) A12 A13	Fe 26 A1 2.520(12) A2 2.478(8)	Co 27 A1 2.506(12) A3 2.499(6) 2.507(6)	Ni 28 A1 2.487(12) A3 2.49(6) 2.49(6)	Cu 29 A1 2.551(12)	Zn 30 A3 2.660(6) 2.907(6)	Ga 31 A11 2.437(1) 2.706(2) 2.736(2) 2.795(2)	Ge 32 A4 2.445(4)
Rb 37 A2 4.87(8)	Sr 38 A1 4.296(12)	Y 39 A3 3.595(6) 3.663(6)	Zr 40 A2 3.13(8) A3 3.166(6) 3.223(6)	Cb 41 A2 2.853(8)	Mo 42 A2 2.720(8)	Ma 43	Ru 44 A3 2.645(6) 2.699(6)	Rh 45 A1 2.684(12)	Pd 46 A1 2.745(12)	Ag 47 A1 2.884(12)	Cd 48 A3 2.973(6) 3.287(6)	In 49 A6 3.242(4) 3.370(8)	Sn 50 A4 2.80(4) A5 3.016(4) 3.175(2)
Cs 55 A2 5.24(8)	Ba 56 A2 4.343(8)	Rare Earths 57–71 See below	Hf 72 A3 3.139(6) 3.200(6)	Ta 73 A2 2.854(8)	W 74 A2 2.735(8) A15 2.816(12) 2.519(2) 2.816(4) 3.085(8)	Re 75 A3 2.735(6) 2.755(6)	Os 76 A3 2.670(6) 2.730(6)	Ir 77 A1 2.709(12)	Pt 78 A1 2.769(12)	Au 79 A1 2.878(12)	Hg 80 A10 2.999(6) 3.463(6)	Tl 81 A1 3.423(12) A3 3.404(6) 3.450(6)	Pb 82 A1 3.492(12)
			Th 90 A1 3.590(12)		U 92 A2 2.97(8) 2.75(2) 2.84(2) 3.25(4) 3.34(4)	Rare Earths							
							La 57 A1 3.754(12) A3 3.727(6) 3.754(6)	Ce 58 A1 3.637(12) A3 3.63(6) 3.65(6)	Pr 59 A3 3.638(6) 3.657(6)	Nd 60 A3 3.620(6) 3.657(6)		Er 68 A3 3.73(6) 3.74(6)	

* This table is taken in the main from the summary by M. C. Neuburger, *Z. Krist.* **93**, 1 (1936). The symbols A1 (cubic closest-packed arrangement), A2 (cubic body-centered arrangement), A3 (hexagonal closest-packed arrangement), A4 (diamond arrangement), etc., are those used in the Strukturbericht. The numbers below these symbols are the smallest interatomic distances (in A), followed by the number of corresponding neighboring atoms in parentheses.

"simple elements" (i.e., those with their *d*-shells either completely filled or completely empty).

Densities of metals can be calculated to a first approximation from known lattice constants obtained by x-ray analysis. This is shown below for copper (F.C.C.).[11] The cube length is 3.608 A.U. Fourteen atoms make up the lattice cell, if considered by itself, as the cube has 8 corners and 6 sides. A geometric cube, 3.608 A.U. on the side, represents

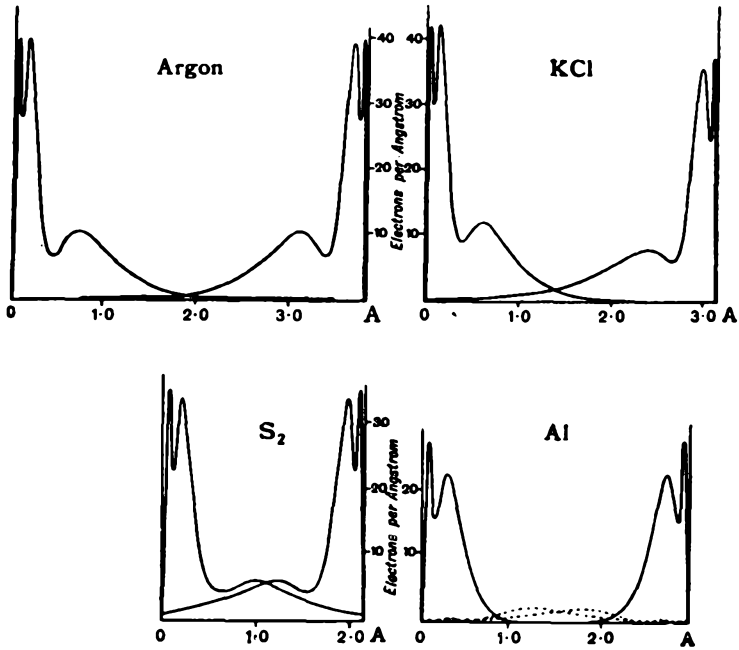

Fig. 7.8. The radial electron distribution in various atoms in relation to the interatomic distance in crystals. After W. L. Bragg[20] (*Courtesy The McMillan Company, London.*)

the unit cell which would cut through the corner atoms and contain $\frac{1}{8}$ atom within its volume at each corner, or a total of $8 \times \frac{1}{8} = 1$ corner atom. Likewise, the unit-cell boundary cuts in half the atoms at the face centers, and thus contains $6 \times \frac{1}{2} = 3$ face atoms within its volume. The total number of atoms contained within the copper unit cell is thus $1 + 3 = 4$. From this information a theoretical figure for the density of ideal copper can be obtained as follows. Density is mass per unit volume in grams per cc. As there are 4 atoms per unit cell, we have to weigh these atoms in grams and express the volume of the unit cell in cc. Avogadro's number gives us the number of atoms per mole; the atomic weight the number of grams per mole, and the volume of the unit cell

gives us the number of unit cells per cc so that the following transformation is obtained:

$$\text{Density} = 4\,\frac{\text{atoms}}{\text{cell}} \times \frac{1}{6.06 \times 10^{23}}\,\frac{\text{mole}}{\text{atom}} \times \frac{1}{(3.608 \times 10^{-8})^3}\,\frac{\text{cells}}{\text{cc}} \times 63.57\,\frac{\text{g}}{\text{mole}}$$
$$= 8.93\,\frac{\text{g}}{\text{cc}} \qquad (7.4)$$

This comes very close to the published density 8.96. Actual crystals may have lattice deformations and an impurity content which would affect the result of this idealized calculation.

TABLE 7.6. THE HEATS OF SUBLIMATION OF MONATOMIC METALS[10]
(In Kcal/mole at room temperature)

Monovalent Metals		*Divalent Metals*	
Li 39	Cu 81.2	Be 75	Zn 27.4
Na 25.9	Ag 68	Mg 36.3	Cd 26.8
K 19.8	Au 92	Ca 47.8	Hg 14.6
Rb 18.9		Sr 47	
Cs 18.8		Ba 49	
		Ra (72.7)	

Trivalent Metals		*Tetravalent Metals*		*Pentavalent Metals*
Al 55	Ga 52	Ti 100	Ge 85	As 30.3
Sc 70	In 52	Zr 142.15[10a]	Sn 78	Sb 40
Yt 90	Tl 40	Hf (> 72)	Pb 47.5	Bi 47.8
La 90		Th 177		

Transition Element Metals		
V 85	Nb (> 68)	Ta 185.5*
Cr 88	Mo 160	W 210
Mn 74	Ma	Re
Fe 94	Ru 120	Os 125
Co 85	Rh 115	Ir 120
Ni 85	Pd 110	Pt 127
	U 220	

* See Table 10.1.

A typical representative of the ionic bond is the sodium-chloride crystal (F.C.C.). Sodium has one valence electron and chlorine seven. The latter tends to acquire one additional electron to complete a shell of eight; this is provided by sodium, thus creating a positive Na ion (Na^+) and a negative Cl ion (Cl^-). These are held together by electrostatic forces of the coulomb type so that they decrease in distance from each other until the electron clouds overlap and repulsive forces establish a balance. The resulting molecules of Na^+Cl^- possess a rather large dipole moment, and the ionic bond is, therefore, also referred to as a "polar bond." The ionic crystals have responded to theoretical treatment because of the relative simplicity of the coulomb force field acting in the ionic lattice in spherical symmetry. Many of the ionic crystals show

close-packed structures and the lattice geometry is of course dictated by the relative sizes of the constituent atoms in a particular case.

The covalent bond, introduced by G. N. Lewis in 1916, is based on the concept that two atoms can share a pair of electrons. This is expressed in structure formulae by the following symbolism:

```
                                 H                                          H
                                 |                                          ..
                                 |                   ..   ..   ..
H—H, Cl—Cl, H—Cl, H—C—H or H : H, : Cl : Cl :, H : Cl :, H : C : H
                                 |                   ..   ..   ..
                                 H                                          H
```

The valence electrons which contribute to the bond formation are expressed by dots or a single dash, and the chemical symbol stands for the atomic nucleus together with its completed shells of orbital electrons. Thus, the diatomic chlorine molecule attains the stable 8-electron shell configuration by adding to its 7 valence electrons, borrowing one from its neighbor and in turn lending one of its seven so that both share two. Covalent bonds are common for the atoms of the 6th and 7th group of the periodic table. Double and triple bonds between two atoms can be represented in a similar manner, as follows:

```
H       H                  H  .     .H
 \     /                    : C ::  C :
  C=C        or →           H  '     'H
 /     \
H       H

H—C≡C—H      or →      H : C ::: C : H

N≡N          or →        : N ::: N :
```

The two electrons shared in the covalent bond must have opposite spins to satisfy Pauli's Exclusion Principle. When two hydrogen atoms approach each other, for example, the normal energy levels $(1s)^1$ of the respective atoms split into two states of slightly different energies, and the combination of these energy states for the molecule can lead either to an increase (repulsion) or a decrease (attraction) of the molecular potential energy. It may be assumed that the covalent bond depends on the sympathetic cooperation of the energy sublevels of the shared electrons. This leads to an exchange-energy release and resultant tight bonding. The term "resonance" is also used to describe this exchange effect. In its more restricted sense resonance bonds imply a continuous oscillation between two or more essentially different bond structures, such as between a covalent and an ionic bond in the case of H:H and H^+H^-. This contributes a further amount of binding energy.

The linking together of two atoms, and not more, by a hydrogen atom

is known as the hydrogen bond. It is largely ionic in character because of the electrostatic attraction of the proton to two anions. It is responsible for the characteristics of the water molecule.

Finally, there is another basic bond type which acts between molecules that may already be formed by covalent or ionic bonds and which leads to crystal structures in which the chemical identity of the molecules is clearly maintained. The SiO_2 lattice is an example. This molecular bond, or van der Waals bond as it is also called, arises between neutral atoms which are in such close proximity that their electron clouds are subject to long-range forces of interaction between the orbital electrons of the two clouds, respectively. By sympathetic resonance between electrons in the respective orbits "polarization forces" arise which lower the over-all potential proportional to $1/r^6$, and thus lead to attraction between the atoms or molecules concerned. These van der Waals forces are relatively weak in comparison to other bonding forces, but they are important in some crystal lattices and especially in surface phenomena. In the gaseous state fluorine and chlorine are bound by covalent bonds; in the solid state they are held by van der Waals forces in the crystal lattice. The low boiling points of the halides (F_2: -187; Cl_2: -34.6; Br_2: 58.78°C) are an indication of the loose bond. When the covalent bonds of higher-valent atoms are distributed among two neighboring atoms, very large molecules result which may take on the form of spiral structures, as in Se and S, or two-dimensional lattices, as in Sb. Four-valent atoms give rise to three-dimensional structures, exemplified by diamond, Si, Sn, and Ge, where each atom is at the center of a tetrahedron and the coordination number is four.

It has been suggested above that the size of the atoms and their relative distances from each other in a crystal lattice have a distinct bearing on the type of lattice developed in a solid crystal. This implies that each atom has a distinct size and that distinct distances are characteristic of the association of like or unlike atoms. The limitation of the concept of size was emphasized in the discussion of electron orbits. It must be added here that interatomic distances are not accurately fixed values for any given atom; they may change with the state of ionization and the type of bond involved. Nevertheless, the values given in Table 7.5 serve as a valuable guide in determining possible structures of metals and alloys. It is well known that the atomic volume is a periodic function of the atomic number Z throughout the table of elements. Interatomic distances in the crystals of the elements show a similar periodicity when plotted as a function of Z, as shown in Fig. 7.9 according to Hume-Rothery.[12] For pure-metal crystals these distances, d, result directly from the geometry of the crystal lattice as soon as the lattice parameter, a, has been found by x-ray analysis. Thus, the following is obtained:

$$\text{for a body-centered cube (B.C.C.): } d = \frac{a\sqrt{3}}{2}$$

$$\text{for a face-centered cube (F.C.C.): } d = \frac{a\sqrt{2}}{2}$$

$$\text{for a diamond-type lattice: } d = \frac{a\sqrt{3}}{4}$$

and somewhat more complicated expressions for more complex lattice structures.

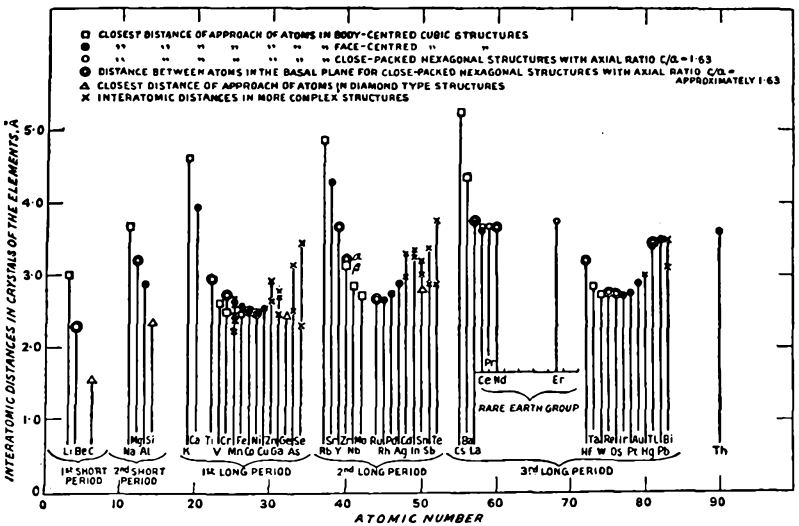

The Atomic Radii of the Elements

Fig. 7.9. The closest distances of approach of the atoms in the crystals of the elements. After Hume-Rothery.[12] (*Courtesy The Institute of Metals, London, England.*)

If solid solutions are formed between two metals, A and B, a distinction is made between "substitutional solid solutions" and "interstitial solid solutions." As the name implies, the added atom B takes the place of atom A in the parent lattice in the first type, and in the second type it leaves all A atoms in their places and pushes itself in between them. In both cases the addition of B is only possible if the atom is small enough to fit into the lattice pattern, either taking the place of an A-atom without crowding its neighbors or fitting into a void between neighbors. Hume-Rothery *et al.*[5] were able to show that solid solutions are likely to be formed when atoms A and B do not differ in size by more than from 14 to 15 per cent, while a greater difference militates against this likelihood. There are many restricting conditions to be considered in special cases, but as a working rule it is most valuable. Duwez[13] has published a chart which facilitates the application of this rule. It is reproduced as Fig. 7.10. From the explanatory notes we quote as follows:

"In this chart, the elements are arranged along a scale of atomic diameter. They are located on several horizontal lines, each corresponding to a given type of electron configuration in the atom. On the first line are the elements having one s electron and no d electrons (column I-A of the periodic table). On the second line are the elements having one s electron and a saturated d shell (column I-B of the periodic table). On the third and fourth horizontal lines are the elements having two s electrons without and with the outermost d shell saturated (columns II-A and II-B of the periodic table). The next four horizontal lines above the atomic diameter scale contain the elements having two s and one, two, three, and four p electrons, respectively (columns III-B, IV-B, V-B, and VI-B of the periodic table). Below the scale of

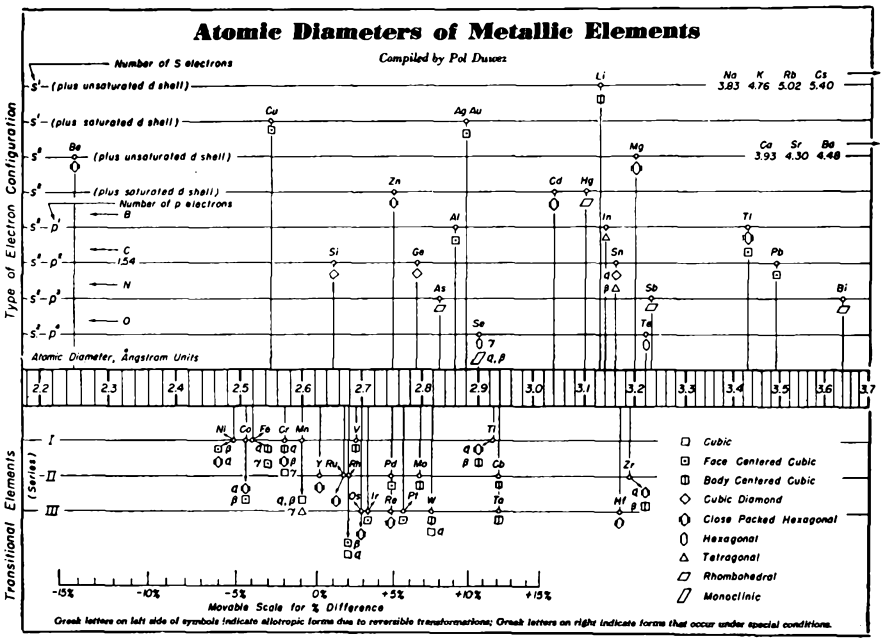

Fig. 7.10. Atomic diameters of metallic elements. After P. Duwez.[13] (*Courtesy of "Metal Progress" The American Society of Metals.*)

atomic diameters the transition elements have been arranged on three separate horizontal lines, corresponding to the three series of transition elements in the periodic table. It is readily seen that the vertical arrangement of the elements adopted here corresponds to what Hume-Rothery has called the 'alloying valence.' This valance is the number of s and p electrons for the elements above the scale, and is zero for the transition elements below the scale.

"The crystal structures of the elements are indicated on the chart by symbols, which are the same as those used in a previous *Metal Progress* Data Sheet, 'Crystallography of the Chemical Elements.' For elements having several allotropic modifications, the symbols are accompanied by the usual Greek letters. In order to distinguish the allotropic modifications that are due to a reversible temperature-dependent transformation (as in iron) from those that occur when the metal is prepared under special conditions (for example, tungsten), the Greek letters are placed on the left side of the symbol in the former case and on the right side in the latter.

"Most of the values of atomic diameters used in the chart are taken from Hume-Rothery's book, 'The Structure of Metals and Alloys.'[12] Because of the more or less empirical character of the atomic diameter, the values reported in various tables may not always agree. For a discussion of the exact measuring of atomic size the reader may refer to the book by Hume-Rothery and also to a more recent discussion by Linus Pauling.[14] All atomic diameters presented in the chart are for coordination number 12. The atomic diameter of silicon, not given by Hume-Rothery, was computed from the lattice parameters of the solid solution of silicon in copper.

"The atomic diameter of manganese has been a matter of controversy. The value adopted here (2.60Å) has been proposed by David Harker in a discussion of a paper by A. R. Troiano and F. T. McGuire[15] and is based on the solid solution of manganese in gamma iron. The elements boron, carbon, nitrogen and oxygen have relatively small atomic diameters and fall outside the chart limits. No definite diameter can be assigned to these elements except for carbon, for which 1.54Å is accepted.

"The scale of atomic diameter used in the chart is logarithmic. The purpose of the log scale is to determine easily which elements have a diameter within a given percentage of any selected element. This is simply done by copying on a piece of paper the small percentage scale at the bottom of the chart and placing it with its zero on the diameter of the element being considered. The application of the Hume-Rothery rule concerned with size factor is thereby greatly simplified."

Once the size factor of the atoms is favorable for alloy formation between two constituent elements, the phase of the alloy, α, β, or γ, is governed by the ratio of valency electrons to atoms. This ratio is called the "electron concentration," according to Hume-Rothery. Thus, a ratio $3/2$ prevails for the B.C.C. crystal structure and the β-manganese structure; $21/13$ for the γ-brass structure and $7/4$ for the C.P.H. structure. Examples for the β-phase of several alloys are the following:[16]

CuZn	1 Cu atom	= 1 valency electron
	1 Zn atom	= 2 valency electrons
Total:	2 atoms	+ 3 valency electrons
Electron Concentration		= $3/2$ = 1.5
Cu_3Al	3 Cu atoms	= 3 valency electrons
	1 Al atom	= 3 valency electrons
Total:	4 atoms	+ 6 valency electrons
Electron Concentration		= $6/4$ = 1.5
Cu_5Sn	5 Cu atoms	= 5 valency electrons
	1 Sn atom	= 4 valency electrons
Total:	6 atoms	= 9 valency electrons
Electron Concentration		= $9/6$ = 1.5

On this assumption that electron concentration alone determined the phase boundaries, H. Jones (1937) was able to calculate these for the Cu-Zn-alloy phase diagram. Lattice distortion and the electrochemical factor may severely limit the applicability of these guiding principles in other alloy systems.

For more detailed study of all these matters discussed above the

reader should consult the references from which much of the presented material has been condensed, and refer also to Chapter 13, where the structures of diamond and graphite are discussed. After the present chapter was written, it was found that an extensive review entitled: "Some Fundamental Concepts of Matter in the Solid State," is contained in the second edition of Norton's book, "Refractories."[17]* This is written in a very similar vein, and it will serve the reader well to recapitulate and extend the present author's presentation. Another review of this subject may be found in an article by Rigby[18]; it is also highly recommended in support of Chapter 15 of this text. Leverenz, in his book on Luminescence of Solids[18a] devotes the first two chapters to the subject presented here. An excellent introduction to the theory of solids is given by Seitz in Ref. 19. The classic treatise by Bragg and Bragg[20] deals with the crystalline state and that of Rice and Teller[21] with the structure of matter in general on the basis of quantum mechanical concepts.

Our present knowledge in this field is well summarized by W. L. Bragg in a review of a book entitled "Progress in Metal Physics"[22]:

> "There is an extraordinary contrast between the extreme simplicity of the perfect crystal of a pure metal, of whose nature the atomic physicists have given us a reasonably complete explanation, and the complexity of behavior when the ideal symmetry is destroyed. When alloys and solid solutions are considered, the complexity is almost infinitely increased. We still await the genius who can order and arrange these facts, and give us a clue to the maze by unifying and simplifying theory. The study of the theory of alloys is the most satisfactory, or perhaps one should say the least unsatisfactory, in this respect. Here one does begin to see bits of the jigsaw puzzle falling into place; the knowledge of atomic arrangement allied to the quantum theory, has for the first time put metal chemistry on a hopeful basis. In the sections on the theory of dislocations and crystal boundaries, and their effects on slip and creep, hardening and fracture, one is still groping in the dark. Advance depends on a much deeper understanding of the number and arrangement of the dislocations, the units in terms of which we seek to define the departure from the perfect crystalline form, by whose movement we seek to explain the flow of the metal. Until more is known about their physical nature, such mathematical theory as has been developed is really little more than a conventional fig leaf to cover the utter nakedness of intuitive guesses. The technologist still has to wait patiently for the advance of pure science which one day will give him a lead. . . . "[23]

As implied in this review, the study of the crystalline state is only the first step necessary in an effort to understand the behavior of solids. The metals and alloys encountered in everyday use are not perfect crystals, and even single crystals are apt to have flaws which profoundly affect their properties. Even a spectroscopically pure metal is a very complicated assembly. On account of the close proximity of many neighbors a metal atom or molecule in the condensed state is subject to the force field of several electronic shells, and consequently is not in

* The third edition does not contain this chapter.

thermodynamic equilibrium with its surroundings. Under perfectly determined conditions of temperature and pressure a pure metal may have a variety of properties which markedly depend on its previous history. This applies especially to mechanical properties which are structure-sensitive* to a high degree. According to the structure produced by treatment certain manganese steels, for example, may be tough, ductile, and nonmagnetic, or hard, brittle, and magnetic. The descriptive terms of "age-hardening," "precipitation-hardening", "work-hardening", "recovery", and "recrystallization" readily bring to mind the many effects of various treatments with which the metal worker is well familiar.

"It is well-known that ordinary metals consist of masses of small crystals, usually referred to as 'crystal grains,' whose existence can be revealed by polishing the metal and attacking its surface with a suitably chosen reagent which has a preferential action on the crystal boundaries and frequently on different crystal faces—for individual chemical reagents usually differ in their rate of reaction on different faces of the same crystal.

"Another method of revealing the structure of metals by treating the surface in a way that shows selective action is by thermal etching, that is, by heating the metal until the surface layers have been removed by vaporization. Chalmers and his collaborators have also studied the attack of gases on heated metals, and have shown that, for instance, oxygen is particularly effective as a revealer of structures."†

The complex behavior of polycrystalline metals and alloys is principally dictated by the existence of crystal grains of a wide size distribution and the boundaries between them.

"The nature of the intercrystalline boundary has long been a matter of dispute, one school holding that the grains are separated by a region some hundreds of atoms thick, in which the atoms are arranged in a disordered manner—the so-called 'amorphous cement'—and the other school maintaining that between two grains, in each of which a crystal order prevails, is a sheet, a few atoms thick only, the members of which, being under the influence of forces from both lattices, constitute a transitional layer. The latter picture is the one more generally accepted, and very recently Chalmers and his collaborators,[25] applying consideration of free energy to the boundaries, have brought forward strong arguments in favor of it."[24]

These crystal boundaries are a source of strength and weakness under certain conditions of strain. On the one hand, they form a barrier to the propagation of dislocations in the lattice of crystals, and thus account for the fact that polycrystalline metals have a greater mechanical strength than single crystals. On the other hand, the boundaries give rise to slip, flow, and creep in the presence of mechanical loads. The "off-setting"

* See page 282.

† The above quotation is contained in a revealing article by E. N. DaC. Andrade,[24] from which several highlights have been extracted here. A recent book by Chalmers, entitled "Progress in Metal Physics,"[22] should contain details on many of the subjects touched upon here only briefly. Barrett[4] also treats these matters extensively.

of tungsten wires, described in the following chapter, is an example (Fig. 8.3). It has also been shown that atoms diffuse into many polycrystalline metals more rapidly along grain boundaries, where the potential barriers that must be overcome during diffusion are lower than those in the interior of the grains. The penetration of silver into "Kovar" during brazing operations and the ensuing boundary cracks present an example of this phenomenon.*

* Recent experience indicates that this effect is predicated on the existence of strain in the Kovar.

REFERENCES

1. Zapffe, C. A., "The Insides of Metals," *Phys. Today*, **3**, 13–19 (1950).
2. Davey, W. P., "A Study of Crystal Structure and Its Applications," New York, McGraw-Hill Book Co., Inc., 1934.
3. Clark, G. L., "Applied X-Rays," New York, McGraw-Hill Book Co., Inc., 1940.
4. Barrett, C. S., "Structure of Metals, Crystallographic Methods, Principles and Data," New York, McGraw-Hill Book Co., Inc., 1943.
5. Hume-Rothery, W., "Atomic Theory for Students of Metallurgy," The Institute of Metals, 4 Grosvenor Gardens, London S.W. (1948).
6. Wagener, S., "Die Oxydkathode," 26, Leipzig, J. A. Barth, 1943.

6a. Seitz, F., "Progress of the Physics of Solids," *J. Franklin Inst.*, **251**, 156–166 (1951).

6b. "Solid State Electronics," National Bureau of Standards Tech. News Bull., **35**, 22–27 (1951).

7. Seitz, F., "The Modern Theory of Solids," New York, McGraw-Hill Book Co., Inc., 1942.
8. Bernal, J. D., "Encyclopedia Britannica," 14 Ed., Vol. 23, 857.
9. Pauling, L., "The Nature of the Chemical Bond," Ithaca, Cornell University Press, 1945.
10. Bichowsky, F. R., and Rossini, F. D., "The Thermochemistry of the Chemical Substances," New York, Reinhold Publishing Corp., 1936.

10a. Skinner, J. B., Edwards, J. W., and Johnston, H. L., "The Vapor Pressure of Inorganic Substances. V Zirconium between 1949 and 2054°K," *J. Am. Chem. Soc.*, **73**, 174–176 (1951).

11. Young, J. F., "Materials and Processes," New York, John Wiley and Sons, Inc., 1946.
12. Hume-Rothery, W., "The Structure of Metals and Alloys," *Monograph Rept.*, Ser. No. 1, Institute of Metals, London (1947).
13. Duwez, P., "Atomic Diameters of Metallic Elements," *Metal Progress*, **57**, 348–348B (1950).
14. Pauling, L., "Atomic Radii and Interatomic Distances in Metals," *J. Am. Chem. Soc.*, **69**, 542–553 (1947).
15. Troiano, A. R., and McGuire, F. T., "A Study of the Iron-Rich Iron-Manganese Alloys," *A.S.M. Transact.*, **31**, 340–359 (1943).
16. Hume-Rothery, W., "Electrons, Atoms, Metals, and Alloys," *Transact. Am. Inst. Min. and Met. Eng. Inst. of Met. Div.*, **171**, 47–62 (1947).
17. Norton, F. H., "Refractories," Chapt. 4, New York, McGraw-Hill Book Co., Inc., 1942; 3rd. Ed., 1949.
18. Rigby, G. R., "The Application of Crystal Chemistry to Ceramic Materials," *Transact. Brit. Ceram. Soc.*, **48**, 1–67 (1949).

18a. Leverenz, H. W., "An Introduction to Luminescence of Solids," New York, John Wiley and Sons, Inc., 1950.
19. Seitz, F., "The Modern Theory of Solids," New York, McGraw-Hill Book Co., Inc., 1942.
20. Bragg, Sir W. H., and Bragg, W. L., "The Crystalline State," **121**, New York, Macmillan Co., 1934.
21. Rice, F. O., and Teller, E., "The Structure of Matter," New York, John Wiley and Sons, Inc., 1949.
22. Chalmers, B., "Progress in Metal Physics," London, Butterworth Scientific Publishers, 1949.
23. Bragg, W. L., Review of above, *Endeavor*, **9**, 35, 160–161 (July, 1950).
24. Andrade, E. N. DaC., The Physics of the Deformation of Metals," *Endeavor*, **9**, 36, 165–177 (1950).
25. Anst, K. T., and Chalmers, B., "The Specific Energy of Crystal Boundaries in Tin," *Proc. Roy. Soc. A.*, **201**, 210–215 (1950).

CHAPTER 8
TUNGSTEN

Among the high melting-point metals tungsten is of unique interest in the electron-tube industry. It is the most commonly used source of electrons in power tubes, the common anti-cathode in x-ray tubes and the filament material in indirectly heated cathodes for most electron tubes. In addition, it is used as a light source in all incandescent lamps. Particularly in this latter application its chief merit is its high melting point, combined with mechanical stability at elevated temperatures.

This extreme refractoriness, on the other hand, is a limitation when it comes to the ease of fabrication of various physical shapes. There are no furnace materials available, which would stand up at these extreme temperatures so that the techniques of powder metallurgy must be resorted to rather than those of casting metal into molds. It is thus necessary, according to the process developed by Coolidge in 1909, to compress the tungsten powder under great pressure and presinter it into porous bars in a hydrogen furnace at 1250°C. The sintering proper then takes place by passing several thousand amperes through the bar in a hydrogen atmosphere, which raises the temperature of the bar almost to its melting point. Grain growth begins at about 1000°C and leads to a coarse crystalline structure accompanied by linear shrinkage of the bar of about 17 per cent. After this treatment, the bar is quite strong, but very brittle. It is then made ductile by a hammering process, called "swaging"; this takes place at an elevated temperature in a series of passes through sets of dies that permit the hammers to strike from all sides, closer each time to the axis, thus gradually reducing the diameter. During swaging the originally coarse crystals are elongated in the axial direction of the rod leading to a fibrous structure of the wire, which is easily apparent on fracture. This long fiber structure is responsible for the ductility of the rod. If the temperature is raised sufficiently to permit recrystallization, the flexibility is lost and a brittle wire results. More will be said about this further on in the text.

From swaged bars wire can be drawn, rods ground by centerless grinding, and ribbon hot-rolled from wire. A ribbon about 2 inches wide is about the maximum width available, and sheet measuring 6″ × 15″ × 0.005″ and 8″ × 20″ × 0.025″ can be had. A tungsten plate,

measuring 2″ × 10″ × 0.060″ thick, was supplied to this laboratory for use as a septum in the cyclotron deflection chamber. Such strips, and strips 2″ wide × 0.100″ thick, are made as long as 18 inches. The edges of such heavy strips have to be ground to dimension. In regard to fineness the art has progressed very far. Wires can be drawn by diamond dies down to 0.0002 inch in diameter, and ribbon is available in thickness as little as 0.001 inch. These can be reduced further by etching in a fused mixture of $Na_2O + NaNO_3$ at 340°C.[1]

Commercial suppliers in the United States are listed below.* The production of seamless tungsten tubing has been disclosed in British Patent 342,648 (Sept., 1939), issued to N. V. Philips Gloeilampenfabrieken in Eindhoven.

"The method consists in depositing the metal by electrochemical means or by thermal decomposition on a core and then dissolving the core away chemically. By this means small seamless tubes can be made from W, Mo, C, Pt, Ti, Zr, Hf, and others. W can be deposited from WCl_6 vapor at 2000°C on a Mo core. The rate of deposition is 5 to 25 microgram per minute, and there is practically no diffusion between the metals. The Mo core is then dissolved in 85 per cent HNO_3 plus 15 per cent concentrated H_2SO_4 at 90°C. The specific gravity of the W tubes is about 19.22 and the tubes are vacuum-tight. Tubes from 1 mm diameter × 3 cm long × 0.1 mm wall thickness to 12 mm diameter × 35 cm long × 1 mm wall thickness can be made. A single crystal W tube can be made by depositing on a single crystal Mo core. Very thin tubes can be made by depositing from a WCl_6 and H_2 mixture on a copper core and melting out the Cu core. The tubes can also be drawn to smaller size before removing the copper core."

Tungsten and other refractory metals can also be deposited on a suitable core from the vapor phase of the appropriate carbonyl in an atmosphere of CO_2, according to a process developed by Commonwealth Engineering Company of Dayton, Ohio, under the name of "Gas Plating."[1a]

"Tungsten carbonyl $W(CO)_6$ exists in the form of white orthorhombic crystals which decompose at 150°C without melting. The vapor phase deposits on any object held at the proper temperature in a metallic form. 'Gas Plating' dates back to the discovery by Ludwig Mond, in 1890, that metallic nickel can be obtained from the decomposition of nickel carbonyls, a process which bears his name. In its improved form, gas plating is applied to the plating of conductors or nonconductors of intricate

* Cleveland Tungsten, Inc., 10200 Meech Ave., Cleveland, Ohio.
Fansteel Metallurgical Corp., North Chicago, Illinois.
General Electric Co., New York 22, N.Y.
Westinghouse Electric Corp., 40 Wall Street, New York, N.Y.
Sylvania Electric Products, Inc., 500 5th Ave., New York 18, N.Y.
North American Philips Co. (Elmet Div.), 100 East 42nd St., New York 17, N.Y.
H. Cross, Inc., 15 Beekman St., New York 7, N.Y.
Sigmund Cohn & Co., 44 Gold St., New York 7, N.Y.
Kulite Tungsten Co., 723–725 Sip Street, Union City, New Jersey.
Radio Corporation of America, Harrison, N.J.
Union City Filament Corp., 540 39th St., Union City, N.J. (Callite Bldg.)

shapes onto which coatings of considerable thickness and density can be deposited in much shorter periods of time than conventional electroplating permits. Continuous wire coating has also been perfected. If the core mandrel is dissolved by chemical means, tubing naturally results. Alloy coating is also possible."

A process for making small metal tubes with diameters from 1 mm down to 0.1 mm or less by electrodeposition on silver-coated nylon fibers has been described by Gezelius.[1b]

Tungsten is relatively expensive, and the cost of very fine wires and ribbon is, of course, higher in proportion to the delicacy of the processing required. Tungsten is bought in units of kilograms for bulk rods and wires, and lengths are measured in meters, this being one industry where the M.K.S. system has been adopted by intuition, it seems. Deliveries, however, are not measured in seconds. Fine wires up to 0.030 inch in diameter are designated in terms of weight per specified length of 200 mm, where the weight, W, is expressed in milligrams. The value of W depends, of course, on the density of the tungsten in process by any one manufacturer, and it is necessary to obtain this information on the basis of which orders are to be placed. In general, the following relations apply:

$$d = 0.7141 \times \sqrt{W} \text{ (mils)}$$
$$W = 1.961 \times d^2 \text{ (mg/200 mm)}$$

It is important to come to an agreement with the manufacturer on such matters as diameter tolerance and elongation under a given load. Guiding principles on such questions and accepted methods of test have been set up by A.S.T.M.* under B 205-45T. On quantity consumption it is very important to maintain careful acceptance tests for incoming stock and quality control on the production line, including life tests on the finished product, if costly failures are to be avoided. This applies in particular when tungsten rod is used for lead seals through glass, where surface fissures can be disastrous.

It is not within the scope of this text to deal extensively with the metallurgy of tungsten and its fabrication, especially since a thorough treatise on this subject is available.[1] Other source material may be found in Refs. 2–5. However, a few basic facts should be summarized to aid in the understanding of some of the unusual properties of tungsten and in its intelligent use. Table 8.1 gives a compilation of physical data of tungsten and Table 8.2 its chemical characteristics. It is seen that W crystallizes in the B.C.C. system, and thus lacks the ductility and plastic yield of the denser structures common to Cu, Ag, and Au. It is hard and brittle after heating to elevated temperatures, quite in contrast to ordinary metals which are soft-annealed by heat treatment. This embrittlement is due to recrystallization which sets in at about 1000°C;

* American Society for Testing Materials, 1916 Race St., Philadelphia 3, Pa.

TABLE 8.1. PHYSICAL CHARACTERISTICS OF TUNGSTEN

Atomic number: 74
Atomic weight: 183.92
Isotopes: 180, 182, 183, 184, 186
Lattice type: B.C.C.
No. of atoms per unit cell: 2
No. of unit cells per cc: 3.1982×10^{22}
Atomic Volume: 9.53 cc/g mole
Atomic Heat: 3.5–8 cal/g mole
Specific Heat: 0.034 (20–100°C)
0.0367 (1000°C)

Atomic valence: 6
Valence orbitals: $5d^4 6s^2$

Lattice constant: 3.1585 KX-units
Closest approach of atoms: 2.734 KX-units

Heat of fusion*: 44 cal/g
Heat of sublimation: 210 kcal/mole
Melting point*: 3,410 ± 20°C
Boiling point: 5,900°C
Vapor pressure†:
at 1800°K—1.93×10^{-15}
2400—7.9×10^{-9}
3000—6.55×10^{-5}
3500—4.68×10^{-3}
mm Hg

Density†: presintered at about 1500°C 10.0–13.0
sintered at 3000°C 16.5–17.5
swaged 18.0–19.0
drawn 18.0–19.3
g/cc
Ref. for lamp industry: 19.35

Brinell Hardness†
Sintered: Rectangular bar, 18 mm 200–250
Swaged bar, 5 mm 350–400
Fused (in arc under H_2) 260–300
(kg/mm²)

Tensile Strength (at 20°C)†:

	kg/mm²	psi	Elongation (% in 2″)
Sintered compact	13	18,500	
Swaged rod	35–150	50,000–71,000	
Drawn wire 1 mm	180	256,000	1–4
Drawn wire 0.5	200	285,000	1–4
Drawn wire 0.2	250	356,000	1–4
Drawn wire 0.1	300	427,000	1–4
Drawn wire 0.02	400–415	570,000–590,000	
Recrystallized wire	110	157,000	0
Single crystal, thoriated, unformed	~ 110	157,000	~ 20
Single crystal, thoriated, formed	180 max.	256,000	
At elevated temperatures:			
Wire 0.6 mm 400°C	120–160	170,000–227,000	2–3
800°	80–100	113,000–142,000	5
1200°	40–60	57,000– 85,000	6
1800°	10–30	14,000– 42,000	

Modulus of rigidity: 21.5×10^6 psi (*vid.* Table 8.5)
Thermal coefficient of modulus of rigidity: -6.6×10^{-5}/°C (Ref. 7) (−50 to +50°C)
Young's Modulus: 41,500 kg/mm², ~ 60×10^6 psi (*vid.* Table 8.5)
Temperature coefficient of Young's Modulus: -9.5×10^{-5}/°C (Ref. 7) (−50 to +50°C)

* Ref. 6.
† Ref. 5, 5a.

TABLE 8.1. PHYSICAL CHARACTERISTICS OF TUNGSTEN. (*Continued*)

Elastic Limit:

		kg/mm²	psi
Annealed wire	0.5–1 mm	72–83	1.0 to 1.2 × 10^5
Unannealed wire	0.5–1 mm	150	2.13 × 10^5

Torsion modulus: 17,000 kg/mm² − 24 × 10^6 psi (for drawn single crystal)

Poisson's ratio: 0.284 (for single crystal)

Coefficient of thermal expansion†:

20–300	44.0 × 10^{-7}	$\frac{cm}{cm}$ /°C
30	44.4 × 10^{-7}	
1030	51.9 × 10^{-7}	
2030	72.6 × 10^{-7}	

°C

Thermal Conductivity: (Ref. 8)

True temp. (°K)	Cal/cm²/cm/sec/°K	Watts/cm²/cm/sec/°K
293	0.31	1.3
1100	.28	1.170
1200	.275	1.153
1300	.272	1.138
1400	.268	1.122
1500	.264	1.106
1600	.260	1.089
1700	.256	1.073
1800	.253	1.058
1900	.249	1.042
2000	.245	1.026

Electrical resistivity†: 20°C 5.5 microhm-cm
1200°C 40.4 microhm-cm
2400°C 85. microhm-cm

Thermal emissivity: (Ref. 9)

e_t =	0.0170 at 300	°K
=	.0320 at 500	
=	.105 at 1000	
=	.192 at 1500	
=	.263 at 2000	
=	.312 at 2500	
=	.346 at 3000	

Electron work function: 4.56 e.V. (Ref. 10, 11, 12)

Richardson constant A: 45 amp/cm² deg² K

Magnetic susceptibility: + 0.28 × 10^{-6}

† Ref. 5, 5a.

tungsten wires which owe their ductility to the peculiar fibrous structure obtained during the swaging and drawing process should not be heated above this temperature during forming operations.

In general, the following schedule is recommended for the winding of coils. Pure tungsten wire, from the smallest size up to 0.010 inch in diameter, can be wound cold on a mandrel of the same diameter as the wire. For diameters from 0.010 to 0.015 inch the minimum mandrel diameter should be 1.5 times the wire diameter; for wires from 0.015 to 0.020 inch in diameter the mandrel diameter should be twice the wire diameter. Wires larger than 0.020 inch in diameter should not be wound

TABLE 8.2. CHEMICAL CHARACTERISTICS OF TUNGSTEN

Atomic number: 74	Atomic valence: 6
Atomic weight: 183.92	Valence orbitals: $5d^4 6s^2$
Heat of fusion: 44 cal/g	Melting point: 3,410 ± 20°C

(A) Reactions of Pure Tungsten:

(1) in air or oxygen at room temperature: none
(2) in air at 400–500°C: onset of oxidation
(3) in air above 500°C: rapid oxidation
(4) in water vapor above 500°C: rapid oxidation
(5) in HCl or H_2SO_4, cold, dilute or conc.: practically none
(6) in HCl or H_2SO_4, warm, dilute or conc.: noticeable attack
(7) in HF, cold or warm, dilute or conc.: none
(8) in HF + HNO_3 (50:50 by vol.), hot: rapid dissolution
(9) in Na(OH) or K(OH) cold: practically none
(10) in molten K(OH) or Na_2CO_3 with access of air: slow oxidation
(11) in molten K(OH) or Na_2CO_3 plus KNO_3 or KNO_2 or $KClO_3$ or PbO_2: rapid dissolution
(12) in molten $NaNO_2$ + $NaNO_3$ at 340°C: rapid etching
(13) in boiling 20% NaOH for 15 min.: suitable cleaning process
(14) in 5 pts HNO_3 + 3 pts H_2SO_4 + 2 pts H_2O (by vol.): cleaning prior to sealing followed by chromic acid and water rinse
(15) in Carbon or hydrocarbons: partial carbide formation up to ~ 1200°C
(16) in Carbon or hydrocarbons: complete carbide formation from 1400–1600°C
(17) in CO: stable up to 1400°C
(18) in CO_2: oxidation above 1200°C
(19) in H_2: none; very little adsorption below 1200°C
(20) in N_2: stable up to 2000°C. Nitride formation at 2300°C
(21) in Hg: none
(22) in contact with Al_2O_3, MgO or ZrO: reduction of oxides above 2000°C, MgO above 1000°C (Ref. 42)
(23) as anode in dilute $NaNO_2$(8N): rapid etching
(24) as anode in solution of 1000 g H_2O + 250 g KOH + .25 g $CuSO_4$ (or $CuCl_2$): uniform etching
(25) in boiling solution of 3% H_2O_2: slow etching
(26) in solution of 305 g $K_3Fe(CN)_6$ + 44.5 g Na(OH) + 1000 cc H_2O: most rapid attack

(B) Oxides of Tungsten

WO_3—greenish yellow—stable up to 600°C. $d = 7.16$
W_2O_5—bluish violet (W_4O_{11})
WO_2—brown—forms at 700°C. $d = 12.11$

Reduction: $\left.\begin{array}{l} WO_2 + 2H_2 \rightleftarrows 2H_2O + W \\ WO_3 + 3H_2 \rightleftarrows 3H_2O + W \end{array}\right\}$ at 600 to 1000°C

(C) Removal of Graphite from Tungsten Wires. This subject has been discussed by Kopelman[12a] and Mesnard and Uzan.[12b]

cold. With the application of heat all sizes of pure tungsten can be coiled on a mandrel of the same diameter as the wire, and the temperature required will increase with the size of the wire. It ranges from 300 to 1000°C. Thoriated tungsten wire, from the smallest size up to 0.010 inch in diameter, can be wound cold on a mandrel not less than 1.5 times the wire diameter. Wires from 0.010 to 0.020 inch in diameter can be

wound cold on mandrels 5 to 10 times the wire diameter. Larger wires should be wound hot and the remarks for hot winding of pure tungsten essentially apply. The forming of hairpin filaments should also be guided by these directions. Pure or thoriated wire from 0.010 to 0.020 inch in diameter can be formed cold around a pin 1.5 times the wire diameter, and below 0.010 inch in diameter the pin diameter may be the same as the wire diameter. Rectangular bends on wire or ribbon must be approximated by round corners; the radius of the corner is chosen on the basis of the remarks above on coil forms. Fig. 8.1 shows a filament basket for a Resnatron; the filaments, in this case, consist of tungsten

Fig. 8.1. Filament basket for a 400 MC resnatron. (*Courtesy Collins Radio Company.*)

ribbons which are formed into U-shaped staples. The short legs of the staples are connected to tantalum lugs which provide some flexibility. The lugs, in turn, are spot-welded to a nickel ring which is brazed to the massive copper end-hats. Some faults of this type of structure are discussed in Chapter 10.

After the desired form of a filament, coil, or other shape has been produced, the tungsten must be cleaned before assembly, particularly when subsequent furnace brazing is to be performed on the part. Immersion in a 50:50 by vol. solution of hot $HNO_3 + HF$ for a few seconds, followed by several rinses in distilled water, has been found most successful. This obviates the need of prior nickel plating in the case of silver brazing.

When the tungsten heater or emitter has been mounted in its final assembly, it is necessary to subject it to a heat treatment, which is often referred to as "flashing." Its purpose is to develop and stabilize a crystal structure which will prevent warping or failure due to excessive grain growth under operating conditions. This is a very important

matter and deserves considerable attention. So many factors have a bearing on the final structure that it is difficult to lay down any general rules, but the following remarks may serve as a guide.

Pure tungsten wire will lose its fibrous structure and begin to grow equi-axed crystal grains above 1000°C, depending on its composition and history of treatment in processing by the manufacturer. The size of the crystal grains will depend on the temperature and duration of heating, and will be strongly affected by small percentage admixtures added to the original powder batch. Fig. 8.2 shows the effect of temperature on grain

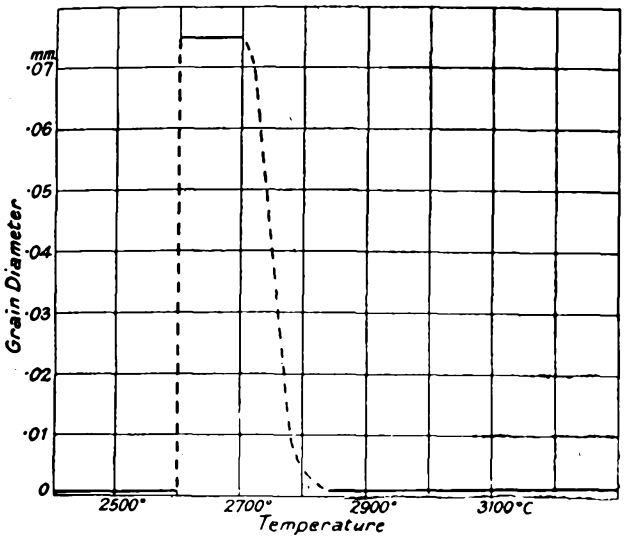

Fig. 8.2. Effect of temperature on the grain size of tungsten bars. After Jeffries.[13]

diameter when presintered bars are sintered for 15 minutes to the temperatures shown on the diagram.[13] There is a critical range from 2600 to 2800°C where development of large grains is most pronounced, and it should be noted that this temperature range lies well above the average temperature of commercial operation in electronic tubes, which is in the vicinity of 2300°C. However, incandescent lamp filaments operate near 2700°C. Approximate equilibrium of grain growth is usually established in 10 to 15 minutes, and prolonged heating does not appear to alter the structure.[1]

The development of large crystal grains is not necessarily confined to wires flashed at the optimum temperature range for growth, but may develop at lower temperatures on prolonged operation. In any case, such crystal grains may assume sufficient size to extend across a full wire diameter, and slip may occur along their boundaries at right angles to the axis of the wire leading to hot spots and burn-outs. This effect is known

as "offsetting", and is associated with equi-axed crystals. Folded heaters may be twisted into unbelievably complex patterns when the crystal structure has not been set or excessive growth prevented. Fig. 8.3 illustrates the development of offsetting on heating in diagrammatic form, and Fig. 8.4 gives a photograph of a faulty wire.

It has been known since 1923, when Irving Langmuir made his basic investigations, that excessive crystal growth can be prevented in tungsten wires by the admixture of thorium oxide to the powder batch from which the wire is made. This benefited electron emission, and resulted in the

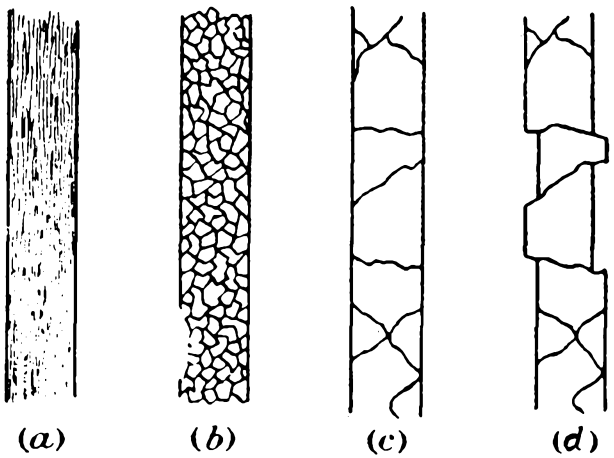

Fig. 8.3. Changes in the structure of pure tungsten filaments heated by alternating current. After Smithells.[1] (*Courtesy Chapman and Hall Ltd.*)

development of so-called "non-sag wire" (N.S.) for the lamp industry. In time other admixtures have made their appearance; these have a similar end-effect of suppressing "offsetting" and "sagging" under gravity when wires or coils are mounted horizontally between supports. The result, however, is achieved in different ways by different admixtures, and it should be emphasized that N.S. wire useful in the lamp industry is not necessarily suitable for electron tubes. The admixture of ThO_2, usually from ½ to 1½ per cent, considerably retards grain growth at elevated temperature, and thus preserves ductility to some extent. This is illustrated in Fig. 8.5a and 8.5b, which show etched metallurgical sections at a magnification × 100 of pure tungsten rod and rod containing 0.75 per cent ThO_2 after being flashed in hydrogen for 2 minutes at 2700°C.[1] ThO_2 is very slowly reduced by tungsten above 2300°C and metallic Th is slightly soluble in tungsten.

The addition of small percentages of alkali oxides and silica to the tungsten oxide brings about exaggerated grain growth, and is often used

for wires from which coiled lamp filaments are made. Long crystals, several millimeters or even centimeters long, are developed in such coils after a few seconds of flashing and remain substantially unchanged after long periods of heating above the recrystallization temperature. Such coils remain ductile after recrystallization, and have many properties of the single crystal wires (Pintsch wires). Additional strain due to coiling increases the potentiality for exaggerated growth in these wires, and straight wires do not show the desired long grain growth as easily.[1] In

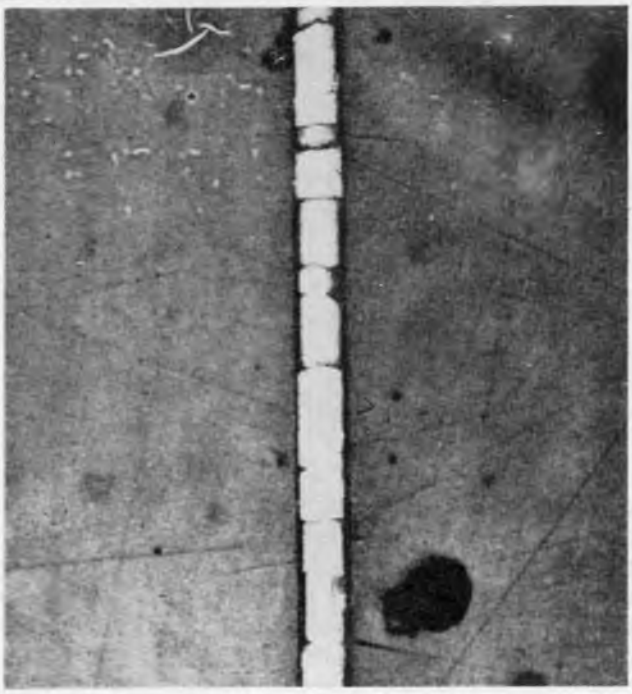

Fig. 8.4. Pure tungsten wire 0.05 mm. diameter after annealing. Etched H_2O_2 ($\times$100). After Smithells.[1] (*Courtesy Chapman and Hall Ltd.*)

the case of straight filaments of substantial diameter, of the order of 0.040 to 0.050 inch, there is also evidence that long grain growth is favored by the presence of strain existing between the inner and outer crystals produced while drawing the wire. The grains should have a length from 6 to 10 times their width and contain from 25 to 40 grains per mm diameter of the wire.[14]

The treatment required to produce the long fibrous structure of the drawn wire after it is flashed in hydrogen under tension at temperatures near 2300°C must be very carefully controlled to give the desired result.

On flashing, the wire is brought up to temperature at a constant rate in a matter of minutes and held at the maximum value for 5 minutes, whereupon the temperature is reduced at a constant rate to a black temperature in one minute. The rate at which the current is raised to the flashing temperature has a pronounced effect on the result obtained. Potentially good wire can be ruined if the heating cycle is carried out too slowly. The effects of the flashing treatment carried out on the wire in a

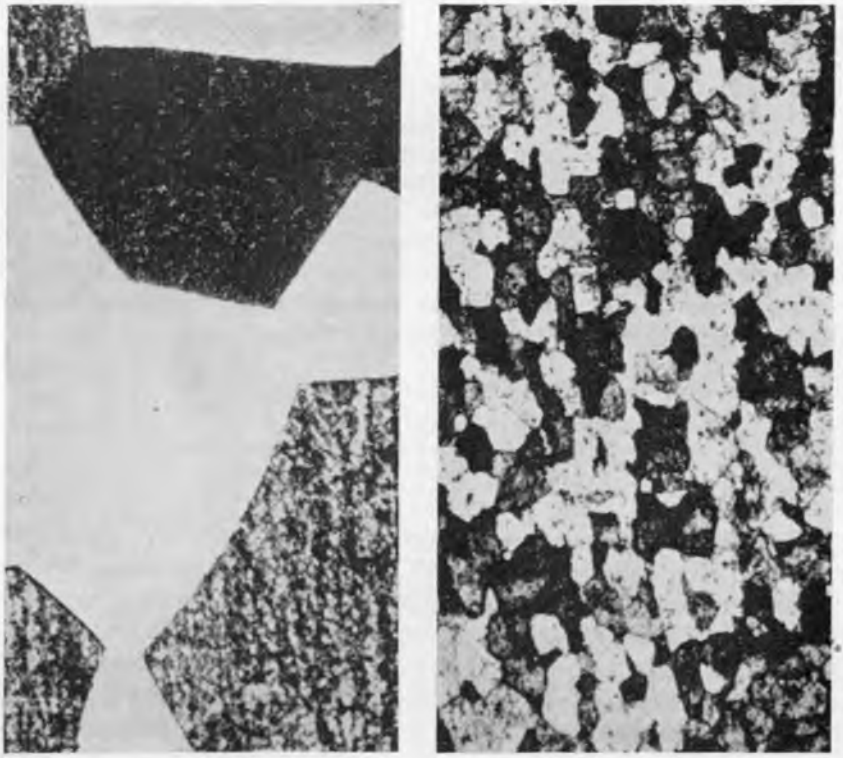

(a) (b)

Fig. 8.5. Metallurgical sections of tungsten rod, annealed at 2700°C for 2 minutes (×100). Etched H_2O_2. (a) Pure tungsten; (b) Tungsten containing 0.75% ThO_2. After Smithells.[1] (*Courtesy Chapman and Hall, Ltd., London.*)

vertical position under tension are easily verified by a subsequent flashing at 2300°C in a horizontal plane for about 5 minutes without tension; the deformation under the force of gravity can therefore be measured on a flat surface upon which the wire is placed for measurement. Micrograph sections will disclose the grain structure under a microscope.

The following procedure for sag-testing tungsten wire was developed by the Federal Telephone and Radio Corporation Vacuum-Tube Division

and proposed as a standard test by ASTM.[14,15] Under the application of external heat the wire is formed into a hairpin by bending it around a pin 0.080 inch in diameter until the free ends are 1 inch apart. Not more than 20 per cent of the hairpin length, measured from the apex, should be heated above a black heat during this forming operation. The legs of the formed hairpin must naturally lie in the same plane. After the specimen is clamped in a fixture which can be rotated by 90°, the exposed length, L, of the hairpin measured from the apex to the clamp should have the following values for given diameters of wire:

Diameter (in.)	Length (in.)
0.030–0.0349	4⅛
0.035–0.0449	4½
0.045–0.0550	4⅝

A hook formed from 0.080-inch diameter tungsten wire is attached to the loop of the hairpin, which has been mounted in the test fixture in a vertical position. Depending on the diameter of the wire under test the following weights are attached to the hook:

Diameter of Wire under Test (in.)	Weight Attached to Hook (lbs)
0.0300–0.0349	3
0.0350–0.0449	4
0.0450–0.0550	6

A bell jar filled with hydrogen is lowered over the assembly. The hydrogen should have a dew point of −65°C or less, and not contain more than 10 parts per million (ppm) of oxygen, 20 ppm of hydrocarbons, and ½ per cent of nitrogen.

The hairpin is flashed according to a predetermined time schedule and with the weight attached. It is cooled after the weight is removed, and then turned through 90° into a horizontal plane and flashed again at the same temperature according to a predetermined schedule. After recooling, the hairpin is inspected in situ and the vertical distance measured in mm by which the apex of the hairpin digresses from the horizontal plane. This is the measure of distortion.

The characteristics of tungsten filaments as a function of temperature have been described in the classical paper by Jones and Langmuir in 1927,[9] from which Table 8.3 is reproduced here for convenience of reference. The figures given refer to a filament 1 cm in diameter and 1 cm long, and conversion to other sizes is readily obtained by setting up the dimensional equations with the aid of factors given in the second line at the top of the table. Thus it is seen, for example, that it takes 1526 amps to heat a 1 cm diameter wire to 2500°K ($A' = 1526$) if end cooling is neglected. To heat a 0.040-inch diameter wire to the same temperature

TABLE 8.3. SPECIFIC CHARACTERISTICS OF IDEAL TUNGSTEN FILAMENTS[9,10]
(For a wire 1 cm in length and 1 cm in diam.)

T (°K)	W', $\frac{W}{ld}$ watts/cm²	$R' \times 10^6$, $\frac{Rd^2}{l} \times 10^6$, ohm-cm	A', $\frac{A}{d^{3/2}}$, amps/cm$^{3/2}$	$V' \times 10^3$, $\frac{V\sqrt{d}}{l} \times 10^3$, volts/cm½	I', $\frac{I}{ld}$, amp/cm²	M', $\frac{M}{ld}$, g/π cm²/sec, evaporation	$\frac{R'_T}{R'_{293°}}$, $\frac{R_T}{R_{293°}}$
273		6.37					0.911
293	0.0	6.99	0	0			1
300	.000100	7.20	3.727	0.02683			1.03
400	.00624	10.26	24.67	.2530			1.467
500	.0305	13.45	47.62	.6404			1.924
600	.0954	16.85	75.25	1.268			2.41
700	.240	20.49	108.2	2.218			4.93
800	.530	24.19	148	3.581			3.46
900	1.041	27.94	193.1	5.393			4
1,000	1.891	31.74	244.1	7.749	3.36×10^{-16}	1.16×10^{-33}	4.54
1,100	3.223	35.58	301	10.71	4.77×10^{-13}	6.81×10^{-30}	5.08
1,200	5.210	39.46	363.4	14.34	3.06×10^{-11}	1.01×10^{-26}	5.65
1,300	8.060	43.40	430.9	18.70	1.01×10^{-9}	4.22×10^{-24}	6.22
1,400	12.01	47.37	503.5	23.85	2.08×10^{-8}	7.88×10^{-22}	6.78
1,500	17.33	51.40	580.6	29.85	2.87×10^{-7}	7.42×10^{-20}	7.36
1,600	24.32	55.46	662.2	36.73	2.91×10^{-6}	3.92×10^{-18}	7.93
1,700	33.28	59.58	747.3	44.52	2.22×10^{-5}	1.31×10^{-16}	8.52
1,800	44.54	63.74	836	53.28	1.40×10^{-4}	2.97×10^{-15}	9.12
1,900	58.45	67.94	927.4	63.02	7.15×10^{-4}	4.62×10^{-14}	9.72
2,000	75.37	72.19	1,022	73.75	3.15×10^{-3}	5.51×10^{-13}	10.33
2,100	95.69	76.49	1,119	85.57	1.23×10^{-2}	4.95×10^{-12}	10.93
2,200	119.8	80.83	1,217	98.40	4.17×10^{-2}	3.92×10^{-11}	11.57
2,300	148.2	85.22	1,319	112.4	1.28×10^{-1}	2.45×10^{-10}	12.19
2,400	181.2	89.65	1,422	127.5	0.364	1.37×10^{-9}	12.83
2,500	219.3	94.13	1,526	143.6	0.935	6.36×10^{-9}	13.47
2,600	263	98.66	1,632	161.1	2.25	2.76×10^{-8}	14.12
2,700	312.7	103.22	1,741	179.7	5.12	9.95×10^{-7}	14.76
2,800	368.9	107.85	1,849	199.5	11.11	3.51×10^{-7}	15.43
2,900	432.4	112.51	1,961	220.6	22.95	1.08×10^{-6}	16.10
3,000	503.5	117.21	2,072	243	44.40	3.04×10^{-6}	16.77
3,100	583	121.95	2,187	266.7	83	8.35×10^{-6}	17.46
3,200	671.5	126.76	2,301	291.7	150.2	2.09×10^{-5}	18.15
3,300	769.7	131.60	2,418	318.3	265.2	5.02×10^{-5}	18.83
3,400	878.3	136.49	2,537	346.2	446	1.12×10^{-4}	19.53
3,500	998	141.42	2,657	375.7	732	2.38×10^{-4}	20.24
3,600	1,130	146.40	2.777	406.7	1,173	4.86×10^{-4}	20.95
3,655	1,202	149.15	2,838	423.4	1,505	7.15×10^{-4}	21.34

the following is derived from the table, Column 4:

$$\frac{A}{d^{3/2}} = 1526 \text{ amps}$$

A is the required current in amps and d the diameter of the wire in cm. By converting 0.040 inch into cm, the following is obtained:

$$A = (0.040 \times 2.54)^{3/2} \times 1526 = 42.2 \text{ amps}$$

In a similar manner all other transformations can be obtained. Fig. 8.6 gives the various tungsten data in graphical form, according to Spangenberg.[9a] Many refinements may have to be considered in more

accurate calculations for which any one of the references (8, 9, 16, 21) should be consulted. "The Design of Tungsten Springs to Hold Tungsten Filaments Taut," is described by Katherine D. Blodgett and Irving Langmuir.[22] Problems relating to electron emission from tungsten are discussed by Reimann[23] and Herring and Nichols,[10] thoriated tungsten filaments by Langmuir,[24] the design of thoriated tungsten filaments by Dailey,[25] and carburizing of thoriated filaments by Andrews and Dushman[26] and Horsting,[27] and the coating of tungsten heaters with alumina by Bidgood and Kent.[27a]

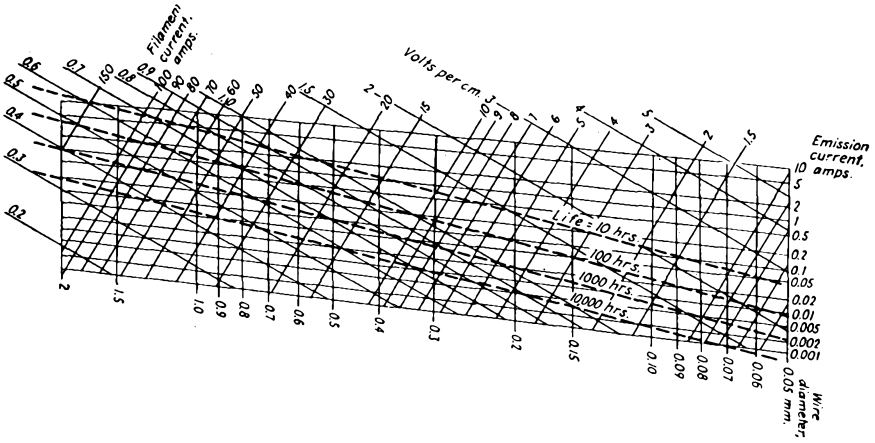

Fig. 8.6. Characteristics of ideal tungsten filaments as given by the data of Langmuir and Jones.[9] Curves are for a 1-cm length of wire. Life is defined as the time required for a 10% reduction in mass through evaporation. (*By permission from "Vacuum Tubes" by K. Spangenberg. Copyright 1948. McGraw-Hill Book Company, Inc.*)

The life of a tungsten filament, either in a lamp or as a heater or emitter in an electron tube, is considered to have reached its end point after the diameter of the filament has been reduced by 10 per cent because of evaporation. At that time a hot spot usually forms which leads to burn-out. For gas-filled lamps or tubes different considerations apply. The rates of evaporation, M, at different values of operating temperature are available from Table 8.3, which gives M' in grams/sec for π cm^2 according to Jones and Langmuir.[9] These data, when applied to filaments operating in tubes with water-cooled copper anodes, fall short by a factor of 2 of actually observed tube life, according to Bell, Davies and Gossling.[40] Revised data by Reimann[41] were found in good agreement with actual tests.*

The author has recently had occasion to compile operating data for large tungsten strips for unconventionally large power tubes. Some of these figures are given in Table 8.4 as a ready reference for orders of

* For further comments see Chapter 19.

TABLE 8.4. TUNGSTEN-STRIP DESIGN DATA

$T' = 2600°K$

	L	Serial Number Length (inches) Aspect Ratio w/t	1 6 6.5	2 6 4.5	3 6 6.3	4 12 6.3	5 12 6.3	6 12 8.3	7 18 6.3
1	w	inches	⅛	⅛	¼	⅛	¼	½	¼
2	t	inches	0.020	0.030	0.040	0.020	0.040	0.060	0.040
3	q	sq. cm	.0162	.0242	.065	.0162	.065	.1933	.065
4	d_q	cm	.1438	.1754	.286	.1438	.286	.495	.286
5	d_s	cm	.2342	.2508	.469	.2342	.469	.906	.469
6	F	d_q/d_s	.612	.70	.611	.612	.612	.546	.612
7	$1/F$	d_s/d_q	1.634	1.43	1.639	1.634	1.639	1.830	1.639
8	S_1	sq. inches	0.750	0.750	1.50	1.50	3	6	4.50
9	S_1	sq. feet	.005	.005	0.0104	0.0104	0.0208	0.0416	0.0313
10	S_1	sq. cm	4.835	4.835	9.670	9.670	19.34	38.680	29
11	A_t	sq. cm	11.218	11.992	22.436	22.436	44.872	86.66	67.314
12	A_t	sq. feet	0.012	0.0129	0.0242	0.0242	0.0484	0.0933	0.0725
13	W	Kilowatts	.94	1.008	1.878	1.878	3.76	7.26	5.64
14	R	Ohms	.072	0.0481	0.0185	0.144	0.037	0.0121	0.0555
15	I	Amperes	114	144.5	318.1	114.2	318.5	777	318.5
16	E	Volts	8.25	7	5.9	16.43	11.8	9.35	17.7
17	I_{s1}	Amperes	4.84	4.84	9.67	9.67	19.3	38.7	29
18	I'	$I_{s1}/6$ Amperes	0.81	0.81	1.61	1.61	3.21	6.45	4.63
19	Wt	Lbs/Strip	.015	.0158	0.042	0.021	0.085	0.025	0.128
20	C	$/Strip	.53	.55	1.47	.75	3	.90	4.50
21	L	Life (hours)	3,100	4,650	6,200	3,100	6,200	9,300	6,200

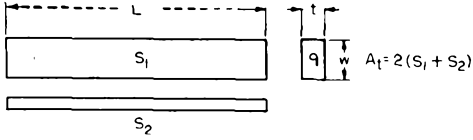

8	9	10	11	12
18	18	24	24	24
10.	12.5	12.5	12.5	16.7
½	¾	½	¾	1
0.050	0.060	0.040	0.060	0.060
.162	.290	.129	.290	.387
.455	.608	.405	.608	.702
.890	1.309	.873	1.309	1.715
.510	0.437	.465	0.437	0.41
1.960	2.286	2.16	2.286	2.44
9	13.5	12	18	24
0.0626	0.0938	0.0832	0.1252	0.168
58.0	87.1	77.45	166.0	155
127.62	188.12	167.29	250.6	328.6
0.137	0.2025	0.1803	0.2703	0.354
10.75	15.7	14.0	21.0	27.6
0.0216	0.0120	0.03618	0.01605	0.01242
703.5	1140	623	1140	1516
15.4	13.8	22.5	18.5	18.2
58	87.1	77.5	116.0	155.0
9.7	14.5	12.90	19.33	25.9
0.312	0.568	0.336	0.755	1.01
11	19.80	11.80	26.4	35.3
7,750	9,300	6,200	9,300	9,300

Legend

$d_q = \frac{2}{\sqrt{\pi}}\sqrt{w \times t}$. Diameter of cylindrical rod with the same cross-section q as the strip.

$d_s = \frac{2(w + t)}{\pi}$. Diameter of cylindrical rod with the same surface A_t as the strip.

$S_q = d_q \times \pi \times l$. Surface of cylindrical rod with the same cross-section q as the strip.

$S_s = d_q \times \pi \times l$. Surface of cylindrical rod equal to the total surface A_t of the strip.

$$F = \frac{S_q}{S_s} = \frac{d_q}{d_s} = \frac{\sqrt{w \times t \times \pi}}{w + t} = \frac{\sqrt{(A.R.) \times \pi}}{(A.R.) + 1}$$

$A.R. = w/t$. Aspect Ratio of strip.

W = Watts $\times 10^2$. Power dissipated by strip at $T = 2600°K$.
$= 263 \times 10^3 \times l \times d_s$

$R = \frac{5.5 \times 10^{-6} \times 14.12 \times l}{q}$. Resistance of strip at 2600°K.

$I = \sqrt{\frac{W \times 10^{-3}}{R}}$. Current in amperes, required to heat strip to 2600°K (neglecting end losses).

$I_{s1} = S_1$. Peak electron emission from one side of strip at rate of 1 amp/cm².

$Wt = w \times t \times L \times 0.7$. Weight of one strip in lbs.

$C = Wt \times 35$. Cost of one strip in dollars at $35/lb. Actual cost will vary widely due to processing cost.

$L = t \times 1.55 \times 10^5$. Life in hours for end point at evaporation of 10% of strip thickness where rate of evaporation $M = 4.4 \times 10^{-9}$ g/cm²/sec.

magnitude in the evaluation of strips of this size range operating at 2600°K. The figures are of slide-rule accuracy and values for cost and life are of necessity only approximate.

The mechanical properties of tungsten are dependent to a large extent on composition, crystal structure, history of mechanical and thermal treatment, and temperature of operation. This has become evident from the previous discussion, and some data will be added here for reference. Mechanical properties of drawn wires at room temperature are given in Table 8.5, according to Smithells.[1]

TABLE 8.5. MECHANICAL PROPERTIES OF DRAWN TUNGSTEN WIRE[1]

Wire Diam.		Tensile Strength			Modulus of Elasticity		Modulus of Rigidity	
mm	Mils	Kg/mm²	Tons/in²	Psi	Kg/mm²	Psi	Kg/mm²	Psi
Sintered Bar		13	9.24	18,486				
5	197.5	40	28.44	56,880				
3	118.5	75	53.33	106,650				
2	79	100	71.10	142,200				
1	39.5	140	99.54	199,080			13,000	18,486,000
0.5	19.75	185	131.54	263,070			15,200	21,614,000
.3	11.85	220	156.42	312,840	9,000	12,798,000	16,000	22,752,000
.15	5.925	270	191.97	383,940	26,000	38,172,000	16,800	23,889,600
.10	3.95	300	213.10	426,200	31,500	44,793,000	17,200	24,458,400
.05	1.975	345	245.60	490,590	33,200	47,210,400	17,800	25,311,600
.03	1.185	385	273.74	547,470	34,000	48,348,000	18,400	26,164,800
.02	0.790	425	302.18	604,350				
.015	.5925	470	334.17	668,340				

Fig. 8.7 represents graphically a log/log plot from which it is evident that the tensile strength is roughly an exponential function of the wire diameter for values below 2 mm. Curve B shows a decrease of tensile strength when the wire was annealed after being drawn to 0.13-mm diameter; however, recovery occurs on further drawing. The effect of annealing at various temperatures is shown in Fig. 8.8. There is an initial rise of tensile strength on annealing up to 600°C, but for higher temperatures the drop is severe. This is, of course, an important consideration for the design of springs, which ideally should not run hotter than 600°C. The very marked differences in values of tensile strength at any given temperature, depending on the mechanical and thermal history of the wire in question, are evident from Fig. 8.9[1]; curve A represents a drawn wire, curve B the same wire after being flashed for 1 minute at 3000°K, and curve C a Pintsch single-crystal wire containing 2 per cent of ThO_2. Curve B indicates a wire consisting of a series of long crystals which occupy the full diameter of the wire. Its weakness in comparison

to the single-crystal Pintsch wire is evident. It would seem desirable to use Pintsch wires wherever possible, but, unfortunately, their manufacture is too complicated to make this commercially feasible.

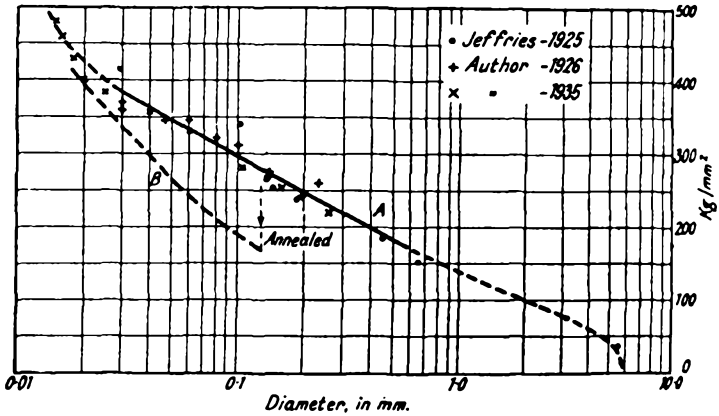

Fig. 8.7. Tensile strength of tungsten wire. (a) Normal drawing; (b) Intermediate anneal at 0.13 mm. After Smithells.[1] (*Courtesy of Chapman and Hall, Ltd.*)

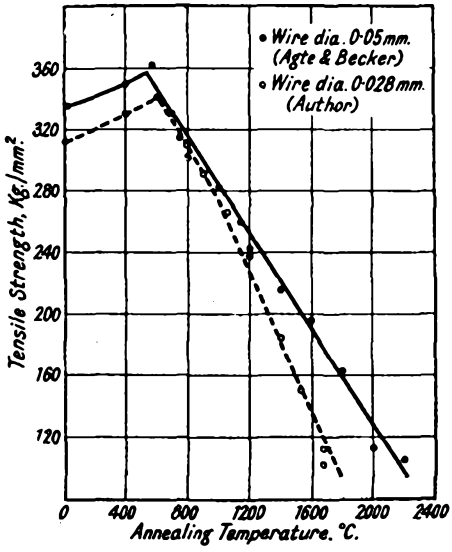

Fig. 8.8. Effect of annealing on the tensile strength of pure tungsten wire. After Smithells and Agte and Becker.[1] (*Courtesy Chapman and Hall, Ltd.*)

For the study of the physical properties of tungsten such single-crystal wires are particularly suitable.[11,28,29,30,31,32,33] When a single crystal is loaded in tension, the time required for fracturing is an exponential function of the load and temperature. In Fig. 8.10 the load per unit area required to fracture a wire in 1 minute is plotted against the temperature; Goucher[28,1] tested wires in the range of 0.093- to 0.195-mm diameter

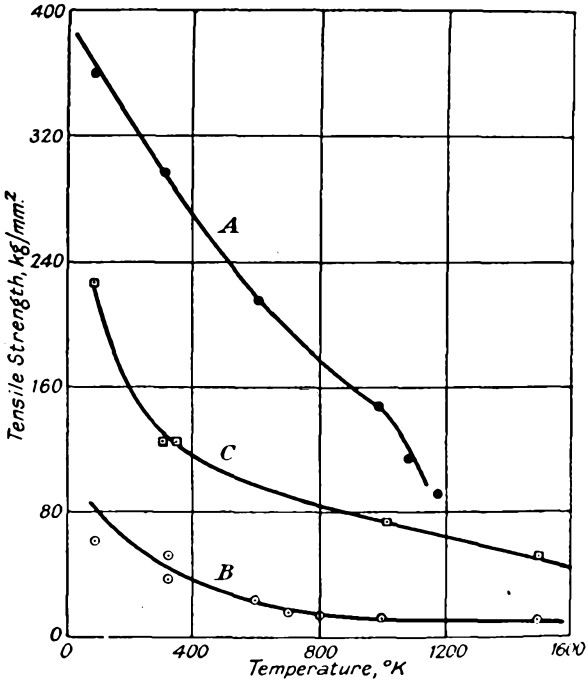

Fig. 8.9. Tensile strength—temperature curves for (a) Drawn tungsten wire; (b) Drawn tungsten wire recrystallized; (c) Pintsch single crystal wire. After Smithells.[1] (*Courtesy Chapman and Hall, Ltd.*)

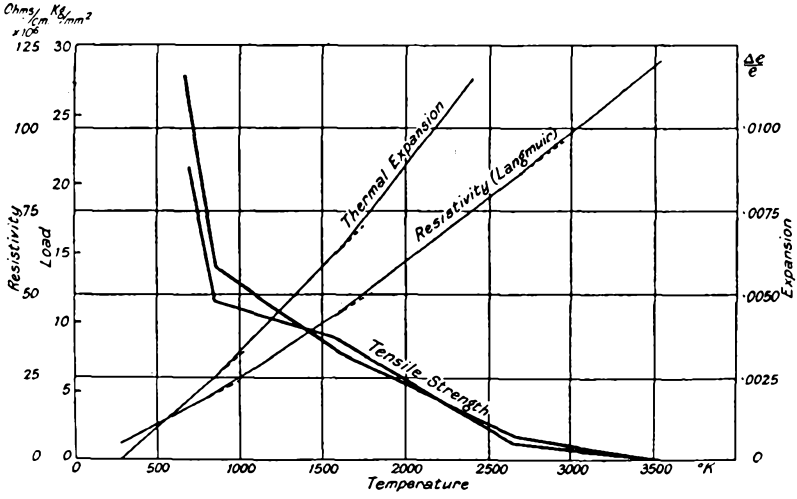

Fig. 8.10. Tensile strength of tungsten single crystals as a function of temperature. After Goucher.[28] Also shown are plots of resistivity and thermal expansion versus temperature. After Smithells.[1] (*Courtesy Chapman and Hall, Ltd.*)

after flashing them for 1 minute at 3000°K. It is interesting to note that the test data fall on one of two curves, thus giving two groups with the same behavior. Most of the fractures obtained below 800°K occurred at intercrystalline boundaries. There are three temperature ranges where distinct discontinuities take place (i.e., at 800–900°K, 1600°K and 2600–2700°K). These breaks in the curves coincide with discontinuities in electrical resistivity observed by Langmuir, and Worthing's data on thermal expansion indicate the break at about 1600°K. The significance of these discontinuities is still obscure.[1]

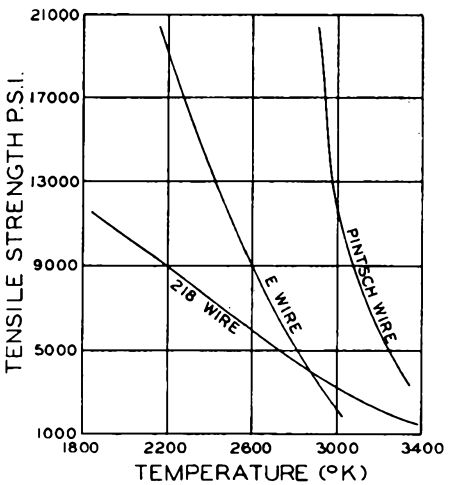

Fig. 8.11. Hot tensile strength of tungsten filaments. After Fonda.[39] (*Courtesy General Electric Company.*)

Fonda[39] has reported measurements on the hot tensile strength of several types of tungsten filaments, which are reproduced in Fig. 8.11. Type 218 wire, developed by the General Electric Company for gas-filled lamps, is a "non-sag", doped wire, which permits the growth of long-grained crystals. It is a popular material for heaters in receiving tubes. The dope consists of a 1 per cent addition of Na_2O, K_2O, $CaCl_2$, Al_2O_3, and SiO_2 before the sintering process, as mentioned earlier. "E" wire is of fine grain, and contains 1.5 per cent of thoria, (ThO_2). Pintsch wire, as used in this experiment, was a single-crystal wire containing 2 per cent of ThO_2. The different values of hot tensile strength shown by these three wires are plotted in Fig. 8.11.

The tensile strength of tungsten is an important consideration not only when tungsten members are supported by springs but also when fine wire grids are wound under tension. For a 0.3-mil wire the required

tension amounts to 300,000 psi, thus approaching the tensile strength of such wire, which is 530,000 psi.[34]

For single-crystal wires the moduli of elasticity, E, and the moduli of torsion, G, have been determined as a function of temperature by Geiss,[30] who finds them well represented by the following equations:

$$E_T = E_o \left(\frac{T_S - T}{T_S}\right) 0.263 \tag{8.1}$$

$$G_T = G_o \left(\frac{T_S - T}{T_S}\right) 0.263 \tag{8.2}$$

E_T and G_T are the respective moduli at temperature T°K in kg/mm^2. T_S is the melting point of Tungsten in °K. $E_o = 40{,}000 \pm 1000$ and $G_o = 17{,}100 \pm 300$, both in kg/mm^2, are the values at 300°K[1]. The modulus of elasticity for drawn wires was found by Schönborn[35] to vary at room temperature from 34,800 to 37,300 kg/mm^2 and to drop to 32,000 kg/mm^2 at 1300°K.[1]

According to Schriever[36] the torsion modulus varies at room temperature from 9,000 to 22,000 kg/mm^2 and decreases only slightly with increase in temperature up to 1000°K. Between 1000 and 2000°K the modulus falls more rapidly, reaching about 3060 kg/mm^2 at 2000°K.

The formation of thin films of oxides and their reduction in hydrogen is of some considerable interest to the vacuum-tube engineer. The common oxides of tungsten are listed in Table 8.2. They are the green-yellow WO_3 which is stable up to 600°C, the chocolate brown WO_2, which forms at 700°C, and the bluish violet W_2O_5. A form W_4O_{11} is sometimes given for this oxide, but the latter is probably a solid solution of WO_3 and W_2O_5. The reduction of these oxides has been calculated over the temperature range 500 to 1000°C to take place according to

$$WO_2 + 2H_2 \rightleftarrows 2H_2O + W$$
$$WO_3 + 3H_2 \rightleftarrows 3H_2O + W$$

Reduction in hydrogen is thus feasible as long as the water-vapor concentration is kept at a low value so that the reactions take place to the right. The rate of reaction of oxide-film formation and reduction has been investigated by Gulbransen and Wysong[37] and others. The reaction rates are dependent on temperature, pressure, and surface conditions. All tungsten oxides are stable in vacuum up to 1000°C (i.e., they do not decompose, but evaporate at much lower temperatures). The reduction of tungstic oxide powder in hydrogen at various temperatures is illustrated by Table 8.6, according to Smithells,[1] which shows the appearance and approximate composition of a 10-g powder sample after being heated for 1 hour in a stream of dry hydrogen.

Norton and Marshall[38] found that tungsten had to be heated in vacuo to 2300°C (true temperature) for about 30 minutes to prevent further gas

evolution at still higher temperatures. The amount of gas evolved was from 15 to 25 per cent of that obtained from a similar sample of molybdenum outgassed at 1800°C (see page 212).

The attractive properties of tungsten, which make it a useful material for many purposes when used in vacuum or in the presence of an inert atmosphere, are offset by its ready reaction with oxygen at moderate temperatures (Table 8.2). The development of a high-temperature porcelain enamel for tungsten, reported by Horsfall,[44] thus extends its

TABLE 8.6. STAGES IN THE REDUCTION OF TUNGSTIC OXIDE[7]

Temp. (°C)	Appearance	Approx. Composition
400	Green-blue	$WO_3 + W_4O_{11}$
500	Intense blue	$WO_3 + W_4O_{11}$
550	Violet	W_4O_{11}
575	Purple-brown	$W_4O_{11} + WO_2$
600	Chocolate-brown	WO_2
650	Brown-black	$WO_2 + W$
700	Grey-black	W
800	Grey	W
900	Metallic grey	W
1000	Coarse metallic	W

application to fields where operation in air is required at elevated temperature up to 1650°C. The batch of the enamel consists of the following ingredients:

9 parts by weight $ZrO_2 \cdot SiO_2$
1.5 parts by weight Al_2O_3
0.5 parts by weight Co_3O_4
0.02 parts by weight $H_2MoO_4 \cdot H_2O$
0.3 parts by weight Dextrose

to which a few drops of formaldehyde are added to prevent fermentation while in storage. The tungsten rod to be coated is cleaned by flashing in a helium atmosphere and then coated with the enamel and fired again according to a prescribed schedule. A firmly adherent coat of enamel is thus obtained.

REFERENCES

1. Smithells, C. J., "Tungsten, a Treatise on its Metallurgy, Properties, and Applications," London, Chapman and Hall, Ltd., 1945.
1a. *U.S. Patent 2,332,309*; *2,344,138*; *2,475,601*; The Commonwealth Engineering Co. of Ohio, "Metal Plating from Carbonyl Gases," *Chem. Eng.* (Oct., 1949).
1b. Gezelius, R. J. E., "Making Small Metal Tubes by Electrodeposition on Nylon Fibres," *Rev. Sci. Inst.*, **21**, 886 (1950).
2. Espe, W., and Knoll, M., "Werkstoffkunde der Hochvakuumtechnik," Berlin, J. Springer, 1936. Obtainable from Edwards Bros., Ann Arbor, Michigan.

3. Li, K. C., and Chung Yu Wang, "Tungsten," New York, Reinhold Publishing Corp., 1946.
4. Schwarzkopf, P., "Powder Metallurgy," New York, Macmillan Co., 1947.
5. Kieffer, R., and Hotop, W., "Pulvermetallurgie und Sinterwerkstoffe," Berlin, J. Springer, 1943.
5a. Kieffer, R., and Hotop, W., "Sintered Metals," *Metal Ind.*, **66**, 342–344, 354–356, 378–380 (1945).
6. "Metals Handbook," Cleveland, Am. Soc. for Metals, 1948.
7. Brombacher, W. G., "Temperature Coefficient of the Elastic Moduli of Spring Materials used in Instrument Design," *Rev. Sci. Inst.*, **4**, 688–692 (1933).
8. Osborn, R. H., "Thermal Conductivity of Tungsten and Molybdenum at Incandescent Temperatures," *J.O.S.A.*, **31**, 428–431 (1931).
9. Jones, H. A., and Langmuir, I., "The Characteristics of Tungsten Filaments as Functions of Temperature," *G. E. Rev.*, **30**, 310–319, 354–361, 408–412 (1927).
9a. Spangenberg, K. R., "Vacuum Tubes," New York, McGraw-Hill Book Co., Inc., 1948.
10. Herring, C., and Nichols, M. H., "Thermionic Emission," *Rev. Mod. Phys.*, **21**, 185–270 (1949).
11. Brown, A. A., Neelands, L. J., and Farnsworth, H. E., "Thermionic Work Function of the (100) Face of a Tungsten Single Crystal," *J. Appl. Phys.*, **21**, 1–4 (1950).
12. Nichols, M. H., "Average Thermionic Constants of Polycrystalline Tungsten Wires," *Phys. Rev.*, **78**, 158–161 (1950).
12a. Kopelman, B., "Clean-up of Graphite Lubricant from Tungsten Wire," *Sylvania Technologist*, **2**, 13–16 (1949).
12b. Mesnard and Uzan, "Some Prevailing Treatments of Tungsten Filaments for Electron Tubes." (In French.) *LeVide* (5) **30**, 896–904 (1950).
13. Jeffries, Z., "Grain-Size Determination and Standardization," *Met. Chem. Eng.*, **16**, 503–504 (1917).
14. Fed. Tel. and Radio Corp., "Report on 'Non-sag' Properties of Tungsten," presented to ASTM, Aug. 18, 1948.
15. ASTM Committee 8.B4, "Proposed Method for Sag-Testing Tungsten Wire," Feb. 10, 1950.
16. Forsythe, W. E., and Worthing, A. G., "The Properties of Tungsten and the Characteristics of Tungsten Lamps," *Astrophys. J.*, **61**, 146–185 (1925).
17. Langmuir, I., McLane, S., and Blodgett, K. B., "Lead-Loss Correction and Temperature Distribution Along a Filament," *Phys. Rev.*, **35**, 478–503 (1930).
18. Forsythe, W. E., and Watson, E. M., "Resistance and Radiation of Tungsten as a Function of Temperature," *J.O.S.A.*, **24**, 114–118 (1934).
19. Langmuir, I., and Taylor, J. B., "Heat Conductivity of Tungsten and Cooling Effect of Leads upon Filaments at Low Temperatures," *Phys. Rev.*, **50**, 68–87 (1936).
20. Ornstein, I., "Tables of Emissivity of Tungsten as a Function of Wave length from 0.23 μ to 2.0 μ in the Temperature Region 1600–3000° K," *Physica*, **3**, 561–562 (1936).
21. Forsythe, W. E., and Adams, E. Q., "Radiation Characteristics of Tungsten and Tungsten Lamps," *J.O.S.A.*, **35**, 108–113 (1945).
22. Blodgett, K. B., and Langmuir, I., "The Design of Tungsten Springs to Hold Tungsten Filaments Taut," *R.S.I.*, **5**, 321–333 (1934).
23. Reimann, A. L., "Thermionic Emission," London, Chapman and Hall, Ltd., 1934.
24. Langmuir, I., "Thoriated Tungsten Filaments," *J.F.I.*, **217**, 543–569 (1934).

25. Dailey, H. J., "Designing Thoriated Tungsten Filaments," *Electronics*, 107–109 (Jan., 1948).
26. Andrews, M. R., and Dushman, S., "Diffusion of Carbon through Tungsten and Tungsten Carbide," *J. Phys. Chem.*, **29**, 462–472 (1925).
27. Horsting, C. W., "Carbide Structures in Carburized Thoriated Tungsten Filaments," *J. Appl. Phys.*, **18**, 95–102 (1947).
27a. Bidgood, E. S., and Kent, G. H., "Cataphoresis and Alundum Coatings," *Transact. Electrochem. Soc.*, **87**, 321–329 (1945).
28. Goucher, F. S., "On the Strength of Tungsten Single Crystals and its Variation with Temperature," *Phil. Mag.*, **48**, 229–249 (1924).
29. Goucher, F. S., "Studies on the Deformation of Tungsten Single Crystals under Tensile Stress," *Phil. Mag.*, **48**, 800–819 (1924).
30. Geiss, W., "The Elastic Constants of Tungsten as a Function of Temperature." (In Dutch), *Physica*, **3**, 322–327 (1923).
31. Johnson, R. P., and Shockley, W., "An Electron Microscope for Filaments: Emission and Adsorption by Tungsten Single Crystals," *Phys. Rev.*, **49**, 436–440 (1936).
32. Nichols, M. H., "The Thermionic Constants of Tungsten as a Function of Crystallographic Direction," *Phys. Rev.*, **57**, 297–306 (1940).
33. Robinson, C. S., Jr., "Rate of Crystal Growth in Drawn Tungsten Wires as a Function of Temperature," *J. Appl. Phys.*, **13**, 647–651 (1942).
34. Walsh, E. J., "Fine Wire Vacuum-Tube Grids," *Bell Lab. Rec.*, **28**, 165–167 (1950).
35. Schönborn, H., "On the Elongation of Tungsten Single-Crystal Wires." (In German.), *Z. Phys.*, **8**, 377–381 (1921).
36. Schriever, W., "The Simple Rigidity of a Drawn Tungsten Wire at Incandescent Temperatures," *Phys. Rev.*, **23**, 255–265 (1924).
37. Gulbransen, E. A., and Wysong, W. S., "Thin Oxide Films on Tungsten," *Am. Inst. Min. and Met. Eng.* (*Metals Tech.*) **14**, T.P. No. 2398, 1-17 (1948).
38. Norton, F. J., and Marshall, A. L., "The Degassing of Metals," *Transact. Am. Inst. Min. and Met. Eng.*, **156**, 351–371 (1944).
39. Fonda, G. R., "Burn-out of Incandescent Lamps," *G. E. Rev.*, **32**, 206–212 (1929).
40. Bell, J., Davies, J. W., and Gossling, B. S., "High-Power Valves: Construction, Testing, and Operation," *J. Inst. El. Eng.*, **83**, 176–198, D. 198–207 (1938).
41. Reimann, A. L., "The Evaporation of Atoms, Ions, and Electrons from Tungsten," *Phil. Mag.*, **25**, 834–848 (1938).
42. Moore, G. E., "Reduction of Magnesium Oxide by Tungsten in Vacuum," *J. Chem. Phys.*, **9**, 427–431 (1941).
43. Reed, E. L., "Tungsten," AECD-2700, Sept. 15, 1947.
44. Horsfall, J. C., "A High-Temperature Porcelain Enamel for Tungsten," *Am. Ceram. Soc. Bull.*, **29**, 314–315 (1950).

CHAPTER 9

MOLYBDENUM

This metal has long been one of the basic materials for electron-tube construction because of its high melting point and great mechanical strength, similar to tungsten. Its high ductility permits parts of considerable size to be fabricated at more reasonable cost. Ingots weighing up to 1000 lbs are now being produced, yielding rolled sheets, some of which are 0.020 × 24 × 60 inches, and various-shaped parts.[1,26] Molybdenum pipe, 2 inches O.D. with a ¼-inch wall, has been recently produced in 3-foot lengths, and seamless tubing of various diameters up to ½ inch is available in 8-foot lengths.* Like tungsten, molybdenum ingots are made by powder metallurgical techniques from molybdenum powder of high purity and small particle size. The powder is pressed in steel dies under pressure of the order of 20 tons per sq inch to form bars which are sintered in hydrogen at a maximum temperature of 2300°C and swaged. Pure molybdenum metal has a silvery white appearance. About 90 per cent of the world's known molybdenum production is located in U. S.[27]

The applications of molybdenum in the tube and lamp industry are manifold. Coiled tungsten filaments for incandescent lamps are wound on molybdenum mandrel wire, which is later dissolved chemically by immersion in a solution of 50 pts HNO_3 + 30 pts H_2SO_4 + 20 pts H_2O at 90°C. Grids for radio receiving tubes and power tubes are generally made of molybdenum. Special surface treatments of the wire, such as the application of thin coatings of graphite, platinum, or gold in combination with tantalum, become necessary when secondary emission is likely to be a serious factor in the operation of the tube and must be suppressed.† Anodes and corona shields are frequently made of molybdenum, and current leads through glass may also be made of molybdenum when special molybdenum sealing glass is used.

Molybdenum is frequently used in electrical furnaces as long as a

* From Fansteel Metallurgical Corporation, North Chicago, Illinois.

† A coated molybdenum anode was introduced by Eitel-McCullough, Inc. under the trade name "Pyrovac." It replaced the earlier tantalum anodes used extensively by this company. Similarly, a preprocessed molybdenum wire under the designation "Y-3," is used for grid wires in place of the earlier "X-grid." "Pyrovac" has a dark, rough surface and excellent gettering power. "Y-3" has a secondary emission characteristic comparable to platinum and low primary emission. (The author is indebted to Eitel-McCullough, Inc., for supplying this information.)

protective atmosphere is provided to prevent oxides from forming. The glass industry employs large amounts for electrodes in glass tanks. Molybdenum is a suitable material for welder tips on spot welders and for thermocouple protection tubes. It has many other important applications which will not be discussed in this chapter.

The physical characteristics of molybdenum are summarized in Table 9.1, its chemical characteristics in Table 9.2. In many respects molybdenum is similar to tungsten as may be expected of members of the

TABLE 9.1. PHYSICAL CHARACTERISTICS OF MOLYBDENUM

Atomic number: 42	Atomic valence: 6/5/3
Atomic weight: 95.95	Valence orbitals: $4d^5 5s^1$
Isotopes: 96, 97, 98, 100	
Lattice type: B.C.C.	Lattice constant: 3.140 KX-units (Ref. 3)
No. of atoms per unit cell: 2	Closest approach of atoms: 2.720 KX-units (Ref. 3)
No. of unit cells per cc: 3.226×10^{22}	Heat of fusion: 70 cal/g.
Atomic volume: 9.41 cc/g mole	Heat of sublimation: 160 kcal/mole
Atomic heat: 5.85 cal/g mole	Melting point: 2630 ± 50°C (Ref. 2)
Specific Heat: 0.061 cal/g (20°) (Ref. 3) 0.08 cal/g (1400°)	Boiling point: 4,800°C (Ref. 5)

Vapor Pressure: 6.4×10^{-9} mm Hg at 1530°C (Ref. 2)
8×10^{-7} mm Hg at 1730°C (Ref. 2)
4×10^{-5} mm Hg at 1930°C (Ref. 2)
10^{-4} mm Hg at 2035°C (Ref. 4)
10^{-3} mm Hg at 2295°C (Ref. 4)
10^{-2} mm Hg at 2533°C (Ref. 4)

Density: (Ref. 2)		
Pressed, not sintered	6.1– 6.3	g/cc
Sintered at 1800–200°C	9.2– 9.4	g/cc
Swaged	9.7–10.	g/cc
Drawn	10.0–10.3	g/cc

Brinell Hardness: (kg/mm^2) (Ref. 2, 2a)

Sintered: Rectangular bar 18 mm	150–160
Rectangular forged rod, 18 mm	200–230
Sheet 2 mm thick	240–250
Sheet 1 mm thick	250–255
Fused (in arc under H_2)	160–200

Tensile Strength: (Ref. 2, 2a) (at 20°C)

		Kg/mm^2	Elongation (%)
Drawn wire 1.2 mm diam.		100–120	2–5
Drawn wire 0.4 mm diam.		150–170	2–5
Drawn wire 0.05 mm diam.		180–250	2–5
Recrystallized wire 1.25 mm diam.		80–100	10–20
Recrystallized wire 0.4 mm diam.		80–120	10–25
Recrystallized wire 0.03 mm diam.		80–120	20–30
Single crystal		~ 30	~ 30
At elevated temperatures:			
0.6 mm diam. wire	200°C	80–100	4–5
	400°C	60–70	4–5
	800°C	50–60	4–5
	1200°C	20–30	5–6

TABLE 9.1. PHYSICAL CHARACTERISTICS OF MOLYBDENUM. (*Continued*)

Tensile stress required to produce 0.5% per hr minimum creep rate for arc-cast molybdenum. Ref. 24.

Temp. (°C)	(°F)	Stress (psi)
982	1800	17,000
1204	2200	8,000
1427	2600	5,000
1649	3000	2,000

Young's Modulus: 33,600 kg/mm² (Ref. 2)
46–49 × 10^6 psi (Ref. 12, 21)

Torsion Modulus: 6,710 psi (Ref. 3) Poisson's Ratio not available:

Coefficient of thermal expansion: 20–300°C: 53–57 × 10^{-7} $\frac{\text{cm}}{\text{cm}}$ / °C
25–700°C: 58–62 × 10^{-7}

Thermal conductivity:
(Ref. 6)

True Temp. (°K)	Cal/cm²/cm/sec/°K	Watts/cm²/cm/°K/sec
293	0.382	1.6
1200	.259	1.083
1300	.244	1.023
1400	.230	0.964
1500	.216	.904
1600	.202	.844
1700	.188	.785
1800	.173	.725
1900	.159	.666

Electrical resistivity:

20 (°C)	4.8	microhm-cm	(Ref. 2)
800	22	" "	(Ref. 2)
1200	33	" "	(Ref. 2)
2000	60	" "	(Ref. 2)
2127	66	" "	(Ref. 9)
2227	69.2	" "	(Ref. 9)
2327	71.8	" "	(Ref. 8)
2527	78.2	" "	(Ref. 8)
2622	81.4	" "	(Ref. 8)

Thermal emissivity (total): at 100°C 0.071 (Ref. 10)
1000°C .13 (Ref. 3)
1500°C .19 (Ref. 3)
2000°C .24 (Ref. 3)

Electron work function: 4.37 e.V. (Ref. 11)

Richardson constant A: 115 amp/cm² deg² K (Ref. 11)

Electron emission: at 1000°C 1 × 10^{-9} ma/cm²
1630°C 8.3 × 10^{-1} ma/cm²
2230°C 800 ma/cm²

Magnetic susceptibility: +0.04 × 10^{-6} (Ref. 12)

TABLE 9.2. CHEMICAL CHARACTERISTICS OF MOLYBDENUM

Atomic number: 42 — Atomic valence: 6/5/3
Atomic weight: 95.95 — Valence orbitals: $4d^5 5s^1$
Heat of fusion: 70 cal/g — Melting point: 2630 ± 50°C
Heat of sublimation: 160 Kcal/mole
Heat of combustion: 1812 cal/g − 173.950 Kcal/g atom (Ref. 22)

(A) Reactions of pure molybdenum
- (1) in air or oxygen at 20°C: practically none
- (2) in air or oxygen at 400°C: weak oxidation sets in at 250°C
- (3) in air or oxygen at 600°C: rapid oxidation to MoO_3 (Ref. 23)
- (4) in water vapor at 700°C: rapid oxidation
- (5) in HCl or H_2SO_4, cold, dil. or conc: practically none
- (6) in HCl, dilute, hot: severe attack
- (7) in H_2SO_4 conc. at 200°C: rapid attack
- (8) in H_2SO_4 dilute at 110°C: none
- (9) in HNO_3 conc. at 20°C: slow reaction to form a layer of MoO_3
- (10) in HNO_3 dil. at 20°C: more rapid; complete dissolution (suitable pickling solution)
- (11) in Aqua Regia, warm, dil. or conc: rapid attack, forming H_2MoO_4
  " " " cold, " " " : none
- (12) in HF, cold or warm, dil. or conc: none
- (13) in HF + HNO_3 (50:50 by vol.) hot: rapid dissolution
- (14) in Na(OH) or K(OH) aqueous, cold: none
- (15) in Na(OH) or K(OH) aqueous, warm: weak
- (16) in Na(OH) or K(OH) molten: rapid dissolution
- (17) in molten oxidizing salts KNO_3, KNO_2, NaO_2, K_2CO_3, Na_2CO_3 + KNO_3, KCl_3, and PbO_2: violent reaction
- (18) in N_2O and NO at red heat: oxidation to MoO_3
- (19) in SO_2 at red heat: oxidation to MoO_2
- (20) in NH_3: none
- (21) in $NH_4(OH)$: moderate general attack
- (22) in H_2S: Mo-Sulfide forms at 1200°C
- (23) in S: none up to 440°C; sulfides form at higher temperatures
- (24) in P: none, even at higher temperatures
- (25) in Si: formation of silicide at high temperatures
- (26) in Hg: no amalgamation; less than 2×10^{-5}% Mo soluble
- (27) in Halogens: F—reaction at room temperature
  Cl—reaction at 300°C (J. Wulff)
  Br—reaction at bright red heat
  I—none at 500°C
- (28) in carbon or hydrocarbons: partial carbide formation at 1100°C; complete carbonization at 1300 to 1400°C
- (29) in H_2: none up to M.P.
- (30) in N_2: none up to 1500°C; nitrides form above 1500°C
- (31) in CO_2: oxidation above 1200°C
- (32) in CO: none up to 1400°C

(B) Oxides of Molybdenum
- (1) M_2O_3—black; hydrated molybdic oxide, Mo-sesquioxide
- (2) MoO_2—violet, red; Mo-dioxide (stable with substrate 300 − 700°C; d = 6.74)
- (3) MoO_3—white, yellow; Mo-trioxide (M.P. = 795°C; d = 4.5) (vapor pressure at 500°C ~ 10^{-5} mm Hg, at 800°C ~ 10mm Hg) volatile at 700°C
- (4) Mo_2O_5—violet, black; Mo-hemipentoxide

TABLE 9.2. CHEMICAL CHARACTERISTICS OF MOLYBDENUM. (*Continued*)

(C) Cleaning and Etching
  (1) Removal of oxides by cathodic treatment in dil. H_2SO_4 at approx. 100 amp/sq ft (Ref. 23)
  (2) Dilute (8N) $NaNO_2$ or K(OH): anodic—rapid etching
  (3) 1000 cc H_2O + 250 g K(OH) + 0.25 g $CuSO_4$ (or $CuCl_2$)—anodic, uniform etching
  (4) $NH_4(OH)$ + H_2O_2: uniform etching
  (5) 1000 cc H_2O + 305 g $K_3Fe(CN)_6$ + 44.5 g Na(OH)—rapid etching
  (6) 50 pts HNO_3 + 30 pts H_2SO_4 + 20 pts H_2O at 90°C—rapid etching
  (7) 95 pts conc. H_2SO_4 + 4.5 pts HF + 0.5 pt conc. HNO_3 + 18.8 g/liter Cr_2O_3 – 10 sec at 90°C for etching prior to resistance welding or brazing with tantalum foil (Ref. 25)

(D) Electrodeposition: See Ref. 19 and 20.

same group in the periodic table. Since recrystallization is not a serious problem, there is no need for preventing it by additions to the base powder. A small amount of recrystallization actually increases the

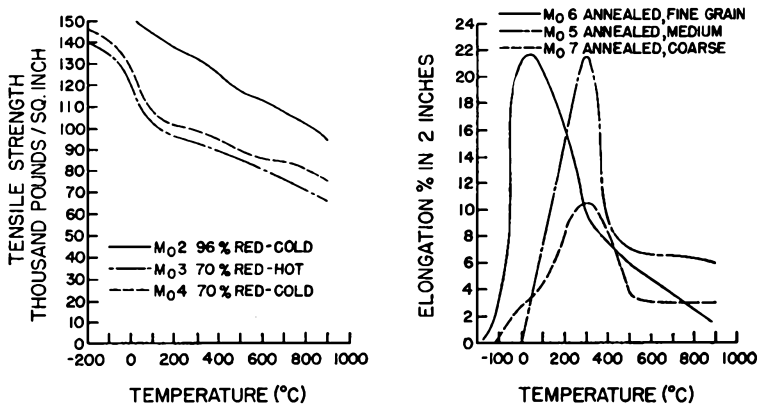

Fig. 9.1. (a) Tensile strength-temperature curves for molybdenum; (b) Elongation-temperature curves for molybdenum. After Sykes.[14] (*Courtesy American Institute for Metals.*)

ductility of the metal.[13] Recrystallized molybdenum has a higher tensile strength and elongation than tungsten. In Fig. 9.1 there are a series of graphs[14] which give the temperature dependence of tensile strength and elongation of wires treated in different ways. Curve 1 refers to a 25-mil diameter wire which was drawn at a temperature from 1300 to 1000°C and had its cross-section reduced on drawing by 93 per cent. This resulted in a fibrous structure of the wire and consequent high tensile strength and reasonable elongation at room temperature. Curve 2 refers to a wire which, in addition to the treatment under 1, was flashed in H_2 for 2 seconds at 65 per cent of the current required to melt the wire. This gives rise to a fine crystalline structure with an average grain size

of 5.3 microns, which lowers the tensile strength but markedly increases the elongation. Flashing a wire, as under 1, at a higher temperature for a longer time in H_2 (i.e., for 5 seconds at 90 per cent of its melting current) brings about a coarse crystalline structure with an average grain size of 30 microns and properties shown in curve 3. Tensile strength is now substantially reduced and useful elongation at room temperature lost completely. The mechanical properties of molybdenum can thus be changed over a wide range by suitable heat treatment; in the purchase of

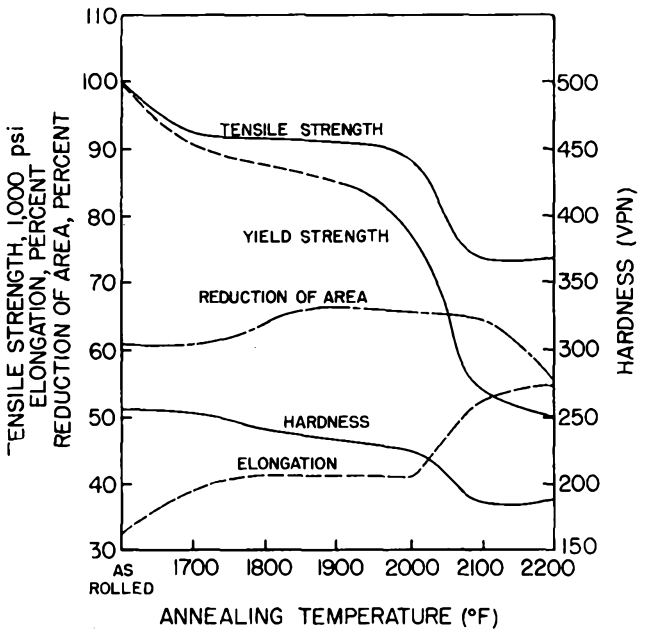

Fig. 9.2. Effect of annealing on properties of arc-cast hot rolled molybdenum bar (½″ diameter) stress relief at 1200–1900°F. After J. J. Harwood.[25] (*Courtesy McGraw-Hill Publishing Company and Climax Molybdenum Company.*)

wire desirable limits of performance must be specified to suit the application. This is of special importance for grid wire, which should be tested for elongation before use. A Scott tester* is a suitable instrument for such tests.

Fig. 9.2 gives the effect of annealing temperature on the mechanical properties of an arc-cast hot-rolled bar, ½ inch in diameter. Within the temperature range of 1200–1900°F stress relief occurs and above 1900°F recrystallization takes place.[25] The high-temperature mechanical properties of pure arc-cast molybdenum are given in Table 9.3 for several

* Obtainable from Scott Company, 65 Blackstone St., Providence, Rhode Island.

conditions of heat treatment.* Above about 1000°C (1832°F), the creep strength of molybdenum is superior to available iron-, nickel- and cobalt-base high-temperature alloys. These properties have given molybdenum a place of prime importance for applications in the field of high-temperature engineering for turbine blades, combustion chambers,

TABLE 9.3. MECHANICAL PROPERTIES OF PURE MOLYBDENUM AT ELEVATED TEMPERATURES[25]

Testing Temp, °F	Condition	Tensile Strength psi	Yield Str. psi 0.2 % offset	Proportional Limit psi	Per cent Elong. in 2 in.	Per cent Red. of Area
Room Temp.	As rolled	95,140			3	2
	Stress relieved (1850°F)	91,000	84,850		10	9
	Recrystallized (2250°F)	67,600	63,500		46	36
1600	As rolled	61,400	50,100	26,000	18	72
	Stress relieved	50,600	44,500	21,500	22	81
	Recrystallized	34,400	11,600	3,500	46	84
1700	As rolled	56,200	49,400	36,500	19	77
	Stress relieved	46,500	36,200	22,500	16	72
	Recrystallized	32,800	11,000		44	76
1800	As rolled	49,900	40,500	23,000	19	81
	Stress relieved	40,500	35,600	22,500	32	81
	Recrystallized	29,000	10,500	5,700	49	75
1900	As rolled	38,700	30,000	16,500		81
	Recrystallized	24,800	8,200	4,500	40	45
1950	Stress relieved	31,400	22,800	16,500	36	84
	Recrystallized	21,500	8,550	4,100	35	52
1950	Hot rolled	38,000	31,600	24,000	29	83

guide vanes and other components of gas turbines, rockets and guided missiles.[25]

Methods of fabrication for molybdenum have been described recently by Chelius.[26] As they are of considerable interest, a large part of the paper is reproduced here, and some data on seamless molybdenum tubing are taken from Fansteel Technical Bulletin 4.304.

Forming

"Most of the procedures in working and fabricating molybdenum are conventional, and can be mastered without too much difficulty. At the outset, however, one important characteristic of molybdenum must be kept constantly in mind; molybdenum should never be formed or bent in a chilled condition. Where the term 'room temperature' is used in this article, a temperature of 70°F or more is meant. A few simple

* With the kind permission of Climax Molybdenum Company.

tests will quickly convince the reader of the substantial difference in workability caused by the slight difference between 40 and 70°F.

"The lighter gages of molybdenum sheet, less than 0.020 in. in thickness, can be formed easily at room temperatures. Cross-rolled molybdenum sheet in this range of thicknesses can be bent to an angle of 180 deg in any direction on a radius equal to its thickness. When material between 0.020 and 0.040 in thick is formed, the sheet should be warmed to a temperature of 200 to 325°F. Sheet heavier than 0.040 in. should be worked at 900 to 1000°F to avoid cracking.

"Mo tubing up to ¼ inch O.D. by 0.030-inch wall thickness can be bent or coiled at temperatures of 200 to 350°F. Heavier tubing should be worked at 900 to 1000°F to avoid cracking. Tubing should be flared at approximately 1000°F.

"*Punching and Shearing:* The same general instructions given for forming are applicable to blanking, punching, or shearing (i.e., sheet thicker than 0.020 in. should be heated to temperatures which increase with thickness). In fact, it is good practice to keep the dies warm with a common heat lamp or infrared lamp. Dies should be kept sharp to avoid laminations and cracking of the molybdenum sheet.

"Sheet of 0.050 in. and thicker should not be sheared to finish dimensions, but should be sheared to within 1/16 to ⅛ in. of desired dimensions, then edge-machined.

"*Drawing and Spinning:* Wherever possible, molybdenum parts should be designed for finishing in one drawing operation, and the diameter of the cup after the first draw should be not less than 60% of the diameter of the original blank. The possibility of cracking increases considerably with each additional draw and, because of this, parts should be designed for a minimum number of draws.

"Dies should be made of aluminum bronze or other material with a low coefficient of friction. If steel dies are used, they should be well lubricated with light oil. Low-melting alloys can be used for experimental work or short runs. Rubber or pneumatic die cushions should be used where required.

"Molybdenum can be spun by conventional techniques, using aluminum-bronze tools or other tools having a low coefficient of friction. Sheet less than 0.020 in. thick can usually be drawn or spun at room temperature although it is better practice to heat the sheet and the dies to 200 to 325°F. Heavier sheet must be heated for drawing, the temperature depending upon the thickness of the sheet and the amount of draw. It would be extremely difficult to list recommended temperatures for all conditions, so that it is probably best to determine these temperatures experimentally.

"Molybdenum sheet can be heated to temperatures up to approximately 750°F on a gas or electric hot plate without too much danger of oxidation, although thin sheet should not be exposed to air at this temperature for too long a time. When higher temperatures are required, the sheet should be heated in electric furnaces in an atmosphere of hydrogen or dissociated ammonia. It should be removed from this protective atmosphere for as short a time as possible for working; and if further working is necessary, it should be returned to the furnace immediately.

"For drawing, spinning, or severe forming operations cross-rolled annealed sheet should always be specified. Such sheet has been properly worked to impart the necessary ductility for forming in any direction.

"*Annealing:* Stresses induced by forming or drawing can be relieved, as with other metals, by annealing. The recommended annealing temperature is 1830°F, and the metal should be held at this temperature not more than 3 min. This time should not be exceeded, nor should the temperature be exceeded. Otherwise recrystallization and embrittlement will occur, regardless of the type of heating, or the type of atmosphere or lack of atmosphere. Molybdenum can be annealed at a lower temperature, which, of course, requires a longer time at heat, the time being dependent on the temperature. The lowest recommended temperature is 1355°F.

Machining

"There has been some mention in the literature of 'free-machining' molybdenum. To use this term in comparison with free-machining brass or free-machining steel is decidedly a misnomer.

"The only property of pure molybdenum which has any influence on its machinability is its grain structure. A molybdenum bar as sintered (i.e., with no working) has been found to be slightly more easily machinable than metal which has been worked. The proper structure of worked molybdenum for best machining properties is a uniform fine fibrous grain. The following information on machining applies to properly wrought molybdenum.

"The machining characteristics of molybdenum cannot be compared easily to those of other metals. Perhaps the nearest comparison that could be made is SAE 1040 or 1045 steel which has been heat-treated to a hardness of 30 Rockwell C. Such a material would have machining characteristics generally similar—but only generally similar—to those of molybdenum.

"Molybdenum machines with the crumbling chip, which is characteristic of hardened SAE 1040 steel. Although it is possible to machine molybdenum with high-speed steel tools, tungsten-carbide tools are recommended. Satisfactory results are obtained with Grade 2A5 Vascoloy-Ramet tools.

"*Turning and Milling:* For inside and outside turning, tools should be ground to angles and rakes similar to those used for cast iron. Correct tool shapes are illustrated in "Machinery's Handbook" and in the literature of carbide tool manufacturers. Speeds up to 100 ft. per min., with a depth of cut up to ⅛ in., are satisfactory for rough turning. The feed should be 0.015 in. For finishing work, speeds up to 100 ft. per min., with a depth of cut of 0.005 inch to 0.015 inch and a feed of 0.005 inch to 0.010 inch, should be used. It is important in turning that the depth of cut always be greater than 0.005 inch. If the depth of cut is less, tool wear will be excessive.

"Sulfur-base cutting oil should be used as a lubricant for roughing cuts, and kerosene or sulfur-base cutting oil should be used for finishing work. If lubricants are not used, tool wear will be excessive.

"Molybdenum has a tendency to chip while being machined, and care must be taken to prevent this. Work should be firmly chucked, tools rigidly supported, and machines should be sufficiently powerful and free from chatter or backlash.

"Face-milling is not generally recommended. It can be done when necessary, however, by the use of carbide-tipped cutters. The speeds and depth of cut should be similar to those used in lathe turning, except that the depth of cut should not exceed 0.050 in.

"Molybdenum plates can be edge-machined. In fact, plates thicker than 0.050 in. should be edge-machined rather than sheared to finished dimensions. This work can be done either on a shaper or milling machine, and the machining should be done along the edge rather than across the edge. The molybdenum should be clasped between steel plates while being machined to avoid chipping the edges.

"*Drilling, Threading and Tapping:* Molybdenum can be drilled with high-speed steel drills although carbide drills are recommended for deep drilling. When using high-speed steel drills the speed should be 30 to 35 ft. per min. with a feed of 0.003 in. A sulfur-base cutting oil should be used for all drilling, tapping, or threading.

"Some difficulty may be experienced in threading or tapping. The thread depth should not be more than 50 to 60% because of the tendency of molybdenum to chip. Re-threading or tapping should not be attempted at any time.

"Molybdenum can be roll-threaded. In this operation the molybdenum stock and the die should be heated to approximately 325°F. It is neither necessary nor

desirable to heat molybdenum beyond this temperature since it attains ample workability at that point. Molybdenum can be heated to this temperature in air without danger of oxidation.

"*Grinding:* In grinding, molybdenum behaves in a manner comparable to cast iron. Aluminum-oxide, silica-bonded wheels have proved satisfactory for most purposes. A 60-grit wheel, such as Norton No. 3860, is suitable for most grinding. When a fine finish is desired, a finer grit wheel can be used, but wheels of a grit finer than 80 tend to load rapidly and require frequent dressing.

"Wheel speeds for either cylindrical or surface grinding should be about 6500 ft. per min. For cylindrical grinding, the work speed should be 250 to 300 ft per min., and the depth of grind not more than 0.0002 in.

"For best results molybdenum should always be ground with plenty of coolant."

Joining

"Molybdenum parts are commonly joined by riveting (headed molybdenum rivets are available) or brazing, and sometimes by welding.

"*Brazing:* Brazing operations for relatively thin sheet can be done in a spot or seam welder, using copper or silver solder as the brazing medium. If all parts are well cleaned, no flux is necessary. Copper-alloy electrodes can be used in the welding machine, but tungsten-faced electrodes are better.

"For electronic tube parts, or other applications where temperatures beyond the melting points of copper or silver solder are encountered, tantalum foil of approximately 0.001-in. thickness is an excellent brazing medium. Brazing should be done under water to prevent oxidation of the tantalum foil.

"Heavier sections of molybdenum can be brazed in hydrogen-atmosphere furnaces without the use of a flux. Experimental copper or silver solder brazes can be made with a torch, but a flux must be used, and the results are largely dependent upon the experience and skill of the operator.

"*Welding*—Molybdenum can be resistance-welded. The preferred method is to stamp or roll a series of serrations or dimples in one of the sheets to be jointed, thus providing a number of projections at which welding will be localized. The resultant weld structure is somewhat brittle.

"Spot welds of fairly satisfactory quality can be made if the surfaces of both sheets to be jointed are etched. Any molybdenum sheet to be brazed or welded should be thoroughly cleaned of grease and oxide immediately before joining.

"Only welding equipment with precise controls should be used as excess heating will result in extremely brittle welds. Current values and timing are best determined by experiment. Electrodes should be kept clean and well-dressed."

Surface Finishing

"Ordinary cleaning and degreasing of parts made from molybdenum sheet present no special problems, and conventional methods and materials can be used.

"*Chemical Cleaning:* Electronic tube parts, which must be chemically cleaned, require somewhat more careful treatment. The hot chromic-acid cleaning solution commonly used for cleaning glass is recommended. A saturated solution of potassium dichromate in hot concentrated sulfuric acid can be used, but chromium trioxide is preferred to potassium dichromate because its use eliminates the possibility of potassium residues in crevices of fabricated parts. This cleaning solution should be used at 194°F, and should be kept red at all times. When the liquid becomes muddy or turns green, it should be discarded.

"After the chromic acid wash, the parts should be thoroughly rinsed, preferably

with hot distilled water. If running distilled water is not available, three dip washes will suffice, but it is important that all cleaning solution be removed. Electropolishing for bright finish can also be done in a chromic acid solution.

"*Etching and Polishing:* Etching, in preparation for resistance welding or brazing with tantalum foil, is accomplished by immersing the molybdenum sheet for 10 sec at 194°F in the following solution:

Sulfuric acid conc.	5 gal
Chromic acid	375 g
Hydrofluoric acid	1 qt
Nitric acid conc.	1/10 qt

The sheet should then be immersed in the chromic-acid cleaning solution, previously described, until the blue oxide disappears.

"For metallography, molybdenum can be polished with emery to No. 000 levigated alumina, and then etched with alkaline potassium ferricyanide. Etching and polishing should be repeated until grain boundaries appear.

"*Grit Blasting:* Molybdenum parts for electronic tubes are often blasted with steel grit to provide greater radiation surface. The recommended procedure is a blast of a few seconds with No. 90 steel grit at a pressure of 20 to 40 psi, followed by thorough cleaning in hydrochloric acid to remove iron particles. Sand, alumina, silicon carbide, or other abrasives should not be used because they become embedded in the molybdenum and cannot be removed with any chemical treatment which would not damage the metal.

"Since the purpose of grit blasting is to increase the amount of surface per unit of area, the blasting should be done in the manner which will produce fine "whiskers" rather than mere indentations on the surface. Sharp particles of grit will do this, while dull ones merely indent the surface. To achieve best results the blasting nozzle should be held at an angle nearly tangential to the work rather than perpendicular to the work.

"Molybdenum parts for electronic tubes are often 'hydrogen-fired' before assembly into the tube. The purpose of this operation is to reduce oxides and make a chemically clean component. The operation also relieves cold strains and set dimensions. The temperature range for hydrogen firing is usually 1470 to 1830°F, and the time is 10 to 30 min. Pure, dry hydrogen gas is recommended. Dissociated ammonia can be used if no further forming is to be done, but precautions must be taken to see that no free ammonia or nitrogen is present in the atmosphere. Fired parts, of course, must be cooled in the same protective atmosphere. Small parts are often loaded into trays or boats made of molybdenum sheet. These are easily made by the user or can be ordered from a supplier."

The tendency of molybdenum to form stable oxides at temperatures as low as 250°C imposes special precautions on handling tube assemblies during processing. Such oxide films will have a marked effect on contact potential between grid and cathode in the sealed-off tube and also on secondary emission, as mentioned above. Thin oxide films on molybdenum have been investigated by Gulbransen and Wysong[15] in oxidizing and reducing atmospheres and in high vacua at elevated temperatures. They have determined reaction rates as a function of temperature and pressure from the weight gained or lost over a period of time by a sample of sheet molybdenum suspended on a microbalance. It was found that

the oxides of molybdenum are essentially nonprotective to the base metal and that the rate of oxidation follows the well-known parabolic law $W = \sqrt{kt}$ from 250 to 450°C. This equation relates the weight increase in g per unit area, W, with the time t (sec), during which oxidation takes place, and k is the rate law constant $(g/cm^2)^2/sec$. It was first observed by G. Tammann in 1920. Deviations from this law set in at 450°C.

The stable oxides formed are MoO_2 and MoO_3 and the rate of formation depends much more markedly on the gas pressure than is the case for the oxides of tungsten. The oxides are volatile at relatively low temperatures, but are stable in high vacua of 10^{-6} mm of Hg up to 1000°C. MoO_2 may be formed at such high vacuum and high temperature; it then tends to inhibit further reaction. At pressures as low as 300 μ at 1000°C the volatile oxide MoO_3 is rapidly formed. A previously formed oxide film will begin to evaporate in a vacuum of 10^{-6} mm Hg when heated to 415°C, but at 400°C the rate of vacuum oxidation overcomes the evaporation phenomena and increases with increasing temperature. The reduction of Mo oxides in hydrogen is difficult to carry to completion. Three equations govern the possible reactions:

$$(1)\ MoO_2(s) + 2H_2(g) \rightleftarrows Mo(s) + 2H_2O(g)$$
$$(2)\ MoO_3(s) + 3H_2(g) \rightleftarrows Mo(s) + 3H_2O(g)$$
$$(3)\ MoO_3(s) + H_2(g) \rightleftarrows MoO_2(s) + H_2O(g)$$

Gulbransen and Wysong state that from a thermodynamic point of view reactions 2 and 3 above are favorable both in dry and wet hydrogen,

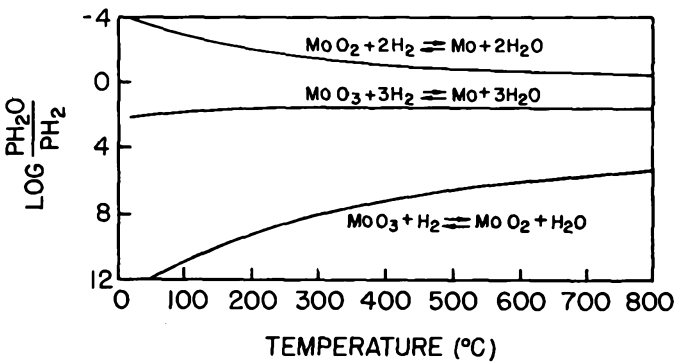

Fig. 9.3. Equilibrium pressure ratio H_2O/H_2 vs. temperature. Hydrogen reduction of oxides of molybdenum. After E. A. Gulbransen and W. S. Wysong.[15]

while reaction 1 is feasible if the water-vapor concentration is maintained below the equilibrium value. With a H_2 pressure of 2.2 cm practically complete reduction of oxide films formed at 400°C for 2 hours at 7.6 cm pressure of O_2 was obtained at 550°C. Fig. 9.3 gives plots of the equilibrium pressure ratio log pH_2O/pH_2 versus temperature for the three reac-

tions. The decomposition pressures of MoO_3 and MoO_2 as a function of temperature are shown in Fig. 9.4. They are negligibly small for practical consideration.

It is also of interest to note that white MoO_3 is turned blue by atomic hydrogen, which reduces MoO_3 to a lower oxide of the form $MoO_3 \cdot Mo_2O_3 \times H_2O$. J. R. Arthur[16] has demonstrated the presence of atomic hydrogen in hydrogen, coal gas, and moist carbon-monoxide flames which bring about this reaction. The oxidation of molybdenum in air at temperatures from 1100°F (593°C) to 1600°F (871°C) has been described recently

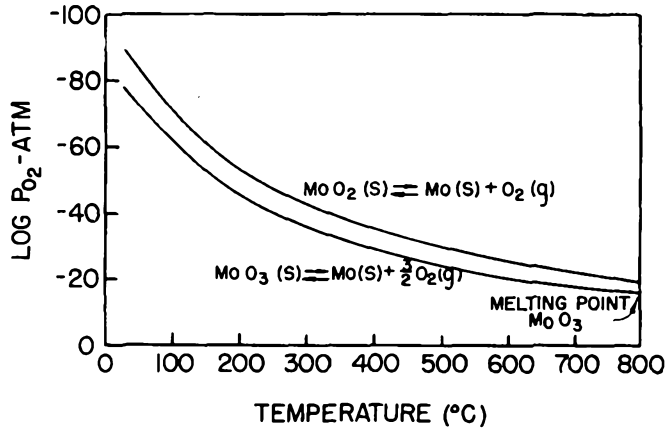

Fig. 9.4. Decomposition pressure MoO_3 and MoO_2 vs. temperature. After E. A. Gulbransen and W. S. Wysong.[15]

by Lustman.[23] At 1100°F the sheet is covered with a loosely adherent yellow scale of MoO_3, which turns white on cooling to room temperature. At higher temperatures the sheet was covered with a crystalline steel-gray oxide with the size of the crystals increasing with increasing temperatures. These oxide scales are nonprotective so that oxidation increases with time and extremely rapidly after the melting point of MoO_3 (795°C) has been passed.

The degassing of molybdenum has been studied by Norton and Marshall.[4,17] For complete outgassing it was found necessary to heat the metal to 1760°C (true temperature) in a vacuum of 10^{-6} mm Hg for a time depending on the thickness of the metal (½ to 1 hour). The gases given off are N_2 (over 60 per cent) CO (15 to 36 per cent), CO_2 (3 to 65 per cent) and H_2 (a small amount, mostly 0 per cent). Molybdenum parts thus treated may be stored in dry air at atmospheric pressure without absorbing gas from the air if they are wrapped in cellophane or paper bags and not handled. Only a monatomic surface film, which is readily removed by short heating in vacuo, is adsorbed during storage. Firing in a hydrogen furnace at atmospheric pressure is also a suitable degassing

process as H_2 is subsequently readily driven off *in vacuo* at relatively low temperatures. The purity of the H_2 used in the furnace has a marked effect on the amount of gas left in the metal. It should be free of N_2, CO, and CO_2. Norton and Marshall found that molybdenum samples from different sources responded to outgassing treatment quite uniformly, but marked difference in the time of treatment required and the amount of gas given off were noted, depending on the method of prior cleaning of the metal. Table 9.4 is reproduced from their paper.[17,4] All samples were 0.070 inch thick.

At the end of the preceding chapter, the development of a high-temperature porcelain enamel for tungsten was described according to Horsfall. Efforts to protect molybdenum against oxidation at elevated

TABLE 9.4. ANALYSIS OF GASES RELEASED BY MOLYBDENUM*

Treatment	Time of Degassing at 1760°C (time) (Min)	Amount of gas per g sample mm³ (N.T.P.)	Gas Composition (%)		
			N_2	CO	CO_2
Filed clean and washed in benzol	70	7.8	35	65	
Caustic dipped	24	4.4	79	16.5	4.5
Electrolyzed in conc. H_2SO_4	20	3.3	88.5	10.5	1

* After Norton and Marshall, Ref. 17.

temperature have similarly met with considerable success recently. The Fansteel Metallurgical Corporation has sponsored research at the Batelle Memorial Institute to solve this problem. It is stated by the investigators[28] that

"Molybdenum can be rendered highly resistant to oxidation by treatment with a hydrogen-silicontetrachloride atmosphere at 1000 to 1800°C so as to produce a molybdenum disilicide coating at its surface. Coatings 0.025 mm thick, thus produced, have completely protected the base metal for over 4000 hrs in air at 100°C. Thicker coatings, within limits, give proportionately longer lives. Although brittle at room temperatures, the coatings have limited ductility at a red heat."

REFERENCES

1. Gelok, J., "Molybdenum—Practical Structural Material," *Westinghouse Engineer*, (Sept., 1947).
2. Kieffer, R., and Hotop, W., "Pulvermetallurgie u. Sinterwerkstoffe," Berlin, J. Springer, 1943.

2a. "Sintered Metals," *Metal Ind.*, **66**, 342–344; 354–356; 378–380 (1945).

3. "Metals Handbook," Cleveland, Am. Soc. for Metals, 1948.
4. Dushman, S., "Scientific Foundations of Vacuum Technique," New York, John Wiley and Sons, Inc., 1949.
5. Kelley, K. K., "Contributions to the Data on Theoretical Metallurgy III. Free Energies of Vaporization and Vapor Pressures of Inorganic Substances," *U.S. Bur. of Mines, Bull. 383* (1935).

6. Osborn, R. H., "Thermal Conductivity of Tungsten and Molybdenum at Incandescent Tenperatures," *J. Opt. Soc. Am.*, **31**, 428–431 (1941).
7. Kannuluik, W. G., "The Thermal and Electrical Conductivities of Several Metals between −183°C and 100°C," *Proc. Roy. Soc.*, London, Ser. A. **141**, 159–168 (1933).
8. Worthing, A. G., "Physical Properties of Well-Seasoned Mo and Ta as a Function of Temperature," *Phys. Rev.*, **28**, 190–201 (1926).
9. Zwicker, C., "Physical Properties of Mo at High Temperatures," *Physica*, **7**, 71–74 (1927).
10. "Temperature, its Measurement and Control in Science and Industry," New York, Reinhold Publishing Corp., 1941.
11. Herring, C., and Nichols, M. H., "Thermionic Emission," *Rev. Mod. Phys.*, **21**, 185–270 (1949).
12. Smithells, C. J., "Metals Reference Book," New York, Interscience Publishers, Inc., 1949.
13. Espe, W., and Knoll, M., "Werkstoffkunde der Hochvakuumtechnik," Berlin, J. Springer, 1936.
14. Sykes, W. P., "Effect of Temperature, Deformation, Grain Size, and Rate of Loading on Mechanical Properties of Metals," *Am. Inst. Min. and Met. Eng.*, **64**, 780–815 (1921).
15. Gulbransen, E. A., and Wysong, W. S., "Thin Oxide Films on Molybdenum," *Am. Inst. Min. and Met. Eng.* (*Metals Tech.*), **14**, T.P. No. 2226, 1–17 (Sept., 1947).
16. Arthur, J. R., "Colour Changes Induced in Mo and W Oxides Under Flame Impact," *Nature*, **164**, No. 4169, 537–538 (1949).
17. Norton, F. J., and Marshall, A. L., "The Degassing of Metals," *Trans. Am. Inst. Mining Met. Eng.*, **156**, 351–371 (1944).
18. Marden, J. W., and Wroughton, D. M., "The Effect of Working on the Physical Properties of Mo," *Trans. El. Chem. Soc.*, **89**, 217–228 (1946).
19. Ksycki, Sister Mary Joecile, and Yntema, L. F., "The Electrodeposition of Mo from Aqueous Solutions," *J. El. Chem. Soc.*, **96**, 48–56 (1949).
20. Seim, H. J., and Holt, M. L., "The Electrodeposition of Mo-Alloys," *J. El. Chem. Soc.*, **96**, 205–213 (1949).
21. Archer, R. S., Briggs, J. Z., and Loeb, Jr., C. M., "Molybdenum, Steels, Irons, Alloys," New York, Climax Molybdenum Company, 1948.
22. Miller, G. L., "Molybdenum; Production, Properties, and Applications," *Metal Ind.*, London, **75**, 411–413; 439–441 (Nov., 1949).
23. Lustman, B., "Oxidation of Molybdenum in Air at 1100 to 1600°F," *Metal Progress*, **57**, 629–630, 674 (1950).
24. Parker, E. R., "High Temperature Properties of the Refractory Metals," *Transact. A.S.M.* **42**.399-404 (1950). (Data due to G. R. Graham, C. E. Swartz, and G. R. Tatum of the Kellex Corporation.)
25. Harwood, J. J., "New Structural Metals," *Prod. Eng.*, **21**, 96–102 (Oct. 1950).
26. Chelius, J., "How to Fabricate Molybdenum," *Mater. and Meth.*, **32**, 45–48 (1950).
27. Swartz, C. E., "Present Status of the Art of Molybdenum Fabrication," *Metal Progress*, **58**, 181–184 (1950).
28. Beidler, E. A., Powell, C. F., Campbell, I. E. and Yntenna, L. F., "The Formation of Molybdenum Disilicate Coatings on Molybdenum," *J. El. Chem. Soc.*, **91**, 21–25 (1951).

CHAPTER 10

TANTALUM

Tantalum has lately advanced to a prominent place among metals employed as structural material in power tubes. Its use for this purpose has been pioneered to a large extent by Heinz and Kaufman, Ltd., of San Francisco, and carried forward by Eitel-McCullough of San Bruno, California, who were the first to take advantage of the unique properties of tantalum on a commercial scale.[1]* Tantalum is produced in the United States by the Fansteel Metallurgical Corporation, where the first commercial ingot was made by C. W. Balke in 1921.[2] It weighed 8½ g while present-day ingots run to 7.5 kg., indicating the advance which has been made in mastering the intricate technique of its manufacture. While tantalum was discovered as early as 1802 by Ekeberg, a Swedish scientist, it was not used commercially until 1910, when tantalum filaments were used in Germany for incandescent lamps before the advent of tungsten. Like tungsten and molybdenum, tantalum is produced by the methods of powder metallurgy; however, it cannot be sintered in hydrogen but is treated in high vacuum at a temperature of 2600 to 2700°C. After cold swaging, a second high-vacuum sintering at close to the melting point of the metal leads to grain growth and liberation of the remaining impurities and gases. A highly ductile ingot of high purity (99.9 per cent Ta) is then produced. The metal has a bluish-white appearance, like platinum.

Tantalum can be rolled into ribbon as thin as 0.0005 inch and in that thickness is available in widths ranging from 0.006 inch to 1½ inches. It can be deep drawn into cups and drawn to tubing and wire at room temperature. Working the metal increases its tensile strength only by a small amount, rarely more than 20 per cent. While the absence of work-hardening is an advantage in cold rolling, there is the danger of tearing in drawing cups or wire.

Physical and chemical characteristics of tantalum are respectively tabulated in Tables 10.1 and 10.2. Its specific gravity of 16.6 makes it twice as heavy as steel, and in the unannealed state its strength is comparable to that of cold-rolled steel. The annealed metal may be com-

* In recent years "Eimac" tubes containing thoriated tungsten filaments and radiation-cooled anodes in glass envelopes employ "Pyrovac" anodes consisting of coated molybdenum (see Chapter IX).

TABLE 10.1. PHYSICAL CHARACTERISTICS OF TANTALUM

Atomic number: 73
Atomic weight: 180.88
Isotopes: 180, 181, 182
Lattice type: B.C.C.

No. of atoms per unit cell: 2

No. of unit cells per cc: 2.79×10^{22}
Atomic volume: 10.9 cc/g mole (Ref. 2)
Atomic heat: 6.5 cal/g mole

Specific heat: 0.036 cal/g (Ref. 2, 3)
Heat of combustion: 1380 cal/g (Ref. 3)

Density: 16.6 g/cc at 20°C (Ref. 2)
Tensile strength: (Ref. 2, 3)

Atomic valence: 5
Valence orbitals: $5d^3 6s^2$

Lattice constant: 3.2959 KX-units (Ref. 2, 3)

Closest approach of atoms: 2.854 KX-units (See Table 7.5)

Heat of fusion:
Heat of sublimation: 185.5 ± 0.3 Kcal/mole at T = 0°K (Ref. 18)
Melting Point: 2,996 ± 50°C (Ref. 2)
Vapor Pressure:
9.525×10^{-11} mm Hg at 1727°C (Ref. 2)
10^{-3} mm Hg at 2820°C (Ref. 4)
10^{-4} mm Hg at 2599°C (Ref. 4)
10^{-5} mm Hg at 2407°C (Ref. 4)
$R \ln p = -(185.5 \times 10^3)/T + 3.7 \times 10^{-4}T - 8.4 \times 10^{-8}T^2 - 32.87$ (p in atm) (Ref. 18)

		Psi	Elongation (% in 2″)	Rockwell Hardness
Sheet annealed	0.010″	50,000	40	60 (E)
Sheet worked	.010″	110,000	1	95 (E)
Wire annealed	.002″	100,000	11	
Wire worked	.002″	180,000	1.5	
Plate hardened	.010″	145,000	18	103 (B)

Young's Modulus: 27×10^6 psi (Ref. 2)
Torsion Modulus: not available
Poisson's Ratio: " "
Coefficient of thermal expansion: 65×10^{-7} cm/cm/°C 0– 100°C
(Ref. 5) 66×10^{-7} " " " 0– 500°C
80×10^{-7} " " " 20–1500°C
$\Delta L/L_0 = 6.080 \times 10^{-6}(T - 291) + 7.50 \times 10^{-10}(T - 291)^2$ (Ref. 19)
Thermal conductivity: 0.130 cal/cm²/cm/sec/°C at 20–100°C
(Ref. 2) .174 " " " 1430°C
.186 " " " 1630°C
.198 " " " 1830°C
Electrical resistivity: 12.4 microhm-cm at 18°C (Ref. 2)
54 " " " 1000°C (Ref. 2)
71 " " " 1500°C (Ref. 2)
15.5 " " " 20°C (Ref. 5)
61 " " " 1130°C (Ref. 5)
71 " " " 1430°C (Ref. 5)
80 " " " 1730°C (Ref. 5)
Temp. coeff. of el. resistivity: 0.00382/°C at 0–100°C (Ref. 2, 3)
Electron work function: 4.10 e.V. (Ref. 6)
Richardson constant A: 37 amp/cm²/deg² (Ref. 6)
Electron yield: 6 ma/watt at 2200°K
Electron emission: 1×10^{-5} ma/cm² at 1273°K
4.7×10^{-3} ma/cm² at 1500°K
19.5 ma/cm² at 2000°K

TABLE 10.1. PHYSICAL CHARACTERISTICS OF TANTALUM. (*Continued*)

Total radiation: (Ref. 7)	7.3 watts/cm² at 1330°C
	12.8 watts/cm² at 1530°C
	41.8 watts/cm² at 1730°C
Radiant emissivity ($\lambda = 0.665\ \mu$): (Ref. 7)	0.493 at 20°C
	.45 at 930°C
	.418 at 1730°C
Magnetic susceptibility: $+0.93 \times 10^{-6}$ c.g.s. (Ref. 2, 3)	

pared with annealed steel. In ultimate strength, fine tantalum wire, and thin sheet tantalum are similar to steel. The ductility of tantalum is comparable to that of stainless steel.

Its high resistance to chemical attack has made tantalum a valuable material in the chemical-process field. When used as an anode in acid solutions the metal becomes covered with a stable oxide film, which has a unidirectional resistance to the passage of current. This property is the basis of the Fansteel "Balkite" rectifier. "Self-healing" electrolytic condensers made from sintered tantalum powder also take advantage of this thin oxide film. Various proposed methods for the electrodeposition of tantalum have recently been analyzed by Seim and Holt,[8] with the conclusion that none of the processes so far suggested is successful. The study was confined to aqueous and nonaqueous solutions, and fused baths were not considered. Van Gilder, very appropriately, has described the electrodeposition of gold on tantalum.[9]

In turning now to the specific application of tantalum for grids and anodes in electron tubes the following data are extracted from *Fansteel Bulletin Ta-3902*, prepared by Hunter.[10]

"The main advantages to be gained from the use of tantalum in electron tubes are due to its high melting point, low vapor pressure, ductility and ease of welding and forming, its chemical affinity for oxygen, nitrogen, and carbon at temperatures within the operating range of the tubes; the possibility to outgas metal at temperatures substantially above operating temperatures and its resistance to chemical attack which equals that of glass. Essentially, this means that components can be produced economically which can be well outgassed on the pump and act as getters during operation after seal-off. In order to utilize these advantages the tube must be designed for the use of tantalum elements. Proper outgassing of tantalum anodes and grids requires that the temperature on the pump be raised to 2000°C, and, to act as getters during normal tube operation it is desirable that the operating temperature of the elements be in the vicinity of 700°C. These temperatures are higher than those encountered with conventional materials, such as nickel or molybdenum, and the heat must be dissipated by radiation through the tube envelope or conducted away by proper cooling without endangering adjacent glass seals or lowering the mechanical rigidity of the structure as a whole.

"While the vapor pressure of Ta itself is very low and comparable to that of W,

care must be taken that no oxides are formed due to improper processing of the Ta parts or other parts giving off oxygen on the pump. Ta-oxides have a much higher vapor pressure and may be volatilized and lead to blackening of the bulb. Furthermore, Ta becomes brittle and even fragile when more than about 0.1% by weight of oxygen, nitrogen or carbon is chemically combined with it. These oxides, nitrides and carbides of Ta are stable at normal operating temperatures and present a hazard primarily at temperatures above 1800°C, when volatilization and possibly decomposi-

TABLE 10.2. CHEMICAL PROPERTIES OF TANTALUM

Atomic number: 73 — Atomic valence: 5
Atomic weight: 180.88 — Valence orbitals: $5d^3 6s^2$
Heat of fusion: — Melting point: 2996 ± 50°C
Heat of sublimation: 185.5 ± 0.3 kcal/mole (Ref. 18)
Heat of combustion: 1379 cal/g
Electrochemical equiv.: 0.3749 mg/coulomb

(A) Reactions of pure tantalum:
- (1) in air or oxygen at 20°C: practically none
- (2) in air or oxygen at 400°C: weak oxidation—blue film
- (3) in air or oxygen at 600°C: weak oxidation—grey film
- (4) in air or oxygen > 600°C: oxidation to Ta_2O_5—whitish
- (5) in water vapor at 700°C: rapid oxidation
- (6) in HCl or H_2SO_4, cold, dil. or conc.: practically none if no SO_3 present
- (7) in HCl or H_2SO_4, warm, dil. or conc.: practically none up to 100°C if no SO_3 present
- (8) in HNO_3 or aqua regia, cold, dil. or conc.: practically none
- (9) in HNO_3 or aqua regia, warm, dil. or conc.: surface attack forming protective layer
- (10) in HPO_3 (85%) cold to 145°C: practically none
- (11) in HPO_3 conc. above 200°C: attack
- (12) in HF cold or warm, dil. or conc.: attack with absorption of H_2
- (13) in HF + HNO_3, cold or warm. dil. or conc.: strong attack–rapid dissolution
- (14) in Na(OH) or K(OH) cold: slight attack
- (15) in Na(OH) or K(OH) warm: strong attack
- (16) in K(OH) or Na_2CO_3: rapid dissolution
- (17) in Carbon(s) or Hydrocarbons: partial carbide formation above 1200°C complete carburization at ~ 1400°C
- (18) in CO: absorption at 600°C
- (19) in H_2: absorption below 700°C
- (20) in N_2: absorption below 600°C
- (21) in rare gases: none
- (22) in Hg: none

(B) Oxides of Tantalum

Ta_2O_4—dark grey to dark brown powder, Ta-tetroxide

Ta_2O_5—white or colorless rhombic crystals, Ta-pentoxide, decomposes at 1470°C (d = 8.74)

tion takes place. The nitrides are formed at higher temperatures than the oxides and also volatilized and decomposed at much higher temperatures than the oxides. Although the carbides of tantalum are neither fusible nor volatile at temperatures below the melting point of tantalum, they can, under some conditions, be reduced by oxide with the consequent liberation of carbon monoxide. At operating temperatures the result of the reaction between carbide and oxide of tantalum would be to segregate

them in different portions of the anode without the liberation of carbon monoxide. At temperatures in the processing range, however, many factors combine to alter this reaction so that carbon monoxide may be liberated and pumped away. The vapor pressure of some oxides of tantalum is so low at temperatures below 2000°C, that excessively long pumping time is required if such a temperature is not reached. In fact, there are indications that tantalum anodes may never reach a satisfactory condition unless they are heated during the exhaust process to a temperature of at least 2000°C. When this temperature is attained, however, oxides and other forms of contamination which may influence tube operation are rapidly ejected so that pumping time may be reduced to a minimum. If the full value of tantalum is to be realized in transmitting tubes containing tantalum electrodes, they should be heated to at least 2000°C.

"Occluded gases on the surface of tantalum are evolved rapidly at temperatures below 1100°C. From there up to 1600°C, there may be little or no gas evolution. In the range from 1600 to 1800°C there may be a slight evolution of gas which, if the temperature is not increased, will be of long duration. At 1800°C the rate of gassing will increase, but because the temperature of the electrode may not be completely uniform, outgassing will not be complete. There is a tendency for oxide and other compounds to migrate to cooler portions of the metal so that processing at this temperature will not produce a complete outgassing.

"At 2000°C all portions of the plate should reach at least 1800°C, and the oxide will be volatilized from all portions of the electrode rapidly. At this temperature, the rate of decomposition or vaporization of oxide is greater than the rate of combination so that gases from other portions of the tube will not be taken up by the tantalum plate but will be either pumped out or converted into nonvolatile compounds which are exhausted or deposited on the bulb. It is necessary, therefore, to outgas as thoroughly as possible all the other portions of the tube before the tantalum electrodes are heated to this final temperature.

"The practice of maintaining the plate temperature at 1500 or 1600°C by high-frequency induction and then periodically boosting the temperature to 2000°C by internal bombardment is useless and may be injurious. The only effective exhaust is obtained while the plate is at the highest temperature, and if the size of the tubulation in combination with the speed of the pump does not permit removal of the gas as rapidly as it is formed, the tantalum will reabsorb it on cooling to lower temperature faster than the pump can remove the gas. Such a procedure greatly prolongs the pumping schedule and may even prevent adequate outgassing of the tube.

"The thermal radiation coefficient of Ta is low when compared with black materials such as carbon. This is an advantage as the resultant higher operating temperature permits optimum rate of absorption of released gases. On the other hand, care must be taken that the temperature of the Ta parts does not rise to the range where gas release takes place. This may require an increase of the radiating surface by roughening it or by attaching radiating fins to the structure. No process has yet been found to produce and maintain a black surface on Ta. The black oxides which can be formed by heating Ta in air dissolve in the metal when the latter is heated *in vacuo* to temperatures above 800°C. The concomitant oxide content is objectionable for reasons stated above. Carbonizing the surface of Ta is also unsatisfactory because carbides are formed during the outgassing process on the pump which may be reduced in the presence of oxides. Frequently, such carbon coatings also peel off. The commonly used and accepted process for increasing radiation intensity from bright metal surfaces is blasting with fine shape particles. Ordinary sand-blasting equipment is satisfactory, but sand should not be used on tantalum. If sand is used, it will become embedded in the tantalum and decompose during the

exhaust process, causing brittle spots in the tantalum and prolonged gassing. Sharp steel grit is the preferred blasting medium, but 'Carborundum' is frequently used. Steel or iron grit is preferred because embedded particles in the tantalum can be removed by acid treatment while 'Carborundum' cannot. Embedded particles of 'Carborundum' may decompose during exhaust and produce additional gas. The reason why 'Carborundum' is frequently preferred to steel is that the particles remain sharp, whereas steel may become dulled; but since methods of sharpening steel grit have become available, this objection is no longer serious. Grit sizes between 60 and 90 on the Pangborn chart appear to give the most satisfactory results.

"Anodes should be fabricated to final size and shape before grit blasting. If the sheet is blasted before fabricating the anode it will distort and become difficult to handle. Also, the effectiveness of the blasting is lost wherever electrodes or tools touch the surface thereafter. Since the purpose of grit blasting is to increase the amount of surface per square inch, the process should be carried out in the manner which will produce fine "whiskers" rather than mere indentations in the surface. Sharp particles do this, whereas dull ones simply make identations. To achieve best results the blasting gun should be held at an angle which is close to tangential to the work rather than nearly 90° to it since a stream of particles which impinges directly on the surface of the metal will indent rather than cut it and in addition may actually perforate it.

"Tube structures made entirely of tantalum can be effectively cleaned before mounting by simple chemical processes. If other metals are included or attached to these structures, the cleaning process will have to be altered.

"Tantalum plates and grids which have been steel-grit blasted should be first immersed in hot hydrochloric-acid solution to remove particles of iron. If they have been blasted with carborundum, this portion of the process may be omitted. After washing in hydrochloric acid, the parts should be thoroughly rinsed with water. Distilled water is preferred but if it is not available, tap water can be used. The objection to tap water is that it frequently contains calcium salts which may be converted to sulfate by the sulfuric acid of the following process, and these salts left on the electrode.

"Following this treatment the electrode should be immersed in hot "cleaning solution" such as is commonly used for cleaning glass. A saturated solution of potassium dichromate in hot concentrated sulfuric acid may be used for this process, but chromium trioxide is to be preferred to potassium dichromate because with it there is no possibility of leaving alkaline salts in crevices or elsewhere on the electrode. This solution should be heated to approximately 110°C and should be kept red at all times. When the liquid becomes muddy or turns green, it should be discarded and fresh solution made up. The time during which electrodes should be left in this solution varies with their size and condition. If they are dirty or have oil or finger prints on them, the treating time should be long enough to insure complete removal of such contamination. No set schedule can be recommended for this treatment as each manufacturer must be guided by the results obtained under his conditions.

"After the chromic acid wash, the tantalum parts should be thoroughly washed. Tap water, preferably warm or hot, is satisfactory for the first wash, but it should be followed by a thorough washing in hot distilled water. If running distilled water is not available, two dip washes will suffice; but it is important to keep the concentration of sulfuric and chromic acids in the final wash at a minimum.

"The parts should be dried in clean, warm air, avoiding all dust or contamination. They should not be wiped with paper or cloth, nor should they be handled with the fingers. They should be stored in dust-tight containers.

"Anodes fabricated by Fansteel are delivered blasted and thoroughly cleaned. If accidentally handled, they should be recleaned, rinsed and washed as outlined above."

Ta members should not be used in conjunction with other metals when the temperature of the junction is sufficiently high for alloying and subsequent embrittlement to take place. This often leads to fracture of the Ta member. Likewise, severe warpage and embrittlement will ensue when Ta members are operated in the vicinity of hot bodies, such as tungsten filaments, and the degree of vacuum is not sufficient to prevent the presence of gases. Their absorption by tantalum will result in severe embrittlement. Experience at the author's laboratory has brought these effects into sharp focus.

Tantalum channels of U-shaped cross section, some 15 inches long, 0.200 inch wide, and 0.250 inch deep, made from 0.005-inch tantalum sheet, were intended as reflectors behind a 15-inch long tungsten ribbon filament in a continuously exhausted tube of large dimensions. Because of the gases evolved continuously from massive metallic members, the U-channel would close up and short to the tungsten filament. This difficulty was overcome by substituting molybdenum for tantalum and making the channel from several stiffened sections.

In regard to the alloying of tantalum it was found that resnatron filament baskets of the type shown in Fig. 8.1* would fail where tantalum tabs were attached to a nickel ring. The tabs supported flat tungsten filaments at the other end, and tantalum was chosen for the tabs so as to minimize heat loss by conduction to the nickel support ring. Fig. 10.1 shows a photomicrograph taken at this laboratory in which the interpenetration of nickel and tantalum is clearly evident. When heavier nickel rings were chosen, the temperature at the junction could be lowered and the alloying action thus greatly minimized.

The properties of nickel-tantalum alloys have been investigated by E. Therkelson (Berlin, 1932),[11] and Fig. 10.2 gives the constitutional diagram for these alloys. Up to a tantalum content of 36 per cent a homogeneous solid solution is formed which has a liquidus falling smoothly from 1450 to 1350°C. There is a maximum at 1545°C, corresponding with nickel tritatantalide Ni_3Ta, and a minimum at 1400°C with 61 per cent of tantalum. The structures of alloys with 50 to 78 per cent of tantalum are very complex and show a transformation in the solid state at 1350°C. Fig. 10.3 shows the variation of hardness, tensile strength, Young's Modulus, and electrical conductivity with increasing tantalum content. It is seen that the resistance increases markedly with increasing tantalum content, and this may have been in part responsible for the failure of the tantalum tabs as considerable currents were passed through them.

* page 183

Tantalum will not alloy with copper at any temperature. Brazing thus presents quite a problem. Silver soldering in air is done at times in a bed of molten potassium-tantalum fluoride. A heavy plating with nickel or platinum is used for vacuum brazing. Spot welding in air, arc-

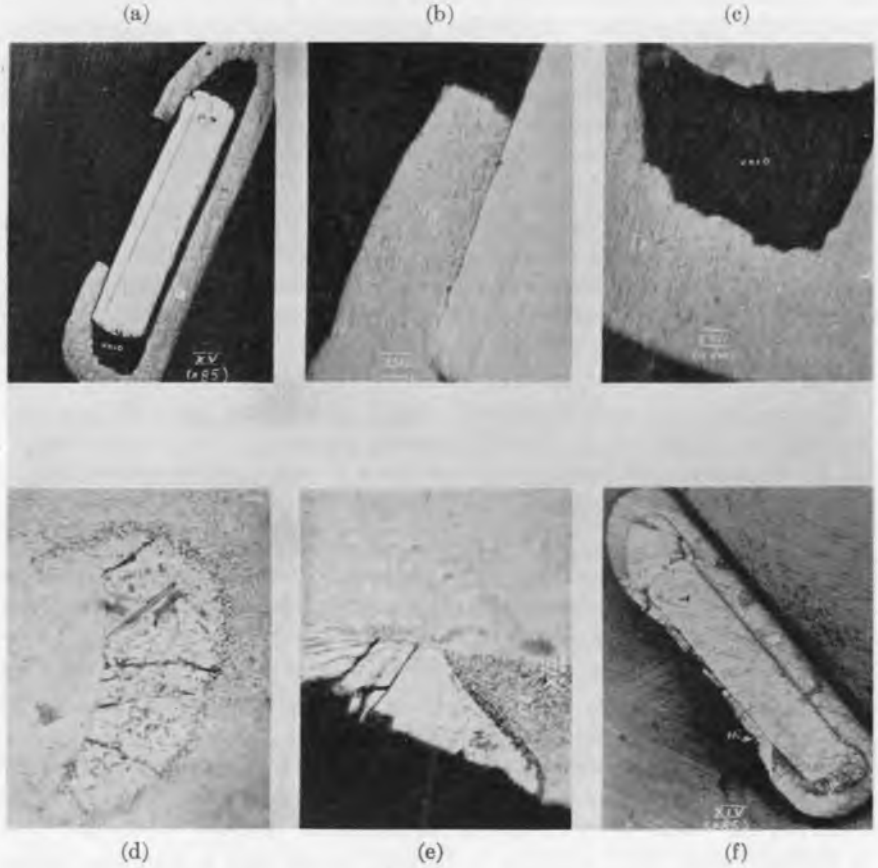

Fig. 10.1. Alloy formation between Ni and Ta. (a) Cross-section of tungsten ribbon (0.010″ × 0.050″) (×42) clamped and spot welded in a tantalum tab which in turn is spot welded to a nickel support ring (not shown). (×200.) (b and c) Enlarged detail of (a). (d) Void of (a) filled with nickel after operating assembly at 2400°C for 30 seconds. (e) Enlarged detail of (f) (where symbol Ni appears in (f)). (f) Same as (a) after operation at 2400°C for 30 seconds. Note: Temperature value approximate only. (*Courtesy Collins Radio Company.*)

welding under carbontetrachloride and seam-welding under water are common techniques. Inert gas welding, using helium and argon has been perfected in recent years and is now being applied to tantalum on a commercial scale.

Tantalum is not only useful as a structural material in electron tubes

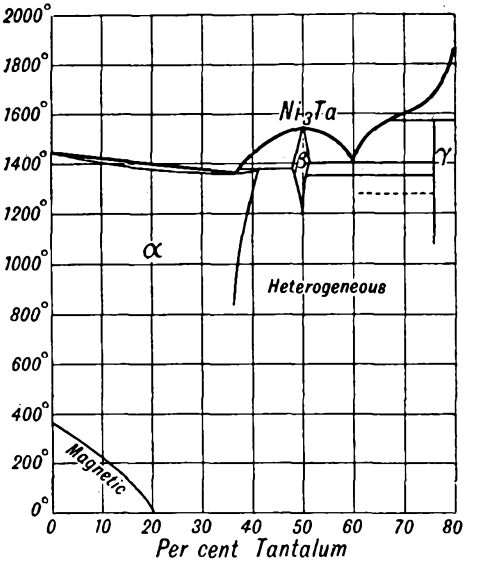

Fig. 10.2. The Constitutional diagram of the Ni-Ta alloys (temperatures in °C). After E. Therkelson, Berlin 1932. (Vid. Ref. 11.) (*Courtesy Longmans Green and Company.*)

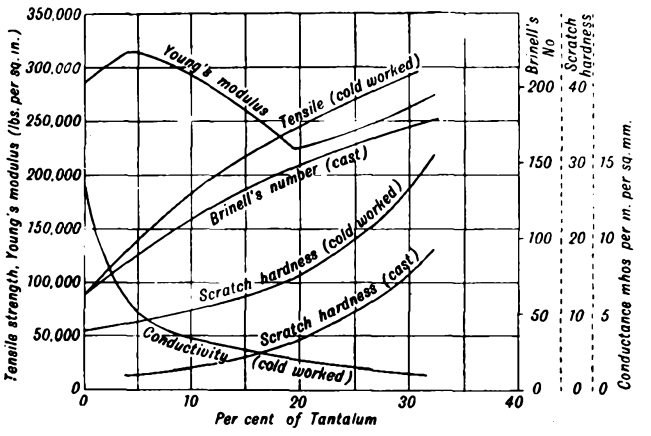

Fig. 10.3. Hardness, tensile strength, and electrical conductivity of the Ni-Ta alloys. After E. Therkelson, Berlin 1932. (Vid. Ref. 11.) (*Courtesy Longmans Green and Company.*)

but also as an efficient electron emitter at elevated temperatures. While its melting point is a few hundred degrees lower than that of tungsten, its work function is less. Consequently, for a given temperature tantalum gives a higher electron emission per unit area than tungsten. At the same time tantalum will operate closer to its melting point, percentage-wise, than tungsten so that the rate of evaporation will be higher for tantalum. This will in turn shorten the life of a tantalum cathode as compared with that of a tungsten cathode when both operate at such a temperature, respectively, as to give the same emission per unit area. These factors have to be weighed carefully against the great advantage

TABLE 10.3. COMPARATIVE DATA FOR PURE METAL CATHODES OPERATING AT A TEMPERATURE T_0 (°K) TO GIVE A SATURATED EMISSION DENSITY $J = 3$ AMP/CM². $T_{M.P.}$ = MELTING POINT (°K); φ = WORK FUNCTION (E.V.); M = RATE OF EVAPORATION AT T_0.[12]

Metal	T_0 (°K) for $J \sim 3$ a/cm²	$\frac{T_0}{T_{M.P.}} \times 100$	φ ev	M g/cm²/sec	$T_{M.P.}$ (°K)
Molybdenum	2580	89.3%	4.37	14×10^{-6}	2893
Columbium	2560	95.2	4.01	0.42×10^{-6}	2685
Tantalum	2585	79.1	4.10	$.043 \times 10^{-6}$	3269
Tungsten	2780	76.2	4.52	$.043 \times 10^{-6}$	3643

of being able to draw and form tantalum in almost any required shape, regardless of size. A good example of the application of these principles is contained in a paper by Jepsen[12] from which Table 10.3 is reproduced. Comparative values are given for temperature of operation, T_0, and rate of evaporation, M, for several pure metal emitters operated at a temperature yielding an electron emission of $J = 3$ amp/cm². The ratio $T_0/T_{M.P.}$, the melting points $T_{M.P.}$, and the work function φ have been added.

Electrical resistance, thermal emissivity, melting point, and rate of evaporation of tantalum have been determined by Malter and Langmuir[13,14]; the earlier measurements of some of these quantities are given by Worthing[15,16] and Utterback and Sanderman.[17] There is a discrepancy between values for resistivity and emissivity measured by Worthing in 1926 and those obtained by Malter and Langmuir in 1939 which may well be ascribed to the advance in processing technique leading to a purer tantalum. A similar apparent change in the properties of tungsten took place between 1922 and 1934 and may likewise be explained by gradually improved material.[12] Rates of evaporation for tungsten given in Table 10.3 above are thus about half those given by Jones and Langmuir in 1927.

Some of the pertinent data from these later measurements on tantalum

are here reproduced for convenience of reference. Fig. 10.4 gives the true temperature T(°K) versus the brightness temperature S(°K) at $\lambda = 0.665\ \mu$, and Table 10.4 summarizes data on resistivity, emissivity, and thermal expansion for tantalum according to Ref. 13. The curve Fig. 10.3 can be represented by the following equation:

$$T = 0.99198 + 37.14 \times 10^{-6}S^2 + 5.74 \times 10^{-9}S^3$$

The percentage error at any point within the measured range is less than

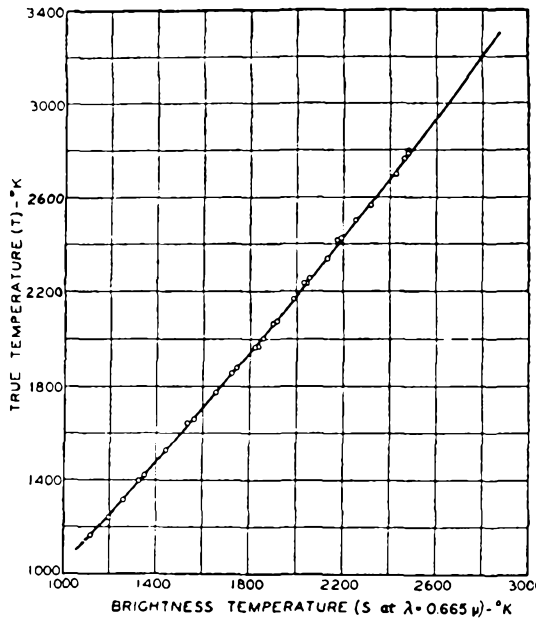

Fig. 10.4. True temperature T vs. the brightness temperature S for the effective wavelength $\lambda = .665$ microns. After Malter and Langmuir.[14] (*Courtesy American Physical Society.*)

0.5 per cent. The spectral emissivity $e_{(0.665\ \mu)}$ as a function of T was determined from the curve of Fig. 10.3 by means of the relation

$$\frac{1}{T} - \frac{1}{S} = \frac{\lambda_e \log e_{(0.665\mu)}}{0.434C_2}$$

C_2 is the Wien-Planck constant 1.433 cm degrees. A smooth curve was drawn through the values thus plotted and the resultant figures entered in Table 10.4. The probable error of emissivity values is 0.01. Electrical measurements were made on wires of diameter d_0, and the values $A' = A/d_0^{3/2}$, $V' = Vd_0^{1/2}/l_0$, $V'A'^{1/3} = VA^{1/3}/l_0$ are entered in Table 10.4, where A is the current in amps., V the measured difference of potential

along the wire, d_0 the filament diameter in cm at room temperature, and l_0 the distance between the potential leads in cm at room temperature. This makes A', V' specific characteristics independent of filament diameter in a manner explained in Chapter 8. The quantity $VA^{1/3}/l_0$ should be kept constant if the temperature of the filament is to remain constant while its diameter is being reduced by evaporation during prolonged

TABLE 10.4. DATA ON RESISTANCE, EMISSIVITY, AND THERMAL EXPANSION OF TANTALUM[13]

T is the true temperature; ρ is the resistivity corrected for thermal expansion; W is the total radiation intensity not corrected for thermal expansion and e_t is the power emissivity corrected for thermal expansion; M and L are the results of Malter and Langmuir; W are those of Worthing, and U and S those of Utterback and Sanderman. The spectral emissivity at 0.665 μ is indicated by $e_{0.665\mu}$. The thermal expansion given by Worthing is designated by l/l_0.

T (°K)	ρ Ohm · cm	W watts/cm²	e_t	A'	V'	$V'A'^{1/3}$	Brightness Temperature			$e_{0.665\mu}$	l/l_0
							M and L	W	U and S		
1000	44.1×10^{-6}	0.793	0.136	211	0.0118	0.0702	967	966		0.481	1.0047
1100	47.3	1.23	.144	254	.0152	.0963	1060			.476	1.0055
1200	51	1.84	.153	299	.0193	.1291	1152	1149		.469	1.0063
1300	54.8	2.73	.163	352	.0244	.1723	1242		1250	.462	1.0071
1400	59	3.95	.174	408	.0304	.2255	1332	1329	1337	.456	1.0079
1500	62.4	5.47	.184	469	.0368	.2855	1421			.449	1.0087
1600	65.8	7.36	.194	528	.0438	.3540	1508	1506	1508	.442	1.0095
1700	69.3	10.10	.205	602	.0527	.4450	1596			.437	1.0103
1800	72.5	13.28	.215	676	.0617	.5415	1682	1682	1678	.432	1.0111
1900	75.8	17.12	.223	751	.0716	.6508	1767			.426	1.0119
2000	78.9	21.63	.232	828	.0821	.7709	1852	1851	1843	.421	1.0127
2100	82	27.11	.240	910	.0936	.9071	1933		1926	.417	1.0135
2200	85.2	34.18	.247	1002	.1072	1.080	2018	2018		.413	1.0144
2300	88.3	42.23	.254	1095	.1212	1.250	2099			.409	1.0152
2400	91.3	51.27	.261	1189	.1357	1.437	2181	2181		.405	1.0161
2500	94.4	62.38	.269	1288	.1522	1.656	2261			.402	1.0170
2600	97.4	75.37	.276	1394	.1699	1.898	2341	2339		.400	1.0179
2700	100.2	89.89	.282	1502	.1880	2.153	2421			.397	1.0188
2800	102.9	105.5	.288	1606	.2064	2.417	2499	2495		.394	1.0197
2900	105.6	123	.293	1715	.2257	2.699	2575			.391	1.0206
3000	108.7	144.4	.298	1830	.2479	3.032	2652	2647		.388	1.0216
3100	111.4	167.4	.302	1948	.2700	3.367	2727			.386	1.0225
3200	113.9	194.2	.306	2075	.2940	3.749	2803			.384	1.0235
3269	115.5	214.5	.309	2164	.3110	4.025	2855			.383	1.0242

operation at elevated temperature. The rate of evaporation as a function of temperature, determined by Langmuir and Malter[14] from weight measurements, can be represented by

$$\log_{10} M = 7.86 - \frac{39{,}310}{T}$$

M is the rate of evaporation in g/cm² sec, and T is the temperature in °K. Fig. 10.5 shows the corresponding graph, and Table 10.5 gives

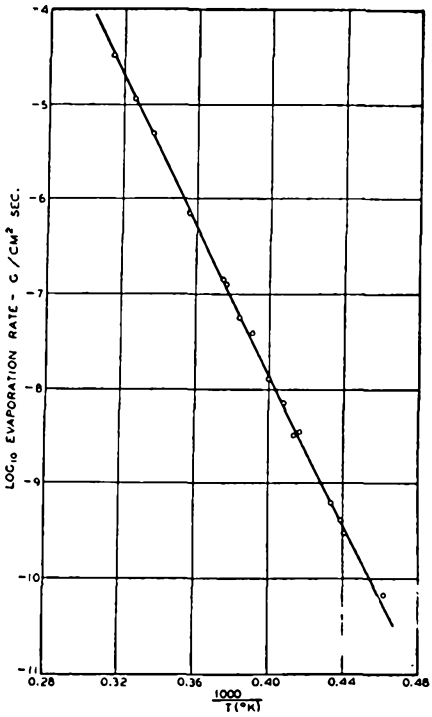

Fig. 10.5. Rate of evaporation of tantalum as a function of temperature. After Langmuir and Malter.[14] (*Courtesy American Physical Society.*)

TABLE 10.5. RATE OF EVAPORATION M AND VAPOR PRESSURE P FOR TANTALUM AT VARIOUS TEMPERATURES
(After Langmuir and Malter, Ref. 14)

T (°K)	M g/cm² sec	P	
		Dynes/cm²	mm Hg*
2,000	1.63×10^{-12}	1.27×10^{-7}	9.53×10^{-10}
2,200	9.78×10^{-11}	8.01×10^{-6}	6.01×10^{-9}
2,400	3.04×10^{-9}	2.58×10^{-4}	1.94×10^{-7}
2,600	5.54×10^{-8}	4.90×10^{-3}	3.68×10^{-6}
2,800	6.61×10^{-7}	6.07×10^{-2}	4.55×10^{-5}
3,000	5.79×10^{-6}	5.40×10^{-1}	4.05×10^{-4}
3,200	3.82×10^{-5}	3.77	2.83×10^{-3}
3,269 (M.P.)	6.80×10^{-5}	6.75	5.06×10^{-3}

* This column added by present author.

values of M and P, the vapor pressure of tantalum at various temperatures in dynes/cm^2, and mm Hg. P is derived from the relation

$$P = 1700MT^{1/2}$$

REFERENCES

1. Wagener, W. G., "Evolution of Tantalum Tubes," *El. Ind.* **108** (June, 1944).
2. Fansteel Metallurgical Corp., *Tech. Data Bull.*
3. "Metals Handbook," Cleveland, Am. Soc. for Metals, 1948.
4. Dushman, S., "Scientific Foundations of Vacuum Technique," New York, John Wiley and Sons, Inc., 1949.
5. Kieffer, R., and Hotop, W., "Pulvermetallurgie u. Sinterwerkstoffe," Berlin, J. Springer, 1943.
6. Herring, C., and Nichols, M. H., "Thermionic Emission," *Rev. Mod. Phys.*, **21**, 185–270 (1949).
7. Espe, W., and Knoll, M., "Werkstoffkunde der Hochvakuumtechnik," Berlin, J. Springer, 1936.
8. Seim, H. J., and Holt, M. L., "Attempts to Electrodeposit Tantalum," *J. El. Chem. Soc.*, **96**, 43–47 (1949).
9. Van Gilder, R. D., "Electrodeposition of Gold on Tantalum," *U.S. Patent 2,492,204* (Dec. 27, 1949).
10. Hunter, F. L., "Processing of Tantalum Anodes and Grids for Transmitting Tubes," *Tech. Data Bull. Ta-3902*, Fansteel Metallurgical Corp.
11. Mellor, J. W., "Inorganic and Theoretical Chemistry," Vol. 15, 237 New York, Longmans, Green and Co., 1936.
12. Jepsen, R. L., "Coaxial Tantalum-Cylinder Cathode for C. W. Magnetrons," *R.C.A. Rev.*, **8**, 301–311 (1947).
13. Malter, L., and Langmuir, D. B., "Resistance, Emissivities, and Melting Point of Tantalum," *Phys. Rev.*, **55**, 743–747 (1939).
14. Langmuir, D. B., and Malter, L., "The Rate of Evaporation of Tantalum," *Phys. Rev.*, **55**, 748–749 (1939).
15. Worthing, A. G., "Physical Properties of Well-Seasoned Molybdenum and Tantalum as a Function of Temperature," *Phys. Rev.*, **28**, 190–201 (1926).
16. Worthing, A. G., "Spectral Emissivities of Tantalum, Platinum, Nickel, and Gold as a Function of Temperature and the Melting Point of Tantalum," *Phys. Rev.*, **28**, 174–189 (1926).
17. Utterback, C. L. and Sanderman, L. A., "Some Thermal Properties of Tantalum" *Phys. Rev.*, **39**, 1008–1011 (1932).
18. Edwards, J. W., Johnston, H. L., and Blackburn, P. E., "Vapor Pressure of Inorganic Substances. IV. Tantalum between 2624 and 2943°K," *J. Am. Chem. Soc.*, **73**, 172–174 (1951).
19. Edwards, J. W., Speiser, R., and Johnston, H. L., "High Temperature Structure and Thermal Expansion of some Metals as determined by X-Ray Diffraction Data. I. Platinum, Tantalum, Niobium, and Molybdenum," *J. Appl. Phys.* **22**, 424–428 (1951).

CHAPTER 11

NICKEL

Nickel has always been in common use in the radio-tube industry. For moderate temperature operation, nickel combines the many advantages claimed for tantalum at higher temperature, with the exception that it has little gettering action. It is available in many forms at low cost and is easily worked into all conceivable shapes required for cathode sleeves, grid supports, anodes, deflector plates, shields, and the like. It has reasonable strength in the commercially pure state and may be alloyed with a variety of metals when special characteristics are required. Wise[1] has described the properties of nickel which are of particular interest to radio engineers. Table 11.1 summarizes the physical characteris-

TABLE 11.1. PHYSICAL CHARACTERISTICS OF CHEMICALLY PURE NICKEL*

Atomic number: 28	Atomic valence: 2, 3
Atomic weight: 58.69	Valence orbitals: $3d^8 4s^2$
Isotopes: 58, 60, 61, 62, 64	
Lattice type: F.C.C.	Lattice constant: 3.5167 KX-units at 24.8°C (Ref. 2)
No. of atoms per unit cell: 4	
No. of unit cells per cc: 2.30×10^{22}	Closest approach of atoms: 2.487 KX-units (See Table 7.5)
Atomic volume: 6.59 cc/g mole (Ref. 2)	Heat of fusion: 73.8 cal/g (Ref. 2)
Atomic heat: 6.16 cal/g mole	Heat of sublimation: 85 Kcal/mole (Ref. 2)
Specific heat: 0.105 cal/g/°C (20°C) (see also Fig. 11.1 page 234)	Melting point: 1453°C (Ref. 6)
0.1123 at 100°C (Ref. 2)	Boiling point: 2730°C (Ref. 7)
.1225 200°C	Vapor pressure: (Ref. 8, 9)
.1367 300°C	7×10^{-8} mm Hg at 1000°C
.1267 400°C	9×10^{-7} mm Hg at 1100°C
.1265 500°C	1.3×10^{-5} mm Hg at 1200°C
.1326 600°C	1.5×10^{-4} mm Hg at 1300°C
	1×10^{-3} mm Hg at 1400°C

Density: computed		8.908 g/cc (20°C)
(Ref. 2)	cast	8.907 g/cc (23°C)
	worked-annealed	8.901 – 8.903 g/cc (25°C)

* Many of the data quoted from Ref. 2 are there in turn credited to other sources listed in Ref. 2. These data apply to chemically pure nickel (99.98) unless otherwise specified.

TABLE 11.1. PHYSICAL CHARACTERISTICS OF CHEMICALLY PURE NICKEL. (*Continued*)

Average coefficient of thermal expansion over various temperature ranges (Ref. 2). (See also Fig. 11.2 page 234)

10.22×10^{-6}	cm/cm/°C	−180 to 0°C
13.3×10^{-6}	cm/cm/°C	0 to 100°C
14.63×10^{-6}	cm/cm/°C	0 to 300°C
15.45×10^{-6}	cm/cm/°C	0 to 500°C
13.3×10^{-6}	cm/cm/°C	25 to 100°C
14.4×10^{-6}	cm/cm/°C	25 to 300°C
15.5×10^{-6}	cm/cm/°C	25 to 600°C
16.3×10^{-6}	cm/cm/°C	25 to 900°C

Instantaneous coefficient of thermal expansion: (Ref. 2)

12.6×10^{-6}	cm/cm/°C	at 20°C
13.5×10^{-6}	cm/cm/°C	at 100°C
14.5×10^{-6}	cm/cm/°C	at 200°C
16.3×10^{-6}	cm/cm/°C	at 300°C
16.3×10^{-6}	cm/cm/°C	at 400°C

Thermal conductivity: (Ref. 2) (See also Fig. 11.3 page 235)

0.198	cal/cm²/cm/sec/°C	at 100°C
.175	cal/cm²/cm/sec/°C	at 200°C
.152	cal/cm²/cm/sec/°C	at 300°C
.142	cal/cm²/cm/sec/°C	at 400°C
.148	cal/cm²/cm/sec/°C	at 500°C

Electrical resistivity: 6.141 microhm-cm at 0°C (Ref. 2) (See also Fig. 11.4 p. 236)
6.844 microhm-cm at 20°C
10.327 microhm-cm at 100°C (Ref. 3)

Temperature coeff. of el. resistivity: 0.0067/°C at 0–100°C (Ref. 2)

Ratio of resistivity at elevated temperatures (R_t) to resistivity at 0°C (R_0) and R_t at elevated temperatures according to Umbreit[2] and Potter[13] (Fig. 11.5 page 236)

$\frac{R_t}{R_0}$	R_t (microhm-cm)	Temp. (°C)	
0.08	0.49	−200	(Ref. 13)
.46	2.82	−100	(Ref. 13)
1.000	6.141	0	(Ref. 13)
1.131	6.844	+ 20	(Ref. 13)
1.681	10.3	+100	(Ref. 13)
2.57	15.8	200	(Ref. 13)
3.75	23	300	(Ref. 13)
4.99	30.6	400	(Ref. 13)
5.57	34.2	500	(Ref. 13)
6.06	37.2	600	(Ref. 13)
6.50	39.9	700	(Ref. 13)
6.97	42.8	800	(Ref. 2)
7.41	45.5	900	(Ref. 2)
7.86	48.3	1000	(Ref. 2)

Spectral emissivity: ($\lambda = 0.65\ \mu$): 0.355 (Ref. 2)

Total emissivity: (black body = 1.00)

0.045	at 25°C	(Ref. 14)
.06	at 100°C	(Ref. 14)
.12	at 500°C	(Ref. 14)
.19	at 1000°C	(Ref. 2)

TABLE 11.1. PHYSICAL CHARACTERISTICS OF CHEMICALLY PURE NICKEL. (*Continued*)

Reflectivity: (yellow green) 0.64 at 0.550 μ (Ref. 2)
(ultra violet) .413 at 0.300 μ
(infrared) .835 at 2μ
.820 at 3 μ
Thermal E.M.F. vs. Pt: 1.485×10^{-3} volts (0–100°C) (Ref. 2)
Electron work function: 4.84 e.V. (Ref. 15, 15a)
Richardson constant A: 50 amp/cm^2/deg^2 (Ref. 15)
Electron emission: 1.86×10^{-19} amp/cm^2 at 1000°K
1.76×10^{-6} amp/cm^2 at 1500°K
Magnetic transformation temp.: 358°C (Ref. 8) (See also Fig. 11.6 page 237)
Magnetic saturation (B-H) = 6080 gauss at 20°C (See also Fig. 11.7 page 238)

Mechanical Properties of Commercial Wrought Nickel

		(Brinell 300 Kg)	Rockwell (B)
Hardness:	Rod and bar, cold drawn		
(Ref. 2)	annealed	90–120	40–65
(See also	as drawn	125–230	70–100
Fig. 11.8)	hot rolled	90–120	40–65
(p. 238)	Plate, as rolled	100–200	50–100
	Sheet, strip and tubing, annealed		40–70

	Tensile Strength psi × 1000	Yield Strength (0.2% offset) psi × 1000	Elongation (in 2″%)
(Ref. 2) (See also Fig. 11.9; 11.10)			
Wire, cold drawn (pp. 238, 239)			
annealed	60–80	15–30	50–30
reg. temper	105–140	90–130	15–4
Rod and bar, cold drawn			
annealed	60–80	15–30	50–35
as drawn	65–115	40–90	35–15
hot rolled	65–80	15–30	50–35
Plate, hot rolled as rolled	70–100	20–75	45–30
Sheet, strip, tubing annealed	60–80	15–30	50–35

Young's Modulus: 30×10^6 psi (20°C) (Ref. 2) (See also Fig. 11.11 page 240)
Torsion Modulus: 11×10^6 psi (Ref. 2)
Poisson's Ratio: 0.31 (Ref. 2)

tics of chemically pure nickel and commercial nickel, and Table 11.2 similarly gives the chemical characteristics. Figures 11.1 to 11.14 further illustrate some of these properties. Table 11.3 is a tabulation of the compositions and main properties of various nickel alloys compiled from trade bulletins and Ref. 22. The International Nickel Company has prepared a number of technical bulletins which cover the many applications of the various materials. The author has drawn heavily from this source in preparing the present chapter. Attention is also directed here to the various Research Papers published by the National Bureau of Standards, Washington, D.C. An index of all their publications has recently been published as Circular 460. Circular C447[23] is a valuable reference text containing numerous tabulations and diagrams relating to

TABLE 11.2. CHEMICAL CHARACTERISTICS OF NICKEL

Atomic number: 28	Atomic valence: 2,3
Atomic Weight: 58.69	Valence orbitals: $3d^8 4s^2$
Heat of Fusion: 73 cal/g	Melting point: 1455°C
Heat of Sublimation: 85 kcal/mole	Boiling point: 2730°C (appr.)

(A) Reactions of Pure Nickel:

(1) In dry air at room temperature: none
(2) In dry air above 400°C: slow oxidation (protective film)
(3) In clean moist air at room temperature: practically none
(4) In sulfurous atmosphere at room temperature with rel. humidity > 70%: fogging of surface (film of Ni-Sulfate)
(5) In H_2: absorption according to $\log \mu_m = 1.732 + 0.5 \log P_{mm} - \frac{645}{T}$ (Ref. 16, 17) Ni and Fe are permeable to H_2 to a much larger extent than Cu at all temperatures
(6) In dry CCl_4; none
(7) In moist CCl_4 at room temperature: blue and yellow spots develop on surface
(8) In Trichlorethylene: none
(9) In water at room temperature: practically none; corrosion less than 0.001 in. per year (i.p.y.)
(10) In salt water at room temperature: very little; corrosion less than 0.005 i.p.y. (suffers pitting)
(11) In steam at red heat: slow reaction ($Ni + H_2O \rightleftharpoons NiO + H_2$)
(12) In HCl or H_2SO_4, cold, dilute: air free HCl—0.005 i.p.y. (Ref. 8)
air sat. HCl—0.10 i.p.y.
air free H_2SO_4—0.003 i.p.y.
air sat. H_2SO_4—0.03 i.p.y.
(13) In HCl or H_2SO_4, warm, dilute: dissolution (Fig. 11.12 p. 241) (Ref. 18)
(14) In HNO_3, cold, dilute: rapid dissolution (Fig. 11.13 p. 241) (Ref. 19)
(15) In aqua regia: attack
(16) In HPO_3, cold, dilute: slow dissolution
(17) In HPO_3, hot, conc.: rapid attack
(18) In HF, in dilute solution at 20–110°C: 0.010–0.110 i.p.y.; in anhydrous HF at 20–150°C: 0.002 i.p.y. (Ref. 8)
(19) In HF + HNO_3: rapid dissolution
(20) In alkalies, cold or hot: practically none
(21) In conc. acetic acid: strong attack

(B) Nickel Oxide:

NiO—olive green to greenish yellow or greyish black—changes color on heating and returns to original color on cooling. (d = 7.45; M.P. = 2090°C) Vapor Pressure in Temperature Range from 1440 to 1566°K: $\log p \text{ (atm)} = \frac{25506}{T} - 7.67 \times 10^{-4} \times T + 7.21 \times 10^{-8} T^2 + 10.198$. (Ref. 20.) The rate of oxidation of "Grade A" Nickel was determined by Campbell and Thomas (Ref. 21). Fig. 11.14 gives their results. (see page 242)

the mechanical properties of metals and alloys. Circular 485 is a revision of Circular 100 (1924), which deals with nickel and its alloys.[3]

"A Nickel" is a commercial wrought nickel for general-purpose use. Chemical limits are specified in ASTM B160, B161, and B162. "A Nickel" for the electronic industry is produced to narrower limits, as

TABLE 11.3. CHEMICAL COMPOSITION AND USES OF NICKEL AND HIGH NICKEL ALLOYS

No.	Material	Ni + Co (%)	Cu (%)	Fe (%)	Mn (%)	Si (%)	C (%)	Mg (%)	Ti (%)	Al (%)	Cr (%)	Nb (%)	Mo (%)	W (%)	S (%)	Availability‖
1	Pure Nickel	99.97[b]	0.01	0.01											0.001	
2	Electronic A-Nickel*†	99[a]	.20[b]	.30[b]	0.35[b]	0.20[b]	0.20[b]								.008[b]	A–R
3	220 Nickel*	99.10[a]	.20[b]	.20[b]	.20[b]	.01–0.05	.15[b]	0.01–0.10							.008[b]	A, B, I, J, L
4	225 Nickel*	99[a]	.20[b]	.20[b]	.20[b]	.15–0.25	.15[b]								.008[b]	A, B, I, J, L
5	330-Nickel*	99[a]	.15[b]	.20[b]	.30[b]	.10[b]	.15[b]	(some)							.008[b]	I, J, L
6	D-Nickel*	93.70[a]	.25[b]	.75[b]	4.5–5	.15[b]	.20[b]								.015[b]	A, F, I, J, L, M, N
7	E-Nickel*	97[a]	.25[b]	.75[b]	1.75–2.25	.15[b]	.20[b]								.015[b]	J
8	Duranickel*	(93[a])	.25[b]	.60[b]	.50[b]	1.00[b]	.30[b]		0.25–1	4–4.75					.01[b]	I, J, K, L, M
9	Permanickel*	(97[a])	.25[b]	.60[b]	.50[b]	.35[b]	.40[b]		.20–.60						.01[b]	I, J, L
10	Low Carbon Nickel	99[a]	.25[b]	.40[b]	.35[b]	.35[b]	.02[b]								.01[b]	A–C, G–J, M, Q
11	326-Monel*	58–61	(33)	2.50[b]	2[b]	.50[b]	.30[b]								.02[b]	A, H–J, L, M
12	Monel*	63–70	(24)	2.50[b]	2[b]	.50[b]	.30[b]			0.50[b]					.02[b]	A–R
13	R-Monel*	63–70	(24)	2.50[b]	2[b]	.50[b]	.30[b]								.025–.60[b]	J, M
14	K-Monel*	63–70	(21)	2.00[b]	1.50[b]	1[b]	.25[b]			2–4						A, B, D, E, H–M, P, S
15	KR-Monel*	63–70	(21)	2.00[b]	1.50[b]	1[b]	.35[b]			2–4						J, M
16	H-Monel*	65	29.5	1.5	0.9	3	.30									F
17	S-Monel*	63	30	2	.9	4	.10									F
18	Inconel*	72[a]	0.50[b]	10.00[b]	1[b]	0.50[b]	.15[b]				14–17				0.015	A, D, F–K, M, O–Q, T
19	Inconel-X*	70[a]	.20[b]	9.00[b]	1.[b]	.75[b]	.08[b]		2.25–2.75	0.4–1.00	14–16	0.50–1.20			.01[b]	B, H–K, M
20	Ni-Span C*	41–43		(45)	0.80[b]	1[b]	.06[b]		2.1–2.5	.3–.8	5.4–5.8				.04	A, I, J, L, M
21	60Ni-15Cr	62		(24)	.1[b]	1[b]	.06[b]				12[b]					A, H–K, M
22	80Ni-20Cr	80		0.5	.2–2	1.25	.1				20					A, H–K, M
23	Illium G‡	58	6	6.	1.25	0.65	.02				22		6			F
24	Hastelloy-A§	57		20.	2	1	.15						20			A, H, M
25	Hastelloy-B§	62		6.	1	1	.15						30			A, H, M
26	Hastelloy-C§	55		6.	1	1	.15				15		17	5		A, H, M

* Trade Marks of the International Nickel Company, Inc., 67 Wall Street, New York 5, N.Y.
† Electronic grade. See page 234 below.
‡ Trade mark of Illium Co., Freeport, Illinois.
§ Trade marks of Haynes Stellite Company, Kokomo, Indiana; Unit of Union Carbide & Carbon Corp.
‖ Availability:

A Tubing, seamless
B Tubing, welded
C Tubing, "Bundyweld"
D Welding electrodes
E Welding rods for gas welding
F Castings, sand, centrifugal, precision
G Plate, hot rolled
H Sheet, cold rolled
I Strip, cold rolled
J Wire
K Forgings
L Ribbon
M Rod and shapes, hot rolled & cold drawn
N Bimetallic strip wire (copper cored Ni wire)
O Screen and gauge
P Accessories: bolts, nuts, rivets
Q M-clad steel plate
R M-clad steel strip
S Rings
T Tube and pipe

( ) Figures in brackets indicate approximate remainder by difference.
[a] Denotes minimum.
[b] Denotes maximum value.

shown in Table 11.3 (Item 2). Special nickel products are available for cathodes, anodes, and grids in vacuum tubes, and will be described later. "A Nickel" is used primarily in the form of wire for miniature base pins and other structural components. All of these nickels are melted; electrolytic nickel is used as the raw material, to which deoxidizing and desulfurizing elements are added which not only provide important mechanical and working properties but also determine the behavior of a

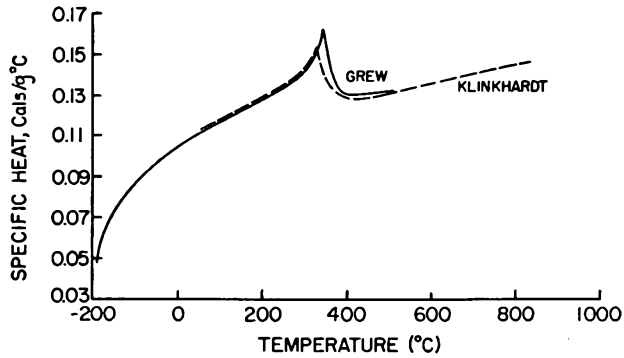

Fig. 11.1. Specific heat of 99.97% nickel (Grew[4]) and nickel with 0.5% manganese (Klinkhardt[6]). From N.B.S. Circular 485.[3] (*Courtesy National Bureau of Standards.*)

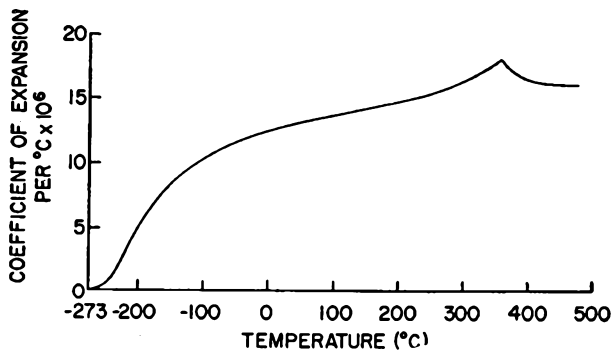

Fig. 11.2. Thermal expansion of nickel. After Nix and MacNair.[11] (See also N.B.S. Circular 485, p. 16.)

vacuum tube. "A Nickel" is easily drawn and worked; it spot-welds readily and can easily be brazed in a hydrogen atmosphere with silver alloy filler metals; its resistance to corrosion is of a high order. Oxidation at high temperatures is low and the oxide film is tightly adherent.

During the early days of power-tube development anodes were made from nickel and purposely oxidized in air to produce a coating of olive-green anhydrous NiO, which has a higher coefficient of thermal radiation than pure nickel. The vapor pressure of nickel is given in Table 11.1

for the temperature range 1000 to 1400°C and that of NiO in Table 11.2 for the temperature range of 1440 to 1566°K. NiO reacts slowly with Al_2O_3 at about 900°C to form nickel spinel.[24] In contact with zirconium, nickel forms a eutectic, and thus should not be used for support of zirconium elements which operate at temperatures above about 1100°C.

Nickel retains sufficient strength at high temperatures to prevent deformation during outgassing. Its modulus of elasticity and damping

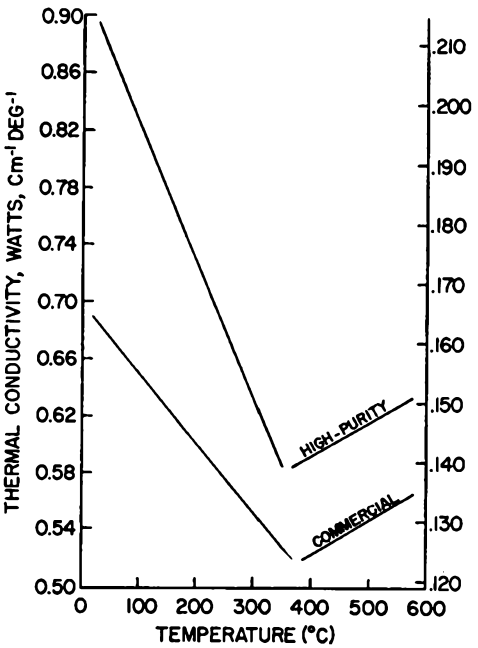

Fig. 11.3. Thermal conduction of nickel. After Van Dusen and Shelton.[12] (See also N.B.S. Circular 485, p. 17.)

factor are high, thus minimizing vibrational and microphonic effects. Its electrical resistivity is moderate, but the temperature coefficient of resistivity is high so that it is easily spot-welded and heated by induction. The electrical resistivity at moderate temperature is low enough to permit the use of nickel as a current-carrying lead. Butt-welded combinations of copper-"Dumet"-nickel are commonly used in the receiving-tube and incandescent-lamp industries. Similar leads, consisting of multistrand copper, tungsten rod, and nickel rod, are used for hard glass seals in power tubes. To insure uniform quality of such leads, which are liable to fail at the butt-welds if oxidized at the junction, flex-tests should be performed regularly on sample lots. The procedure for such tests has been formulated in ASTM Spec. B.113-41.

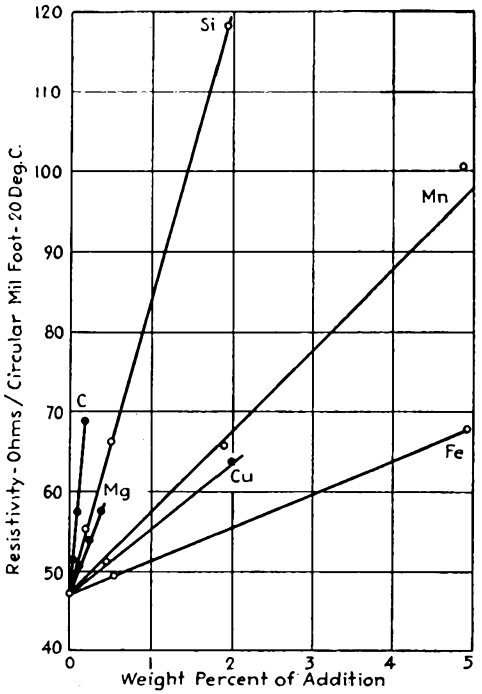

Fig. 11.4. Effect of alloying on the resistivity of nickel at 20°C. After E. M. Wise and R. H. Schaefer.[2] (*Courtesy of Metals & Alloys.*)

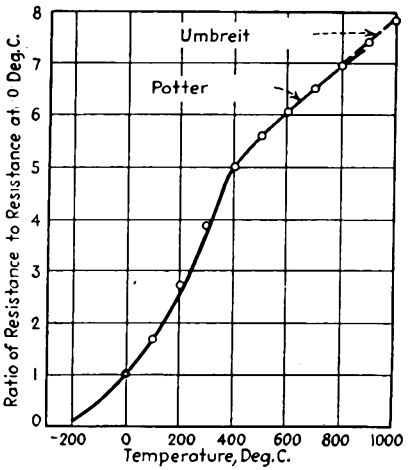

Fig. 11.5. Variation of electrical resistance of nickel with temperature. After Umbreit and Potter.[2,13] (*Courtesy of Metals & Alloys.*)

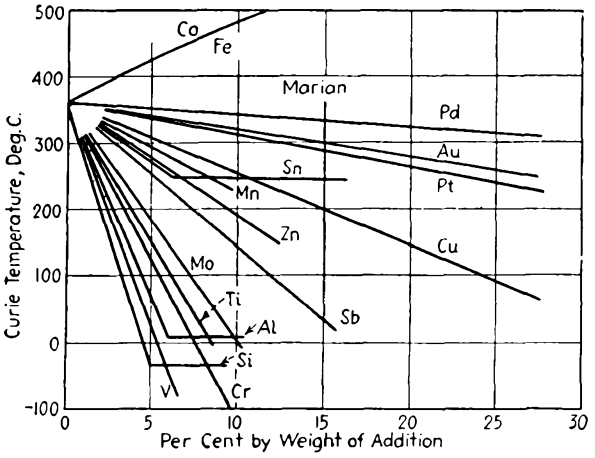

Fig. 11.6. The effect of specific single alloying additions on the Curie point of nickel. After E. M. Wise and R. H. Schaefer.[2] (*Courtesy of Metals & Alloys.*)

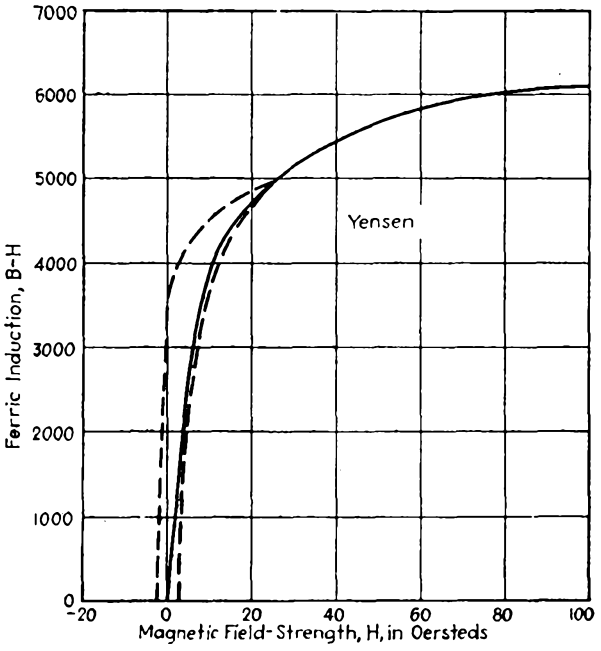

Fig. 11.7. Magnetic induction of very pure polycrystalline nickel. After Yensen. (*Courtesy of Metals & Alloys.*)

"220 Nickel" is used as a base metal for oxide-coated cathodes, where fairly easy activation without liberation of excessive amounts of free barium is required. This falls into the group of normal cathode materials proposed by ASTM, with silicon and magnesium content restricted to the limits given in Table 11.3 (see page 233)

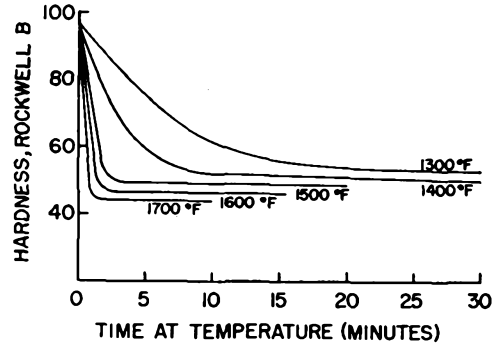

Fig. 11.8. Effect of annealing time and temperature on the hardness of nickel.[10] (*Courtesy International Nickel Company.*)

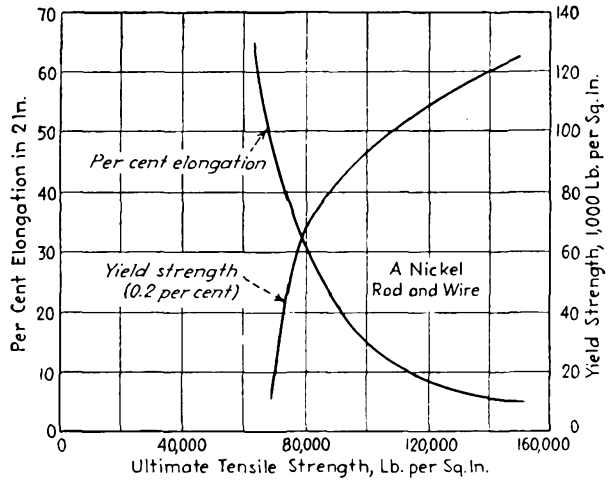

Fig. 11.9. Approximate relationship between tensile strength, yield strength and per cent elongation. After E. M. Wise and R. H. Schaefer.[2] (*Courtesy of Metals & Alloys.*)

"225 Nickel" has the highest silicon content (0.15 to 0.25 per cent) of the three cathode nickels, and is used where activation of oxide coatings is required under adverse conditions. Silicon in all these cathode nickels acts as a strong reducing agent and liberates free barium from the oxide BaO during the activation cycle.

"330 Nickel" is the material developed primarily for anodes in vacuum tubes, and it is preferred to "A Nickel" for this application. Therefore, it constitutes the bulk of nickel shipped in the form of strip to the electronics industry. The mechanical, electrical, and corrosion properties are the same as for "A Nickel," but "330 Nickel" is deoxidized and desulfurized in a different manner to provide optimum performance in its special application.

"D Nickel" is characterized by its manganese content (from 4 to 4.5 per cent), which gives it a strength and base hardness when fully

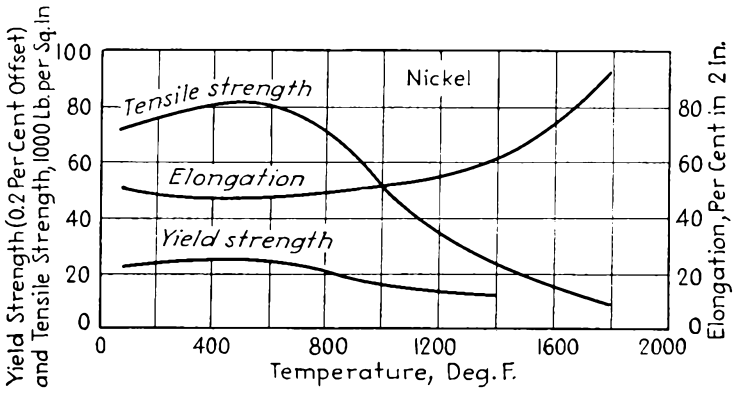

Fig. 11.10. Tensile properties of hot-rolled nickel at elevated temperatures. After E. M. Wise and R. H. Schaefer.[2] (*Courtesy of Metals & Alloys.*)

annealed which are slightly above that of "A Nickel." The annealing temperature is also higher so that greater hardness is retained after degassing. This makes it a desirable material for structural elements and, in particular, for support rods. Its high manganese content imparts some tolerance to attack by oxidizing sulfur compounds at elevated temperature. For this reason it has been used for supports sealed into glass where embrittlement by sulfur in the heating flames is a factor. However, the resulting oxidation is somewhat greater than with "A Nickel" or "E Nickel" so that the latter is more generally used under these circumstances. The electron emission from "D Nickel" is lower than that from "A Nickel"; this is true even when the "D Nickel" is contaminated with barium which has distilled over from the cathode so that it is used at times for grid wires. In this drawn form for grid laterals, "D Nickel" wire carries the trade name "Mangrid"* wire or "Gridnic-E" wire.† "Magno-Nickel" is another name frequently used for "D Nickel" wire.

* Wilbur B. Driver Co., Newark, N.J.
† Driver-Harris Co., Harrison, N.J.

"E Nickel" contains from 1.75 to 2.25 per cent Mn, and has mechanical properties intermediate between "A Nickel" and "D Nickel." Its corrosion resistance at moderate temperatures is comparable to that of "A Nickel." As "Mangrid-E" wire it is widely used for support wires in incandescent lamps and also for grid laterals.

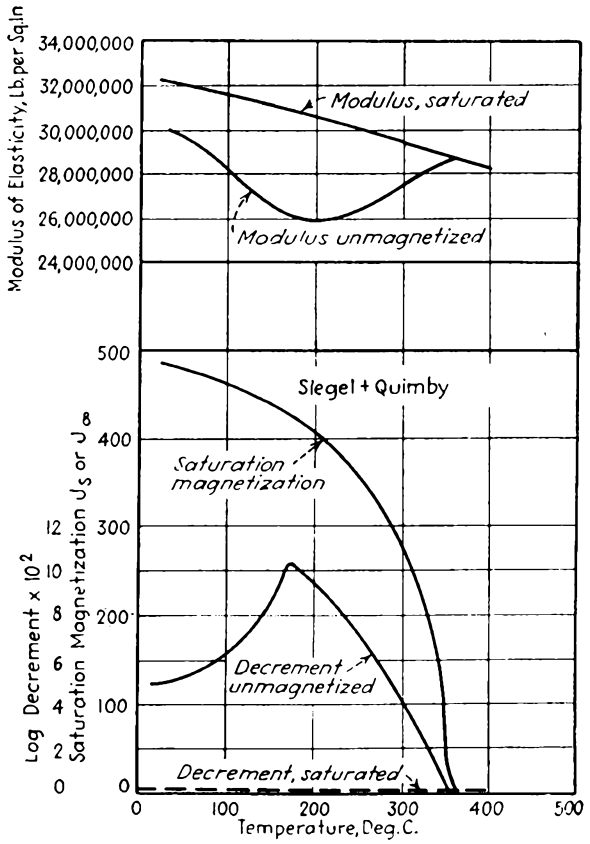

Fig. 11.11. Modulus of elasticity (top) and intensity of magnetization (bottom) on nickel at various temperatures.[2] (*Courtesy of Metals & Alloys.*)

"Duranickel," formerly known as "Z Nickel," is an age-hardenable wrought-nickel alloy, having an aluminum content of 4.00 to 4.75 per cent. Its mechanical properties lie between those of "K Monel" and "Inconel X." The properties of the alloy in the soft condition may be increased by cold work. Soft as well as annealed material may be hardened by heat treatment. Its selection over the softer nickels is usually based on mechanical considerations rather than other physical characteristics. In the annealed and aged condition it exhibits low

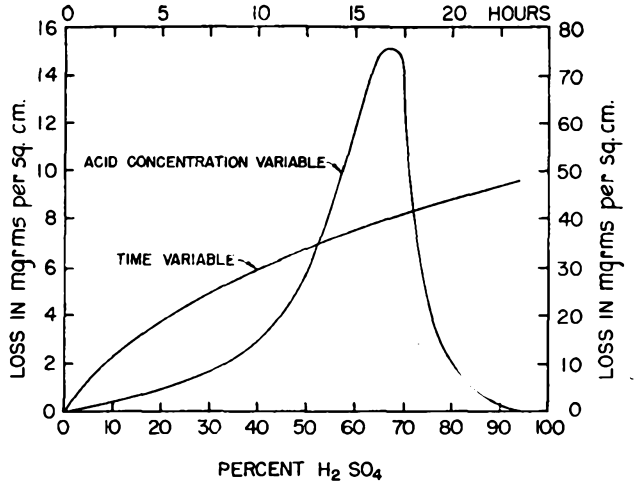

Fig. 11.12. The action of sulfuric acid on nickel. After R. Irman.[18]

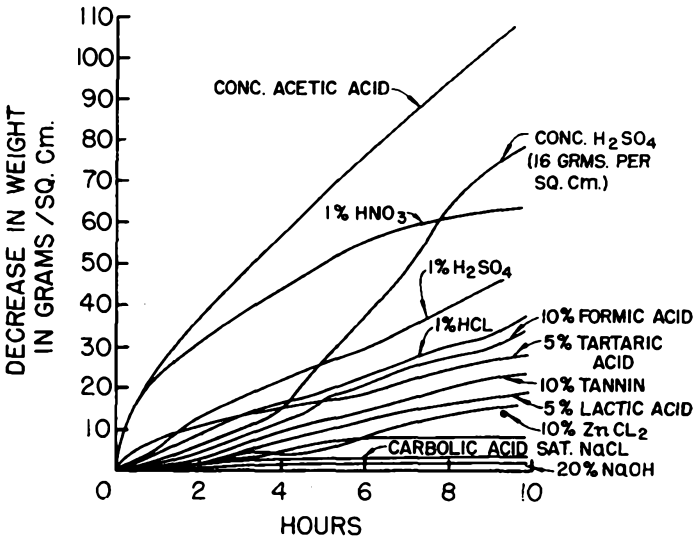

Fig. 11.13. The dissolution of nickel in various solutions. After R. Krulla.[19]

relaxation; this is useful for spring parts subjected to relatively high stress up to 350°C for prolonged times, and may be employed up to 400°C at low stress and short time at elevated temperature. In the soft condition the alloy is slightly magnetic at room temperature and magnetic after age hardening. It has corrosion resistance comparable with "A Nickel." For best surface condition, aging in dry hydrogen is recommended; but

even in this gas a thin tenacious aluminum oxide film is formed which must be removed prior to welding or soldering.

"Permanickel," formerly known as "Z Nickel Type B," is the original age-hardenable high-nickel alloy developed for high strength, corrosion-resistant applications. It is sometimes referred to as the *old* "Z Nickel" to distinguish it from its companion alloy, and care should be exercised to avoid confusing the older material, "Permanickel," with "Duranickel," which has largely replaced it. They require different annealing and aging treatments and have different physical characteristics. "Permanickel" is magnetic at room temperature in all conditions and has an electrical

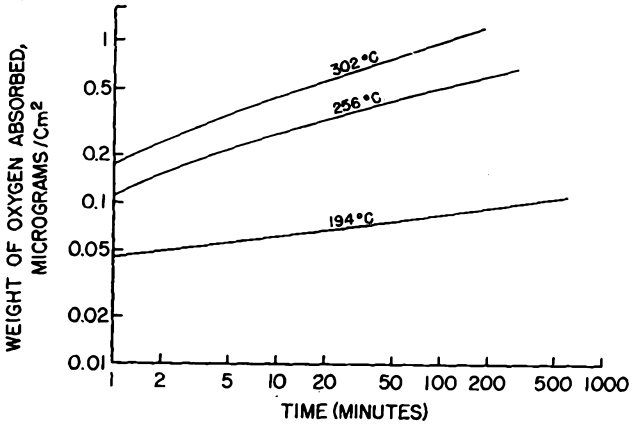

Fig. 11.14. Oxidation rate curves for commercial "Grade A" nickel at various temperatures. After W. E. Campbell and U. B. Thomas.[21] (*Courtesy Electrochemical Society.*)

conductivity higher than "Duranickel," but lower than that of "A Nickel." The mechanical properties are the same as for "Duranickel," and its resistance to corrosion is comparable with that of "Duranickel." Its resistance to relaxation is somewhat inferior to that of "Duranickel." "Permanickel" would be used in place of "Duranickel" only when high electrical conductivity and magnetic properties are essential. After aging, its surface must be cleaned before welding or soldering. Its electrical resistivity is about 43×10^{-6} ohm-cm.

"Low-Carbon Nickel" (formerly called "L Nickel") has a maximum carbon content of 0.02 per cent. This results in a grade of nickel that is soft and ductile, and one that anneals at low temperature and is most suitable for spinning operations. It is also used to a large extent for lead wires and spud wires in glass tube stems for receiving tubes. During sealing "Low-Carbon Nickel" forms a good bubble sheath around the wires, which acts as a protecting buffer in the glass, minimizing the strains

set up by the relatively large differential expansion between glass and metal. It is resistant to molten caustic soda, nitrates, and certain chemicals. T. H. Briggs, now with Burroughs Research Laboratory, reports that "Low-Carbon Nickel" has a lower rate of sublimation than "220 Nickel," but slightly higher than "499 Nickel." It is thus desirable for use where high operating temperatures and low leakage levels are required.*

"326 Monel" is similar to wrought "Monel"; but has a slightly lower nickel content, making this wrought alloy substantially nonmagnetic at and above room temperature. Fabricating and welding characteristics are the same as "Monel." Another advantage of "326 Monel" over nonmagnetic alloys containing substantial quantities of easily oxidized elements is that it can be fired and bright annealed at a lower temperature and in a hydrogen atmosphere possessing a higher dewpoint. It will not become magnetic on cold working. The approximate permeability at 20°C is 1.025 and at −10°C is 1.1.

"Monel," a wrought nickel-copper alloy, with its combination of high strength, ductility, weldability, and excellent corrosion resistance, is useful in many electronic applications, particularly where atmospheric corrosion in industrial, rural, or sea locations is a factor. It is also highly resistant to corrosion by chlorinated solvents and glass-etching agents, as well as by many other acids and alkalies. Regular "Monel" is somewhat magnetic at room temperature. Where a nonmagnetic material is required, "326 Monel," "K Monel," or "Inconel" is recommended. If parts are to be made by machining rather than by drawing, "R Monel," a wrought free-machining grade of "Monel," or "KR Monel" may be used. "Monel" can be welded, brazed or soldered, deep drawn, spun, and blanked. For annealing, a reasonably dry hydrogen atmosphere is entirely adequate, but the work must be free from grease or cutting oil prior to annealing. Its electrical resistivity is about 48×10^{-6} ohm-cm.

"R Monel" is a variation of the basic wrought alloy, "Monel," to which a small amount of sulfur has been added. It was designed specifically for improved machining behavior, particularly on automatic screw machines. It has the same general resistance to corrosion as "Monel" and has comparable physical and mechanical properties and welding characteristics. It may be machined at relatively high feeds and speeds if properly ground high-speed tools or tools of high red hardness, such as stellite alloys or cemented tungsten carbides, are used. The work should be well flooded with cutting compound. For sizes up to ½-inch diameter the use of cold-drawn rod, No. 1 temper, is suggested, while for larger sizes cold-drawn, as-drawn, stress-equalized temper, is

* Private communication to the author.

recommended. Its electrical resistivity is the same as that of regular "Monel."

"K Monel" is an age-hardenable wrought high nickel-copper-aluminum alloy. Like "Monel," it possesses excellent corrosion resistance and offers the added advantage of high strength and hardness comparable to heat-treated steels. Since it is nonmagnetic down to −100°C, it is useful where a strong nonmagnetic material is required. It has good high-temperature strength properties up to about 580°C, but where creep at maximum temperature is of controlling importance, "Inconel X" is recommended. For maintaining the best surface condition, aging in dry hydrogen is recommended; but, in any event, the thin oxide film formed must be removed before the material is welded or soldered. The permeability at 20°C is approximately 1.0015 and at −120°C about 1.1. The electrical resistivity at 20°C is about 58×10^{-6} ohm-cm.

"KR Monel" is a wrought alloy similar to "K Monel" except for a slightly higher carbon content. This alloy was developed to provide improved machining characteristics. In general, its machinability in the annealed condition is comparable to cold-drawn (as-drawn) "Monel," but is inferior to "R Monel." It has the advantage that parts may be machined in the annealed state and subsequently age hardened. Its nonmagnetic characteristics are important in some uses. This alloy, after aging, has physical and mechanical properties comparable to those of annealed and aged "K Monel."

"Inconel" is a nonmagnetic, nickel-chromium-base alloy that is resistant to oxidation at elevated temperatures and to oxidizing corrosive solutions. It is also resistant to a wide variety of inorganic and organic compounds, as well as many heat-treating atmospheres. "Inconel" possesses considerable tolerance for sulfur. The oxide scale formed at elevated temperatures is tightly adherent, and this, plus the elevated temperature-strength characteristics of the alloy, make it useful for many structural applications for such service. For spring parts, the heavily cold-worked and stress-equalized material shows low relaxation at temperatures up to 370°C at relatively high stresses and prolonged exposure. At higher temperatures it has been used as a spring element for parts with relatively low stresses and short time exposure to temperature. The alloy work-hardens more rapidly than nickel or "Monel," but is readily fabricated or welded. The permeability at 20°C is approximately 1.007, and at −100°C is 1.1. The electrical resistivity at 20°C is about 98×10^{-6} ohm-cm.

"Inconel X" is a wrought, nonmagnetic, age-hardenable modification of "Inconel," developed primarily for gas turbines and jet engines in which high rupture strength and low creep rates under high stress at temperatures up to 815°C are essential. It retains about 80 per cent of its room temperature short-time tensile strength at 650°C. For spring

parts subjected to relatively high stresses the soft or mildly cold-worked and aged material shows low relaxation for prolonged times at temperatures up to 455°C. For minimum creep at the highest temperatures cold work must be avoided. In the heavily cold-worked and aged condition the alloy has a tensile strength of about 250–300,000 psi. In this condition the alloy has low relaxation up to about 400°C and offers useful characteristics at higher temperatures for short-time exposure. After aging, its surface should be cleaned chemically or mechanically before welding or soldering. Its electrical resistivity at 20°C is about 120×10^{-6} ohm-cm.

"Ni-Span C" is an age-hardenable iron nickel base alloy which has a substantially constant modulus of elasticity over the range −20°C to 90°C. Its thermoelastic coefficient can be adjusted by suitable heat treatment and prior cold work so that small negative, zero, or small positive coefficients can be obtained. This alloy is useful for springs that must exert a constant force over a considerable temperature range, as in accurate weighing systems and in vibrating systems where constant frequency of vibration is desired (i.e., watches, clocks, and the like). Its electrical resistivity at 20°C is about 110×10^{-6} ohm-cm.

Present Views on Nickel for Oxide Cathodes

The availability of the various wrought nickels listed above indicates the importance of choosing the proper base metal for oxide-coated cathodes. Steps are usually taken in a manufacturing plant to insure constancy of the composition of the nickel by chemical analysis and control runs of tubes made with known source material. The theory of thermionic emission from oxide-coated cathodes is not as yet firmly established and differences of opinion still exist concerning the optimum composition of nickel for cathodes. The importance of this point is demonstrated by the fact that nickel producers and representatives of most radio-tube companies have carried on an extensive program of study under the auspices of the American Society for Testing Materials (ASTM), Committee B-4, Subcommittee 8, Section A, which started in 1945 and is still continuing. Five subsections were originally set up under Section A (cathode), of which the author was a member from the beginning. These were

Subsection 1 Data
Subsection 2 Diode
Subsection 3 Chemical
Subsection 4 Metallurgical
Subsection 5 Physical Testing

Up to this time, the acceptance of a new 10,000-lb melt of nickel by the tube industry for production of cathode sleeves by the sleeve manu-

facturer was a very time-consuming and often ambiguous procedure. The tube manufacturer would receive sample sleeves and use them for trial runs of radio tubes then in production. The differences of processing technique prevailing at various plants were liable to lead to conflicting results so that some would accept the new melt and others refuse it. It was thus the purpose of the Subsection 1 to establish coordinated, industry-wide methods of tests and their evaluation. As a result of these efforts "Recommended Practice for Cathode Melt Prove-in" has been issued by ASTM under the designation B238-49T.

Subsection 2 set out to develop a standard diode for melt approval in the laboratory and to investigate variations in composition of the nickel or effects of different processing procedures[25,26,26a]. This diode is readily made from standard component parts, and eliminates the hazards of testing new sleeve material on a variety of different tubes. A sufficient quantity of a control melt (No. 66), which had been generally found acceptable, was set aside, and sleeves made from it were used for control runs. Melt 66 is a typical grade "220 Nickel."

Subsection 3 was concerned with methods of chemical analysis and Subsection 4 with metallurgical test procedures, while Subsection 5 carried on developments of physical test methods begun at a much earlier date. Subsections 1 and 2 have recently been combined into one. Cathode materials are known under three classifications: Normal, Active, and Passive. The amount of reducing material contained in the melt determines the classification.

Table 11.4 gives the tentative specifications for circular cross-section nickel-cathode sleeves for electronic devices (ASTM Designation B239-49T), which applies to sleeves or tubing having 0.005-inch wall thickness or less.

The effects of reducing agents usually present and desired in cathode nickel were summarized by the ASTM Cathode Committee in 1948, and commented on by E. M. Wise* and T. H. Briggs,† as follows:

General

"Pure nickel is believed to have no reducing effect on the coating of an oxide-coated cathode. It is therefore common practice to introduce a reducing agent into the nickel cathode in order to obtain a slight reduction of the oxide coating to produce sufficient barium for high electron emission from the cathode.

"Excessive amounts of reducing agents may reduce unnecessarily large amounts of barium. In certain types of tubes reducing agents in the nickel must be excluded to minimize reduction of Ba. Power-output pentodes and other tubes with very close cathode to grid spacing and/or high cathode-operating temperatures therefore employ

* In charge of Platinum Metals and Electronics Sections, Development and Research Division, International Nickel Company.

† Research Division, Burroughs Adding Machine Company, Philadelphia 23, Pa. Formerly, Superior Tube Company, Norristown, Pennsylvania.

'passive' cathodes, such as the 499 type. When large amounts of cathode poisons are likely to be released from tube parts and the glass wall, an 'active' cathode alloy, such as Type 225, is used to advantage.

"The reaction with carbon produces volatile compounds which are pumped out during the tube exhaust or are cleaned up by getter action. The products of the reaction with other reducing agents result in the formation of compounds, such as barium silicate, titanate, aluminate, magnesium oxide, etc., at the surface of the

TABLE 11.4. ASTM SPECIFICATION B239-49T FOR CIRCULAR CROSS-SECTION NICKEL CATHODE SLEEVES

	Cu %	Fe %	Mn %	C* %	Mg %	Si %	S %	Ti %
Active Alloy; Type Composition	0.20 max.	0.20 max.	0.20 max.	0.08 max.		0.05/0.25	0.008 max.	
Grade 1	0.20 max.	0.20 max.	0.20 max.	0.08 max.	0.01/.10	0.12/0.20	0.008 max.	0.02 max.
2	0.04 max.	0.05 max.	0.05 max.	0.08 max.	0.01/.10	0.12/0.20	0.005 max.	0.01 max.
3	0.20 max.	0.20 max.	0.20 max.	0.08 max.	N.S.	0.15/0.25	0.008 max.	N.S.
4	0.04 max.	0.05/0.10	0.10 max.	0.08 max.	0.01 max.	0.15/0.25	0.005 max.	N.S.
5	0.04 max.	0.05/0.10	0.10 max.	0.08 max.	0.05/0.15	0.05/0.15	0.005 max.	N.S.
6	0.04 max.	0.05 max.	0.02 max.	0.08 max.	0.01 max.	0.15/0.25	0.005 max.	N.S.
Normal Alloy; Type Composition	0.20 max.	0.20 max.	0.20 max.	0.08 max.	0.01/0.10	0.01/0.05	0.008 max.	N.S.
*Grade 11	0.20 max.	0.20 max.	0.20 max.	0.08 max.	0.01/0.10	0.01/0.05	0.008 max.	N.S.
Passive Alloy; Type Composition	0.05 max.	0.05 max.	0.05 max.	0.05 max.	0.02 max.	0.02 max.	0.008 max.	0.01 max.
Grade 21	0.04 max.	0.05 max.	0.02 max.	0.05 max.	0.01 max.	0.01 max.	0.005 max.	N.S.

* The carbon content of these alloys in the form of lockseam sleeves averages 0.01% per 0.001 in. thickness while seamless tubing averages slightly higher.

Note—The melting, processing and application of some material melted to Grade 21 composition limits may be limited by U.S. Patents. N. S. indicates: Not specified.

nickel sleeve and are called 'interfacial compounds' or the 'interface layer.' This interface layer may have harmful effects on the operation of the cathode such as lowering the cathode temperature, introducing a high resistance (in the cathode circuit) and some oxides may not bond well, and result in peeling of the coating from the base material. There are other complicating effects on tube performance in addition to the above."

General Effects of Individual Reducing Agents

"Aluminum—gives good emission and, when present in small percentage, does not vaporize at the temperatures reached during the tube processing or on life. The color of the interface layer formed between base metal and oxide coating is a function of the

percentage content of aluminum in the base metal. In cathode sleeves the interface is light grey for 0.05 to 0.01% aluminum. At about 0.25% the interface becomes black. The percentage of aluminum for satisfactory operation of cathode sleeves is much lower than for directly heated filaments.*

"Carbon—a good reducing agent and produces good emission; no interface. The quantity of carbon is difficult to control because of the high rate of diffusion of carbon in nickel and because carbon reacts with hydrogen, oxygen, and water vapor. It is a potent hardener for nickel.

"Magnesium—excellent reducing agent; produces a light interface. The metal vaporizes from the cathode if present in sufficient quantity, and may cause leakage. Aside from its activating effect it is used to control the effects of sulphur and improves rolling properties of strip; stiffens the metal.

"Manganese—is not a reducing agent to BaO and may be harmful to emission if present in quantities greater than about 0.2%; produces some interface with consequent lowering of the cathode temperature. It is somewhat volatile. Desired only by supplier and user for its effect in improving working properties of nickel.

"Silicon—a good reducing agent; emission holds up on life. It does not volatilize but produces a somewhat darker interface then magnesium, with a consequent lowering of the cathode temperature. Amounts greater than 0.25% Si may cause peeling of the cathode coating. The resistance of the interface may be objectionable in pulsed tubes for computers, etc.

"Titanium—a strong reducing agent but produces a dark and heavy interface, therefore only a small quantity can be tolerated if a thermally efficient cathode is desired; it does not vaporize appreciably and confers improved working properties. It may improve the transconductance during life of critical tubes."

Effect of Minor Impurities

"Cobalt—may replace nickel in any moderate amount without affecting the cathode performance. Small quantities have only a very slight effect upon the mechanical properties of nickel at ordinary temperature; its effect at higher temperature is unknown, but probably small. Recent heats of cathode alloys have dropped in cobalt content from 0.7 to 0.4% and some to 0.15%.

"Copper—has no effect on emission but if present in considerable quantities copper will vaporize.

"Iron—may have no effect on emission and life when alloyed with the nickel in small amounts. When concentrated on the surface because of pick-up during manufacture of cathode base material it must be removed in order to obtain satisfactory emission and to avoid spots in the coating."

The specified and typical analyses of commercial cathode alloys produced in the United States have been tabulated by Briggs,[27] as shown in Table 11.5. The effects of the various cathode constituents on cathode performance are tabulated in Table 11.6, and the probable choice of alloy for emphasis of any one given performance aspect is shown in Table 11.7, also derived from Briggs.†

* According to reports from the Superior Tube Company kindly communicated to the author by T. H. Briggs.

† Tables 11.5, 11.6, 11.7 are taken from Electronics Laboratory Report #22 (April 6, 1950) of the Superior Tube Company, Norristown, Pa. This report, prepared by T. H. Briggs, C. D. Richard, Jr., and T. Small, is entitled: "The Relation of the Base

TABLE 11.5. SPECIFIED AND TYPICAL ANALYSIS OF COMMERCIAL U.S. CATHODE ALLOYS[27]

Alloy	Element						
	Cu %	Fe %	Mn %	Mg %	Si %	Ti %	C %
399 spec.	0.04	0.05	0.02	0.01	0.15–0.25		
ave.	.018	.055	.020	.010	.190	.004	
499 } spec.	.04	.05	.02	.01	.01		.02 max.
999 } ave.	.013	.017	.001	.004	.008	.001	
							.023
599 spec.	.04	.05–.10	.10	.01	.15–.25		
ave.	.015	.078	.056	.009	.182	.004	
699 spec.	.04	.05–.10	.10	.05–.15	.05–.15		
ave.	?	.07	.05	.13	.08	?	
799 spec.	.04	.05–.10	.05	.01–.10	.12–.20	.02	
ave.	no analysis available						
220 spec.	.20	.20	.20	.01–.10	.01–.05		
ave. 3	.02	.06	.10	.035	.035	.023	
225 spec.	.20	.20	.20		.15–.25		
ave.	.02	.04	.15	.05	.22	.033	

The following elements are not specified. However, they have been checked and are found to be held at satisfactorily low levels in commercial heats:

$$\text{Al, B, Ca, Cr, Pb, Zn, } < 0.005\%$$

For cathodes with 0.002–0.003″ wall thickness of any form the carbon content is about 0.02–0.05% by weight.

Cobalt content formerly averaged 0.7%. By improved refining processes it has been reduced to 0.4% and will drop to 0.15% as soon as practical.

$$\frac{\text{Approximate atomic \% of element X}}{100} = \frac{\dfrac{\text{\% by weight of X element}}{\text{Atomic wt. of X element}}}{\dfrac{\text{\% by weight Ni and Co}}{\text{Atomic wt. of Ni}} + \dfrac{\text{\% by weight of X element}}{\text{Atomic wt. of X element}}}$$

Methods of testing oxide-coated nickel sleeves for their emission capabilities in the standard diode and the evaluation of the results by a figure of merit have been described by McCormack.[26] The position of the knee of the curve giving emission versus heater voltage at a constant anode voltage of 40 volts was taken as the basis of the figure of

Metal to the Performance of Thermionic Cathodes." The author is indebted to Mr. Briggs and the Superior Tube Company for making this and other reports available to him.

TABLE 11.6. ELEMENTS IN CATHODE ALLOY IN PROBABLE RELATION TO PERFORMANCE CHARACTERISTICS[27]

Element	Relative Rate of Reaction with BaO	Relative Rate of Sublimation	Relative Effect upon Interface Resistance	Effect upon D.C. Emission Initially or During Life	Other Comments
B	5		?	+?	
C	4		6	+*	* More effective as other elements are reduced in quantity
Ca	5?		?	*	* Harmful in quantity to metallurgical properties of Ni
Cr	2?		1	−	
Cu		3		0?	
Fe		*			* Sublimes with Ni + Co in presence of other elements
				−Δ	Δ Especially damaging if in surface of sleeve
Mg	1	2	5	++*	* Highly transient, progressively lost during life
Mn		3*		−−	* Probable when in compound form
S				*	* Harmful to metallurgical properties of Ni and to cathodes
Si	2	4	3	++	
Ti	4	5	2	+	
W	3	6	4	++*	* Probably requires large quantities
Co		*		0	* Sublimes with Ni + Fe in presence of other elements
Pb-Sn-Zn		1			

Greatest effect = 1
Least effect = Highest number

TABLE 11.7. CHOICE OF CATHODE ALLOYS FOR SPECIFIC REQUIREMENTS[27]

Alloy	Rapid Activation	Low Sublimation	High DC Y_s Level	Low Interface Resistance	Good I_s Life	Good Gm Life
399	4	2	4	4*	Dependent upon tube processing and application	High silicon alloys probably poorest
499–999	7*	1	7*	1		
599	4	2	4	4*		
699	1	5*	1	?		
799	2	3	3	3		
220	6	3	6	2		
225	2	3	2	4*		
"A"	5	4*	5	2		

Lowest figure is best; highest figure poorest; * = very bad.

merit in most of the diode tests. At a later stage in the program, data were also taken at low field conditions, with an anode voltage of 4.0 volts to avoid poisoning effects known to occur from breakdown of oxides and chlorides at the surface of the anode at anode voltages equal to 4.5 volts and higher.

Still more recently, a new figure of merit was adopted by the Data and Diode Committee, which is based on work by Richard and Briggs.[28]

Pulse tests were also carried out in some cases, but the main work in this first effort by the Cathode Section was aimed at static tests.

Factory-approval runs with commercial tubes were evaluated on the basis of initial shrinkage, initial tube characteristics, and life-performance tests, which formed the basis of a figure of merit different from the one referred to above in the discussion of diode tests.

While much remains to be clarified, this cooperative program sponsored by ASTM has been and will continue to be a worthwhile undertaking. It is an excellent example of the modern approach to a common problem by competitive groups in industry, where cooperation will benefit all concerned.

An extensive study of cathode nickels was recently reported from France; this formed part of a broad investigation of factors affecting the performance of oxide cathodes. Violet and Riethmuller[29] devised a test assembly with two diodes and an ionization gauge in one envelope. Directly heated filamentary cathodes (0.4 mm diameter—16 mils), coated with coprecipitated Ba/Sr/Ca-carbonates by cataphoresis (Ba:Sr:Ca = 1:1.18:0.24 moles) to a coating thickness of 0.050 mm (2 mils), were used. This arrangement makes it possible to mount a standard reference cathode in the same tube where the unknown material is being studied, thus insuring that vacuum conditions and spurious contaminations are the same for both. The tests applied use sinusoidal voltage pulses which permit evaluation of the cathodes in the vicinity of the onset of saturation without overloading the cathode. Thus, while average emission amounted to 70 ma/cm^2, peak currents of 10 amps/cm^2 were observed. Activation or fatigue effects could be followed on a cathode-ray oscillograph by application of rectangular voltage pulses.

As this study was confined to one laboratory, much more rigorous conditions could be imposed on all processing schedules and materials used. All these varied widely with different manufacturers in the ASTM. program, as was expected. Violet and Riethmuller came to similar conclusions. Their reference alloy M10, which is found most stable and conducive to high-emission yields and good life under operating conditions, contains 0.21 per cent of (Mg + Si + Al + Ca) and 0.21 per cent of (Mn + Fe + Cu). By designating the additives shown in brackets as the Mg group and the Mn group, respectively, they found that emission

decreases with increased percentage content of the Mn group; but even an increase by a factor of 4 does not decrease emission to the low level shown by very pure Ni. The decrease of the Mn-group content below 0.21 per cent by itself increases emission only by a small amount. Aging runs were carried out for 300 hours and correlated with pulsed emission tests from which the conclusion was drawn that two groups of cathodes had to be distinguished. These are referred to as "normal" and "abnormal" cathodes to throw some light on the phenomenon of "emission slumping" observed with cathodes which, according to pulse-test data, should have performed satisfactorily. Pure nickel and nickel containing less than 0.20-per cent additives of the magnesium group behave "normally" and become definitely active when this percentage exceeds 0.40 per cent. Additives of the manganese group act in the same sense but to a lesser degree.

For the sake of completeness, additional data are given in Table 11.8 on commercial nickel-alloy filaments used for oxide-coated emitters in receiving tubes. "In addition, a 5-per cent nickel, 95 per cent-platinum alloy coated with barium and strontium oxides was used as a base for long-life thermionic cathodes used in telephone-communication tubes with service life of the order of 50,000 hours. This type of cathode is the only one known which can be reactivated after exposure to the atmosphere, and for this reason cathodes of this nature are employed in certain types of ionization gauges.[30]

This discussion of nickel would not be complete without referring to carbonized nickel, which is so commonly used for receiving-tube anodes. Nickel-plated cold rolled steel and nickel clad steel can be used for carbonized parts but require much closer control over material, temperature, surface conditions and gas content than does pure nickel.[31] Aluminum-clad iron (P2 Iron) has been used in Europe as a substitute for nickel in receiving tubes during the last war. This material takes on a dark color on firing at about 700°C in vacuum. Not much has been published on the subject of carbonized nickel, except in patent literature. The only paper known to the author is that by Briggs.[32] Power dissipation from various anode materials is discussed in Chapter 13 and tabulated in Table 13.4. The substantial increase of power dissipated from nickel when it is carbonized is thus evident. The total emissivity of bright nickel was given as 0.16 and for carbonized nickel as 0.85, both at 727°C (1000°K), according to Barnes.[33] The thickness of the carbon film usually runs between 0.002 and 0.003 inch, and the methods of application described in the patent literature are many. According to Briggs:[32]

"The carbonization of nickel is accomplished through formation of a green oxide by heating the nickel in air to about 925°C, then almost immediately placing it in another furnace at the same temperature in a hydrocarbon-gas atmosphere. The

TABLE 11.8. NICKEL ALLOYS FOR FILAMENTS AND GRIDS

Ser. No.	Name*	Supplier†	Typical Composition	M.P. °C	Sp Gr.	Resistivity microhm-cm		Tensile Strength kg/cm²		Use
						20°C	800°C	20°C	800°C	
1	Ballast nickel	W.B.D.	Ni: 99.7; Co: 0.08; Mn: nil; Fe: 0.17	1,455	8.90	8.30	48	3,960	740	
2	Silicon nickel	W.B.D.	Ni: 96; Si: 2.5; Mn: 1.5	1,420	8.52	38	65.6	5,350		
3	Sylvaloy	W.B.D.	Ni: 97; Si: 3; Mn: nil	1,420	8.61	26.5	51	5,370	1,115	
4	Hilo	W.B.D.	Ni: 75; Co: 18; Fe: 5; Ti: 2	1,450	8.56	42	114	7,480	1,840	
5	Modified Hilo	W.B.D.	Ni: 79; Co: 18; Fe: 2, Ti: 0.8	1,450	8.71	25	79.5	5,790	1,540	
6	Cobanic	W.B.D.	Ni: 54.5; Co: 44.5; Fe: 1	1,500	8.84	12.5	81.2	6,060	1,255	
7	Tensite	W.B.D.	Ni: 98; Al: 2	1,425	8.76	15	54.8	3,990	965	
8	Mangrid (D-Nickel)	W.B.D.	Mn: 4.5–5; Fe: 0.75; Si: 0.15; C: 0.20; Cu: 0.20	1,427	8.78	18.3	43.9	6,050		Grid supports
9	W-4	S.C.C.	C: 0.04; Co: 0.90; Fe: 0.01–0.04; Si: 0.04; S: Tr; Cu: 0.01–0.03; Bal: Ni							Fil. for 71A, 47, 45
10	210	S.C.C.	Al: 0.10; C: 0.34; Co: 0.62; Fe: 0.09; Mn: 0.06; Si: 0.08; Mg: 0.21; Bal: Ni							Fil. for battery tubes
11	C-43	S.C.C.	Mn: 0.10; Si: 3.52; Ni: 96.38							Rectif. fil.
12	925-C	S.C.C.	Al: 1.90; C: Tr; Ni: 98.10							Fil. batt. tubes
13	213	S.C.C.	Al: 1.90; U: 2.10; W: 1; Ni: 96.10							
14	531	S.C.C.	Al: Tr.; Co: 19; Fe: 2.50; Si: 1.50; Ni: 77							Rect. fil.
15	213-M	S.C.C.	Al: 1; C: 0.25; Mo: 2; Ni: 96.75							Grid wire
16	Filnic-F	D.H.C.	Co: 17; Fe: 7.50; Ti: 2.25; Ni: Bal.	1,450	8.59	35.0	100	7,270		
17	Filnic-J	D.H.C.	Si: 3; Bal: Ni	1,420	8.60	27.3	52.5	5,270		
18	Filnic-M	D.H.C.	Co: 45; Bal: Ni	1,480	8.84	12.9	81			
19	Filnic-T	D.H.C.	Ni: 98 Min.	1,450	8.75	16.6	48.2	7,030		
20	Gridnic-A	D.H.C.	Ni: 50.5; Bal: Fe	1,425	8.25	43.2	115.9	4,950		
21	Gridnic-C	D.H.C.	Cr: 15; Mn: 1.75; Fe: 1; Bal: Ni	1,390	8.53	94.3	99.4	7,740	1,760	
22	Gridnic-D	D.H.C.	Cr: 20; Bal: Ni	1,400	8.41	108	114.7	9,200	850	
23	Gridnic-E	D.H.C.	Mn: 4.5; Bal: Ni	1,435	8.75	20	57.9	5,270	2,530	
24	Gridnic-F	D.H.C.	Co: 17; Fe: 7.50; Ti: 2.25; Bal: Ni	1,450	8.59	35	100	7,270		
25	Gridnic-T	D.H.C.	Ni: 98 Min.	1,450	8.75	16.6	48.2	7,030		
26	D-Nickel	I.N.C.	See Table 11.3; same as Gridnic E	1,435	8.13	14				Grid support
27	E-Nickel	I.N.C.	See Table 11.3; also Mangrid E							
28	N9	R.C.A.	Mn: 0.20; Si: 0.16; Mg: 0.05; C: 0.10; Bal: Ni	1,448	8.88	9.82	47	81,910	1,605	Fil. for 45 cbc
29	N97	R.C.A.	Co: 40; Si: 0.16; Mn: 0.10; C: 0.04 Min; Bal: Ni	1,449	8.88	13.16	77.9	13,025	1,263	Rectif. fil.
30	N91	R.C.A.	Co: 20; Si: 0.10; Mn: 0.10; C: 0.04 Min; Bal: Ni	1,443	8.88	13.87	67.2	10,858	1,066	Rectif. fil.
31	N100	R.C.A.	W: 2; Al: 1; C: 0.10; Mg: 0.05; Bal: Ni	1,443	8.77	19.89	51.5	12,282	1,652	Miniat. fil.

* All names and codes are Registered Trademarks of the respective companies.
† W.B.D.—Wilbur B. Driver Company, Newark, N.J. S.C.C.—Sigmund Cohn Corp., 44 Gold St., New York 7, N.Y.
D.H.C.—Driver Harris Company, Harrison, N.J.
I.N.C.—International Nickel Company, Inc. New York 5, N.Y.
R.C.A. Radio Corporation of America, RCA Victor Division, Harrison, N.J.

nickel oxide may act as a catalyst and crack the gas into its carbon and hydrogen components. The hydrogen reduces the oxide, and the water formed and the excess hydrogen are carried off with the surplus hydrocarbon gases. The carbon at once deposits on the active nickel surface. The oxidation and reduction of the nickel surface itself tends to open up the grain boundaries and generally roughen the nickel surface. Other roughening is frequently used, such as by mechanical, or chemical means, or an earlier carbonization and oxidation. Above all a clean, active nickel surface is necessary, uncontaminated by old, deep-grown oxides, finger marks, oil, dust, or mechanical scars. The speed of carbon deposit and its depth or darkness of color depend largely upon the effectiveness of the preparation of the original nickel strip. Once the carbon begins to deposit on the strip it does so rapidly and after that any increased time in the furnace will have little additional effect."

Continuous carbonization of nickel-strip is carried out in large furnaces with careful control of temperature, rate of gas flow, and speed of travel. Carbonization by cataphoretic deposition of a colloidal graphite suspension is a useful technique, notably developed by the Philips Company in Eindhoven.

A number of tests for the quality and adherence of carbon coating on nickel anodes are in use. "This may be done by exposing a sample to a hydrogen atmosphere in a furnace at 1000°C for 1 to 2 minutes or by exposing it for 30 minutes in a vacuum furnace at from 1100 to 1300°C. Good material will show little or no damage in color under this test, while poor material will be partially or entirely decarbonized."[32]

Available from commercial suppliers are a variety of different carbon finishes, which should be selected with the type of tube in mind for which the coated nickel is to be used.

REFERENCES

1. Wise, E. M., "Nickel in the Radio Industry," *Proc. I.R.E.*, **25**, 714–752 (1937).
2. Wise, E. M., and Schaefer, R. H., "The Properties of Pure Nickel," *Metals and Alloys*, **16**, 424–428; 891–893; 1067–1071 (1942).
3. "Nickel and Its Alloys," *U.S. Dept. of Commerce N.B.S. Circular 485*, (Mar., 1950). (For sale by the Superintendent of Documents, U.S. Govt. Printing Office, Washington 25, D.C.)
4. Grew, K. E., "The Specific Heat of Nickel and of Some Nickel-Copper Alloys," *Proc. Roy. Soc.*, London, **145**, 509–522 (1934).
5. Von Klinkhardt, H., "Measurement of the True Specific Heat at High Temperatures by Electron Bombardment." (In German.) *Annalen d. Phys.*, **84**, 167–200 (1927).
6. Stimson, H. F., "The International Temperature Scale of 1948," *J. Res. Nat. Bur. Stand.*, **42**, 209–217 (1949).
7. "Metals Handbook," Cleveland, Am. Soc. for Metals, 1948.
8. Wise, E. M., Private Communication, International Nickel Co., Inc., 1950.
9. Jones, H. A., Langmuir, I., and Mackay, G. M. J., "The Rates of Evaporation and the Vapor Pressures of W, Mo, Pt, Ni, Fe, Cu, and Ag," *Phys. Rev.*, **30**, 201–214 (1927).
10. "Nickel and Nickel Alloys," International Nickel Co., Inc., 1941.
11. Nix, F. C., and MacNair, D., "The Thermal Expansion of Pure Metals Cu, Au, Al, Ni, and Iron, *Phys. Rev.*, **60**, 597–605 (1941).

12. Van Dusen, M. S., and Shelton, S. M., "Apparatus for Measuring Thermal Conductivity of Metals up to 600°C," *J. Res. Nat. Bur. Stand.*, **12**, 429 (1934). (RP668.)
13. Potter, H. H., "The Electrical Resistance of Ferromagnetics," *Proc. Phys. Soc.*, London, **49**, 671–678 (1937).
14. Roeser, W. F., and Wensel, H. T., "Temperature, Its Measurement and Control in Science and Industry," Table 18, 1314, New York, Reinhold Publishing Corp., 1941.
15. Cardwell, A. B., "Photoelectric and Thermionic Properties of Nickel," *Phys. Rev.*, **76**, 125–127 (1949).
15a. Michaelson, H. B., "Work Functions of the Elements," *J. Appl. Phys.*, **21**, 536–540 (1950).
16. Armbruster, M. H., "The Solubility of Hydrogen at Low Pressure in Iron, Nickel, and Certain Steels at 400 to 600°," *J. Am. Chem. Soc.*, **65**, 1043–1054 (1943).
17. Dushman, S., "Scientific Foundations of Vacuum Technique, 561, New York, John Wiley and Sons, Inc., 1949.
18. Irman, R., "The Action of Sulfuric Acid on Nickel," *Metall. Erz.*, **12**, 358 (1915); **14**, 21, 37 (1917). Also, Mellor, **15**, 150 (1936).
19. Krulla, R., "The Corrosion Resistance of Nickel." (In German.) *Chem. Ztg.*, **54**, 429–431 (1930). Also, Mellor, **15**, 147 (1936).
20. Johnston, H. L., and Marshall, A. L., "Vapor Pressures of Ni and NiO," *J. Am. Chem. Soc.*, **62**, 1382–1390 (1940).
21. Campbell, W. E., and Thomas, U. B., "The Oxidation of Metals," *Transact. Electrochem. Soc.*, **91**, 623–640 (1947).
22. Betty, B. B., and Mudge, W. A., "Some Engineering Properties of Ni and High-Ni Alloys," *Mech. Eng.*, **67**, 123–129 (1945).
23. Everhart, J. L., *et al.*, "Mechanical Properties of Metals and Alloys," *National Bureau of Standards, Circular C447*, U.S. Gov't Printing Office, Washington, D.C. (1943).
24. Thirsk, H. R., and Whitmore, E. J., *Faraday Soc. Transact.*, **36**, 565–574 (1940).
25. Acker, J. T., "Testing Cathode Materials in Factory Production," *Proc. I.R.E.*, **37**, 688–690 (1949).
26. McCormack, R. L., "A Standard Diode for Electron-Tube Oxide-Coated Cathode-Core Material Approval Tests," *Proc. I.R.E.*, **37**, 683–687 (1949).
26a. ASTM Committee B-4, Annual Report 1950, Appendix thereto, "Proposed Method of Test for Relative Thermionic Emissive Properties of Materials Used in Electron Tubes," *Proc. A.S.T.M.* **50**, 142–158 (1950).
27. Briggs, T. H., "The Performance of Nickel Alloys in Oxide-Coated Cathodes," presented before ASTM Committee B4-VIII-A, June 7, 1950.
28. Briggs, T. H., and Richard, C. D., Jr., "Development and Use of a D.C. Emission Figure of Merit for Oxide-Coated Cathodes," *ASTM Bull.* No. 171, 66–70 (Jan. 1951).
29. Violet, F., and Riethmuller, J., "Contribution to the Study of Oxide Cathodes." (In French.) *Annales de Radioél.*, **4**, 184–215 (1949).
30. Wise, E. M., "The Platinum Metals: A Review of Their Properties and Uses," *J. Electrochem. Soc.*, **97**, 57–64(C) (1950).
31. Espe, W., and Steinberg, E. B., "Aluminum-Clad Iron for Electron Tubes," *Tele-Tech.*, **10**, 28–30, 77 (1951).
32. Briggs, T. H., "Carbonized Nickel for Radio Tubes," *Metals and Alloys*, **9**, 303–306 (1938).
33. Barnes, B. T., "Total Radiation from Polished and from Soot-Covered Nickel," *Phys. Rev.*, **34**, 1026–1030 (1929).

CHAPTER 12

COPPER

The great importance of this metal to our economy is easily brought into focus if it is remembered that nearly a million tons of copper are processed in the United States each year. From gleaming kitchen kettles to bus bars in modern power houses a multitude of divers applications have made copper a byword, and national fortunes are staked on its availability in time of war. Depending on its application, copper is used in various degrees of purity, and many alloys are available in the form of brass, bronze, nickel-silver, beryllium copper, aluminum-bronze, and others. For convenience of reference the compositions of these various alloys are listed in Table 12.1.[1]

The special field which concerns us here (i.e., electron tubes) calls almost exclusively for pure copper; but external gear, such as radiators and larger components used in particle accelerators, may at times be made from alloys. Copper finds little use in receiving tubes, except for lead wires external to the tube envelope, and beryllium copper is used occasionally for special support wires of larger diameter. (For properties and processing of beryllium-copper see Ref. 3.) For thin members copper is too soft and its melting point too low to make it useful whenever high temperatures are encountered during the processing cycle. Such a situation exists to a certain extent with lead wires of tube stems. Excessive oxidation during the sealing operation may weaken the copper and cause breakage on basing when tension is applied to straighten the wires. Most tube engineers must have attempted to solder a broken lead within the dome of the stem flare and no doubt enjoyed the experiment.

To reduce such costly hazards heat-resistant, nickel-clad copper wires were made for many years under the trade name "Kulgrid" by the former Callite Company, and are now produced under the same name by Sylvania Electric Products, Inc.* in size ranges from 5 to 10 mil diameter for multistrand wire and up to 0.060 inch in diameter for single wires. Nickel-clad copper conductor is also available in various shapes and sizes (0.031 to ½ inch in diameter) from the Alloy Metal Wire Company, Inc.† The current-carrying capacity of "Kulgrid" wire and strand

* Parts Division, Warren, Pa.

† Prospect Park, Pennsylvania.

TABLE 12.1. PER CENT NOMINAL COMPOSITION OF COPPER AND COPPER ALLOYS*

99.993 Cu	Gas free high purity copper (NRC see Table 12.6)
99.96[a] (Cu + Ag)	Certified OFHC
99.92[a] (Cu + Ag)	Oxygen free high conductivity copper (OFHC)
99.90[a] Cu-0.04 O-P: nil-Ag: nil	Electrolytic tough pitch copper
99.90[a] Cu-Ag: 10 oz/ton	Silver bearing or lake copper
99.90[a] Cu-0.025 P	Deoxidized or phosphorized copper
99.50 Cu-0.50 Te	Tellurium copper
99.40[a] Cu-0.30 As	Arsenical copper (tough pitch)
99.40[a] Cu-0.30 As-0.025 P	Arsenical copper (phosphorized)
99 Cu-1.00 Pb	Leaded copper
Wrought Alloys	
95 Cu-5 Zn	Gilding metal, 95%
90 Cu-10 Zn	Commercial bronze, 90%
85 Cu-15 Zn	Red brass, 85%
80 Cu-20 Zn	Low brass, 80%
70 Cu-30 Zn	Cartridge brass, 70%
65 Cu-35 Zn	Yellow brass
60 Cu-40 Zn	Muntz metal
89 Cu-9.25 Zn-1.75 Pb	Leaded commercial bronze
64.5 Cu-35 Zn-0.5 Pb	Low-leaded brass
67 Cu-32.5 Zn-0.5 Pb	Low-leaded brass (tube)
64.5 Cu-34.5 Zn-1 Pb	Medium-leaded brass
67 Cu-31.4 Zn-1.6 Pb	High-leaded brass (tube)
62.5 Cu-35.75 Zn-1.75 Pb	High-leaded brass
62.5 Cu-35 Zn-2.5 Pb	Extra-high-leaded brass
61.5 Cu-35.5 Zn-3 Pb	Free-cutting brass
60 Cu-39.5 Zn-0.5 Pb	Leaded Muntz metal
60.5 Cu-38.4 Zn-1.1 Pb	Free-cutting Muntz metal
60 Cu-38 Zn-2 Pb	Forging brass
57 Cu-40 Zn-3 Pb	Architectural bronze
71 Cu-28 Zn-1 Sn	Admiralty metal
60 Cu-39.25 Zn-0.75 Sn	Naval brass
60 Cu-37.5 Zn-1.75 Pb-0.75 Sn	Leaded naval brass
58.5 Cu-39.2 Zn-1 Fe-1 Sn-0.3 Mn	Manganese bronze—Grade A
76 Cu-22 Zn-2 Al	Aluminum brass
95 Cu-5 Sn	Phosphor bronze, 5%—Grade A
92 Cu-8 Sn	Phosphor bronze, 8%—Grade C
90 Cu-10 Sn	Phosphor bronze, 10%—Grade D
98.75 Cu-1.25 Sn—Trace P	Phosphor bronze, 1.25%—Grade E
70 Cu-30 Ni	Cupro-nickel, 30%
65 Cu-18 Ni-17 Zn	Nickel silver, 65–18
55 Cu-27 Zn-18 Ni	Nickel silver, 55–18
65 Cu-20 Zn-15 Ni	Nickel silver, 65–15
65 Cu-23 Zn-12 Ni	Nickel silver, 65–12
65 Cu-25 Zn-10 Ni	Nickel silver, 65–10
94.8[a] Cu-3 Si	High-Silicon Bronze, Type A

TABLE 12.1. PER CENT NOMINAL COMPOSITION OF COPPER AND COPPER ALLOYS.* (*Continued*)

Wrought Alloys (*Continued*)

96.0[a] Cu-1.5 Si	Low-Silicon bronze, Type B
95 Cu-5 Al	Aluminum bronze, 5%
92 Cu-8 Al	Aluminum bronze, 8%
Cu-10 Al	Aluminum bronze, 10%
82.5 Cu-10 Al-5 Ni-2.5 Fe	Aluminum bronze
Cu-2 Be-0.25 Co (or 0.35 Ni)	Beryllium copper
93.5 Cu-6.5 Ag 88.0 Cu-12.0 Fe	High strength, high conductivity alloys (Ref. 2)

Casting Alloys

88 Cu-6 Sn-1.5 Pb-4.5 Zn	Leaded tin bronze
87 Cu-8 Sn-1 Pb-4 Zn	Leaded tin bearing bronze
85 Cu-5 Sn-9 Pb-1 Zn	High-leaded tin bronze
83 Cu-7 Sn-7 Pb-3 Zn	High-leaded tin bronze
80 Cu-10 Sn-10 Pb	High-leaded tin bronze
78 Cu-7 Sn-15 Pb	High-leaded tin bronze
70 Cu-5 Sn-25 Pb	High-leaded tin bronze
85 Cu-5 Sn-5 Pb-5 Zn	Leaded gunmetal or red brass
83 Cu-4 Sn-6 Pb-7 Zn	Leaded red brass
81 Cu-3 Sn-7 Pb-9 Zn	Leaded semi-red brass
76 Cu-3 Sn-6 Pb-15 Zn	Leaded semi-red brass
71 Cu-1 Sn-3 Pb-25 Zn	Leaded yellow brass
66 Cu-1 Sn-3 Pb-30 Zn	Leaded yellow brass
60 Cu-1 Sn-1 Pb-38 Zn	Leaded yellow brass
62 Cu-26 Zn-3 Fe-5.5 Al 3.5 Mn	High-strength yellow brass
58 Cu-39.25 Zn-1.25 Fe-1.25 Al-0.25 Mn	High-strength yellow brass
59 Cu-0.75 Sn-0.75 Pb-37 Zn-1.25 Fe-0.75 Al-0.5 Mn	Leaded manganese bronze
66 Cu-5 Sn-1.5 Pb-2 Zn-25 Ni	Nickel silver
64 Cu-4 Sn-4 Pb-8 Zn-20 Ni	Nickel silver
57 Cu-2 Sn-9 Pb-20 Zn-12 Ni	Nickel silver
60 Cu-3 Sn-5 Pb-16 Zn-16 Ni	Leaded nickel brass
89 Cu-1 Fe-10 Al	Aluminum bronze
87.5 Cu-3.5 Fe-9 Al	Aluminum bronze
86 Cu-4 Fe-10 Al	Aluminum bronze
79 Cu-5 Fe-11 Al-5 Ni	Aluminum bronze

[a] Indicates minimum.

* According to a tabulation in the Metals Handbook[1] with permission of the Society for Metals. Additions and corrections were made by the present author in collaboration with various manufacturers.

is approximately 70 per cent that of a copper conductor of equivalent cross-sectional area. The nickel sheath occupies from 27 to 29 per cent of the cross section of the clad wire.

Thin copper foil, several hundred feet long and 7¼ inches wide, can now be obtained as thin as 0.00012 inch, according to a recent announce-

ment.* The foil is said to be of hard temper and may be easily handled in spite of its thinness. Its electrical resistivity is 1.64 microhm cm minimum, which corresponds to an electrical conductivity of 105.13 per cent I.A.C.S. (International Annealed Copper Standard).† Its chemical

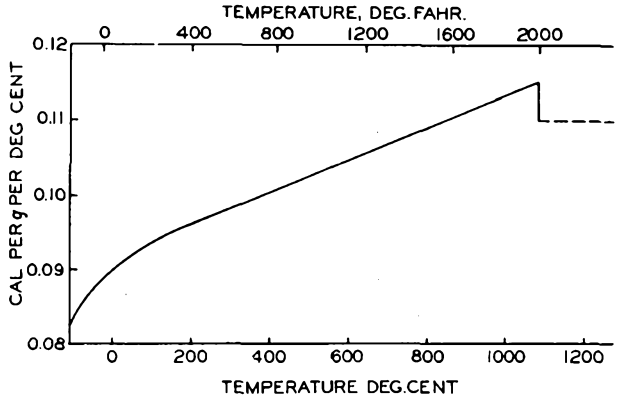

Fig. 12.1. The specific heat of pure copper as a function of temperature. After K. K. Kelley.[1] (*Courtesy U.S. Bureau of Mines.*)

composition is that of electrolytic copper. In the light of experience in this country where 101% IACS applies to electrolytic and 102% to OFHC, the figure 105.13% given for the foil appears high. The foil is supplied with one side polished and may, if necessary, have one or both sides plated with gold, silver, nickel, zinc, cadmium, or tin.

Copper has been the choice material for anodes in power tubes ever since the "Housekeeper Seal" made a reliable joint to glass possible by

* N. M. Rothschild and Sons, Royal Mint Refinery, 19 Royal Mint St., London E. 1, England.[4]

† The international standard for the resistivity of annealed copper is 0.15328 ohm (meter, gram) at 20°C (68°F) and corresponds to 100% conductivity. This means that a wire 1 meter long and weighing 1 gram would have a resistance of 0.15328 ohm. This is equivalent to a resistivity of 1.7241 microhm-cm for a bar 1 cm long and of 1 cm² cross-section. Other relationships are the following:

Conductivity % I.A.C.S. at 20°C	100	97.16	96.16
Resistivity at 20°C			
ohms (mile, pound)	875.20	900.77	910.15
ohms (meter, gram)	0.15328	0.15775	0.15940
ohms (foot, mil)	10.371	10.674	10.785
ohms (meter, mm²)	0.017241	0.017745	0.017930
microhm-inch	0.67879	0.69863	0.70590
microhm-cm	1.7241	1.7745	1.17930

A complete discussion of this subject is contained in Circular No. 31 of the National Bureau of Standards.

means of a machined feather edge (Chapter 4). Magnetrons, klystrons, and T-R tubes also use copper extensively; but, wherever power dissipation is a factor, proper cooling of the copper members by forced air or water circulated through cooling jackets is necessary to maintain mechanical rigidity and prevent vaporization of the metal. The unique properties of copper which outweigh this disadvantage are its high electrical and thermal conductivity, the ease with which it can be formed or cast into all conceivable shapes, and its ready availability at a reasonable cost. Copper is easily joined to other metals by soldering, brazing,

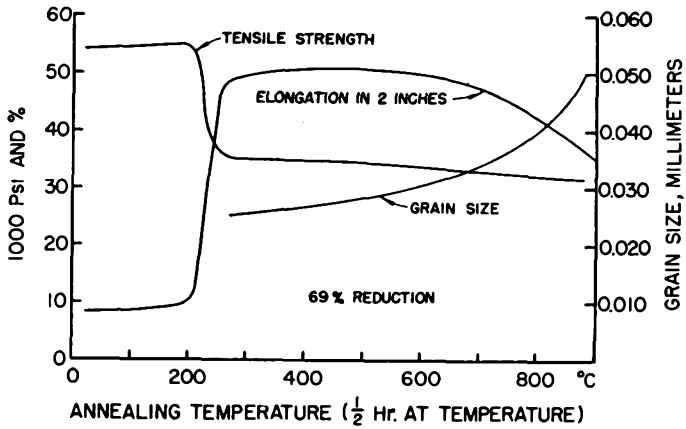

Fig. 12.2. Recrystallization diagram for electrolytic tough pitch copper giving tensile strength, elongation and grain size on one-half hour anneal at temperature. (*Courtesy American Brass Company.*[1])

or torch welding. Spot welding, however, is very difficult and tough pitch copper is difficult to torch-weld.

Machining of OFHC copper is not altogether easy, especially when it has to be done to close tolerances. On account of the extreme toughness of the metal the cuttings are long shavings rather than chips. Dalzell[5] recommends the following procedures:

"In preparing the metal for further machining in volume production carbide-tipped standard slitting or high-speed steel saws are recommended. For cutting with carbide-tipped tools, a top rake angle of 20 to 30 degrees and a 5- to 8-degree side-clearance angle are best; cut at 250 to 300 feet per minute.

"Precision-ground taps should be used for internal threading, maintaining close tolerances on the pitch diameters of the tap. In some cases standard gun taps can be used. External threading can be done with self-opening die heads on which the chasers have a 15-degree radial hook to facilitate chip clearance. (Landis, Geometric or Jones and Lampson tapping heads have been used with suceess.) Coolants must be free of sulfur to avoid contamination. (Paragon Lard Oil, Cutrite, and sulfur-free

Acorn No. 10 cutting oils give good results; others can be used.) Spiral milling cutters are preferred, four flute-fast spiral-end-mills producing the best results for end milling."

To improve machinability small percentages of lead, tellurium, or selenium are alloyed with the copper at the mill. Such copper is generally not used for vacuum-tube components. Tellurium-Copper* is an example. It contains 0.5 per cent of tellurium, and has an average electrical conductivity of 90-per cent IACS (annealed) (Table 12.3) and a machinability of 90-per cent free-cutting brass; the latter is assigned a machinability of 100 per cent for reference purposes in the machine trade. However, carbide-tipped tools are recommended on account of the hardness of copper-telluride particles. A method has recently been disclosed by R. A. Harris[6] which permits the use of tellurium copper for "Housekeeper Seals" by the expedient of plating the feather edge with pure copper and sealing thereto. It is stated that tellurium-copper forms a flaky nonadherent oxide if not protected in this manner. The vapor pressure of tellurium is given in the literature as follows:[7]

14.26 mm Hg at 671°C
3.34 mm Hg at 578°C
0.46 mm Hg at 488°C

From these data it seems questionable whether such a process should be recommended.

The metallurgy of copper has been treated in many texts, of which the following are listed:[1,8,9,10, and 11]. Physical characteristics of copper are presented in Tables 12.2 and 12.3, and chemical characteristics in Table 12.4. Jenkins and Digges[12] have reported on the "Creep of High-Purity Copper" and Backofen[12a] on the "Torsion Texture of OFHC and Electrolytic, Tough-Pitch Copper."

TABLE 12.2. PHYSICAL CHARACTERISTICS OF PURE COPPER†

Atomic number: 29	Atomic valence: 1, 2
Atomic weight: 63.54	Valence orbitals: $3d^{10}4s^2$
Isotopes: 63, 65	Lattice type: F.C.C.
Lattice constant: 3.6080 KX	
No. of atoms per unit cell: 4	
No. of unit cells per cc: 2.13×10^{22}	
Closest approach of atoms: 2.551 KX	
Atomic volume: 7.09 cc/g. mole	
Atomic heat: 5.848 cal/g mole	
Heat of fusion: 50.6 cal/g	
Heat of sublimation: 81.2 Kcal/mole (Ref. 13)	

* Patented Alloy, Chase Brass & Copper Co.
† Ref. 1 unless otherwise stated.

TABLE 12.2. PHYSICAL CHARACTERISTICS OF PURE COPPER.† *(Continued)*

Melting point: 1083 ± 0.1°C
Boiling point: 2595°C
Specific heat (at 20°C): 0.092 cal/g (see Fig. 12.1 page 259)
Vapor pressure (Ref. 8)

$$\log p \text{ (mm Hg)} = -\frac{18{,}350}{T(°\text{K})} + 14.01 - 1.275 \times \log T(°\text{K}) \text{ (for } T \rightarrow 800 \text{ to } 1356°\text{K)}$$

$$\log p \text{ (mm Hg)} = -\frac{17{,}700}{(T°\text{K})} + 13.51 - 1.275 \times \log T(°\text{K}) \text{ (for } T \rightarrow 1356 \text{ to } 2400°\text{K)}$$

Representative values of p (mm Hg) (Ref. 14)

1 mm Hg at 1628°C (1901°K)
10^{-1} mm Hg at 1432°C (1705°K)
10^{-2} mm Hg at 1273°C (1546°K)
10^{-3} mm Hg at 1141°C (1414°K)
10^{-4} mm Hg at 1035°C (1308°K)
10^{-5} mm Hg at 946°C (1219°K)

Composition limits for continuously cast, high purity copper (3/8 rod):

Fe— 0.0005% max.	Ag—0.00003% max.
Sb— .0001% max.	As— .0001% max.
Pb—.00005% max.	Te— .0001% max.
Sn—.00005% max.	Se— .0001% max.
Ni— .0001% max.	S— .0001% max.
Bi— .0001% max.	C— .0008% max.
	O_2—nil

Density (at 20°C): 8.96 g/cc
Thermal expansion (at 20°C): 165×10^{-7} per °C
from 0 to 300°C:

$$L_t = L_0[1 + (16.23t + 0.00483t^2) \times 10^{-6}] \text{ cm}$$

from 0 to 1000°C:

$$L_t = L_0[1 + (16.733t + 2.626 \times 10^{-3}t^2 + 9.1 \times 10^{-7}t^3) \times 10^{-6}] \text{ cm}$$

Thermal conductivity (at 20°C): 0.941 ± 0.005 cal/cm²/cm/°C/sec
Electrical resistivity (at 20°C): 1.6730 microhm-cm (This corresponds to an electrical conductivity on the volume basis of 103.5% I.A.C.S.)
Temperature coeff. of electr. resistivity: 0.0068 microhm-cm/°C (for any sample of copper at any temp.)
Temperature coeff. of electr. resistance (at 20°C): 0.00405 microhm-cm/°C. (This value applies for 103.5% I.A.C.S.)
Spectral emissivity (at 20°C) (Ref. 8: Hagan & Rubens 1900):

0.56 for $\lambda = 0.5\ \mu$
.28 for $\lambda = 0.6\ \mu$
.10 for $\lambda = 1.0\ \mu$
.03 for $\lambda = 3.0\ \mu$
.02 for $\lambda = 5.0\ \mu$
.02 for $\lambda = 9.0\ \mu$

Total emissivity: 0.02 (at 100°C) (Ref. 8)
0.12 (at 1200°C)
Magnetic susceptibility:

-0.086×10^{-6} c.g.s. at 18°C
-0.077×10^{-6} c.g.s. at 1080°C
-0.054×10^{-6} c.g.s. at 1090°C

Electron work function ϕ: 4.46 e.V. (Ref. 15)

TABLE 12.3. PHYSICAL CHARACTERISTICS OF VARIOUS GRADES OF COPPER
(See Table 12.1)

No.	Copper Grade	% Cu	Density g/cc lbs/c in.	Hardness Rockwell B	Hardness Rockwell F	Tensile Strength (psi)	Elongation % in 2 in.	Apparent Elastic Limit (psi)	Endurance Limit (psi) 20×10^6 Reversals	Young's Modulus (10^6) (psi)	M.P. (°C) (°F)	Coeff. Thermal Expansion (25-300°C) $\times 10^{-6}$	Thermal Conductivity cal/cm²/cm/sec/°C Btu/sq ft/ft/hr/°F	Electrical Conductivity % I.A.C.S. (annealed)
1	Gas-Free high purity copper	99.993	8.9436 0.3231			as cast: 21,300 hard: 54,300	52.5 21.			16				100.3 (as cast) 101.1 (worked)
2	Certified OFHC	99.96+	8.9310 0.3227							16				
3	Oxygen free high conductivity copper (OFHC)	99.92+	8.921 0.3223	h: 53-59 s:	90-92	h: 50-56,000 s: 32,000	h: 3 s: 43	h: 38-43,000 s: 3,000	h: 17,000	16	1082 1980	17.7	0.9426 228	101.85
4	Electrolytic tough pitch copper (Fig. 12.2)	99.90+	8.89-8.94 0.322	h: 55 s:	90 25	h: 55,000 s: 33,000	h: 6 s: 45	h: 40,000 s: 4,000	h: 15,000 s: 10,000	16	1082.56 1981	17.7	1.1386 227	101.6
5	Silver bearing copper or lake copper	99.90+	8.913 0.322	h: 56-64 s:	90-95 34	h: 52-58,000 s: 33,000	h: 5 s: 40	h: 39-46,000 s: 5,000	h: 15,000	16	1079.78 1975	17.4	0.9426 228	101.6
6	Deoxidized or phosphorized copper (tube)	99.90+	8.94 0.323	h: 65 s:	98 42	h: 59,000 s: 35,000	h: 5 s: 45	55,000 12,000	s: 12,000	16	1080.9 1977	17.7	0.728-0.848 176-205	75-90
7	Tellurium copper (Rod)	99.50	8.94 0.323	h: 48 s:	86 40	h: 53,000 s: 32,000	h: 7 s: 40	h: 42,000 s: 5,000		16	1082 1980	17.7	0.847 205	90 min.
8	Arsenical copper tough-pitch (sheets, strip)	99.50	8.913 0.322	h: 60-65 s:	93-97 41	h: 55-60,000 s: 34,000	h: 4 s: 47-42	h: 38-47,000 s: 2,000	h: 17,000 s: 13,000	17	1082.56 1981	17.4	0.4217 102	45
9	Arsenical copper (phosphorized)	99.45+	8.94 0.323	h: 65 s:	98 42	h: 60,000 s: 37,000	h: 4 s: 43	h: 55,000 s: 9,000	s: 15,000	16	1081.44 1978	17.4	0.4217 102	45
10	Leaded copper (rod)	99.00	8.94 0.323	h: 52 s:	90 30	h: 55,000 s: 35,000	h: 10 s: 50	h: 38,000 s: 5,000		15	1082 1980	17.7	0.9136 221	98

Wherever copper is used in a vacuum, it is essential to choose oxygen-free-high-conductivity (OFHC) grade, or its equivalent. Many costly failures will be avoided by observing this rule strictly. Oxide and other nonmetallic inclusions will lead to porosity after hydrogen firing, and

TABLE 12.4. CHEMICAL REACTIONS OF PURE COPPER

Atomic number: 2 — Atomic valence: 1 or 2
Atomic weight: 63.54 — Valence orbitals: $3d^{10}4s^{1}$
Heat of fusion: 50.6 cal/g — Melting point: 1083 ± 0.1°C
Heat of sublimation: 81.2 kcal/mole — Boiling point: 2600°C
Electrochemical equivalent: 0.3294 mg/coulomb for Cu^{++} (Ref. 8)
0.6588 mg/coulomb for Cu^{+} (Ref. 10)
Normal hydrogen electrode potential: +0.344 volts

(A) Reactions of Pure Copper
- (1) in dry air at room temperature: none
- (2) in dry air at 100°C: formation of invisible protective oxide
- (3) in dry air at 200°C increasing to red: oxidation colors: brown-orange, rose-red, violet, steel-blue, brass-yellow, red, greenish-grey, grey, black.
- (4) in moist air at room temperature: practically none
- (5) in sulfurous atmosphere at room temp.: tarnishing to a purplish color in 1–2 weeks when concentration of reactive sulfur corresponds to 1 vol. H_2S in 35. × 10^6 vol. of air. Formation of Copper Basic Sulfate $CuSO_4 \cdot 3Cu(OH)_2$ known as Verdigris or Green Patina
- (6) in water at room temp.: practically none
- (7) in salt water at room temp.: slow corrosion
- (8) in steam at 450°C: oxidation
- (9) in dry carbontetrachloride and dry trichlorethylene: practically none
- (10) in moist carbontetrachloride and moist trichlorethylene: some corrosion
- (11) in HCl or H_2SO_4, unaerated cold, warm, dilute or concentr. solutions, below 80%: practically none
- (12) in HNO_3, cold, warm, dil. or conc.: dissolution
- (13) in HNO_3 + HF (1:1 by vol.): rapid dissolution
- (14) in HF: none
- (15) in aqua regia: dissolution
- (16) in NH_4Cl, warm, dilute: dissolution (due to dissolution of oxide in NH_4Cl)
- (17) in NH_4OH: rapid dissolution; other alkalies, some corrosion
- (18) in cyanides: rapid dissolution

(B) Oxides of Copper
- (1) Cu_2O—cuprous oxide (d = 6.0) red, octahedral or cubic: insoluble in H_2O, dissolves in NH_4Cl
- (2) CuO—cupric oxide (d = 6.4) black, tetrag. cubic, tricl.: insol. in H_2O, dissolves in NH_4Cl
- (3) $CuO_2 \cdot H_2O$—monohydrated copper dioxide, brownish black: insoluble in H_2O, dissolves in acids

bring about intergranular cracks which result in leaks. Gas bursts may cause high-voltage breakdowns. The importance of these facts is easily confirmed by studying the photomicrographs in Figs. 12.3 and 12.4.[16,17] It is easy to test copper for verification of its grade, and such tests should be made whenever new stock is received.

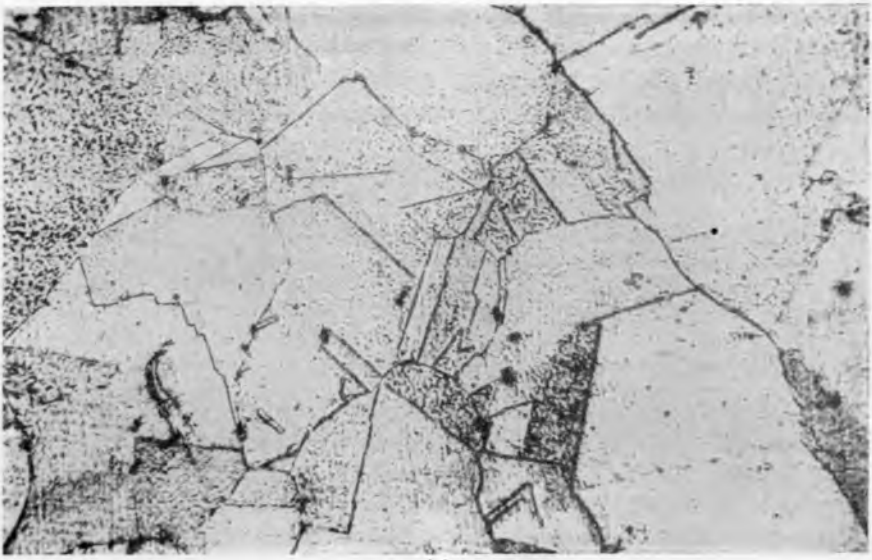

(a)

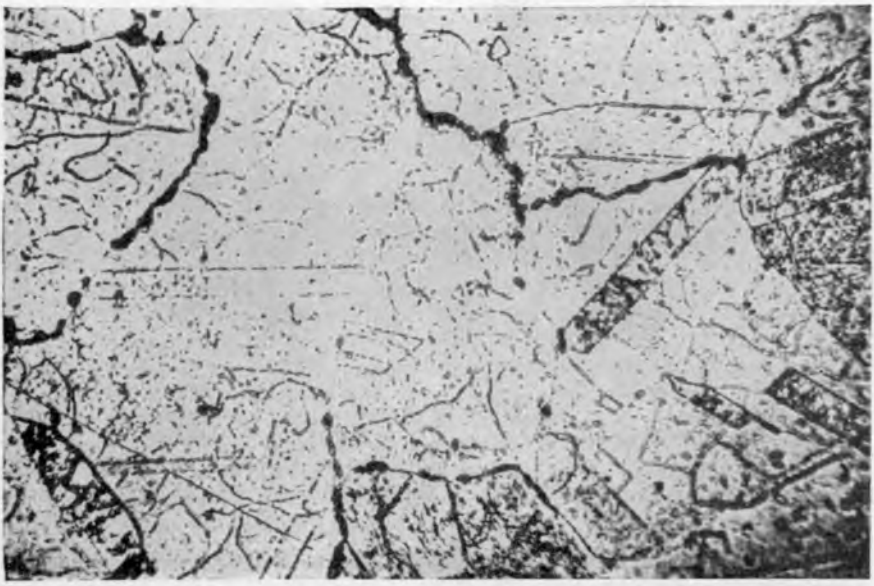

(b)

Fig. 12.3. Photomicrographs of copper taken to detect inclusions of Cu_2O. (a) "Good" copper, magnification 250×; (b) "bad" copper, magnification 405×. (*By permission from "Microwave Magnetrons" edited by George B. Collins.*[16] *Copyright, 1948. McGraw-Hill Book Company, Inc.*)

In its bulletin on OFHC copper the American Metal Corp.* recommends the hydrogen bend test as the most satisfactory procedure:

"If copper containing oxygen is heated in hydrogen, the latter gas penetrates into the copper and decomposes the oxides, leaving voids representing the difference in

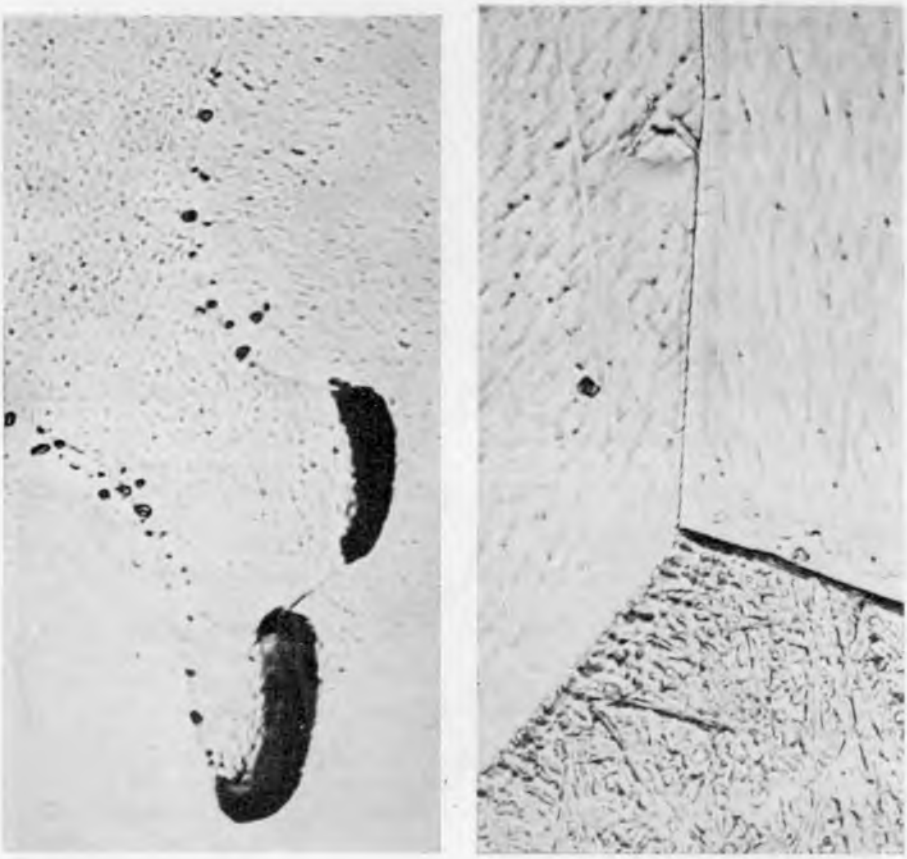

(a) (b)

Fig. 12.4. Photomicrographs of copper. (a) O.F.H.C. ingot (1000×). (b) Gas-free high purity copper (1000×). After Stauffer et al.[17] (*Reprinted by permission, The American Chemical Society and National Research Corporation, Cambridge, Mass.*)

volume between oxide and its reduced metal. There is also probably some opening up of grain boundaries because of the expansion of the steam formed in the reaction between oxygen and hydrogen. The hydrogen bend test comprises heating a piece of wire (or strip) in hydrogen at 850°C for 30 minutes and then, after quenching, bending it over a mandrel until it breaks. If the copper of which the wire (or strip) is made contains any oxygen, the number of bends is below a specified figure (at least four 90° bends in alternate directions). This test is sensitive and reliable."

* 61 Broadway, New York, 6, N.Y.

Both electrolytic tough pitch and OFHC copper will produce a tenacious oxide film but electrolytic tough pitch is not satisfactory for vacuum tube purposes because of its susceptibility to hydrogen embrittlement. Partridge[18] gives the following test for copper to be used for glass seals:

"Specimens not exceeding 1/16 inch in thickness are cleaned in a weak solution of sulfuric and nitric acids, washed in running water and placed on a rack in a furnace at a temperature of 820°C. After half an hour they are removed and plunged immediately into cold water. Copper suitable for seal-making should, after this treatment, be coated with a film of black matt oxide, lying on the surface of red cuprous oxide which adheres very tenaciously to the metal. A loose oxide film indicates unsatisfactory material, arising from the presence in the copper of deoxidizers which reduce the cuprous oxide to spongy copper. The copper should not be handled between the cleaning and the oxidizing treatments."

It is also a common observation that copper which has been embrittled by exposure to hydrogen at elevated temperature does not resume its original size after a heat cycle, but remains oversize. On 2½-inch diameter cylinders the excess on diameter has been reported as high as from 0.010 to 0.018 inch, while OFHC will return to its original size within 0.001 inch.[16]

The most definite test might appear to be the preparation of microphotographs. Inclusions of Cu_2O, a crystal-growth inhibitor, can then be readily seen under the microscope, and the grain size in general appraised. When viewed with polarized light, Cu_2O particles show a distinctive ruby-red color. The following procedure has been described by G. B. Collins[16] for the preparation of sections:

"A small piece of the copper under suspicion is cut from the billet. If the examination is concerned with grain structure, the sample is then annealed in an H_2 oven at 800°C. The copper is not annealed if detection of Cu_2O grains is desired. The metal is mounted in a molded bakelite cylinder to facilitate holding it during the polishing operations, which must be carried out with some care. Beginning with a coarse abrasive such as '320 Aloxite' cloth, progressively finer ones are used until the final polishing is done with a very fine alumina solution on 'Miracloth.' These polishings should be done on a slowly rotating wheel, and care should be taken not to carry over any abrasive from one stage to the next. Polishing should continue until no scratches are visible at a magnification of 200 diameters.

"If one wishes to study the grain structure, it is necessary to etch the surface of the copper after the polishing has been completed. If one is looking only for Cu_2O inclusions, etching is not necessary or desirable because the reagent may destroy the inclusions. Under microscopic powers of 200 to 500×, Cu_2O appears as small particles with a distinct bluish color. Their presence indicates that the copper will become porous when fired in an H_2 atmosphere. To develop the grain structure of the copper an etch of equal parts of NH_4OH and H_2O_2 is applied to the specimen with a soft cloth. Only fresh solutions of this reagent will etch satisfactorily. Because the polishing process usually alters superficially the grain structure of the metal it is good practice to etch lightly, then polish off this etch on the last wheel, and repeat this process until one has taken off the altered surface. Two etching and polishing cycles are usually sufficient to do this."

It has been pointed out, however, that the microscopic examination for cuprous oxide is not a definite test for the suitability of the copper for electron-tube applications. Traces of other compounds may be found which appear similar to oxide inclusions, yet are still not harmful. Thus, it is the general experience of the industry that the embrittlement test, together with the results from test seals to glass, give a more foolproof check on the quality of the copper for use in electron tubes.

There are two grades of OFHC available: regular and certified (Chapter 4). Regular OFHC is produced in accordance with ASTM specification B170-47, covering wire bars, billets, and cakes produced without the use of residual metallic or metalloidal deoxidizers. The minimum content of (Cu + Ag) is 99.92 per cent. The resistivity is specified as not exceeding 0.15328 international ohms per meter g at 20°C in the annealed state, which corresponds to an electrical conductivity of 102 per cent IACS. Annealing is carried out at approximately 500°C for 30 minutes. Cuprous oxide must not be detectable by microscopic examination at a magnification of 75 diameters. Samples must withstand the hydrogen bend test when clamped between jaws having edges with a radius 2.5 times the diameter (thickness in case of strip) of the specimen. One flexure of the wire through 90° and back to its original position is counted as one bend; a specimen of regular OFHC must withstand at least four such bends alternately made in opposite directions.

Certified OFHC carries a stricter specification, and is preferred for tube components. Its minimum (Cu + Ag) content is 99.96 per cent; it must withstand at least ten bends on the hydrogen bend test and a micrograph section should not show Cu_2O inclusions at a magnification of 200 diameters. In addition, the maximum impurity content is specified as follows:

	Per Cent
Phosphorus	0.0003
Sulfur	0.0040
Zinc	0.0003
Mercury	0.0001

Copper of somewhat higher impurity content is used when the better grade is not available. Partridge[18] gives the following typical specification for inferior grades, and points out that the oxide film will not adhere when the phosphorus content is as high as 0.005 per cent.

Copper	99.9 per cent min
Phosphorus	0.003 " " max
Arsenic	0.002 " " "
Oxygen	0.04 " " "
Other Constituents	0.005 " " "

The sensitivity of copper to impurities is further emphasized by pointing out that as little as 0.05 per cent of arsenic will lower the electrical conductivity (100-per cent IACS) by about 14 per cent, that the same amount of iron will reduce it by about 19 per cent, and that the same amount of phosphorus will lower it by about 30 per cent.[19,20]

OFHC copper is produced from electrolytic copper cathodes by continuous melting in an electric induction furnace and casting in water-cooled copper or steel molds, the entire operation being maintained at all times in a reducing atmosphere. An assay of OFHC copper is given in Table 12.5. Another high-conductivity copper, known under the trade

TABLE 12.5. ASSAY OF OFHC COPPER*

Gold	trace	Phosphorus	0.0000%
Silver	0.37 ozs/ton	Bismuth	.0001%
Iron	.0005%	Selenium	.0002%
Sulfur	.0018%	Tellurium	.0001%
Arsenic	.0002%	Tin	.0001%
Lead	.0006%	Nickel	.0009%
Antimony	.0005%	Copper	99.98+

Conductivity 101.85% IACS; bends after hydrogen anneal—10 average
* Courtesy of American Metal Corporation, New York, N.Y.

mark "PDCP Copper,"* is also obtained from electrolytic copper; however, the latter is not melted again, but is converted into the desired shapes of bar, rod, and strip by exposure to tremendous pressure at elevated temperature in a reducing atmosphere. Its analysis and conductivity in general compare with that of certified OFHC. The latter is considered to have better ductility.

During recent years the National Research Corporation† has developed the art of vacuum-casting copper ingots of substantial size,[17] thus showing how the gas content can be reduced substantially while other impurities remain about equal to those present in OFHC copper. Table 12.6 gives the analysis of this gas-free, high-purity copper, compared with one for regular OFHC.

Table 12.7 gives the typical analysis of a 200-pound ingot of N.R.C. gas-free high-purity copper which has an electrical conductivity of 100.3-per cent IACS. The tensile properties of N.R.C. gas-free high-purity copper in comparison with those of OFHC copper are given in Table 12.8.[17]

Large-scale production of vacuum-fused metals was pioneered in

* Phelps Dodge Copper Products Corp., 40 Wall St., New York, N.Y.
† 70 Memorial Drive, Cambridge 42, Massachusetts.

TABLE 12.6. ANALYSIS OF VACUUM CAST COPPER*

Element	OFHC	GFHPC	Method of Analysis
Hydrogen	0.00012%	0.00001%	Vac. fusion
Oxygen	.00045	.00004	Vac. fusion
Sulfur	.0023	.0001	Wet method
Selenium	.00013	.00005	Wet method
Tellurium	.0001	.00005	Wet method
Lead	.0005	.0001	Spectroscopic

* Courtesy National Research Corporation, Cambridge, Mass.

TABLE 12.7. TYPICAL ANALYSIS OF A 200 LB INGOT OF GAS-FREE HIGH-PURITY COPPER*

Nitrogen	<0.0001%
Oxygen	<0.0001%
Hydrogen	<0.0001%
Iron	<0.002%
Nickel	<0.0005%
Arsenic	0.001% or less
Lead	.0001% or less
Silver	.003% or less
Sulfur	.0001% or less
Bismuth	trace
Tin	trace
Zinc	trace

* The author is indebted to NRC for supplying these data.

TABLE 12.8. TENSILE PROPERTIES OF VACUUM CAST COPPER[17]

	As Cast		Forged and Drawn			
			Full Hard		Full Annealed	
	OFHC	Vacuum	OFHC	Vacuum	OFHC	Vacuum
Tensile strength (psi)	23,200	21,300	54,500	54,300	36,000	36,000
Reduction in area (%)			76	88		
Elongation (%)	48.5	52.5	17	21		

Germany by Heraeus and reached considerable proportions by 1929. A paper by W. Rohn[21] describes the technique and properties of vacuum-fused metals known at that time. The advance made during recent years is readily appreciated by comparing the absolute pressure at which vacuum casting was carried out then (several mm Hg), with the pressures prevailing in modern techniques (several microns). Ingots up to 400 pounds are now cast to any desired shape.

REFERENCES

1. "Metals Handbook," Cleveland Am. Soc. for Metals.
2. Hodge, W., and Rose, K., "New Copper-Base Alloys Combine High Strength with High Conductivity," *Mater. and Meth.*, **31**, 64–65 (1950).
3. Richard, J. T., "Beryllium Copper," *Mater. and Meth.*, **31**, 76–90 (1950). *Manual No. 58.*
4. "Thin Copper Foil," *J. Sci. Inst.*, **27**, 173 (1950).
5. Dalzell, R. C., "Copper in Electronic Tubes," *Electronics*, **22**, 164–170 (Apr. 1949).
6. Harris. R. A.. and Patton. C. C., "Composite Structure for Forming a Seal with Glass," *U.S. Patent 2,482,178* (Sept. 20 1949).
7. Doolan, J. J., and Partington, J. R., "Intern. Crit. Tables."
8. Smithells, C. J., "Metals Reference Book," New York, Interscience Publishers, Inc., 1949.
9. Mellor, J. W., "Inorganic and Theoretical Chemistry," Vol. 3, New York, Longmans, Green and Co., 1923.
10. Ellis, O. W., "Copper and Copper Alloys," Cleveland, Am. Soc. for Metals.
11. Wilkins, R. A., and Bunn, E. S., "Copper and Copper-Base Alloys," New York, McGraw-Hill Book Co., Inc. 1943.
12. Jenkins, W. D., and Digges, T. G., "Creep of High-Purity Copper," *J. Res. Nat. Bur. Stand.*, **45**, 153–161 (1950). (RP2121).

12a. Backofen, W. A., "The Torsion Texture of Copper," *Transact. Am. Inst. Min. and Met. Eng. J. of Metals*, **188**, 1454–1459 (1950).

13. Seitz, F., "The Modern Theory of Solids," New York, McGraw-Hill Book Co., Inc., 1942.
14. Dushman, S., "Scientific Foundations of Vacuum Technique," New York, John Wiley and Sons, Inc., 1949.
15. Anderson, P. A., "The Work Function of Copper," *Phys. Rev.*, **76**, 388–390 (1949).
16. Collins, G. B., "Microwave Magnetrons," *Rad. Lab. Ser. No. 6*, 696, New York, McGraw-Hill Book Co., Inc. (1948).
17. Stauffer, R. A., Fox, K., and DiPietro, W. O., "Vacuum Melting and Casting of Copper," *Ind. and Eng. Chem.*, **40**, 820–825 (1948).
18. Partridge, J. H., "Glass-to-Metal Seals," *Soc. Glass Tech.*, Sheffield 10, England (1949).
19. Archbutt, S. L., and Prythench, V. E., "Effect of Impurities in Copper," *Research Monograph No. 4.* London, British Nonferrous Metals Res. Assoc. (1937).
20. Parker, E. R., "The Effect of Impurities on Some High-Temperature Properties of Copper," *Trans. Am. Soc. Metals*, **29**, 269 (1941).
21. Rohn, W., "Technical Properties of Vacuum-Fused Metals." (In German.) *Zs. Metallkunde*, **21**, 12–18 (1929). Also, *J. Inst. Metals*, **24**, 203 (1929).

CHAPTER 13
CARBON AND GRAPHITE

The applications of carbon and graphite in the electron-tube industry are manifold indeed. This material will withstand a higher temperature *in vacuo* than any other element, and its position halfway between metals and semiconductors enables it to perform the most varied functions. From the carbon filament in the original incandescent lamp to graphite anodes in power tubes of present-day design a long series of developments has refined the processes employed to make them perform to the best advantage in a given application. Graphite molds are used for vacuum casting metals and x-ray tube targets as well as for forming glass components from glass powder. Graphite electrodes are employed in glass furnaces and arc lamps. In combination with metals and insulators and produced by powder metallurgical techniques, interesting graphitized combinations result which range from graphite-filled "Oilite"* bearings to graphitized "Teflon."† As lampblack and colloidal graphite applied in thin films, it may be used to suppress secondary emission on tube electrodes or provide a conductive path for the screen current return in cathode-ray tubes. It may be employed as an intermediate layer between luminescent material and supporting metal to reduce "blocking effect" and screen poisoning in tuning indicators, as demonstrated by Parker and Kohl.[1] In special cases carbonizing of tungsten filaments may be accomplished by depositing colloidal graphite by cataphoresis although flashing in a hydrocarbon atmosphere is the generally accepted technique. Very thin sheets of pure carbon can be obtained by hydrogen-firing filter paper between two metal blocks. Finely divided carbon in the form of charcoal has a powerful getter action, and is used in liquid air traps. Thin carbon films on glass or ceramics form stable high resistances. This gives a random selection of the main uses and will serve to emphasize the fact that carbon plays an important role in electronics. One is tempted to refer also to graphite in "lead" pencils, a misnomer which dates back to the time when lead was believed to be a constituent of graphite. Following the procedure adopted in earlier chapters, the physical and chemical properties of carbon and graphite are summarized in Tables 13.1 and 13.2.

* Chrysler Corporation, Amplex Division.

† United States Gasket Company, 602 N. 10th St., Camden, N.J.

TABLE 13.1. PHYSICAL CHARACTERISTICS OF CARBON AND GRAPHITE

Atomic number: 6 — Atomic valence: 2, 4
Atomic weight: 12.010 — Valence orbitals: $2s^2\ 2p^2$
Isotopes: 12, 13 14* (radioactive)

	Diamond	Graphite	Carbon
Lattice type	A4: diamond	A9: hexagonal	
Lattice constant (Ref. 3)	$a = 3.56$	$a = 2.46$ $c = 6.7$	
No. of atoms/unit cell	8	4	
Closest approach of atoms (Ref. 3)	$d_c = 1.54$	1.42 in layers 3.35 between layers	
Atomic volume		5.41 cc/g atom (Ref. 4)	6.7–8.0 (Ref. 2)
Atomic heat cal/g atom/°C (Ref. 4)		26– 76 1.98 26– 280 2.35 25– 490 2.70 30– 540 2.80 30– 750 3.47 35– 900 3.90 40– 925 3.90 48–1193 4.20 56–1450 4.69	
Heat of sublimation		140 Kcal/mole (Ref. 5)	
Heat of vaporization at B P.	143 Kcal/g atom (Ref. 6)	11,900 cal/g (Ref. 2)	11,900 cal/g (Ref. 2)
Melting point (Ref. 4)	> 3,500°C	3,700 ± 100°C	
Boiling point (Ref. 4)	4,830°C	4,830°C	4,830°C
Specific Heat (cal/g/°C)(Ref. 7)			
0– 24°C	0.12 (at 20°)	0.166	0.165
26– 76	.160	.165	.168
26– 282	.315	.195	.200
26– 538 (Ref. 2)	.415	.234	.234
36– 902		.324	.315
47–1193		.350	.352
56–1450		.390	.387

Vapor pressure (mm Hg) (Ref. 8)

10^{-5} mm Hg at 2129°C
10^{-4} mm Hg at 2288
10^{-3} mm Hg at 2471
10^{-2} mm Hg at 2681
10^{-1} mm Hg at 2926
1 mm Hg at 3214

Thermal emissivity (Ref. 9) — Rough dull surface: 0.89; Smooth shiny surface: .82

According to H. T. Wensel[10] carbon is believed to be a true grey body having the same emissivity at all wavelengths and temperatures, so that spectral and total emissivities can be used interchangeably. Barnes, Forsythe and Adams[11] give the following values for total emissivity:

Carbon (Rough)	0.77 (100°C)	0.77 (320°C)	0.72 (500°C)
Graphitized Carbon (Rough)	.76 (100°C)	.75 (320°C)	.71 (500°C)

TABLE 13.1. PHYSICAL CHARACTERISTICS OF CARBON AND GRAPHITE. (*Continued*)

	Diamond	Graphite	Carbon
Density	3.51	2.1 -2.3	1.8-2.1
Hardness (Mohs)	10	0.5 -1	
Refractive index	2.40242-2.45922	1.93-2.07	
Dielectric constant (Ref. 2)	5.26-5.35		2.4
Coeff. lin. therm. exp. (40°C)	1.18×10^{-6}/°C	1.2×10^{-6}/°C	2.2×10^{-6}/°C
Electron work function (e.V.)			4.60 (Ref. 12)
Richardson constant A (amp/cm² deg²)			46

Physical Properties of Baked Carbon (Ref. 13)

Elasticity (Young's modulus) psi	434,000-955,000
Transverse breaking strength (psi)	
Extruded carbon	700-2000
Molded carbon	2000-6000
Electrical resistivity at 20°C (ohm-cm)	
Coke base	0.0036-0.0046
Lampblack base	0.0046-0.0056
Specific heat, cal/g	0.20
Thermal conductivity, cal/cm²/cm/sec/°C	.01
Coefficient of linear expansion (per °C)	$.65 \times 10^{-6}$
Hardness, sceleroscope	
Coke base	70-90
Lampblack base	70-110
Radiation (total emissivity) 1000-1500°C	0.52
1800-2400°C	.79
3900°C	.84
Apparent density (lb/cu ft)	
Amorphous carbon electrodes	97.5
Large electrothermal electrodes	100.0

Physical Properties of Anthracite-Base and Petroleum-Coke-Base Electrodes (Ref. 13)

	Carbon Electrodes	
	Anthracite Base	Petroleum-Coke Base
Carbon (%)	91.5 or more	97.5 or more
Specific gravity	1.9-2.1	2-2.1
Apparent density, g/cc		
Extruded	1.45-1.67	1.53-1.64
Molded	1.55 min	
Porosity, av. (%)	22	24
Tensile strength (psi)	330-1310	700-1200
Electrical resistivity (ohm-cm)	0.0036-0.0064	0.0036-0.0046
Thermal conductivity, cal/cm²/cm/sec/°C		
20- 40°C		0.0079
40-340°C		.016
340-600°C		.012
Specific heat, cal/g		
26- 76°C		.168
26- 538°C		.199
56-1450°C		.387
Coefficient of linear expansion (per °C)		
220-1820°C	0.000011	
180-1920°C		0.0000072

TABLE 13.1. PHYSICAL CHARACTERISTICS OF CARBON AND GRAPHITE. (*Continued*)

Physical Properties of Electrographite Electrodes (Ref. 13)	
Specific gravity	2.21–2.25
Apparent density, g/cc	1.50–1.75
Elasticity (Young's modulus) psi	60,000–300,000
Transverse breaking strength, psi	1000–1400
Crushing strength (psi)	3000–5000
Electrical resistivity (ohm-cm)	0.00063–0.00113
Specific heat (76–1450°C.) cal/g	0.166–0.39
Thermal conductivity, cal/cm²/cm/sec/°C	
At 50°C	0.369
At 900°C	0.15
Coefficient of linear expansion (per °C)	
Longitudinal section	$1.1–2.2 \times 10^{-6}$
Transverse section	$2.2–4.6 \times 10^{-6}$
Temperature of vaporization (°C)	3200–4200
Oxidation begins at (°C)	500
Ash content (%)	0.10–1.80

Fig. 13.1–13.3 give electrical and thermal conductivities as a function of temperature according to Powell[14] and Buerschaper.[15]

Fig. 13.4 shows the Thermal Expansion of National Carbon Company Graphite Grade C-18 and AGX.*

Fig. 13.5 presents data on the electrical resistance vs. temperature of C-18 and AGX graphite, measured perpendicular to the direction of molding pressure.*

Fig. 13.6 gives the short-time breaking strength of various grades of National Carbon Company graphites as a function of temperature.*

Fig. 13.7 shows a typical creep curve for grade ECA graphite.*

Fig. 13.8 presents the steady creep rate obtained with ECA graphite as a function of stress for various temperatures.*

Fig. 13.9 gives Young's Modulus of ECA graphite versus temperature.*

Fig. 13.10 shows the strength-to-weight ratio for several materials as a function of temperature.*

Three allotropic forms of carbon, diamond, graphite, and amorphous, can be readily distinguished by chemical and physical tests. Their densities are quite distinctly different (Table 13.1), and the following chemical test has been described. One part of the material to be tested is treated with three parts of $KClO_3$ and sufficient concentrated HNO_3 to render the mass liquid, the mixture being heated in a water bath for several days. Diamond carbon is entirely unaffected; graphite carbon is converted into golden yellow flakes of graphitic acid and amorphous carbon into a brown substance which is soluble in water.[2]

* Figures 13.4 to 13.10 are based on measurements made at the Atomic Energy Research Department of North American Aviation, Inc. Fig. 13.6–13.10 are contained in their report NAA-SR-79 by Malmstrom, Keen and Green of Sept. 28, 1950. The author is indebted to Dr. C. Malmstrom for kindly sending him these data and permitting their inclusion in this text prior to publication of the report in the Journal of Applied Physics under the title: "Some Mechanical Properties of Graphite at Elevated Temperatures."[54]

TABLE 13.2. CHEMICAL PROPERTIES OF CARBON AND GRAPHITE

Atomic number: 6		Atomic valence: 2, 4	
Atomic weight: 12.010		Valence orbitals: $2s^2 2p^2$	
Heat of combustion:	94,310 cal/g mole (diamond)	94,810 cal/g mole (graphite)	96,960 cal/g mole (charcoal)

(A) Reactions of Carbon and Graphite

(1) in air, dry or moist up to 170°C: none. Carbon begins to oxidize in air at about 350°C and graphite at about 450°C (Ref. 2). Murphy (Ref. 16) gives 600°C as the onset of oxidation in air for bulk graphite while thin colloidal graphite films will show oxidation at 450°C. The oxidation rates of carbon and graphite in controlled atmospheres have been investigated by A. S. Bemis and G. P. McKnight* of which a partial account is given in Ref. 17. The rate of combustion depends largely on temperature and the supply of oxygen, i.e. the rate of flow of the gas passing over the hot sample. If the oxygen supply does not limit the combustion rate, carbon burns about 20 times as fast as graphite. Thus graphite can be heated nearly 100°C hotter than carbon without increasing the rate of combustion. At temperatures below 600°C (dark cherry red) the burning rate of graphite is so low that it is negligible. At about 850°C (light red) the oxygen supply limits the oxidation rate. These characteristics are illustrated in Fig. 13.11 and Fig. 13.12 which are taken from Ref. 17 (see page 281 and 282).

(2) in water up to 100°C: none

(3) in CCl_4 up to B.P.: none

(4) in trichlorethylene: none

(5) in 75% H_2SO_4 up to 135°C: none

(6) in 96% H_2SO_4 up to 80°C: none

(7) in HCl up to B.P.: none

(8) in HNO_3, conc.: attack with formation of mellitic acid, hydrocyanic acid or $CO_2 + N_2O$ (Ref. 2)

(9) in aqua regia: none

(10) in 15% HF up to B.P.: none, except in electrolysis with C anode

(11) in 20 cc conc. HNO_3 + 40 cc conc. H_2SO_4 + 20 g $KClO_3$/g of graphite: dissolution of graphite to form graphitic acid (Ref. 18)

(12) in $H_2Cr_2O_7 + H_2SO_4$: oxidation

(13) in molten alkalies: none

(14) in alkali hydroxides: none in solution but attack in molten alkali hydroxides (Ref. 2)

in oxygen: diamond ignites at about 800°C, graphite at 700°C, charcoal above 400°C

in chlorine, bromine, iodine, nitrogen: none

in fluorine: formation of CF_4 (B.P.—130°C)

in dry hydrogen at 1100–1500°C: formation of CH_4 (0.1% yield) (yield decreasing with increasing temp.) (Ref. 19)

in dry hydrogen with Ni as catalyst: formation of CH_4 at 500°C (Ref. 2)

in water vapor above 1000°C: nearly complete conversion into $CO + H_2$ (Ref. 19)

in wet Hydrogen passed through H_2O at 50°C: 12% conversion into $CO + H_2$ above 1000°C (Ref. 19)

in wet Hydrogen passed through H_2O at 25°C: 3% conversion above 1000°C (Ref. 19)

* Speer Carbon Company, St. Marys, Pennsylvania. Tech. Report No. 3030 (1948).

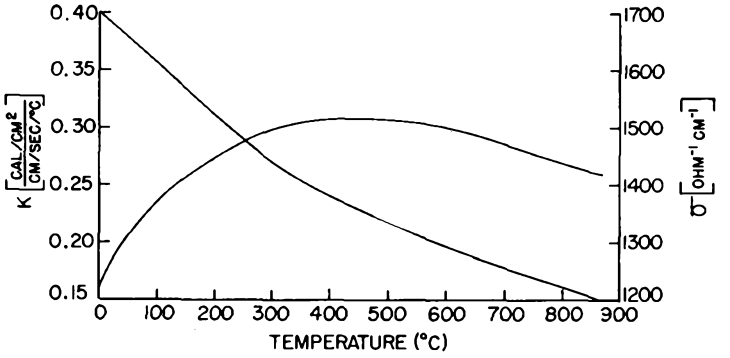

Fig. 13.1. Variation of electrical and thermal conductivity of Acheson graphite with temperature. After Powell.[14] (*Courtesy Cambridge University Press.*)

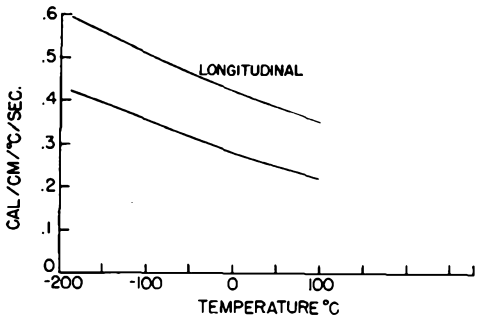

Fig. 13.2. Thermal conductivity of graphite vs. temperature. After R. A. Buerschaper.[15] (*Courtesy American Institute of Physics.*)

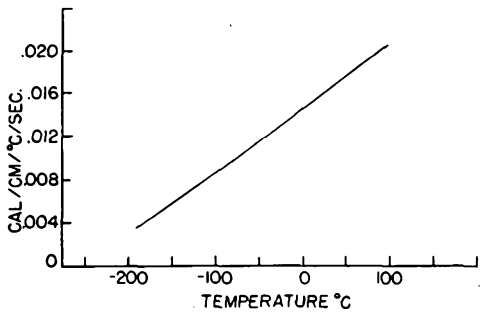

Fig. 13.3. Thermal conductivity of carbon vs. temperature. After R. A. Buerschaper.[15] (*Courtesy American Institute of Physics.*)

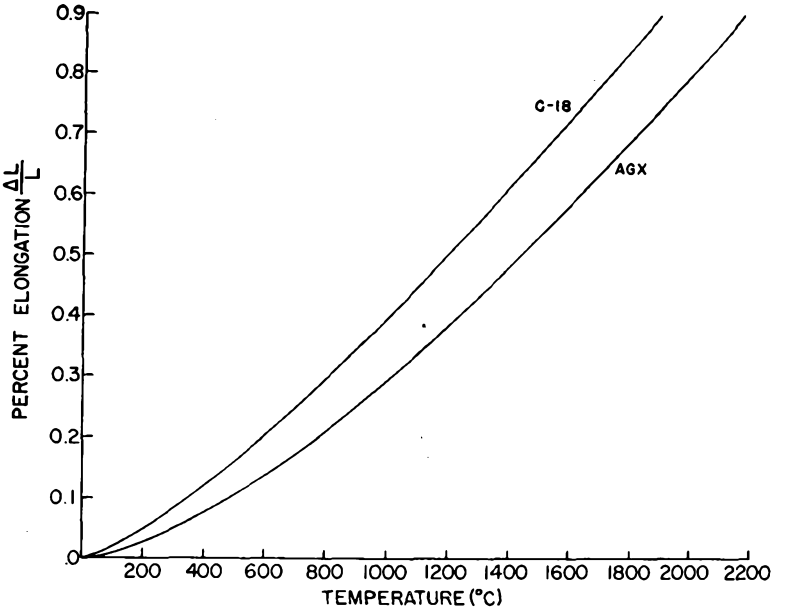

Fig. 13.4. Thermal expansion of National Carbon Company graphite grade C-18 and AGX. (*Courtesy North American Aviation, Inc.*[54])

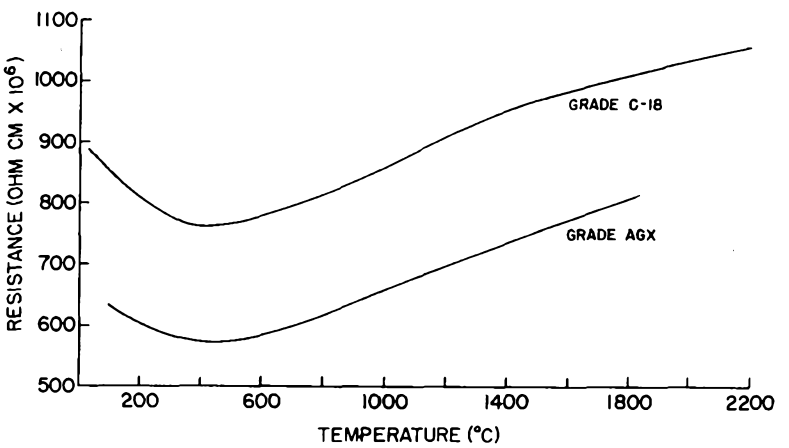

Fig. 13.5. Electrical resistance vs. temperature for C-18 and AGX graphite, measured perpendicular to the direction of molding pressure. (*Courtesy North American Aviation, Inc.*[54])

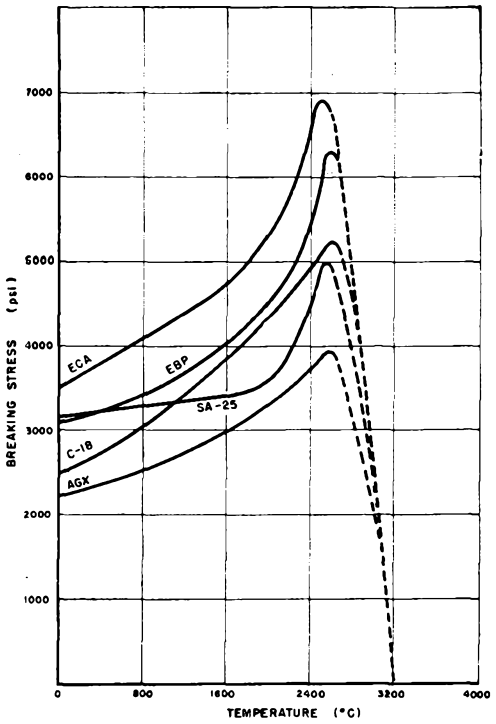

Fig. 13.6. Short-time breaking strength of various grades of National Carbon Company graphites as a function of temperature. (*Courtesy North American Aviation, Inc.*[54])

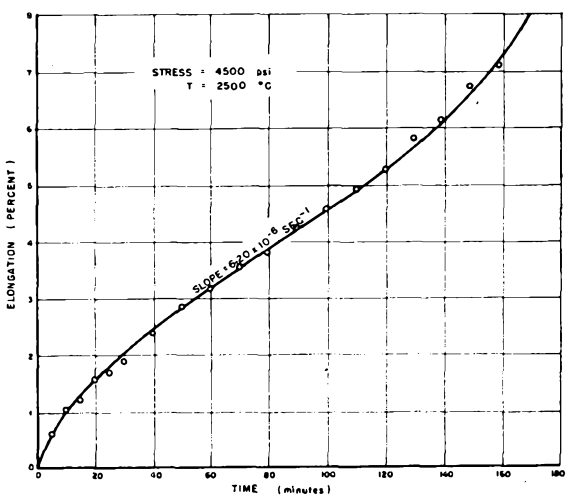

Fig. 13.7. Typical creep curve for Grade ECA graphite. (*Courtesy North American Aviation, Inc.*[54])

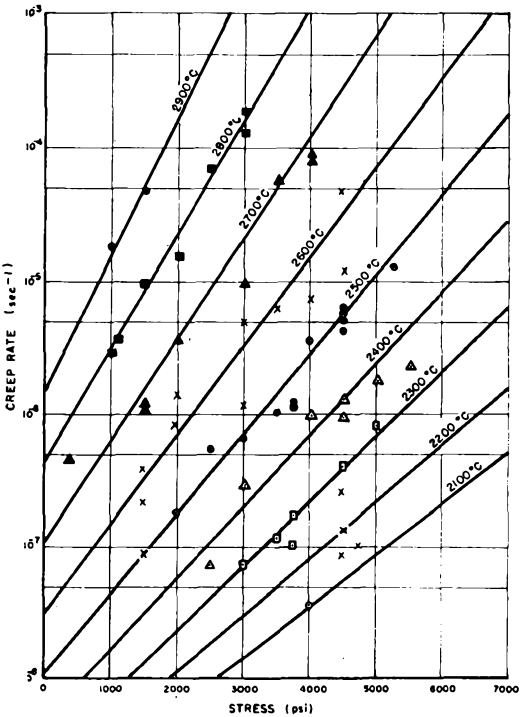

Fig. 13.8. Steady creep rate obtained with ECA graphite as a function of stress for various temperatures. (*Courtesy North American Aviation, Inc.*[54])

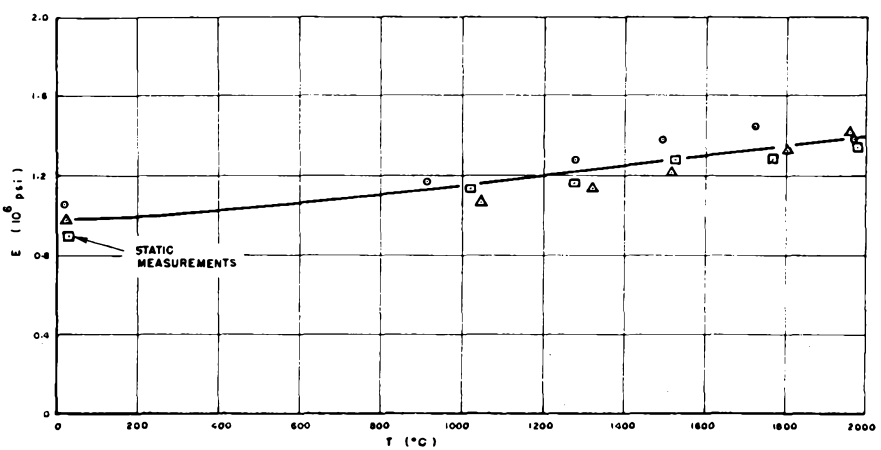

Fig. 13.9. Young's modulus of ECA graphite vs. temperature. (*Courtesy North American Aviation, Inc.*[54])

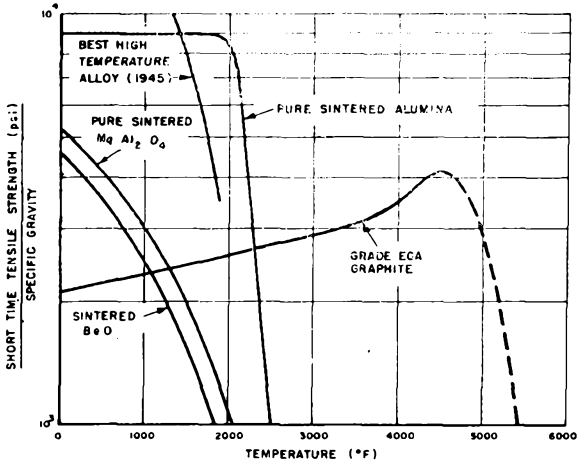

Fig. 13.10. Strength to weight ratio for several materials as a function of temperature. (*Courtesy North American Aviation, Inc.*[54])

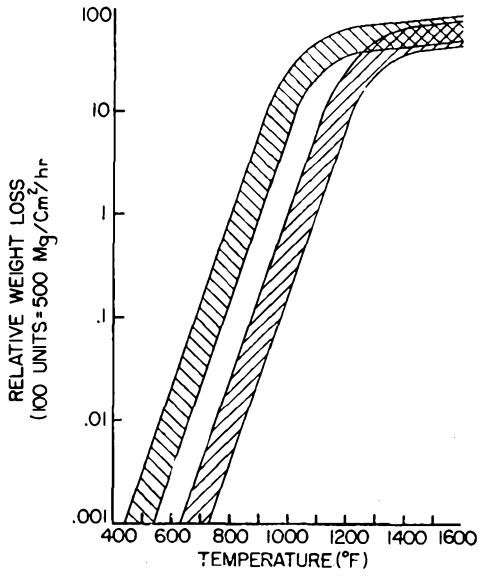

Fig. 13.11. Combustion rate of carbon and graphite in terms of relative weight loss per hour vs. temperature. (*Courtesy Speer Carbon Company and International Graphite & Electrode Corp.*[17])

The fact that diamond is the hardest material ($H = 10$ on Mohs, scale) and graphite one of the softest ($H = 1$) emphasizes their "structure-sensitive properties." This term was introduced by Smekal[20] in conjunction with "structure-insensitive materials" as a classification of crystals. Some properties, such as hardness, are more dependent on structure, others, such as density, are less. In the case of hardness a correlation with structure is quite evident when the minerals of Mohs'

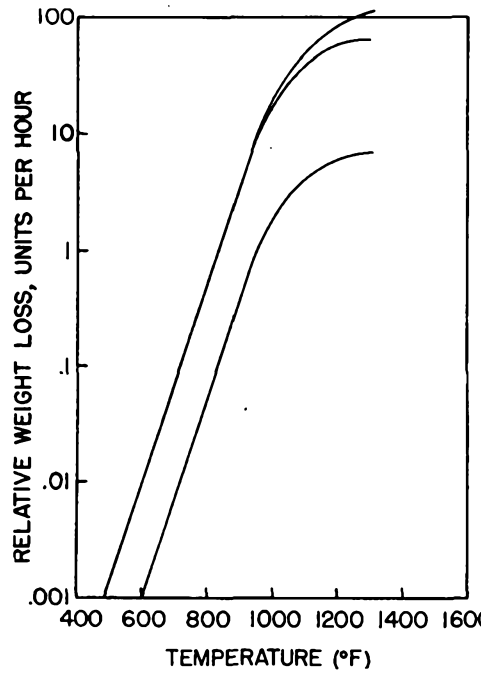

Fig. 13.12. Effect of different atmospheres on the oxidation rate of graphite. (a) Normal air flow. (b) Velocity doubled. (c) Oxygen content $\frac{1}{10}$ normal. (*Courtesy of Speer Carbon Co. and International Graphite & Electrode Corp.*[17])

scale of hardness are compared with the lattice structure found in these crystals, as shown in Table 13.3.[21]

Hardness changes gradually with the type of bond, and graphite and diamond stand at the two extremes of the scale. It is of interest to note that a difference in hardness in a probable ratio 100:1 exists in a single diamond in different directions of the crystal. Diamond hardness is thus a vector property.[22]

Diamond crystallizes in what is often called the "diamond-like lattice," in which each carbon atom is surrounded by four other carbon atoms. The latter are located at the corners of a tetrahedron (Fig. 13.13), and all atoms are linked by homopolar bonds (See Chapter 7).

This structure was listed under A4 as the diamond cubic lattice in which germanium and tin crystallize, and it is also familiar from the SiO_4 subgroups in glasses (Chapter 1). The fact that a cubic lattice is associated with tetrahedrons is easily recognized when the corner of a cube is

TABLE 13.3. HARDNESS AND CRYSTAL STRUCTURE[21]

Mohs Hardness	Mineral	Chem. Composition	Bond Type
1	Talc	$3\ MgO{\cdot}4\ SiO_2{\cdot}H_2O$	Layer lattice
2	Gypsum	$CaSiO_4{\cdot}2H_2O$	Layer lattice
3	Calcite	$CaCO_3$	Layer lattice
4	Fluorite	CaF_2	Ionic bond
5	Apatite	$CaF{\cdot}Ca_4(PO_4)_3$	Ionic bond
6	Orthoclase	$KAlSi_3O_8$	SiO_4 sceleton
7	Quartz	SiO_2	SiO_4 sceleton
8	Topaz	$Al_2F_2SiO_4$	Ionic and covalent (mixed)
9	Corundum	Al_2O_3	Covalent
10	Diamond	C	Covalent

cut by a plane containing three adjacent corners. Graphite, on the other hand, forms sheetlike hexagonal lattices. The forces within the sheet are attributed to conjugated double bonds and those from layer to layer to much weaker van der Waals forces (Fig. 13.14). This accounts on the

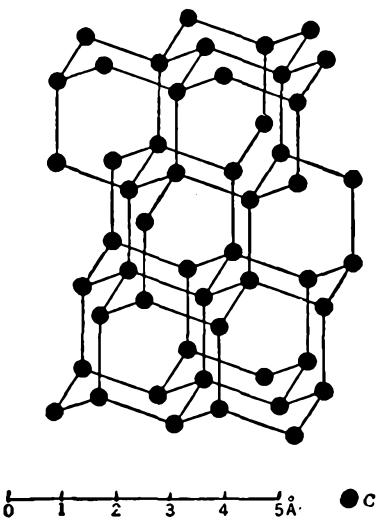

Fig. 13.13. The structure of diamond. After Rice and Teller.[23] (*Courtesy John Wiley and Sons, Inc.*)

one hand for the splitting of natural graphite and on the other for the metallic conductivity of graphite due to the essentially metallic binding within the sheets. Across the sheets the electrical conductivity is correspondingly smaller.

Many types of carbon blacks and graphite have been studied by means of x-ray diffraction by Clark, Eckert and Burton[24] and by White and Germer,[24a] and with the electron microscope by Watson, Ladd, and others.[25] It is of interest to note the staggered alignment of the lattice layers, as determined by x-ray analysis by Lipson and Stokes.[26] They found that in most of the crystals the successive layers have the position ababa, etc. although about 15 per cent are arranged abcabc, etc. (Fig. 13.15). Quite recent investigations by Hoerin and Weigle[27] suggest that the unit cell of the graphite lattice is twice as large as assumed. Diamond

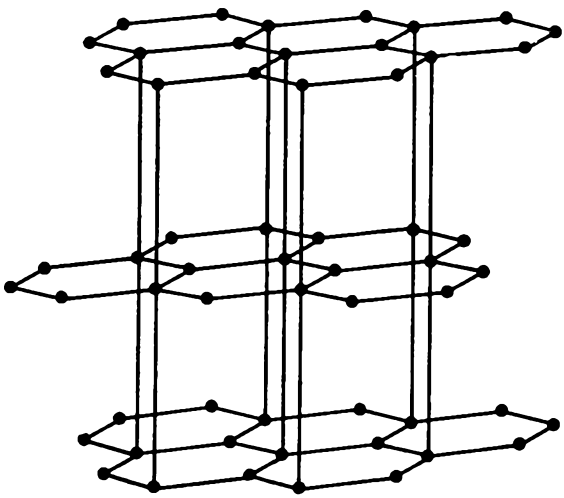

Fig. 13.14. The graphite lattice. After C. Zwicker.[21] (*Courtesy Verlag J. Springer, Berlin.*)

is considered to be a metastable phase at all temperatures; under high pressure of the order of 50,000 atm it goes over to the stable phase of graphite. The inverse transformation—from graphite to diamond—is not possible (monotropic allotropy).

Apart from its appeal as a gem, diamonds are used industrially to an ever increasing extent. The world production in 1944 amounted to 11,402,000 carats,* of which 2,280,000 were employed for gem stones and 9,122,000 carats or 80 per cent of the total production found their way into industrial uses.[22] Diamond dies are used for drawing fine tungsten and molybdenum wires for electron tubes.[53] The shortage of diamond dies during World War II made strict control of allocation of such wires necessary. All the small diamond dies for drawing 0.002 to 0.004-inch diameter wire had previously been imported from Europe. A need for still finer wires, down to 0.0004 inch diameter, arose early during the war,

* 1 Intern. Carat = 200 mgrms = 3.08647 grains troy.

and conventional methods for drilling such dies required from 75 to 125 hours without yielding the quality desired. A project (NRC-535), set up by the National Bureau of Standards in January, 1943, resulted in the development of an electrolytic method for drilling such dies which reduced the necessary time to a few hours; the need for highly skilled operators was eliminated and the end product compared favorably with mechanically drilled dies.[22] This is only one of many examples where the urgent need for a product formerly controlled by foreign monopolies brought forth new techniques and a better understanding of the problems involved.

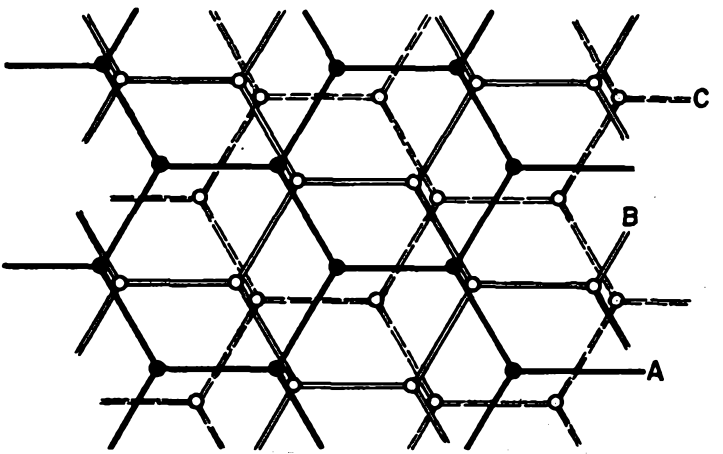

Fig. 13.15. Layers in the graphite lattice. After A. Lipson and A. R. Stokes.[26] (*Courtesy Cambridge University Press.*)

Diamond powder is an important lapping agent for diamonds and hard metals. It is available in various particle sizes, and standards have been set up by the NBS and its production described.[22] That graphite may be used as a carrier of such powders and is required for the lubrication of diamond dies brings well into focus the diverse properties of these two allotropic modifications of carbon. The cutting of glass with diamonds is a well-known technique but intricate in its interpretation.[28]

Amorphous carbon is often taken to include coke, gas carbon, anthracite, soot, lampblack, animal charcoal, wood charcoal, and the forms of carbon which separate during the decomposition of many chemical compounds. The term "amorphous carbon" was used originally to imply that these varieties of carbon are noncrystalline; but now it refers to carbon which is not diamond or graphite.[29] Colloidal carbon and colloidal graphite might thus best be classed with amorphous carbon as the latter has been disintegrated and lost its identity. Mantell[2] refers to

amorphous graphite as one of the natural forms found as minute particles distributed more or less uniformly in feebly metamorphic rocks, such as slates or shales.

"For many electrical and mechanical uses carbon is too hard, too abrasive, or not low enough in electrical resistance. Carbon if heated to a high enough temperature can be transformed into graphite. Although it is sometimes called 'artificial' graphite, the term 'electrographite' is more descriptive and accurate. All carbon materials can be transformed into electrographite, but not all have the same degree of softness, unctuousness, high density, and low resistance that can be obtained from carbon material made from petroleum coke. Petroleum coke is, therefore, the predominant raw material for electrographite. Pitch coke, lampblack, carbon black, and charcoal are difficult to graphitize, and the characteristics are only slightly different from the original values. Although the material has become softer, the resistivity is slightly decreased and analysis for graphitic acid usually shows less than 10%.

"After the baked carbon material has been cleaned and inspected, it may be packed in an electric furnace and transformed to electrographite. These are resistance-type furnaces and the process was developed by E. G. Acheson about 1896 as a result of observations made while developing silicon carbide, which was discovered somewhat earlier. Noticing that at high enough temperatures silicon carbide was decomposed leaving an unctuous graphitic form of carbon, he made one further step by heating petroleum coke and coal with enough carbide-forming material to produce electrographite. It was Acheson's theory that carbides must be formed first, which on heating to a higher temperature decomposed leaving graphitic carbon. Acheson's patents specify the addition of silicon dioxide, boric oxide, ferric oxide, or other metallic oxides to facilitate the formation of graphite. This practice is no longer common since it has been found that the carbon material itself contains enough carbide-forming material. Since the dissociation temperature of silicon carbide is considered to be 2250°C, graphitizing probably begins at a minimum of 2200°C and is completed at 2300–2400°C. Graphite volatilizes without melting at an even higher temperature. Dissociation of silicon carbide is complete at 2700°C.

"Graphitizing furnaces may be of any size, from small ones using a single 18-in. diameter electrode at each end, used for graphitizing small lots of material, to the large steel-furnace-electrode graphitizer, which may hold 100,000 lbs. or more.

"Graphitizing not only lowers the resistivity, but reduces the ash content by the high temperature volatilizing the ash constituents. The ash on electrodes may run from 0.2 to 0.5%. Graphite for electron-tube anodes, electrolytic anodes, and certain other purposes must have minimum ash. By careful selection of raw materials and proper methods of furnace loading, with a sufficiently high furnace temperature, graphite can be made that has less than 0.10% of ash.

"Analyses on grades of material in the carbon industry vary from 99% or over graphitic acid for extremely well-graphitized material to below 70% for partially graphitized or superbaked grades. Graphite having less than 0.05% ash is required in some electrolytic processes and many tons of high purity graphite were made during World War II for the Manhattan Project."[13]

The purity of electronic-grade graphites has been continuously increased during recent years. It is reported that the ash content has been decreased from 0.10 to an average of 0.015 per cent for most grades and to 0.003 per cent on others.[30]

Graphite is available in various grades from commercial sources, and

the material should be selected with its final application in mind. A grade suitable for molds is not likely to be suitable for anodes. Furthermore, it must be pointed out that on the basis of the findings by Malmstrom and his co-workers[54] the characteristics of polycrystalline graphite vary not only from grade to grade but from piece to piece within a given grade. Within a given piece, moreover, the physical and mechanical properties may be functions of orientation and position of the grain. However, the remarkable increase in breaking strength of graphite with increasing temperature (Fig. 13.6)* has, so far, defied an explanation on the basis of structural changes.

Porous graphite of various pore diameters is useful for filters. Graphite anodes fabricated by the manufacturer to finished dimensions usually do not require special treatment before assembly although previous outgassing in a separate evacuated envelope is good practice. Graphite releases gas more readily in high vacuum, and carbonized metals are apt to be coated with tacky carbonyls when treated in H_2. Graphite releases adsorbed oxygen only when heated in high vacuum from 1500 to 1800°C.[18] There is at times danger of dust remaining in the pores of graphite and surface contaminations being present from handling or machining if the latter has been done from bulk stock in the user's shop. These contaminations must be removed by heat treatment either in air or in a vacuum. Heating by induction or in a suitable furnace serves this purpose. According to measurements by Norton and Marshall,[8] graphite treated *in vacuo* at 1800°C will release 1.5–12 cm^3 gas at S.T.P. as against 270 cm^3 and more when not treated. To prevent further release of gas on subsequent heating to higher temperature they found it necessary to degas graphite at 2150°C *in vacuo*. Some manufacturers quench the red-hot graphite part in boiling distilled water.[51] The steam formed in crevices and pores will blow out dust and loosely held particles.

Winter and McPherson[9] have reported on the effect of surface finish and wall thickness on the operating temperature of graphite anodes for radio tubes, and found that the difference in surface temperature for thin or thick and smooth or rough anodes does not exceed 30°C. Back-arcing in rectifier tubes can be greatly minimized when the graphite anode is electrolytically polished to a mirror finish.[31] This is accomplished in a bath of molten potassium hydrofluoride (KHF_2), where the graphite part to be treated is used as anode and a current is drawn at a density ranging from 0.1 to 1. amp/cm^2 for a duration ranging from 1 minute to 1 hour, depending on the size and shape of the part.

The choice of anode material for a particular application is affected by a variety of factors which have been discussed from time to time by different authors;[2,30,32] however, a possible bias in interpretation must be

* p. 279.

guarded against when a concern engaged in the manufacture of the favored material is its proponent. A list of the desirable properties of anode materials may be compiled, as follows:

Thermal
1. High melting point
2. High thermal emissivity
3. Moderately high thermal conductivity
4. Low coefficient of thermal expansion, resulting in dimensional stability
5. Low vapor pressure and gas content
6. High gettering action in operation

Electrical
1. High electrical conductivity
2. High electron work function, preventing emission of electrons at maximum operating temperature
3. Good weldability

Mechanical
1. High modulus of elasticity
2. Sufficiently high strength at elevated temperatures
3. Ease of fabrication and mounting

Chemical
1. Low content of impurities
2. High resistance to chemical reactions

Economical
1. Low cost of raw material
2. Ready availability

Not all of the above requirements can be satisfied by any one material. Nickel, iron, copper, molybdenum, tantalum, tungsten, and graphite all find their use as anodes in various types of electron tubes. Nickel and iron are the most common materials in receiving tubes for low-temperature operation. In power tubes, molybdenum, tantalum, and graphite compete for first place, while tungsten is ruled out on the basis of high cost and difficulty of fabrication. For large power tubes with forced air or water cooling, copper is the most suitable material. An effort has been made in Table 13.4 to compile available data on power-tube anode materials so that an unbiased selection of the most suitable material can be made in the light of the design problem at hand.

Colloidal graphite is produced from electrographite by disintegration, deflocculation, and stabilization with suitable protective colloids, followed by suspension in a liquid medium to form a concentrated dispersion. Sometimes it exhibits thixotropic properties (i.e., liquefaction on application of stress). The thick paste may be used directly or in a diluted form, depending on the desired application. These pastes are available under the trade names "Aquadag," "Oildag," "Glydag," "Castordag,"* and "Dixonac."† They may be dispersions in water, oil,

* Acheson Colloids Corp., Port Huron, Mich.

† Joseph Dixon Crucible Company, Jersey City 3, N.J.

TABLE 13.4. PHYSICAL CHARACTERISTICS OF ANODE MATERIALS FOR POWER TUBES

Physical property	Electro-Graphite	Molybdenum	Tantalum	Copper (OFHC)
Melting point (°C)	3,700 ± 100	2,630 ± 50	2,996 ± 50	1,083 ± 0.1
Outgassing temp. (°C)	1800–2000	1800–2000	2000	800
Typical operating temp. (°C)	350	500	700	60–120
Thermal radiation coefficient in % of black body	89 (at all temperatures)	13 (1000°C) 19 (1500°C) 24 (2000°C)	19.6 (1330°C) 21.4 (1530°C) 46 (1730°C)	2 (100°C) 12 (1200°C)
Power dissipation (W/cm^2)	0.76 (350°C) 13.35 (1000°C) 50.7 (1500°C) 137 (2000°C)	1.95 (1000°C) 10.67 (1500°C) 36.5 (2000°C)	7.3 (1330°C) 12.8 (1530°C) 41.8 (1730°C)	0.0022 (100°C)
Thermal conductivity ($cal/cm^2/cm/sec/°C$)	0.337 (25–390°C) .330 (25–500°C) .284 (25–1000°C) .275 (25–1500°C)	0.346 (17°C) .259 (927°C) .159 (1627°C)	0.130 (20°C) .174 (1430°C) .186 (1630°C) .198 (1830°C)	.941 (20°C)
Specific Heat (cal/g/°C)	.234 (26–538°C) .324 (36–902°C) .390 (56–1450°C)	.061 (20°C) .08 (1400°C)	.036	.092 (20°C)
Linear thermal exp. coeff. (cm/cm/°C) $\times 10^{-7}$	12 (0–100°C)	53–57 (20–300°C) 58–62 (25–700°C)	65 (0–100°C) 66 (0–500°C) 80 (20–1500°C)	165 (20°C) 177 (25–300°)
Vapor pressure (mm Hg)	10^{-3} (2471°C) 10^{-4} (2288°C) 10^{-5} (2129°C) (10^{-6}) (2000°C) (10^{-7}) (1870°C)	10^{-3} (2295°C) 10^{-4} (2095°C) 10^{-5} (1900°C) 10^{-6} (1725°C) (10^{-7}) (1580°C)	10^{-3} (2820°C) 10^{-4} (2599°C) 10^{-5} (2407°C) (10^{-6}) (2220°C) (10^{-7}) (2100°C)	10^{-3} (1141°C) 10^{-4} (1035°C) 10^{-5} (946°C) 10^{-6} (860°C) 10^{-7} (805°C)
Getter Action	some	none	good	none
Electrical conductivity (micromhos cm^{-1})	0.00127 (20°C) .00137 (100°C) .00152 (450°C) .00144 (800°C)	0.208 (20°C) .046 (800°C) .030 (1200°C) .017 (2000°C)	0.081 (18°C) .019 (1000°C) .014 (1500°C)	0.5800 (20°C)
IACS at 20°C (%)	.22	35.8	14	101.85
Magnetic susceptibility per unit mass $X \times 10^6$	−0.49	+0.04	+0.93	−0.077 (1080°C) −0.086 (18°C)
Electron work function (ev)	4.6	4.37	4.10	4.9
(Apparent) density (g/cc)	1.5–1.7	10.4	16.6	8.931
Young's modulus (psi) $\times 10^6$	1.3–2.4	47.7–49.4	27	16
Tendency to warp with heat	none	slight	hardly any	none
Recommended Use	Internal anodes Heavy Wall Med. high freq.	Internal anodes Thin Wall Any frequency	Internal anodes Thin Wall Any frequency	Internal or external anodes with forced cooling

volatile hydrocarbons, and alcohol, and may have special admixtures to impart desired surface properties suitable for special applications. Aqueous dispersions of electrographite carry a negative charge on the individual particles while oil dispersions carry a positive charge. Filter paper usually carries a negative charge, thus permitting the passage of negatively charged aqueous suspensions but rejecting positively charged oil suspensions. The colloidal nature of these suspensions requires precautions in handling to prevent flocculation which takes place in contact with electrolytes. A number of semicolloidal dispersions in various media are also available for uses wherein the highly refined product is not economically justified. The supplier should be consulted in regard to the most suitable product. Colloidal graphite dispersions have interesting potentialities and are useful in many ways to the electronic engineer and research worker. A number of publications deal with their physical characteristics and describe practical applications,[36–42] which range over a wide field. Some of the latter have been mentioned in the introduction to this chapter. The production of highly resistive thin films[33] and the treatment of glass mold surfaces[16,34] may also be included here. The effect of a graphite coating on grids and plates upon the thermal radiative power was studied by Szymanowitz,[35] from which Table 13.5 is reproduced. The values determined by Barnes[52] at 727°C have been added.

By far the most wide-spread application today is the coating of the interior and at times also the exterior wall of glass envelopes for cathode-ray tubes (C.R.T.), television-receiving tubes, camera tubes, and the like. "Aquadag" or "Dixonac" is widely used for this purpose and several techniques are available. As an object lesson in the development of process technique the following pages will deal at some length with the various procedures that have been used over a period of years for coating C.R.T. bulbs. During the earlier days of development the glass envelope was held in a vertical position and the suspension made to rise in the bulb by syphoning it from a main container connected by a rubber hose. This could be done by the application of pressure on the main container or by lifting the container to the desired level. After the suspension had risen to the prescribed level—without touching the luminescent screen on the face of the bulb—the liquid column was lowered and, if conditions were favorable, a uniform film of the colloidal graphite would adhere to the glass wall. This was then dried superficially by circulating hot air and finally baked at about 450°C for 1½ hours to remove the organic binders. A smooth and well-adhering coating was thus obtained. However, the pitfalls were many, as the writer can well remember from his experiences at that time.

One of the more obvious annoyances related to the rubber stopper,

TABLE 13.5. EMISSIVE POWER OF RECEIVING TUBE ANODE MATERIALS*
(In Terms of Watts/Sq Cm)

	Temp. °F										
	150	200	250	300	350	400	450	500	550	600	1341
Plain nickel	0.003	0.005	0.007	0.010	0.014	0.018	0.022	0.027	0.033	0.038	0.78‡
Plain N.P.C.R.S.†	.003	.006	.010	.015	.022	.029	.038	.048	.058	.071	
N.P.C.R.S. acid etched	.003	.007	.012	.018	.026	.034	.046	.059	.073	.089	
N.P.C.R.S. sand blasted	.007	.013	.022	.033	.047	.064	.082	.105	.130	.160	
Oxidized nickel	.004	.010	.018	.031	.047	.068	.094	.125	.162	.208	
Nickel with polished graphite coating	.008	.016	.028	.044	.066	.090	.121	.159	.200	.245	
N.P.C.R.S. with matte graphite coating	.007	.016	.028	.044	.066	.093	.125	.165	.210	.260	
Oxidized nickel graphite coated	.008	.017	.031	.048	.072	.097	.130	.170	.215	.265	
Nickel with matte graphite coating	.009	.019	.033	.051	.075	.102	.135	.176	.220	.270	4.8‡
N.P.C.R.S. with polished graphite coating	.009	.018	.032	.049	.073	.100	.132	.172	.218	.270	
N.P.C.R.S. acid etched and graphite coated	.012	.023	.039	.053	.081	.110	.143	.183	.223	.275	
N.P.C.R.S. sand blasted and graphite coated	.009	.019	.033	.050	.076	.104	.139	.184	.228	.282	
N.P.C.R.S. acid etched and strip carbonized	.008	.018	.032	.051	.078	.108	.145	.194	.245	.310	
Oxidized nickel batch carbonized	.013	.027	.049	.076	.114	.156	.210	.275	.346	.430	
N.P.C.R.S. sand blasted and strip carbonized	.015	.031	.054	.083	.122	.166	.220	.286	.360	.445	

* According to Szymanowitz.[35]
† Nickel plated cold rolled steel.
‡ According to Barnes.[52]

which was recommended for closing the tube to be coated, at its neck. A glass tube penetrated the stopper at its center and served as a feeder for the suspension. A rubber hose was usually connected to the end of the tube and to the main container of the graphite suspension, thus permitting the container to be raised and lowered during the syphoning. The stopper, when pressed into the neck of the bulb, is supposed to stay there as long as the coating operation lasts. Graphite, however, is an ideal lubricant and not only penetrates filter paper but also enters the crevices between stopper wall and glass. This, added to the weight of the rising liquid column, causes the black "Aquadag" to spill out. A clamp, then, has to be provided which keeps the stopper in place and removes some of the weight.

In addition to the feeder tube which penetrated the stopper there must also be an exit tube for the air, which naturally is compressed as the liquid rises. This tube must be just a little longer than the final height of the column, but it must not scratch the screen. A third tube through the stopper is conveniently provided for drainage of the "Aquadag." This one is very short and need not protrude above the top level of the stopper. On the outside it has a piece of rubber hose with a pinch cock.

If the liquid column is forced to rise at such a rate that equalization of pressure inside and outside the bulb cannot take place quickly, the air above the rising liquid column is still being compressed, its dew point is lowered, and condensation of moisture on the wall and liquid surface results. The graphite suspension will then slide over this film of water without contacting the glass and likewise recede over this film without leaving a trace of coating on the wall. Such condensation of moisture is especially severe when the liquid column within the bulb is forced to rise not by external pressure but by internal suction. This causes the water from the suspension to evaporate more freely and condense on the wall. The difference of the two procedures is easily demonstrated by pushing the liquid column up halfway by external pressure and then raising it by partial vacuum the rest of the way. On receding, the upper half of the wall will be free of coating and the lower half coated. To eliminate this condensation problem it is then necessary to further complicate the feeder apparatus by additional tubes which permit the circulation of hot dry air (80°C) above the rising and receding column. This is done by providing two concentric glass tubes entering through the center of the stopper. A distributor cap at the top should prevent direct impact of the air stream on the screen. One of the two concentric tubes will take over the function of the exit tube mentioned above. The air intake should be filtered through a cotton or glass wool plug in order to reduce the number of condensation nuclei present (Fig. 13.16).

With these refinements at hand consistently good coatings were

obtained by the author after draining the liquid. The wet coating is immediately dried in situ by raising the temperature of the circulating air to about 200°C. During the first few minutes it is necessary to heat the screen with a large flame from the outside to prevent water condensation on the screen. When the "Aquadag" coating has taken

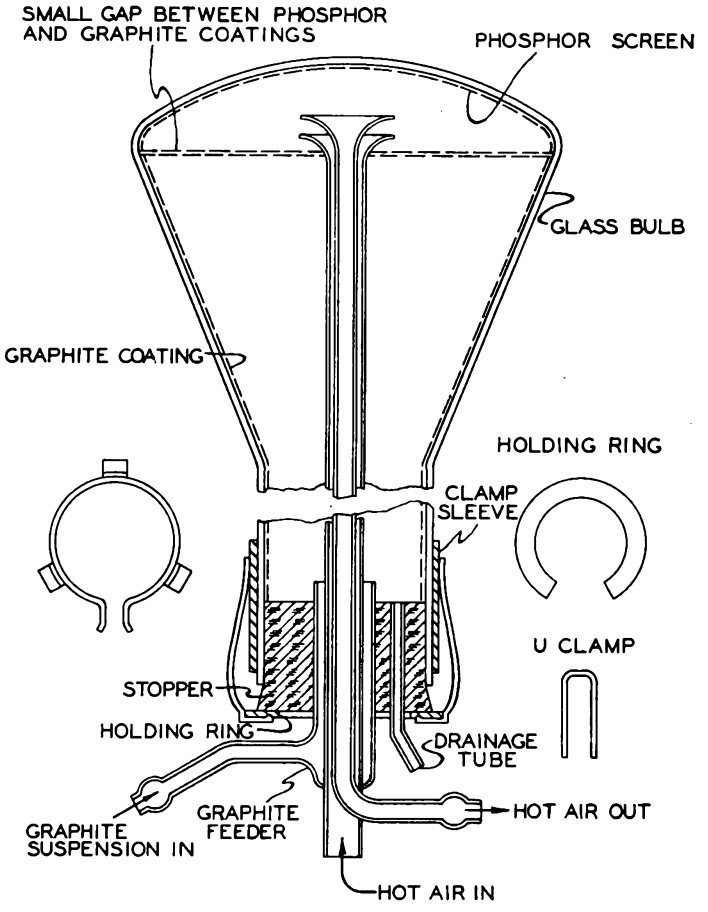

Fig. 13.16. Apparatus for coating the inner wall of cathode ray tube bulbs with graphite suspension by the syphon-method.

on a dry glossy finish, the feeder apparatus is disconnected and the tube placed in a preheated baking oven where it is baked for about 2 hours or less at 450°C to remove the binders in the colloid. Hot air should again be circulated during this baking cycle and careful attention paid to the position of the heater elements (unless heating is done entirely by air) in

relation to the tube so that uniform heating is obtained and no chilling results from supporting members.

Further control is necessary in handling and preparing the "Aquadag" suspension. A ratio 1:3 by volume was found satisfactory in diluting the stock paste with distilled water. It is ball-milled to advantage for 20 hours, and a record should be kept of the optimum viscosity. Prolonged storing of the coating solution is not advisable and careful stirring before use is necessary. Building up the thickness of the coating by repeated coating operations is feasible only after each layer has gone through the baking cycle in the oven.

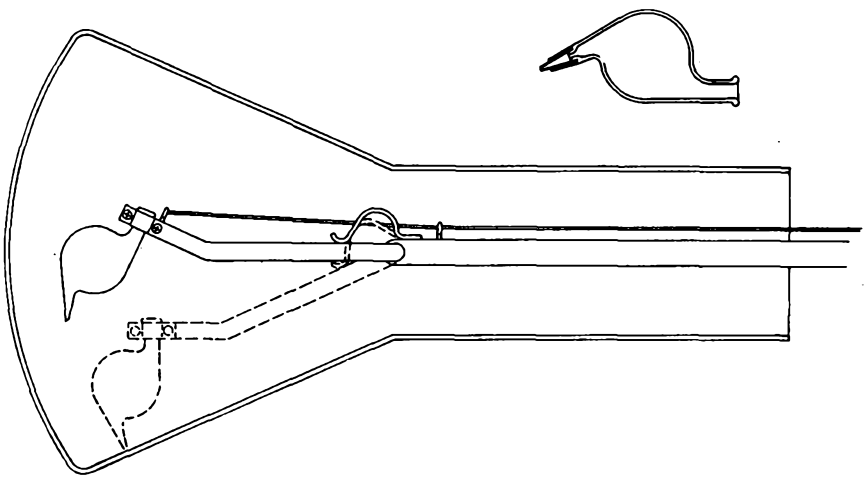

Fig. 13.17. Apparatus for coating the inner wall of cathode ray tube bulbs with graphite suspension by the scriber-method.

When all these measures had resulted in good coatings, a new idea presented itself which simplified the procedure immeasurably. The handling of a large volume of liquid in order to give the wall of the container a thin coat is wasteful and awkward. Means were thus developed to scribe a spiral onto the wall by using a small feeder cup which contained little more than the total amount of liquid required for one spiral. This cup is held on a flexible support which enters the tube until the tip rests near the screen edge. The tube is mounted horizontally in the chuck of a lathe and the scriber is mounted in the tail stock. By rotating the tube and slowly withdrawing the scriber a spiral of any desired pitch can be obtained. An outline of the scriber is shown in Fig. 13.17.

The main problem in this technique is, of course, the production of a continuous line, and it was found that this could best be achieved by sealing a seamless nickel cathode sleeve (0.030 inch dia. × 5 mm long)

into the tip of the soft-glass pen. The nib of this pen is then ground to the desired angle. As a protection against a possible break in the spiral, all turns are connected lengthwise by a line of "Aquadag." Connection to the outside of the tube is made by means of a "Dumet" spiral sealed into the wall (Fig. 13.18). To further insure good contact the getter, if used, may be flashed onto this contact. For "Pyrex" envelopes a tungsten wire is sealed into the wall and the area around it coated with a suspension of AgO, which is reduced to Ag by application of heat. "Aquadag" is coated over this silver layer and a good contact thus

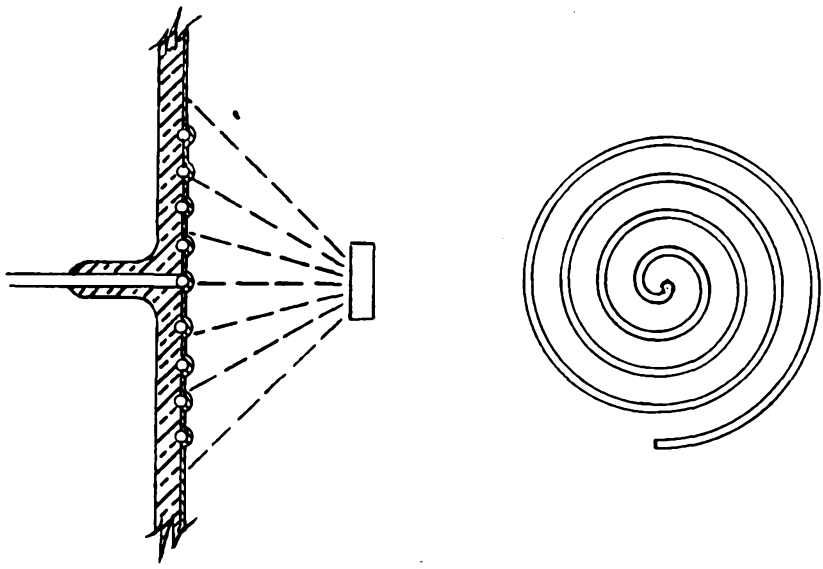

Fig. 13.18. Outline of a method for making electrical contact with a graphite coating on the inner wall of a tube by partly embedding in the glass wall a metallic spiral and flashing a getter onto it.

ensured.[43,44] This spiral coating may have advantages when it is desirable to observe the inside of the tube during operation. A fluorescent coating may be deposited over it to obtain emission patterns from thermionic emitters.[45] Kohl has described a simple method for the application of luminescent screens[46] which lends itself to cylindrical surfaces. A different application of spiral graphite coatings is made in infrared-sensitive thalofide cells.[47]

The scriber method, however, is still "too nice" to be commercially practical for C.R.T. coatings. By replacing the scriber with an old toothbrush completely satisfactory results can be obtained, and this is indeed the technique used today on a large scale in television-tube manufacture. The brushes are, of course, shaped to suit the size of the tube.

To further improve the adhesion of the colloidal graphite and especially to prevent the release of fine carbon particles in the presence of high electrical field gradients, a small amount of K_2SiO_3 is added to the suspension.[48] "Dixonac" is now available as a ready mixed solution with silicate added for direct application by brushing. It is said that "Dixonac" contains less organic material than other products of this type.

The experience of the present author was spread over about 2 years before World War II and probably illustrates how things are often done the hard way before the simple solution is found. Since this is very costly, a few steps in the procedure may be skipped by consciously searching for simpler solutions which may not be immediately obvious. The research worker is also advised to have in his laboratory some bright young lad who is not steeped in modern theories, but is well equipped with common sense.

Before leaving the subject of graphite coating and as an insertion after the main text had been written, it is gratifying to learn from a recent announcement by Corning Glass Works[49] that glass bulbs for television tubes are now given an electrically conductive, opaque coating on the inside wall during the manufacturing process so that all the laborious hand-operations at the tube factory are eliminated. This should be welcome news, especially in the light of remarks by Moss,[50] who states that the various organic materials used in the preparation of the colloidal graphite wall coating are an insidious source of trouble and may result in screen staining and/or cathode poisoning during the baking and pumping operation. These effects may be avoided in many cases by pre-vacuum-baking the graphite wall coating before the fluorescent screen is applied. It should also be mentioned that the advent of rectangular television bulbs has reinstated the old syphon method in part.

REFERENCES

1. *U.S. Patent 2,105,818* (Jan. 18, 1938).
2. Mantell, C. L., "Industrial Carbon," 2nd. Ed., New York, D. Van Nostrand Co., 1946.
3. Smithells, C. J., "Metals Reference Book," New York, Interscience Publishers, Inc., 1949.
4. "Metals Handbook," Cleveland, Soc. for Metals, 1948.
5. Pauling, L., and Sheehan, W. S., "Association Energies of Carbon Monoxide and Heat of Sublimation of Graphite," *Proc. Nat. Acad. Sci.*, **36**, 359–363 (1949).
6. Lange, N. A., "Handbook of Chemistry," Ohio, Handbook Publishers, Inc., 1946.
7. National Carbon Division, Union Carbide and Carbon Corp.
8. Dushman, S., "Scientific Foundations of Vacuum Technique," 496, New York, John Wiley and Sons, Inc., 1949.
9. Winter, L. L., and MacPherson, H. G., "Effect of Surface Finish and Wall Thickness on the Operating Temperature of Graphite Radio-Tube Anodes," *Proc. I.R.E.*, **33**, 834–837 (1945).

10. "Temperature, Its Measurement and Control in Science and Industry," 1149, New York, Reinhold Publishing Corp., 1941.
11. Barnes, B. T., Forsythe, W. E., and Adams, E. Q., "The Total Thermal Emissivity of Various Materials at 100°–500°C," *J.O.S.A.*, **37**, 804–807 (1947).
12. Ivey, H. F., "Thermionic Electron Emission from Carbon," *Phys. Rev.*, **76**, 567 (1950).
13. Kirk, R. E., and Othmer, D. F., "Encyclopedia of Chemical Technology," Vol. 3, 1–34, New York, Interscience Encyclopedia, Inc., 1949. Abbott, H. W., "Carbon."
14. Powell, R. W., "Thermal and Electrical Conductivity of Acheson Graphite from 0° to 800°C," *Phys. Soc. Proc.*, **49**, 419–426 (1937).
15. Buerschaper, R. A., "Thermal and Electrical Conductivity of Graphite and Carbon at Low Temperatures," *J. Appl. Phys.*, **15**, 452–454 (1944).
16. Murphy, J. R., "Colloidal Graphite Treatment of Mold Surface," *Glass Ind.*, **31**, 250–253 (1950).
17. McKnight, G. P., "The Oxidation Rate of Carbon and Graphite," *Intern. Digest*, **2** (Dec. 1949).
18. Espe, W., and Knoll, M., "Werkstoffkunde der Hochvakuumtechnik," Berlin, J. Springer, 1936.
19. Kopelman, B., "Clean-up of Graphite Lubricant from Tungsten Wire," *Sylvania Technologist*, **2**, 13–16 (1949).
20. Smekal, A., "Structure-Sensitive Properties of Crystals," *Handbuch der Physik*, Berlin, 2nd Ed. Vol. 24.2. (1933).
21. Zwicker, C., "Technische Physik der Werkstoffe," Berlin, J. Springer, 1942.
22. "Third Symposium on Diamonds," *Am. Mineralogist*, **31**, 135–167 (1946).
23. Rice, F. O., and Teller, E., "The Structure of Matter," New York, John Wiley and Sons, Inc., 1949.
24. Clark, G. L., Eckert, A. C., Jr., and Burton, R. L., "Commercial and Experimental Carbon Blacks," *Ind. and Eng. Chem.*, **41**, 201–208 (1949).
24a. White, A. H., and Germer, L. H., "The Structure of Black Carbon," *J. Chem. Phys.*, **9**, 492–497 (1941).
25. Burton, E. F., and Kohl, W. H., "The Electron Microscope," 2nd Ed., New York, Reinhold Publishing Corp., 1945.
26. Lipson, A., and Stokes, A. R., "The Structure of Graphite," *Proc. Roy. Soc.*, London, A, **181**, 101–105 (1942).
27. Hoerin, J., and Weigle, J., "Structure of Graphite," *Nature*, **164**, 1088 (Dec. 24, 1949).
28. "The Mechanism of Glass Cutting" (Translated from the German), *Glass Ind.*, **25**, 23–25, 68–69. (1944).
29. Mellor, J. W., "Inorganic and Theoretical Chemistry," Vol. 5, New York, Longmans, Green, and Co., 1924.
30. Winter, L. L., and Alexander, F. L., "New Graphite Developments for Electronic Applications," *El. Manuf.*, **41**, 86–91 (Jan., 1948).
31. Bakker, J., "Electrolytically Polished Graphite Anode," *U.S. Patent 2,494,425* (Jan. 10, 1950).
32. "Power-Tube Anode Materials," *Elec. Markets*, 14 (May 1945).
33. Szymanowitz, R., "Colloidal Graphite Films—Properties and Applications," *El. Ind.*, **2**, 96–98, 162, 164, 166, 168 (Oct. 1943).
34. Szymanowitz, R., "Colloidal Graphite and Its Uses in the Glass Industry," *Glass Ind.*, **26**, 125–127, 151 (1945).
35. Szymanowitz, R., "The Emissive Power of Typical Grid and Plate Surfaces," *Electronics*, **16**, 93, 178 (1943).

36. Porter, B. H., "Research Applications of Colloidal Graphite," *Rev. Sci. Inst.*, **7**, 101–106 (1936).
37. Porter, B. H., "Impregnation Studies with Colloidal Graphite," *J. Appl. Phys.*, **8**, 479–482 (1937).
38. Szymanowitz, R., and Porter, B. H., "Notes on the Wettability of Highly Polished Metal Surfaces by Graphite Hydrosols," *Rev. Sci. Inst.*, **11**, 230–231 (1940).
39. Vennto, L. J., "Colloidal Carbons," *Am. Paint J.*, **31**, 68–72 (1947).
40. Vold, R. D., and Konecny, C. C., "Suspensibility of Carbon in Detergent Solutions," *J. Phys. and Coll. Chem.*, **53**, 1262–79 (1949).
41. Savage, R. H., "Graphite Lubrication," *J. Appl. Phys.*, **19**, 1–10 (1948).
42. Szymanowitz, R., "Colloidal Graphite," *Alexander's Colloid Chemistry*, Vol. 6, 436–458, New York, Reinhold Publishing Corp., 1946.
43. Maloff, I. G., and Epstein, D. W., "Electron Optics in Television," 286, New York, McGraw-Hill Book Co., 1938.
44. Zworykin, V. K., and Morton, G. A., "Television," 335, New York, John Wiley and Sons, Inc., 1940.
45. Johnson, R. P., "Simple Electron Microscopes," *J. Appl. Phys.*, **9**, 508–516 (1938).
46. Kohl, W. H., "A New Method for the Application of Luminescent Screens to Glass Surfaces," *Can. J. Res. A.*, 126–132 (1935). Further remarks on above title, *J. El. Chem. Soc.*, **96**, 3, 123–131 (1949).
47. Hewlett, C. W., "High-Sensitivity Photoconductive Cell," *G.E. Rev.*, **50**, 22–25 (Apr., 1947).
48. Myers, L. M., "Electron Optics," 378, London, Chapman and Hall, Ltd., 1938.
49. *Glass Ind.*, **31**, 105 (Feb., 1950).
50. Moss, H., "Cathode-Ray Tube Progress in the Past Decade with Special Reference to Manufacture and Design," *Advances in Electronics*, Vol. 2, New York, Academic Press, Inc., 1950.
51. Briggs, T. H., "Carbonized Nickel for Radio Tubes," *Metals and Alloys*, **9**, 303–306 (Nov., 1938).
52. Barnes, B. T., "Total Radiation from Polished and Soot-Covered Nickel," *Phys. Rev.*, **34**, 1026–1030 (1929).
53. Paterson, Sir Clifford, and Leads, R. E., "Diamond Dies for Wire Drawing," *Research*, **1**, 2–10 (1947).
54. Malmstrom, C., Keen, R., and Green, L. Jr., "Some Mechanical Properties of Graphite at Elevated Temperatures," *J. Appl. Phys.* **22**, 593–600 (1951).

CHAPTER 14

JOINING METALS BY SOLDERING AND BRAZING

Since the metals most commonly used in the construction of electron tubes have been discussed in the preceding chapters, the available methods for joining various metals will now be considered. Again, a great deal has been written on this subject.[1–8] By pointing out some of the difficulties that can arise the present chapter may serve as a guide to this literature. We shall confine ourselves, in the main, to the production of permanent joints by the application of heat (i.e., soldering and brazing), and disregard semipermanent joints by clamping devices.

Soldered and brazed joints are much better for electrical circuits on account of the greater electrical conductivity of the joint. The need for joining two different metals may exist for several other reasons. It may be a matter of economy to use as little of an expensive material as possible and confine it to the location where its special properties are required. The three-piece welds for lead-in wires, described in Chapter 4, are an example. Costly tungsten is here confined to the seal area and nickel and copper are butt-welded at either end. The flexibility and high conductivity of copper make this material also preferable to tungsten for the outside lead. Thus, economical and functional considerations together determine the choice of a metal combination. A "Kovar"-to-copper braze for a glass-to-metal seal is another example (Chapter 4) and so is the tungsten anticathode in an x-ray tube which is embedded in a copper block. Bimetal strips for the production of motion under the influence of heat at a given temperature level dictate a purely functional selection of metal on the basis of their relative expansion coefficients. When such bimetals are intended to keep hot tungsten filaments taut, the selection and joining of the components becomes a very difficult problem.

In making one solid out of two parts the greatest attention must be given to the interface. In the last analysis the cohesion at the interface becomes a question of intermolecular forces and the main problem is reduced to the effort of bringing the two components as closely together as possible without the interference of oxide barriers or other films. If this can be achieved at room temperature, it will result in

"cold welds" which are just as strong, if not stronger, than conventional fusion welds. A recent development by Sowter of the General Electric Company, Ltd., England* for cold welding of nonferrous metals and particularly aluminum at room temperature promises to put this technique on a commercial basis.[12,13] Usually, however, joints are made either by the application of heat, which causes the two components to interpenetrate directly as in spot welding and inert gas tungsten-arc welding, or by introduction of an intermediary component which "wets" both metals throughout the junction as in soft soldering and brazing. We shall consider some of these techniques each in turn.

In naming these various techniques old-fashioned words were employed which will probably be in common usage for a long time to come. They make sense in a way, but are difficult to differentiate from one another. The American Welding Society (A.W.S.) has therefore prepared a list of standard welding terms. It will surprise many that soldering, be it soft or hard, does not appear; there is, however, a chapter on soft soldering in the "Welding Handbook."[6] Soft solders are defined therein as "metals or alloys, used for joining most common metals, which melt at temperatures below the melting point of the base metal and in all cases below 800°F (427°C)." For some time another term for hard soldering has been brazing; it is covered by the following definitions which are authorized by the A.W.S.

"*Brazing* a group of welding processes wherein coalescence is produced by heating to suitable temperatures above 800°F and by using a nonferrous filler metal having a melting point below that of the base metals. The filler metal is distributed between the closely fitted surfaces of the joint by capillary attraction.

"*Braze Welding* is a method of welding whereby a groove, fillet, plug, or slot is made using a nonferrous filler metal, having a melting point below that of the base metals but above 800°F. The filler metal is not distributed in the joint by capillary attraction. ('Bronze Welding,' formerly used, is a misnomer for this term.)

"*Welding*, used by itself, is a generic term which describes a variety of metal-joining processes whereby a localized coalescence of metal is produced by heating to suitable temperatures, with or without the application of pressure, and with or without the use of filler metal. The filler metal, if used, either has a melting point approximately the same as the base metals or has a melting point below that of the base metals but above 800°F."

Forge welding, thermit welding, flow welding, gas welding, arc welding, resistance welding, induction welding, and brazing are all different specializations of welding. We shall confine ourselves in the following to soft soldering and brazing.

Soldering

A comprehensive brochure, entitled "Notes on Soldering," has recently been issued by the Tin Research Institute and is distributed free

*U.S. Representative, Kold Weld Corp., 10 East 40th St., New York 16, N.Y.

of charge.[1] It runs to 88 pages and contains a bibliography on the subject of soldering. Rather than leave the reader with this reference and others, such as a review article on the practical aspects of soldering by Mample,[9] a few highlights are extracted from various sources at the present author's discretion and amplification. It is an all too common experience to have engineers and designers underestimate the importance of details once soldering must be used.

There probably is still a widespread tendency among technicians to use any kind of solder that happens to be within reach, no matter what the particular job requires. This attitude naturally requires correction by consistent educational campaigns. Once various types of solders get mixed up in the shop, the situation is almost beyond control. A portable, direct reading indicator for the determination of the ratio of lead and tin in solder has been announced by Wheelco Instruments Company, which makes possible rapid analysis of lead alloys containing up to 7 per cent of tin.

Most of the soldering jobs in conventional tube manufacture apply to the outside of the tube where lead wires are soldered to terminal pins and caps and where radiator fins and cooling jackets are soldered to anodes. In continuously pumped tubes, however, many of the internal components are soft soldered for ease of disassembly when components are replaced after failure. Such joints in large power tubes, of which the resnatron is an example, are water-cooled to preserve the strength of the joint. The use of solders within a high-vacuum tube in the conventional sense, as well as in larger high-vacuum structures such as particle accelerators, deserves great discrimination. Any material component present in such a system which has a vapor pressure higher than that of the coldest part is a virtual leak. Such a material may, in addition, act as a poison not only to the vacuum but to an electron emitter, especially if the latter is an oxide cathode. There may be oxides present at a solder joint which by themselves do not have an excessive vapor pressure. If they should be exposed to electron bombardment or to an excessive operating temperature, they may decompose and result in products of excessive vapor pressure. Great caution is thus necessary when selecting solders for internal use. Table 14.1 gives the vapor pressures of Bi, Cd, In, P, Pb, Sn, Sb, and Zn at various temperatures.[14]

Quite apart from the application to tubes, soldered joints are an essential part of vacuum plumbing on exhaust systems and of feeder pipes for gas-supply lines. Even experienced plumbers have been known to have their "bad days," and it behooves the tube engineer to be familiar with the essentials of this art and to watch the joints carefully when his vacuum system refuses to merit this name.

One of the most important considerations, which is all too frequently neglected, is that parts to be joined must be designed with the require-

ments of the particular technique in mind so that the operator has a chance to do a good job within the limitations of the working medium. A little discussion with the operator while the design is still on paper will often save endless trouble and costly reworking of the parts. Soft solders are essentially weak metals in comparison with copper, brass, and steel, with which they are used primarily. The function of the solder is that of sealing and solidifying the assembly. Joined components should be interlocked mechanically as the solder film cannot be depended on to hold them together. Clean surfaces are a prerequisite for a good joint, as pointed out above. The parts should thus be cleaned and preferably

TABLE 14.1. VAPOR PRESSURE OF SOLDER COMPONENTS (mm Hg) AT TEMPERATURES SHOWN (°C)

Metal	M.P.	10^{-7}	10^{-6}	10^{-5}	10^{-4}	10^{-3}	10^{-2}	10^{-1}	10^{0}
Bi	271	(350)*	(400)	474	536	609	698	802	934
Cd	321	(95)	(120)	148	180	220	264	321	
P							(195)	(220)	(270)
Pb	328	(360)	(420)	483	548	625	718	832	975
Sn	232	(640)	(730)	823	922	1042	1189	1373	1609
In	157	(520)	(590)	667	746	840	952	1088	1260
Sb	630	(340)	(395)	466	525	595	678	779	904
Zn	419	(140)	(175)	211	248	292	343	405	

* Figures in parentheses extrapolated from curves.

pretinned before interlocking folds are made into which cleaning agents cannot penetrate readily. The flux cannot be relied on at any time to do the cleaning. Adjacent solder joints should be spaced well apart so that the heat applied to one joint does not soften the one made previously. For the same reason, low-melting materials, such as fibre insulation and plastics, should be at a sufficient distance from the joint. Fixtures designed to hold components in alignment during the soldering operation are frequently helpful, but consideration must be given to the differential thermal expansion of all components involved.

On joining different metals in the form of coaxial cylinders with an overlap, it is thus preferable to have the high-expansion metal on the outside. A sufficient gap, to be filled with the solder, should be allowed when both metals are hot. Fairly rapid cooling and the selection of a solder composition which will retain plasticity for some time will then result in a good joint which is in compression. If the high-expansion metal were on the inside, the gap for the solder might be closed before the solder can enter or, if allowance were made for this, the solder might be fractured on cooling because of the tension at the interface. As long as the solder is molten, there is a continuing alloying action between it

and the parent-metal, which results in the formation of intermetallic compounds or phases which are generally extremely hard and brittle. In the case of steel and copper the principal compounds formed are $FeSn_2$ and Cu_6Sn_5. To minimize the formation of these intermetallic compounds joints should be made as quickly as possible and at the proper temperature, depending on alloy composition. Excess solder around the joint does not contribute to its strength so long as sharp corners are provided with fillets. On steel, copper, and brass the strongest joints are obtained with a joint clearance of 0.005 inch. Thicker fillers are less dependable and films thinner than 0.003 inch may be weak from poor penetration and flux inclusions.

In various countries the composition of solders is governed by a standard code which limits the permissible amounts of impurities. The working properties of solders are acutely affected by small traces of certain metals, particularly zinc and aluminum. As little as 0.001 per cent of either of these two metals may cause lack of adhesion, grittiness, or liability to "hot-short cracking." This "hot shortness" refers to a mechanical weakness of soft solders in a temperature range below the solidus which extends down to about 140°C, as a rule, where solders are liable to fracture from mechanical shock or vibration. It is particularly noticeable in solders low in tin content. Antimonial solders are less liable to this defect. The temperature range from solidus to about 140°C should, therefore, be passed as quickly as possible to reduce the opportunity for cracking.

Table 14.2 lists compositions and properties of a variety of solders, as shown in the appendix of ASTM Specification B32–49 for soft-solder metal. Table 14.3 gives the chemical composition of the alloys in this specification, according to grades with the imposed limits.

"Other nominal compositions, as agreed upon by the manufacturer and the purchaser may be provided under these specifications. The alloy grade classification, limits on impurities, and permissible variations in desired elements shall conform to the requirements for similar alloy grades in Table I. The letters A, B, C designate increasing antimony content. The letter S, with nominal silver content, is used for silver-lead alloys."

Table 14.4 gives the U. S. Federal Specification for soft solders (QQ-S-571b—Sept. 30, 1947) and Table 14.5, the British Standard B.S. 219 of 1932 for tin-lead solders, which were applied again after wartime restrictions were removed.

The equilibrium diagram for the Pb-Sn system is shown in Fig. 14.1. From this it is apparent that pure Pb melts at 327°C, pure Sn at 232°C, and alloys containing more than 19.2-per cent Sn and less than 97.5-per cent Sn solidify as solid solutions of the α or β phase in a matrix of the smaller crystals of the eutectic at 183°C. The eutectic consists of

TABLE 14.2. ASTM SPECIFICATIONS FOR SOFT SOLDER METAL (B 32–49)
Properties of Soft Solder Alloys

Nominal Composition (%)			Specific Gravity[a]	Melting Ranges				Uses
				Solidus		Liquidus		
Tin	Lead	Antimony		(°C)	(°F)	(°C)	(°F)	
				Tin-Lead Alloys				
70	30		8.32	183	361	192	378	For coating metals.
60	40		8.65	183	361	190	374	"Fine Solder." For general purposes, but particularly where the temperature requirements are critical.
50	50		8.85	183	361	216	421	For general purposes. Most popular of all.
45	55		8.97	183	361	227	441	For automobile radiator cores and roofing seams.
40	60		9.30	183	361	238	460	Wiping solder for joining lead pipes and cable sheaths. For automobile radiator cores and heating units.
35	65		9.50	183	361	247	477	General purpose and wiping solder.
30	70		9.70	183	361	255	491	For machine and torch soldering.
25	75		10.00	183	361	266	511	For machine and torch soldering.
20	80		10.20	183	361	277	531	For coating and joining metals. For filling dents or seams in automobile bodies.
15	85		10.50	227[b]	440[b]	288	550	For coating and joining metals.
10	90		10.80	268[b]	514[b]	299	570	For coating and joining metals.
5	95		11.30	270	518	312	594	For coating and joining metals.
				Tin-Lead-Antimony Alloys				
40	58	2	9.23	185	365	231	448	Same uses as (50-50) tin-lead but not recommended for use on galvanized iron.
35	63.2	1.8	9.44	185	365	243	470	For wiping and all uses except on galvanized iron.
30	68.4	1.6	9.65	185	364	250	482	For torch soldering or machine soldering, except on galvanized iron.
25	73.7	1.3	9.96	184	364	263	504	For torch and machine soldering, except on galvanized iron.
20	79	1	10.17	184	363	270	517	For machine soldering and coating of metals, tipping, and like uses, but not recommended for use on galvanized iron.
				Silver-Lead Alloys				
0	97.5	2.5	11.35	304	579	304	579	For use on copper, brass, and similar metals with torch heating. Not recommended in humid environments due to its known susceptibility to corrosion.
1	97.5	1.5	11.28	309	588	309	588	For use on copper, brass, and similar metals with torch heating.

[a] The specific gravity multiplied by 0.0361 equals the density in lb/cu. in.

[b] For some engineering design purposes it is well to consider these alloys as having practically no mechanical strength at 183 C (361 F).

TABLE 14.3. ASTM SPECIFICATIONS FOR SOFT SOLDER METAL (B 32–49)
Chemical Composition[a,b,c]

Alloy Grade	Tin Desired (%)	Lead, Nominal (%)	Antimony (%)			Silver (%)		
			Min	Desired	Max	Min	Desired	Max
70A	70	30			0.12			
70B	70	30			.50			
60A	60	40			.12			
60B	60	40			.50			
50A	50	50			.12			
50B	50	50			.50			
45A	45	55			.12			
45B	45	55			.50			
40A	40	60			.12			
40B	40	60			.50			
40C	40	58	1.8	2.0	2.4			
35A	35	65			0.25			
35B	35	65			.50			
35C	35	63.2	1.6	1.8	2.0			
30A	30	70			0.25			
30B	30	70			.50			
30C	30	68.4	1.4	1.6	1.8			
25A	25	75			0.25			
25B	25	75			.50			
25C	25	73.7	1.1	1.3	1.5			
20B	20	80			0.50			
20C	20	79	0.8	1	1.2			
15B	15	85			0.50			
10B	10	90			.50			
5A	5[d]	95			.12			
5B	5[d]	95			.50			
2A	2[e]	98			.12			
2B	2[e]	98			.50			
2.5S	0[f]	97.5			.40	2.3	2.5	2.7
1.5S	1[g]	97.5			.40	1.3	1.5	1.7

[a] For elements other than those mentioned in the table, the maximum content in the alloy shall be as follows:

Bismuth		0.25 %
Copper	Alloy grades 70A to 2B, incl.	0.08 %
	Alloy grades 2.5S and 1.5S	0.3 %
Iron		0.02 %
Aluminum, Zinc	each shall not exceed	0.005 %

[b] Analysis shall regularly be made only for the elements specifically mentioned in the above table and footnote a. If, however, the presence of other elements is suspected, or indicated in the course of routine analysis, further analysis shall be made to determine that the total of these other elements is not in excess of 0.08 per cent.

[c] The chemical requirements of S.A.E. Specifications Nos. 1A, 2A, 2B, 3B, 4A, 4B, 5A, 5B, 6A, and E-07 conform substantially to the requirements for alloy grade Nos. 45B, 40B, 40C, 30B, 30C, 25B, 25C, 20B, 20C, 15B, and 2.5S, respectively.

[d] Permissible tin range, 4.5 to 5.5%.

[e] Permissible tin range, 1.5 to 2.5%.

[f] Tin max., 0.25%.

[g] Permissible tin range, 0.75 to 1.25%.

61.9-per cent Sn + 38.1-per cent Pb and represents the only composition which transforms from the liquid to the solid state without passing through an intermediate pasty state. At 182°C, eutectic solder is completely solid, but at 184°C it is entirely liquid. At 183°C, however, the eutectic may be either liquid or solid or a mixture of both states in

TABLE 14.4. UNITED STATES FEDERAL SPECIFICATIONS FOR SOFT SOLDER (QQ-S-571b, SEPTEMBER 30, 1947)
Chemical Composition

	Per cent composition[1]										Approx. melting range (°F)[2]	
Composition[3]	Tin[4] (range)	Lead (max)	Antimony (max)	Silver (max)	Copper (max)	Iron (max)	Bismuth (max)	Zinc (max)	Aluminum (max)	Others (max)	Solidus	Liquidus
Sn 70	69.5 to 71.5	Remainder	0.50		0.08	0.02	0.25	0.005	0.005	0.08 total	360	378
Sn 60	59.5 to 61.5	Remainder	.50		.08	.02	.25	.005	.005	.08 total	360	372
Sn 50	49.5 to 51.5	Remainder	.50		.08	.02	.25	.005	.005	.08 total	360	420
Sn 40	39.5 to 41.5	Remainder	.50		.08	.02	.25	.005	.005	.08 total	360	460
Sn 35	34.5 to 36.5	Remainder	1.6 to 2		.08	.02	.25	.005	.005	.08 total	360 to 365	490 to 500
Sn 30	29.5 to 31.5	Remainder	1.4 to 1.8		.08	.02	.25	.005	.005	.08 total	360	500 to 510
Sn 20	19.5 to 21.5	Remainder	0.8 to 1.2		.08	.02	.25	.005	.005	.08 total	360	525 to 545
Ag 2.5		Remnindder	0.40	2.3 to 2.7	.30	.02	.25	.005	.005	.30 total	580	585
Ag 5.5		Remainder	.40	5 to 6	.30	.02	.25	.005	.005	.30 total	579	689
Sb 5	94.0, min	0.2	4 to 6		.08	.08	Cadmium 0.03	.03	.03	.30 total	450	464

[1] Specified percentage is for solder metal only. In flux-cored wire solder, the weight of the flux shall be subtracted from the total weight to obtain the weight of the solder metal.

[2] For information only.

[3] Tin-lead solders (prefixed by "Sn") may be furnished as flux-cored wire as well as plain wire and other forms. The weight of the flux in ROSIN-flux-cored wire shall not exceed 4 per cent of the total weight. The weight of the flux in CHLORIDE-flux-cored wire shall not exceed 6 per cent of the total weight.

[4] When tin-lead solders (prefixed by "Sn") are furnished as flux-cored wire, the minimum permissible tin content shall be 0.5 per cent less than the minimum values specified in the table.

TABLE 14.5. THE PROPERTIES OF TIN-LEAD SOLDERS
(British Standard)

B.S. 219 Grade	Nominal Tin Content	Limits of Tin Content		Limits of Antimony Content		Melting Temperature				Sp. Gr.	Electrical Conductivity (% of Copper)	Applications
	(%)	Min. (%)	Max. (%)	Min. (%)	Max. (%)	Solidus (°C)	Liquidus (°C)	Solidus (°F)	Liquidus (°F)			
	100					232	232	450	450	7.3	13.9	Pretinning; special instrument work
E	95	94.5	95.5		0.5	183	223	361	434	7.5	13.7	Electrical instruments
A	65	64	66		1	183	186	361	367	8.4	11.9	High strength; quick setting
	63					183	183	361	361	8.4	11.8	No plastic range; lowest melting point
K	60	59	61		0.5	183	189	361	372	8.5	11.6	Fine electrical and tinsmiths' work; quick setting
F	50	49	51		.5	183	214	361	417	8.9	10.9	General purposes; tinsmiths' and machine soldering; non-antimonial
B	50	49	51	2.5	3	185	203	365	398	8.7	9.8	General purposes; where an antimonial solder can be used
	45					183	225	361	437	9.1	10.5	General purposes; non-antimonial
M	45	44	46	2.3	2.7	185	215	365	419	8.9	9.5	General purposes; antimonial
G	42	41	43		0.4	183	232	361	450	9.2	10.3	General purposes; dipping galvanized work
	40					183	236	361	457	9.3	10.1	Can soldering
C	40	39	41	2.0	2.4	185	228	365	443	9.1	9.2	General purpose but slow setting
H	35	34	36		0.3	183	246	361	475	9.5	9.6	Non antimonial for wiping joints on cables
L	32	31	33	1.6	1.9	185	245	365	474	9.5	8.8	Post office cable wiping solder
J	30	29	31		0.3	183	255	361	491	9.7	9.3	Non-antimonial; wiped joints and dipping baths
D	30	29	31	1.0	1.7	185	248	365	478	9.6	8.6	Plumbers' wiped joints
N	18.5	18	18.5	0.75	1	185	275	365	527	10.2	8.1	War-time dipping solder
	Lead	0				327	327	621	621	11.4	7.9	Pure lead

any proportion. Eutectic solder has the greatest strength of any composition in bulk, and it excels by its ease of application, the wettability of metals to be joined and penetration into joints. As the eutectic solder melts and freezes almost instantly, it may in some instances run right through the joint; 45 Sn/55 Pb is thus preferred for most uses. A tabulation of mechanical properties of various solders and their composition is given in Table 14.6.[15] This includes data on S.T. (save tin) solders, which were introduced during World War II and of which some have found permanent usefulness because of their lower cost.

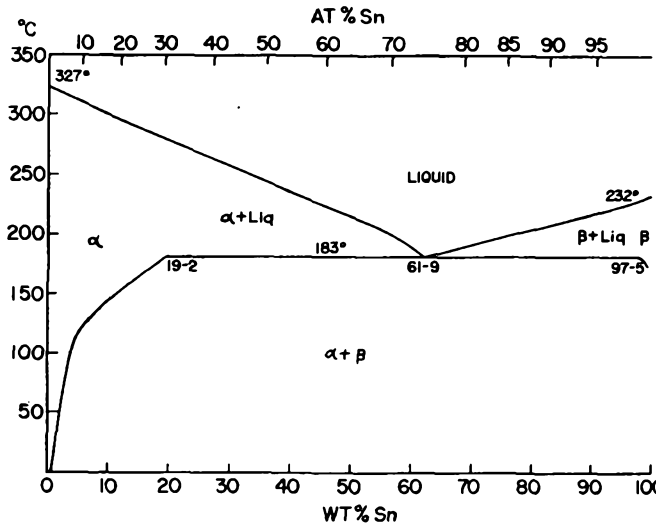

Fig. 14.1. Lead-tin phase diagram. After Smithells.[7] (*Courtesy Interscience Publishers, Inc., New York.*)

A number of low-temperature solders are available for special applications. They contain substantial amounts of bismuth, as evident from Table 14.7. Because of the approach of their melting point to room temperature low-melting alloys are often exceedingly weak. Published data on their mechanical strength may refer to thin films tested for short times only and may not be applicable to joint strength.

"Bismuth is one of the few elements which does not shrink when it solidifies. Water and antimony are two other substances which expand on solidification, but bismuth expands more than the former, namely, 3.3% of its volume. When bismuth is alloyed with other metals, this expansion is somewhat modified according to the relative percentages of bismuth and other components present. For example, in many alloys of more than 48% bismuth, expansion occurs on freezing and some of them continue to expand or grow for many hours in the solid state. In some alloys of the above type, containing lead, the greatest growth occurs after solidification. Some alloys, containing Pb and from 35 to 45% Bi will show slight shrinkage during

TABLE 14.6. MECHANICAL PROPERTIES OF VARIOUS SOLDERS[15]

Alloy	Composition (%)					Liquidus		Tens. Str. (psi)	Elongation, (% in 2 in.)	Bond Strength Lap Joint psi	
	Tin	Silver	Bismuth	Antimony	Lead	(°F)	(°C)			Copper	Steel
"S.T." Solders											
ST-10	10	1.50		0.5	Bal.	554	290.2	5335	11.5	4830	4430
ST-16N	16	0.75		1.50	Bal.	511	266.6	6600	18	4280	4330
ST-20N	20	1.25		1.50	Bal.	503	261.7	7800	11.5	6030	4850
ST-21	21	0.75		1.50	Bal.	503	261.7	7100	10	5900	5400
ST-30	30	1.25	0.5	0.5	Bal.	478	243.4	7625	15	5800	5200
ST-30H	30	1.25		2	Bal.	480	249	8125	20.5	5960	4830
Standard Tin-Lead Solders											
10-90	10			0.5	89.50	568	293.4	4850	21.5	4960	4090
20-80	20			.5	79.50	527	271.4	4940	24.7	5680	4285
25-75	25			.5	74.50	503	261.7	4990	26	5700	
30-70	30			.5	69.50	495	256.8	5390	38.5	5770	
35-65	35			2.00	63	480	249	5670	40	5960	
40-60	40			0.5	59.50	460	238	5660	62.5	6270	
50-50	50			.5	49.50	414	212.2	5790	90	6510	

solidification and aftergrowth in the solid phase that is enough to compensate for the initial shrinkage. Alloys containing 50% or more Bi but no Pb expand during solidification, with only slight shrinkage during cooling to room temperature."[16]

A number of indium-bearing alloys have been developed in recent years and are marketed under the trade name "Cerrolow."* They are eutectic alloys with sharp melting points or zero freezing ranges, but their composition can be modified to produce a plastic range when desired. Indium melts at 155°C and the "Cerrolow" compounds have their liquidus extending down to as low as 41°C. "Cerroseal" adheres

TABLE 14.7. COMPOSITION OF LOW TEMPERATURE SOLDERS

	Pb	Sn	Bi	Cd	M.P. (°C)
Woods metal	25	12.5	50	12.5	70
Woods metal	30.8	15.4	38.4	15.4	77–80
Lipowitz metal	26.7	13.3	50	10	70
Ternary eutectic	32	16	52		95
Rose's alloy	28	22	50		100
	42	33	25		150
"Cerro tru"*		42	58		138

* Registered Trademark, Cerro de Pasco Copper Corp., 40 Wall St., New York 5, N.Y.

to glass and may be used for glass joints to glass and metal within the limited temperature range dictated by the softening point of the alloy. The mechanical properties of several widely used bismuth alloys have recently been described by Seeds,[16] from whose article Table 14.8 is taken.

"In the case of regular lead-tin solders, tinning occurs when the solders are molten and an active flux is present to keep the metal surfaces clean and free of oxides. But Cerro Alloys do not tin when they are just at their liquidus points. Therefore, to satisfactorily solder with a Cerro Alloy, the parts must be pretinned before assembly, using enough heat to activate the flux and secure an alloy bond. Pretinning may be done with regular solders or with a Cerro Alloy chosen for the work at hand. After pretinning, parts are assembled and reheated sufficiently to melt the Cerro Alloy required to complete the joint."†

Special alkali-resistant, indium-bearing solders were recently developed at the Battelle Memorial Institute. These resist the corrosive action of strong alkaline solutions much better than ordinary soft solders, according to Grymko and Jaffee.[17] The authors report from their tests that

(1) "The alloys with 25% or more of indium by wt. are high in resistance to attack by alkaline solutions. They proved satisfactory in a one-month test of immersion in

* Cerro de Pasco Copper Corp., 40 Wall St., New York 5, N.Y.

† *Cerro Bulletin E9-12-49.*

TABLE 14.8. PROPERTIES OF SEVERAL WIDELY USED BISMUTH ALLOYS[16]

Properties	1 "Cerrolow-117"	2 "Cerrolow-136"	3 "Cerrobend"	6 "Cerrosafe"	15 "Cerro-matrix"	16 "Cerrobase"	18 "Cerrotru"	19 "Cerrocast"
Yield temp. (°F)	117	136	158	162.5	240	255	281	302
Weight, lb/cu in	0.32	0.31	0.339	0.341	0.343	0.380	0.315	0.296
Tensile strength (psi)	5,400	6,300	5,990	5,400	13,000	6,400	8,000	8,000
Elong. in 2 in. (slow load), %	1.5	50	200	220	< 1	60–70	200	200
Brinell hardness	12	14	9.2	9	19	10.2	22	22
*Spec. heat (liquid), Btu/lb/°F	0.035	0.032	0.040	0.04	0.04	0.042	0.045	0.047
*Spec. heat (solid), Btu/lb/°F	.035	.032	.040	.04	.045	.03	.045	.047
*Latent heat of fusion, Btu/lb	6	8	14	10		7.2	20	22
*Coeff. of thermal expan. (°F)			1.2×10^{-5}	1.3×10^{-5}			0.9×10^{-5}	0.9×10^{-5}
Elect. cond. (% of Copper)	3.9	3	4	4	3.2	3	4.5	4.6
*Max. load (30 sec) psi			10,000	9,000	16,000	8,000	15,000	15,000
*Max. load (5 min) psi			4,000	3,800	10,000	4,000	9,000	9,500
*Safe sustained load, psi			300	300	300	300	500	500
Cumulative growth and shrinkage per in. compared to cold mold dimensions (test bar: ½ × ½ × 10 in)								
Time after casting:								
2 min	+0.0005	+0.0003	+0.0025	−0.0004	+0.0008	−0.0008	+0.0007	−0.0001
30 min	0.0000	+0.0001	+0.0045	−0.0009	+0.0047	−0.0010	+0.0006	−0.0001
1 hr	−0.0001	0.0000	+0.0051	0.0000	+0.0048	−0.0008	+0.0006	−0.0001
5 hr	−0.0002	−0.0002	+0.0051	+0.0018	+0.0049	0.0000	+0.0005	−0.0001
24 hr	−0.0002	−0.0002	+0.0051	+0.0022	+0.0051	+0.0008	+0.0005	−0.0001
96 hr	−0.0002	−0.0002	+0.0053	+0.0025	+0.0055	+0.0015	+0.0005	−0.0001
500 hr	−0.0002	−0.0002	+0.0057	+0.0025	+0.0061	+0.0022	+0.0006	−0.0001

* Approximate values.

25% potassium hydroxide at 120°F, and would be expected to withstand considerably longer exposures.

(2) "The strongest of the alkaline-resistant solders contains 25% indium, 37.5% lead, and 37.5% tin.

(3) "The solders containing 25% indium show an appreciable increase in shear strength after the one-month immersion test cited above.

(4) "The alloys without indium or with only 10% In are penetrated by the alkaline solution and lose some strength in a month's exposure."

The cost of a solder containing 25-per cent indium is about 17 times higher than that for 50 Pb-50 Sn solder. The advantage of corrosion resistance to alkaline solutions is thus obtained at a considerable price.

It is at times important to know the low-temperature properties of solders and soldered joints when tubes and associated equipment are

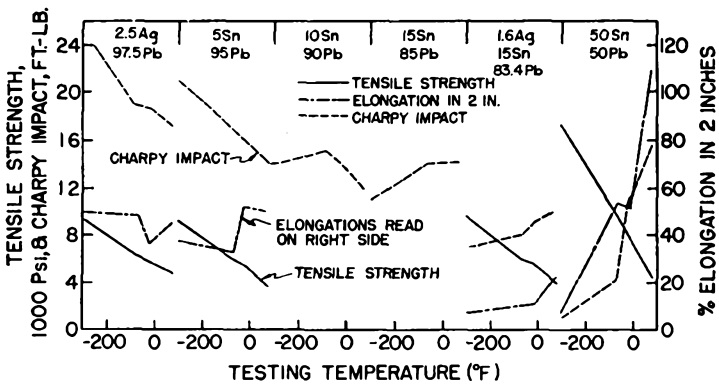

Fig. 14.2. Mechanical characteristics of soft solders at low temperatures. After R. I. Jaffee, E. J. Minarcik and B. W. Gonser.[18] (*Courtesy The American Society for Metals.*)

installed in aircraft flying at high altitudes or when refrigerating units are soldered to vacuum systems. The National Lead Company has sponsored research on this subject with Battelle Memorial Institute,[18] and their findings are summarized in Fig. 14.2 for a number of solder compositions which were tested over a temperature range from 75 to −295°F (23.9 to −181.7°C). Tests of soldered joints were also made and the following conclusion reached:

"Soft solders that contain a high percentage of face-centered cubic lead retain their ductility and increase in impact strength at low temperatures. This is in agreement with recent concepts concerning the relation of structure to low-temperature properties. When the percentage of tetragonal tin becomes as high as 50%, serious embrittlement and decrease in impact strength occur. Tin contents up to 15% have no serious embrittling effect.

"The increase in the tensile strength of solder alloys and in the breaking load of soldered joints is linear with decreasing temperature. The solder containing the most tin (50%) shows the greatest increase in strength, and the solder with the most

lead (97.5%) shows the least increase in strength. Breaking loads of soldered copper tubing at low temperatures are nearly independent of the kind of lead-base solder used. The impact strength and ductility of such joints would probably be influenced by low temperatures, in view of the properties of the solders alone."

To facilitate the removal of oxide films and the spreading of the solder a number of fluxes are in common usage. These may be classified as corrosive fluxes, such as zinc chloride, ammonium chloride, hydrochloric acid, phosphoric acid, and noncorrosive or resin-type fluxes. The most commonly used flux for soft soldering is zinc chloride ($ZnCl_2$)

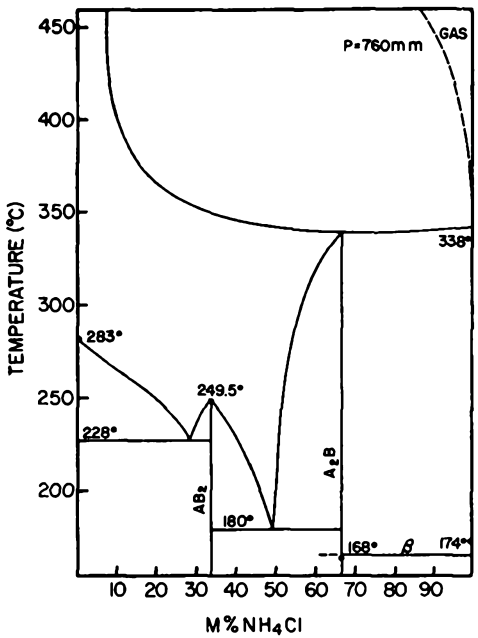

Fig. 14.3. Phase diagram of zinc chloride-ammonium chloride system. After K. Hachmeister.[18a]

dissolved in water. The water, or other solvent used, quickly evaporates when the flux is applied to the hot joint, and the $ZnCl_2$ then melts and combines with surface oxides which are present. To reduce the melting point of $ZnCl_2$ (365°C), ammonium chloride (NH_4Cl) is usually added to $ZnCl_2$ in such proportion so as to form a eutectic mixture of the lowest melting point. Figure 14.3 gives the phase diagram of these two components.[18a] The eutectic mixture contains 71 weight per cent of ZnCl and 29 weight per cent of NH_4Cl, and melts at 180°C. To become fully active and to perform its useful function it is of course necessary that the flux melts before the solder is molten. The correct selection of flux com-

position as well as that of the solder will have a distinct bearing on the strength and reliability of the joint.

The so-called "organic fluxes" occupy an intermediate position between acid- and resin-type fluxes. Because of their organic components they char, burn, or decompose at the soldering temperature, and are not recommended for use in conjunction with a torch.

Resin, rosin, or colophony, familiar to the player of string instruments, is the gum exuded from wounds or cuts in the bark of pine trees and consists chiefly of abietic acid and related substances. At ordinary temperatures it is solid and does not cause corrosion, but at or near the soldering temperature it reacts mildly. It melts readily at 125°C.

"Rosin is generally not considered an acid-type flux, but this is not true. Rosin does contain an acid, but it has certain rather unusual physical properties which prevent the acid from being active at normal temperatures. Furthermore, the residue of a rosin flux is nonconducting, noncorrosive, and nonhygroscopic. It should, in general, be used as the standard flux in electrical applications. One of the frequent errors in handling rosin is that of overheating. Too much heat disintegrates the rosin, reduces its active fluxing properties, and carbonizes the residue. Rosin should thus always be applied to the parts being soldered and not to the soldering iron. The same rule applies to the use of rosin-core solder, which should be applied to the parts as they are being brought up to the soldering temperature and not after they have reached a temperature approaching that of the soldering iron. Good practice involves efficient heat transfer through the medium of the solder itself."[9]

Usual solvents for rosin are methyl or ethyl alcohol, propyl or butyl alcohol, or turpentine. Resin flux may be made more active (and corrosive) by addition of oleic or lactic acid. "Activated" resin fluxes contain additions which decompose at the temperature of the soldering operation and become noncorrosive. Hydrochlorides of amines, such as aniline, naphthylamine, and hydroxylamine, or the tetrachloride of naphthalene are examples. Certain activated rosins contain surface-active agents that do not cause corrosion and do not depend on heat to decompose them. Flux pastes of either the corrosive or noncorrosive type are often a convenience when liquid fluxes are liable to run off the work. When they are mixed with powdered solder, solder paints* are obtained. Flux-core solder contains the paste flux in a tube of solder. Common paste-forming ingredients are petroleum jelly or vaseline, tallow and lanoline, with glycerine as the moisture-retaining substance. Much ingenuity has gone into the preparation of a wide variety of solder paints and flux-core solders for different applications. New products should, however, be carefully tested unless they are sponsored by reputable suppliers.

The selection of fluxes is controlled by the design of the joint, the

* Powder solders mixed with flux are generally termed "solder paints" to differentiate them from the solder-free flux pastes, sometimes called "solder pastes."

materials involved, and the degree of possible removal of corrosive fluxes after the joint is made. Flux should be removed from pretinned parts before the actual joint is made. For joints forming part of a sealed-off vacuum tube fluxes should not be used. They are liable to have components or decomposition products of a high vapor pressure and act as poisons to oxide cathodes in most cases.

A compilation of soldering and brazing materials and their fluxes is given in Table 14.9 and is intended as an over-all reference and guide. In its original form this table was first prepared by R. O. McIntosh for use at the Westinghouse Research Laboratory and published later by Feldmeier.[4] The present author has brought it up to date after consultation with several advisers and firms, and has also re-arranged it slightly for more convenient use.[4a] The applications and materials listed are not confined to the field of electron tubes directly, but cover other phases of processing likely to arise in electronics in general.

It is evident that the soft solders proper are of no avail when temperatures above 150°C are encountered during the operation of the joint because of the low strength between this temperature and the tin-lead solidus at 183°C. Antimony solders are then used to advantage. The alloy Sn97-Sb3 has a melting point of 235°C and retains its strength well up to 200°C, provided that lead-free materials are used. Tinning should be done with this solder or pure tin in order to exclude the possibility of formation of the Sn-Pb-Sb eutectic, which even in small amounts may cause embrittlement at temperatures above 185°C. The tin-antimony high-temperature solder is applied by the usual means, but at a slightly higher temperature. The usual fluxes are sufficiently active and there is no difficulty from drossing. Tin-Silver eutectic (Sn 96.5-Ag 3.5) is sometimes used as an alternative in fine instrument work. It melts at 221°C and is easy to apply with resin-type flux. Pure tin which melts at 231.9°C is objectionable on account of its high shrinkage, brittleness, and cost. Pure lead does not wet steel, cast iron, copper, and its alloys. A tin-silver-lead alloy (Sn 1-Ag 1.45-Pb 97.55), however, is a satisfactory solder which melts at 300°C. Good fluxing is essential and the temperature must be strictly controlled. This alloy has the highest resistance to creep above 150°C.[3]

The many factors which enter into the production of a satisfactory solder joint have eluded critical evaluation for a long time. Of recent years distinct progress has been made, however, and several methods have been described which aim at a quantitative approach to this problem. Soldering is to a large extent a problem of heat flow. It is thus important to take into account the heat capacities of the components and to know the thermal characteristics of the solder itself.

Table 14.10 gives data published by Mample.[9] It is evident from

(Text continued on p. 332)

TABLE 14.9. SOLDERS AND BRAZING MATERIALS[4a]

Ser. No.	M.P. (°C)	Flow P. (°C)	Material and Supplier	Composition (%)	Flux	Comments	M.P. (°F)	Flow P. (°F)
(A) Fusible Alloys								
1	38	43	"Cerrolow"-105 C.D.P.	Bi: 42.91; Pb: 21.70; Sn: 7.97; Cd: 5.09; In: 18.33; Hg: 4		Pretinning required on all Cerro alloys. Acid flux gives best results with Bi-alloys.	100	110
2	47.2	47.2	"Cerrolow"-117 C.D.P.	Bi: 44.70; Pb: 22.60; Sn: 8.30; Cd: 5.30; In: 19.10			117	117
3	47.2	52.2	"Cerrolow"-117B C.D.P.	Bi: 44.70; Pb: 22.60; Sn: 11.30; Cd: 5.30; In: 16.10			117	126
4	56.7	65.0	"Cerrolow"-140 C.D.P.	Bi: 47.50; Pb: 25.40; Sn: 12.60; Cd: 9.50; In: 5			134	149
5	57.8	57.8	"Cerrolow"-136 C.D.P.	Bi: 49; Pb: 18; Sn: 12; In: 21			136	136
6	57.8	68.9	"Cerrolow"-136B C.D.P.	Bi: 49; Pb: 18; Sn: 15; In: 18			136	156
7	61.1	65.0	"Cerrolow"-147 C.D.P.	Bi: 48; Pb: 25.63; Sn: 12.77; Cd: 9.60; In: 4			142	149
8	70	73.9	Wood's Metal C.D.P.	(a) Bi: 50; Pb: 25; Sn: 12.50; Cd: 12.50			158	165
				(b) Bi: 50; Pb: 24; Sn: 14; Cd: 12			158	165
9	78.9	78.9	"Cerrolow"-174 C.D.P.	Bi: 57; Sn: 17; In: 26			174	174
10	91.9	91.9	Bi-Pb-Cd	Bi: 51.60; Pb: 40.20; Cd: 8.20			197	197

11	95	95	Newton's Alloy	(a) Bi: 52.50; Pb: 32; Sn: 15.5 (b) Bi: 50; Pb: 31.25; Sn: 18.75
12	95	115	Darcet's Alloy	Bi: 50; Pb: 25; Sn: 25
13	100	100	Rose's Alloy	(a) Bi: 50; Pb: 28; Sn: 22 (b) Bi: 46; Pb: 20; Sn: 34
14	115.6	126.7	"Cerroseal"-35 C.D.P.	Sn: 50; In: 50
15	134.2	181.4	Alkali-resistant solder	Sn: 37.5; Pb: 37.5; In: 25
16	138.6	138.6	"Cerrotru" C.D.P.	Bi: 58; Sn: 42
17	144	144	Bi-Cd-eutectic	Bi: 60; Cd: 40
18	177	177	Sn-Cd-eutectic	Sn: 67.75; Cd: 32.25
(B) Soft Solders				
1	156.4		Pure indium I.C.A. C.D.P.	In: 100
2	182.0		Alkali-resistant solder	In: 50; Pb: 50
3	183	183	Eutectic soft solder	Sn: 61.9; Pb: 38.1
4	183	190	Lead-tin solders	Sn: 60; Pb: 40
5	183	216	No. 111 N.L.C.	Sn: 50; Pb: 50

	(a) B-Sealing solder for wiped joints (Bell Laboratories Record, July 1950).	203	203
		203	239
		212	212
No flux on nonmetals	Low vapor pressure, adheres to glass, metal, mica, quartz (and glazed ceramic).	240	260
A	Strong and corrosion resistant.[20]	274	358
		281	281
		291	291
		351	351
	Very expensive, rarely used.	313.5	313.5
A	Strong and corrosion resistant.	360	
		361	361
		361	374
A	Works easily; strong; adheres and covers well for all metal fabrication.	361	421

TABLE 14.9. SOLDERS AND BRAZING MATERIALS. (*Continued*)

Ser. No.	M.P. (°C)	Flow P. (°C)	Material and Supplier	Composition (%)	Flux	Comments	M.P. (°F)	Flow P. (°F)
6	183	227		Sn: 45; Pb: 55			361	440
7	183	238	Lead-tin solders	Sn: 40; Pb: 60			361	460
8	183	247		Sn: 35; Pb: 65			361	476
9	183	255		Sn: 30; Pb: 70			361	491
10	183	266		Sn: 25; Pb: 75			361	511
11	183	277		Sn: 20; Pb: 80	A	Weak.	361	531
12	183	288		Sn: 15; Pb: 85			361	550
13	183	299		Sn: 10; Pb: 90			361	570
14	270	312		Sn: 5; Pb: 95			518	594
15	184	263	Lead-tin-antimony solders	Sn: 25; Pb: 73.7; Sb: 0.96			363	504
16	184	270		Sn: 20; Pb: 79; Sb: 1			363	517
17	184			Sn: 34.5; Pb: 64.1; Sb: 1.25; As: 0.11		E-Wiping Solder (Bell System).	363	
18	185	231	Lead-tin-antimony solders	Sn: 40; Pb: 58; Sb: 2			365	448
19	185	243		Sn: 35; Pb: 63.2; Sb: 1.8			365	470
20	185	250		Sn: 30; Pb: 68.4; Sb: 1.6			365	482
21	219	232	"Eutec Rod" 199B E.W.A.	Sn: 90–92; Zn: 8–9; Ni: 0.75–1.25	E199B	Soft solder for Aluminum, ferrous and non-ferrous alloys	425	450
22	230.3		Alkali resistant solder	Pb: 75; In: 25	A	Strong and corrosion resistant.[20]	446	

23	231.9	231.9	Pure tin	Sn: 100
24	232	240		Sn: 95; Sb: 5
25	302	304	"Eutec Rod" 153 E.W.A.	Pb: 93–95; Ag: 5–6; Sn: 1–2
26	304	304	Lead-silver eutectic	Pb: 97.5; Ag: 2.5
27	304	380		Pb: 94–95; Ag: 6–5
28	309	309		Sn: 1; Pb: 97.5; Ag: 1.5
29	314	314	C.D.P.	Pb: 95; In: 5
30	327.4	327.4	Pure lead	Pb: 100
31	385	391	"Eutec Rod" 155 E.W.A.	Cd: 94–95; Sn: 1–2; Ag: 5–6
32	400		Intermed. solder I.C.A.	Sn: 75; Ag: 20; Cu: 3; Zn: 2
(C) Brazing Filler Metals				
1	550	632	Gold-indium I.C.A.	Au: 80; In: 20
2	591	719	"RT-SN" H. & H.	Ag: 60; Cu: 30; Sn: 10
3	600	630	Low-melting hard solder	Ag: 42; Cu: 33; Sn: 25
4	600	640	Low melting hard solder	Ag: 46.5; Cu: 32.5; Sn: 21
5	607	618	"Easy-Flo" 45 H. & H.	Ag: 45; Cu: 15; Zn: 16; Cd: 24

A	Shrinks, Cu-Sn alloys brittle. Low strength, rarely used.	450	450
	Sweating Cu tubing joints.	450	464
E153	Ferrous and non-ferrous alloys	575	580
A		579	579
A		579	715
		588	588
		598.5	598.5
		621	621
E155	Ferrous and non-ferrous metals; high strength	725	735
A	Allow time for Sn to diffuse.	752	
H_2	Hard, brittle.	1022	1170
C		1095	1325
H_2	F. C. Hull, Westinghouse Res. Lab. Hard, brittle.	1100	1162
H_2	F. C. Hull, Westinghouse Res. Lab. Hard, brittle.	1110	1180
C, F A.P.1	Narrow melting range. For ferrous and non-ferrous metals.	1125	1145

TABLE 14.9. SOLDERS AND BRAZING MATERIALS. (*Continued*)

Ser. No.	M.P. (°C)	Flow P. (°C)	Material and Supplier	Composition (%)	Flux	Comments	M.P. (°F)	Flow P. (°F)
			"Silvaloy" 45 A.P.W. Sil-Bond-45 U.W.S.		A.P.1 A.P.2 S	Very free flowing		
6	613	677	"Eutec Rod" 1700X E.W.A.	Ag: 34–36; Cu: 24–28; Zn: 19–23; Cd: 17–19	E1700X	Wide melting range. For ferrous and non-ferrous metals when fillets are required. Free flowing	1135	1250
	607	702	"Easy-Flo" 35 H. & H.		C, F		1125	1295
			"Silvaloy" 35 A.P.W. "Sil-Bond"-35 U.W.S.		A.P.1 A.P.2 S			
7	613	621	Type 154 G.P.	Ag: 45; Cu: 17; Zn: 16.5; Cd: 20.5; Sn: 0.5; Pb: 0.5		Extremely wetting on ferrous and non-ferrous metals.	1135	1150
8	613	652	"Silvaloy" 40 A.P.W.	Ag: 40; Cu: 18; Zn: 15; Cd: 27	A.P.1 A.P.2	For ferrous and non-ferrous metals and their alloys including Inconel, Monel and other nickel alloys.	1135	1205
9	616	816	"ATT" H. & H.	Ag: 20; Cu: 45; Zn: 30; Cd: 5	C, F	ASTM Spec. B-73-29. No. 3. Brass Yellow.	1140	1500
	621	643	"Sil-Bond"-45 WE U.W.S.	Ag: 45; Cu: 18; Zn: 18; Cd: 19	S	For ferrous and non-ferrous metals. War Emergency substitute for Sil-Bond-45	1150	1190
10	621	732	"Sil-Lon" U.W.S.	Ag: 40; Cu: 30.5; Zn: 29.5	S	For general use with ferrous metals, especially for loose fitting parts.	1150	1350

11	623	650	"Silvaloy" 355 A.P.W.	Ag: 56; Cu: 22; Zn: 17; Sn: 5	A.P.2 F
12	627	635	"Easy Flo" H & H "Silvaloy" 50 A.P.W. KH-7 G.P. "Sil-Bond"-50 U.W.S.	Ag: 50; Cu: 15.5; Zn: 16.5; Cd:	C A.P.1 A.P.2
13	630	643		Ag: 50; Cu: 15; Zn: 25; Cd: 10	
14	630	754	"Sil-Bond"-31 U.W.S.	Ag: 31.5; Cu: 34; Zn: 15.5; Cd: 19	S
15	632	688	"Easy-Flo" #3 H. & H. "Silvaloy" 503 A.P.W. KH-7 G.P. "Sil-Bond"-50N U.W.S.	Ag: 50; Cu: 15.5; Zn: 15.5; Cd: 16; Ni: 3	C A.P.1 A.P.2 S
16	641	704	"Sil-Fos" H. & H.	Ag: 15; Cu: 80; P: 5	C
	641	693	"Silvaloy" 15 A.P.W.		A.P.1 A.P.2
	643	820	"Sil-Lo" U.W.S.		S
17	641	741	"Phoson" U.W.S.	Ag: 6; Cu: 86.88; P: 7.12	

White; for stainless steel and other white metals.	1152	1203
Narrow melting range. For ferrous & non-ferrous metals. Yellow, mech. strong. Fed. Gov. Agencies Spec. QQ-S-561d. No. 4.	1160	1175
	1166	1190
For ferrous metals. Slow flowing	1165	1390
Wide melting range. For ferrous & non-ferrous metals when fillets are required. Yellow, strong. Fed. Gov. Agencies Spec. QQ-S-561d. For carbide tool tipping and building of fillets.	1170	1270
Wide melting range, hard and strong. For copper and its alloys but not for ferrous metals. Gray-white. Fed. Gov. Agencies Spec. QQ-S-561d. Grade 3.	1185	1300
	1185	1280
	1190	1508
For copper and its alloys	1185	1380

TABLE 14.9. SOLDERS AND BRAZING MATERIALS. (*Continued*)

Ser. No.	M.P. (°C)	Flow P. (°C)	Material and Supplier	Composition (%)	Flux	Comments	M.P. (°F)	Flow P. (°F)
18	660	779	"SS" H. & H.	Ag: 40; Cu: 30; Zn: 28; Ni: 2	C	Pale yellow. For carbide tool tipping at higher temperatures.	1220	1435
	661	769	"Silvaloy" 250 A.P.W.		A.P.1 A.P.2		1222	1416
19	663	985	SN #7 H. & H.	Ag: 7; Cu: 85; Sn: 8	C		1225	1805
20	669	710	"Easy" H. & H.	Ag: 65; Cu: 20; Zn: 15	C	ASTM B-73-29. No. 6. Silver white for sterling silver. Fed. Gov. Agencies Spec. QQ-S-561d, Grade 2.	1235	1310
			A.P.W.		A.P.1 A.P.2		1285	1325
			"Sil-Loy" U.W.S.		S			
	696	719	SK4 G.P.					
21	670	700	Low melting hard solder	Ag: 53; Cu: 32; Sn: 15	H_2	F. C. Hull, Westinghouse Res. Labs. Very hard, brittle, low vapor pressure.	1238	1290
22	677	727	"Silvaloy" A-28 A.P.W.	Ag: 50; Cu: 28; Zn: 22	C, F A.P.1 A.P.2	Yellow white.	1250	1340
23	677	743	"DE" H. & H.	Ag: 45; Cu: 30; Zn: 25	C, F	Yellow white. ASTM B-73-29. No. 4. Fed. Gov. Agencies Spec. QQ-S-561d, No. 1.	1250	1370
			"Silvaloy" A-18 A.P.W.		A.P.1 A.P.2			
			"Sil-Tite" U.W.S.		S			

24	682	718	"RT" H. & H. "Silvaloy" A-33 A.P.W. "Sil-Tex" U.W.S.	Ag: 60; Cu: 25; Zn: 15	C A.P.1 A.P.2 S	Silver white (for Tungsten to Copper with NaCN flux).	1260	1325
25	685	710	"Incosil" W.G.P.	Ag: 63; Cu: 27; In: 10	H_2	For electron tube step brazing.	1265	1310
26	688	704	"SH-7" G.P.	Ag: 60; Cu: 20; Zn: 7; Cd: 10; Sn: 3	A.P.1, F A.P.2	All ferrous and non-ferrous metals and alloys.	1270	1300
27	691	774	"E.T.X." H. & H.	Ag: 50; Cu: 34; Zn: 16	C, F	ASTM B-73-29. No. 5.	1275	1425
	689	774	"Silvaloy" A-25 A.P.W.		A.P.1 A.P.2		1272	1425
	691	802	"Sil-Gon" U.W.S.		S		1275	1475
28	691	738	"Medium" H. & H. A.P.W. "Sil-Co" U.W.S.	Ag: 70; Cu: 20; Zn: 10	C A.P.1 A.P.2 S	ASTM Spec. B-73-29. No. 7. For sterling silver; silver white.	1275	1360
29	696	724	"SB-2" G.P.	Ag: 60.50; Cu: 22.5; Zn: 7; Cd: 10		Atmosphere for non-ferrous only.	1285	1335
30	704	729	"TR #1" H. & H.	Ag: 75; Zn: 25	C, F		1300	1345
31	704	755	"KK-5" G.P.	Ag: 55; Cu: 31.5; Zn: 11.7; Ni: 1.8	H_2	Fluxless brazing, particularly of ferrous metal.	1300	1355
32	707	750	Phos copper— Westinghouse	Cu: 93; P: 7		For non-ferrous metals. Hard and strong, very free flowing.	1304	1382

TABLE 14.9. SOLDERS AND BRAZING MATERIALS. (*Continued*)

Ser. No.	M.P. (°C)	Flow P. (°C)	Material and Supplier	Composition (%)	Flux	Comments	M.P. (°F)	Flow P. (°F)
33	708	813	"Phosco" U.W.S.	Cu: 92.5; P: 7.12		For non-ferrous metals. Hard and strong; very free flowing.	1308	1495
34	719	857	"AMS-4772" H. & H.	Ag: 54; Cu: 40; Zn: 5; Ni: 1			1325	1575
35	720	740	Low melting hard solder	Ag: 59; Cu: 31; Sn: 10	H_2	F. C. Hull. Very hard; can be swaged, low vapor pressure.	1328	1360
36	721	779	"DT" H. & H.	Ag: 40; Cu: 36; Zn: 24	C, F	Pale yellow.	1330	1445
			"Silvaloy" A-14 A.P.W.		A.P.1 A.P.2			
	727	763	"CH-1" G.P.				1340	1405
37	730	760	"MA-1" G.P.	Ag: 72.15; Cu: 22.8; Zn: 5.05			1345	1400
38	732	774	"Hard #1" H. & H.	Ag: 75; Cu: 20; Zn: 5	C, F		1350	1425
39	732	777	"LM-1" G.P.	Ag: 27; Cu: 40.15; Zn: 32.85			1350	1430
40	738	757	"SM-1" G.P.	Ag: 66.7; Cu: 28.25; Zn: 5.05			1360	1395
41	738	810	"I.T." H.& H.	Ag: 80; Cu: 16; Zn: 4	C	ASTM Spec. B-73-39. No. 8. White.	1360	1490
			"Silvaloy" A-49 A.P.W.		A.P.1 A.P.2			

42	741	788	"Hard" H. & H. A.P.W.	Ag: 75; Cu: 22; Zn: 3
43	743	760	"SI-1" G.P.	Ag: 68; Cu: 26.6; Sn: 5
44	743	766	"N.T." H. & H. "Silvaloy" A-13 A.P.W. "Sil-30" U.W.S.	Ag: 30; Cu: 38; Zn: 32
45	752	785	"RE-Mn" H. & H.	Ag: 65; Cu: 28; Mn: 5; Ni: 2
46	754	912	"Eutec Rod" 16 E.W.A.	Cu: 46–48; Ni: 10–11; Ag: 1 max; P: 0.2–1; Si: 0.15 max; Zn: Bal.
47	777	799	"KC-4" G.P.	Ag: 54; Cu: 40; Zn: 5; Ni: 1
48	777	816	"AT Special" H. & H. "Silvaloy" A-11 A.P.W.	Ag: 20; Cu: 45; Zn: 35
49	777	816	"Silvaloy" 20 A.P.W.	Ag: 20; Cu: 45; Zn: 30; Cd: 5
50	779	779	Silver-Copper Eutectic W.G.P.	Ag: 72; Cu: 28

C, F		1365	1450
A.P.2			
	Suitable for vacuum equipment and tubes.	1370	1400
C	Pale yellow.	1370	1410
A.P.2 S			
C, F	For stellites, carbides and refractory alloys containing tungsten.	1385	1445
E16	For ferrous and non-ferrous metals and alloys. High strength, very fluid.	1390	1675
A.P.1 A.P.2 H_2, F	Ferrous or non-ferrous metals.	1430	1470
C, F A.P.2	ASTM Spec. B-73-29. No. 2 Fed. Gov. Agencies Spec. QQ-S-561d. No. 0.	1430	1500
A.P.2	ASTM Spec. B-73-29. No. 3.	1430	1500
C, H_2,	Excellent for copper. White.	1435	1435

TABLE 14.9. SOLDERS AND BRAZING MATERIALS. (*Continued*)

Ser. No.	M.P. (°C)	Flow P. (°C)	Material and Supplier	Composition (%)	Flux	Comments	M.P. (°F)	Flow P. (°F)
	779	779	"B.T." H. & H. "Silvaloy" 301 A.P.W. "Sil-72" U.W.S. ML G.P.	Ag: 72; Cu: 28 (ct'd.)	H_2 A.P.2 F, S	Low vapor pressure alloy. Suitable for vacuum equipment and tubes. Fast melting, free flowing except on ferrous metals.	1435	1435
51	782	816	"LH-3" G.P.	Ag: 19.45; Cu: 47.75; Zn: 32.8			1440	1500
52	788	852	"T.L." H. & H.	Ag: 9; Cu: 53; Zn: 38	C, F	ASTM Spec. B-73-29. No. 1. Brass yellow.	1450	1565
53	813	866	"BH-1" G.P.	Ag: 10; Cu: 50; Zn: 40			1495	1590
54	816	857	"N.E." H. & H.	Ag: 25; Cu: 52.5; Zn: 22.5	C, F		1500	1575
55	820	950	Tobin brazing bronze	Cu: 60; Zn: 39.25; Sn: 0.75	M, E146	Good wear resist. & high tensile strength for cast iron or steel.	1500	1740
56	821	871	"Silvaloy" A-4 A.P.W.	Ag: 10; Cu: 52; Zn: 38	A.P.2		1510	1600
57	827	843	"Spelter Bronze"	Cu: 49–52; Sn: 3–4; Pn: 0.5: Fe: 0.1; Zn: Bal.			1520	1550
58	857	871	"T.E. Special" H. & H.	Ag: 5; Cu: 58; Zn: 37	C, E181		1575	1600
59	871	882	"Spelter" or brazing solder	Cu: 49–52; Pb: 0.5; Fe: 0.1; Al: 0.1; Zn: Bal.		Common brazing solder for metal work shops.	1600	1620

TABLE 14.9. SOLDERS AND BRAZING MATERIALS. (*Continued*)

Ser. No.	M.P. (°C)	Flow P. (°C)	Material and Supplier	Composition (%)	Flux	Comments	M.P. (°F)	Flow P. (°F)
60	875		Brazing compound	Cu: 54; Zn: 46	D	Ref. J. Strong; Proc. Exp. Phys. '42.	1607	
61	890	890	Gold-copper eutectic	Au: 80; Cu: 20	D, H_2	Beware brittle joints.	1634	1634
62	899	960	Brazing solder	Cu: 68–72; Pb: 0.3; Fe: 0.1; Zn: Bal.			1650	1760
63	941	996	Brazing solder	Cu: 78–82; Pb: 0.2; Fe: 0.1; Zn: Bal.			1725	1825
64	950	990	Gold-copper alloy	Au: 37.5; Cu: 62.5	H_2	For vacuum tube components.	1742	1814
65	950	950	Gold-nickel eutectic	Au: 82.5; Ni: 17.5	D, H_2	" " " "	1742	1742
66	950	980	Gold-copper alloy	Au: 94; Cu: 6	D, H_2	" " " "	1742	1796
67	960	960	Pure silver	Ag: 100	D, H_2	" " " "	1760	1760
68	960	970	"Silvaloy" 850 A.P.W. H. & H.	Ag: 85; Mn: 15	A.P.2 H_2	For stainless steel. When high brazing temp. required.	1760 1745	1778 1760
69	970	1010	Gold-copper alloy W.G.P.	Au: 35; Cu: 65	H_2	For vacuum tube components.	1778	1850
70	980	1025	"Nicoro" W.G.P.	Au: 35; Cu: 62; Ni: 3	H_2	For vacuum tube components.	1796	1877
71	1010	1038	"Nicrobraze" W.C.C.	Ni: 70; Cr: 18; B: 3.2; Fe + Si + C: 9 max	H_2*	For stainless steel, Inconel, etc. High strength and corrosion resistance at elevated temperatures of the order of 1500°F.	1850	1900

72	1063	1063	Pure gold	Au: 100	D, H_2		1945	1945
73	1080	1085	"Eutec Rod" 183 E.W.A.	Cu: 97–98; Ag: 1–1.5; Mn: 0.05–0.875; Fe: 0.25–0.50	E183	For high-conductivity copper.	1975	1985
74	1082	1082	Pure copper (OFHC)	Cu: 100	H_2		1980	1980
75	1160		Platinum solder	Ag: 73; Pt: 27	H_2	Wets tungsten.	2120	
76	1205		Nickel coinage (Pre war)	Cu: 75; Ni: 25	H_2	Wets tungsten.	2201	
77	1450		Nickel	Ni + Co: 99–99.5; Traces: C, Mn, S	H_2	Wets tungsten and molybdenum.	2642	
78	1966	1966	Rhodium	Rh: 100	H_2	For joining tungsten and molybdenum to each other respectively. (With permission of British Admiralty Services Electronics Research Laboratory according to development by G. F. Gittins.)	3574	3574

* For furnace brazing of stainless steels, pure dry hydrogen of dew-point −40°F. or below should be used. Dissociated ammonia forms nitrides and is not recommended.

(D) Fluxes

Code

A (1) Liquid: 40 pts. Zinc Chloride + 20 pts. Ammonium Chloride + 40 pts. Water
(2) Paste: 90 pts. Petroleum + 10 pts. Ammonium Chloride
(3) Solution of Resin in Alcohol

B NU Braze Wonderflux No. 4. (M.P. 480°F—Water thin at 800°F)—SH

C (1) Handy Flux (Fluid 1100–1600°F) (B: 1; F: 1.8; K: 2.6; Na: 0.1). Addition of 5 to 10 per cent KOH will facilitate fluxing with certain refractory oxides.
(2) Special Handy Flux Type LT contains less fluorine, has higher M.P., is more viscous, less active and longer lived.
(3) Special Handy Flux Type H contains still less fluorine, is more difficult to wash off; for brazing above 1600°F.

TABLE 14.9. SOLDERS AND BRAZING MATERIALS. (*Continued*)

D	(1) 10 pts. Powdered Borax + 1 pt. Boracic Acid (2) Borax Applied Dry
E	Eutector Fluxes. E.W.A.
F	Flotectic Flux 1100 (1100–1500°F). E.W.A.
H_2	Hydrogen
M	Marvel (1450–1900°F) A.R.S.
A.P.1	Low Temperature Flux No. 1100. A.P.W.
A.P.2	All Purpose Flux No. 1200. A.P.W.
S1	Sil-Flux (Red) (700–1500°F). U.W.S.
S2	Sil-Flux (Blue) (800–1600°F). U.W.S.

(E) Suppliers

	Code	Products
American Platinum Works N.J.R.R. Ave. at Oliver St. Newark 5, N.J.	A.P.W.	Solders, Brazes, Fluxes, Precious Metals
Belmont Smelting & Refining Works 330 Belmont Avenue Brooklyn, N.Y.	B.S.R.	Solders, Brazes, Fluxes
Cerro De Pasco Copper Corporation 40 Wall St. New York 5, N.Y.	C.D.P.	Solders
Eutectic Welding Alloys Corporation 40-40 172nd Street Flushing, New York, N.Y.	E.W.A.	Eutectic Low Temperature Welding Alloys
General Plate Division Metals & Controls Corporation Attleboro, Massachusetts	G.P.	Solid and Laminated Precious and Base Metals
Handy & Harman 82 Fulton Street New York 7, N.Y.	H. & H.	Solders, Brazes, Fluxes

TABLE 14.9. SOLDERS AND BRAZING MATERIALS.* (*Continued*)

Indium Corp. of America 1557 Lincoln Bldg. 60 E. 42nd Street New York 17, N.Y.	I.C.A.	Solders, Brazes, Fluxes
Kester Solder Company 4201 Wrightwood Avenue Chicago 39, Illinois	K.S.C.	Solders, Fluxes
D. E. Makepiece Company Attleboro, Massachusetts	D.E.M.	Solders, Brazes, Fluxes Solid and Laminated Precious and Base Metals
National Lead Company 111 Broadway New York, N.Y.	N.L.C.	Solders, Fluxes
J. M. Ney Company 71 Elm Street Hartford, Connecticut	N.C.	Gold & Platinum Solders
Sherman & Company 36-07 Pringe Street Flushing, New York	SH	Solders, Brazes, Fluxes
United Wire & Supply Corporation Providence 7, Rhode Island	U.W.S.	Brazing Alloys
Wall Colmonoy Corporation 19345 John R Street Detroit 3, Mich.	WCC	Hard facing alloys
Western Gold & Platinum Works 589 Bryant Street San Francisco, Calif.	W.G.P.	Brazing Alloys for Electron Tubes
Wildberg Bros. Smelting & Refining Co. 742 Market Street San Francisco, Calif.	W.B.	Gold, Platinum & Silver Solders

TABLE 14.9. SOLDERS AND BRAZING MATERIALS. (*Continued*)

Air Reduction Sales Company 60 East 42nd St. New York 17, New York	A.R.S.	Welding Torches & Fluxes, Equipment
Hoke, Inc. 148 S. Dean Street Englewood, N.J.	H.I.	Precision Torches, etc.

(F) Notes

(1) Original compilation by R. O. McIntosh, Westinghouse Research Labs., East Pittsburgh. 11–16–43[4]
Revised compilation by W. H. Kohl, Collins Radio Co., Res. Labs., Cedar Rapids, Iowa. 8-15-50[4a]

(2) An effort has been made to give a fairly representative list of available compositions and their suppliers. There are many others and the selection has been arbitrary to a degree and does not imply that products not included are in any way inferior to those listed. The cooperation of the various manufacturing concerns is gratefully acknowledged.

this compilation that 20 Sn/80 Pb solder, for example, takes less heat per pound than 50 Sn/50 Pb solder to reach the liquidus temperature. It would thus be incorrect to assume from the higher liquidus temperature of 20 Sn/80 Pb solder that a hotter iron is required to do the same job that had previously been done with eutectic solder. Similarly, it is incorrect to assume that a binary solder of higher liquidus temperature results in a stronger joint than a solder of lower liquidus temperature. The "solidus" would be the better reference point although the strength of a joint is appreciably affected at half the temperature interval between room temperature and solidus.

TABLE 14.10. SPECIFIC, LATENT AND TOTAL HEAT FOR TIN-LEAD ALLOYS—BTU/LB[9]

Alloy		Mean Sp. Ht.		Latent Heat of Fusion	Total heat in Liquid at 100°F above Liquidus Btu
Sn (%)	Pb (%)	60°F to Liquidus	Liquid		
100	0	0.069	0.060	24.9	57.8
69.5	30.5	.0579	.0516	30.6	53.76
50	50	.051	.046	23	45.65
37	63	.044	.041	14.8	43.3
20	80	.0394	.0376	16.2	38.5
0	100	.032	.032	9.9	31.1

When published data on mechanical strength are evaluated, the effect of short-time loads must be carefully distinguished from continuous loads and the temperature at which the tests were performed taken into account. Table 14.11 gives comparative data[9] of the maximum safe load in psi for short-time and continuous loading for eutectic Sn/Pb versus 20/80 solder at different temperatures. Kies and Roeser[19] have reported on short-time tests of 13 solders of various compositions used for scarf joints of copper, brass, and steel with different fluxes. Schumacher, Bouton, and Phipps[20] devised a simple test for the determination of the wetting ability of solders which also permits the study of the effect of different fluxes.

"The test consists of the vertical immersion of a twisted pair of wires, at room temperature, into the solder bath at a predetermined temperature, for a given time, and the measurement of capillary rise of liquid between the wires from the surface of the solder bath to the point of maximum rise. The time of immersion used was 15 sec. The wires were of 0.040 inch diameter so twisted that adjacent turns were 0.5 inch apart, to give the equivalent of 1.0-inch pitch. The wire specimens were 2.5 inches long and were chemically cleaned and fluxed before immersion. Capillary rise is interpreted as a measure of the wetting ability of the solder under the conditions used."

Figs. 14.4 to 14.6 give some of their results. It is to be noted that the solders rise higher than tin alone, which is presumably the active wetting

TABLE 14.11. SHORT-TIME LOADS AND CONTINUOUS LOADS FOR SOLDERED JOINTS—SINGLE LAP JOINT[9]

Base Metal	Short-Time Load (Max. safe load psi)						Continuous Loads (Max. safe load psi)					
	Load at 70°F		Load at 180°F		Load at 362°F[4]		Load at 70°		Load at 180°F		Load at 362°F[4]	
	62/38	20/80	62/38	20/80	62/38	20/80	62/38	20/80	62/38	20/80	62/38	20/80
Copper[1]	4420	2100	1020	425	0	0[3]	570	275		105	0	0[3]
Copper[2]		3750			0	0[3]	785	375		175	0	0[3]
Brass[1]	6950	3300	1620	670	0	0[3]	630	300		87	0	0[3]
Brass[2]		3550			0	0[3]	730	350		150	0	0[3]
Iron-Bl[1]	5450	2600	1260	520	0	0[2]	520	250		100	0	0[3]
Iron-Bl[2]		3200			0	0[3]	680	325		135	0	0[3]
Iron-Tin[1]	4000	1900		380	0	0[3]		210		95	0	0[3]

[1] Thin sheet metal members—bend under load—shear angle 173°.

[2] Heavy metal members—no bend under load—shear angle 180°.

[3] 361°F is the solidus point at equilibrium for alloys containing 19.5 to 98.0% tin. For engineering design purposes the solidus point may well be taken as 361°F for alloys containing 10 to 98% tin.

[4] 362°F is used to avoid confusion of the state of the alloy at 361°F. With a deficiency of BTU at this point, the temperature of the alloy could be 361°F and yet most of the alloy be in a solid state.

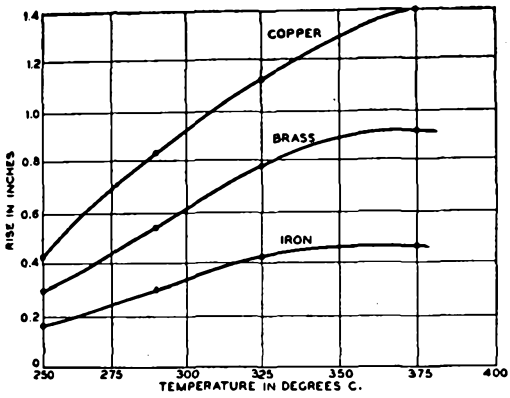

Fig. 14.4. Extent of rise for 45/55 tin-lead solder in relation to temperature, using cleaned wires. $ZnCl_2/NH_4Cl$ flux, indicated wire materials and 15 seconds immersion. After Schumacher et al.[20] (*Courtesy Materials and Methods.*)

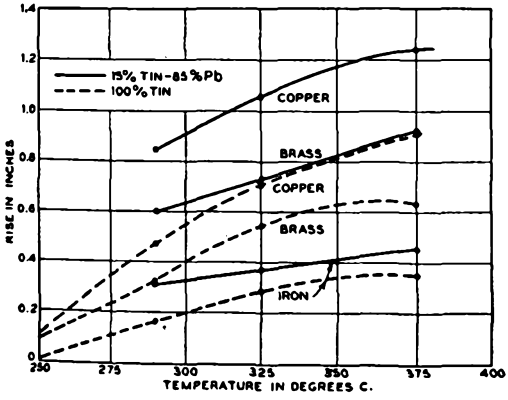

Fig. 14.5. Extent of rise of 15/85 tin-lead solder and pure tin vs. temperature, using cleaned wires of indicated materials, $ZnCl_2/NH_4Cl$ flux and 15 seconds immersion. After Schumacher et al.[20] (*Courtesy Materials and Methods.*)

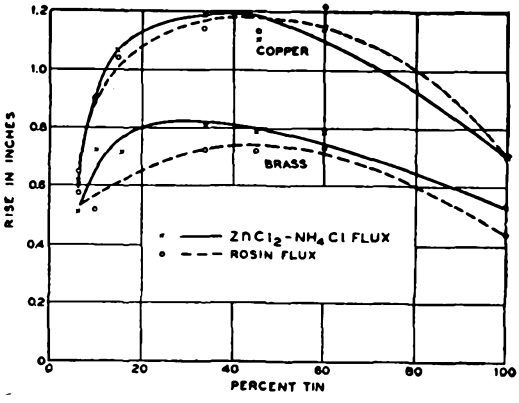

Fig. 14.6. The effect of flux on the capillary rise of tin-lead solder. Conditions as for Fig. 14.5. After Schumacher et al.[20] (*Courtesy Materials and Methods.*)

agent. There was a relatively small difference observed in the extent of rise between the 15/85 Sn/Sb and the 45/55 Sn/Pb solders; the difference in the quantity of solder that rose was rather large. Photomicrographs taken of the twisted wire section at different levels above the bath disclose a change in solder composition with height. The mechanism of this action is similar to that of a fractionation process. The low-melting components of the solder will travel farther than the high-melting components. Such segregation undoubtedly also occurs in practical solder application. Biondi[11] has reported the interesting fact that solder will not travel any farther along twisted wires than the point to which they have been immersed in hydrochloric acid. With other fluxes, such as eutectic $ZnCl_2/NH_4Cl$, wetting takes place beyond the point of flux immersion.

Earle[21] describes an ingeneous device, called the "kollagraph," which serves to measure quantitatively the jointing capacity of solders. By means of a sensitive balance and an automatic recorder the minimum effective wetting temperature (M.E.W.T.) is determined for a given solder-flux-stock combination. A flat plate of the metal under test is attached to one arm of the balance and is edge-dipped into the liquid solder, the temperature of which is controlled to within 1°C. The resultant surface-tension pull on the plate is measured by adding weights to the opposite pan of the balance in the form of a chain which keeps the balance in zero adjustment with a sensitivity of 0.2 gram. If no wetting takes place, no resultant pull will be exerted. When, on the other hand, wetting occurs, it is possible to obtain quantitative measurements of the interfacial tension exerted; and, moreover, as a nonwetting system begins to wet, observations of the change in resultant pull with time will give a clear picture of the changing conditions of the system. The apparatus records as short a period as one-fifth of a second.

Fig. 14.7 shows a typical kollagram. Time is recorded on the abscissa from right to left and the ordinate gives the interfacial pull in dynes/cm. The dip below the horizontal axis, if it occurs, represents the up-thrust on the specimen while it is resting on the unbroken surface of the molten solder before wetting begins. Its duration measures the time taken by the solder to wet the fluxed stock. Fig. 14.7 was obtained by testing copper sheet 0.012 inch thick with 40/60 Sn/Pb solder, using $ZnCl_2/NH_4Cl$ flux. The curve to the right was obtained at a solder temperature of 240°C. The solder was slow to wet and a period of 3⅝ seconds elapsed before initial wetting occurred. This may be attributed to insufficient activity of either flux or solder at this temperature, which is only a few degrees above the liquidus. During the following 5⅘ seconds this relative inactivity persisted after wetting and interfacial tension developed only gradually to an equilibrium at 258 dynes/cm. In the curve

to the left in Fig. 14.7 the solder-bath temperature is raised to 350°C and immediate development of interfacial tension results on immersion of the edge of the specimen. The equilibrium value, in this case, is 290 dynes/cm.

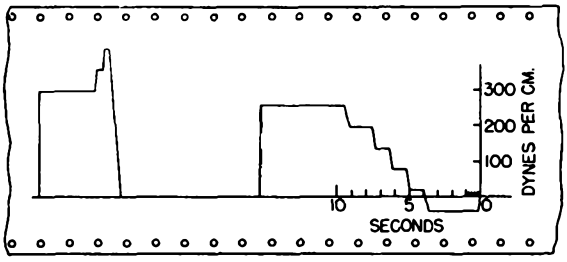

Fig. 14.7. Two typical kollagrams showing rapid and slow wetting. After L. G. Earle.[21] (*Courtesy Metal Industry, London, and Institute of Metals, London.*)

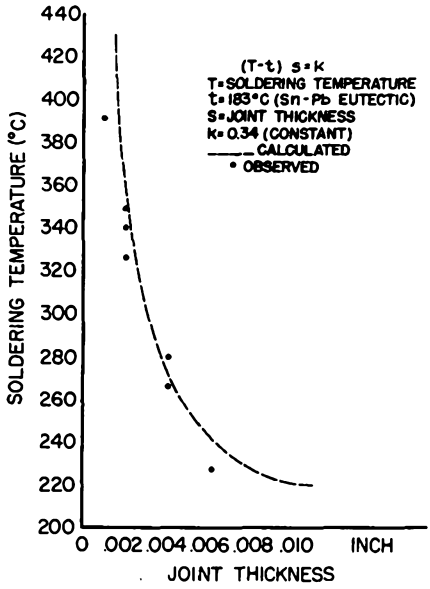

Fig. 14.8. Relation between joint thickness and soldering temperature for maximum joint strength. After S. J. Nightingale.[10] (*Courtesy British Non-Ferrous Metals Research Association and Chemical Publishing Co., New York.*)

Extensive data are reported in Earle's paper, which cannot be reproduced here in detail. Nightingale[10] has described the relation existing between joint thickness and soldering temperature for maximum joint strength, which is reproduced in Fig. 14.8.

Brazing

According to the definition given above, brazing takes place above a temperature of 800°F (427°C). The materials used for joining metals by brazing techniques are called "brazing filler metals" (formerly hard solders). Table 14.12 includes the chemical composition and permissible variations of eight silver-copper-zinc alloys, according to ASTM Standard Specification for Silver Solders,* Designation B-73-29. Table 14.13 gives U.S. Federal Specification QQ-S-561d of June 3, 1944 for Silver Solder, which comprises six classes, 0 to 6; and Table 14.14 yields U.S. Federal Specification QQ-S-551 of June 28, 1932 for Brazing Solder, consisting essentially of copper and zinc. The physical mechanism of bonding is essentially the same as with soft soldering, except that it takes place at a higher temperature. The bond is achieved below the melting point of the joined metals by the interfacial penetration of the filler metal or alloy. These alloys are non-ferrous, and are either of the silver-base or copper-base type. The former melt between 635 and 843°C and the latter from 704 to 1177°C. A subdivision into low-temperature and high-temperature brazing is thus made.

The remarks made above on the need for cleanliness of joints, for careful design and assembly, for selection of fluxes, and for control of temperature fully apply to brazing. Heat may be applied by gas torch, a chemical or metal bath, induction heating, resistance heating, or a controlled atmosphere furnace. Surrounding the work with a reducing atmosphere rich in hydrogen will generally make the use of fluxes unnecessary. Otherwise a suitable flux must be used. Several of these are listed in Table 14.9. Borax is a common brazing flux but it will not work on stainless steel. Most of the commercial brazing fluxes are alkali-fluoride-borates. A flux must not only be able to dissolve oxides but its viscosity at brazing temperature be such that it can be displaced by the brazing alloy. When the flux has become saturated with oxide it will no longer act as a flux and also be difficult to remove during clean-up. Very active, fluid fluxes are generally short-lived and viscous, sluggish fluxes are long-lived. The latter have a higher melting point and are preferable during prolonged brazing operations at high temperatures.†

The acceptable tolerances for fits of parts to be joined are much smaller and more critical than with soft-soldered joints. For electron-tube work Goodman[22] recommends 0.0005 to 0.001 inch when a base-metal filler, such as Cu, Ag, and Ni, is used; 0.0015 to 0.003 inch for eutectic alloys, such as Ag 72-Cu 28 or Au 80-Cu 20; 0.0035 to 0.002 inch for other eutectic alloys, such as Ag 50-Cu 50 or Ni 70-Cu 30, if furnace-

* "Silver Brazing Alloys" would be the correct heading for this table.

† Handy and Harman, *Tech. Bull. T*-8 (1951).

TABLE 14.12. ASTM SPECIFICATIONS FOR SILVER SOLDERS (B 73-29)
Chemical Composition

Grade	Silver (%)	Copper (%)	Zinc (%)	Cadmium (%)	Impurities (max %)	Melting Point		Flow Point		Color
						°F	°C	°F	°C	
No. 1	10	52	38	[a]	0.15	1510	820	1600	870	Yellow
No. 2	20	45	35	[a]	.15	1430	775	1500	815	Yellow
No. 3	20	45	30	5	.15	1430	775	1500	815	Yellow
No. 4	45	30	25	nil	.15	1250	675	1370	745	Nearly white
No. 5	50	34	16	nil	.15	1280	695	1425	775	Nearly white
No. 6	65	20	15	nil	.15	1280	695	1325	720	White
No. 7	70	20	10	nil	.15	1335	725	1390	755	White
No. 8	80	16	4	nil	.15	1360	740	1460	795	White

[a] The addition not to exceed 0.50% of cadmium to assist in fabricating grades Nos. 1 and 2 shall not be considered as a harmful impurity.

TABLE 14.13. UNITED STATES FEDERAL SPECIFICATIONS FOR SILVER SOLDER (*QQ*-S-561d, JUNE 3, 1944)
Chemical Composition

Class	Silver, range (%)	Copper, range (%)	Zinc, range (%)	Phosphorus, range (%)	Cadmium range (%)	Nickel, range (%)	Total other elements. (% max.)	Melting point		Flow point		Color
								(°F)	(°C)	(°F)	(°C)	
0	19–21	44–46	33–37				0.15	1,430	775	1,500	815	Yellow
1	44–46	29–31	23–27				.15	1,250	675	1,370	745	Nearly white
2	64–66	19–21	13–17				.15	1,280	695	1,325	720	White
3	14.5–15.5	79–81		4.75–5.25			.15	1,200	650	1,300	705	Gray-white
4	49–51	14.5–16.5	14.5–18.5		17–19		.15	1,160	627	1,175	635	Yellow-white
5	49–51	14.5–16.5	13.5–17.5		15–17	2.5–3.5	.15	1,195	645	1,270	688	Yellow-white
6	49–51	14.5–16.5	23–27		9–11		.15	1,166	630	1,190	641	Yellow-white

brazed. Large fillets are objectionable. The brazing alloy is usually located at the joint to be made in the form of rings, washers, disks, or foil, or applied in paste form with provisions to prevent the alloy from "running off" before entering the joint. When the heat is controlled manually, the brazing alloy or a sample thereof, located near the joint, should be visible to the operator so that overheating or inadequate heating can be avoided. With massive parts in the furnace the temperature distribution at the joint to be made is often difficult to ascertain, even from controlled furnaces, unless carefully calibrated thermocouples are directly attached to the joint.

TABLE 14.14. UNITED STATES FEDERAL SPECIFICATION FOR BRAZING SOLDER (*QQ*-S-551, JUNE 28, 1932)

Chemical Composition

Composition	Copper (%)	Tin (%)	Lead (max.) (%)	Iron (max.) (%)	Aluminum (max.) (%)	Zinc (%)
A	49–52	None[1]	0.50	0.10	0.10	([2])
B	49–52	3–4	.50	.10		([2])
C	68–72	None[1]	.30	.10		([2])
D	78–82	None[1]	.20	.10		([2])

[1] As determined on a 1-gram sample.
[2] Remainder.

The alloy phases which may occur during brazing operations are often complex and depend not only on the constituents of the brazing alloy proper but also on the base metals or alloys which are to be joined. Thus, enrichment of the brazing alloy may take place at elevated temperature by absorbing or robbing the parent-metal. In this process the "filler metal" may change its liquidus temperature and also the resulting mechanical properties unless allowance is made for this change in composition by biasing the original filler metal in the desired direction and by controlling the heat cycle in such a way that undesired changes in composition are minimized.

The eutectic 72/28 silver-copper alloy (known by various trade names which are given in Table 14.9) is very commonly used in vacuum-tube brazing because of its freedom from high-vapor-pressure components. It may well serve as a prototype for the discussion of interalloying problems. Fig. 14.9 shows the Ag-Cu equilibrium diagram from which the composition of the eutectic is seen to be Ag 71.5-Cu 28.5, with a melting point at 779.8°C or 1435°F. Any composition of this binary alloy which contains more than 28.5 weight per cent of copper, or less, will melt over a range of temperatures, which is delineated by the liquidus and solidus lines in the equilibrium diagram. A vertical line in the dia-

gram defines constant composition, and is called an "isopleth." The sloping curves AD and DF describe the solid solubility of component B in component A as a function of temperature, and correspondingly, curves BE and EG the solid solubility of component A in component B. The areas marked α and β thus represent a solid solution of copper in silver and silver in copper, respectively. In the area $ADEB$, marked $\alpha + \beta$, mixed solid solutions exist.

If a pot full of liquid brazing alloy of eutective composition* were allowed to cool slowly so that equilibrium could be established through-

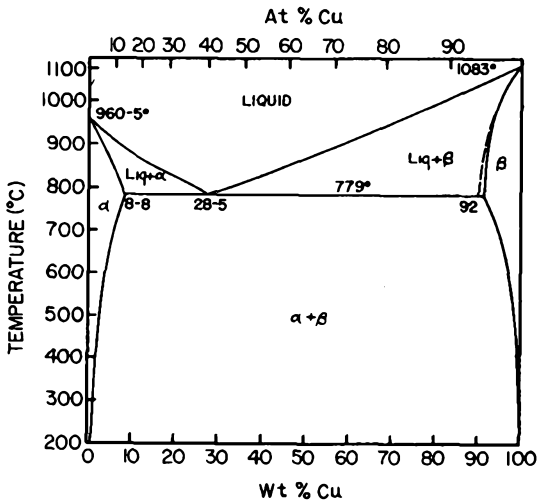

Fig. 14.9. Phase diagram for silver-copper system. After C. S. Smithells.[7] (*Courtesy Interscience Publishers, Inc., New York.*)

out its volume at any temperature level, the isopleth through C in Fig. 14.10 would permit analysis of the changes in the system as the temperature was lowered gradually from T_7 to T_1. The system will remain in the liquid phase until the eutectic point C is reached at a temperature T_3. There, the two liquidus lines CF and CG intersect and all three phases,, L, α, and β, are in equilibrium.

Applying the phase rule (Chapter 17) there are two components (i.e., Cu and Ag [C = 2]) and three phases ($P = 3$) so that $F = C + 2 - P = 1$, which makes the eutectic a univariant system as defined. Changing any of the variables temperature, pressure, or concentration would prevent the three phases from coexisting. Thus, the temperature of the sample of brazing alloy will remain constant at T_3 until all of the liquid phase has solidified and the composition of the entire volume has

* It is assumed that no reaction takes place between the wall of the container and its content.

readjusted itself continuously to conform with the one prescribed by the isopleth through C. On cooling further to T_2 and T_1 the solubility curves AD and BE will govern the redistribution of the α-phase and β-phase within the mixture of solid solutions until room temperature is reached. The cooling curve over the entire temperature range through which the experiment was carried would be represented by Fig. 14.11(a).

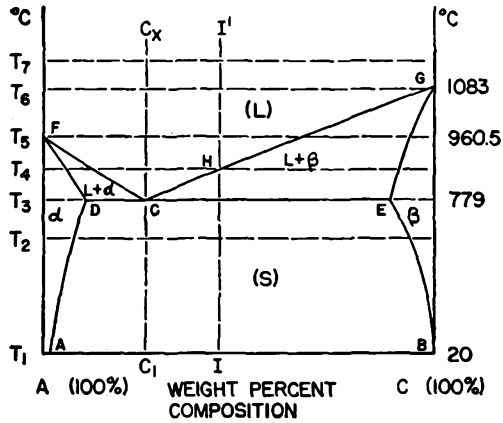

Fig. 14.10. Phase diagram for silver-copper system.

It is quite evident that the experiment would have taken a different course if some granular copper had been added from time to time to the pot containing the eutectic alloy while it was cooling from T_7 to T_3. This would have been equivalent to shifting the isopleth in Fig. 14.10 to the right toward a composition richer in copper, as indicated by $I - I'$. The liquidus at point H is at a higher temperature; on cooling, the plastic

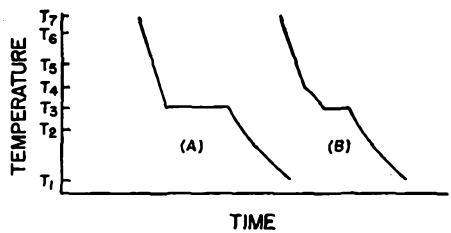

Fig. 14.11. Cooling curves for solder alloys.

region $(L + \beta)$ would be traversed, as shown by the melting curve Fig. 14.11b.

Such shifts in composition can easily occur in brazing operations when one or both of the parent metals of the joint has a tendency to dissolve in one or both of the constituent metals of the brazing alloy, or vice versa. Assuming that a braze between copper members is to be made in a furnace

with reducing atmosphere, it is relatively easy to shift the composition of the brazing alloy by large amounts; there is a very small volume of brazing alloy in comparison with the large reservoir of parent copper. At elevated temperature copper will diffuse into the brazing alloy to form a solid solution according to *DF* and silver from the brazing alloy into parent copper according to *EG* (Fig. 14.10), thus enriching the brazing alloy with copper on both counts. If the liquid phase has a chance to run out of the joint because of poor design, fractional crystallization will occur which will continue to rob the copper until the melting point of copper is reached. For these reasons it is essential to hold the joint about 50°C above the eutectic temperature for a minimum of time and then cool it quickly as soon as the brazing alloy has run into the joint. The amount of brazing alloy supplied should not be greater than necessary to fill the very small interface between members, and it is poor practice to aim for large fillets. When cooling a brazed joint quite rapidly to room temperature, so that there is not time for equilibrium to be established between the various phases of the solid, the solid solutions α and β may become supersaturated on account of the decreasing solubility with decreasing temperature (Fig. 14.10). Proper annealing may be required to re-establish or improve the mechanical properties of the structure according to the principles of precipitation hardening. When steel assemblies are to be treated thus, it is necessary to use a filler of higher melting point than exhibited by silver-copper alloys. Pure copper is most satisfactory. Copper flows very freely in the liquid state and clearance between parts should not exceed 0.001 inch. Interference fits up to 0.002 inch are recommended. These are also commonly known as "shrink fits," "drive fits," or "press fits."

"An assembly comprised of two steels having different transformation characteristics (such as a deep-hardening steel and a shallow or nonhardening steel) may also give trouble in combined brazing and heat treatment. When a steel is cooled from the heat-treating temperature, it first contracts; then, as transformation occurs it expands, and after transformation is completed, there will be further contraction. In a deep-hardening steel, the transformation will be delayed on quenching more than in a shallow-hardening steel. We then have a situation where during cooling, one part may be expanding and the other contracting at one time, and the converse situation at a later time during the quench. There are so many possible combinations of movement that it is impossible to prescribe a generally applicable cure. In one situation, a brazing alloy that will remain molten at a lower temperature may be indicated; in another situation, a higher melting point alloy may be required. In many instances, an increase in clearance will suffice."*

During the processing of intricate assemblies the need for "step brazing" often arises where the first joint is made at the highest temperature permissible and subsequent brazes are performed at progressively

* Handy and Harman, *Tech. Bull. T-7* (1950).

lower temperatures after intervening assembly operations. It is, of course, necessary that the previous joint is not weakened during the following brazing operation. Table 14.9 will offer a number of choices in any given temperature range, but proper selection must be dictated by the materials involved, the method of brazing, and the final application. For vacuum-tube components this choice narrows down to 72–28 Ag-Cu eutectic, silver, gold, and copper. The melting points of gold and copper are rather too close for comfort when a copper assembly is brazed

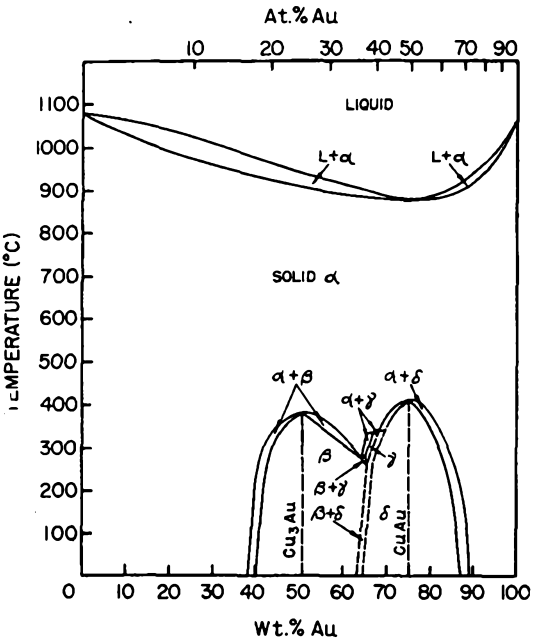

Fig. 14.12. Phase diagram for gold-copper system. After Smithells.[7] (*Courtesy Interscience Publishers, Inc.*)

with gold. Caution should prevail when several lower melting-point alloys of gold are used. The tendency toward erosion of copper by gold is even more pronounced than it is with silver and copper as copper and gold form continuous solid solutions at any percentage composition. Fig. 14.12 gives the phase diagram for the binary system Au-Cu, which discloses a congruent melting point at 884°C for the alloy Au 81.5-Cu 18.5. At temperatures below 400°C this alloy forms an intermetallic compound Au-Cu, which is brittle and hard. Its formation may be avoided by quenching from 500°C to room temperature, resulting in a ductile joint. This, however, is an awkward procedure to follow. The tendency of gold to enrich itself with copper at the brazing temperature

will shift the isopleth in the phase diagram toward the left in the composition range, 40- to 90-per cent Au, where other brittle intermetallic phases occur. Therefore, it is best to start with an alloy containing less than 40 per cent of gold by weight.

Nelson[25] reports on an alloy containing Au 37.5-Cu 62.5, which has a melting range from 950 to 990°C and gives satisfactory joints between copper and copper, copper and steel, and copper and "Fernico." A furnace temperature of 1040°C was found to be successful in most cases. The alloy is harder than annealed copper. When used as a gasket material in the form of wire rings between copper members successful diffusion seals were made by clamping the members together and baking them at 450°C for 2 hours during exhaust. The tube was then vacuum tight on removal of the clamps. Diffusion seals with pure gold have been known for some time, but are subject to the limitations mentioned above.

Electroplating parts prior to the brazing operation is at times necessary. This may serve one of two objectives. The brazing metal may be applied in this manner to assure correct placement and intimate contact over the surfaces to be joined. Ferrous and nonferrous metals are available in sheet form coated with a thin layer of silver braze, and are known as "silver solder-flushed metal." This material lends itself to many applications where the joint area is large and reliance on capillary forces to cover the joint area with brazing alloy is not safe.* Brazing sheet has been common for aluminum for some time. On the other hand, an intermediate metal coating is applied where the braze metal may not easily wet the parent-metal or where excessive grain penetration by the brazing alloy is to be avoided.

Thus, tungsten is frequently silver-plated although successful brazes of unplated tungsten filaments to copper with "BT" have been made in the author's laboratory. This was successful only after the tungsten was cleaned thoroughly by a rinse in a 50:50 by volume mixture of concentrated nitric and hydrofluoric acid, with subsequent rinses in distilled water and methyl alcohol. Platinum is being used to braze tungsten to molybdenum, and molybdenum is a brazing metal for joints between tungsten members.[26] According to J. F. Gittins of the British Admiralty Services Electronics Research Laboratory, rhodium has been used successfully as a brazing material for tungsten and/or molybdenum.

"It has been found most convenient to use 0.010-inch diameter rhodium wire. The brazing operation is performed in an atmosphere of hydrogen or argon in which the pieces to be joined are heated until the rhodium melts and held at that temperature for about 20 sec. The temperature is then lowered to prevent over-alloying between rhodium and molybdenum or tungsten. For the same reason, only the minimum

* Communication from Sherman & Company, Flushing, N.Y.

amount of rhodium should be used. No particular care is needed in cleaning the workpieces before brazing as any oxides are volatile well below the melting point of rhodium."*

Electroplating is a convenient method for applying these metals economically. Processes have been developed recently at the National Bureau of Standards for the electrodeposition of tungsten alloys containing iron, nickel, and cobalt.[27] The codeposition of tungsten and nickel was described by Vaaler and Holt.[28]

Reinartz[29] describes industrial brazing by pulse techniques, with particular application to electron tubes. During the final assembly of delicate tube parts it often happens that conventional brazing techniques cannot be used for fear of oxidizing or overheating adjacent components of the assembly. Induction heating of short duration in combination with a flux concentrator coil permits concentration of the power at the braze joint.[30] The 15 KW-400 KC-0.3 sec. pulse-type electronic brazer described by Reinartz fulfills this purpose.

* Personal communication from Mr. J. F. Gittins, to whom the writer is grateful for the release of this information. Reference to it was made during the Ann Arbor I.R.E. Tube Conference, June, 1950 by Mr. Lea Wilson of the British Joint Services Mission, Washington, D.C. Rhodium wire can be obtained from Sigmund Cohn Corp. 44 Gold St. New York 7. N.Y.

REFERENCES

1. Lewis, W. R., "Notes on Soldering," Tin Research Institute, 1948. Available in England, Fraser Rd., Greenford, Middlesex; in the United States, 492 West Sixth Avenue, Columbus 1, Ohio.
2. McKeown, J., "Properties of Soft Solders and Soldered Joints," *Res. Monogr. No.* 5, London N.W.1. Brit. Nonferrous Metals Res. Assoc., (1948).
3. National Bureau of Standards Letter Circulars 937, 938, 939, "Soldering and Brazing," *Rev. Sci. Instr.*, **20**, 707–709 (1949).
4. Feldmeier, J., "Brazing and Soldering." See Collins, G. B., "Microwave Magnetrons," *Radiation Laboratory Series No. 6*, Chap. 17, New York, McGraw-Hill Book Co., Inc., 1948.

4a. Kohl, W. H., "Solders and Brazing Materials," *Mater. and Meth. File Facts* **204**, 205 (Jan.–Feb. 1951).

5. "Metals Handbook," Cleveland, Am. Soc. for Metals, 1948.
6. "Welding Handbook," 3rd ed., New York, Am. Welding Soc., 1950.
7. Smithells, C. J., "Metals Reference Book," New York, Interscience Publishers, Inc., 1949.
8. Moss, A. R., and Brooker, H. R., "Some Aspects of German Soldering, Brazing, and Welding Methods," *Final Report No. 184*, Item No. 21, Brit. Intell. Objectives Sub-Committee, H. M. Stationary Office, London (1946).
9. Mample, A. Z., "Soldering with Tin-Lead Alloys," *Mater. and Meth.*, **21**, 702–707 (1945); **21**, 1000–1006 (1945).
10. Nightingale, S. J., "Tin Solders," London, Brit. Nonferrous Metals Research Assoc., 2nd ed. 1942.

11. Biondi, F. J., "Metal Fabrication, Soldering, and Brazing," Bell Telephone Laboratories, Inc. (Talk given on 4/21/47 before the New York Section of the American Society of Metals.)
12. Sowter, A. B., "Materials Joined by New Cold Welding Process," *Mater. and Meth.*, **28**, 60–63 (1948).
13. "Cold Welding," *Fortune*, 114–116, 120, 122 (Sept., 1950).
14. Dushman, S., "Scientific Foundations of Vacuum Technique," New York, John Wiley and Sons, Inc., 1949.
15. Rose, K., "Low-Tin Solders," *Mater. and Meth.*, **22**, 1125, File Facts No. 93 (Oct., 1945).
16. Seeds, O. J., "How to Select and Use Low-Melting Alloys as Production Aids," *Mater. and Meth.*, **32**, 64–68 (Sept., 1950).
17. Grymko, S. M., and Jaffee, R. I., "New Indium-Bearing Solders Have Improved Alkali Resistance," *Mater. and Meth.*, **31**, 59–60 (1950).
18. Jaffee, R. I., Minarcik, E. J., and Gonser, B. W., "Low-Temperature Properties of Lead-Base Solders and Soldered Joints," *Metal Progress*, **54**, 843–845 (1948).
18a. Hachmeister, K., "The Phenomena of Melting, Freezing, and Boiling for Mixtures of Ammoniumchloride and other Chlorides." (In German.) *Zs. Anorg. Allg. Chem.* **109**, 145–186 (1919).
19. Kies, J. A., and Roesser, W. F., "Solders and Soldered Joints," *Mech. World*, **116**, 434–435, 448 (1944).
20. Schumacher, E. E., Bouton, G. M., and Phipps, G. S., "Soft-Solder Selection Aided by Simple Test," *Mater. and Meth.*, **22**, 1407–1410 (1945).
21. Earle, L. G., "Soft Solders, Determination of 'Jointing Capacity' by the Kollagraph," *J. Inst. of Metals*, **71**, 45, 1945; also *Metal Ind.*, 308–311, 322–325 (May, 1945).
22. Goodman, I. S., "Welding and Brazing Techniques in the Electron-Tube Industry," *Transact. El. Chem. Soc.*, **87**, 261–274 (1945).
23. *Welding Journal*, **17**, 26–33 (1938); **19**, 754–758 (1940).
24. Setapen, A. M., "Silver-Alloy Brazing with Induction Heating," *Transact. El. Chem. Soc.*, **86**, 1–22 (1944).
25. Nelson, R. B., "A Gold-Copper Alloy Solder, Pb-15151," General Electric Co., OEMsr-931 (1944); *U.S. Patent 242467*, (Aug. 26, 1947).
26. "New Outlook in Brazing," *Fortune*, 127–132 (Oct., 1948).
27. Breuner, A., Burkhead, P., and Seegmiller, E., "Electrodeposition of Tungsten Alloys Containing Iron, Nickel, and Cobalt," *J. Res. Nat. Bur. Stand.*, **39**, 351–383 (1947). (RP1834.)
28. Vaaler, L. E., and Holt, M. L., "Tungsten and Nickel," *Metal Ind.* (Nov. 22, 1946).
29. Reinartz, J. L., "Industrial Brazing by Pulse Techniques," *Electronics*, **23**, 78–80 (1950).
30. Babat, G., and Losinsky, M., "Concentrator of Eddy Currents for Zonal Heating of Steel Parts," *J. Appl. Phys.*, **11**, 816–823 (1940).

CHAPTER 15
CERAMICS AND MICA

Introduction

In a broad sense we come now to the treatment of the "earthy materials," which have occupied an important position in the design and production of electron tubes from the very beginning of the tube art. Glass is, of course, a member of this family, but on account of its transparency and noncrystallinity it occupies a special position which has been dealt with at length in the early chapters. The tube engineer thinks of ceramics primarily in regard to refractory insulators. Cathode heaters for receiving tubes were inserted in ceramic sleeves in the early days in order to insulate the heater from the nickel sleeve. Now, this insulation is provided by coating the heater wire directly with a water suspension of aluminum oxide, which is sintered onto the wire by high-temperature firing in a neutral atmosphere.[1,1a] It is still a ceramic coating. In an effort to simplify the heater problem conductive ceramic rods* have recently been introduced commercially.[2] Porous ceramics are treated with hydrocarbon gases at elevated temperature to obtain the desired conductivity. Such heater rods may then be inserted into conventional nickel sleeves which carry the cathode coating, or they may be coated directly. High current density thoria-emitters represent another application of ceramic bodies which has interested tube engineers for many years. (See Chapter 19.) Various types of ceramic spacers for insulation and support of tube electrodes are employed in both large and small tubes. The use of ceramics for tube envelopes has gained in importance over glass since the latter is too fragile and has a low softening point.

If we add to this enumeration the extensive use of ceramics for circuit components, such as resistors, condensers, transducers, printed circuits, coil forms, etc., there can be little doubt that a ceramist should be included on the staff of a modern tube laboratory. Or, to put it differently, the tube engineer must have a workable knowledge of ceramics, powder metallurgy, and solid-state physics. This will be necessary at least to the extent of being able intelligently to appraise a problem that

* The author made a variety of extruded ceramic heaters early in 1940.

might arise and to recognize the scope of special investigations required and equipment needed to carry the investigation to a conclusion.

All that this chapter can hope to convey is an appreciation of the complexity of this field and of its many applications in electronics. For more detailed study the reader is again referred to the references.[3–8] In following this course the tube designer and development engineer, who are not ordinarily trained in the field of ceramics, then find themselves confronted with a vast new terminology. This handicap will at least be eliminated in this chapter as the basic terminology and description of materials will be given. To go much further would be beyond the scope of this text.

The word "ceramics" derives from the Greek "Keramos," standing for potters' earth or clay. It is a noun used to describe pottery or earthenware but the use of ceramic as an adjective has also been suggested. A definition given by Thurnauer[9] states that ceramics are inorganic materials which are brought to permanent shape and hardness by high-temperature firing. Such materials as abrasives, cements, enamels, glass, clay products, refractories, terra cotta, and white ware are thus covered by this definition. High-melting point metals, which are often called "refractory metals," are not ceramics, but are often produced by methods akin to those used in the field of ceramics (i.e., pressing from powders and firing at high temperatures). The term "powder metallurgy" covers these procedures when a metallic body is the end product.

Mica, which is a natural mineral and is used in its natural form without firing, is not a ceramic although many ceramics contain similar oxide constituents as mica. In view of the importance of natural mica in the tube industry this material will be discussed in this chapter. Glass-bonded mica, known under the trade names of "Mycalex,"* "Mykroy,"† and others, is a compound of ground mica and low-melting glasses—in most cases lead borate—obtained by pressing and heating the powdered materials in a mold; it is a ceramic *product.*

A new class of materials called "Cerametals," "Cermets" or "Ceramals" is reaching an increasing importance for high-temperature applications. These are metal ceramics consisting of mixtures of metal powders and metal-oxide powders processed into solids by the methods of powder metallurgy.[10,11] Powdered iron cores and permanent magnet materials, which comprise a mixture of finely powdered iron and powdered organic plastics or metal oxides for the insulation of the metal particles, could be mentioned in this connection although they are not used at high temperature and not classified as "Cerametals."

* Mycalex Corporation of America, 60 Clifton Blvd., Clifton, N.J.

† Electronic Mechanics, Inc., 70 Clifton Blvd., Clifton, N.J.

Raw Materials and Their Fabrication

The constituents of porcelain are clay, feldspar, and flint, in varying proportions, depending on the desired characteristics of the end product. Clay is the plastic component while feldspar and flint are nonplastic. Flint is rock quartz of high purity (SiO_2) and provides the skeleton, so to speak, of the composite structure. Feldspar is an alkaline aluminum silicate (Na_2O/K_2O-Al_2O_3-$6SiO_2$), which occurs also in rock formations. It fuses on heating and dissolves part of the clay and flint, thus acting as a flux. Clay or kaolin (Al_2O_3-$2SiO_2$-$2H_2O$) is a hydrous aluminum silicate which results from the natural decomposition of feldspars. It may be regarded as the filler of the skeleton of flint. All three components are in interaction during the firing process, leading to a complex re-orientation of the crystal structure of the whole body.

The natural minerals, refractory rocks, clays, and earths which go into the blending of ceramics are of various origins, and they usually differ in their properties, depending on the place of origin for one specific material. Tube engineers may have come to appreciate the high quality of Italian lava grade talc, or soapstone, after its supply was cut off before World War II. There is only one deposit in the United States (in Montana) which furnishes a satisfactory grade of soapstone from which blocks for tube insulators can be cut and machined for experimental samples.* The early refractories industry in the United States used large amounts of clays imported from Europe until the 1850's, when native deposits came into use. Siliceous rock for the lining of iron furnaces had to be transported by wagons over long distances, and the same applied to New Jersey clay, which was used for firebrick, replacing the rock lining of furnaces after 1800.

For the purpose of reference Table 15.1 lists the names of some natural minerals, together with their formula of composition, fusion point, occurrence, specific gravity, and hardness.[3] Table 15.2 similarly gives refractory rocks, clays, and earths from the same reference. Mohs' hardness was given for the basic minerals of this scale in Table 13.3 (p. 283). While there are more than 1500 species of minerals, only a few hundred occur in significant deposits. Table 15.1 is confined to the refractory minerals. (*Text continued on p. 358*)

* Due to the scarcity of mica in Germany during World War II, spacers for small electron tubes were made of block talc by cutting the material into small slices of 0.5 to 0.6 mm thickness and punching the holes into the soft material which subsequently was hardened by firing. Hardened German block talc had a very small shrinkage on firing, of the order of 2 per cent, and the accuracy of the hole distances was far superior to any common ceramic discs or plates. This technique was initiated by Dr. Albers-Schoenberg and production grew to considerable proportions. (The author is indebted to Dr. Albers-Schoenberg for submitting this information.)

TABLE 15.1. NATURAL MINERALS[3]

Material	Formula	Fusion Point (pure)	Occurrence	Sp. Gr.	Hardness
Allophane	$Al_2SiO_5 \cdot nH_2O$		Few deposits	1.88–1.94	3
Alumian	$Al_2O_3 \cdot 2SO_3$ (perhaps)		Very rare	2.70–2.78	2–3
Aluminite	$Al_2O_3 \cdot SO_3 \cdot 9H_2O$		Not common	1.66	1–2
Alunite	$K_2O \cdot 3Al_2O_3 \cdot 4SO_3 \cdot 6H_2O$		Commercial deposits	2.63–2.73	3.5–4
Alunogen	$Al_2O_3 \cdot 3SO_3 \cdot 16H_2O$		Rare	1.72–1.74	1.5–2
Amesite	$(Mg,Fe)_4 \cdot 4Al_2 \cdot 2Si_2 \cdot 4O_{10}(OH)_8$		Very rare	2.77	2.5–3
Anauxite	$Al_8(Si_4O_{10})_3(OH)_{12} \cdot 3H_2O$		Uncommon	2.5–2.4	2.5
Ancylite	$2Ce_2O_3 \cdot 3SrO \cdot 7CO_2 \cdot 5H_2O$		Very rare	3.82	4.5
Andalusite	Al_2SiO_5	1816°C (3301°F)	A few workable deposits	3.12–3.29	7.5
Ankerite	$(Ca,Mg,Fe)CO_3$		Occurs with dolomite	2.99–3.19	3.5–4
Apjohnite	$MnO \cdot Al_2O_3 \cdot 4SO_3 \cdot 22 \pm H_2O$		Very rare	1.78	1.5
Aragonite	$CaCO_3$	2570°C (4658°F)	Uncommon	2.86–3.15	3.5–4
Augelite	$2Al_2O_3 \cdot P_2O_5 \cdot 3H_2O$		Very rare	2.77	4.5–5
Aurichalcite	$5(Zn,Cu)O \cdot 2CO_2 \cdot 3H_2O$		Uncommon	3.27–3.64	2
Baddeleyite	ZrO_2	2700°C (4892°F)	Few deposits	5.5–6.03	6.5
Barite	$BaSO_4$	1580°C (2876°F)	Commercial deposits	4.62	2.5–3.5
Barylite	$BaBe_2Si_2O_7$		Very rare	4.03	7
Beckelite	$Ca_3(Ce,La,Di)_4Si_3O_{15}$		Very rare	4.15	5
Beidellite	$Al_8(Si_4O_{10})_3(OH)_{12} \cdot 12H_2O$		Widespread		
Bertrandite	$Be_4Si_2O_7(OH)_2$		Rare	2.59–2.60	6–7
Beryl	$Al_2Be_3Si_6O_{18}$	1410–1430°C (2570–2606°F)	Commercial deposits	2.55–2.91	7.5–8
Brookite	TiO_2	1900°C (3451°F)	Rare	3.97	5.5–6
Brucite	$Mg(OH)_2$	2800°C (5072°F)	Commercial deposits rare	2.38–2.39	2.5

Bunsenite	NiO
Calcite	$CaCO_3$
Cassiterite	SnO_2
Celsian	$BaAl_2Si_2O_2$
Cerite	$(Ce,Y,Pr,Nd)_2Si_2O_7 \cdot H_2O$
Chalcedony	SiO_2
Chalcophanite	$(Mn,Zn)O \cdot 2MnO_2 \cdot 2H_2O$
Chondrodite	$Mg_5(SiO_4)_2(OH,F)_2$
Chromite	$FeCr_2O_4$
Chrysoberyl	$BeAl_2O_4$
Chrysocolla	$CuSiO_3 \cdot 2H_2O$
Churchite	$(Ce,Ca)PO_4 \cdot 2H_2O$
Clinoenstatite	$Mg_2Si_2O_6$
Clinohumite	$Mg_9(SiO_4)_4(OH,F)_2$
Columbite	$(Fe,Mn)(Nb,Ta)_2O_6$
Cordierite	$(Mg,Fe,Mn)_2(Al,Fe)_4\ Si_5O_{18} \cdot H_2O$
Corundum	Al_2O_3
Cristobalite	SiO_2
Derbylite	$6FeO \cdot Sb_2O_3 \cdot 5TiO_2$
Diamond	C
Diaspore	$AlO(OH)$
Dickite	$Al_2Si_2O_5(OH)_4$
Dioptase	H_2CuSiO_4
Dolomite	$CaMg(CO_3)_2$

	Very rare	6.40	5.5
2570°C (4658°F)	Commercial deposits	2.70–2.82	3
	Commercial deposits (not in U.S.A.)	6.72–6.91	6–7
	Very rare	3.3–3.45	6–6.5
	Very rare	4.86–4.91	5.5
1715°C (3119°F)	Commercial deposits	2.55–2.63	6
	Rare	3.91	2.5
	Rare	3.18	6–6.5
2180°C (3956°F)	Numerous workable deposits	4.32–4.57	5.5
	Commercial deposits rare	3.49–3.73	8.5
	Uncommon	2.40–2.42	2–4
	Very rare	3.14	3–3.5
	Rare	3.19	6
	Rare	3.1–3.21	6–6.5
	Uncommon	5.15–6.85	6
		2.57–2.66	7–7.5
2050°C (3722°F)	Commercial deposits	3.97–4.03	9
1715°C (3200°F)	Very rare	2.32–2.36	6–7
	Very rare	4.51–4.53	5
	Very rare	3.51–3.51	10
2035°C (3695°F)	Many deposits	3.39	6.5–7
1785°C (3245°F)	In some clays; uncommon	2.62	2.5
	Very rare	3.30–3.32	5
2570–2800°C (4658–5072°F)	Commercial deposits	2.83–2.99	3.5–4

TABLE 15.1. NATURAL MINERALS (*Continued*)

Material	Formula	Fusion Point (pure)	Occurrence	Sp. Gr.	Hardness
Dumortierite	$AlB_3Si_3O_{19}(OH)$		Very rare	3.30–3.36	7
Dysanalyte	$7(Ca,Ce,Fe,Na_2)O{\cdot}6TiO_2{\cdot}Cb_2O_5$		Very rare	4.26	5–6
Euxenite	Columbate and titanite of Y, Er, Ce, U, etc.		Very rare	4.59–4.99	6.5
Evansite	$2AlPO_4{\cdot}4Al(OH)_3{\cdot}12H_2O$		Very rare	1.92–1.93	3.5–4
Fergusonite	$Y(Nb,Ta)O_4$		Very rare	4.98–5.78	5.5–6
Fermorite	$(Ca,Sr)_4[Ca(OH,F)][(P,As)O_4]_3$		Rare	3.52	5
Fluellite	$AlF_3{\cdot}H_2O$		Very rare	2.17	3
Fluocerite	$(Ce,La,Di)F_3$		Very rare	5.73	4
Forsterite	Mg_2SiO_4	1910°C (3470°F)	Uncommon	3.22–3.27	6–7
Franklinite	$(Zn,Fe,Mn)(Fe,Mn)_2O_4$		Uncommon	5.09	5.5–6.5
Gadolinite	$(Al,Fe''',Ti)_2Fe''Be_2(SiO_4)_2O_2$		Very rare	4.0–4.6	6.5–7
Gahnite	$ZnAl_2O_4$		Rare	4.48–4.60	7.5–8
Garnierite	Perhaps $H_2(Ni,Mg)SiO_4 + H_2O$ very variable		Widespread	2.27–2.87	1–3
Geikielite	$(Mg,Fe)TiO_3$		Rare	3.98–4	6
Gibbsite (hydrargillite)	$Al(OH)_3$	2035°C (3695°F)	Common	2.3–2.42	2.5–3.5
Goethite	$HFeO_2$		Widespread	4.18–4.48	5–5.5
Goslarite	$ZnSO_4.7H_2O$		Rare	1.9–2.1	2–2.5
Grandidierite	$2Na_2O{\cdot}4FeO{\cdot}8(Fe,Al,B)_2O_3{\cdot}5SiO_2$		Very rare	2.99	7.5
Graphite	C		A few deposits	2.22	1–2
Greenockite	CdS		Rare	4.82	3–3.5
Grothine	Silicate of Ca, Al, Fe (uncertain)		Very rare	3.08–3.09	
Gummite	Doubtful composition, alternative product of uraninite		Rare	5.08	2.5–3
Halloysite	$Al_4Si_4O_{10}(OH)_8{\cdot}H_2O$	1775°C (3227°F)	A few deposits	2.44–2.71	1–2

Hambergite	$Be_2BO_3(OH)$		Rare	2.36	7.5
Hatchettolite	Tantalocolumbate of U, Ca, etc.		Very rare	4.42–4.51	5
Hausmanite	Mn_3O_4		Uncommon	4.78–4.84	5–5.5
Hematite	Fe_2O_3		Common	5.17–5.26	5–6.5
Hematolite	$8MnO\cdot(Al,Mn)_2O_3\cdot As_2O_5\cdot 8H_2O$		Very rare	3.30–3.40	3.5
Hercynite	$FeAl_2O_4$		Rare	4.01	7.5–8
Hinsdalite	$2PbO\cdot 3Al_2O_3\cdot 2SO_3\cdot P_2O_5\cdot 6H_2O$		Rare	3.65	4.5
Hisingerite	Fe_2O_3,MgO,FeO, SiO_2, H_2O, etc.		Rare	2.50	3–3.5
Högbomite	$MgO\cdot 2(Al,Fe)_2O_3$, some TiO_2		Rare	3.81	6.5
Humite	$Mg_7(SiO_4)_3(OH,F)_2$		Rare	3.1–3.2	6–6.5
Hydromagnesite	$4MgO\cdot 3CO_2\cdot 4H_2O$		Uncommon	2.15–2.16	3.5
Hydrotalcite	$6MgO\cdot Al_2O_3\cdot CO_2\cdot 12H_2O$		Rare	2.04–2.09	2
Hydrozincite	$7ZnO\cdot 3CO_2\cdot 4H_2O$		Uncommon	3.58–3.8	2.0–2.5
Iddingsite	$MgO\cdot Fe_2O_3\cdot 3SiO_2\cdot 4H_2O$		Widespread	2.54–2.80	2.5–3
Ilmenite	$FeTiO_3$		Common	4.44–4.86	5–6
Incobsite	$MnFe_2O_4$		Uncommon	4.75–4.76	6
Kaliophilite	$(K,Na)(Al,Si)_2O_4$		Uncommon	2.56–2.61	6
Kaolinite	$Al_2Si_2O_5(OH)_4$	1785°C (3245°F)	Common in clays	2.6–2.63	2–2.5
Kehoeite	$3(Zn,Ca)O\cdot 2Al_2O_3\cdot P_2O_5\cdot 27 \pm H_2O$		Very rare	2.34	
Koppite	$2(Ca,Ce,\text{etc.})O\cdot Cb_2O_5\cdot \frac{2}{5}NaF$		Rare	4.45–4.56	5.5
Kornerupine	Near $MgAl_2SiO_6$		Very rare	3.27–3.34	6.5
Kreittonite	$(Zn\cdot Fe)(Al\cdot Fe)_2O_4$		Uncommon	4.48–4.89	7–8
Kyanite	Al_2SiO_5		Small deposits	3.28–3.59	4–7
Langbanite	Sb_2O_3, Fe_2O_3,Mn_2O_3,SiO_2		Very rare	4.6–4.8	6.5
Lansfordite	$MgO\cdot CO_2\cdot 5H_2O$		Very rare	1.69–1.73	2.5
Lazulite	$AlPO_4(Fe,Mg)(OH)_2$		Rare	2.96	5–6
Limonite	$Fe_2O_3\cdot nH_2O$		Common	3.87	4–5.5
Mackintoshite	$(U,Ce,Th,La,Y,Pb)_2SiO_5$		Very rare	5.44	5.5
Magnesioferrite	$MgFe_2O_4$		Rare	4.57–4.65	6–6.5
Magnesite	$MgCO_3$	2800°C (5072°F)	Commercial deposits	2.95–3.12	3.5–4.5

TABLE 15.1. NATURAL MINERALS. (*Continued*)

Material	Formula	Fusion Point (pure)	Occurrence	Sp. Gr.	Hardness
Manganite	$Mn(OH)O$		Uncommon	4.29	4–5
Manganosite	MnO		Very rare	5.36	5–6
Martinite	$H_2Ca_5(PO_4)_4 \cdot \frac{1}{2}H_2O$		Very rare	2.89	
Melanocerite	$Ca_{16}Na_4(Y,La)_8(Zr,Ce)6Be_3Si_{12}O_{57}F_{12}$		Very rare	4.13	5–6
Mesitite	$(Fe,Mg)CO_3$		Widely distributed	3.38	
Metavansite	$Al_2O_3 \cdot P_2O_5 \cdot 4H_2O$	> 1500°C (> 2732°F)	Rare	2.54	4
Microlite	Essentially $Ca_2Ta_2O_7$		Very rare	5.41–5.56	5.5
Miloschite	$(Al,Cr)_2O_3 \cdot 2SiO_2 \cdot 2H_2O$		Very rare	2.13	1.5–2.5
Moissanite (natural) (silicon carbide synthetic)	SiC	2500°C (4532°F)	Unique	3.2	9.5
Molybdenite	MoS_2		A few extensive commercial deposits	4.62	1–1.5
Monazite	$(La,Ce,Y)PO_4$		A few deposits	5.11–5.31	5–5.5
Montmorillonite	$(OH)_2 \cdot Al_2[Si_2O_5]_2 \cdot nH_2O$		Common	2.04–2.52	Soft
Morenosite	$NiSO_4 \cdot 7H_2O$		Fairly rare	2	2–2.5
Nacrite	$Al_2Si_2O_5(OH)_4$	1785°C (3245°F)	Very rare	2.5+	2.5
Nephelite	$(Na,K)(Al,Si)_2O_4$	1526°C (2779°F)		2.53–2.66	5.5–6
Nontronite	Member of beidellite group		Uncommon	2.29–2.30	
Norbergite	$Mg_3(SiO_4)(OH,F)_2$		Rare	3.13–3.15	6.5
Octahedrite	TiO_2	1900°C (3452°F)	Rare	3.95	5.5–6
Olivine	$(Mg,Fe)SiO_4$	1700–1910°C (3092–3470°F)	Common	3.2–3.3	6.5–7
Opal	$SiO_2 \cdot nH_2O$	1715°C (3119°F)	A few deposits	2.06–2.22	5.5–6.5

Parisite	$2(Ce,La,Di,Th)OF \cdot CaO \cdot 3CO_2$
Periclase	MgO
Perovskite	$CaTiO_3$
Phenacite	Be_2SiO_4
Picotite	$(Mg,Fe)(AlCr)_2O_4$
Pigeonite	$(Ca,Mg)(Mg,Fe)Si_2O_6$
Polianite	MnO_2
Polycrase	Columbate and titanate of Y, U, Th, Fe, etc.
Polymignite	Columbate, titanate, zirconate of Ce, etc.
Prosopite	$CaF_2 \cdot 2Al(F,OH)_3 \cdot H_2O$
Pseudobrookite	Fe_2TiO_5
Pyroaurite	$6MgO \cdot Fe_2O_3 \cdot CO_2 \cdot 12H_2O$
Pyrochlore	Columbate and titanate of Ce, Ca, et. with Th, F, etc.
Pyrolusite	MnO_2
Pyrope	$Mg_3Al_2(SiO_4)_3$
Pyrophanite	$MnO \cdot TiO_2$
Pyrophyllite	$Al_2Si_4O_{10}(OH)_2$
Quartz	SiO_2
Ralstonite	$(Na_2,Mg)F_2 \cdot 3Al(F,OH)_3.2H_2O$
Retzian	Arsenate of Y, Mn, Ca, etc., and H_2O
Rhabdophanite	$(Y,Er,La,Di)_2O_3 \cdot P_2O_5 \cdot 2H_2O$
Rhodochrosite	$MnCO_3$
Rhodolite	$3(Mg,Fe)O \cdot Al_2O_3 \cdot 3SiO_2$
Risörite	$Cb_2O_5(Y,Er)_2O_3 \cdot H_2O$ some Ta, Ti, Ce, La, etc.
Rosieresite	Hydrous phosphate of Al, Pb and Cu

	Rare	4.32	4.5
2800°C (5072°F)	Rare	3.64–3.67	5.5–6
	Commercial deposits unknown	3.95–4.04	5.5
2000°C (3632°F)	Rare	2.94–3.04	7.5–8
	Rare	4.08	
	Widespread	3.2–3.4	6
	Rare	4.84–5.03	6–6.5
	Rare	4.97–5.04	5–6
	Very rare	4.77–4.85	6.5
	Rare	2.88–2.89	4.5
	Rare	4.60	6
	Rare	2.07	2–3
	Very rare	4.2–4.36	5–5.3
	Uncommon	4.75–4.89	2–2.5
	Uncommon	3.51–3.75	7–7.5
	Very rare	4.54	5
	Rare	2.66	1–3
1715°C (3119°F)	Very plentiful	2.65–2.70	7
	Very rare	2.61	4.5
	Very rare	4.15	4
	Very rare	3.94–4.01	3.5
	Small deposits	3.31–3.74	3.5–4.5
	Rare	3.75–3.84	7–7.5
1720°C (3128°F)	Very rare	4.18	5.5
	Very rare	2.2	

TABLE 15.1. NATURAL MINERALS. (*Continued*)

Material	Formula	Fusion Point (pure)	Occurrence	Sp. Gr.	Hardness
Rowlandite	$(Y,Ce,La)_4Fe''(Si_2O_7)_2 \cdot F_2$		Very rare	4.52	6–7
Rutile	TiO_2	1900°C (3452°F)	Few large deposits but widely distributed	4.12–4.27	6–6.5
Saponite	$(Mg,Fe'')_{3.28}(Al,Fe''')_{.72}Si_{3.64}O_{10}$-$(OH)_{3.28} \cdot 4H_2O$			2.18–2.31	Soft
Sapphirine	$Mg_5Al_{12}Si_2O_{27}$		Rare	3.3–3.5	7.5
Schneebergite	$2CaO \cdot Sb_2O_4$		Rare	5.41	6.5
Schroetterite	$3Al_2O_3 \cdot SiO_2 \cdot nH_2O$		Rare	1.95–2.05	3–3.5
Sillimanite	Al_2SiO_5	1816°C (3300°F)	A few commercial deposits	3.23–3.24	6–7.5
Sipylite	Columbate of Er, La, Di, U, etc.		Very rare	4.89	6
Smithsonite	$ZnCO_3$		Widespread	4.19–4.41	4.5–5
Sphaerocobaltite	$CoCO_3$		Rare	4.02–4.13	3–4
Spinel	$MgAl_2O_4$	2135°C (3875°F)	Small deposits	3.68–3.92	8
Spurrite	$5CaO \cdot CO_2 \cdot 2SiO_2$		Rare	3.01	5
Stibiconite	$Sk_2O_4 \cdot nH_2O$		Rare	5.1–5.3	4–5
Stichtite	$6MgO \cdot Cr_2O_3 \cdot CO_2 \cdot 12H_2O$		Rare	2.16	1.75
Symplesite	$3FeO \cdot As_2O_5 \cdot 8H_2O$		Very rare	2.96	2.5
Szmikite	$MnO \cdot SO_3 \cdot H_2O$		Very rare	3.15	1.5
Tantalite	$(Fe,Mn)O \cdot (Ta,Ch)_2O_5$			6.5–8.20	6
Tapiolite	$FeO \cdot (Ta,Cb)_2O_5$		Very rare	7.19–7.91	6
Tavistockite	$3CaO \cdot Al_2O_3 \cdot P_2O_5 \cdot 2H_2O$		Very rare		
Thalenite	$(Al,Fe''',Ti)_2Si_2O_7$		Very rare	4.45	6.5
Thaumasite	$3CaO \cdot CO_2 \cdot SO_3 \cdot SiO_2 \cdot 15H_2O$		Rare	1.85–1.88	3.5
Thorianite	Chiefly $(Th, U)O_2$	1660°C (3020°F)	Very rare	9.33	6.5
Thorite	$ThSiO_4$		Rare	5.2–5.4	4.5–5

Topaz	$Al_2SiO_4(F,OH)_2$
Tridymite	SiO_2
Tungstite	$WO_3 \cdot H_2O$
Turquoise	$CuO \cdot 3Al_2O_3 \cdot 2P_2O_5 \cdot 9H_2O$
Uraninite	A uranate of U, Pb, Th, Zr, and metals of La and Y groups
Uranophane	$CaU_2Si_2O_{11} \cdot 7H_2O$
Uranothallite	$2CaO \cdot UO_2 \cdot 4CO_2 \cdot 10H_2O$
Uvarovite	$Ca_3Cr_2(SiO_4)_3$
Variscite	$Al_2O_3 \cdot P_2O_5 \cdot 4H_2O$
Vashegyite	$3Al_2O_3 \cdot 2P_2O_5 \cdot 18 \pm H_2O$ (about)
Voelckerite	$10CaO \cdot 3P_2O_5 P_2O_5$
Volchonskoite	$(Al,Fe''',Cr)_4(Si_4O_{10})(OH)_8$
Voltzite	$ZnO \cdot 4ZnS$
Wavellite	$3Al_2O_3 \cdot 2P_2O_5 \cdot 13(H_2O \cdot 2HF)$
Whewellite	$CaO \cdot C_2O_3 \cdot H_2O$
Wiikite	Columbate, titanate, and silicate of Fe and rare earths
Willemite	Zn_2SiO_4
Xenotime	YPO_4
Yttrialite	$(Y,Th)_2O_3 \cdot 2SiO_2$
Yttrocrasite	Hydrous titanate of Th, Y, etc.
Zebedassite	$5MgO \cdot Al_2O_3 6SiO_2 \cdot 4H_2O$
Zepharovichite	$Al_2O_3 \cdot P_2O_5 \cdot 6H_2O$
Zincaluminite	$6ZnO \cdot 3Al_2O_3 \cdot 2SO_3 \cdot 18H_2O$
Zincite	ZnO
Zircon	$ZrSiO_4$
Zirkelite	$(Ce,Fe,Ca)O \cdot 2(Zr,Ti,Th)O_2$
Zunyite	$Al_8(SiO_4)_3(F,Cl,OH)_{12}$

	Commercial deposits scarce	3.35–3.59	8
	Rare	2.27–2.27	7
	Rare	5.5	2.5
	Rare	2.84	5
	Rare	7.13–9.79	5.5
	Rare	3.81–3.96	2–3
	Rare		2.5–3
	Rare	3.42–3.81	6.5–7.5
	Rare	2.47	4
	Rare	1.96	2–3
1540°C (2804°F)	Not common	3.06–3.10	
	Rare	2.2–2.3	2.5
	Very rare	3.66–3.80	4.0–4.5
	Uncommon	2.33	3.5–4
	Rare	2.23	2.5
	Very rare	3.8–4.8	6
	Uncommon	3.89–4.19	5.5
	Uncommon	4.55	4–5
	Very rare	4.58	5–5.5
	Rare	4.80	5.5–6
	Very rare	2.19	2
> 1500°C (> 2732°F)	Very rare	2.37	5.5
	Very rare	2.26	2.5–3
	Rare	5.43–5.7	4.0–4.5
2550°C (4622°F)	Few deposits	4.05–4.75	7.5
	Very rare	4.3–5.22	5.5
	Very rare	2.88	7

The fabrication of the raw materials into finished ware comprises a number of steps, each of which has a critical influence on the quality of the end product. As these lines are not written for the specialist in this field but for the novice in the art who may wish to try his skill on a new article of which only a few are required, it should be emphasized that the success or failure of his experiment may well hinge on his appreciation of the critical importance of each step in preparing a ceramic body. The raw minerals must be reduced to a powder of suitable particle-size distribution and freed of undesirable impurities. Fortunately, most

TABLE 15.2. REFRACTORY ROCKS, CLAYS, AND EARTHS[3]

Material	Approximate Formula	Fusion Point (pure)	Density	Hardness	Occurrence
Bauxite (mixture of gibbsite and kaolin)	$Al_2O_3 \cdot nSiO_2 \cdot nH_2O$	3722°C (6732°F)	2–2.6		Scattered deposits
Chrome ore	$(FeCr)_2O_3$	2185°C (3965°F)	4.3–4.6	5.5	A few deposits
Diaspore	Al O(OH)	3722°C (6732°F)	3.4–3.6	6.5–7	Small deposits
Diatomaceous earth	SiO_2	1715°C (3119°F)	0.8–1.2 (bulk)		Widespread
Dolomite	$(Ca, Mg, Fe)CO_3$		2.5–3	4	Common
Ganister	SiO_2	1715°C (3119°F)	2.65	7	A few large deposits
Gibbsite	$Al(OH)_3$	2035°C (3695°F)	2.4 ±	2.3–2.4	A few deposits
High-grade fireclay	$Al_2O_3 \cdot 2SiO_2 \cdot 2H_2O$		2.62	2	Widespread
Kaolin	$Al_2O_3 \cdot 2SiO_2 \cdot 2H_2O$	1785°C (3245°F)	2.62	2	Many deposits
Limestone	$CaCO_3$	2570°C (4658°F)	2.4–2.8	3	Common
Low-grade fireclay	$Al_2O_3 \cdot 2SiO_2 \cdot 2H_2O$		2.62	2	Widespread
Magnesite	$MgCO_3$	2800°C (5072°F)	2.96	3.5–4.5	Numerous deposits

minerals, powdered and refined, can be obtained from mineral dealers. The critical amounts of constituent powders must be intimately mixed either in the dry or wet state and sufficient amounts of water or organic binder added to produce the desired plasticity. A prolonged kneading process generally achieves this objective. In mechanized operations this is done by a pugmill, which often removes occluded air at the same time in order to obtain a denser body. In forming the body into the desired shape there are three alternatives: wet forming, slip casting, or dry pressing.

Wet forming might be called the "mud-pie technique." It implies shaping the clay by hand or with simple tools on the potter's wheel, an art dating back to prehistoric times. On the other hand, the raw cake in its wet condition, containing about 25 per cent of water, may be

pressed into a plaster of Paris mold. This may be done by rotating the mold on a potter's wheel and by pressing the clay against its surface by means of a contour-shaping tool (jiggering). The porous wall of the mold will then absorb some of the moisture of the body and cause it to set dry and to shrink away from the mold. After removal from the mold the body is in the "green" state, and preliminary oven drying will make it "leather-hard" and permit trimming to dimension and removal of mold marks. Firing or "maturing" at the requisite temperature for the proper duration (bisque-fire) and controlled cooling will transform the body into a hard permanent form, after which it may then be glazed by a second firing at a lower temperature (glost-fire), if desired.

The extrustion of tubes or cylinders or rods from dies is another wet-forming process. This may be done in auger machines or hydraulic presses.[12,13,14] During the firing or sintering of the body a substantial shrinkage in volume occurs, depending on the composition and to some extent the shape of the body. Allowance must naturally be made for shrinkage when shaping the body before firing. Common tolerances are established for different body types. Finish grinding is necessary when closer tolerances are required.

Slip casting or casting of ceramics requires a creamlike fluidity of the raw material. To obtain a uniform distribution of the components in the suspension medium and maintain its colloidal nature deflocculants, such as silicates of soda and soda ash, are added. The proper preparation of slip is still an art which depends to a large extent on established formulas and on the know-how of the operator. The water content of the slip is about 40 per cent. The slip is poured into a mold of plaster of Paris, which takes up moisture from the slip and causes a solid shell to form. The slip in the center is then poured out (drain casting), and after further drying the body is removed from the mold, whereupon the subsequent treatment is the same essentially as for wet forming. The thickness of the body may be built up by successive pourings of the slip.

Dry pressing refers to the pressing of a relatively dry granular mass containing from 0 to 12 per cent of water in steel dies under considerable pressure. The processes of drying and firing are again similar to those used with wet forming.

Two methods of forming are gaining in importance. Isostatic pressing permits the compacting of powders in rubber molds. These molds are inserted in a liquid to which pressure is applied.[15] The other method consists of combining the ceramic powder with a temporary plastic binder, molding the heated and soft mass, and burning out the binder before sintering.[16]

After the firing process of the ceramic body is completed, a glaze may be applied and fired at a lower temperature. This may serve to seal the

pores to provide nonperveance to gases on less dense bodies, reduce water absorption and thus increase volume resistivity (although the surface resistivity may be decreased), or just add luster and color. Glazes are also used to increase the mechanical strength of ceramics. For this purpose the thermal expansion coefficient of the glaze is chosen to be less than that of the body to which it is applied so that the glaze is in a state of compression. This compression must not be excessive as otherwise "chipping" or "peeling" will occur. In the opposite case, with the glaze having a higher expansion than the body, it will be in tension and liable to develop numerous cracks (crazing). Variations in glaze fit can affect the mechanical strength of porcelain by 300 to 400 per cent.[17] Self-glazing bodies (cordierites) have also been developed.

Special Ceramic Compositions

In considering the various ceramic compositions available it is difficult to select one which will satisfy all the needs of the worker in the field of electronics. There is hardly a body which does not fulfill a particular need in one of the many problems that arise from time to time in the laboratory or factory. There are many grades of firebrick for furnace linings. Permeable bricks can be used for interesting furnace designs, where combustible gas mixtures are fed through the furnace wall to burn on the inside of a muffle or through pipes and make them burn on the outside, as the author has demonstrated. Sometimes furnace trays which stand up under severe heat shock when passing from the hot to the cool zone in hydrogen furnaces are a problem, requiring careful selection of the ceramic body, if such has to be used. Thermocouple protective tubes for high-temperature service often need special attention. Ceramic coil forms with low coefficient of thermal expansion for stable oscillator circuits are a critical item. High dielectric-constant ceramics for condensers represent a special group where great advances have been made in recent years. Finally, the very extensive use of ceramics for electrical insulation under the most varying conditions of operation covers an application with which the electronics engineer is most intimately concerned. The tube engineer, in particular, will distinguish between insulators used inside or outside the tube or as an integral part of the tube envelope. Different types of ceramic bodies have been developed for applications where low-voltage or high-voltage and low-frequency or high-frequency predominate in different combinations.

Table 15.3 gives the general composition of typical white-ware bodies.[18] Also indicated in this table are the firing ranges in terms of cone-numbers and their equivalent temperatures. Table 15.4 gives the pertinent data on pyrometric cones. A cone is a trihedral pyramid made of a mixture of materials as used in classical bodies (Table 15.3); thus, they behave similarly in a thermochemical sense and provide useful

pyrometric guides for the proper firing of ceramics in terms of time and temperature. ASTM Specification C-24-46 covers the details of preparation and mounting cones and the Pyrometric Cone Equivalent (P.C.E.), based on the work of Fairchild and Peters.[19]

TABLE 15.3. GENERAL COMPOSITION OF SOME CERAMICS[18]

	Chemical Porcelain	Normal Porcelains	Electrical Porcelains	Vitreous China	Sanitary Porcelain	Fine Earthenware
	Cone 12–14 (2390–2534F)	Cone 12–14 (2390–2534F)	Cone 11–13 (2345–2462F)	Cone 10–11 (2300–2345F)	Cone 9–11 (2282–2345F)	Cone 8–9 (2237–2282F)
Feldspar or Nepheline Syenite	20–5	20–28	28–38	10–18	30–36	10–16
Whiting	0–1	0–1	0–3	0–1.5		
Dolomite				0–3.0		
Ball Clay	0–5		15–35	10–20	16–25	20–35
Kaolin, China Clay	50–58	40–50	20–35	20–30	20–30	20–35
Silica (200 Mesh "Flint")	10–15	22–35	15–25	30–38	20–30	32–36

Electrical Porcelain

Electrical porcelains for high-voltage insulation at low frequencies are generally produced by wet-forming the intimately mixed raw materials (on the average, 50 per cent clay, 25 per cent feldspar, and 25 per cent flint). After firing near 1400°C a dense vitrified ware, which has good mechanical strength and a high dielectric strength, is produced. However, its power factor is rather high, its heat shock resistance only fair, and its electrical resistivity rapidly decreasing with increase in temperature. Very large shapes can be produced at reasonable cost.[20] Typical characteristics are given in Table 15.5.

Porcelains are essentially two-phase bodies, consisting of approximately 60 per cent crystalline matter (silica and mullite) imbedded in 40 per cent glass. It is the presence of glass components, in particular, which causes the high loss factor of porcelains. This is readily understood if one bears in mind that the high polarizability of sodium ions present in glasses derive from sodaspar. A decrease of the feldspar component would lessen the dielectric strength of the porcelain and require higher firing temperatures, both undesirable consequences from the standpoint of the user and manufacturer, respectively. For high-frequency application, where a low loss factor is of prime importance, new bodies thus had to be developed. For convenience, Equation 5.4, which gives the power dissipated in a dielectric, is repeated here:

$$\frac{\text{Watts}}{\text{cm}^3} = 0.555 \times \text{loss factor} \times \text{frequency (MC)} \times \left[\text{field strength}\left(\frac{\text{kv}}{\text{cm}}\right)\right]^2$$

TABLE 15.4. CHARACTERISTICS OF PYROMETRIC CONES

Definition: Pyrometric Cone Equivalent (P. C. E.)—In the case of refractories, the number of that standard pyrometric cone whose tip would touch the supporting plaque simultaneously with a cone of the material being investigated when tested in accordance with the Standard Method of Test for Pyrometric Cone Equivalent of Refractory Materials (A. S. T. M. Designations C-24) of the American Society for Testing Materials.

Note: The terms "fusion point," "softening point," "deformation point" and "melting point" have heretofore been loosely used for "pyrometric cone equivalent."

Pyrometric Cone Equivalents in Degrees Fahrenheit and Centigrade

	No. of Cone	150°C. End Point			No. of Cone	150°C. End Point	
		Degrees Cent.	Degrees Fahr.			Degrees Cent.	Degrees Fahr.
The Soft Series	022	605	1121	The Intermediate Temperature Series	7	1250	2282
	021	615	1139		8	1260	2300
	020	650	1202		9	1285	2345
	019	660	1220		10	1305	2381
	018	720	1328		11	1325	2417
	017	770	1418		12	1335	2435
	016	795	1463		13	1350	2462
	015	805	1481		14	1400	2552
	014	830	1526		15	1435	2615
	013	860	1580		16	1465	2669
	012	875	1607		17	1475	2687
	011	905	1661		18	1490	2714
					19	1520	2768
The Low Temperature Series	010	895	1643		20	1530	2786
	09	930	1706	The High Temperature Series	23	1580	2876
	08	950	1742		26	1595	2903
	07	990	1814		27	1605	2921
	06	1015	1859		28	1615	2939
	05	1040	1904		29	1640	2984
	04	1060	1940		30	1650	3002
	03	1115	2039		31	1680	3056
	02	1125	2057		32	1700	3092
	01	1145	2093		33	1745	3173
	1	1160	2120		34	1760	3200
	2	1165	2129		35	1785	3245
	3	1170	2138		36	1810	3290
	4	1190	2174		37	1820	3308
	5	1205	2201		38	1835	3335
	6	1230	2246				

NOTE: Pyrometric cones do not give an accurate measurement of temperature. Where it is desired to interpret P. C. E. values approximately in terms of temperature the table above may be used. This table has been approved by the A. S. T. M. It is based on the work of Fairchild and Peters, J. Amer. Cer. Soc. 9, 701–43, 1926. Heating rate 150°C per hour cone 022 to 20 and 100°C per hour cone 23 to 38. The temperatures do not apply to the slower rates of heating common in the commercial firing and the use of refractory materials.

TABLE 15.5. TYPICAL CHARACTERISTICS OF ELECTRICAL PORCELAIN

Dielectric constant	6.5–7.0
Power factor (1000 KC–50 MC)	0.007–0.02
Loss factor (1000 KC–50 MC)	5.2–105
Dielectric strength	
(For 2.5 cm thickness)	130–150 volts/mil
Volume resistivity at 22°C[21]	3×10^{14} ohm-cm
Surface resistivity at 22°C[21]	
Unglazed	6×10^{11} (50 % Humidity)
Unglazed	5×10^{6} (90 " ")
Glazed	2×10^{12} (50 " ")
Glazed	5×10^{8} (90 " ")

Steatites

Steatites were first introduced in Germany for low-frequency, high-voltage insulation in 1890,* and became commercially available for high-frequency insulation under the trade names "Frequenta,"* "Steatit,"* "Calit,"† and "Calan"† in the late 1920's. In the United States they were introduced as "Alsimag 35"‡ in 1930, and continuously improved. "Ultra-Steatite"§ and "Isolantite"‖ are other examples of these bodies, produced in very large quantities in this country for military requirements during World War II. The demand was such that in 1943 six companies yielded 14 times the volume produced in 1939.[22]

Steatites are essentially one-phase bodies, consisting of a close-knit crystal lattice of magnesium metasilicate $MgO{\cdot}SiO_2$ in the form of clinoenstatite or one of its polymorphous forms. The silicates are bonded together with an alkaline or alkaline-earth glass in most cases, and cristobalite (SiO_2) may be present as a result of the thermal dissociation of the talc or clay. A typical batch composition would be 60 per cent or more talc ($3\ MgO\text{-}4\ SiO_2\text{-}H_2O$); 30 per cent or less clay or kaolin ($Al_2O_3\text{-}2\ SiO_2\text{-}2\ H_2O$), to which alkali or alkaline earth oxides are added as flux, and organic binders, such as natural water, soluble gums, starches, dextrines, methyl cellulose, polyvinyl alcohol, or waxes. The mix is fired in the range from 1300 to 1400°C, depending on its composition.

Steatites are characterized by a very "short firing range," by which the ceramist describes the temperature span in which vitrification takes place. Staying below this range will produce porosity because of "underfiring" and exceeding the prescribed firing range will lead to distortion or vesicular development because of "over-firing." The firing range for steatites may vary from 10 to 20°C for ultra low-loss

* Steatit Magnesia A. G. Lauf, Bavaria, Germany.

† Hermsdorf-Schönberg Isolatoren Ges. Hermsdorf, Thuringia, Germany.

‡ American Lava Corp., Chattanooga, Tennessee.

§ General Ceramics Company, Keasby, N.J.

‖ Formerly, the Isolantite Inc., Belleville, N.J.

TABLE 15.6. AMERICAN WAR STANDARD C-75.1—1943. CERAMIC RADIO-INSULATING MATERIALS, CLASS L. AMERICAN STANDARDS ASSOCIATION (A.S.A.)

Grade	Loss Factor
L-1	0.150 or less
L-2	0.070 or less
L-3	0.035 or less
L-4	0.016 or less
L-5	0.008 or less
L-6	0.004 or less

types to possibly 30 to 40°C for ordinary types. By comparison, many porcelains have firing ranges of 50 to 90°C.[23] Very accurate temperature control is thus necessary during the firing of steatites.

TABLE 15.7. TYPICAL APPLICATIONS AND PHYSICAL PROPERTIES

	Vitrified Products			
	Chemical and High Voltage Porcelain	Alumina Porcelain	Zircon Porcelain	Steatite
Typical Applications	Chemical laboratory ware, power line insulation	Sparkplug cores, thermocouple insulation, protection tubes	Sparkplug cores, high voltage-high temp. insulation	High frequency insulation, electrical appliance insulation
Specific gravity (g/cc)	2.3–2.5	3.1–3.9	3.0–3.8	2.5–2.7
Water absorption (%)	0	0	0	0
Mohs hardness	7	8.5–9.0	7.5–8.5	7:0–7.5
Coefficient of linear thermal expansion per °C (20–700)	$5.0–6.8 \times 10^{-6}$	$5.5–8.1 \times 10^{-6}$	$3.5–5.5 \times 10^{-6}$	$8.6–10.5 \times 10^{-6}$
Safe operating temp. (°C)	1,000	1,350–1,500	1,000–1,200	1,000–1,100
Thermal conductivity (cal/cm²/cm/sec/°C)	0.002–0.005	0.007–0.05	0.010–0.015	0.005–0.006
Tensile strength (psi)	3,000–8,000	8,000–30,000	10,000–15,000	8,000–10,000
Compressive strength (psi)	25,000–50,000	80,000–250,000	80,000–150,000	65,000–130,000
Flexural strength (psi)	9,000–15,000	20,000–45,000	20,000–35,000	16,000–24,000
Impact strength, ft-lb	0.2–0.3	0.5–0.7	0.4–0.5	0.3–0.4
Modulus of elasticity (psi)	$7–14 \times 10^6$	$15–52 \times 10^6$	$20–30 \times 10^6$	$13–15 \times 10^6$
Thermal shock resistance	moderately good	excellent	good	moderate
Dielectric strength (volts/mil) (¼-in. thick specimen)	250–400	400	250–350	200–350
Resistivity (ohm-cm) at room temp.	$10^{12}–10^{14}$	$10^{14}–10^{15}$	$10^{13}–10^{15}$	$10^{12}–10^{15}$
Te-value (C)	300–500	700	700	450–1000
Power factor at 1 mc	0.006–0.010	0.001–0.002	0.0002–0.0020	0.0002–0.0035
Dielectric constant	6–7	7.3–11.0	8.0–10.5	5.5–7.5
Loss factor at 1 mc	0.036–0.070	0.007–0.022	0.0016–0.0210	0.001–0.026

The proper selection of the raw materials is also very critical. The mines located in California and Montana yield grades of talc which are suitable for steatite production, but none reach the purity of Manchurian or Indian talc. Thus, for extremely low-loss steatites imported talc is still being used in the United States. For the latter type, extremely small crystal size is also very important. Furthermore, it has been found

that it is possible to obtain materials which have as their main crystalline constituent magnesium orthosilicate (forsterite). These bodies have such low dielectric losses that they can be classified under designation L-6 of the Joint Army Navy Air Force Specification Jan-I-8. Table 15.6 gives this classification, originally written by the American Standards Association.

A porous, low loss body containing forsterite was produced in Germany under the trade name "Ergan" and used extensively during World War II for supports in Cathode Ray Tube mounts. Ergan was machined in the fired state by hard alloy tools to close tolerances. Its dielectric constant was 4.5 and its power factor 3 to 5 $\times 10^{-4}$.

OF SOME TECHNICAL CERAMIC MATERIALS (AND 2 GLASSES)*

			Porous and Refractory Products			
Titania, Titanate Ceramics	Corning 7070 Glass	Fused Silica†	Low Voltage Porcelain	Cordierite Refractories	Alumina, Aluminum Silicate Refractories	Massive Fired Talc, Pyrophyllite
Ceramic capacitors, lightning arrester insulation	Low Loss insulation	Low loss, high temp. insulation	Switch bases, low voltage wire holders, light receptacles	Resistor supports, burner tips, heat insulation, arc chambers	Vacuum spacers, high temp. insulation	High frequency insulation, vacuum tube spacers, ceramic models
3.5–4	2.13	2.2	2.2–2.4	1.6–2.1	2.2–2.4	2.3–2.8
0	0.0–0.01	0	0.5–2.0	5–15	10–20	1.0–3.0
7–8	7	4.9	7	7	7–8	6
7.0–10.0 $\times 10^{-6}$	3.2 $\times 10^{-6}$	0.55 $\times 10^{-6}$	5.0–6.5 $\times 10^{-6}$	2.5–3.0 $\times 10^{-6}$	5.0–7.0 $\times 10^{-6}$	3.6 pyrophyllite, 11.5 talc
800–1,000	230–430 (annealed)	900–1,200	900	1250	1,300–1,600	1200
0.008–0.01	0.0028‡	0.0033	0.004–0.005	0.003–0.004	0.004–0.005	0.003–0.005
4000–10,000			1,500–2,500	1,000–3,500	700–3,000	2,500
40,000–120,000	See Table 1.2 and text		25,000–50,000	20,000–45,000	15,000–60,000	20,000–30,000
10,000–22,000	Chap. 1 p. 5		3,500–6,000	1,500–7,000	1,500–6,000	7,000–9,000
0.3–0.5			0.2–0.3	0.2–0.25	0.17–0.25	0.2–0.3
10–15 $\times 10^6$	6.8 $\times 10^6$	1.02 $\times 10^7$	7–10 $\times 10^6$	2–5 $\times 10^6$	2–5 $\times 10^6$	4–5 $\times 10^6$
poor	good	excellent	moderate	excellent	excellent	good
50–300	200–400	410	40–100	40–100	40–100	80–100
10^8–10^{16}	> 10^{17}	$10^{10.5}$	10^{12}–10^{14}	10^{12}–10^{14}	10^{12}–10^{14}	10^{12}–10^{15}
	10^9 at 350°C	(at 350°C)				
200–400			300–400	400–700	400–700	600–900
0.0002–0.050	0.0006	0.00023	0.010–0.020	0.004–0.010	0.0002–0.010	0.0008–0.010
15–5000	4.0 (at 1 MC)	4.1	6.0–7.0	4.5–5.5	4.5–6.5	5–6
	0.0024 (at 1 MC)	0.0009	0.060–0.140	0.018–0.055	0.0009–0.065	0.004–0.060
	0.008 (at 10^4 MC)					

* According to H. Thurnauer[24] with addition of data on Corning Glass 7070 and Silica by present author.
† Ref. 25.
‡ Approximate.

The over-all physical characteristics of steatite in comparison to those of other ceramic materials may be gleaned from Table 15.7, which has been taken, with some extension and revision, from Ref. 24. Table 15.8

(*Text continued on p. 372*)

TABLE 15.8. MECHANICAL AND ELECTRICAL PROPERTIES OF ALSIMAG CERAMICS††

Materials shown have been grouped according to vitrification, impervious dense materials on the left with increasing porosity toward the right, classified by moisture absorption, as follows:

Impervious.. 0 to .02% Technically Vitreous.. .5 to 3%
Vitrified..... .02 to .5% Semivitreous..... 3 to 10%
Highly Porous..... Above 10%

Measurements shown are average values from test pieces. Production articles may vary slightly, depending on size, shape and method of manufacture.

			Vitreous Ceramic Materials								
			Fine Texture								
			Steatite—Chiefly Clinoenstatite Crystals $MgO \cdot SiO_2$				Forsterite $2MgO \cdot SiO_2$	Titanium Dioxide TiO_2	Zircon $ZrO_2 \cdot SiO_2$	Alumina Al_2O_3	Alumina Al_2O_3
			Alsimag 35 L-3	Alsimag 196 L-4	Alsimag 228 L-4 Unglazed L-5 Glazed	Alsimag 197*	Alsimag 243 L-5Unglazed L-6 Glazed	Alsimag 192 (Patented)	Alsimag 475	Alsimag 491†	Alsimag 513†
Property	A. S. T. M. Test Number	Unit	High strength insulators with good electrical characteristics, made to close tolerances for household equipment and appliances.	Lower dielectric losses than Alsimag 35. High strength insulators made to accurate dimensions for radio frequency circuits.	Excellent mechanical properties with lower electrical losses than Alsimag 196. For use in high frequency equipment.	Mechanically strong with high electrical resistance at elevated temperatures. For heater wire supports in appliances.	For service where very low loss insulators are required. For ceramic to metal seals. Close tolerances obtainable by grinding.	Ceramic for polished thread guides. Alsimag 193 is the same mechanically but made an electrical conductor to dissipate static.	Vitrified ceramic with excellent electrical properties, high strength and good resistance to thermal shock.	Fine texture, extremely hard, resistant to abrasion, chipping and corrosion. Best adopted to small size machined or pressed parts.	High Strength alumina ceramic for somewhat larger size articles than possible in 491, made by both machining and pressing methods.
Water Absorption	D116-42(A)	%	0 to .02 Impervious	0 to .02 Impervious	0 to .02 Impervious	.02 to 1 Vitrified to Techn. Vitreous	0 to .02 Impervious	0 to .02 Impervious	0 to .02 Impervious	0 to .02 Impervious	0 to .02 Impervious
Specific Gravity	—	—	2.5	2.6	2.7	2.6	2.8	4.0	3.7	3.5	3.4
Density	—	Lbs. per cu. in.	.090	.094	.098	.094	.101	.144	.134	.125	.122
Standard Body Colors[a]	—	—	White	White	White	White	Buff	Tan	White	Blue	Gray
Alternative Body Colors	—	—	206 Gray 207 Brown	—	—	209 Gray 210 Brown	—	—	—	—	—
Softening Temperature	C24-46	°C °F	1 450 2 642	1 440 2 624	1 440 2 624	1 445 2 633	1 440 2 624	1 450 2 642	1 440 2 624	1 750 3 182	1 700 3 092
Safe Temperature at Continuous Heat	--	°C °F	1 000 1 832	1 000 1 832	1 000 1 832	1 000 1 832	1 000 1 832	1 000 1 832	1 100 2 012	1 400 2 552	1 350 2 462

Hardness	—	Mohs' Scale[b]	7.5	7.5	7.5	7.5	7.5	8	8	9	9
Thermal Expansion Linear Coefficient	—	Per °C 25–100°C 25–700°C	6.9×10^{-6} 8.7×10^{-6}	7.3×10^{-6} 8.6×10^{-6}	6.4×10^{-6} 8.9×10^{-6}	7.7×10^{-6} 10.2×10^{-6}	9.1×10^{-6} 10.6×10^{-6}	7.3×10^{-6} 8.7×10^{-6}	3.2×10^{-6} 4.1×10^{-6}	6.2×10^{-6} 7.7×10^{-6}	3.3×10^{-6} 7.5×10^{-6}
Tensile Strength	D116-42	Lbs. per sq. in.	8 500	10 000	10 000	8 500	10 000	7 500	12 000		
Compressive Strength	D667-42T	Lbs. per sq. in.	75 000	85 000	85 000	75 000	85 000	80 000	90 000	100 000	100 000
Flexural Strength	D667-42T	Lbs. per sq. in.	18 000	20 000	20 000	20 000	20 000	20 000	22 000	45 000	45 000
Resistance to Impact (½" rod)	Charpy D667-42T	Inch-Lbs.	4.5	5.0	4.0	4.5	4.0	6.5	5.5	6.0	7.0
Thermal Conductivity[c] (Approximate Values)	—	g. cal. × cm. thick / cm² × sec. × deg. C	.006	.006	.006	.006	.008	.009	.012	.02	.02
Dielectric Strength (step 60 cycles) Test discs ¼" thick	D667-42T	Volts per mil	225	240	240	210	240	100	250	250	250
Volume Resistivity at Various Temperatures: 25°C	—	Ohms per centimeter cube	$>10^{14}$	$>10^{14}$	$>10^{14}$	$>10^{14}$	$>10^{14}$	$>10^{12}$	$>10^{14}$	$>10^{14}$	$>10^{14}$
100°C			2.1×10^{12}	1.0×10^{13}	$>10^{14}$	8.1×10^{13}	5.0×10^{13}	9.8×10^{11}	2.0×10^{13}	$>10^{14}$	$>10^{14}$
300°C			6.0×10^{7}	6.5×10^{9}	8.0×10^{10}	2.5×10^{10}	7.0×10^{11}	1.0×10^{9}	5.5×10^{11}	1.7×10^{11}	6.3×10^{8}
500°C			3.2×10^{5}	4.0×10^{7}	3.0×10^{8}	8.8×10^{7}	1.2×10^{10}	1.7×10^{6}	5.5×10^{8}	2.0×10^{7}	1.7×10^{8}
700°C			2.3×10^{4}	1.8×10^{6}	5.0×10^{6}	4.2×10^{6}	1.0×10^{8}	2.5×10^{4}	1.4×10^{7}	6.2×10^{5}	8.0×10^{4}
900°C			7.0×10^{3}	3.0×10^{5}	4.0×10^{5}	6.8×10^{5}	3.0×10^{6}	$>1 \times 10^{4}$	8.2×10^{5}	8.0×10^{4}	1.4×10^{4}
Te Value[d]	—	°C °F	440 824	750 1 382	820 1 508	840 1 544	>1 000 >1 832	520 968	870 1 598	670 1 238	525 977
Dielectric Constant: 60 Cycles	D667-42T	—	6.1	5.9	6.2	6.3	6.3	85	—	—	—
1 MC			5.9	5.8	6.1	6.0	6.2	85	9.1	8.6	7.9
10 MC			5.8	5.7	6.1	5.8	6.2	85	—	—	—
100 MC			5.7	5.6	6.0	5.7	6.1	85	—	—	—
Power Factor[e]: 60 Cycles	D667-42T	—	.0150	.0022	.0013	.0020	.0014	.0010	—	—	—
1 MC			.0035	.0021	.0013	.0012	.0004	.0005	.0008	.002	.004
10 MC			.0030	.0015	.0011	.0010	.0003	.0006	—	—	—
100 MC			.0028	.0014	.0010	.0009	.0003	.0007	—	—	—

TABLE 15.8. MECHANICAL AND ELECTRICAL PROPERTIES OF ALSIMAG CERAMICS†† (*Continued*)

			Vitreous Ceramic Materials								
			Fine Texture								
			Steatite—Chiefly Clinoenstatite Crystals $MgO \cdot SiO_2$				Forsterite $2MgO \cdot SiO_2$	Titanium Dioxide TiO_2	Zircon $ZrO_2 \cdot SiO_2$	Alumina Al_2O_3	Alumina Al_2O_3
			Alsimag 35 L-3	Alsimag 196 L-4	Alsimag 228 L-4 Unglazed L-5 Glazed	Alsimag 197*	Alsimag 243 L-5Unglazed L-6 Glazed	Alsimag 192 (Patented)	Alsimag 475	Alsimag 491†	Alsimag 513†
Property	A. S. T. M. Test Number	Unit	High strength insulators with good electrical characteristics made to close tolerances for household equipment and appliances.	Lower dielectric losses than Alsimag 35. High strength insulators made to accurate dimensions for radio frequency circuits.	Excellent mechanical properties with lower electrical losses than Alsimag 196. For use in high frequency equipment.	Mechanically strong with high electrical resistance at elevated temperatures. For heater wire supports in appliances.	For service where very low loss insulators are required. For ceramic to metal seals. Close tolerances obtainable by grinding.	Ceramic for polished thread guides. Alsimag 193 is the same mechanically but made an electrical conductor to dissipate static.	Vitrified ceramic with excellent electrical properties, high strength and good resistance to thermal shock.	Fine texture, extremely hard, resistant to abrasion, chipping and corrosion. Best adopted to small size machined or pressed parts.	High Strength alumina ceramic for somewhat larger size articles than possible in 491, made by both machining and pressing methods.
Loss Factor[e] 60 Cycles	D667-42T	—	.090	.013	.008	.013	.002	—	—	—	—
Loss Factor[e] 1 MC			.021	.012	.008	.007	.002	—	.007	.017	.032
Loss Factor[e] 10 MC			.017	.008	.006	.006	.002	—	—	—	—
Loss Factor[e] 100 MC			.016	.008	.006	.005	.002	—	—	—	—
Capacity Change Per °C	—	Parts per million	+160	+160	+160	+160	+130	−750	—	+120	+160

* Alsimag 202 is porous, will withstand heat shock, whereas 197 is dense and is intended for service where high Te value is essential.
† Economic, limitations on sizes and shapes.
[a] Standard glaze is white. Brown and other colors available on some bodies.
[b] Ceramic materials cannot be measured by Rockwell or Brinell methods.
[c] Conversion factor:

$$\frac{\text{g. cal.} \times \text{cm. thick}}{\text{cm}^2 \times \text{sec.} \times \text{deg. C.}} = 2903 \frac{\text{BTU} \times \text{in. thick}}{\text{sq. ft.} \times \text{hr.} \times \text{deg. F.}}$$

[d] Te value is the temperature at which a centimeter cube has a resistance of one megohm.
[e] Alsimag 35, 196, 228 and 243 measured wet, after immersion in water for 48 hours. (JAN-1-10)
†† American Lava Corporation, Chattanooga 5, Tennessee.

TABLE 15.8. MECHANICAL AND ELECTRICAL PROPERTIES OF ALSIMAG CERAMICS (*Continued*)

Materials shown have been grouped according to vitrification, impervious dense materials on the left with increasing porosity toward the right, classified by moisture absorption, as follows:

Impervious.. 0 to .02% Technically Vitreous.. .5 to 3%
Vitrified.... .02 to .5% Semivitreous..... 3 to 10%
Highly Porous..... Above 10%

Measurements shown are average values from test pieces. Production articles may vary slightly, depending on size, shape and method of manufacture.

			Lava		Refractories					
			Made from Natural Stone		Medium Grain	Fine Texture				Granular
			Aluminum Silicate	Magnesium Silicate	Cordierite $2MgO \cdot 2Al_2O_3 \cdot 5SiO_2$	Zirconium Oxide ZrO_2	Zircon $ZrO_2 \cdot SiO_2$	Alumina Al_2O_3	Magnesium Silicate	Zirconium Oxide ZrO_2
			Lava Grade A	Lava 1136	Alsimag 202*	Alsimag 530†	Alsimag 504	Alsimag 393	Alsimag 222†	Alsimag 508†
Property	A. S. T. M. Test Number	Unit	Good electrical and heat resistance, excellent for close tolerances. Available in larger sizes than any other grade of Lava.	Excellent electrical properties, made to close tolerances. For insulating spacers in small size vacuum tubes.	Low coefficient of expansion, high resistance to heat shock. For heating elements, thermocouple insulators and burner tips.	Fine grain high mechanical strength refractory for the simpler extruded shapes. Has excellent resistance to heat shock.	Very fine grain refractory with good resistance to heat shock. Suitable for firing plates and supports, brazing jigs, etc.	Easily degassed refractory with good electrical resistance of high temperature. Porous body principally used for vacuum tube insulators.	Refractory which is machinable in the fired state. Solid in rods, tubes, plates and blocks. For model making and repair parts.	Refractory body excellent for heat shock. Made only in plates, rods and simple shapes manufactured by pressing or casting methods.
Water Absorption	D116-42(A)	%	2 to 3 Technically Vitreous	2 to 3 Technically Vitreous	See footnote[f]	6 to 10 Semi-vitreous	8 to 14 Highly Porous	12 to 18 Highly Porous	14 to 18 Highly Porous	12 to 16 Highly Porous
Specific Gravity	—	—	2.3	2.8	2.1	3.8	2.9	2.4	2.0	2.9
Density	—	Lbs. per cu. in.	.085	.102	.076	.136	.105	.087	.072	.106
Standard Body Colors[a]	—	—	Pink	Tan	See footnote[f]	Orange	White	White	Light Brown	Orange
Alternative Body Colors	—	—	—	White[g]	See footnote[f]	—	—	—	—	—
Softening Temperature	C24-46	°C °F	1 600 2 912	1 475 2 687	1 430 2 606	2 400 4 352	1 610 2 930	1 800 3 272	1 625 2 957	2 400 4 352
Safe Temperature at Continuous Heat	—	°C °F	1 100 2 012	1 250 2 282	1 250 2 282	1 600 2 912	1 350 2 462	1 400 2 552	1 300 2 372	1 600 2 912

Hardness	—	Mohs' Scale[b]	6	6
Thermal Expansion Linear Coefficient	— —	Per °C 25–100°C 25–700°C	2.9×10^{-6} 3.6×10^{-6}	11.3×10^{-6} 11.9×10^{-6}
Tensile Strength	D116-42	Lbs. per sq in.	2 500	
Compressive Strength	D667-42T	Lbs. per sq. in.	20 000	25 000
Flexural Strength	D667-42T	Lbs. per sq. in.	9 000	9 000
Resistance to Impact (½" rod)	Charpy D667-42T	Inch-Lbs.	3.3	—
Thermal Conductivity[c] (Approximate Values)	—	g. cal. × cm. thick / cm² × sec. × deg. C	.003	.005
Dielectric Strength (step 60 cycles) Test discs ¼" thick	D667-42T	Volts per mil	80	100
Volume Resistivity at Various Temperatures: 25°C	—	Ohms per centimeter cube	$>10^{14}$	$>10^{14}$
100°C			6.0×10^{11}	9.0×10^{12}
300°C			2.0×10^{9}	1.2×10^{10}
500°C			5.0×10^{6}	1.1×10^{8}
700°C			3.5×10^{5}	3.3×10^{6}
900°C			5.0×10^{4}	4.2×10^{5}
Te Value[d]	—	°C °F	620 1 148	810 1 490
Dielectric Constant: 60 Cycles	D667-42T	—	—	—
1 MC			5.3	5.8
10 MC			5.3	—
100 MC			5.2	—
Power Factor[e]: 60 Cycles	D667-42T	—	—	—
1 MC			.01	.0003
10 MC			.009	—
100 MC			.007	—

7	—	—	—	6	—
1.6×10^{-6} 2.8×10^{-6}	6.7×10^{-6} 8.1×10^{-6}	5.3×10^{-6} 5.3×10^{-6}	5.1×10^{-6} 7.2×10^{-6}	8.0×10^{-6} 10.0×10^{-6}	7.2×10^{-6} 8.3×10^{-6}
3 500	—	—	—	2 500	—
40 000	30 000	16 000	11 000	25 000	11 000
8 000	10 000	13 000	10 000	8 000	4 000
2.5	5.0	5.0	3.0	1.9	4.0
.003	.004	.003	.004	.005	.004
100	—	—	50	50	—
$>10^{14}$	$>10^{14}$	$>10^{14}$	$>10^{14}$	$>10^{14}$	$>10^{14}$
3.0×10^{13}	$>10^{14}$	$>10^{14}$	5.0×10^{12}	$>10^{14}$	$>10^{14}$
2.0×10^{10}	4.6×10^{9}	3.6×10^{9}	1.0×10^{10}	6.0×10^{11}	4.5×10^{9}
9.0×10^{7}	1.2×10^{7}	1.8×10^{7}	7.5×10^{7}	4.6×10^{9}	8.2×10^{6}
3.0×10^{6}	3.2×10^{5}	1.0×10^{6}	3.6×10^{6}	1.7×10^{8}	2.5×10^{5}
3.5×10^{5}	2.4×10^{4}	2.2×10^{5}	5.6×10^{5}	1.1×10^{7}	4.0×10^{4}
780 1 436	625 1 157	700 1 292	835 1 535	>1 000 >1 832	610 1 130
—	—	—	—	—	—
5.0	—	—	5.5	5.5	—
5.0	—	—	5.4	5.5	—
4.9	—	—	5.3	5.5	—
—	—	—	—	—	—
.004	—	—	.0025	.0002	—
.003	—	—	.0025	.0002	—
.003	—	—	.0020	.0002	—

TABLE 15.8. MECHANICAL AND ELECTRICAL PROPERTIES OF ALSIMAG CERAMICS (*Continued*)

			Lava		Refractories					
			Made from Natural Stone		Medium Grain	Fine Texture				Granular
			Aluminium Silicate	Magnesium Silicate	Cordierite $2MgO \cdot 2Al_2O_3 \cdot 5SiO_2$	Zirconium Oxide ZrO_2	Zircon $ZrO_2 \cdot SiO_2$	Alumina Al_2O_3	Magnesium Silicate	Zirconium Oxide ZrO_2
			Lava Grade A	Lava 1136	Alsimag 202*	Alsimag 530†	Alsimag 504	Alsimag 393	Alsimag 222†	Alsimag 508†
Property	A. S. T. M. Test Number	Unit	Good electrical and heat resistance, excellent for close tolerances. Available in larger sizes than any other grade of Lava.	Excellent electrical properties, made to close tolerances. For insulating spacers in small size vacuum tubes.	Low coefficient of expansion, high resistance to heat shock. For heating elements, thermocouple insulators and burner tips.	Fine grain high mechanical strength refractory for the simpler extruded shapes. Has excellent resistance to heat shock.	Very fine grain refractory with good resistance to heat shock. Suitable for firing plates and supports, brazing jigs, etc.	Easily degassed refractory with good electrical resistance of high temperature. Porous body principally used for vacuum tube insulators.	Refractory which is machinable in the fired state. Solid in rods, tubes, plates and blocks. For model making and repair parts.	Refractory body excellent for heat shock. Made only in plates, rods and simple shapes manufactured by pressing or casting methods.
Loss Factor[e] 60 Cycles	D667-42T	—	—	—	—	—	—	—	—	—
Loss Factor[e] 1 MC	D667-42T	—	.053	.002	.020	—	—	.014	.001	—
Loss Factor[e] 10 MC	D667-42T	—	.048	—	.015	—	—	.014	.001	—
Loss Factor[e] 100 MC	D667-42T	—	.036	—	.010	—	—	.011	.001	—
Capacity Change Per °C	—	Parts per million	—	—	—	—	—	+100	+100	—

[a] Standard glaze is white. Brown and other colors available on some bodies.
[b] Ceramic materials cannot be measured by Rockwell or Brinell methods.
[c] Conversion factor:

$$\frac{\text{g. cal.} \times \text{cm. thick}}{\text{cm}^2 \times \text{sec.} \times \text{deg. C.}} = 2903 \frac{\text{BTU} \times \text{in. thick}}{\text{sq. ft.} \times \text{hr.} \times \text{deg. F.}}$$

[d] Te value is the temperature at which a centimeter cube has a resistance of one megohm.
[e] Alsimag 35, 196, 228 and 243 measured wet, after immersion in water for 48 hours. (JAN-1-10)
[f] Furnished in various densities:
202, porous, 10 to 15% (tan)
178, porous, 10 to 15% (white)
047, semi-vitreous, 2 to 7% (brown)
[g] Hydrogen fired.
Values omitted because specimens according to A.S.T.M. cannot be made in this material or the values have no industrial significance.

is included as an example of ceramic products from one manufacturer. This should not be regarded as discrimination against other manufacturers, who have similar and sometimes better bodies available and who should be consulted before a body is chosen for a particular application. Table 15.9 gives physical and chemical properties of several ceramic materials and graphite and carbon according to Sabol.[26] In studying these tables carefully a great deal of valuable information can be obtained for the application of any of these ceramic bodies to a particular problem. It is apparent, for example, that there are a variety of different steatites which have different properties and which lend themselves to a greater or lesser extent to the performance of certain functions. The engineer is well advised to consult the manufacturer before making a final selection and to give him all the necessary data that enter into the problem.

Zircon Porcelain

For some time the mineral zircon ($ZrO_2 \cdot SiO_2$) has been used as an admixture with other high-grade ceramic bodies; this improves the temperature and frequency characteristics of the latter.[27] The highly abrasive nature, which gives excessive wear on press tools, is a disadvantage in fabrication. The relatively high dielectric constant (Table 15.7) and its variation with temperature is also a limitation, especially in high frequency insulation. Zircon porcelains were extensively used for spark plugs;[15] but their application as high-frequency insulation was not introduced until 1943 after extensive studies of their usefulness in this field had been carried out at two industrial laboratories.* Russell and Mohr[28] describe the properties of zircon porcelains as follows:

"The general superiority of commercial zircon porcelain to all except the expensive, noncompetitive sintered alumina is readily apparent. It is 50 to 200% stronger than mullite and high voltage porcelains and 10 to 50% stronger than steatite, heretofore the strongest of the porcelain-type materials. Thermally, zircon porcelain is equal or superior to all other porcelains. It has the highest thermal conductivity of any porcelain and approaches the low thermal expansion of mullite porcelain. It has been observed to have good thermal shock resistance, as is also true of mullite porcelain. High-voltage porcelain is mediocre in this respect, and steatite porcelain is decidedly inferior. All of the porcelains have good resistance to all alkalis and acids except hydrofluoric. Sintered alumina, however, is known to resist corrosive vapors and reducing conditions at high temperatures more effectively than any porcelain, and also to resist hydrofluoric acid.

"Zircon porcelains generally fall within the three best classes of ceramic high-frequency insulators, namely, L-4, L-5, L-6. The somewhat higher dielectric constant is offset by its lower power factor at high frequencies."

* Titanium Alloy and Manufacturing Company, Buffalo, New York.
Westinghouse Research Laboratories, East Pittsburgh, Pennsylvania.

Contained in Figs. 15.1 to 15.3 are curves showing the variation of loss factor with frequency and temperature and that of volume resistivity with temperature for a number of ceramic insulating materials.[28] The trend of the dielectric constant with frequency and temperature is given for similar bodies in Fig. 15.4 and 15.5 from an earlier report of Russell

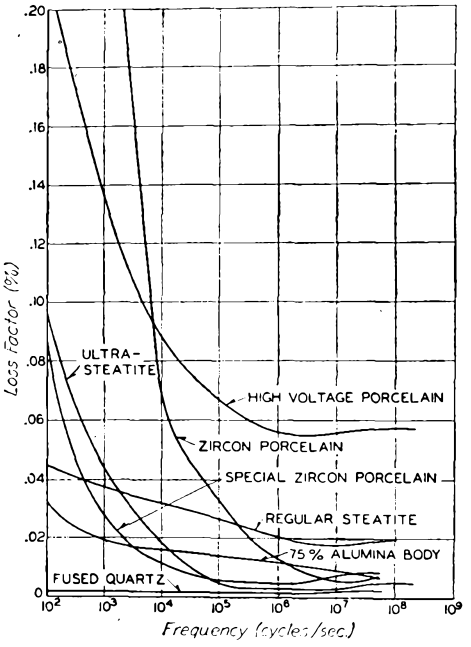

Fig. 15.1. Relationship of loss factor to frequency of several ceramic insulating materials. After R. Russell, Jr., and W. G. Mohr.[28] (*Courtesy American Ceramic Society.*)

and Berberich.[23] They should be compared with the corresponding curves for glasses, given in Chapter 5 (Figs. 5.11, 5.12, and 5.2).

"Mineral zircon is found in igneous rocks throughout the world, but the most important commercial deposits are the beach sands of certain districts of Florida, Brazil, Australia, and India. These deposits are particularly useful because in most cases they are constantly replenished by the sea and because the pure zircon is readily separated from the accessory minerals. Since the preparation of zircon consists largely of purification and grinding, its characteristics can be controlled much more closely than most ceramic raw materials.

"Zircon-porcelain compositions, as the name implies, contain a major portion, at least 50% by weight, of the mineral, zircon. Fluxes are present in amounts under 30% and are usually added as double zirconium silicates of the alkaline-earth oxides. Special fluxes and auxiliary materials are sometimes used. Clay is added in amounts generally not exceeding 30% by weight, and small additions of bentonite are often made to increase plasticity and dry strength.

TABLE 15.9. PHYSICAL AND CHEMICAL PROPERTIES OF TEN CERAMIC REFRACTORIES*

Material	Specific Gravity	Melting Point °C & °F	Hardness, Mohs Scale	Mean Specific Heat Cal/gm/°C	Thermal Conductivity Btu/hr/ft²/in/°F	Thermal Expansion $n \times 10^{-6}$	Thermal Shock Resistance	Modulus of Elasticity psi	Tensile Strength at 25°C psi	Compressive Strength at 25°C psi	Transverse Strength at 25°C psi	Resistance to Abrasion	Resistance to Chemical Corrosion	Resistance to Oxidation by air	Resistance to Reduction by Carbon	Cost per Pound Approx. Dollars
Alumina Al_2O_3	4.0	2050°C 3722°F	9.0	20°-1000°C 0.304	2400°F 30.0	25°-800°C 8.5	Good	5.24×10^7	35,800	412,500	46,800	Good	Acid Alkali HF	Not Affected	Attacked by amorphous carbon at M.P. but not readily by graphite	.055
Beryllia BeO	3.0	2570°C 4658°F	9.0	900°C 0.497	High	25°-1260°C 9.2	Very Good	4.28×10^7	13,800	103,100	20,600	Good	Alkali	Not Affected	Not Affected	4.00
Magnesia MgO	3.5	2800°C 5072°F	6.0	30°-1100°C 0.283	2012°F 40.8	20°-1800°C 13.4	Fair	1.24×10^7				Very Poor	Alkali	Not Affected	Slightly reduced at 1450°C Rapidly reduced above 2000°C	.05
Silicon Carbide SiC	3.17	>2700°C >4892°F	9.0-10.0	1000°C 0.1216	2012°F 70.7-121.8	0°-1700°C 4.3-4.7	Good					Very Good	Reacts readily with basic fluxes	Dissociates at 2200°C Dissociates at 2240°C	Not Affected	.15-.20
Thoria ThO_2	9.69	3030°C 5486°F	7.0	25°C 0.06	Very Low	25°-800°C 9.5	Fair	1.79×10^7		220,000	17,900	Good	Basic	Not Affected	Reduced by carbon at high Temp.	7.00

Zirconia ZrO_2	5.6	2720°C 4928°F	Fused 8.5 Sintered 7.0	25°–1000°C 0.157	2400°F 14.3	0°–1400°C 5.0	Fair
Zircon $ZrO_2 \cdot SiO_2$	4.7	2550°C 4622°F	8.0	36°C 0.131	11.6	20°–700°C 4.9	Very Good
Spinel $MgO \cdot Al_2O_3$	3.53	2135°C 3875°F	8.0	50°–1025°C 0.290 0°–1042°F 0.257	2400°F 14.6	25°–800°C 8.5	Fair
Graphite C	2.25	3527°C 6380°F	0.5–1.0	26°–76°C 0.165 56°–1450°C 0.390	400°F 730.0 2000°F 220	25°–40°C 7.8	Very Good
Carbon C	1.8–2.1	Sublimes 3537°C 6399°F		26°–76°C 0.168 56°–1450°C 0.387	1600°F 18.5 2000°F 22.0	500°C 1.5–5.5	Very Good

* Ohio State Univ. Research Foundation Proj. 252—F.P. Sabol (1947).

2.48×10^7	17,900	302,500	26,100	Good	Acid and Neutral Material	Not Affected	Forms Carbides at high Temp.	.90
2.40×10^7	12,700	90,000	25,000	Good	Acid HF	Not Affected	Decomposes above 1900°C	.12
3.17×10^7	18,600	247,500	24,100	Good	Acid Bases	Not Affected	Not Readily Reduced	
Plain $.14 \times 10^7$ Impervious $.22 \times 10^7$	Plain 800 Impervious 2400	Plain 5500 Impervious 10,000	Plain 2800 Impervious 4800	Poor	Chemically Inert	Oxidizes in air appreciably at 640°C	Not Affected	C.P. .50–.75
Plain $.19 \times 10^7$ Impervious $.28 \times 10^7$	Plain 900 Impervious 1800	Plain 7000 Impervious 10,500	Plain 2700 Impervious 4400	Good	Chemically Inert	Oxidizes in air appreciably of 640°C	Not Affected	C.P. .25– 45

"Mixing of the body constituents may be accomplished by either the wet- or dry-mixing processes. The body may be formed by extrusion, turning, dry or semi-wet pressing, or casting. The hardness of zircon causes tools and dies to be abraded more than with conventional white-ware bodies.

"The glazing of zircon porcelain presents a considerable problem. Ordinary white-ware glazes are absorbed by the body during firing unless an extremely heavy coat is applied. Because of the low thermal expansion of zircon porcelain, ordinary glazes also tend to craze and decrease the strength of the product. Special glaze

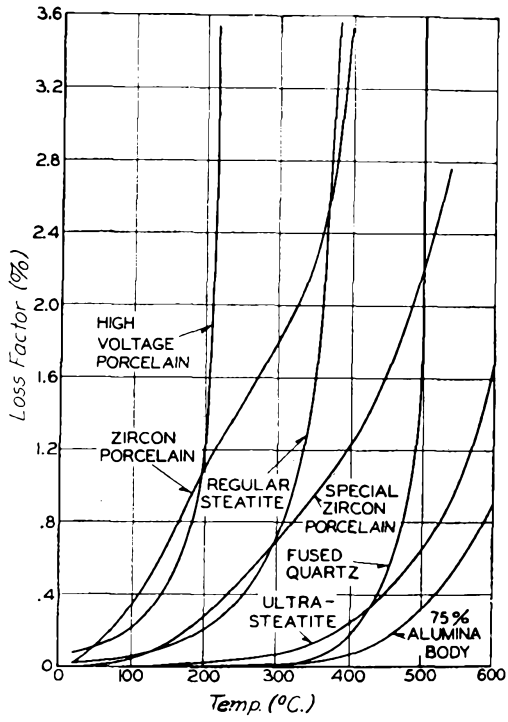

Fig. 15.2. Relationship of loss factor to temperature of several ceramic insulating materials. After R. Russell and W. G. Mohr.[28] (*Courtesy American Ceramic Society.*)

compositions and application techniques, however, have been developed, and zircon porcelain is now manufactured with compression-type glazes which even improve the strength of the already strong material.

"Zircon-porcelain bodies may be developed with possible maturing temperatures from as low as cones 4 or 5 up to the softening point of zircon. The vitrification range of zircon porclain is often 30 to 50°C., which compares favorably with that of feldspar-clay-flint bodies. The problem of warpage is sometimes encountered, but this factor can usually be eliminated by prudent design and improved kiln-setting techniques. The current commercial zircon porcelains are made by the one-fire process."[28]

The properties of zircon and zirconia (ZrO_2) at elevated temperatures were recently described by Curtis and Laurie.[29] Their discussion is concerned with heat-transfer rates and hot-load resistance, and also

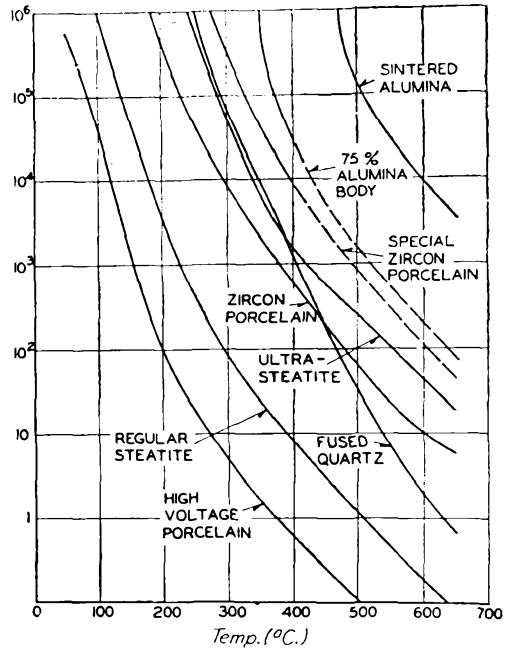

Fig. 15.3. Relationship of resistivity to temperature of several ceramic insulating materials. After R. Russell and W. G. Mohr.[28] (*Courtesy American Ceramic Society.*)

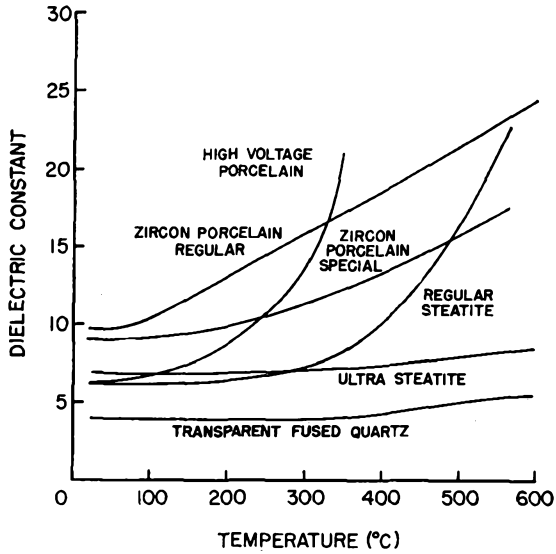

Fig. 15.4. Dielectric constant of various ceramic bodies at 25°C as a function of frequency. After R. Russell, Jr., and L. J. Berberich.[23] (*Courtesy McGraw-Hill Publishing Company, Inc., New York.*)

with the limiting temperatures at which these relatively expensive super-refractories begin to react chemically with other refractories used as backing-up materials in furnace construction:

"Zircon was found to be as resistant as zirconia to reaction when in contact with alumina, aluminum silicate and silica refractories. It is less resistant to chrome, chrome magnesite and magnesite, however, since reaction begins at 1540°C (2800°F) which is 100°C lower than in the case of zirconia. In hot-load tests zircon failed at about 2040°C (3700°F), zirconia bodies failed at temperatures varying from 2090

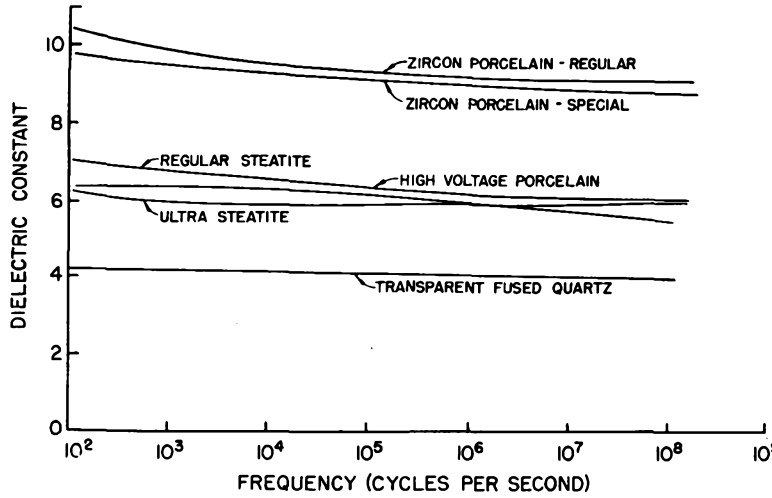

Fig. 15.5. Dielectric constant of various ceramic bodies at 100 KC as a function of frequency. After R. Russell, Jr. and L. J. Berberich.[23] (*Courtesy McGraw-Hill Publishing Company, Inc., New York.*)

to 2430°C (3800 to 4400°F), the load resistance tending to increase with increasing density of body. The use of high-density zirconia bodies is therefore advisable when unusual resistance to load at high temperatures is essential."[29]

Reactions at High Temperatures

A recent investigation by Johnson[30] in this field of high-temperature reactions of refractories is of more direct concern to the tube engineer as it describes conditions prevailing *in vacuo* and covers the interaction with the high-melting metals molybdenum and tungsten and also includes carbon. Samples were produced from pure raw materials with suitable binders by dry pressing in a hydraulic press, and were heated in a high-temperature vacuum-induction furnace over the range of 1500 to 2300°C. Individual test readings departed from the average by not more than 3 per cent in any case. Table 15.10 gives the result of Johnson's observations and Table 15.11 the temperature in °C, at which stability no

longer exists in surface-to-surface contact between the materials indicated in Table 15.10. The pressure range during the tests was 0.1 to 0.5 microns and the superscripts to the figures give the duration of tempera-

TABLE 15.10. REACTION BETWEEN DIFFERENT REFRACTORIES IN VACUO (After Johnson[30])

Combination	Lowest Temp. of Reaction (°C)	Type of Reaction	Remarks
Carbon-tungsten	1500	Carbide formation	
Carbon-molybdenum	1500	Carbide formation	
Carbon-thoria	2000	Reduction of thoria	Carbide at higher temperatures
Carbon-zirconia	1600	Reduction of zirconia	Carbide at higher temperatures
Carbon-magnesia	1800	Reduction of magnesia	Some adherence
Carbon-beryllia	2300	Reduction of beryllia	Metal coating on carbon
Beryllia-tungsten	2000	Yellow metallic deposit on beryllia	Deposit increased with temperature
Beryllia-molybdenum	1900	Silvery deposit on beryllia	Decomposition of reaction products evident at 2300°C
Beryllia-thoria	2100	Liquid formed	Complete fusion at 2200°C
Beryllia-zirconia	1900	Slight adherence due to liquid formation	Definite liquid at 2000°C
Beryllia-magnesia	1800	Liquid phase	Strong adherence of melt to molybdenum
Magnesia-tungsten	2000	Reduction of magnesia	Slight adherence
Magnesia-molybdenum	1600	Silvery deposits on magnesia	No magnesia and strong erosion of molybdenum at 2100°C
Magnesia-thoria	2200	Vapor reaction	Thoria eroded but no adherence
Magnesia-zirconia	2000	Liquid phase	Specimens welded at 2000°C.
Zirconia-tungsten	1600	Yellow deposits at interface	Little change up to 2300°C where decomposition of zirconia evident
Zirconia-molybdenum	2200	Slight adherence due to sintering	Decomposition of zirconia at 2300°C
Zirconia-thoria	2200	Slight adherence	No liquid phase evident at 2300°C
Thoria-tungsten	2200	Slight thoria reduction	Little reaction up to 2300°C but adherence evident
Thoria-molybdenum	1900	Slight deposits with adherence	Little reaction up to 2300°C, no adherence above 2000°C
Molybdenum-tungsten	2000	Slight adherence due to sintering	Greater adherence up to 2300°C

ture exposure in minutes. In summarizing his results Johnson comes to the following conclusions:

(1) "At high temperatures, in a vacuum, the limiting factor for many refractories is not the melting point but stability when in contact with other substances and the rate of volatilization. As an example, magnesia cannot be used *in vacuo*, even for short periods, above the 1600 to 1700°C range, nor beryllia above 2100°C. Carbon, zirconia, thoria, molybdenum, and tungsten can be used for extended periods at least to 2300°C.

(2) "Maximum density of some oxides, such as magnesia and beryllia, cannot be obtained at the higher temperature ranges, owing perhaps to internal volatilization. This indicates the advisability of using high-temperature atmospheric furnaces for these substances.

(3) "Of the oxides tested, beryllia is the most stable in contact with carbon, zirconia is most stable in contact with molybdenum, and thoria is most stable in contact with tungsten.

(4) "The most stable combinations of oxides are ZrO_2–ThO_2 and MgO–ThO_2.

(5) "Unstabilized zirconia may be fired to a dense, mechanically strong mass at 2200°C and above in vacuum."

TABLE 15.11. TEMPERATURE (°C) AT WHICH STABILITY NO LONGER EXISTS IN SURFACE-TO-SURFACE CONTACT BETWEEN THE MATERIALS INDICATED IN TABLE 15.10
(After Johnson[30])

	W	Mo	ThO_2	ZrO_2	MgO	BeO
C	1500^8	1500^8	2000^4	1600^4	1800^8	2300^2
BeO	2000^2	1900^4	2100^4	1900^2	1800^2	
MgO	2000^2	1600^4	2200^4	2000^4		
ZrO_2	1600^4	2200^4	2200^4			
ThO_2	2200^4	1900^4 (?)				
Mo	2000^8					

Superscripts indicate time in minutes.
Pressure range 0.1–0.5 micron.

TABLE 15.12. COMPOSITION OF VARIOUS PORCELAIN BODIES
(After Lindsay and Berberich[31])

Constituent	Composition (%)		
	High Tension Porcelain	Zircon Porcelain	Alumina* Porcelain
SiO_2	68.72	36.96	6.69
Al_2O_3	23.90	6.08	90.98
TiO_2		0.24	0.06
ZrO_2		49.72	
Fe_2O_3	1.80	0.25	0.20
$Na_2O + K_2O$	5.46	.13	.21
CaO	0.25	6.48	1.08
MgO	.12	0.14	0.66
Total	100.25	100.00	99.88
Total flux	5.83	6.75	1.95
Main crystalline constituent	Mullite ($3Al_2O_3 \cdot 2SiO_2$) Quartz (SiO_2)	Zircon ($ZrO_2 \cdot SiO_2$)	Alumina (α-Al_2O_3)

* This high alumina body is not commercially available.

The electrical behavior of a number of ceramics, including high-tension porcelain (H.T.P.), zircon porcelain (Z.P.), and a special high alumina porcelain (A.P.) has been investigated at high temperature (up to 1000°C) by Lindsay and Berberich.[31] The composition of these bodies is given in Table 15.12. Muskovite mica (M.M.) and fused

silica (F.S.) are shown to obey the same relations which were found to exist for the above-mentioned materials and which will now be described. Fig. 15.6 gives a representative graph obtained for zircon, showing the variation of dielectric strength and volume resistivity with temperature. When the first two quantities are plotted on a logarithmic scale versus the reciprocal of temperature, each is represented by two straight-line

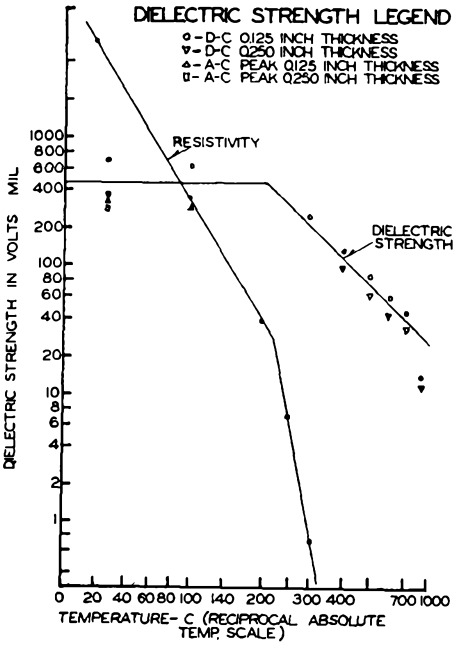

Fig. 15.6. Variation of dielectric strength and volume resistivity of zircon porcelain with temperature. After E. W. Lindsay and L. J. Berberich.[31] (*Courtesy American Institute of Electrical Engineers.*)

sections joining at a transition temperature which was found to be approximately the same for dielectric strength and resistivity for one given material. These transition temperatures are listed for the various materials in Table 15.13.

"The region below the transition temperature (*T.T.*) is known as the disruptive or electric-breakdown region while that above it is known as the thermal-breakdown region. Von Hippel and Maurer[32] report similar results for glass and show that such a behavior is to be expected of amorphous materials. (See Chapter V.) In crystals the situation is somewhat different in that the *d-c* breakdown strength increases with temperature in the low temperature region until the *T.T.* is reached when it decreases again, as is the case for amorphous materials."[31]

Figure 15.7 shows that the power factor, as measured at 100 KC, can also be represented approximately by two straight lines. The dashed vertical lines indicate the *T.T.*, as determined by the resistivity data.

That the two *T.T.* do not exactly coincide can readily be ascribed to the fact that the respective measurements were taken on different samples which may have varied slightly in their composition. It is interesting to note that zircon porcelain behaves differently from the other materials in so far as the high-temperature branch of its power factor curve rises less steeply than the low-temperature brands.

The authors point out that not too much emphasis should be placed on the absolute values of breakdown strength obtained in these tests,

TABLE 15.13

Material	Transition Temperature °C
High-tension porcelain	100
Zircon porcelain	220
Alumina porcelain	250
Fused silica	280
Muscovite mica	380

but that the relative values among the various materials have considerable significance. The ASTM Spec. D149-44, which prescribes one

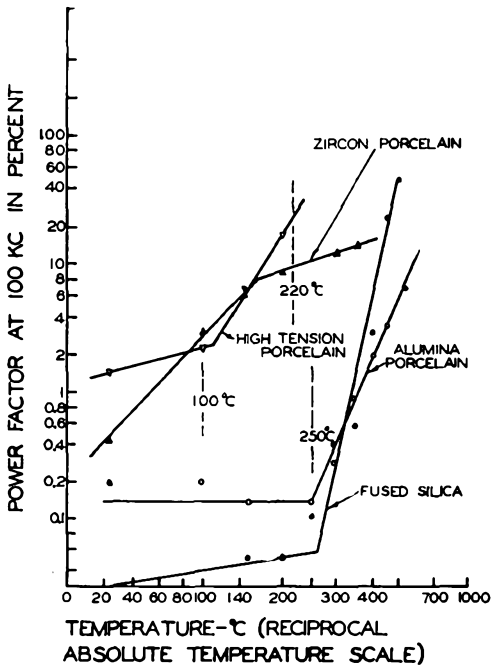

Fig. 15.7. Variation of power factor of various procelain bodies with temperature. After E. W. Lindsay and L. J. Berberich.[31] (*Courtesy The American Institute of Electrical Engineers.*)

minute step-by-step rise of voltage, was used in this work. Other test conditions might well affect the values obtained but hardly the relative

order. The interesting correlation between breakdown and conduction mechanisms which is suggested by the common transition temperature remains to be explained fully on theoretical grounds as the authors point out. Meanwhile, the electronic engineer is well advised to take note of these data as they naturally indicate the inadvisability to apply a sizable fraction of the breakdown voltage above the transition temperature.

Design Considerations

Experience has shown that many ceramic problems can be solved either the hard way or the easy way as far as the selected shape is concerned. The eagerness with which complicated shapes are at times

Fig. 15.8. Pagoda insulator for cyclotron deflector. (*Courtesy Collins Radio Company.*)

dreamed up by the designer in the tube laboratory is not often appreciated by the ceramic manufacturer. It involves costly dies, long delivery dates, and an unnecessarily high cost. One such design of the author for the support of a cyclotron deflector is shown in Fig. 15.8. It had to support a 150-pound pipe 3½ inches in diameter, resting in an outer coaxial pipe 9½ inches in diameter, and to withstand 100 kv D.C. There was nothing wrong with it, functionally, except that it could not be made in one piece by the manufacturer. It was constructed in two pieces so poorly joined that it broke down consistently at the rated voltage. The "pagoda insulator" fortunately makes a most attractive paper weight. Some notes on die-pressed ceramics are copied below from Gleason,[33]* who represents the manufacturer's viewpoint.

"To form the simplest article, the die consists of a stationary block, or die case, with a movable top and bottom punch. A solid article, round or square, in cross

* With the kind permission of the editor of the *J. of the Brit. Inst. of Radio Eng.*

section, as the requirements may be, needs these three parts. If holes are required, stationary pins are added running up through the bottom punch and into the top punch. If several steps in thickness are required in an article, this necessitates moving parts within the bottom punch to distribute the pressure evenly to the various thicknesses. The cross section of the die case and the punches are shaped to the design required by the customer, allowing for the shrinkage of the body in the firing operation. The finest die steels are used and the various die parts are machined and polished to a high degree of accuracy.

"A few suggestions to the prospective purchaser of die-pressed insulators may aid in the intelligent design of the ceramic part and enable it to be manufactured more economically, effecting smaller production losses and thus making possible lower selling prices.

"(1) Give the ceramic supplier full information as to the size of parts that fit into or around the ceramic. Whenever possible, the supplier should be furnished with a sample assembly so that the economical design may be checked. Usually, the metal stamping dies are cheaper than the steatite-pressing dies and can be altered more easily.

"(2) Always allow as liberal tolerances as possible. It may seem paradoxical that the ceramic manufacturer boasts of his ability to hold exacting tolerances and then asks for broad tolerances, but it reduces to this: The supplier can furnish ceramics to close tolerances; but when they are more restrictive than ordinary commercial tolerances, he must resort to costly individual gauging.

"(3) Bevelled edges are very helpful. As the die parts wear, the material crowds into the resulting crevice between punch and block and forms a fin or flash on the ceramic. Where a bevel is allowed the supplier will profile his punch faces and the ceramic will be neater and the dies last longer.

"(4) Bosses, counterbores, or depressions should be kept as low or shallow as possible and their walls should be tapered about three degrees.

"(5) The number of different levels should be kept at a minimum.

"(6) Wall thickness between the edge of the ceramic and holes or depressions should be as substantial as possible, else cracks will have a tendency to result.

"(7) Avoid very small pins, and all designs that necessitate dies of weak construction.

"(8) Holes can only be pressed-in when parallel to the axis of pressing. Other holes must be drilled into the article individually after pressing.

"(9) Pressed ceramics should not be too long in direction of pressing. They will have a tendency to have a center section smaller than the ends.

"(10) Thin sections, no matter where, should be avoided. They tend to crack, warp, or blister, thus making the ceramic hard to control.

"(11) Bosses should be used wherever flat, ground, parallel surfaces are required, thus keeping the ground area at a minimum.

"(12) Threads of tapped holes cannot be pressed in. Unless special binders are used the pressed ceramic crumbles to some extent in the tapping operation, especially with fine pitches; so as large and coarse a thread as possible should be chosen. If the screw must enter the ceramic quite a distance, it would be advisable to counterbore a fraction of the hole so that any variation in firing shrinkage and its accompanying variation in pitch will still allow the screw to enter. Holes tapped into a ceramic perpendicular to the pressing axis will invariably fire out oval-shaped."

High Dielectric-Constant Ceramics

High dielectric-constant ceramics form a special group of bodies based primarily on the mineral rutile (TiO_2) and the titanates of the alkaline-

earth elements. Voluminous literature has accumulated during the relatively short time in which these materials have occupied the attention of ceramist and physicist alike. The writer can do no better than to quote here in full a paper by Roup,[34]* which summarizes the history and gives the trend of recent developments. References 35 to 61 are taken from this paper as quoted, and the same applies to Figures 15.9 to 15.16.

"Of the various branches that comprise the ever expanding ceramic family tree, perhaps the youngest of the group is titania dielectrics. Sixteen years ago condensers comprising titania dielectrics came onto the market for the first time in Germany.

"To go back a little farther historically the dielectric constant of the rutile form of TiO_2 was measured by W. Schmidt[35] in 1902. He found a K value of 173 in the direction parallel to the principal axis and 89 in the direction perpendicular to it. The Landolt-Börnstein tables[36] of 1912 record a value of 110 for the dielectric constant of a fired TiO_2 body. In 1921 Liebisch and Rubens[37] showed that the high dielectric constant of rutile persisted at very high frequencies of the order of 10^{12} cycles per second. A German patent,[38] appearing in 1925, covered the use of TiO_2 as a high-frequency dielectric.

"From 1928 to 1933 tubular condensers were made in Germany using low-loss steatite as the dielectric. In 1933 and 1934 production finally was started using as the dielectric titanium dioxide alone and with admixtures of clay and magnesium titanate for varying amounts of temperature compensation.†

"In 1935 Hans Thurnauer came to the United States from Germany and started a similar program at American Lava Corp. That same year, Titanium Alloy Mfg. Co. (now a division of National Lead Co.) started a research program along this line and in March, 1936, opened the field to other manufacturers by supplying samples of heavy grade TiO_2.

"A United States' patent,[39] filed in 1938, covers the use of rare-earth oxides in dielectrics and the use of these materials to counteract the negative temperature coefficient of TiO_2. Substantial improvements in dielectric constants over the previous art were obtained.

"About a decade ago, other alkaline-earth titanates were prepared and tested, and over a period of several years the unusual and many times higher dielectric constants were found. This set off a tremendous surge of research and a rush to get materials of higher dielectric constant into production. Mixtures of strontium and barium titanates proved especially interesting, and many complex formulas of alkaline earth and lead titanates, zirconates, stannates, etc. were made, tested, and put into production.‡

"Many eminent scientists, such as Wainer,[40–42] Thurnauer, Howatt,[43] Navias,[44] Shelton,[45] von Hippel,[46] deBretteville,[47] Wul,[48–51] Roberts,[52] Donley,[53] Megaw,[54]

* Globe-Union, Inc., Milwaukee, Wisconsin. Presented at the Whiteware Symposium at the 51st Annual Meeting of The American Ceramic Society, Cincinnati, Ohio, April 27, 1949. With permission of the editor, *The Journal of the American Ceramic Society.*

† Dr. Albers-Schoenberg, now with General Ceramics and Steatite Corporation, informs the writer of this book that he was the first who made a titanate dielectric, the magnesium titanate in 1934. (German patent 684,932, June 6, 1934.)

‡ A very fine group of materials, developed in Germany, are the titania-zirconia dielectrics which are especially adapted to the use as high power condensers and were described by W. Soyck and A. Ungewiss (U.S. Pat. 2,069,903).

Rooksby,[55] Matthias,[56] and their associates, and dozens of others too numerous to list here, went to work on the various aspects of research. Many were practical ceramists and many were physicists interested in determining the exact properties and structures and the reasons for these unusual characteristics.

"During 1942 and 1943 anomalous properties of $BaTiO_3$ and solid solutions of $BaTiO_2$, $SrTiO_2$, and allied materials were reported by E. Wainer and A. N. Solomon.[40] Wainer was in all probability the first to observe piezoelectric characteristics in high barium-titanate ceramics. His patent,[41] filed June 11, 1943, discloses these properties. Studies in the Laboratory for Insulation Research at M.I.T. further established the fact, as reported during 1944 and 1945, that these materials constitute a new class

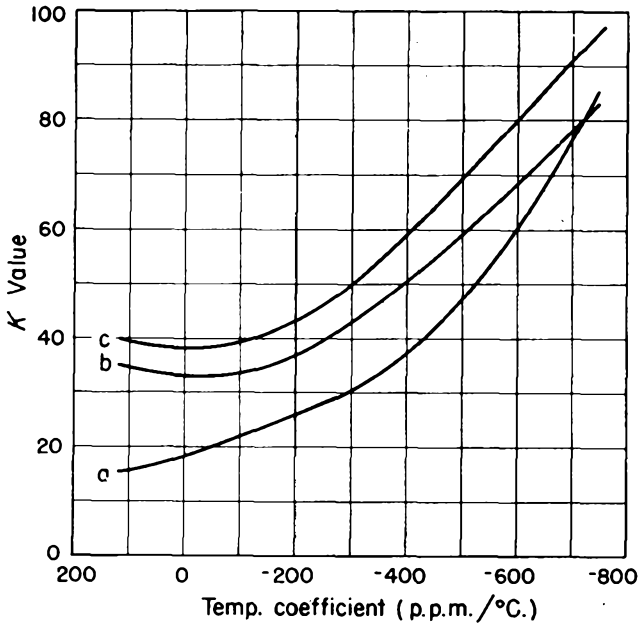

Fig. 15.9. Temperature coefficient vs. K value for commercial low-K dielectrics at 1 MC. After R. R. Roup.[34] (*Courtesy American Ceramic Society.*)

of ferroelectric dielectrics.[57] Confirmation by other workers followed in rapid order.[46,51,53]

"In 1947 it was further reported by S. Roberts[52] that fired barium titanate, although polycrystalline, exhibits piezoelectric properties when polarized in a *d-c* field.

"In addition to compositional studies, developments also proceeded int he direction of making thinner dielectric films.[43] Films are now being produced commercially that are 0.003 in. thick, and successful films down to 0.001 in. have been reported.

Industrial Accomplishments

"To review briefly some of the progress made to date Fig. 15.9 shows the dielectric constant versus temperature coefficient of three commercially available series of titanate compositions. The measurements were made at one megacycle. Curve (a) represents the well-proved titania-magnesium titanate series. Curve (b) shows a

titania-rare-earth oxide series incorporating a few per cent of clay; and curve (c) shows a similar series with further increased dielectric constants gained by replacing the clay by a similar amount of strontium titanate.

"Figure 15.10 shows K value versus temperature curves for the composition series (c) of Fig. 15.9.

"Figure 15.11 shows a different presentation of the same thing, in which the variation in K value is expressed as a percentage of its dielectric constant at room temperature.

"Figure 15.12 shows an extended temperature coefficient compositional series in which K value is plotted against temperature coefficient.

"Figure 15.13 shows the K value versus temperature of a number of commercially available dielectrics. These, tested at one kilocycle, are representative of literally

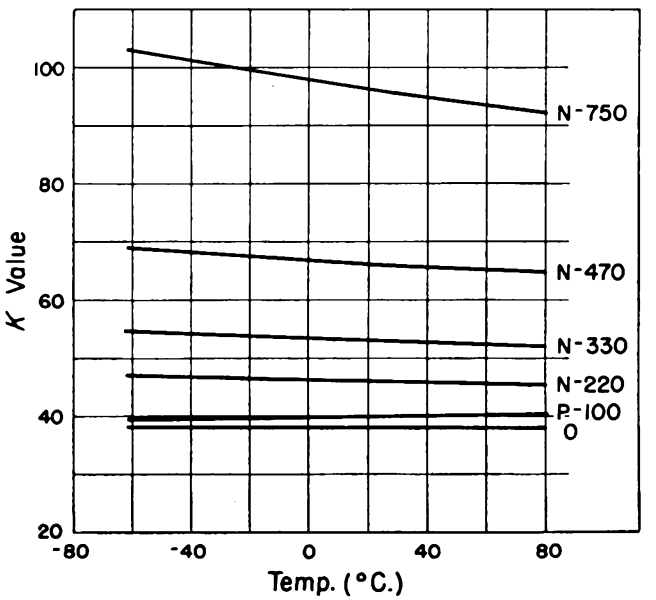

Fig. 15.10. K value vs. temperature for standard titania composition dielectrics at 1 MC. After R. R. Roup.[34] (*Courtesy American Ceramic Society.*)

thousands of compositions with varying curve shapes that are known and available for special applications.

"The adaptability for commercial uses where smaller temperature ranges are to be encountered is illustrated in Fig. 15.14, which shows these same curves over the smaller temperature range of 10 to 65°C. Curves of like materials are given similar identification on both graphs.

"Figure 15.15 illustrates one of many peculiarities that are encountered in the high K value field. Curve (a) shows the K versus temperature curve of high K material pressed and fired into a disk 0.020 inch thick; (b) shows the K of the same material pressed and fired to 0.140 in. thickness. The thick piece exhibits a much lower effective K than does the thinner piece, regardless of higher or longer firing to compensate for the additional mass. Curve (c) shows the K value of a thin section

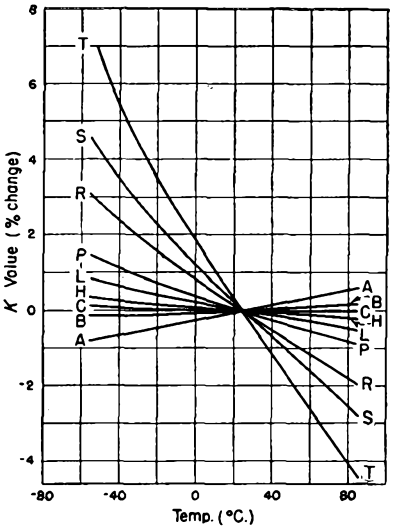

Fig. 15.11. K-change per cent vs. temperature for standard titania composition dielectrics. Temperature coefficients: A, 100; B, 30; C, 0; H, −30; L, −80; P, −150; R, −220; S, −330; T, −470; U, −750. K Values: A, 40; B, 38; C, 38; H, 38; L, 39; P, 41; R, 46; S, 53; T, 66; U, 96. After R. R. Roup.[34] (*Courtesy American Ceramic Society.*)

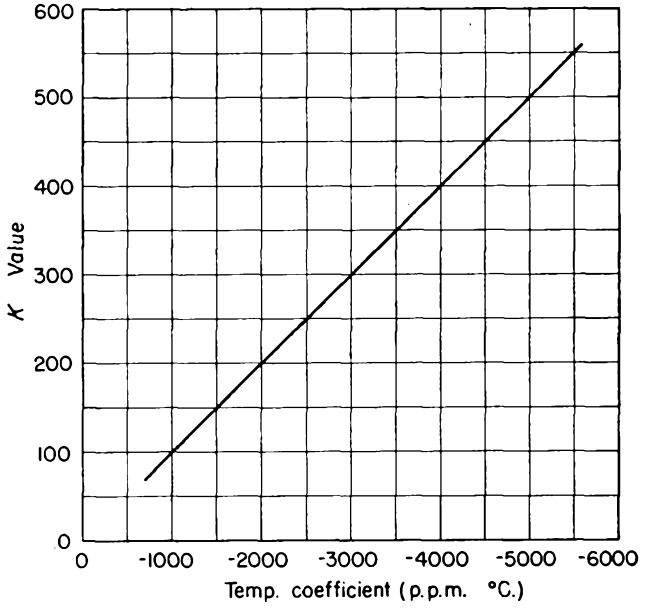

Fig. 15.12. Temperature coefficients vs. K value of highly negative titania composition dielectrics. After R. R. Roup.[34] (*Courtesy American Ceramic Society.*)

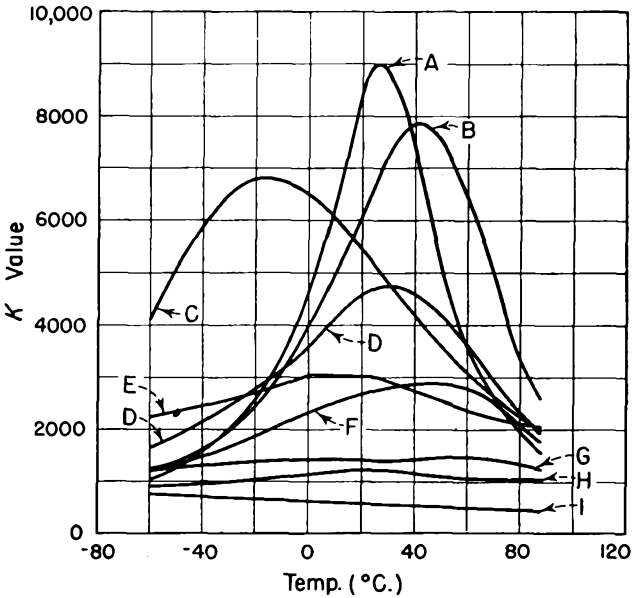

Fig. 15.13. K-value vs. temperature for commercial dielectrics. After R. R. Roup.[34] (*Courtesy American Ceramic Society.*)

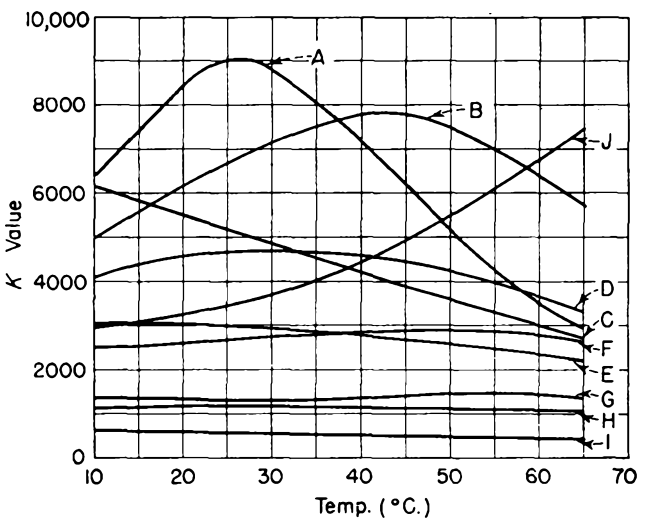

Fig. 15.14. K-value vs. temperature for commercial dielectrics; temperature range 10 to 65°C. After R. R. Roup.[34] (*Courtesy American Ceramic Society.*)

cut off the surface of a disk similar to that used in (b), and (d) is the curve of a similar section cut from the center of that same type of disk. The variations of this nature often require adjustments in compositions, depending upon the size of the piece to be made.

"Figure 15.16 illustrates another characteristic, aging, which is a factor to be considered in the development of high K materials. Curve (a) shows K versus temperature for a high K-value material, the curve being run 5 hours after cooling from a temperature well above the peak temperatures for the material. Curve (b) shows the same material after 8 days' aging, and (c) after 67 days' aging. At any time heating to 50 or 100°C above the peak K value will restore the curve to its original shape.

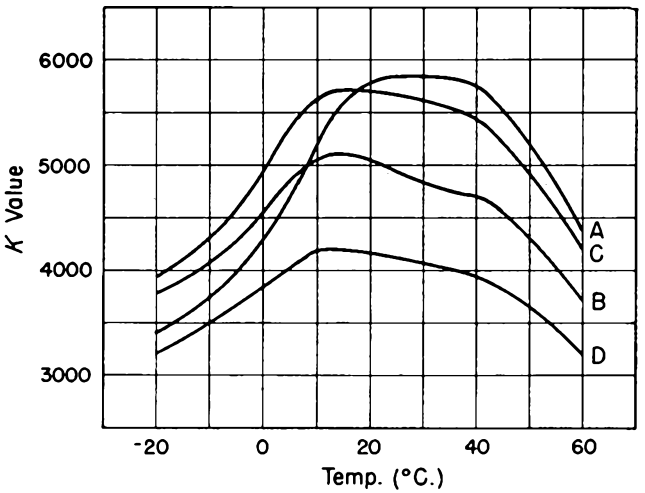

Fig. 15.15. Effect of thickness on K-value. After R. R. Roup.[34] (*Courtesy American Ceramic Society.*)

"Time does not permit a discussion of this phenomenon. It must suffice to say that this aging effect is caused by delayed inversions of the various domains that made up the structure.

Direction of Research

"Research will continue on the $BaTiO_3$-type materials, particularly along the line of single crystal studies and x-ray diffraction of single domains. The electrostrictive aspects will be thoroughly explored. Attempts will be made to get more complete effective polarization of polycrystalline materials, and efforts will be made to manufacture large single crystals for commercial applications.

"Compositional research will be directed toward obtaining higher K values and greater temperature stability of the high K materials; also toward lower aging rates, improved power factors, higher dielectric strengths, and thinner films.

"In the low K fields, higher K values with respect to the temperature coefficient will be striven for. Efforts will also be directed toward the general improvement of power factors and dielectric strengths and the making of still thinner films.

Prediction of Future Accomplishments

"Out of all this research will come rather complete explanations for the unusual properties of these new types of ceramics, and the knowledge of how to make further improvements.

"Reasonably temperature-stable dielectrics can be predicted which will have K values of more than 10,000 for a fair range of temperatures. Effective K values 10 to 100 times higher than this may also be possible. This tremendously high K material, however, will have much higher power factors and will be suitable for very limited applications only. In fact, the greatest problem would probably be finding

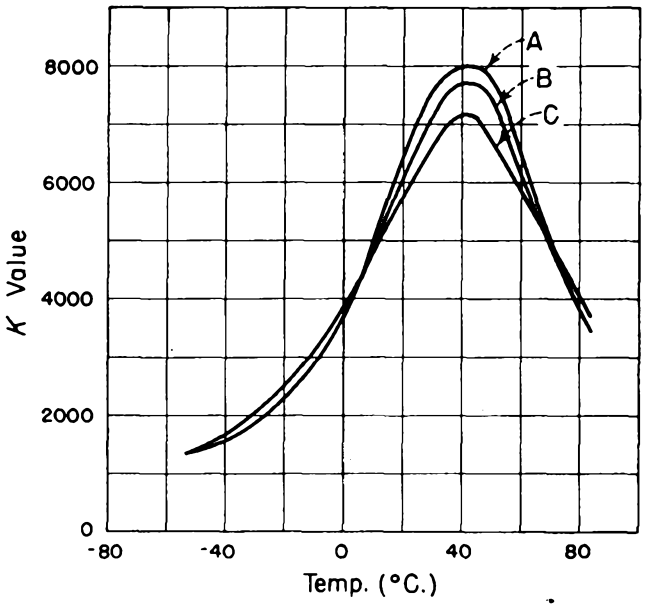

Fig. 15.16. Effect of Aging on K-value. After R. R. Roup.[34] (*Courtesy American Ceramic Society.*)

an application which can utilize the high K and tolerate the very high power factors involved.

"Methods of growing single crystals commercially will probably be accomplished for special applications where performance rather than cost is the major consideration.

"The present K value of 38 for extremely temperature-stable, zero-temperature coefficient dielectrics, will probably be doubled.

"Useful film thicknesses of well below 0.001 in. have been predicted with the expected accomplishment of about five microns or 0.0002 in.

"Improved power factors of lower than 0.01% will permit large ceramic capacitors to make inroads into the massive oil-filled paper capacitor field.

Acknowledgment

"The author wishes to express his appreciation for the contributions of K. B. Thews and A. R. Rutkowski, and E. Wainer, H. Thurnauer, and A. P. deBretteville,

Jr., for historical information, present achievements, the direction of research, and predictions of future accomplishments."

Magnetic Ferrites

Ferromagnetic ferrites are compounds of various metal oxides and have the general formula $MOFe_2O_3$, where M stands for a bivalent metal ion such as Ni, Zn, Mg and others. They are ceramic materials with a crystalline structure of the spinel type and are produced according to the common techniques of ceramic manufacture outlined earlier in this chapter. The mineral magnetite ($FeOFe_2O_3$) is the ferro-ferrite occurring in nature and well known for its magnetic properties. Synthetic ferrites were first proposed by G. Hilpert in Germany as core materials for high frequency application in 1909. (German Patents No. 226347, 227787, 227788.) Kawai, Noboru, Takei and others in Japan investigated various compositions of ferrites in 1934 and the following years.[58–60] They succeeded in making ferrites with both "soft" and "permanent" magnetic properties and studied the effect of composition on different magnetic characteristics. J. L. Snoek[61] published a book on the work carried out during World War II at the Philips Laboratories in Eindhoven which led to the development of the different types of Ferroxcube."[62] E. Albers-Schoenberg* and W. Soyck began work on ferrites in Germany in 1942 and development of ferrites has been active by several companies in U.S.A. since the end of World War II.[63–65]

Due to the absence of metal components and in view of their dense structure, ferrites have a high volume resistivity and high permeability in comparison to conventional iron powder core materials. Their specific gravity lies between 4 and 5 and the dielectric constant is about 9. Table 15.14 gives the physical characteristics of ferrites as produced by one manufacturer under the trade name "Ferramic."[64] Their interesting properties are evident and will lead to a wide field of applications, especially if the relatively high temperature coefficient of permeability can be reduced and the Curie point shifted to higher temperatures. Some of these implications have been treated by Strutt.[65a]

Mica

Mica is not a ceramic, as was pointed out previously, but a natural mineral which is used in its natural form. The heat treatment to which it is usually subjected before use in electron tubes does not alter its form, but serves to drive out water and gases. Some physical properties of mica, principally those of thermal expansion and power factor, have been described at length by Hidnert and Dickson of the National Bureau of

* Now Director of Research with General Ceramics and Steatite Corp., Keasbey, N.J.

TABLE 15.14. PHYSICAL CHARACTERISTICS OF SOME TYPICAL FERRITES*

Property	Unit	A 34	B 90	C 159	D 216	E 174	G 254	H 419	I 141	J 472
Initial permeability at 1 Mc/sec		15	95	220	400	750	410	850	900–1000	330
Maximum permeability†		100	190	710	1030	1710	3300	4300	1010	750
Saturation flux density†	Gauss	840	1900	3800	3100	3800	3200	3400	1550	2900
Residual magnetism†	Gauss	615	830	2700	1320	1950	1050	1470	660	1600
Coercive force†	Oersted	3.7	3.0	2.1	1.0	0.65	0.25	0.18	0.40	.80
Temperature coefficient of initial permeability	%/°C	0.65	0.04	0.4	0.3	0.25	1.3	0.66	0.3	0.22
Curie point	°C	280	260	330	165	160	160	150	70	180
Volume resistivity	Ohm-cm.	1×10^9	2×10^6	2×10^6	3×10^7	4×10^5	1.5×10^8	1×10^4	2×10^5	
Loss Factor:										
at 1 Mc/sec			.00016	.00007	.00005	.00008	.00008	.00030	.0003	.000055
at 5 Mc/sec		.0004	.0011	.0008	.0012	.002	.00075	.00155	.005	
at 10 Mc/sec		.0005					.0017	.00275		

* Courtesy of General Ceramic and Steatite Corporation.

† Measurements made on D.C. ballistic galvanometer.

Standards,[66] where extensive references are given to the earlier literature. The classification of various grades of mica and methods of test are covered by the following ASTM Specifications:

D 351-49T	Natural muskovite mica, based on visual quality.
D 352-49	Testing pasted mica, used in electrical insulation.
D 652-43	Measuring mica stampings, used in electronic devices and incandescent lamps.
D 748-49	Natural block mica and mica films, suitable for use in fixed mica-dielectric capacitors.
D 374-42	Methods of tests for thickness for solid electrical insulation.
D 1039-49T	Glass-bonded mica, used as electrical insulation.
D 1082-49T	Power factor and dielectric constant of natural mica.
D 149-44	Standard methods of tests for dielectric strength of electrical insulating materials at commercial power frequencies.

The titles of these specifications in themselves indicate the wide scope of application of mica.

There are eight different kinds of mica, of which the first five are commercially important. They are known under the following names:

(1) Muscovite	$H_2KAl_3(SiO_4)_3$
(2) Phlogopite	$HK(MgF)_3Mg_3Al(SiO_4)_3$
(3) Biotite	$(H, K)_2(Mg, Fe)_2(Al, Fe)_2(SiO_4)_3$
(4) Lepidolite	$KLiAl(OHF)_2Al(SiO_3)_3$
(5) Roscoelite	$H_8K(Mg, Fe)(Al{\cdot}V)_4(SiO_3)_{12}$
(6) Zinnwaldite	$(KLi)_3FeAl_3Si_5O_{16}(OH, F)_2$

Only the first two of these are generally used in the electrical industry and the tube industry in particular.

Muscovite, also called "white mica" or "India mica," received its name from the locality where it was found (i.e., Muskovia in Russia). The prime source is India, but it also occurs in South America, South Africa, Korea, Mexico, Canada, and U.S.

Phlogopite, or amber mica, comes mainly from Madagascar. Muscovite is harder and is preferred for use in vacuum tubes. Phlogopite is darker in color (amber to brown) and used chiefly for heating appliances. It will stand 800°C without disintegration.[20] The tube industry thus essentially depends on a proper supply of India mica, of which it has been said that it is probably the most important single strategic material in time of a national emergency. The success obtained recently in producing synthetic mica thus appears in a proper perspective.[67] The physical

properties of electrical grade mica are given in Table 15.15.[66,68–70] The thermal expansion coefficient for phlogopite can assume very large values in the direction at right angle to the cleavage plane, as shown by Hidnert and Dickson.[66] It is many times that of any other known solid, and phlogopite piles can thus be readily used for temperature-responsive

TABLE 15.15. PHYSICAL CHARACTERISTICS OF MICA

	Muscovite	Phlogopite
Density* (g/cc)	2.6–3.2	
Mohs' hardness* (Shore's Test)	2.8–3.2 80–150	2.5–3.0 70–100
Temperature of disintegration† (°C)	975	925
Softening temperature† (°C)	> 1550	(1550)
Shear modulus‡ (kg/mm²)	23.5–26.5	10–13
Proportional limit‡ (kg/mm²)	35–39	20–28
Elastic yield‡ (kg/mm²)	35–39	20–28
Modulus of elasticity‡ (kg/mm²)	16,000–21,000	
Specific heat* (20–100°C) (cal/g. °C)	~ 0.207	
Thermal conductivity‡ (cal/cm²/cm/sec/%)	0.0008–0.0014	
Coefficient of thermal expansion§ (perpendicular to cleavage plane) (cm/cm °C)	17–25 × 10^{-6} (20–300°C) 15–34 × 10^{-6} (300–600°C)	much larger
Electrical resistivity (20°C)* (ohm cm)	2 × 10^{13}–1 × 10^{17}	somewhat less
Dielectric strength at 20°C* (1–3 mil thick) (kv/mil)	3–6	3–4.2
Dielectric constant*	6.5–8.7	5–6
Power factor (tan δ × 10^4)	8–10 (100 KC)§ 6–8 (1000 KC)	2–8‡(50–800 cy) 1.7 1 MC 1.6 50 MC ~ 2 500 MC
Refractive index*	1.56–1.60/61	1.58–1.61
Optic axial angle*	50°–75°	5°–25°
Acid reaction*	affected only by HF	decomposed in H_2SO_4

* Ref. 68.
† Ref. 69.
‡ Ref. 70.
§ Ref. 66.

devices, without the need for mechanical amplification as customarily employed with lower expansion materials. On some samples of phlogopite the expansion coefficient is as high as 0.0478 cm/cm/deg C over a short range of temperature. It usually is much lower (up to about

100°C), rises between 100 and 200°C, and then drops again above 200°C. Values obtained for one sample of Madagascar phlogopite were:

0.000097	26 to 100°C
0.00729	100 to 150°C
0.00152	200 to 300°C
0.00143	300 to 600°C

It had been concluded by earlier investigators that muscovite and phlogopite micas withstand heating between 400 and 600°C without appreciable change in their physical properties. Hidnert and Dickson find that this essentially applies to muscovite mica, but there were appreciable changes in some of the samples of phlogopite when heated to 600°C. Powell and Griffiths[71] investigated the thermal conductivity of some muscovite and phlogopite micas up to 600°C in a direction perpendicular to the cleavage plane. Five specimens of Indian muscovite mica showed slight variations of thermal conductivity with temperature over the range of 100 to 600°C. However, Canadian and Madagascan phlogopite micas indicated a pronounced decrease in thermal conductivity between 150 and 250°C, which was only partially reversible on cooling. The power factor, studied by Hidnert and Dickson, was also found to be affected by heat treatment.

"The power factors of nearly all specimens of muscovite mica from Brazil and Guatemala were slightly greater at 100 kc/s than at 1,000 kc/s. The power factor of each specimen of phlogopite mica was considerably greater at 100 kc/s than at 1,000 kc/s. The power factors of the samples of phlogopite mica from Madagascar and Mozambique are considerably larger than the power factors of the samples of muscovite mica from Brazil and Guatemala. Heating the samples of phlogopite and muscovite micas to 600°C, with or without a load on each sample, caused considerable increases in the power factors of the phlogopite micas and only slight changes in the power factors of the muscovite micas. The power factors of the phlogopite mica from Madagascar which was heat treated without a load, are less than the power factors of this mica heat treated with a load. However, the power factors of the phlogopite mica from Mozambique heat treated without a load are considerably greater than the power factors of this mica heat treated with a load."[66]

As mentioned above, it is customary and beneficial to air-bake mica wafers used as structural or insulating members in electron tubes. This is done either by holding them with tweezers in the flame of a Bunsen burner until a yellow color appears in the flame or, more reliably, by baking the micas in an electric furnace for a period of 8 to 15 hours at about 450°C. Some manufacturers prefer hydrogen firing for about 1 minute at about 900°C. Sudden heat shock like that encountered by putting the micas into a flame or a hot oven is likely to affect the mica structure adversely. In critical applications like camera tubes for television the affect of the heat treatment on physical characteristics, such as thickness,

thermal and electrical conductivity, transparency, and color, must be carefully born in mind. Storing of fired micas in a dust-free, dry atmosphere is essential, and they should be used within 2 to 3 days. Otherwise, refiring is necessary. The effectiveness of heat treatment and the importance of the time factor is well illustrated by Fig. 15.17, according to Roy,[69] who studied four species of micas which were pulverized and then decomposed by heat, water vapor under pressure, and electrodialysis.

Thus, Fig. 15.17 shows the weight loss of pulverized (80 per cent + 200 mesh) muscovite when exposed to the various temperatures indicated on the curves in a platinum crucible in air. It is apparent that dehydra-

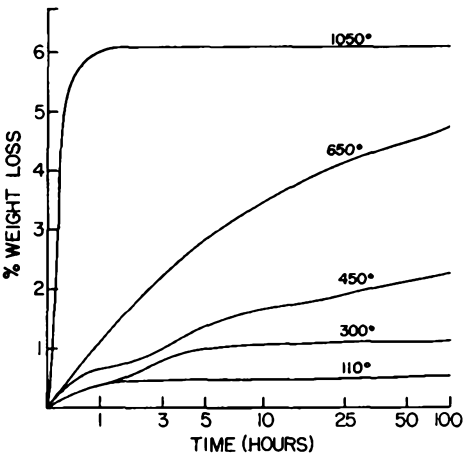

Fig. 15.17. Change of total percentage weight loss as a function of time when muscovite is held at various temperatures. After R. Roy.[69] (*Courtesy The American Ceramic Society.*)

tion at 450°C continues even after 100 hours and that only a heat treatment at 1050°C brings about total water loss in 1 hour. This must be correlated with the fact that the mica lattice breaks down at about 975°C. A baking treatment at about 900°C is thus indicated as most effective for tube applications. The common assumption, related above, that phlogopite is more heat resistant than muscovite was disproved by Roy, who showed that both have very similar weight-loss curves and that phlogopite loses its micaceous structure about 50°C lower than muscovite, which decomposes at about 975°C. To reduce surface leakage an insulating coating is frequently sprayed onto the mica and dried with hot air at about 80°C. The coating mix consists of magnesium oxide in distilled water, zirconium oxide or aluminum oxide in methyl alcohol or polyvinyl alcohol, or mixtures of these constituents. Elaborate conveyor-belt furnaces have been built for spraying and drying on a mass-production basis, but barrel coating seems to be generally preferred. The micas are

tumbled in a barrel made from wire mesh and exposed to the spray material at the same time. A hot-air blast takes care of the drying during spraying, which is followed by a baking cycle.

The fabrication of mica spacers, according to specifications worked out by the tube engineer, is a highly specialized art. The remarks made above in regard to the design of ceramics must be restated with even more emphasis (i.e., consult the manufacturer before freezing a design). For general guidance the following remarks are quoted from a pamphlet issued by the former Mica Fabricators Association.[68]

"Practically all of the mica of the qualities used in the electrical industry must be blasted or dug out of the ground by hand. In India all mining operations are brought to a standstill during the monsoon season, from June to October, each year. Cobbing is the first operation after getting the mica out of the ground. This consists of separating the books of mica from the mine-run scrap and removing all rock and earth adhesives. The next operation, known as rifting, consists of opening up the crude mica books and splitting them into blocks of from 0.007 in. to 0.030 in. thick. There are three methods of 'trimming,' namely thumb, knife, and shear. Thumb trimming is the breaking off of loose edges by hand. Knife trimming consists of cutting out all cracks and other imperfections, leaving a bevelled edge all around. Shear trimming is similar to knife trimming except that there are no bevelled edges and the trim usually results in a rectangular shape. The final operation in the preparation of the raw material is 'sorting' the block mica and classifying it into grades and qualities in accordance with commercial specifications.

"Splitting the 0.007-in. to 0.030-in. thick mica blocks to the required smaller thickness is a highly skilled manual operation, performed with knives especially designed for the purpose. Some mica must be split to as fine as one thousandth of an inch or less within very close tolerances. Here again no form of mechanization has been developed that can replace the essential accuracy and skill of experienced mica workers. At least six months' training is required before they are reasonably proficient.

"Each mica pattern or part requires a special precision die to produce clean-edged parts, free from burrs, delaminations, and cracks. This die, even for the simplest design, must be made of special steel, and requires expert tool-making and precision equipment in its manufacture. A new die is required not only for each change in pattern, but also for each change in thickness. For instance, a die which has been designed to stamp out condenser films 3 mils thick cannot be used for films 1.2 mils thick; of course, the reverse is also true. Mica dies are so highly specialized in their design and construction that ordinary tool-making experience is insufficient to make a die capable of producing parts accurately and in satisfactory quantities.

"The physical characteristics of mica make it impractical to have tolerances less than 0.0005 in. The cost decreases as the tolerance increases. Since a mica die cannot be lubricated and mica must be punched dry, dust particles and mica flakes tend to distort the holes that have been punched, and, therefore, make inspection difficult for closer tolerances. Several punched parts must be checked in order to arrive at a satisfactory average reading.

"Holes in sheet metal may be pierced and other operations performed before the blanks are cut, but not so with mica, which comes in individual pieces. For this reason, compound dies must be used for fabricating the mica patterns. A compound die punches the outside shape and all the inside holes with one stroke of the press.

"Since the design of the die has direct bearing on the cost of the fabricated part, it is recommended that either a mica fabricator or a mica die-maker be consulted before designs are adopted. The limitations of the material necessitate that certain factors in design be considered by die engineers. Although, for the most part, problems of design vary with each pattern, there are certain rules that should apply to all designs.

"One rule is that the maximum thickness should not exceed 50% of the diameter of the smallest hole. Holes cannot be placed too close to the outside edge because the material will break down through cracking and delamination. The distance, however, depends on the thickness of the mica and the size of the hole. The minimum wall, either between the hole and the edge of the blank, or between two holes, should be 80 to 100 mils for condenser films, and on other parts not less than 20 to 25 mils."

For the laboratory worker who undertakes his own fabrication of mica Strong[72] suggests splitting by introducing a drop of water after the edge has been pried open with a dissecting needle. The sealing of mica to glass and metal to form vacuum tight-joints has been described by Donal[73] and others.[74,75] An extensive treatment of mica "dealing with natural and built-up mica and mica products in all aspects, including geology, prospecting, mining, production, manufacture, utilization, and marketing of mica" has been published by Chowdhury.[76]

REFERENCES

1. Bidgood, E. S., and Kent, G. H., "Cataphoresis and Alundum Coatings," *Transact. Electrochem. Soc.*, **87**, 321–329 (1945).

1a. Klemperer, H., "Heater-Cathode Insulation Performance," *El. Eng.*, **55**, 981–985 (1936).

2. Palumbo, T. R. (Ceramic Heater Cathode Resistor Company, Keyport, N.J.), "Ceramic Heaters and Cathodes for Electron Tubes," Symposium on Thermionics held at New York University (Jan./Feb. 1950).

3. Norton, F. H., "Refractories," New York, McGraw-Hill Book Co., 1942: 3d Ed., 1949.

4. *J. Am. Ceram. Soc.*, 20th & Northampton Streets, Easton, Pa.

5. *Ceram. Bull., Ibid.*

6. *Transact. Brit. Ceram. Soc.*, The North Staffordshire Technical College, Stoke-on-Trent, England. (The General Secretary).

7. *J. of the Soc. of Glass Tech.*, "Elmfield," Northumberland Rd., Sheffield 10, England.

8. Rigby, G. R., "The Application of Crystal Chemistry to Ceramic Materials," *Transact. Brit. Ceram. Soc.*, **48**, 1–67 (1949).

9. Thurnauer, H., "Ceramic Insulating Materials," *El. Eng.*, **59**, 451–459 (1940).

10. Hausner, H. H., "Metal Ceramics, a New Field in Powder Metallurgy," *Proc. of Fourth Annual Spring Meeting*, Metal Powder Assoc. 420 Lexington Ave., New York 17, N.Y. (1950).

11. Campbell, J. B., "Metals and Refractories Combined in High-Temperature Structural Parts," *Mater. and Meth.*, **31**, 59–63 (1950).

12. Navias, L., "Extrusion of Refractory Oxide Insulators for Vacuum Tubes," *J. Am. Ceram. Soc.*, **15**, 234–251 (1932).

13. Partridge, J. H., and Lait, J. R., "The Manufacture of Refractory Carbides from Pure Oxides of High Melting Point," *J. Soc. Glass Tech.*, **20**, 200–217 (1936).

14. Ijdens, R. A., "Ceramics and Their Manufacture," *Philips Tech. Rev.*, **10,** 205–213 (1949).
15. Riddle, F. H., "Ceramic Spark-Plug Insulators," *J. Am. Ceram. Soc.*, **32,** 333–346 (1949).
16. Schwartzwalder, K., "Injection Molding of Ceramic Materials," *Bull. Am. Ceram. Soc.*, **28,** 459–461 (1949).
17. Rowland, D. H., "Porcelain for High-Voltage Insulators," *El. Eng.*, **55,** 618–626 (1936).
18. Koenig, J. H., "Ceramics for Engineering Applications," *Mater. and Meth., Manual 62*, **32,** 69–84 (Sept. 1950).
19. Fairchild, C. O., and Peters, M. F., "Characteristics of Pyrometric Cones," *J. Am. Ceram. Soc.*, **9,** 701–743 (1926).
20. Miner, D. F., "Insulation of Electrical Apparatus," New York, McGraw-Hill Book Co., 1941.
21. "Handbook of Chemistry and Physics," 31st. Ed., Cleveland, Chemical Rubber Publishing Co., 1949.
22. Thurnauer, H., "High-Frequency Insulation," *Ceram. Bull.* **29,** 158–160 (1950).
23. Russell, R., Jr., and Berberich, L. J., "Low-Loss Ceramics," *Electronics*, **17,** 136–142, 338 (1944).
24. Thurnauer, H., "Properties and Uses of Technical Ceramics," *Mater. and Meth.*, **26,** 87–92 (1947).
25. Sosman, R. B., "The Properties of Silica," New York, Reinhold Publishing Corp., 1927.
26. Sabol, F. P., "Ohio State Univ. Res. Found. Proj., No. 252," 1947.
27. Albers-Schönberg, E., "Hochfrequenz-Keramik," Dresden and Berlin, Theodor Steinkopff, 1939.
28. Russell, R., Jr. and Mohr, W. G., "Characteristics of Zircon Porcelain," *J. Am. Ceram. Soc.*, **30,** 32–35 (1947).
29. Curtis, C. E., and Laurie, D., "Investigation of Various Properties of Stabilized Zirconia at Elevated Temperatures 1–3," *J. Am. Ceram. Soc.*, **33,** 198–207 (1950).
30. Johnson, P. D., "Behavior of Refractory Oxides and Metals, Alone and in Combination, *in Vacuo* at High Temperatures," *J. Am. Ceram. Soc.*, **33,** 168–171 (1950).
31. Lindsay, E. W., and Berberich, L. J., "Electrical Properties of Ceramics as Influenced by Temperature," *Transact. Am. Inst. El. Eng.*, **67,** 734–742 (1948).
32. Von Hippel, A. and Maurer, R. J., "Electric Breakdown of Glasses and Crystals as a Function of Temperature," *Phys. Rev.*, **59,** 820–823 (1941).
33. Gleason, J. M., "Steatite for High-Frequency Insulation," *J. Brit. Inst. Rad. Eng.*, **6,** 20–32 (1946).
34. Roup, R. R., "Titania Dielectrics," *Ceram. Bull.*, **29,** 160–163, (1950).
35. Schmidt, W., "Determination of the Dielectric Constant of Crystals by Means of Electric Waves" (In German), *Ann. Physik*, **9,** (Ser. 4), 919–937 (1902). Pt. 2, *Ibid.*, **11,** (Ser. 4) 114–126 (1903).
36. Landolt-Börnstein, *Phys. Chem.-Tabellen*, 1221, (1912).
37. Liebisch, T., and Rubens, H., "Preuss. Akad. Wiss. Berlin Ber.," **8,** 211 (1921).
38. *Ger. Patent 545,402* (1925).
39. Ehlers, G. M., and Roup, R. R., Assignors to Globe-Union, Inc., "Electrical Capacitor and Dielectric for Same," *U.S. Patent 2,398,088.*
40. Wainer, E., and Solomon, A. N., *Ind. Repts.*, Nos. 8, 9, and 10, Titanium Alloy Mfg. Co. (1942–1943).
41. Wainer, E., Assignor to Titanium Alloy Mfg. Co., "High Dielectric Material and Method of Making the Same," *U.S. Patent 2,402,515* (June 18, 1946).

42. Wainer, E., "High-Titania Dielectrics," *Trans. Electrochem. Soc.*, **89,** 47–71 (1946).
43. Howatt, G. N., Breckenridge, R. G., and Brownlow, J. M., "Fabrication of Thin Ceramic Sheets for Capacitors," *J. Am. Ceram. Soc.*, **30,** 237–41 (1947).
44. Navias, L., "Compositions and Properties of Some High-Titania Ceramics," *J. Am. Ceram. Soc.*, **24,** 148–155 (1941).
45. Shelton, G. R., Creamer, A. S., and Bunting, E. L., "Properties of Barium-Magnesium Titanate Dielectrics," *J. Am. Ceram. Soc.*, **31,** 205–212 (1948).
46. von Hippel, A., Breckenridge, R. G., Chesley, F. C., and Tisza, L., "High Dielectric Constant Ceramics," *Ind. Eng. Chem.*, **38,** 1097–1109 (1946).
47. deBretteville, A. P., "Oscillograph Study of Dielectric Properties of Barium Titanate," *J. Am. Ceram. Soc.*, **29,** 303–307 (1946).
48. Wul, B. M., "Dielectric Constant of Barium Titanate at Low Temperatures," *J. Phys. U.S.S.R.*, **10,** 64–66 (1946).
49. Wul, B. M., and Goldman, I. M., "Dielectric Hysteresis in Barium Titanate," *Compt. rend. acad. sci. URSS,* **51,** 21–23 (1946).
50. Wul, B. M., and Goldman, I. M., "Dielectric Constants of Titanates of Metals of the Second Group., *Ibid.*, **46,** 141 (1945).
51. Wul, B. M., and Vereschlagin, L. F., "Dependence of Dielectric Constant of Barium Titanate on Pressure," *Ibid.*, **48,** 634–66 (1946).
52. Roberts, S., "Dielectric and Piezoelectric Properties of Barium Titanate," *Phys. Rev.*, **71,** 890–895 (1947).
53. Donley, H., "Effect of Field Strength on Dielectric Properties of Barium Titanate," *R.C.A. Rev.* **8,** 539–533 (1947).
Donley, H., "Barium Titanate and Strontium Titanate Resonators," *Ibid.*, **9,** 218–228 (1948).
54. Megaw, H. D., "Crystal Structure of $BaTiO_3$," *Nature*, **155,** 484–485 (1945).
55. Rooksby, H. P., "Compounds of the Structural Type of Calcium Titanate," *Ibid.*
56. Matthias, B. T., Breckenridge, R. G., and Beaumont, D. W., *Phys. Rev.*, **72,** 532 (1947).
57. *N.D.R.C. Rept.*, Div. 14, No. 300 (Aug., 1944). *Ibid.*, No. 540 (Oct. 1945).
58. Kawai, Noboru, "Formation of Solid Solution between Some Ferrites," *Jour. Soc. Chem. Ind., Japan,* **37,** 4 (1934).
59. Takei, T., "Metallic Oxides as Magnetic Materials," *Machinery and Electr., Japan,* Vol. 1, 2, 3, Jan., Feb., Mar. (1937).
60. Takei, T., "Metallic Oxides as Ferromagnetic Materials," *Electr. Eng. Soc. Jour., Japan* **59,** 6 (1939).
61. Snoek, J. L., "New Developments in Ferromagnetic Materials," New York, *Elsevier Publ. Comp.* (1947).
62. Snoek, J. L., "Non-metallic Material for High Frequencies," *Philips Tech. Rev.*, **8,** 353–360 (1946).
63. Javitz, A. E., "Ten New Magnetic Materials," *El. Mfg.*, **40,** 74–78, 194, 196 (1947).
64. Snyder, C. L., Albers-Schoenberg, E. and Goldsmith, H. A., "Magnetic Ferrites, Core Materials for High Frequencies," *El. Mfg.*, **44,** 86–91 (Dec. 1949).
65. Albers-Schoenberg, E., "Ferromagnetic Oxide Bodies, a Counterpart to the Ceramic Dielectrics," *Cer. Age.*, **56,** 14–16, 41 (Oct. 1950).
65a. Strutt, M. J. O., "Ferromagnetic Materials and Ferrites," *Wireless Eng.*, **27,** 277–284 (1950).
66. Hidnert, P., and Dickson, G., "Some Physical Properties of Mica" (RP1675), *J. Res. Nat. Bur. Stand.*, **35,** 309–353 (1945).
67. Jackel, R. D., "Progress in Synthetic Mica," *El. Manuf.*, **45,** 99–103, 190, 192 (1950).

68. "Handbook on Fabricated Natural Mica," New York, Mica Fabricators' Assoc., 1949. (Stewart N. Clarkson Associates, Inc.)
69. Roy, R., "Decomposition and Resynthesis of the Micas," *J. Am. Ceram. Soc.*, **32,** 202–209 (1949).
70. Espe, W., and Knoll, M., "Werkstoffkunde der Hochvakuumtechnik," Berlin, J. Springer, 1936.
71. Powell, R. W., and Griffiths, E., "The Variation with Temperature of the Thermal Conductivity and the X-Ray Structure of Some Micas," *Proc. Roy. Soc.*, London (A), **163,** 189 (1937).
72. Strong, J., "On Splitting Mica," *Rev. Sci. Inst.*, **6,** 243 (Aug. 1935).
73. Donal, J. S., Jr., "Sealing Mica to Glass or Metal to Form a Vacuum-Tight Joint," *Rev. Sci. Inst.*, **13,** 266 (1942).
74. Wu, C. S., Meaker, C. L., and Glassford, H. A., "Thin Window Counter with Special Mica-to-Glass Seal," *Rev. Sci. Inst.*, **18,** 693–695 (1947).
75. Labeyrie, J., "Vacuum-Tight Sealing of Glass and Mica," (In French), *J. de Physique et le Radium*, **11,** 20 (1950).
76. Chowdhury, R. R., "Handbook of Mica," Brooklyn, Chemical Publishing Co., Inc., 1941.

CHAPTER 16

CERAMIC-TO-METAL SEALS

The joining of ceramic bodies to each other or to glass and metal members is a problem that naturally arises in the construction of electronic devices. The required joints may be temporary and demountable or permanent, and in all cases must be vacuum-tight. Temporary seals can of course be made by a variety of gaskets and sealing compounds. These will not be discussed in this chapter. Ceramic seals of various kinds were first developed in Germany,[1–4] and during World War II ceramic-to-metal seals were applied on a larger scale to small radar tubes by Telefunken A.-G.[5–7] Partridge[8] gives a review of ceramic-sealing techniques in his monograph on glass-to-metal seals. In recent years ceramic sealing has been paid increasing attention in the United States. Apart from developing and improving known techniques original contributions have been made. Bondley[9]* described the titanium-hydride process in highly purified hydrogen, Pearsall[10]† the zirconium-hydride process in conjunction with zirconium alloys, and Nolte and Spurck[11]* metal-ceramic sealing with manganese. Under the sponsorship of the Bureau of Ships‡ a tetrode ceramic version of the planar triode 2C39 was developed with the designation ML-281. During this development an improved version of the Telefunken Process was used which eliminated the danger of seal leakage.[12] Similarly, a miniature ceramic "Lighthouse" triode (ML-280) was developed from the British Prototype VX-7021, under the sponsorship of the Bureau of Ships.[13]§ The first ceramic x-ray tube (Fig. 16.1) was constructed by Machlett Laboratories, Inc.,[14] using the same technique. McPhee and Soderstrom[15]|| applied the Telefunken technique to a novel seal structure which permits the joining of any suitable metal to any suitable ceramic regardless of size and relative thermal expansion coefficient.

The advantages of ceramic seals have been well summarized by Rheaume,[13] from which the following is quoted:

* General Electric Company, Schenectady, N.Y.
† M.I.T., Cambridge, Massachusetts.
‡ Contract NObsr-30150.
§ Contract No. NObsa-30045.
|| Collins Radio Company, Research Laboratory, Cedar Rapids, Iowa.

"From a large-scale production viewpoint the metallized ceramic silver solder seal method has important potential advantages for many different kinds of electron tubes, and is well adapted for the manufacture of miniature tubes. In general, after metallizing ceramics and electroplating metal parts, all that remains for assembling tubes is to stack these components with rings of silver solder in precision jigs and pass them through an atmosphere furnace. The mechanical strength and alignment of these seals, and consequently of the internal electrodes, appear to be superior to those of conventional metal-glass tubes.

"The elimination of glass permits the tube to be outgassed during evacuation to higher temperatures than heretofore, and the subsequent sealing-off operation is

Fig. 16.1. Ceramic X-ray tube with a wide angle beryllium window for reproduction of Greuz Rays. Anode voltage 4 to 25 kv. Diameter of ceramic cylinder is 2 inch, over-all length $3\frac{13}{16}$".[4] (*Courtesy Machlett Laboratories, Inc.*)

performed by severing the copper-anode tubulation to form a vacuum-tight cold-welded joint. The use of a copper anode affords optimum electrical conductivity and heat dissipation, and takes advantage of the gettering capability of thoroughly outgassed copper surfaces for maintaining high vacuums. No other gettering procedure is needed."

To provide a bond between metal and ceramic a thin film of metal or alloy is first applied to the ceramic body in such a way as to become an integral part of it. This usually entails a firing operation at elevated temperature. The art of metallizing nonconductors[1,16,17] is very old, and includes the decorative art of the ancient cultures. Enameling steel and producing printed circuits[18] involve similar problems. There is one case, however, where this intimate junction can be obtained at room temperature. Wooster and MacDonald[19] have reported on smears of titanium metal, obtained when the metal is rubbed against many hard surfaces. All silicates, except beryl, are readily attacked in this manner. Thus, it is possible to remove the polished surface of glass by rubbing it with

titanium, then dissolving the metallic smear in hydrochloric acid. Gillett[20] reported this effect of titanium on glass several years earlier, and found that zirconium behaves in a similar manner. He showed that decorative patterns can be applied to glazed china without the need of firing, and remarked that "more utilitarian applications for an adherent metal surface of zirconium or titanium or of some other metal, plated upon these adherent coatings upon glass and glazed ceramic wares, can readily be thought of, such, for example, as a type of gasket in glass-to-glass seal." It has always appeared reasonable to the present author to expect vacuum tight seals after an assembly of polished glass or ceramic surfaces, treated with a titanium or zirconium smear, is subjected to a moderate heat treatment. In France such "cold seals" have been made between polished quartz surfaces, even without the intervening metal,[21] and cold seals between metallic surfaces have also been realized. It is interesting to consider in this light a statement by Weyl,[22] which reads as follows:

"Pressing a metal against a glass surface produces locally a chemical reaction. On removal of the metal, parts of it are retained by the glass. This is particularly true for the metals, such as titanium and zirconium, which are ductile and form highly charged ions. But even those metals, such as iron, which produce no visible marks on the glass, leave traces on the surface which can be 'developed' by means of silvering solutions. Among the metal ions, those of tin seem to have the greatest affinity for the glass surface."

In many ways the joining of two ceramic bodies has features in common with the problems encountered in metal-brazing. In his early seals Handrek[1] utilized a glass as bonding layer which constitutes a ceramic of lower softening point entering the matrix of the adjoining high-melting ceramic. At the same time, many considerations entering into the design of glass-to-metal seals (Chapter 4) apply to ceramic-metal seals, and the principles of glaze-fit, discussed in the previous chapter, play an important role. As an example, we may consider the joining of two tubular members, one of which is made of ceramic with a heavy wall and the other of glass with a relatively thin wall. The glass may be joined to the inside or outside of the ceramic tube. Depending on the relative magnitude of the expansion coefficient of the glass to that of the ceramic the stresses occurring at the joint are as listed in Table 16.1. Compression in the axial, tangential, or radial direction is indicated by C and tension by T.[3]

Since glass is the weaker member of the two materials joined, it should not be put into tension. It has been shown that the stresses at the surface, both in an axial and tangential direction, are the most important and that the radial tension is less critical. It is thus evident from the tabulation below that the glass should have the smaller thermal expansion coefficient and that a seal with the glass inside would be the safer although

an outside seal is also practical. If the ceramic is the weaker member in terms of thickness, conditions may be quite different. Among the many practical applications of this type of ceramic-to-glass seal are the betatron gun and target seals. To seal directly to the ceramic side arms of the doughnut 7050 or 3320 Corning glass is used. After a glaze-fit having $\alpha_{glaze} < \alpha_{ceramic}$ is chosen, the ceramic body is glazed on the outside to improve strength and resistance to thermal shock and the inside is unglazed and metallized with a solution of liquid-bright palladium solution in an equal volume of acetone. Commercial platinum solution can also be used in the same manner.[23] Metallizing an unglazed or slightly rough-surface ceramic is usually easier than a glazed surface.

TABLE 16.1. STRESSES OCCURRING AT THE INTERFACE OF GLASS-TO-CERAMIC SEALS (T = TENSION; C = COMPRESSION)*

	$\alpha_{glass} > \alpha_{ceramic}$				$\alpha_{glass} < \alpha_{ceramic}$			
	Glass Outside		Glass Inside		Glass Outside		Glass Inside	
	Glass	Ceramic	Glass	Ceramic	Glass	Ceramic	Glass	Ceramic
Axial	T	C	T	C	C	T	C	T
Tangential	T	C	T	C	C	T	C	T
Radial	C	C	T	T	T	T	C	C

* After Albers-Schönberg.[3]

The successful realization of the betatron ceramic tube is an excellent example of advanced ceramic technique.

When it comes to joining a rod and a cylinder or two cylindrical bodies, where one is a metal and the other a ceramic, glass may again be used as an intermediate bond if its thermal expansion coefficient is suitably chosen. The limitations are severe, however. The expansion of the metal and ceramic must also be matched within fairly close limits. It is possible to visualize, for example, a rod-disk seal where all three components, metal, ceramic and glass, are similar in expansion within about 10 per cent. Fig. 16.2 shows such an assembly, which closely follows glass-to-metal sealing technique. The range of thermal expansion coefficients for ceramics, given in Table 15.7,* encompasses values from 25×10^{-7} to 105×10^{-7}, while copper has a value of 165×10^{-7} and steel covers 75×10^{-7} to 190×10^{-7}. Copper is thus ruled out, but some alloy steels or "Kovar" (50×10^{-7}) might be acceptable despite their higher electrical resistivity. Molybdenum and tungsten are other alternatives. In these cases it would be advisable to use short lengths of the sealing metal, butt-welded to copper at each end in the fashion of three-piece welds (Chapter 4), to reduce to a minimum the high resistance path.

* page 364.

Using 7040 as intermediate bond Bahls[24] has described seals between "Kovar" and electrical porcelain. Handrek[1] has pointed out the desirability of reducing the cross-section of such current leads into ceramics and keeping their sealing surface large. The expansion stresses set up by the metal rod tend to rupture the seal, increase with the square of the diameter, while the adhesive forces of the seal surface are directly proportional to the first power of the diameter. Smaller diameters thus give a more favorable balance. Handrek carried this reasoning to the extreme by reducing the current-carrying member to a thin metal film of a few microns thickness which he applied to a ceramic rod.

The metal film then takes on the expansion characteristics of the ceramic itself, and is bonded to the disk by a thin glaze. Outside of the

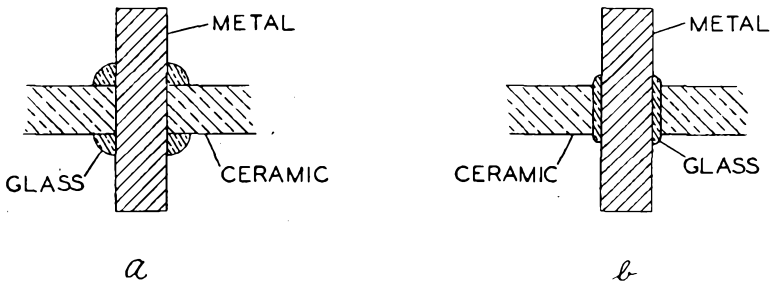

Fig. 16.2. Schematic outline of metal-rod ceramic-disk seals.

seal area the metal film can be reinforced and brazed to a heavy metal sleeve. Several hundred amperes have been passed through such seals (*Metallhaut Einschmelzungen*), and it is said that the current-carrying capacity in amperes is twice the diameter of the seal circle in mm. Fig. 16.3 gives an outline sketch of such a "metal-film seal." Arrangements where thin flexible metal members take up the stresses involved during expansion are readily visualized. Fig. 16.4 gives one such outline in cross section where a thin metal coupling is brazed to the metal rod at the center and to a reinforced metal film on the ceramic disk. Similar assemblies have been used widely in soldered ceramic-to-metal seals.[25]

The proper metallizing of ceramic surfaces permitting high-temperature brazing of bulk metals was the outstanding advance represented by the Telefunken process.[5] It consisted of coating the ceramic with a paste of very fine molybdenum powder to which a few per cent of iron powder was added. After sintering this paste to the ceramic in a hydrogen atmosphere at about 1400°C, or just below the ceramic softening point, a paste of nickel powder is applied in a similar manner and fired at 1000°C. The metal, which may be silver- or nickel-plated at the joint surface, is then silver-brazed to the metallized ceramic in a conventional manner,

with the reservation that the composition of the furnace atmosphere and the time of firing are much more critical than in ordinary metal brazing. "Alsimag 243"* is the ceramic body commonly used for such seals, and the nickel-iron alloys, Driver-Harris "Alloy 52" and "Alloy 14," sufficiently match the ceramic over the low temperature range to give satisfactory seals.

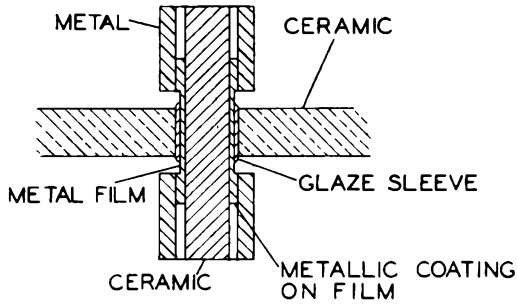

Fig. 16.3. Schematic outline of metal film seal. After Handrek.[1] (*Courtesy Verlag Johann Ambrosius Barth, Leipzig.*)

Referring to Chapter 4 and Figs. 4.12 and 4.13 (p. 67), it will be recalled that the expansion coefficient of Ni-Fe alloys varies over a wide range with percentage composition. For glass-to-metal seals an alloy was chosen which is without phase transformation within the range of temperatures encountered by the alloy during sealing and operation. By developing special glasses which closely match the expansion charac-

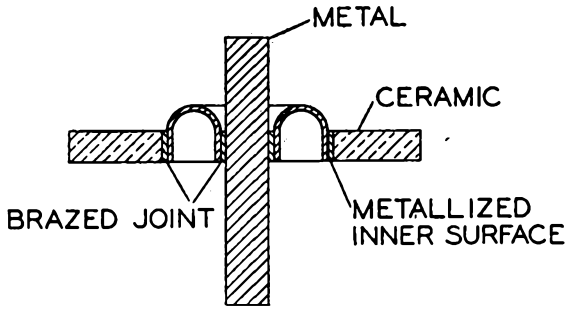

Fig. 16.4. Schematic outline of a flexible cup ceramic-metal seal.

teristic of the alloy over the entire range between room temperature and sealing point, satisfactory seals were obtained. For ceramic seals the sealing point may be as high as 1000°C, depending on the brazing metal or alloy chosen for the joint. A match of the expansion characteristics of ceramic and Ni-alloy over such a wide range is clearly impossible on

* American Lava Corporation, Chattanooga, Tennessee.

account of the wide digression of the alloy expansion after it has passed the inflection point. Fig. 16.5 makes this statement more plausible by comparing the thermal expansion characteristics of "Alsimag 243" and "42 Alloy." Fig. 16.6 gives the thermal expansion characteristics of several nickel alloys and "Alsimag 243" over the low temperature range 0–300°C.* These two materials or their equivalents represent the best match possible within present-day materials technology. To allow for

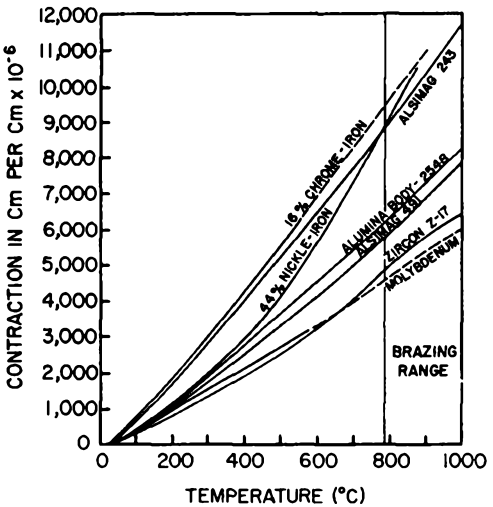

Fig. 16.5. Elongation vs. temperature for various ceramic bodies and sealing alloys. After H. J. Nolte and R. F. Spurck.[11] (*Courtesy Bryan Davis Publishing Company, New York.*)

the expansion differential at elevated temperatures careful design of the seal geometry and slow cooling rates are necessary. The ceramic body of the completed seal should be under compression to take advantage of the very much greater strength of ceramics under compression as against tension. Some of the physical characteristics of materials for ceramic-to-metal seals are given in Table 16.2 (see page 411).

Alloy No. 52 is used for cylindrical seals where the metal is on the outside and alloy 14 where the metal is on the inside of "Alsimag 243" cylinders. Under sponsorship of the Bureau of Ships† Machlett Laboratories, Inc. have carried on an extensive program of investigation of the various ceramic sealing processes, and Doolittle reports his findings in regard to the Telefunken Process as follows:‡

* Average of five samples measured by Bell Telephone Laboratories.

† Contract No. NObsr-39365.

‡ The author is indebted to Dr. H. D. Doolittle of Machlett Laboratories, Inc., for making these data available to him.

"The details of processing worked out agree well with those given by Telefunken. The ceramic must be heated to within 50°C of the softening point of the ceramic in order to obtain a bond between the molybdenum and the ceramic. A slight oxidizing of the molybdenum must take place (i.e., the oven atmosphere must not be devoid of water vapor or oxygen). Satisfactory results depend upon developing the technique for painting the molybdenum powder solution onto the ceramic. The coating must not be too thick or too thin and must wet into the ceramic pores. In this connection

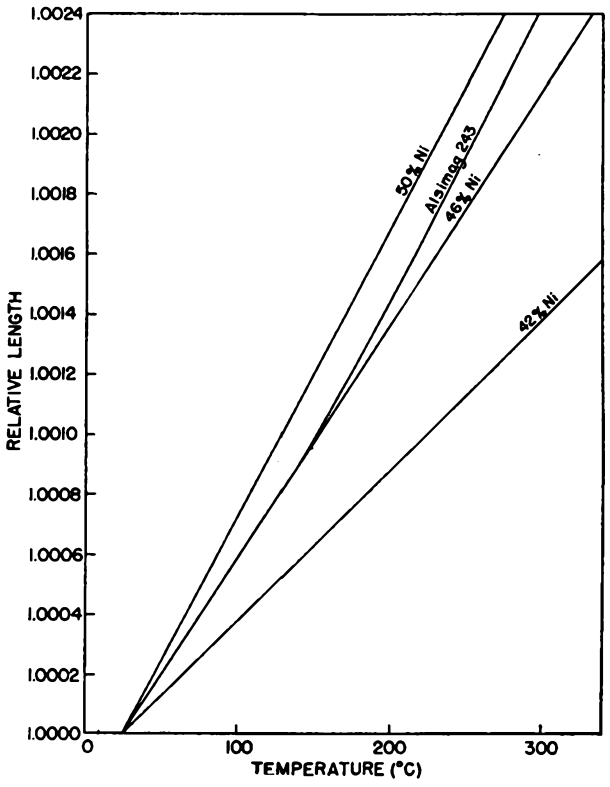

Fig. 16.6. Thermal expansion characteristics of "Alsimag 243" and several nickel-iron alloys. (*Courtesy Machlett Laboratories, Inc. and U.S Bureau of Ships.*)

a proper ceramic surface is essential. Several hundred ceramic parts were obtained which had a mottled surface appearance. It was impossible to obtain good results with these parts. Apparently, the grain structure of the ceramic must be fine and uniform. Satisfactory joints were made with seven different types of commercial ceramics but only the 'Alsimag 243' was made up in large quantities for complete testing.

"It was not a simple procedure to pick proper metals for sealing. A great variety of low-expansion alloys were obtained and tested. Alloys containing chromium were difficult to use since firing in any atmosphere other than extremely dry hydrogen produced oxides even through a silver-plated layer. In such cases failure to hold a vacuum might well be due to the chromium oxide in the bond rather than expansion

TABLE 16.2. CHARACTERISTICS OF MATERIALS FOR CERAMIC-TO-METAL SEALS
(See also Tables 15.7–15.9)

Ser. No.	Material	Type Composition	Thermal Expansion Coefficient (Range °C) $\frac{cm}{cm}/°C \times 10^7$	Compressive Strength (psi)	Resistance to Thermal Shock	Softening Point (°C)	Loss Factor (at MC) 25°C	Dielectric Constant (at MC) 25°C	Volume Resistivity (Temp. °C) ohm-cm
1	Alsimag 243[a]	Forsterite ($2\ MgO \cdot SiO_2$)	91 (25–100) 107 (25–700)	85,000	Low	1440	0.002 (1) .0011 (10^4)	6.2 (1) 6.1 (100)	10^{14} (25) 1×10^8 (700)
2	Alsimag 491[a]	Alumina (Al_2O_3)	62 (25–100) 77 (25–700)	100,000	High	1750	.017 (1)	8.6 (1)	1.7×10^{11} (300)
3	Alsimag 505[a]	Steatite ($MgO \cdot SiO_2$)	66 (25–100) 91 (25–700)			1420	.0094		7×10^{11} (300)
4	Coors AI-200[b]	Alumina (Al_2O_3)	66.7 (25–200) 91.4 (25–1000)	275,000–290,000			.0031 (1) .0031 (100)	8.81 (1) 8.80 (100)	4.0×10^{14} (100) 3.3×10^{10} (500)
5	Coors ZI-4[b]	Zircon Type ($ZrO_2 \cdot SiO_2$)	54.3 (25–800)	64,600– 76,000			.0021 (1)	6.82 (0.1)	7.7×10^{15} (25) 4.9×10^{10} (300)
6	Coors AB-2[b]	Alumina (Al_2O_3)	56.8 (25–200) 78.9 (25–1000)	> 200,000			.0074 (1) .0074 (100)	8.16 (1) 8.16 (100)	
7	Stupakoff 6486[c]								
8	Alumina 2548[d]	Alumina (Al_2O_3)			High	1750			
9	Zircon Steatite[e] BN3030	Steatite ($MgO \cdot SiO_2 + ZrO_2 \cdot SiO_2$)	60 (20–100) 73 (20–400)	80,000	Medium	1380	.004 (4)	6.3	$> 10^{14}$ (20) 2×10^{13} (200) 3×10^{12} (300)
10	Zircon Porcelain M400[e]	Zircon Type ($ZrO_2 \cdot SiO_2$)	28 (20–100) 49 (20–400)	88,000	Med. High	1450	.0143	$> 10^{14}$ (20°C) 5×10^{14} (200°C) 3×10^{12} (300°C)	
11	Driver Harris No. 42[f]	Ni: 42; Fe: Bal.	53 (20–400)						66.5×10^6
12	Driver Harris No. 46[f]	Ni: 46; Fe: Bal.	80 (25–425)						45.7×10^6
13	Driver Harris No. 52[f]	Ni: 50–51; Fe: Bal.	95 (20–500)						43.2×10^6
14	Carpenter No. 42[g]	Ni: 42; Fe: Bal.	50 (20–350)						71×10^6
15	Carpenter No. 49[g]	Ni: 49; Fe: Bal.	90 (20–350)						43×10^6
16	Carpenter No. 426[g]	Ni: 42; Fe: Bal.	93 (20–350) 99 (20–400)						94×10^6
17	Allegheny HC-1[h]	Cr: 28; Fe: Bal.	105 (20–500)						72×10^6

[a] American Lava Corporation.
[b] Coors Porcelain Company.
[c] Stupakoff Ceramic & Manufacturing Company.
[d] General Electric Company.
[e] General Ceramic and Steatite Corporation.
[f] Driver Harris Company.
[g] Carpenter Steel Company.
[h] Allegheny Ludlum Steel Corporation.

properties. Good seals could be made with such alloys of the proper expansion characteristics, but the yield was poorer than that obtained with pure nickel-iron alloys; 46- and 50% nickel alloys with iron were the most reliable materials for use with 'Alsimag 243' ceramic.

"Pieces from 0.3 to 2 inches in diameter show torsion strength equivalent to 'Kovar'-to-7052 glass seals. Failure is always due to the ceramic rather than the metal.

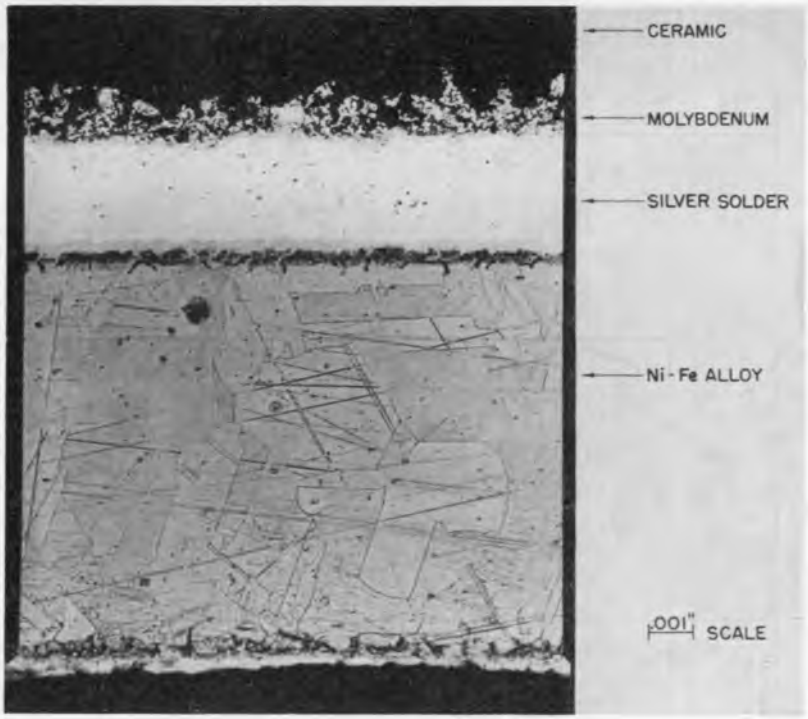

Fig. 16.7. Microphotograph (240×) of molybdenum ceramic seal (etched) made according to Telefunken process. (*Courtesy Machlett Laboratories, Inc., through American Cyanamide Company and U.S. Bureau of Ships.*)

"Repeated temperature cycling from 20 to 600°C with slow heating and cooling does not cause the seals to leak and does not impair the thermal shock resistance. The structures were heated to 600°C and allowed to cool in ordinary room ambient air. Presumably the silver anneals and relieves any strain once its temperature exceeds 200°C.

"For seals larger than 3 inches in diameter, going up to 6 and 8 inches, the use of 'Alsimag 243' was thought to be impractical and substitution of 'Alsimag 505' was suggested by the manufacturer. This latter ceramic is similar to that used by Telefunken in their radio tubes and has so far not been found wholly satisfactory, even in small diameters. Some difficulties in its manufacture remain to be overcome."

Fig. 16.7 shows a microphotograph (240X) of a ceramic seal made according to the Telefunken technique by the Machlett Laboratories,

The photograph itself was obtained through the courtesy of American Cyanamid Company.

"It is seen that some molybdenum penetrates about 1 or 2 thousands of an inch into the ceramic, but there is not a general fusion of metal and ceramic. The plating on the nickel-iron alloy has a peculiar boundary layer between metal and plating, indicating that the plating methods leave something to be desired. Grain boundaries in the nickel-iron alloy and also some foreign inclusions are clearly visible in the etched photograph."

In regard to the hydride-sealing technique[9,10] Doolittle found that satisfactory seals could be made only in a vacuum at pressures below 10^{-4} mm Hg.

"Although it has been reported by M.I.T.[10] that zirconium hydride seals could be made in nitrogen, we have had no success. Even with prepurified nitrogen the silver fails to wet the ceramic surface evenly and zirconium nitride forms. The pieces stick together, but the seal is not vacuum tight. Zirconium hydride is a little easier to use than titanium hydride because good seals can be made at a somewhat poorer vacuum (i.e., very good seals can be made at a pressure of 10^{-4} mm Hg). Using the same set-up and pressure, titanium seals show considerable oxidation. Zirconium does not wet metal as easily as titanium, and hence is easier to confine to the location where the seal is wanted. Although many vacuum-tight joints were obtained with titanium hydride at this pressure, these seals still were not considered satisfactory. Upon tearing them apart, a bond was seen to exist only at the solder fillets with little or no bond between. The use of silver-copper eutectic braze and copper instead of pure silver gave the same trouble."

Only when the pressure was kept at 2×10^{-5} mm Hg, or less, throughout the entire sealing operation was consistent success obtained with hydride seals. Fig. 16.8 shows a photograph of a tetrode (ML-329), where a number of coaxial seals were made simultaneously with the zirconium-hydride technique. The seals were made by induction heating *in vacuo.*

"The heating cycle on large ceramic bodies must be slow enough not to crack the ceramic by thermal shock. The bombarder output is increased gradually until all parts inside the furnace have reached a sufficiently high equilibrium temperature to insure complete melting of the silver and alloying with the zirconium. As the melting point of silver is reached, a great deal of vaporized silver is deposited on the inside of the container and parts of the assembly. All ceramic-soldered assemblies must, therefore, be sand-blasted to remove the thin film of vaporized metal."

In comparing the relative merits of the various sealing techniques tested by the Machlett Laboratories, Doolittle arrives at the following conclusions:

"The Mo-metallizing process derives its chief advantage from the fact that a vacuum is not necessary, thereby greatly simplifying the equipment required. This is of particular interest when production quantities are involved where jigging is also simplified. Two coating operations and three separate firings in a carefully controlled atmosphere are required with a different time schedule for each size or shape of the

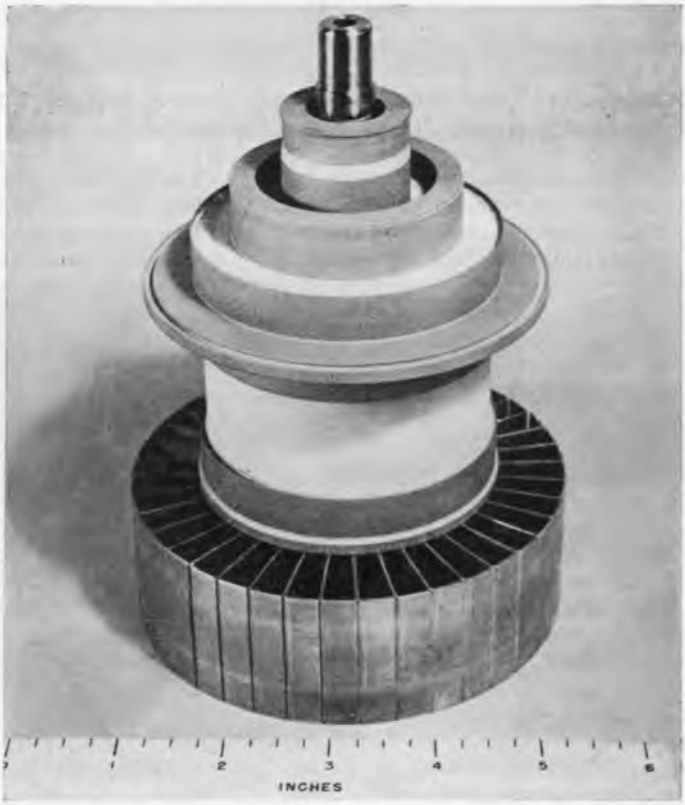

(A)

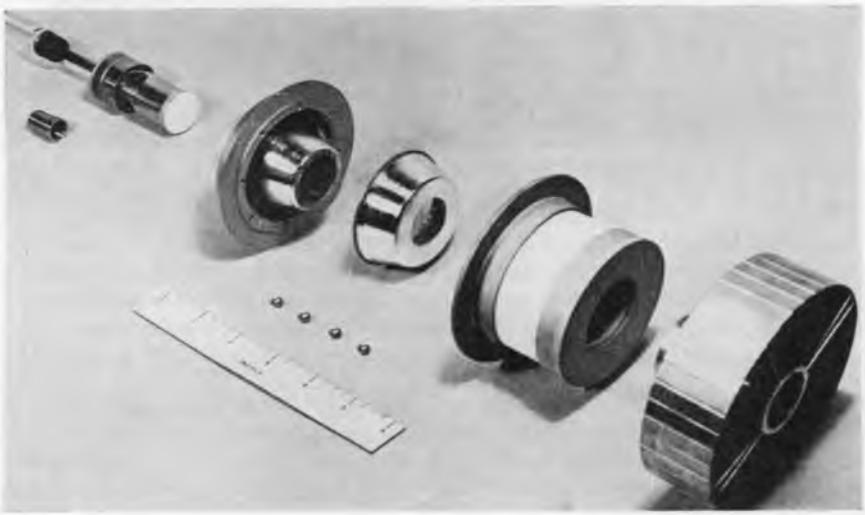

(B)

Fig. 16.8. (A) Photograph of a 1000 G Ceramic Tetrode (ML-329) sealed by the zirconium-hydride technique. (B) Exploded view showing components before final brazing of the assembly. (*Courtesy Machlett Laboratories, Inc., through U.S. Bureau of Ships.*)

(C)

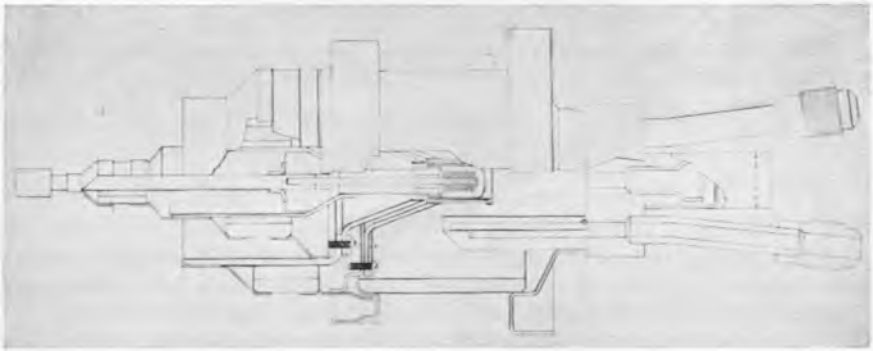

(D)

Fig. 16.8. (C) A power tetrode using ceramic construction. (D) Structural detail of same tube. (*Courtesy General Electric Company, Schenectady, N.Y.*)

ceramic part. Radiographs of Mo-metallized seals have shown evidence of voids or gas pockets. Such gas may slowly leak into the tube rendering it inoperable.

"The vacuum-hydride process is preferred chiefly because no special atmospheres are necessary. Brazing in vacuum, too, aids in the outgassing of parts, cutting down pumping time. A single painting operation preceded by one hydrogen firing or vacuum bombarding shortens sealing time appreciably. Another favorable point is that high-chrome alloys may be used for the metal member, desirable because their expansion characteristics more closely parallel the ceramics than do the high-nickel alloys. The chrome will oxidize in hydrogen atmosphere furnaces even under heavy nickel and silver plating. The vacuum-hydride process has disadvantages also, of course, primarily due to the fact that a high vacuum is needed. This may mean elaborate vacuum equipment, and more difficult jigging since the parts to be brazed must be suspended in such a manner that they are heated uniformly.

"In summarizing, the following conclusions may be reached:

(1) For small assemblies not required to insulate high voltages at high frequencies the Mo-metallizing process is to be preferred. Such small parts would probably not have to be sand-blasted. Quantity production set-ups are feasible for fairly rapid production.
(2) The vacuum-hydride process is preferable for larger assemblies:
  (a) The brazing cycle is faster, consisting of fewer operations.
  (b) Parts are more thoroughly outgassed, with no gas pockets remaining.
  (c) Controlled atmospheres are eliminated.
  (d) High-chrome alloy metal parts may be used."

Knecht[10a] has reported on the use of hydrides of active materials in vacuum tube techniques and found thorium hydride to give a stronger seal with "Alsimag 243" than does zirconium hydride. Tantalum and "Alsimag 243" were sealed successfully with zirconium hydride.

Nolte and Spurck[11] have modified the Telefunken Process by the addition of manganese to the molybdenum powder, thereby stimulating the formation of eutectics or solid solutions between metals and ceramics at the interface. The preparation of the metallizing material is described as follows:

"For over-all good performance with all ceramics the metallizing mixture is prepared by ball-milling a mixture of five materials for 24 hours:

160 grams Mo-powder (200 mesh)
40 grams Mn-powder (150 mesh)
100 cc Pyroxiline binder ('Dupont 5511')
50 cc Amyl acetate
50 cc Acetone

Sufficient amyl acetate-acetone (1:1 by vol) solution should then be added to the ball-milled mixture to give a viscosity reading of 22 seconds with a Zahn viscosimeter. The resultant metal suspension should be suitable for brushing or spraying.

"The metallizing mixture can then be applied to the areas to be brazed by brushing or spraying to a thickness of 0.001 to 0.002 inches. To insure a uniform layer when dry the coating should be moist a short time after application. Firing of the coated ceramic then proceeds in hydrogen (or other protective atmosphere) at 1350°C for ½ hour.

"The sintered and bonded molybdenum layer, like ordinary Mo or W, is not easily wetted by brazing materials; therefore, further treatment of this surface may be necessary before brazing. If silver braze is to be used, the metallized areas should be nickel-plated first, then copper-plated. Each plating should be applied for 5 minutes at 2 volts. Then these platings should be sintered in hydrogen for 10 minutes at 1000°C. If copper brazing is to be done, the treatment is the same, except that the nickel-plating is omitted. Brazing is done in a protective atmosphere in much the same way as ordinary metal-to-metal brazing.

"Four ceramic bodies in combination with three sealing metals, have been found to give good results: 'Alsimag 243' with 16% chrome-iron; 'Alsimag 491' and 'Alumina 2548' with 44% nickel-iron; and 'Zircon 217A' with molybdenum.

"Vacuum and strength tests have been made on the junctions of a large number of metal-ceramic envelopes brazed with the process. Seals have been found to be

mechanically strong, to withstand high bake-out and operating temperatures, and to be vacuum-tight over a period of several years."

Figure 16.8a shows a Power Tetrode (Type GL-6019) which utilizes Ceramique Technique. Fig. 16.8b gives an outline of its internal structure.*

McPhee and Soderstrom[15] have developed a ceramic-to-metal seal† which is based on one of the metallizing techniques just described and incorporates a novel method of coupling a flexible membrane to the metal.

Fig. 16.9. Photograph of 4-inch diameter test seal. According to Soderstrom and McPhee. (Somac) (*Courtesy Collins Radio Company.*)

Only a small number of these seals have been made so far, but they were found to be vacuum-tight over a period of many months. Fig. 16.9 shows a photograph of a 4-inch diameter test seal comprising a cylindrical ceramic body ("Alsimag 196") between two cold-rolled steel end plates, one of which has a "Kovar" insert with a 7052 glass tubulation. The details of this seal, which was christened the "Somac Seal"† by the originators, are apparent from the exploded view given in Fig. 16.10. The end faces F and a short length of the cylinder wall W near the two ends are ground by the manufacturer to meet dimensional tolerances within ± 0.005 inch. These end faces and the wall bands near them are metallized by one of the methods mentioned above. So far, only the Telefunken Process has been used in this laboratory, but the titanium-hydride or the zirconium-hydride braze should be applicable. An adapter

* The author is indebted to the General Electric Company, Schenectady, N.Y., for making these photographs available.

† U.S. Patent Applied For.

ring A is formed to the contour; it is pressed out of 0.005-inch thick nickel sheet in a die. A bearing ring B with milled slots S is machined from stainless steel. The metal end-plate E is provided with grooves G for braze rings $R2$ on one or both sides, depending on whether a one-ended or two-ended seal is to be made to the end plate, and also for the rim of the adapter ring A. All components are pressed into position and silver brazed in a neutral atmosphere. The seal components are shown only

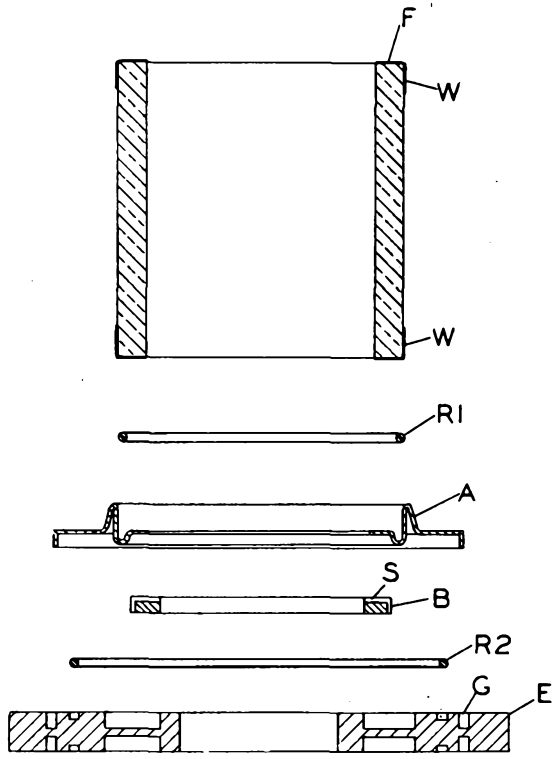

Fig. 16.10. Exploded view of "Somac Seal." (*Courtesy Collins Radio Company.*)

for the lower end of the ceramic cylinder. The same parts apply to the upper end and both seals are made in one furnace pass.

It can readily be visualized that the braze ring $R1$ will effect a seal between the metallized ceramic and the adapter ring A by flowing into the interspace between the two when brought to its flow point. The braze ring $R2$, in its turn, will seal the adapter ring to the end plate. The bearing ring B has been prefired in wet hydrogen so as to develop at its surface a thin coating of chromium oxide which will prevent any bond to the brazing alloy if an excess should penetrate to the inner space. The bearing ring B has a loose fit in the undercut of the end plate. Its func-

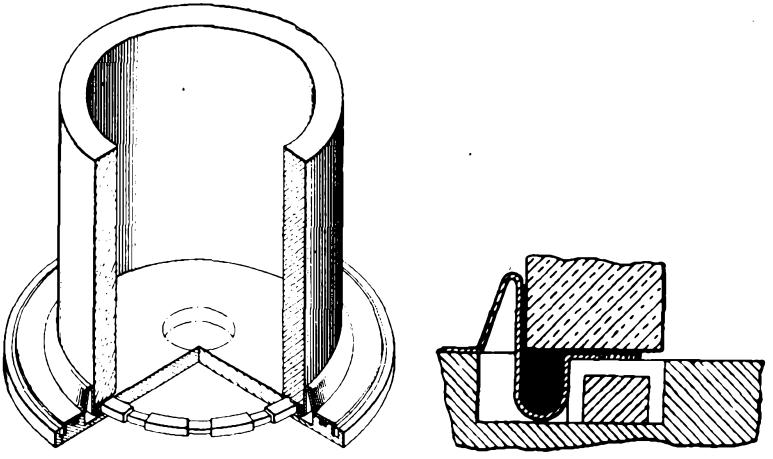

(a) (b)

Fig. 16.11. (*a*) Cut-away view of "Somac Seal." (b) Enlarged view of "Somac Seal." After Brazing. (*Courtesy Collins Radio Company.*)

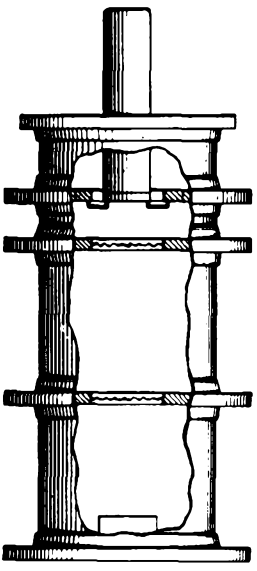

Fig. 16.12. Schematic outline of tetrode assembly comprising several "Somac Seals." (*Courtesy Collins Radio Company.*)

tion is to provide a seat for the adapter ring and to take up the axial load. All relative expansion between the ceramic and the end plate is taken up by the adapter ring, both in a radial and axial direction. It can slide freely on the bearing ring when small movements are imposed by differential expansion. The atmospheric pressure exerted on an evacuated seal will of course produce axial compression of the seal and make it rest on the bearing ring. Slots *S* are provided in this ring to evacuate the

space bounded by the convolution of the adapter ring A. This convolution acts as a spring and exerts radial pressure onto the ceramic wall seal. Details of the assembly are apparent from Figs. 16.11a and 16.11b. The possibilities of this sealing technique, particularly for large high-frequency power tubes, are suggested by Fig. 16.12, where a tetrode assembly is shown in schematic outline.

The attention of the reader is also directed to an article by Bondley[26] where a number of pertinent graphs are given and Reapplication of low-melting solders to metal ceramic seals is described; The binary alloys investigated include lead-silver, lead-indium, and lead-copper.

REFERENCES

1. Handrek, H., "Novel Current Leads for Vacuum Tubes," (In German), *Z. Tech. Phys.*, **15**, 494–496 (1934); "Novel Vacuum-tight Ceramic-to-Metal Seals," (In German), *Z. Tech. Phys.*, **17**, 456–459 (1936).
2. Espe, W., and Knoll, M., "Werkstoffkunde der Hochvakuumtechnik," Berlin, J. Springer, 1936.
3. Albers-Schönberg, E., "Hochfrequenz-Keramik," Dresden and Leipzig, Theodor Steinkopff, 1939. Part 3 by Handrek.
4. Haase, T., *Ker. Rundschau*, **50**, 181–184 (1942).
5. *U.S. Dept. of Commerce Rept. PB-52343*, German Metal Ceramic Technique and Metal Ceramic Decimeter Tube Series.
6. Warde, J. M., "Status Report on the German Ceramic, Glass, and Refractories Industries in the U.S. Zone of Occupation," *Am. Ceram. Soc. Bull.*, **25**, 321–332 (1946).
7. Williams, N. T., "Metal-Ceramic Vacuum Seals," *Rev. Sci. Inst.*, **18**, 394–396 (1947).
8. Partridge, J. H., "Glass-to-Metal Seals," *Soc. of Glass Tech. Monograph*, Chap. 13, "Elmfield," Northumberland Road, Sheffield 10, England (1949).
9. Bondley, R. J., "Metal-Ceramic Brazed Seals," *Electronics*, **20**, 97–99 (July, 1947).
10. Pearsall, C. S., "New Brazing Method for Joining Nonmetallic Materials to Metals," *Mater. and Meth.*, **30**, 61–62 (July 1949).

10a. Knecht, W., Hydrides of Active Metals in Vacuum Tube Techniques. U.S. Air Force Air Material Command, Wright-Patterson Air Force Base, Dayton, Ohio. Report No. 6108 (Sept. 1950).

11. Nolte, H. J., and Spurck, R. F., "Metal-Ceramic Sealing with Manganese," *Telev. Eng.*, **1**, 14–18, 39 (1950).
12. Rheaume, R. H., "A Ceramic Planar Power Triode," **7**, 6–9, 30–31, Machlett Laboratories, Springdale, Conn., Machlett Cathode Press, Spring, 1950.
13. Rheaume, R. H., "A Miniature Ceramic 'Lighthouse' Tube," Machlett Laboratories, Springdale, Conn., Machlett Cathode Press, Summer, 1950.
14. Machlett, R. R., "The First Ceramic-X-Ray Tube," **7**, 2–5, Machlett Laboratories, Springdale, Conn., Machlett Cathode Press, Winter, 1949–50.
15. McPhee, K. H., and Soderstrom, H. W., "A Vacuum Seal between Metals and Ceramics for High-Temperature Applications," presented at the I.R.E. National Convention, New York, March 1950.
16. Wein, S., "Metallizing Nonconductors," New York, Metal Industry Publishing Co., 1945.

17. Monack, A. J., "Metallizing Glass and Ceramic Materials," *Glass Ind.*, **28,** 21–25, 40–44 (1947).
18. Brunetti, C., "Printed Circuit Techniques," *Proc. I.R.E.*, **36,** 121–161 (1948).
19. Wooster, W. A., and MacDonald, G. L., "Smears of Titanium Metal," *Nature*, **160,** 260 (1947).
20. Gillett, H. W., "Some Features of Ductile Zirconium and Titanium," *Foote Prints*, **13,** 1–11 (1940). Foote Mineral Company, 16th and Summer Sts., Philadelphia, Pa.
21. Danzin, A., and Despois, E., "Optically Polished Surfaces for Vacuum Tube Seals," (In French), *Annales de Radioél.*, **3,** 281–289 (1948).
22. Weyl, W. A., "The Dielectric Properties of Glass and Their Structural Interpretation," *J. Soc. Glass Tech.*, **33,** 153, 220–238 (1949).
23. Hursh, R. K., "Development of a Porcelain Vacuum Tube," *J. Am. Ceram. Soc.*, **32,** 75–80 (1949).
24. Bahls, W. E., "A New Type Vacuum Seal," *El. Eng. Transact.*, **57,** 373–378 (1938).
25. Jenny, A. L., "Soldered Ceramic-to-Metal Seals," *Prod. Eng.*, **18,** 154–157 (1947).
26. Bondley, R. J., "Low Melting Temperature Solders in Metal Ceramic Seals," *Ceramic Age*, **58,** 15–18 (1951).

SUMMARIES OF MISCELLANEOUS TOPICS

In the remaining chapters a number of topics are treated in the form of condensed summaries. Some of this material was originally contained in the manuscript for earlier chapters where it seemed to overload the text. Excellent monographs on most of these items are available as well as an extensive literature in technical journals. It was felt that the usefulness of this book would be enhanced by providing a guide to this literature and by including a number of tables which may be a convenience to the reader.

CHAPTER 17

THE PHASE RULE

In 1876 J. Willard Gibbs established a general relationship which applies to heterogeneous systems in real chemical or physical equilibrium and from which the number of permissible variations, degrees of freedom F, can be derived if the number of components C of the system and the number of phases P present are known. The relationship reads

$$P + F = C + 2 \tag{17.1}$$

and is known as Gibb's Phase Rule. It was derived from the first and second law of thermodynamics. The phase rule serves as a guide not only to the understanding of glass compositions but also in determining the compositions of alloys on solidification from a melt and the intricate equilibria established in furnace-brazing different metals; therefore, it will be useful to elaborate a little more on the phase rule and lay down its definitions of terms.[1–3]

Phases are understood to be aggregates, physically separate from each other, which are present in the system. There are as many of these as can be distinguished by different chemical composition as long as they are present as physically separable domains. Thus, there may be several solid phases in the system, several liquid phases when they are present in separate layers, but only one gas phase, as gases and vapors of different composition will always mix.

The number of components C is given by the smallest number of chemical compounds which by means of chemical equations will determine the compositions of all the phases present. There is frequently a choice possible as to which particular compounds should be selected as basic, but the number C is always uniquely defined.

The variability, or degree of freedom F, of the system is given by the relation $F = C + 2 - P$. It determines how many of the variables temperature, pressure, and concentration can be altered simultaneously without disturbing the equilibrium of the system. It should be pointed out here that "real" equilibrium implies that the state of the system varies continuously when any one of the parameters is changed and that the equilibrium is the same no matter from which direction it is approached. Depending on the number of variables temperature, pres-

sure, and concentration (volume) which must be fixed in order that the system is completely defined, one speaks of invariant, univariant, bivariant, or multivariant systems, where $F = 0, 1, 2$ or more.

A liquid in equilibrium with its vapor has one component (liquid and vapor have the same chemical composition) and 2 phases (liquid and gaseous) so that $F = 1 + 2 - 2 = 1$. It is univariant as the temperature or pressure each define the system. This is graphically described by the vaporization curve (Fig. 17.1). Water and ice in equilibrium with

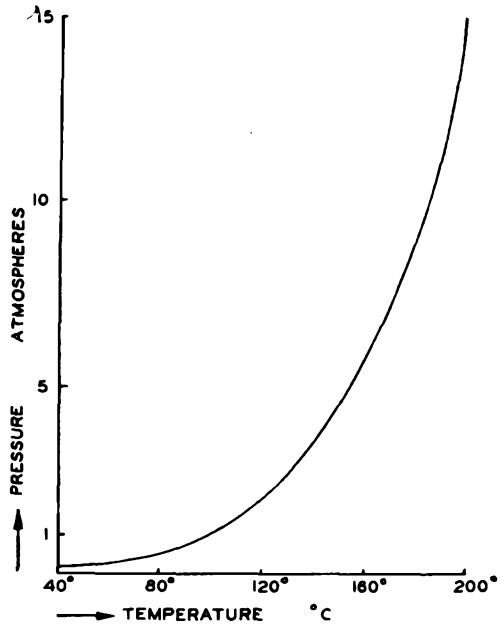

Fig. 17.1. Vapor pressure curve of two-phase system.

vapor have one component and three phases so that $F = 1 + 2 - 3 = 0$. It is an invariant system and the three phases can co-exist only at a definite temperature and a definite pressure where the sublimation curve AO, the vaporization curve BO, and the fusion curve CO meet at the triple point O in the phase diagram (Fig. 17.2). From the slope of the fusion curve CO it is apparent that the melting point decreases with increasing pressure or that the specific volume of the solid is greater than that of the liquid, as is the case for water and ice. For other substances the fusion curve CO generally slopes to the right. The dotted lines in Fig. 17.2 indicate meta-stable states. The three curves emanating from the triple point mark off three distinct domains where only one phase solid, liquid, or vapor can exist *within* the domain marked accordingly in Fig. 17.2. Along the boundary of any two phase regions the two phases

$(S + L)$, $(S + V)$, and $(L + V)$, respectively, can coexist, and at the triple point all three phases coexist. The phase rule applies to the discontinuous changes along the boundaries of the phase diagram. Transitions from one phase to another can be visualized at constant pressure or constant temperature by drawing lines parallel to the coordinate axes. Since the triple point is not identical with the melting point, as ordinarily determined in an open vessel at atmospheric pressure, it is seen from Fig. 17.2 that at pressures above 4.6 mm Hg water vapor will condense to liquid which in turn will freeze to ice when the temperature is gradually lowered. In a vacuum tube, where the pressure is only a few microns,

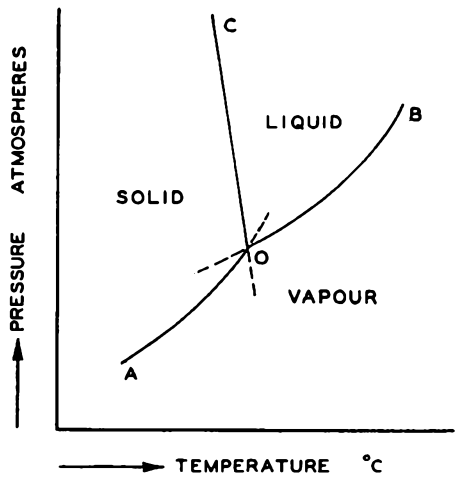

Fig. 17.2. Phase diagram of three-phase system—liquid-solid-vapor.

the liquid phase cannot exist at any temperature, and vapor is frozen to ice at the low temperatures prevailing in a freezing trap attached to the vacuum system. When organic vapors or different gases are present in the system, it can be determined from their phase diagrams how low they must be cooled in order to freeze such vapors in the trap at various pressure ranges.

The graphic representation of three-component systems is achieved with the aid of equilateral triangles. The three components are indicated by the corners A, B, and C, and their combined weight in the system is taken as the reference unit. Each component is expressed as a percentage of the total $\left(\text{i.e., } \frac{A \times 100}{A + B + C}\right)$. If the sides of the triangle are chosen respectively to represent 100 per cent, and are divided into 10 equal parts, a raster is obtained, as shown in Fig. 17.3, when lines are drawn through each division point parallel to the other 2 sides of the

triangle. Starting from corner A, which represents 100 per cent of component A (no B or C present), and moving along the side A-B all the possible compositions of the 2-component system $A + B$ are scanned, where the percentage of A decreases and that of B increases. Similarly, side BC represents the compositions of $B + C$ with no A present. Rising from the center of $B - C$ toward corner A compositions will be prescribed where the content of A gradually increases and B and C are present in equal but decreasing amounts. Point P represents 30 per cent A + 50 per cent B + 20 per cent C. Each point within the triangle gives a

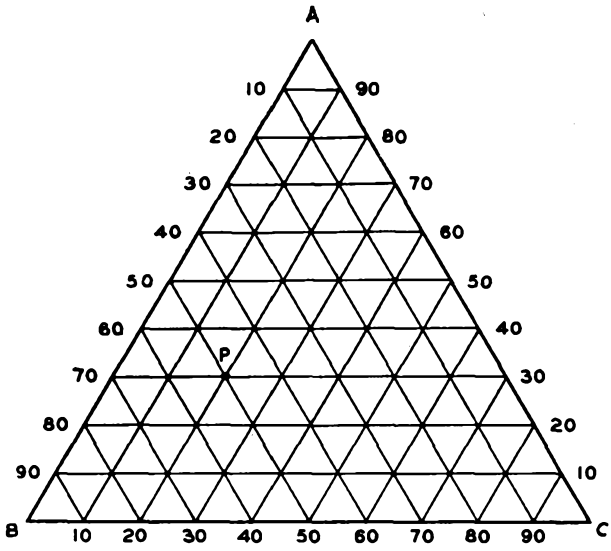

Fig. 17.3. Graphic representation of three-component system according to Rooseboom.

unique composition which is read off by drawing lines parallel to the sides of the triangle through this point. The amount of a component present is represented by the number of units intersected on a side when the side opposite the corner representing 100 per cent is moved parallel to itself to point P. This presentation is due to H. W. B. Rooseboom (1893), who greatly contributed to the application of the phase rule. The original presentation by W. Gibbs amounts to the same thing; however, he divided the height of the triangle into equal subdivisions, and the percentages are read at right angles rather than parallel to the sides (Fig. 17.4).

To portray the variability of the three-component system as a function of temperature the phase triangle (Fig. 17.3) is extended into the third dimension to form a right-angle prism (Fig. 17.5) and temperature

is indicated by the vertical elevation over the base triangle. Any one vertical side of this prism will give the variation of a two-component system with temperature when taken by itself. Before exploring the

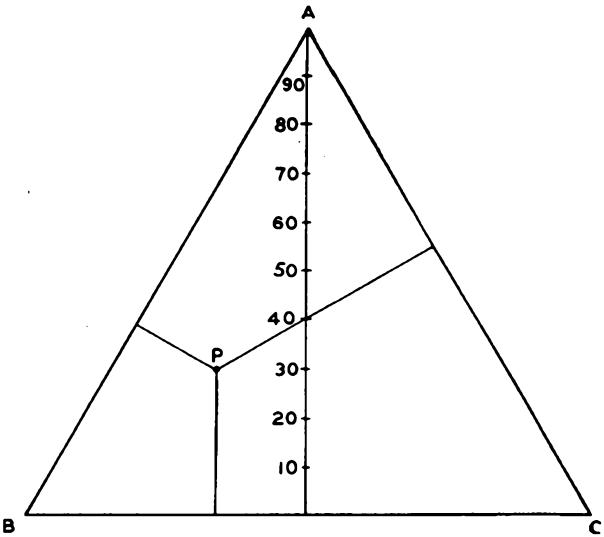

Fig. 17.4. Graphic representation of three-component system according to Gibbs.

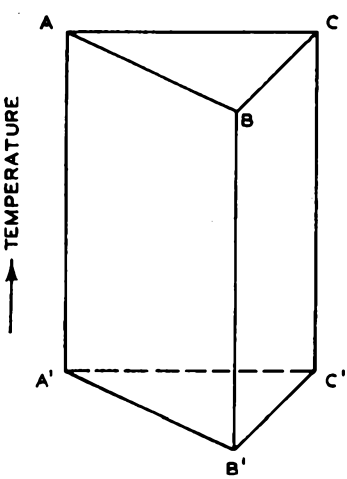

Fig. 17.5. Extension of the phase triangle into a pyramid in order to represent the variation of composition with temperature.

three-component system further an example of such a two-component diagram will be given.

Fig. 17.6[4] describes the system Na_2O-SiO_2, to which reference was made above.* It is at once apparent how the M.P. of pure SiO_2 at 1713°C is substantially lowered on addition of Na_2O until at 793°C mixed crystals of (quartz + $Na_2O{\cdot}SiO_2$) are in equilibrium with (quartz + liquid),

* Chapter 1, p. 13.

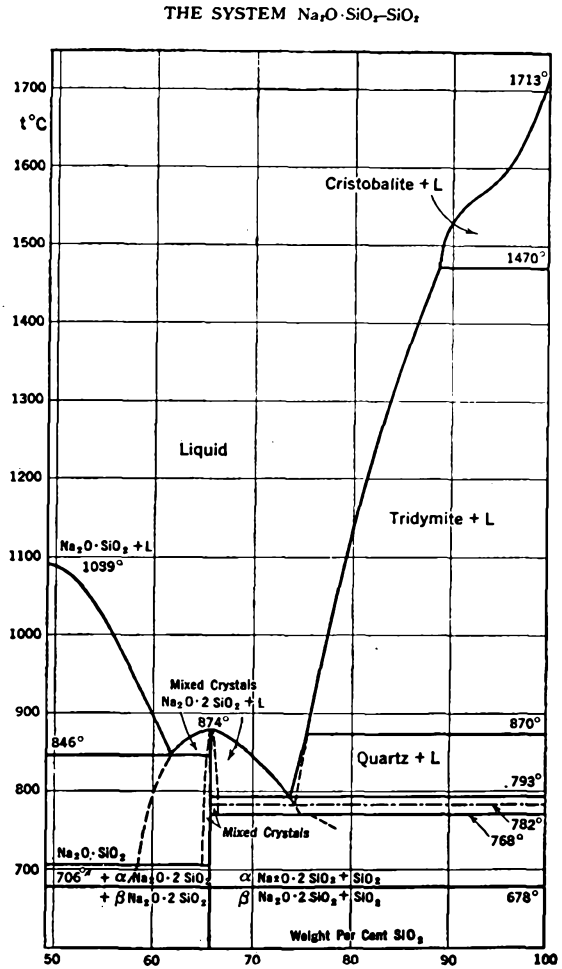

Fig. 17.6. Phase equilibrium diagram of the binary system, Na_2O-SiO_2. Composition is expressed in weight per cent SiO_2. After Kracek.[4] (*Courtesy American Chemical Society.*)

($Na_2O \cdot SiO_2$ + liquid), and liquid alone. This is the lowest temperature at which these phases can co-exist, and it is a eutectic point.* On further lowering of the temperature, the liquid phase will disappear and the solid phase exists in the form of $Na_2O \cdot 2SiO_2$ + quartz for concentrations of SiO_2 above 67 per cent. It should be noted that the solid phase, which crystallizes out below the eutectic point when the temperature is lowered, is a mixture of two solid phases and not a homogeneous compound.

* Derived from Greek meaning "easy melting."

There are two other eutectic points at 846°C and 1024°C, where other mixed crystals are in equilibrium with their liquids.

The representation of a ternary system (three-components) following the outline given in Fig. 17.5 is shown in Fig. 17.7 for a hypothetical case giving the perspective drawing of a space model.[5] The peaks A, B, and C, represent the melting points of the components A, B, and C individually. Points e_1, e_2, and e_3 on the prism faces give eutectics of respective binary compounds if the third component is absent. The M.P.'s of the binary systems are further lowered in the presence of the third

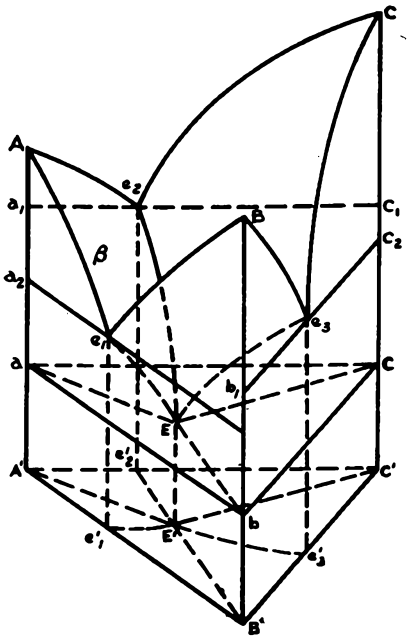

Fig. 17.7. Graphical representation of a ternary system in the form of temperature dependent equilibria. After G. Masing.[5]

component, resulting in the formation of the ternary eutectic E at the bottom of the multidomed roof. At E the solid phases AB, AC, and BC are in equilibrium with their respective liquid phases, while below the level a, b, and c parallel to the base $A'B'C'$ through E the solid phases only exist. The projection of the phase contours onto the base triangle leads to diagrams of the type shown in Fig. 17.8, which depicts the phase equilibrium diagram of the ternary system Na_2O-CaO-SiO_2 where, in addition, isotherms are drawn in the manner of contours of elevation on maps.[6] The figure gives only a section of the complete diagram as it will be noticed that the concentration of SiO_2 begins with 50 per cent and that of CaO and Na_2O does not exceed 50 per cent. This is indeed the practical range in which the glassmaker is interested, as indicated above. It would be beyond the scope of this text to elaborate all the fine points

that these diagrams contain, and the reader is therefore referred to the literature for further elucidation.

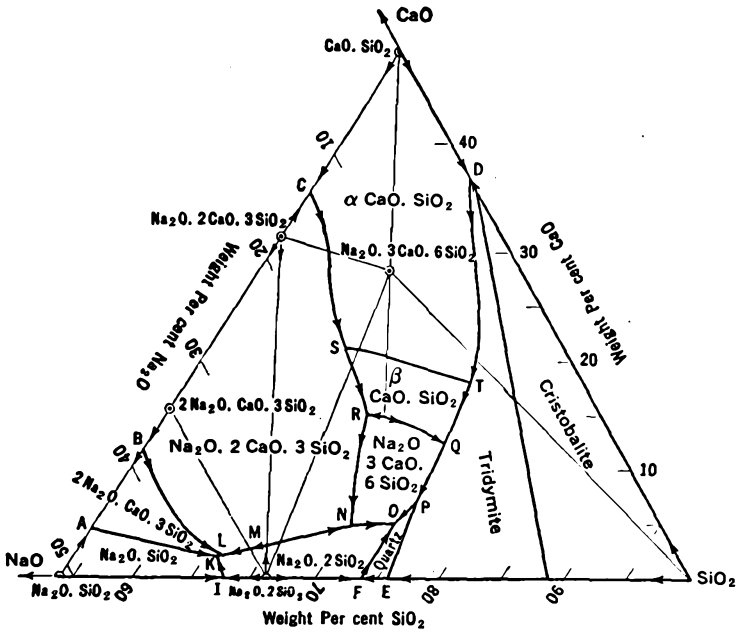

Fig. 17.8. Phase equilibrium diagram of the ternary system $Na_2O \cdot SiO_2$-$CaO \cdot SiO_2$-SiO_2. Composition is expressed in weight per cent of Na_2O, CaO and SiO_2. After Morey and Bowen.[6] (*Courtesy British Society of Glass Technology.*)

REFERENCES

1. Campbell, A. N., "The Phase Rule and Its Application," 8th Ed., New York, Dover Publications, 1945.
2. Findlay, A., "The Phase Rule and Its Applications," London, Longmans Green and Co., Ltd., 1927.
3. Glasstone, S., "Textbook of Physical Chemistry," 2d Ed., New York, D. Van Nostrand Co., Inc., 1949.
4. Kracek, F. C., "The System Sodium Oxide-Silica," *J. Phys. Chem.*, **34**, 1583–1598 (1930).
5. Masing, G., "Handb. d. Metallphysik," Vol. 2, 370, Fig. 266P, 1937: also, *J. Am. Ceram. Soc.*, **30**, 10 (1947).
6. Morey, G. W., and Bowen, N. L., "The Ternary System Sodium Metasilicate-Calcium Metasilicate-Silica," *J. Soc. Glass Tech.*, **9**, 226–264 (1925).
7. Foster, W. R.," Contribution to the Interpretation of Phase Diagrams by Ceramists," *J. Am. Cer. Soc.*, **34**, 151–160 (1951).
8. Hall, F. P. and Insley, H., "Phase Diagrams for Ceramists," *J. Am. Cer. Soc.*, **30** (Pt. 2) (Nov. 1947).
9. McMurdie, H. F., and Hall, F. P., "Phase Diagrams for Ceramists," *Supplement No.* 1, ibid., **32** (Pt. 2) 154–164 (Dec. 1949).

CHAPTER 18

HIGH-VACUUM TECHNIQUE

As an introduction to this intriguing subject it is difficult to find a better review than the 5-page illustrated article by Philip and Emily Morrison.[1] It scans the enormous development that has taken place from ancient times to the present and puts into proper perspective the tasks to be met in the endeavor to produce a good vacuum. The history and development of high-vacuum pumps has been described in detail by Neumann[2] and high-vacuum gauges by Pirani and Neumann.[3] The papers presented at the Cambridge Symposium on High Vacuum in October, 1947[4] give a good review of the industrial applications of high-vacuum engineering in the chemical and metallurgical field. The scientific foundations of vacuum technique are most extensively treated by Dushman[5] and the large-scale applications of vacuum engineering during World War II in the various phases of the Manhattan Project by Guthrie and Wakerling.[6] Vacuum pumps and systems, as well as seals and valves and leak-detection methods, are well covered in this treatise. Refs. 7 and 8 also refer to these subjects. The problem of leak detection on a very large scale at the gaseous diffusion plant for separation of "Uranium 235" led to the perfection of the helium-mass spectrometer,[9] which is now available commercially in several types. White[10] points out, however, that the positive ion emitter, operating in air at atmospheric pressure in conjunction with small admixtures of "Freon" gas, offers a much simpler method for leak detection. This device was perfected in recent years and is now used for testing refrigerators and other welded structures; recently it has found commercial application to vacuum equipment. The introduction of halogen compounds into vacuum containers would seem to be very hazardous unless they can be completely removed afterwards. Possibly other gases or vapors can be found to produce the increase in positive ion current of this detector.

Kohl[11] has published a tabulation of the performance data of commercially available high-vacuum pumps in the United States. These data have been revised and are shown in Tables 18.1 and 18.2. Table 3.1, showing conversion factors for pressure and stress units, should also be useful in this field.* Table 18.3 gives characteristics of oils for mechanical pumps; Table 18.4 those of diffusion-pump fluids; Table 18.5 character-

* page 38.

(Text continued on page 441)

TABLE 18.1. HIGH VACUUM FORE-PUMP DATA

Pump Designation	Number of Stages	Limiting Pressure, microns	Free Air Displacement at Intake (P = 1 Atm)		Pumping Speed at						Pump Revol., rpm	Motor Size, hp	Pump Cost Excl. Motor $
					100 Micron		10 Micron		1 Micron				
			Liter/Sec	CFM	L/S	CFM	L/S	CFM	L/S	CFM			
Class D RP 15*	1	2	8	17	5.8	12.3	3.5	7.5	0	0	200	½	450
RP 30	1	2	16.5	35	11.5	24.5	7.1	15	0	0	200	1	550
RP 50	1	2	27.35	58	19.4	41	11.5	245	0	0	200	2	700
RP100	1	2	54.2	115	36.7	78	19.8	42	0	0	200	5	995
RP250	1	2	141.5	300	95.4	202	56.6	120	0	0	200	10	1,590
RP375	1	2	202.5	430	139	295	83.1	176	0	0	200	15	2,490
RP750	1	2	388	845	278	590	162.8	345	0	0	200	40	3,600
Hyvac 91105†	2	0.2	0.18	0.38	0.1	0.21	0.09	0.19	0.08	0.17	350	⅛	63
Megavac 92110	2	.05	.52	1.1	.3	.64	.28	.6	0.20	.42	325	⅛	160
92015	2	.07	.95	2	.78	1.66	.52	1.1	0.37	.79	600	½	160
Hypervac-23; 93006	2	.2	4	8.5	3.0	6.4	2.20	4.7	0.30	.64	510	½	335
-25; 93020	2	.05	4.40	9.3	2.9	6.15	2.50	5.3	2.10	4.45	570	½	450
-100; 933033S	2	.02	16	34	12.0	25.4	11	23.3	11.0	23.3	450	2	745
Pressovac-4; 90515	1	3	0.58	1.2	0.5	10.6	0.34	0.72	0	0	600	⅛	60
VSD 556‡	1	5	5.2	13.1	3.9	8.3	1.5	3.2	0	0	450	½	295
778	1	5	12.73	27	7.9	16.8	3.3	7	0	0	360	1½	484
8811	1	5	22	46.7	13.7	29	5.7	12	0	0	360	2	667
DVD 8810	1	5	51.8	110	33	70	14.1	29.9	0	0	450	5	925
12814	1	5	103	218	64	135.7	28.2	59.9	0	0	415	10	1,633
14918	1	5	146.8	311	92	195	37.8	80.2	0	0	360	15	2,229
141418	1	5	229	485	144	305	59	125	0	0	360	25	2,821
181420	1	5	331	702	205	435	82.5	175	0	0	360	40	4,302
CVM[1] 3153	2	0.1	0.94	2	0.73	1.55	0.65	1.38	0.5	1.07	755	¼	—
3534	2	0.1	2.3	4.9	1.8	3.9	1.5	3.2	1	2.1	600	⅛	287
556	2	.1	7.2	15.2	5.6	11.9	4.7	10	3.8	8.1	525	1	532
8610	2	.1	21.7	46	16.3	34.6	13.9	29.4	11.1	23.6	500	3	1,149
Microvac 146F§	1	10	7.1	15	4.71	10	0	0	0	0	500	1	316
148F	1	8	15.1	32	11.8	25	5.7	12	0	0	370	1½	512
149F	1	5	28.2	60	21.2	45	9.4	20	0	0	385	3	636
212F	1	2	54.2	115	42.5	90	18.9	40	0	0	385	5	897
412F	1	2	110.7	235	89.7	190	37.7	80	0	0	400	7½	1,618
612F	1	2	246.5	500	189	400	82.5	175	0	0	500	2–7½	2,775

[1] Kinney compound pumps were formerly designated CVD.

TABLE 18.1. HIGH VACUUM FORE-PUMP DATA. (*Continued*)

Pump Designation	Number of Stages	Limiting Pressure, microns	Free Air Displacemental Intake (P = 1 Atm)		Pumping Speed at						Pump Revol., rpm	Motor Size, hp	Pump Cost Excl. Motor
					100 Micron		10 Micron		1 Micron				
			Liter/Sec	CFM	L/S	CFM	L/S	CFM	L/S	CFM			
Miniat. Duo Seal 1395	1	< 25	0.20	0.42	0.09	0.19	0	0	0	0	1725	½	100
Vac. Distillation 1404	1	< 20	.56	1.18	.38	.81	0	0	0	0	300	⅓	75
Duo Seal 1406"	1	5	.56	1.18	.48	1.03	0.30	0.63	0	0	300	⅓	75
1403	1	5	1.67	3.53	1.30	2.78	.58	1.23	0	0	375	½	135
1400	2	0.05	0.35	0.74	0.17	0.37	.16	0.35	0.13	0.28	450	⅓	65
1405-H	2	.05	.56	1.18	.40	.85	.33	.71	.23	.50	300	⅓	200
1405B	2	.05	.97	2.05	.64	1.36	.53	1.15	.39	.83	525	½	215
1397B	2	.10	5	10.6	41	8.5	3.33	7.1	2.5	5.5	300	¾	490

* Beach-Russ Company, New York 7, N.Y.
† Central Scientific Company, Chicago 13, Ill.
‡ Kinney Manufacturing Company, Boston 30, Mass.
§ F. J. Stokes Machine Company, Philadelphia 20, Pa. Complete with motor belt, pulleys and base.
‖ W. M. Welch Scientific Company, Chicago 10, Ill.

TABLE 18.2. HIGH VACUUM DIFFUSION-PUMP DATA

Ser. No.	Pump Designation	Material M—Metal G—Glass	Type Number	Catal. No.	Number of Stages	Limiting Pressure mm Hg	Fore Pressure Microns	Fore Pump Speed		Pump Speed at Various Pressures (mmHg)					
										1		10^{-1}		10^{-2}	
								L/S	CFM	L/S	CFM	L/S	CFM	L/S	CFM
1	Mercury Diffusion Supervac*	M		93201	1	5×10^{-6} 2×10^{-6}	10 1	0.1	0.2						
2	Vertical Diffusion†	G/M	HV-1		3	4×10^{-7}	20	0.1–2.0 at 1 Micron	0.2–4.2			With Stand. Baffle Without Baffle			
3	Vertical Diffusion‡	M	250		2	(a) 1×10^{-6} (b) 5×10^{-8} (c) 5×10^{-7}	10	Depends on through volume							
4	Vertical Purifying§	M	H-2-P	01–0220	3	2×10^{-7}	250	0.55	1.17						
5	Vertical Booster	M	B-6	01–0630	2	1×10^{-4}	900	47.2	100			71	150	378	800
6	Vertical Purifying	M	H-6-D	01–0620	3	4×10^{-7}	200	11.8	25						
7	Vertical Diffusion	M	H-10	01-1010	3	1×10^{-6}	450	23.6	50			47.2	100	189	400
8	Vertical Purifying	M	H-16-P	01–1620	3	2×10^{-7}	300	47.2	100					368	780
9	Vertical Booster	M	B-1	01–0130	2	1×10^{-4}	330	0.55	1.17			0.6	1.3	4.0	8.5
10	Vertical Purifying	M	H-4-P	01–0420	3	2.5×10^{-6}	300	5.9	12.5						
11	Vertical Diffusion "Microjet"‖	M	147-C		3	1×10^{-5}	200	7.0	14.8			0	0	117.5	250
12	Vertical Diffusion "Microjet"	M	147-D		1	1×10^{-4}	2,000	54.3	115			70.5	150	258	550
13	Mercury Diffusion¶	G	GHG-10	8032	2	$< 1 \times 10^{-6}$	1,600	0.3	0.7			0.2	0.5	6	12.7
14		G	GHG-10S	8076	2	$< 1 \times 10^{-6}$	4,000	.3	7			0.2	0.5	6	12.7
15		G	GHG-15	8155	3	$< 1 \times 10^{-6}$	4,000	.3	7			4.0	8.5	20.5	44.0
16		M	MHG-50	8020	2	$< 1 \times 10^{-6}$	350	.3	.7			0.3	0.6	11	23.0
17	Vertical Single Stage	G	G-4	8022	1	7×10^{-6}	100	.5	1.1			1.0	2.12	6	12.7
18	Horizontal Fractionating	G	GF-7A	8088	2	8×10^{-7}	120	.5	1.1					1.8	3.8
19		G	GF-20A	8143	2	5×10^{-7}	200	.1	0.2					12	25
20		G	GF-20W	8142	2	5×10^{-7}	200	.1	.2					12	25
21		G	GF-25A	8014	3	8×10^{-8}	160	.1	.2					8	17
22		G	GF-25W	8013	3	8×10^{-8}	160	.1	.2					8	17
23	Vertical High Speed	G/M	GM-220AB	8097	3	1×10^{-6}	300	.5	1.1					10	22
24		G/M	GM-220WB	8098	3	1×10^{-6}	300	.5	1.1					10	22
25	Horizontal Booster	G	GB-25	8204	2	1×10^{-4}	900	.5	1.1					30	64

26	Vertical Booster	M	VMB-7	8137	1
27		M	MB-100	8087	2
28		M	MB-200-06	8008	2
29		M	MB-200-02		2
30		M	MB-300	8197	2
31	Vertical Ejector	M	VKB-8	8156	1
32		M	VKB-150	8160	1
33	Horizontal Ejector	M	KB-300	8090	1
34	Vertical Booster	M	KS-100		2
35	4 in. Diam. Vertical High Speed	M	MC-275	8006	3
36	6 in. Diam. Vertical High Speed	M	MC-500	8004	3
37	14 in. Diam. Vertical High Speed	M	MC-3000	8186	3
38	20 in. Diam. Vertical High Speed	M	MC-7000	8024	3
39	32 in. Diam. Vertical High Speed	M	MC-15000		3
40	Vertical Fractionating	M	VMF-2A	8082	2
41		M	VMF-2W	8074	2
42		M	VMF-5A	8063	2
43		M	VMF-5W	8064	2
44		M	VMF-10A	8054	2
45		M	VMF-10W	8058	2
46		M	VMF-20A	8056	2
47		M	VMF-20W	8055	2
48		M	VMF-50	8062	2
49		M	VMF-80	8221	3
50		M	VMF-100	8081	2
51		M	VMF-260	8148	3
52	2 in. Diam. Vert. Fractionating	M	MCF-60	8263	3
53	4 in. Diam. Vert. Fractionating	M	MCF-300	8242	3
54	6 in. Diam. Vert. Fractionating	M	MCF-700	8286	3
55	10 in. Diam. Vert. Fractionating	M	MCF-1400	8243	4
56	16 in. Diam. Vert. Fractionating	M	MCF-5000		2
57	16 in. Diam. Vert. Fractionating	M	MCF-5000		3
58	20 in. Diam. Vert. Fractionating	M	MCF-7000		3
59	32 in. Diam. Vert. Fractionating	M	MCF-15000		3

* Central Scientific Co., Chicago, Ill.
† Eitel-McCullough, Inc., San Bruno, Cal.
‡ Litton Industries, San Carlos, Cal.
§ National Research Corporation, Cambridge, Mass.
‖ F. I. Stokes Machine Company, Philadelphia, Pa.
¶ Distillation Products, Inc., Rochester, N.Y.

5×10^{-4}	400	0.5	1.1			3	6.4	5	10.1
5×10^{-5}	270	5	10.6			5	11.2	65	138
5×10^{-5}	235	5	10.6			25	53	115	244
5×10^{-5}	405	5	10.6			50	106	200	424
5×10^{-5}	420	40	85			70	148	300	636
1.5×10^{-3}	500	1	2.1			5.8	12.3	3.5	7.4
5×10^{-4}	300	40	85	60	127	175	371	250	530
5×10^{-3}	750	40	85	120	254	300	636	200	425
1×10^{-5}	1000	5	10.6					130	275
5×10^{-6}	135	5	10.6			10	21.2	60	127
5×10^{-6}	275	5	10.6			50	110	90	190
5×10^{-6}	200	40	85			40	85	100	212
5×10^{-6}	65	40	85			40	85	400	848
5×10^{-6}	60	40	85			50	106	500	1060
1×10^{-6}	100	0.1	0.2					0.1	0.2
1×10^{-6}	100	.1	.2					0.1	0.2
1×10^{-6}	100	.1	.2					0.1	0.2
1×10^{-6}	100	.1	.2					0.1	0.2
1×10^{-6}	100	.1	.2					0.1	0.2
1×10^{-6}	100	.1	.2					0.1	0.2
1×10^{-6}	100	.1	.2					0.1	0.2
1×10^{-6}	100	.5	1.1					0.5	1.1
5×10^{-7}	120	.5	1.1			2.0	4.2	18	38.2
1×10^{-6}	100	.5	1.1					0.5	1.1
1×10^{-6}	100	.5	1.1					43	91
5×10^{-7}	215	1	2.12						
5×10^{-7}	175	5	10.6					75	159
5×10^{-7}	100	5	10.6						
5×10^{-7}	275	10	21					250	530
1×10^{-6}	22	40	85					20	42
5×10^{-7}	170	40	85					21	44
5×10^{-7}	65	40	85					400	848
5×10^{-7}	60	40	85			50	106	500	1060

TABLE 18.2. HIGH VACUUM DIFFUSION-PUMP DATA.—*Continued*

Ser. No.	Pump Speed at Various Pressures (mm Hg)								Recommended Pump Fluid	Amount of Pump Fluid	Heater Power Watts	Cooling A—Air W—Water	Overall Dimensions (in.)			Inlet Flange (in.)		Pump Cost $
	10^{-3}		10^{-4}		10^{-5}		10^{-6}											
	L/S	CFM	L/S	CFM	L/S	CFM	L/S	CFM					H	W	L	O.D.	I.D.	
1			7.0	14.8					Mercury	300 g	250	W				2⅞	2¾	48
2	32.5 60.5	69 126.0	32 68	68 144	34 71.5	72 152	19.5 40	41.4 85	Eimac Type A	150 cc	180	A	25	5¼	11¼			125
3	(a) Pump only, at inlet				280	595			Litton Type C	130 cc	375							195
	Pump + Water Baffle, at inlet				200	424			Silicone DC702	4.5 oz	400	W	18½	7¼		3½	3⅜	210
	(b) Pump, W.B. + Charcoal B., at inlet				85	180			Siilcone DC703	110 g	425							250
	(c) Pump, W.B. + Ch. B. + Valves, at inlet				65	138												325
4	52	110	70	148	67	142	35	74	Narcoil 30 or 20	70 cc	200	W	15½	7	3	2¼		137
5	472	1000							Narcoil 10	3 gal	6000	W	49	18¾		11		930
6	565	1200	707	1500	565	1200	189	400	Narcoil 20	400 cc	950	W	28	16	11	11		370
7	1225	2600	1462	3100	708	1500			Narcoil 10	1000 cc	2250	W	41½	22⅞	16	16		495
8	1790	3800	5420	11,500	5,200	11,000	1890	4,000	Narcoil 30	800 cc	3500	W	53	30	23½	23½		1,600
9	11	23.3							Narcoil 10	25 cc	85	W	7	2½	7	1¼		54
10	340	720	350	740	210	445			Narcoil 30	300 cc	500	W	22⅜	5	13	4		250
11	470	1000	470	1000	0	0			Arochlor 1254	1½ pt	1,200	W	33	20	45	6⅝	6.065	350
12	127	270	117.5	250					1254	8 qts	5,000	W	54¾	25	86½	6⅝	6.065	500
13	4.7	10	3.3	7	0.9	1.9			Mercury	1090 g	200	W	25	8	8	1⅛	1 1/16	130
14	4.7	10	3.3	7	0.9	1.9				1500 g	360	W	28	10	10	1⅛	1 1/16	180
15	19.0	40	14	30	5	10.6				2170 g	500	W	28½	8	12	4¼	2	225
16	55.0	107	65	138	40	85.0				2590 g	500	W	16	10	6	6	3⅞	140
17	9.3	19.7	4.8	10.2	0.5	1.1			Octoil	65 g	40	A	14	5	9	1¼	1⅛	45
18	7.5	15.9	7.5	15.9	5	10.6	0.3	0.64	Octoil or Octoil S	75 g	64	A	10	4	12	1¼	1⅛	165
19	26.0	55.0	26	55	22	47.6	0.2	0.5		130 g	167	A	14	5	16	1¼	1⅛	165
20	26.0	55.0	26	55	22	47.6	0.2	0.5		130 g	167	W	14	5	16	1¼	1⅛	195
21	27.0	57.0	31	66	31	66	17	36		200 g	120	A	14	5	24	2	1 13/16	260
22	27.0	57.0	31	66	31	66	17	36		200 g	120	W	14	5	24	1¼	1 1/16	290
23	100	212	235	498					Amoil S or Octoil	200 g	230	A	24	7	11	5½	4	160

24	100	212	235	498						200 g	230	W	24	7	11	5½	4	205
25	28	59							Butyl phthalate	125	280	W	22 5/16	4⅝	9⅜	2⅛	1 15/16	240
26	7.0	14.8								100 g	300	W	12⅛	5¼	5¼	2½	1 7/16	115
27	120.0	250	80	170					Butyl Sebacate	225 g	375	W	16⅝	6	10½	6	3⅞	125
28	240.0	510	150	318						600 g	640	W	23½	9	13½	9	6	195
29	130	275	50	106						1000 g	1450	W	23¼	9⅝	15½	9	6	250
30	280	594	130	276						2800 g	2000	W	30½	14	18½	12	8⅜	390
31									Myvane-10	700 g	815	W	24	9⅝	9⅝	3¾	1¼	325
32	100	212							Myvane-20	9500 g	3250	W	57⅜	12⅛	28⅞	11	6	850
33									Myvane-10	21,000 g	4700	W	72	24	76	11	6	1,550
34	120	250	100	212					Myvane-20	1,000 g	900	W	24½	8¾	13¾	6	3⅝	296
35	210	445	175	372	95	202			Octoil or Amoil S	200 g	350	W	20	6	12	6	3⅞	155
36	410	870	470	1000	330	700				600 g	730	W	30	9	15	9	6	230
37	3200	6800	3000	6360	2100	4450			Octoil or Myvane 20	4500 g	2960	W	42½	19	27	19	14 5/16	600
38	4100	8700	6800	14410	5100	10820	1400	2970		7500 g	3500	W	62¼	28	36	28	23½	1,300
39	500	10600	15000	31800	12000	25400	3500	7400		15,000 g	6000	W	80	38	52¼	38	32	3,100
40	2.6	5.5	2.3	5	0.7	1.5			Octoil or Octoil S	35 g	85	A	4½	3	3	1	15/16	62
41	2.6	5.5	2.3	5	0.7	1.5				35 g	85	W	4½	3	3	1	13/16	62
42	3.2	6.8	4.2	8.9	1.3	2.8				35 g	85	A	5⅞	3	3	1⅛	1 1/16	65
43	3.2	6.8	4.2	8.9	1.3	2.8				35 g	85	W	5⅞	3	3	1⅛	1 1/16	65
44	11	23	11	23	4	8.5				55 g	135	A	7 5/16	3⅞	3⅞	1½	1 7/16	75
45	11	23	11	23	4	8.5				55 g	135	W	7 5/16	3⅞	3⅞	1½	1 7/16	75
46	22	47	20	42	9	19.2				100 g	200	A	9⅝	5¼	5¼	2	1 15/16	85
47	22	47	20	42	9	19.2				100 g	200	W	9⅝	5¼	5¼	2	1 15/16	85
48	30	64	50	106	25	53				150 g	325	W	11⅜	6¼	6¼	2½	2 7/16	110
49	66	140	60	127	60	127	25	53		150 g	350	W	18⅝	6⅛	7	2½	2 7/16	120
50	50	106	108	229	85	180				300 g	375	W	14 7/16	7 5/16	7 5/16	3½	3 7/16	140
51	137	290	100	212	27	57.2				300 g	340	W	16	7⅜	9½	6	3⅜	195
52	65	138	65	138	65	138	20	42.4		100 g	300	W	10¾	6	5¾	3¾	1 29/32	118
53	240	509	260	552	250	530	105	223		325 g	460	W	18	6	9½	6	3⅞	215
54	380	805	650	1380	480	1018	100	212		300	775	W	29	9	14	9	6	300
55	1450	3080	1500	3180	1400	2970	400	850		2500	3300	W	36⅛	19⅛	22½	14½	10	900
56	1500	3160	4600	9730	3400	7180				5800	1800	W	39	23	42	23	16	1,000
57	2000	4240	5000	10600	5000	10600	2000	4240		5800	3610	W	42¾	23	36½	23	16	1,200
58	4100	8700	6800	14410	5100	10820	1400	2970		7500	3500	W	62¼	28	36	28	23½	1,500
59	5000	10600	15000	31800	12000	25400	3500	7400		15000	6000	W	80	38	52¼	38	32	3,400

TABLE 18.3. CHARACTERISTICS OF MECHANICAL PUMP OILS

Ser. No.	Trade Name	Supplier*	Type	Chemical Type	Viscosity in Saybolt Units		Resistance to (a) Cl_2; (b) HCl; (c) H_2O	Ref.
					100°F	210°F		
1	Calol Deturbo Oil-11	Std.O.C.	Turbine	Paraffin	229	48	Good for a, b, and c	M†
2	Cenco-Hyvac, Light	Cenco	Vacuum					
3	Cenco-Hyvac, Heavy	Cenco	Vacuum					
4	D.P.I. Pump Oil	D.P.I.	Vacuum					
5	Gulf Mechanism Oil E	G.O.C.	Vacuum	Naphthene	205	44.8	Good for a, b, and c	M
6	Gulf Paramount Oil A	G.O.C.	Vacuum	Naphtnene	305	49.4	Good for a, b, and c	M
7	Gulf Paramount Oil D	G.O.C.	Vacuum	Naphthene	710	65.6	Good for a, b, and c	M
8	Kinney Super X	K.M.C.	Vacuum					
9	McMillan Vacuum Pump Oil		Vacuum	Mixed	350	50	Poor for a and b	
10	Shell Turbo 41	S.O.C.	Turbine					6
11	Gargoyle D.T.E. Oil Light	S.V.C.	Turbine	Paraffin	155	43		6
12	Gargoyle Vacuum Pump Oil	S.V.C.	Vacuum	Paraffin	310	54		6
13	Texaco Regal B	T.C.	Turbine	Paraffin	186	45	Fair for a and b; good for c	M
14	Texaco Regal	T.C.	Turbine	Paraffin	304	47	Fair for a and b; good for c	M
15	Texaco URSA P-10	T.C.	Turbine	Paraffin	168	45	Fair for a and b; good for c	M
16	Welch Duo-Seal	W.S.C.	Vacuum					

* List of Suppliers

Std.O.C. Standard Oil Company of California, San Francisco, California.
Cenco Central Scientific Company, Chicago, Illinois.
D.P.I. Distillation Products Industries, Rochester, N.Y.
G.O.C. Gulf Oil Corp., Pittsburgh, Pennsylvania.
K.M.C. Kinney Manufacturing Co., Boston 30, Massachusetts.
S.O.C. Shell Oil Company, San Francisco, California.
S.V.C. Socony Vacuum Oil Company, New York, N.Y.
T.C. Texas Company, Chrysler Tower, New York N.Y.
W.S.C. W. M. Welch Scientific Company, Chicago 10, Illinois.

† Manufacturer's data.

Note: Gulf-crest Oil B and Gulf-crest Oil C are most desirable for use in high vacuum pumps where the operating pressure is 10 microns and more. Gulf Harmony Oil E is particularly suitable for use in high vacuum pumps requiring oils of a viscosity greater than 600 sec S.U.V. at 100°F.

istics of greases, waxes, and cements; Table 18.6 the effectiveness of drying agents; Table 18.7 the gettering power of metals; and Table 18.8 a tabulation of getters and their operating characteristics.

Characteristics of diffusion pumps have recently been discussed by Witty,[12] who deals in some detail with the measurement and significance of the intrinsic speed of a pump and the operational speed of a pump system. The intrinsic speed is often several times larger than the operational speed. With increasing heater wattage input there is a definite tendency for the intrinsic speed to decrease continuously while the operational speed passes through a maximum. The fine pressure will in general decrease with decreasing fore pressure, and will depend on the throughput of the system. With increasing throughput the limiting pressure will increase. When the critical fore pressure is exceeded, the diffusion pump will cease to operate efficiently. Efficiency of a diffusion pump is defined as the ratio of the intrinsic speed to the speed of a perfect pump (i.e., the conductance of the annular gap).

"Since intrinsic speed and efficiency depend on the heat input, it follows that it is not possible to specify a pump by any single value. Care must therefore be taken in assessing the relative efficiencies of pumps for which only single values have been quoted in the literature. The apparent superiority of one jet system over another, for example, may in reality be due more to the operating conditions than to the jet system itself; similar remarks apply to the comparison of the performance of pumps with different fluids."[12]

As far as the entries for ultimate vacuum are concerned, these remarks should be borne in mind when the data given in Tables 18.1 and 18.2, in particular, are evaluated. Additional texts and articles from which miscellaneous information on pumps and gauges is available are listed in Refs. 13 to 16.

A very complete review of "Getter Materials for Electron Tubes" has recently been given by Espe, Knoll, and Wilder.[17] This article still shows zirconium wire mounted on a molybdenum wire support. Tungsten should be used instead for high-temperature operation above 1000°C as interalloying between zirconium and molybdenum or tantalum takes place at these elevated temperatures.

A method for measuring the efficiency of getters at low pressures is described by Wagener.[18] This is probably the most revealing paper on the subject of gas clean-up which has appeared for some time. The observations reported therein, when combined with recent discussions on pumps and gauges by several authors, bring to light an interesting refinement of the modern viewpoint on measurements in the high-vacuum field. With pumps, gauges, and getters the critical importance of the conditions of measurement has become more evident in recent years. It matters a great deal, as we have seen above, whether the intrinsic speed or the

(Text continued on page 448)

TABLE 18.4. CHARACTERISTICS OF DIFFUSION PUMP OILS

Ser. No.	Trade Name	Supplier*	Chemical Composition	Mol. Wt.	Sp. Gr. (25°C)	Ultimate Vacuum	Resistance to Oxidation	Ref.
1	Amoil S	D.P.I.	Amyl sebacate	342.5	0.9251	2×10^{-6}	Poor	6, 7
2	Apiezon A	J.G.B. S.O.C.	Mixture of hydrocarbons; refined from petroleum sources		.8735	10^{-5}	Fair	6, 7
3	Apiezon B	J.G.B. S.O.C.	Mixture of hydrocarbons; refined from petroleum sources		.871	10^{-7}	Fair	6, 7
4	Arocolor 1254	M.C.C.	Mixture of polychlorinated biphenyls similar to pentachlor biphenyl	326	1.54	2×10^{-5}	Fair	7
5	Apiezon Oil C	J.G.B.	Mixture of hydrocarbons			10^{-8}	Fair	
6	Apiezon Oil G	J.G.B.	Mixture of hydrocarbons			10^{-6}	Fair	
7	Butyl Phthalate	D.P.I.		278.3	1.0465	4×10^{-5}	Fair	6
8	Butyl Sebacate	D.P.I.		314.4	0.933	2×10^{-5}	Fair	6
9	Eimac Type A	E.M.C.	Mixture of hydrocarbons; refined from petroleum		.877	4×10^{-7}	Fair	M†
10	Litton Molecular C	L.I.	Mixture of hydrocarbons; refined from petroleum			2×10^{-6}	Fair	6
11	Myvane-20	D.P.I.	Mixture of hydrocarbons; refined from petroleum		.853	10^{-6}	Fair	7
12	Narcoil-10	N.R.C.	Mixture of polychlorinated biphenyls similar to pentachlor biphenyl	326	1.54	2×10^{-5}	Fair to Good	M, 7
13	Narcoil-20	N.R.C.	2-Ethyl hexyl sebacate	426.3	0.9103	5×10^{-8}	Poor	M
14	Narcoil-30	N.R.C.	2-Ethyl hexyl phthalate	390.3	.9796	2×10^{-7}	Poor	M
15	Octoil	D.P.I.	2-Ethyl hexyl phthalate	390.5	.9796	2×10^{-7}	Poor	M

Ser. No.	Trade Name	Supplier*	Chemical Composition	Mol. Wt.	Sp. Gr. (25°C)	Ultimate Vacuum	Resistance to Oxidation	Ref.
16	Octoil-S	D.P.I.	2-Ethyl hexyl sebacate	426.7	.9103	5×10^{-8}	Poor	6, 7
17	Silicone DC-702	D.C.C.	Mixture of organic silicone molecules	530	1.07	2×10^{-7}	Good	7
18	Silicone DC-703	D.C.C.	Mixture of organic silicone molecules	570	1.09	5×10^{-8}	Good	7

* List of Suppliers

J.G.B. James G. Biddle Company, Philadelphia 7, Pa.
S.O.C. Shell Oil Company, San Francisco, California.
D.P.I. Distillation Products Industries, Rochester, N.Y.
E.M.C. Eitel McCullough, Inc., San Bruno, California.
L.I. Litton Industries, San Carlos, California.
N.R.C. National Research Corp., Cambridge, 42, Massachusetts.
D.C.C. Dow Corning Corporation, Midland, Michigan.
M.C.C. Monsanto Chemical Co., St. Louis 4, Missouri.

† Manufacturer's data.

TABLE 18.5. CHARACTERISTICS OF VACUUM GREASES, WAXES AND CEMENTS

	Trade Name	Class	Supplier*	M.P. (°C)	Vapor Pressure mm Hg	Solubility	Application Notes	Ref.
1	Apiezon Grease L	Grease	J.G.B.	47	10^{-10} to 10^{-11} at 20°C 10^{-3} at 300°C		Closely fitting ground joints. Not for stopcocks. Max. temp. 30°C. Note 1	5, 6, 12
2	Apiezon Grease M	Grease	J.G.B.	44	10^{-7} to 10^{-8} at 20°C 10^{-3} at 200°C		More viscous than Apiezon L. Moderately low vapor pressure. Max. temp. 30°C.	5, 6, 12
3	Apiezon Grease N	Grease	J.G.B.	43	10^{-8} to 10^{-9} at 20°C 10^{-3} at 200°C		Stopcock grease. Max. temp. 30°C	M†
4	Apiezon Sealing Compound Q	Soft wax	J.G.B.	45	10^{-4} at 20°C		Sealing compound. Max. temp. 30°C	M
5	Apiezon Wax W-40	Med. soft wax	J.G.B.	45	10^{-3} at 20°C		Sealing compound for unground joints. Max. temp. 30°C. Semi-permanent joints at room temperature. Joints subject to vibration	M
6	Apiezon Wax W-100	Med. hard wax	J.G.B.	55	10^{-3} at 20°C		Sealing compound for semi-permanent joints. Joints subject to vibration. Max. temp. 50°C	M
7	Apiezon Wax W	Hard wax	J.G.B.	85	10^{-3} at 180°C	Sol. in Xylene	Softening point 60–70°C. Max. temp. 80°C. Sealing compound for permanent joints. Note 2.	5, 6, 12 M
8	Apiezon Grease T	Grease	J.G.B.	25	10^{-8} (approx.) at 20°C		For places where a grade of high M.P. is required. Max. temp. 110°C	M
9	Apiezon Oil J	Moderately viscose oil	J.G.B.		10^{-8} (approx.) at 20°C 10^{-8} at 250°C		For oil lubricated taps and places where a moderately viscose oil of low vapor pressure is required	M
10	Apiezon Oil K	Exceedingly viscose oil	J.G.B.		10^{-7} to 10^{-9} at 20°C 10^{-3} at 300°C		For places where an exceedingly viscose oil of very low vapor pressure is required	M
11	Bakelite Cement	Cement	L.S.H.	80		Sol. in methylated spirits	Radio tube bases	
12	Beeswax	Wax	L.S.H.	60		Sol. in CCl_4 and alcohol	Mixture of beeswax and resin melted together	
13	Celvacene Light	Grease	D.P.I.	90	10^{-6} at 20°C		Stopcocks, ground joints. (Pale yellow transparent)	M
14	Celvacene Med.	Grease	D.P.I.	120	$< 10^{-6}$ at 20°C		Stopcocks, ground joints and gaskets. (Yellow to brownish transparent)	M

TABLE 18.5. CHARACTERISTICS OF VACUUM GREASES, WAXES AND CEMENTS. (*Continued*)

	Trade Name	Class	Supplier*	M.P. (°C)	Vapor Pressure mm Hg	Solubility	Application Notes	Ref.
15	Celvacene Heavy	Grease	D.P.I.	130	$< 10^{-6}$ at 20°C	Sol. in chloroform or acetone	Rubber gaskets & metal joints. (Dark yellow to reddish brown, transp.)	M
16	DeKhotinsky Cement	Cement	L.S.H.		$\sim 10^{-3}$ at 20°C	Insol. in usual organ. liquids and common acids	Softens at 50°C. Available as hard and soft–non-plastic and slightly plastic at room temp. Operate below 40°C	5, 6
17	Dennison's Sealing Wax	Wax	J.G.B.		$\sim 10^{-5}$ at 20°C	Sol. in alcohol	Softens at 60–80°C. Hard	M
18	Lubriseal	Grease	A.H.T.	40	$< 10^{-5}$ at 20°C	Insol. in water	General use	M
19	Lubriseal H.V.	Grease	A.H.T.	50	$\sim 3 \times 10^{-6}$ at 20°C	Insol. in water	High vacuum systems	
20	Myvawax-S	Wax	D.P.I.	72.5	1×10^{-6}	Sol. in petroleum ether, CCl_4, C_6H_6	Not affected by acetone, alcohol, octoil pump fluid	M
21	Myvacene-S	Grease	D.P.I.	215	1×10^{-6} at 20°C	Sol. in warm decalene	Stopcocks and joints	M
22	Shellac		L.S.H.			Sol. in alcohol and butyl phthalate	Often used mixed with Beeswax	
23	Dow Corning High Vacuum	Grease	D.C.	None	$< 10^{-6}$ at 20°C	Clean glassware in a solution of 10 to 15 cc of 50% KOH in 100 cc of ethanol	Stopcocks and ground joints. −40 to 200°C	M
24	Silverchloride		L.S.H.	455		Sol. in sod. thiosulfate	Applied at 450°C. Sealing compound for high temp. application	
25	Picein	Wax	L.S.H.		10^{-8} at 20°C 3–10 at 50°C	Inert to usual org. liquids and inorg. acids	Hard black sealing compound. Softens at 50°C. Use as W wax	5, 6
26	Vacuseal Light	Grease	Cenco	50	10^{-5} at 20°C		Stopcocks and ground joints	M
27	Vacuseal Heavy	Grease	Cenco	60	10^{-5} at 20°C		Stopcocks and ground joints	M
28	Cello-seal	Grease	E.A.	100	10^{-6} at 20°C	Sol. in $CHCl_3$	Stopcocks, joints, rubber gaskets and tubing	M
29	Cello-grease	Grease	E.A.	120	$< 10^{-6}$ at 20°C	Sol. in $CHCl_3$	Stopcocks, joints, rubber gaskets and tubing	M

* *List of Suppliers*

J.G.B. James G. Biddle Company, Philadelphia 7, Pennsylvania.
L.S.H. Laboratory Supply Houses, various sources.
D.P.I. Distillation Products Industries, Rochester, N.Y.
A.H.T. Arthur H. Thomas Co., Philadelphia 5, Pennsylvania.
Cenco Central Scientific Company, Chicago, Illinois.
E.A. Eimer and Amend, Fisher Scientific Company, Pittsburgh, Pennsylvania.

† Manufacturer's data.

Note 1: "When Apiezon greases, sealing compounds or waxes are being used for sealing purposes, care should be taken that joint faces are clean and dry when put together. Then the rough vacuum may be applied so as to pull the faces together. The vacuum so obtained will indicate whether the joint is free from grit. Lastly, apply the sealing medium around the outside of the joint to prevent the entrance of external air. In no case should the sealing medium be applied to the actual faces or ground joint connecting parts."

Note 2: "None of the Apiezon waxes will become brittle at room temperatures. Wax W may become brittle at temperatures of 30 to 40°F under which condition the use of W-40 or W-100 is suggested."

TABLE 18.6. EFFECTIVENESS OF DRYING AGENTS FOR ABSORPTION OF WATER VAPOR[6]

Drying Agent	Formula	Residual Water Vapor in Gas* (mg/liter)
Phosphorus pentoxide	P_2O_5	2×10^{-5}
Magnesium perchlorate	$Mg(ClO_4)_2$	5×10^{-4}
Melted caustic potash	KOH	2×10^{-3}
Aluminum oxide	Al_2O_3	3×10^{-3}
Sulfuric acid	H_2SO_4	3×10^{-3}
Sulfuric acid, 95.1%	H_2SO_4	0.3
Calcium oxide	CaO	0.2
Calcium chloride (granular)	$CaCl_2$	0.14–0.25
Calcium chloride (fused)	$CaCl_2$	0.36
Copper sulfate	$CuSO_4$	1.4
Zinc chloride	$ZnCl_2$	0.8
Sodium hydroxide (fused)	NaOH	0.16

* Dried at 25°C

TABLE 18.7. THE GETTERING POWER OF METALS
(Volume of Gas Cleaned Up per Unit Mass of Metal)[16,5]

Getter	Gas	Micron-liters/mg cleaned up		
		Bright Deposit	Diffuse Deposit	Theoretical Value
Aluminum	O_2	7.5	38.6	516.9
	N_2, H_2, CO_2	None	None	
Magnesium	O_2	20	202	382.2
	CO_2	None	Slight	
	N_2, H_2	None at room temperature	None at room temperature	
Thorium	O_2	7.45	33.15	80.1
	H_2	19.45	53.7	120.2
Uranium	O_2	10.56	9.26	53.6
	H_2	8.9	21.5	
Misch metal	O_2	21.2	50.9	100–133
	H_2	46.1	63.9	200–265
	N_2	3.18	16.1	66
	CO_2	2.2	44.8	
Barium	O_2	15.2	45	67.7
	H_2	87.5	73.0	135.4
	N_2	9.5	36.1	45.1
	CO_2	5.21	59.5	

TABLE 18.8. OUTGASSING, FLASHING AND OPERATING TEMPERATURES OF TYPICAL GETTERS[17]

Material	Ta	Cb	Zr	Th	Ceto	Mg	Al-Mg	Ba and Ba Compounds	Bato	Reaction-Type Getters		Phosphorus
										Batalum	Ba-Berylliate	
Form of application	bulk coating	bulk	bulk coating	coating	coating	flash	flash	flash	flash	flash	flash	flash
Form of getter	sheet, powder	pellets	sheet, wire, powder	powder	powder	ribbon, wire	powder, paint	metal-clad wire pellets	Ni-clad	$BaCO_3$ paint	$BaBeO_2$ paint on Ta	powder suspension
Outgassing-preheating Temp. (°C)	1,600–2,000	1,650	700–1,300 (up to 1,700 in compound wires)	for metal base 800–1,000; for graphite 1,500–1,600	800–1,200	400	400	600–700		800–1,100	900–1,000	
Flashing Temp. (°C)						500		900–1,300	750–800 (900)	1,200–1,300	1,300	200
Operating Temp. (°C)	700–1,200	500	800 (up to 1,600 in compound wires)	400–500	200–500	Absorbs gases only during flashing		20–200 max	20–200	20–200	20–200	100–200
Applications reported	D, E, M	D, E	C, D, E, F, I, K, L, M, N	C, D	P	I, K	A, F	A, B, D, F, G, H, I, (L), N	D, M	A, F	A, F	O

A—Small receiving tubes
B—Miniature tubes
C—UHF tubes
D—Medium-size transmitting tubes
E—High-power transmitting tubes
F—Oxide-cathode tubes
G—Cathode-ray tubes
H—Phototubes
I—Gaseous-discharge tubes
K—Hg-vapor tubes
L—X-ray tubes
M—High-power vacuum tubes
N—Tubes with thoriated cathodes
O—Incandescent lamps
P—Vacuum tubes in which neither flashing getters nor the high temperatures necessary for Ta and Zr may be used

operational speed of a pump is discussed, or whether the throughput or backing pressure is held constant. Where the leak is put is also an important consideration. If it is on the fine side, it makes a difference whether or not a large enough dome is put on the mouth of the pump and how the leak-orifice is directed.[19] With ionization gauges the importance of position has also been demonstrated by the same author and by others. A connecting tubulation of small diameter, combined with gas clean-up within the gauge, makes the readings often quite illusory. Even within the gauge the position, size, and shape of the collector element is critical in view of the effect of intercepted x-rays released by the impact of electrons on the positive electrode.[21–24] Photoelectrons emitted by the collector will register in the same sense as positive ions received by it and thus produce a minimum gauge reading which is independent of pressure and a linear function of anode voltage.*

The position of getters is equally critical, as Wagener has demonstrated. Their ability to clean up gases varies widely for different materials, and in appraising their effectiveness the strong gettering action of clean metal surfaces or cathodes, which are located within the same envelope, has to be eliminated. The aim is to measure the intrinsic gettering power of the getter and not the operational gettering power of the whole system, getter and all other surfaces combined. After taking care of these refinements Wagener obtained the results illustrated in Fig. 18.1.

The ratio of ion current to electron current, measured in a triode which is operated as an ionization gauge and known as the vacuum factor K, is plotted in $\mu\mu a/ma$ versus the manifold pressure p_{man}. The ionization gauge was attached to the manifold by a short length of small diameter tubing, 40 mm long and 2 mm I.D. The vacuum factor K was measured under these conditions and is shown by the dotted line in Fig. 18.1. When various getters were added to the gauge tube the other curves were obtained in accordance with the lower pressure then prevailing in the tube. Due allowance was made for the pumping action of the gauge tube itself and also for the minimum gauge reading K_{rad} due to intercepted radiation which had been separately measured.

The curve marked Mg in Fig. 18.1 refers to two magnesium getters located at the center of the gauge tube on opposite sides of the mount

* Kohl[20] has described an ionization gauge in which an electron gun is separated from the main gas space by a small slit aperture. The collector consists of a rectangular plate in the gas space; however, to intercept a minimum of x-radiation it should be made in the form of a wire loop. The gauge is designed for the measurement of pressure in large metal containers, to which it can be clamped by flanges leaving the collector entirely open to the volume where the gas pressure is to be measured. The electron gun is protected from the harmful effects of sudden gas bursts by the high impedance of the slit aperture.

where they were flashed from nickel ribbons onto which *Mg* had been coated in powder form. The getter deposit covered an area of 8 cm² on the glass wall.

The curve marked *Ba I* refers to two "KIC"* getters mounted on opposite sides next to the stem pinch below a mica disk which had four holes 3.5 mm diameter. During flashing of the getters the pressure was kept as low as possible in order to avoid a deterioration of the getter by residual gas. ($p_{man} = 5 \times 10^{-6}$ mm Hg.) After flashing, the getter deposit covered a total area of about 10 cm² on the glass wall.

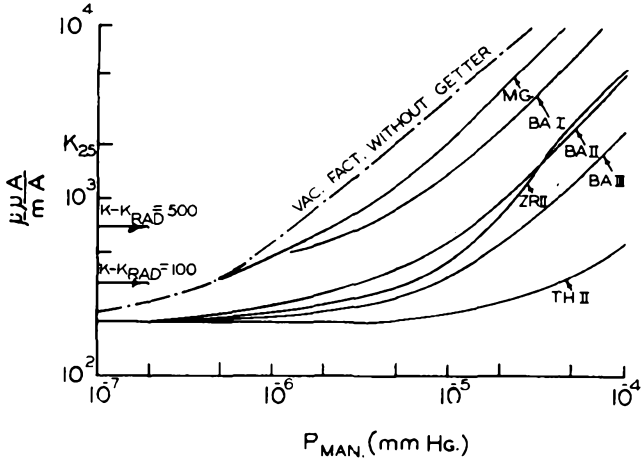

Fig. 18.1. Vacuum factor K in $\mu\mu a/ma$ as a function of manifold pressure (p_{man}) for different getters. After S. Wagener.[18] (*Courtesy The Institute of Physics, London, S.W. 1, England.*)

The curve marked *Ba II* refers to the case where two KIC getters were mounted at the center of the tube opposite the electrode assembly. They were flashed in the same manner as Ba I.

The curve marked *Ba III* refers to a condition where two KIC getters, mounted in the same way as Ba II, were flashed in an argon atmosphere at about 5 mm pressure. In this way, as shown by Ehrke and Slack[16] a black barium deposit is obtained which, owing to its larger surface, adsorbs larger quantities of gas than the bright deposit obtained by flashing in a high vacuum. The getter area in this case was 5 cm².

The curve marked *Zr II* depicts the gettering action of zirconium powder of particle size between 3 and 20 microns, applied onto separate indirectly heated sleeves by spraying. The total coated area was 7.5 cm² and the sleeves were parallel to the tube structure and operated at 1000°K.

* Trade name, Kemet Laboratories Company, Inc., Cleveland, Ohio, for Kemet Iron Clad (KIC) Barium Getter Assemblies.

The curve marked *Th II* refers to a similar arrangement of coated indirectly heated sleeves onto which thorium powder of particle size between 1 and 10 micron was deposited by cataphoresis. The coated area was about 4 cm^2 and the sleeves were operated at 1000°K.

TABLE 18.9. GETTERING RATES OF VARIOUS GETTERS AT TWO PRESSURES ABOVE THE GETTERS

Type of Getter	$p_1 = 3 \times 10^{-7}$	$p_2 = 1.5 \times 10^6$ mm Hg
Mg	— cm^3/sec	9 cm^3/sec
Ba I	— "	22 "
Ba II	125 "	135 "
Ba III	400 "	260 "
Th II	1650 "	1500 "
Zr II	230 "	190 "

The relative rates of gettering action for different getters can be readily obtained from Fig. 18.1 by drawing a line K = const. parallel to the abscissa. Two such lines are indicated as $K - K_{rad} = 500$ ($p_g = 1.5 \times 10^{-6}$ mm Hg) and $K - K_{rad} = 100$ ($p_g = 3 \times 10^{-7}$ mm Hg).

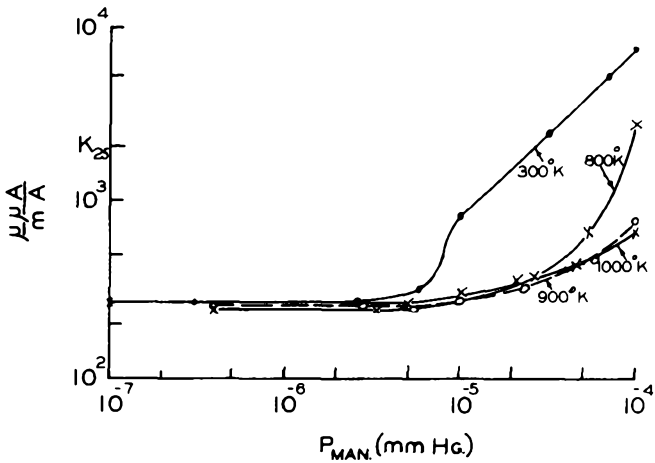

Fig. 18.2. Vacuum factor K as a function of manifold pressure (p_{man}) for a thorium getter at different temperatures. After S. Wagener.[18] (*Courtesy The Institute of Physics, London, S.W. 1, England.*)

With the knowledge of the conductance of the connecting tubulation the gettering rates can be expressed in cm^3/sec as shown in Table 18.9 above. The great differences in gettering rates between different getters and between identical getters at different locations are evident from this table. When thorium powder was applied directly to the inner surface

of the anode it was many times more effective than when applied to the outside. Being exposed to direct bombardment by electrons on the inside, the temperature of the powder was correspondingly higher than when applied to the outer anode surface. Fig. 18.2 shows the dependence of the vacuum factor K on the temperature of operation of indirectly heated sleeves coated with thorium.

Haase[25] has demonstrated that Ba-films evaporated at a pressure of 10^{-8} mm Hg. are still active as getters at room temperature. Ba-films dispersed in an Argon atmosphere at a pressure of 5 mm Hg. are active at 10^{-8} mm Hg. when the surface on which the Ba is deposited is cooled by liquid air.

REFERENCES

1. Morrison, E., and Morrison, P., "High Vacuum," *Sci. Am.*, **182,** 20–24 (1950).
2. Neumann, R., "High-Vacuum Pumps, Their History and Development," *El. Eng.*, **20** (Jan.–May 1948).
3. Pirani, M., and Neumann, R., "High-Vacuum Gauges," *El. Eng.*, **17** (Dec. 1944); (Jan.–Mar. 1945).
4. "Symposium on High Vacuum," *Ind. and Eng. Chem.*, **40,** 778–847, 938–944 (1948).
5. Dushman, S., "Scientific Foundations of Vacuum Technique," New York, John Wiley and Sons, Inc., 1949.
6. Guthrie, A., and Wakerling, R. K., "Vacuum Equipment and Techniques," National Nuclear Energy Series, Manhattan Project Technical Section, Div. 1, Vol. 1, New York, McGraw-Hill Book Co., Inc., 1949.
7. Sullivan H. M., "Vacuum-Pumping Equipment and Systems," *Rev. Sci. Ins.*, **19,** 1–15 (1948).
8. Kurie, N. D., "Vacuum Systems, Seals, and Valves," *Ibid.*, **19,** 485–493 (1948).
9. Jacobs, R. B., and Zuhr, H. F., "New Developments in Vacuum Engineering," *J. Appl. Phys.*, **18,** 34–48 (1947).
10. White, W. C., "Positive Ion Emission, a Neglected Phenomenon," *Proc. I.R.E.*, **38,** 852–858 (1950).
11. Kohl, W. H., "Performance Data for High-Vacuum Pumps," *Iron Age*, **164,** 59–63 (1949).
12. Witty, R., "Characteristics of Diffusion Pumps," *Brit. J. Appl. Phys.*, **9,** 232–237 (1950).
13. Yarwood, J., "High-Vacuum Technique, 2nd. Ed., New York, John Wiley and Sons, Inc., 1945.
14. Inananda, S., "High Vacua, Principles, Production, and Measurement," New York, D. Van Nostrand Co., 1947.
15. Cloud, R. W., and Philip, S. F., "Vacuum Tests of Rubber, Lead, Teflon Gaskets, and Vinyl-Acetate Joints," *Rev. Sci. Inst.*, **21,** 731–733 (1950).
16. Ehrke, L. F., and Slack, C. M., "Gettering Powers of Various Metals for the Gases; H_2, O_2, N_2, CO_2, Air," *J. Appl. Phys.*, **11,** 129–137 (1940).
17. Espe, W., Knoll, M., and Wilder, M. P., "Getter Materials for Electron Tubes," *Electronics*, 80–86 (Oct. 1950).
18. Wagener, S., "A Method for Measuring the Efficiency of Getters at Low Pressures," *Brit. J. Appl. Phys.*, **1,** 225–231 (1950).
19. Dayton, B. B., "Measurement and Comparison of Pumping Speeds," *Ind. and Eng. Chem.*, **40,** 795–803 (1948).

20. Kohl, W. H., "Vacuum Gauge of the Ionization Producing Type," *U.S. Patent 2,516,704* (July, 25, 1950).
21. Metson, G. H., "Vacuum Factor of the Oxide-Cathode Valve," *Brit. J. Appl. Phys.*, **1**, 73–77 (1950).
22. Bayard, R. T., and Alpert, D., "Extension of the Low Pressure Range of the Ionization Gauge," *Rev. Sci. Instr.*, **21**, 571–572 (1950).
23. Lander, J. J., "The Ultra-High Vacuum Ionization Manometer," *Rev. Sci. Instr.*, **21**, 672–673 (1950).
24. Metson, G. H., "The Physical Basis of the Residual Vacuum Characteristic of a Thermionic Valve," *Brit. J. Appl. Phys.*, **2**, 46–48 (1951).
25. Haase, G., Getter Action of Thin Barium Films at Low Pressures," (In German), *Zs. f. angew Phys.*, **2**, 4, 188–191 (1950).

CHAPTER 19
THERMIONIC EMISSION

Introduction

Some remarks relating to electron emission were made in Chapters 8 to 10, in which tungsten, molybdenum, and tantalum were described. Chapter 11 on nickel contains fairly extensive data on the effect of base-metal composition on oxide cathodes. Much has been learned during the past 50 years about the mechanism of electron emission and the fabrication of cathodes, but the most pertinent progress has been made during the past decade. This research was stimulated for the most part by the surprisingly high peak emission currents observed with magnetrons under pulsed conditions during World War II. The severe operating conditions encountered in these tubes called for new types of cathodes. The progress of theory and practice has been reviewed in several books and articles[1–5] which will be familiar to the specialist. In the following some highlights are reported which may help to lead the tube engineer to the proper sources for more detailed information.

Pure-Metal Emitters

The electron emission from all types of cathodes is described by Richardson's Equation, as modified by Dushman:

$$I_s = A \times T^2 \times \epsilon^{-\frac{e\phi}{kT}} \tag{19.1}$$

where I_s = saturation current in amps/cm²
A = emission constant expressed in amps/cm² (= 120 for pure metals)
T = absolute temperature in degrees Kelvin
ϵ = 2.71828, the base of natural logarithms
e = the electron charge (1.60×10^{-19} coulombs)
ϕ = the electron work function in e. V.
k = Boltzmann's Constant (1.38×10^{-23} joule/degree)

For a given cathode area and operating temperature the available emission current thus depends on the work function ϕ and the effective value of A. The lower the work function, the greater the available emission at any temperature. With increasing operating temperature the available saturation current grows rapidly so that a high work function can be compensated for by high operating temperature as long as the melting

point of the cathode material is not approached too closely. The life of the cathode will decrease correspondingly because of more rapid evaporation of the cathode. The economics of practical operation will thus dictate an acceptable compromise. Figure 19.1 gives a plot of saturation current versus temperature for various values of the work function ϕ.[3] Michaelson[5] has tabulated the work functions of 57 elements, and has shown a correlation of their periodicity, when plotted against the atomic number of the elements, with that of the first ionization potential E_i and the electrode potential E^0. The quantity of any one of various metals which is vaporized from one square centimeter per second may be found in Table 19.1.[6–11] In Figure 19.2 there are plots giving the life of a square film of 1 mil thickness for various metals as a function of temperature. From this graph the required thickness of flat strips, as shown in Table 8.4, can be derived for a given temperature of operation, or, vice versa, the life of a strip of given thickness at a given temperature.

If the shell evaporated from a rod or filament is converted into an equivalent square film, the life of filaments or the required filament diameter for a desired life at a given temperature can also be derived from these graphs. If L is the desired life of the filament and L' the life of a square film of 1 mil thickness, the relations shown on the graph facilitate this conversion. The data for tungsten are based on the evaporation rates given by Reimann,[6] and are generally accepted in the industry. The evaporation rates given earlier by Jones and Langmuir[12] were found to be too high by about a factor of 2. The actual life of a filament is thus about twice that determined on the basis of Jones and Langmuir's figures, which are given in Table 8.3* (see page 189).

* These figures, incidentally, have to be divided by the factor π to obtain the rate of evaporation in g/cm^2 sec because the surface of a filament of 1 cm diameter and 1 cm long is π cm^2. This fact is often overlooked. Further confusion arises from the statement that the end point of life is reached when 10 per cent of the mass of the filament has been evaporated rather than a mass giving rise to a 10-per cent reduction of the diameter of the filament. A mass reduction by 10 per cent is equivalent to a reduction of the filament diameter by 19 per cent so that the life is nearly twice as long as it should be, if Reimann's figures are used. With Jones and Langmuir's figures it gives about the right answer because it cancels out the factor ½ applying to the evaporation rates. For this reason the legend of Figure 8.6 has been left to read as it does since it refers to Jones and Langmuir's figures.

Recent investigations by Enis Bas-Taymaz[12a] deal with the life of a tungsten helix (or filament) and the rate of evaporation of tungsten in vacuo as given by Zwikker.[12b] On the basis of these data, the end point of life is reached when 15% of the weight of the tungsten filament has been evaporated per unit length. Zwikker's data on evaporation rates, measured in 1925, are substantially lower than those given by Reimann, which explains the different result for the life end point. There is evidently a difference of opinion between European and American workers as to the most reliable figures. In Europe, Zwikker's data are still being used while in America, Reimann's data are made the basis of design calculations.

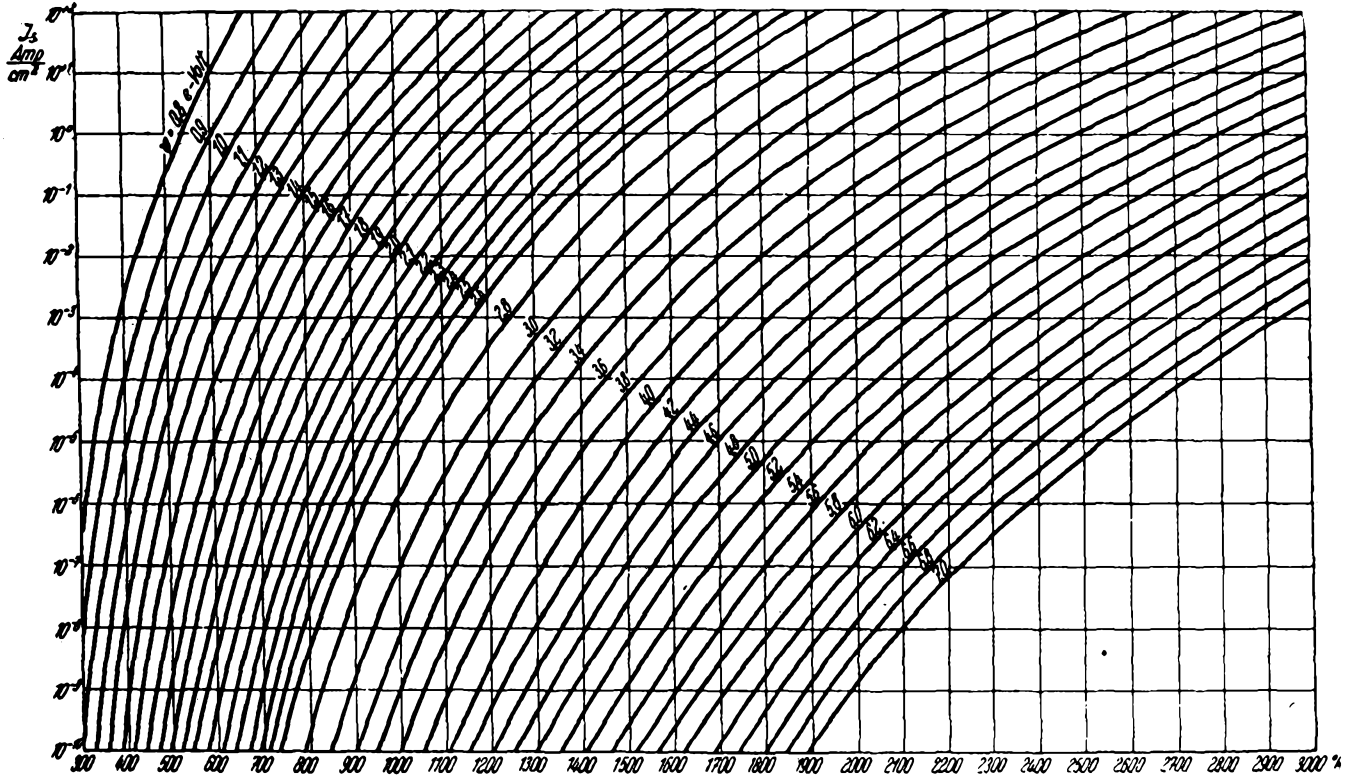

Fig. 19.1. Electron saturation current I_s in amperes/cm² as a function of temperature T in degrees kelvin for various values of the work function φ in e.V. After S. Wagener.[3] *(Courtesy Verlag Johann Ambrosius Barth, Leipzig.)*

TABLE 19.1. RATE OF EVAPORATION (IN G/CM² SEC) FOR VARIOUS METALS USED IN VACUUM TUBES

T °K	T °C	W*	Ta†	Mo‡	Pt‡	Fe‡	Ni‡	Cu‡	Ag§	Ba§§
700	427					1.25×10^{-20}	8.41×10^{-21}	1.16×10^{-18}	3.26×10^{-15}	1.7×10^{-8}
800	527				1.29×10^{-26}	3.17×10^{-17}	2.35×10^{-17}	1.64×10^{-15}	1.64×10^{-12}	9.1×10^{-7}
900	627				7.21×10^{-23}	1.38×10^{-14}	1.08×10^{-14}	3.64×10^{-13}	2.10×10^{-10}	2.0×10^{-5}
1000	727			1.37×10^{-24}	6.70×10^{-20}	1.82×10^{-12}	1.42×10^{-12}	3.96×10^{-11}	9.97×10^{-9}	2.5×10^{-4}
1100	827		1.33×10^{-28}	9.77×10^{-22}	1.81×10^{-17}	9.35×10^{-11}	7.48×10^{-11}	1.51×10^{-9}	2.29×10^{-7}	1.9×10^{-3}
1200	927	8.2×10^{-28}	1.27×10^{-25}	2.44×10^{-19}	2.06×10^{-15}	2.43×10^{-9}	2.00×10^{-9}	3.11×10^{-8}	3.13×10^{-6}	1.0×10^{-2}
1300	1027	3.16×10^{-25}	4.18×10^{-23}	2.53×10^{-17}	9.73×10^{-14}	3.89×10^{-8}	3.19×10^{-8}	3.94×10^{-7}		4.3×10^{-2}
1400	1127	1.26×10^{-23}	6.04×10^{-21}	1.29×10^{-15}	2.92×10^{-12}	4.04×10^{-7}	3.38×10^{-7}	3.5×10^{-6}	1.6×10^{-4}	0.15
1500	1227	7.83×10^{-21}	4.50×10^{-19}	3.81×10^{-14}	5.23×10^{-11}	3.04×10^{-6}	2.55×10^{-6}			0.43
1600	1327	4.36×10^{-19}	1.95×10^{-17}	7.60×10^{-13}	6.56×10^{-10}	1.74×10^{-5}	1.46×10^{-5}	1.0×10^{-4}	2.9×10^{-3}	1.1
1700	1427	1.51×10^{-17}	5.45×10^{-16}	1.05×10^{-11}	6.18×10^{-9}	8.11×10^{-5}	6.82×10^{-5}			2.5
1800	1527	3.52×10^{-16}	1.05×10^{-14}	1.06×10^{-10}	4.42×10^{-8}	3.08×10^{-4}	2.5×10^{-4}	1.4×10^{-3}	2.6×10^{-2}	5.2
1900	1627	5.92×10^{-15}	1.36×10^{-13}	7.52×10^{-10}	2.57×10^{-7}					10.0
2000	1727	7.48×10^{-14}	1.60×10^{-12}	5.34×10^{-9}	1.24×10^{-6}	2.9×10^{-3}	2.2×10^{-3}	1.1×10^{-2}	1.5×10^{-1}	18.0
2100	1827	7.43×10^{-13}	1.38×10^{-11}	2.82×10^{-8}						
2200	1927	6.00×10^{-12}	9.78×10^{-11}	1.30×10^{-7}	1.7×10^{-5}	2.6×10^{-2}	1.2×10^{-2}	5.9×10^{-2}	6.0×10^{-1}	
2300	2027	4.03×10^{-11}	5.88×10^{-10}	5.00×10^{-7}						
2400	2127	2.31×10^{-10}	3.04×10^{-9}	1.80×10^{-6}	1.5×10^{-4}	6.9×10^{-2}	5.0×10^{-2}	2.3×10^{-1}	1.9	
2500	2227	1.16×10^{-9}	1.37×10^{-8}	5.62×10^{-6}						
2600	2327	5.07×10^{-9}	5.54×10^{-8}	1.57×10^{-5}	8.5×10^{-4}	2.2×10^{-1}	1.6×10^{-1}	7.3×10^{-1}		
2700	2427	2.01×10^{-8}	2.00×10^{-7}	4.18×10^{-5}						
2800	2527	7.20×10^{-8}	6.61×10^{-7}	1.04×10^{-4}	4.0×10^{-3}					
2900	2627	2.36×10^{-7}	2.00×10^{-6}	2.35×10^{-4}						
3000	2727	7.15×10^{-7}	5.79×10^{-6}	5.00×10^{-4}						
3100	2827	2.01×10^{-6}	1.51×10^{-5}							
3200	2927	5.32×10^{-6}	3.82×10^{-5}							
3300	3027	1.27×10^{-5}								
3400	3127	3.13×10^{-5}								
3500	3227									
3600	3327									

* Ref. 6. † Ref. 6a. ‡ Ref. 7. § Ref. 10. §§ Ref. 9.

A convenient nomogram for the design of tungsten filaments which are expected to operate at a given temperature was published by Espersen.[13] Data for designing thoriated tungsten filaments were given by Dailey.[14] Nomographs for the evaluation of Richardson's Equation were developed by Ivey and Shackelford.[15] These nomographs make possible the evaluation of temperature when the other emission constants for Richardson's Equation are given; this is usually an awkward procedure when attempted numerically.

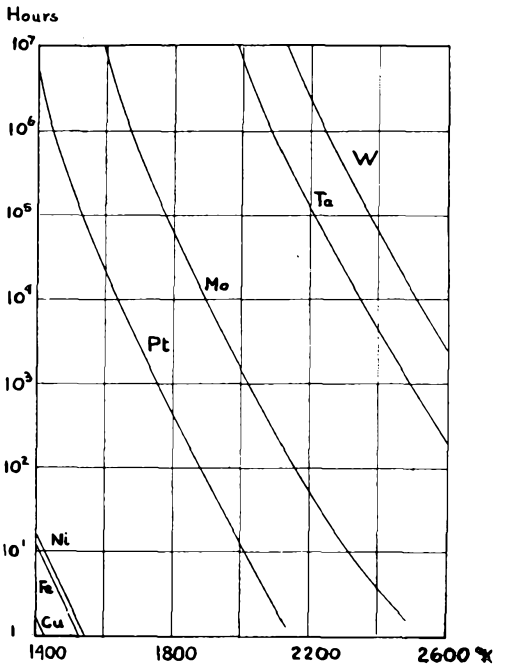

Fig. 19.2. Rate of evaporation of a square film of metal (1 cm × 1 cm × 1 mil).

Composite Cathodes

Efforts to obtain large emission yields for high-power, high-voltage operation were limited, in the past, by the physical characteristics of tungsten. Practically, a yield of 1 amp/cm^2 at 2600°K was about the maximum that could be obtained at the cost of reduced life. For more conservative operation 0.5 amp/cm^2 is the maximum. The enhanced emission available from thoriated cathodes is limited to operation at relatively low-voltage gradients on account of sputtering of the surface film of thorium by gas ions. Such filaments are in common use in power tubes in the presence of anode voltages of the order of 30 kv, and their application in 100 kv rectifiers has been reported by Atlee.[16] Thoriated

tungsten, usually containing up to 1.5 per cent of ThO_2, is very difficult to work mechanically; therefore, the fabrication of large-area cathodes from this material is almost impossible. Its use is thus generally restricted to the form of wire. Cylindrical cathodes made of tungsten, molybdenum, or tantalum can, of course, be wound with a layer of thoriated wire which is brazed or anchored to the base metal; a large-area thoriated tungsten emitter may thus be obtained.* The possibility of interalloying between the base metal and the wire must be borne in mind. Carbonization of a thoriated tungsten surface is common practice since it has been found that the evaporation of thorium from tungsten carbide (W_2C) is much less than that from a pure tungsten surface and the life accordingly much longer.[17]

Thoria cathodes, which consist of the ceramic ThO_2, have been studied extensively,[18–27] but so far have found only limited commercial application. After World War II they were introduced for magnetrons, where they excel by high-current yields, freedom from sparking and poisoning, and low rate of evaporation in comparison with conventional Ba/Sr oxide cathodes. Much of the research on and development of thoria cathodes has been carried out at the Bartol Research Foundation of the Franklin Institute, under sponsorship of the U.S. Bureau of Ships. Danforth[28] reported on their work in a summary, as follows:

"Composite results for well-activated cathodes from several laboratories are in fair agreement with a Richardson curve, in which $A = 0.33$ and $\phi = 2.0$ e.v.† Direct current from thoria is limited to approximately 5a/cm² by decay, and investigations of this subject are continuing. No short-time decay of 10^{-5} sec time constant, as often observed with Ba/Sr oxide, is present, the smallest time constant being some tenths of one second, a fact which recommends thoria for long pulse applications.

"Rates of evaporation and of disappearance of the material with passage of current have been measured and the observations are continuing. On the basis of evaporation alone a coating of 1 mil thickness will completely evaporate in 350 hours at 1800°C (true), a temperature where the primary thermionic emission is 14 amp/cm². At 1650°C ture temperature, where the primary emission is about 5 amp/cm², the evaporation life is 4000 hours per mil thickness. The passage of high d.c. accelerates the disappearance, preliminary results indicating that for coatings the passage of 1 amp/cm² decreases life by a factor of 2, a figure which is roughly independent of temperature.

* Observation presented by W. G. Wagener of Eitel-McCullough, Inc., in a talk on "Recent Developments at Eimac" before the Cedar Rapids Section of the Institute of Radio Engineers on November 21, 1950.

† "Readers may be puzzled by the value $\phi = 2.0$ in view of the higher values presently accepted. The values for A and ϕ quoted above are based on a curve which passes through a mass of data taken from many sources and are regarded as valid for design purposes. Individuals at Bartol and elsewhere, performing careful measurements, report values for ϕ in the neighborhood of 2.5 or 2.6. These latter values rather than 2.0 are to be regarded as appropriate for theoretical purposes." (Comments by W. E. Danforth submitted to the author.)

"Thermionic emission studies have been made with thoria plus numerous admixtures, none of which, to date, has increased its emission. Studies have also been made with coated cathodes of ZrC, TaB, TaC, and TiC, among which ZrC is the most interesting, its emission exceeding that of thoria in the temperature region below about 1400°C."

Haddad and co-workers[29–29a] report the following data for ZrC: A = 0.2 to 0.5 amp/cm^2/deg^2; ϕ = 2.16 volts; b = 11,605. At 1500°C$_b$ stable emission of 0.6 amp/cm^2 d.c. is obtained. At 1700°C$_b$ 6 amp/cm^2 currents are obtained with microsecond pulses. The spectral emissivity is 0.96 ± 0.04.

The fabrication of thoria cathodes is an elaborate procedure at best. Solid bodies, such as cylinders and sleeves, are produced by powder metallurgical methods. Particle-size distribution and purity of the raw materials must be carefully controlled. The paste of ThO_2 with a suitable binder ($ThCl_4$) is submitted to pressure of the order of 100 tons per square inch in hardened dies lubricated with a suitable wax and fired afterwards in a neutral atmosphere at temperatures ranging from 1850 to 2000°C. Tungsten heaters may be embedded in the powder or inserted separately into sleeves. Directly heated sleeves and rods have been produced by imparting a suitable conductivity to the thoria body by admixture of tungsten and other powders.[30–32] Molybdenum electrodes are attached to the ends to serve as current leads. For magnetron application the cathodes have suitable "end hats" of molybdenum, which are brazed to the cathode and serve as heat radiators. If the molybdenum "end hats" are coated with titanium dioxide, the power dissipation in the cathode can be nearly doubled.[33]

The basic limitations encountered when trying to heat a cylinder to a high temperature by means of an inserted heater have been described by Danforth and Haddad.[34] They find that the temperature region from 1700 to 1800°C, true surface temperature, appears to be a practical upper limit consistent with reasonable life of the tungsten heater. This applies equally to ceramic or metal sleeves. The thickness of the sleeve and its thermal conductivity are not determining factors. The excessively high heater temperature and the large temperature drop in the sleeve wall are dictated by radiation transfer from heater to sleeve and radiation from the surface of the sleeve. In a separate paper, Danforth has given the theoretical treatment of this surprising result.[35]

Cataphoretic coating of tungsten filaments with thoria and other rare-earth elements offers a simpler technique for the utilization of these cathode materials when other limitations can be endured. Mesnard and Uzan[36,37] have described the most recent developments of this technique. They coated tungsten wires 6 mil in diameter and refined the procedures described earlier by Weinreich[38] and Hanley.[39]

Lanthanum oxide (La_2O_3) cathodes have been investigated at the Battelle Memorial Institute by Todd, Rueger, and others, and were found to give promising yields. The hexaborides of the alkaline-earth and rare-earth metals and thorium have been investigated by Lafferty of the General Electric Research Laboratory.[40]

"Boride cathodes require no special activation. When they are heated for a few minutes at 1400°C to 1600°C for outgassing, they are found to be completely active. The pulsed emission is the same as the d.c. emission. LaB_6 gives a higher emission than is usually obtained from thoria. These cathodes stand up well under positive ion bombardment and are not affected by air or moisture. They have thus found wide use in experimental demountable systems.

"Lanthanum boride gave the highest emission, and was found to have a relatively low evaporation rate, corresponding to a latent heat of evaporation of 169 Kcal/mole. The emission constants obtained from Richardson plots for the hexaborides are shown in Table 19.2.

TABLE 19.2. HEXABORIDE ELECTRON EMISSION CONSTANTS DETERMINED FROM DUSHMAN'S EQUATION[40]

Boride	A	ϕ
CaB_6	2.6 amp/cm²/°K²	2.86 volts
SrB_6	0.14	2.67
BaB_6	16	3.45
LaB_6	29	2.66
CeB_6	3.6	2.59
ThB_6	0.53	2.92

"If these cathode materials are operated in contact with the refractory metals, the boron atoms diffuse into their metal lattices, forming interstitial boron alloys with them. When this occurs, the boron framework which holds the alkaline-earth or rare-earth metal atoms collapses, permitting them to evaporate. The hexaborides may be operated in contact with tantalum carbide or carbon."[40]

Several successful attempts have been made in the past to produce long-life cathodes of high yield by embedding the active emitter material in a porous metal base or a wire mesh, from which it could continue to diffuse to the surface. A thoriated tungsten wire represents an atomic matrix through which the thorium diffuses to the wire surface. Hull's "Stocking Cathodes" for long-life thyratrons[41] utilized a molybdenum stocking filled with granules of fused $BaO\text{-}Al_2O_3$ mixture, and achieved cathode operation of 24,000 hours in mercury-filled thyratrons. Perforated molybdenum sleeves containing a sintered ThO_2 body have been used for magnetron cathodes.* Porous ceramic bodies or carbon impregnated with alkalies or alkaline-earth metals have been described by Espe

* Dr. Brown, R.C.A. report at NRL conference on Thoria Cathodes, July 14, 1947.

and Evers,[42] who claim a reduced rate of evaporation of the active material when it is dispersed within the pores of the carrier, thus permitting operation at higher temperatures. A German patent[43] describes a porous tube of tungsten or molybdenum, produced by powder metallurgical means and impregnated with thorium, as giving high emission and freedom from sparking in high-voltage power tubes. The so-called "matrix-cathodes," developed at the Bell Telephone Laboratories[44] for magnetron use, should also be mentioned here as they consist of a metallic matrix through which the active coating is dispersed. In another version the conventional carbonates of barium and strontium are mixed with coarse nickel powder to form a paste which is pressed and sintered onto a recessed nickel sleeve. The average size of the nickel particles was 55 microns and that of the carbonates 1 to 2 microns. These matrix-cathodes superseded the earlier mesh cathodes, in which the active coating was pressed into a nickel mesh which was spot welded or sintered directly to the nickel sleeve. The mesh was made of 6-mil diameter nickel wire woven with 75 wires to the inch. The radial thickness of the mesh on the cathode was 10 mils. The average amount of active double carbonate mixture which the cathode holds was 23 mg per sq cm.

A remarkably successful realization of the principles underlying these earlier efforts has been achieved by the Philips Laboratories at Eindhoven, where the so-called "L Cathode" was developed. It combines practically all of the desirable characteristics for cathodes which are to be used in high-voltage, high-frequency tubes, and is bound to have a decisive effect on tube design. Figure 19.3 gives an outline of two typical cathode structures of this type, as described by Lemmens, Jansen, and Loosjes.[45] It is apparent from the diagram that a pressed tablet or cylinder of (Ba/Sr) CO_3 is supported by a molybdenum base and enclosed by a porous tungsten member. After the thermal decomposition of the carbonates at about 1100°C the reduction of the oxides of Ba and Sr takes place at 1270°C. The alkali metals and BaO have a considerable vapor pressure at this temperature (Table 19.1 and Figure 19.4) so that they will escape into the pores of the tungsten and form a monatomic layer of barium and oxygen over its inner and outer surface. This leads to a substantial reduction of the work function and permits the high yield of electron currents.* Table 19.3 compares the thermionic constants of the L cathode with those of other conventional cathodes. Figure 19.5 gives the corresponding Richardson Plots and Figure 19.6 the curves for

* Pertinent observations on the mechanism of adsorption of barium on tungsten have been made recently by Biguenet[46] and by Moore and Allison,[47] who describe thermionic emission of thin films of alkaline-earth oxide deposited by evaporation on tungsten or molybdenum surfaces. They show "evidence that films of pure alkaline-earth oxide, from 1 to 25 molecular layers thick deposited by evaporation, can lower the thermionic work function of clean receiver metals by as much as 3.5 volts."

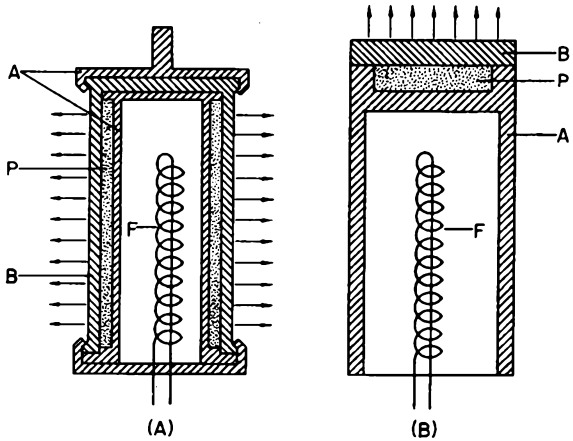

Fig. 19.3. Cross-section of two basic forms of the L cathode. (A) With cylindrical emitting surface; (B) With flat, circular emitting surface. A is wall of molybdenum, B is wall of porous tungsten, P is tablet of barium-strontium carbonate, F is filament. After H. J. Lemmens et al.[45] (*Courtesy Philips Gloelampenfabrieken, Eindhoven, Netherlands.*)

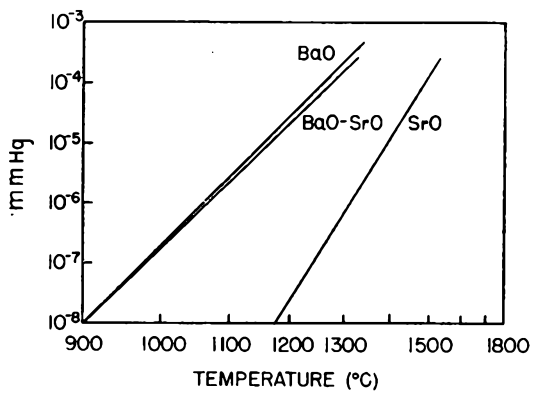

Fig. 19.4. Vapor pressure of BaO, BaO-SrO and SrO as a function of temperature. After Claasen and Veenemans.[8] The mixture of BaO and SrO had a molecular ratio of 42.8:57.2. Its vapor does not contain any measurable quantity of SrO. (*Courtesy Philips Gloelampenfabrieken, Eindhoven, Netherlands.*)

saturation emission currents as a function of temperature. L cathodes operate in the temperature range from 900 to 1350°C, compared with a range of 700 to 900°C for oxide-coated cathodes. The theoretical thermal efficiency of the L cathode is thus somewhat less, as evident from Figure 19.6. The life of the L cathode is some thousands of hours at 1000 to 1100°C, some hundreds of hours at 1250°C, and some tens of hours at 1350°C. The saturation emission currents at these temperatures are 3,

TABLE 19.3. THERMIONIC CONSTANTS FOR VARIOUS TYPES OF CATHODES[45]

Type of Cathode	ϕ (e.v.)	A (Amp/cm²/deg²)
Tungsten	4.44–4.63	22–210
Thoriated tungsten	2.6 –2.9	3– 15
Oxide coated cathode	1.0 –1.5	0.01– 5
L cathode	1.6 –2.0	1– 15

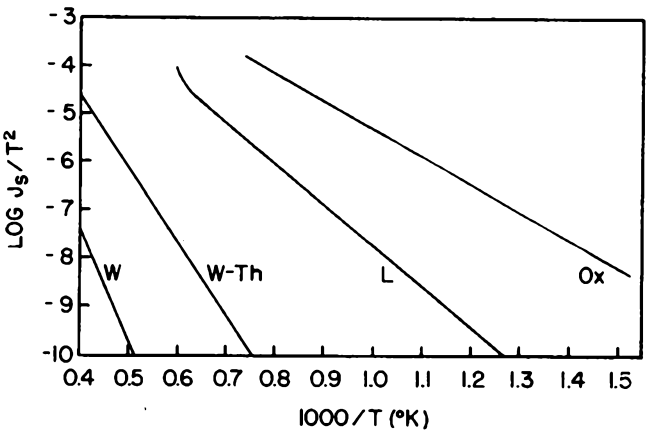

Fig. 19.5. Richardson plots for the L cathode, pure tungsten, thoriated tungsten and conventional oxide cathodes. After Lemmens et al.[45] (*Courtesy Philips Gloelampenfabrieken, Eindhoven, Netherlands.*)

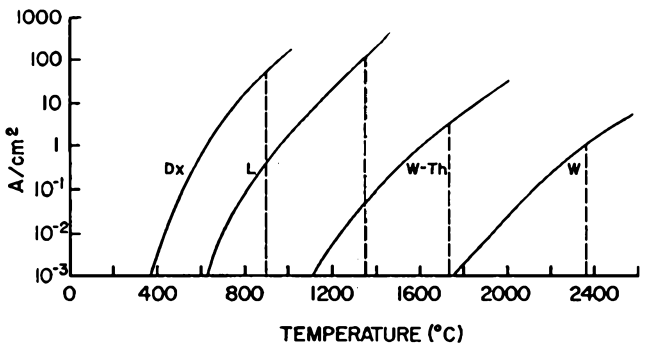

Fig. 19.6. Saturation emission I_s (in amperes/cm²) as a function of true temperature (in degrees centigrade) for the L cathode and three other types of cathodes. After H. J. Lemmens et al.[45] (*Courtesy Philips Gloelampenfabrieken, Eindhoven, Netherlands.*)

100, and 250 amp/cm^2, respectively. L cathodes are mechanically stable, can be fabricated to close tolerances and withstand heavy electron bombardment and bombardment by gas ions. Resistance to sparking and a secondary emission yield greater than one makes the L cathode especially suitable for use in magnetrons. Its physical size is small; samples of L cathodes obtained from the Philips Laboratories at Irvington measured $\frac{1}{8}$ inch diameter for a button type and $\frac{9}{32}$ inch length (Figure 19.3B). The heater is rated at 10 volts 0.8 amp for operation at 1050°C, where an emission density of 2 amps/cm^2 is obtained after suitable activation. Button sizes up to 1 inch diameter are considered to be practical although the limitations mentioned above in relation to heater design will begin to play a part.

Oxide Cathodes

The conventional oxide cathodes, consisting of a mixture of Ba, Sr, Ca oxide generally applied to the base metal in the form of carbonates, remain the most economical source of electrons for the bulk of commercially produced electron tubes. Radio receiving tubes, CR tubes, TV tubes, klystrons, and TR tubes fall in this class. It is now generally recognized that the interface between coating and core-metal plays an important role in determining the available emission. The interface resistance is decidedly non-ohmic and considerably higher than the ohmic coating resistance. The interface shows a lower resistance for electron flow from coating to core metal than in the opposite, normal direction of flow of electrons. The limitation to the passage of large currents thus lies primarily in the breakdown strength of the interface. The phenomenon of sparking after a certain operational life is evidence of such breakdown, which leads to the formation of craters in the coating and subsequent erratic behavior. Pronounced sparking of unaged, fresh cathodes clears up in time, leaving a statistical probability of further sparking during life. Peak emission currents of the order of 100 amp/cm^2 have been obtained under pulsed conditions with microsecond pulses. For continuous duty in commercial devices a saturated emission of about $\frac{1}{100}$ the peak value obtainable under pulsed conditions can be drawn if a reasonable life is expected. This then gives a figure of about 1 a/cm^2 temperature limited emission and about 200 ma/cm^2 for space-charged limited emission. Commercial receiving-tube cathodes are often designed for not more than 100 ma/cm^2 emission in order to give a few thousand hours of life.

Oxide-coated cathodes are subject to emission decay and poisoning when exposed to deleterious gases and vapors, such as oxygen, chlorine, and sulfur. Herrmann and Krieg[48] have recently investigated this effect for rare gases, hydrogen, carbon monoxide, carbon dioxide, and several

hydrocarbons. These data may be useful to a wider circle than ordinarily reached by a foreign publication so that a brief summary of the results obtained may not be out of place in this text.*

"The investigations were carried out with indirectly heated cathodes, consisting of a cathode-nickel sleeve coated with mixed carbonates of Ba/Sr (1:1 by weight) to a thickness of 2.4 to 2.8 mils and a density of about 5 mg/cm^2. A nickel anode, 10 mm in diameter, was arranged in three sections in the usual manner and current drawn from the central section of the cathode where the temperature was constant to within $\pm 1\%$. The assemblies were sealed into soft-glass envelopes, the cathodes activated and aged by drawing currents from 30 to 70 ma/cm^2 for as long as 2 hours at the best obtainable vacuum on the pump. The state of optimum activation was ascertained by measuring saturation emission at low temperatures with 10-volt anode potential. Purified gases and vapors were then admitted and the change of emission with time observed for various gas pressures and cathode temperatures. Saturation currents were limited to 1.7 ma/cm^2 and values for higher temperatures obtained by extrapolation in order to maintain the anode potential at 10 volts.† A distinction was made between physical and chemical effects of the various gases and vapors. The admission of rare gases (He, A, Kr) and hydrogen equally affected the temperature of the cathode due to the thermal conductivity of the gas but had no permanent effect on the emission when the gas was removed. In accordance with earlier measurements by Espe and Knoll[49] this cooling effect becomes noticeable only at temperatures above 550°K and pressures higher than 10^{-3} mm Hg. It remains independent of the gas up to 10^{-1} mm Hg. The influence of ion bombardment was investigated on sealed-off tubes for the rare gases He and A for cathode temperatures from 1000 to 1070°K with 100-volt anode potential and emission densities from 10 to 20 ma/cm^2 during periods ranging from 300 to 700 hours. Considerable sputtering and gas clean-up occurred, but no decrease of emission was observed as long as any coating was left on the cathode. Not fully activated cathodes showed an improvement of emission during bombardment.

"When an activated oxide cathode is exposed to free oxygen, the well-known poisoning occurs, which is the more pronounced the lower the temperature of the cathode. After short-time exposure partial recovery of the emission takes place and, even when the cathode was exposed to an oxygen atmosphere at constant pressure for as long as 20 minutes, recovery was observed in many cases after the oxygen had been pumped out. Poisoning by oxygen is due to the oxidation of the surface film of barium and, on longer exposure, to the oxidation of interstitial Ba within the bulk of the coating. The core metal seemed to be unaffected as was shown by tests with platinum core cathodes.

"Carbon dioxide similarly poisons the emission although much smaller quantities of gas are consumed in the reaction than is the case in the presence of oxygen. Under equal gas pressure the relative poisoning effect of CO_2 is less severe than that of O_2. After poisoning by CO_2 the cathode can be reactivated a few times only when the gas has been removed. The reactivation follows the same schedule as the original activation of the cathode.

* The paper is based on work submitted by O. Krieg as a thesis at the Technical University, Berlin-Charlottenburg under the tutelage of Prof. A. Gehrts. Work was carried out at the Telefunken Laboratory from 1940 to 1943.

† This is necessary to avoid ionization, gas clean-up, and gas release from the anode.

"The chemical reaction of CO_2 with the oxide coating may proceed according to either one of the following equations:

$$M + CO_2 = MO + CO \tag{19.2}$$
$$MO + CO_2 = MCO_3 \tag{19.3}$$

where M stands for the metal component, either Ba or Sr or both. In order to ascertain whether the formation of the carbonates can, by itself, be responsible for the poisoning effect of CO_2, the dissociation pressure of the carbonates was plotted in the form $\log p = f(1/T)$, which results in the familiar straight lines shown in Figure 19.7. To the right of these lines the carbonates are stable; in the singly hatched region SrO is stable, and to the left, in the doubly hatched region, BaO is stable also. If the formation of carbonates is responsible for emission poisoning under the influence of CO_2, the decrease of emission must occur at such gas pressures and cathode temperatures as delineated by the region to the right of the respective straight line plots. Herrmann and Krieg confirmed this by entering into the graph lines of constant

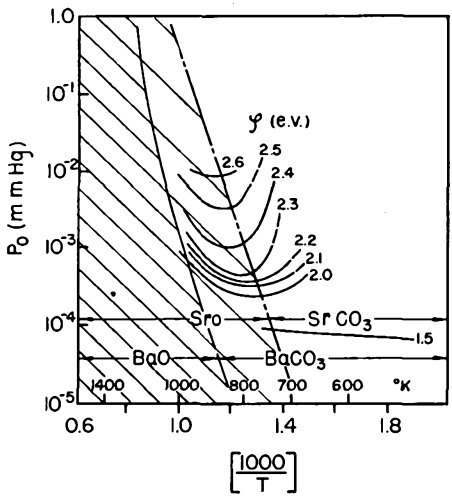

Fig. 19.7. Pressure-temperature diagram for the decomposition of $BaCO_3$ and $SrCO_3$. Curves of constant work function φ indicate the degree of poisoning of oxide cathodes by CO_2 after 10 minutes exposure. After Herrmann and Krieg.[48] (*Courtesy Verlag Johann Ambrosius Barth, Leipzig.*)

work function which they obtained from saturation-current decay measurements at different pressures and temperatures after exposing the cathodes to CO_2 for 10 minutes. The Richardson Constant A was taken to be 120 amps/cm^2/deg^2 for these calculations. The curves of constant φ in Figure 19.7 thus indicate the pressures and temperatures for which the same degree of poisoning was observed after 10 minutes exposure to CO_2. The higher the value of φ, which is entered on the curves as parameter, the greater, of course, is the poisoning effect. It is evident that the φ-values increase toward higher pressures, which is to be expected. For any given pressure there is a maximum tendency towards poisoning in the middle temperature range. The decreasing poisoning effect toward higher temperatures coincides well with the decomposition range of the carbonates. Maximum poisoning occurs in the range where the carbonates are stable when formed by the reaction of CO_2 with the alkaline oxide. Fully active cathodes, in the absence of CO_2, were found to have a work function lower than 1.5 e.v. The φ-values on the left ascending branch of the curves in Figure 19.7 are still considerably higher than 1.5 e.v. This suggests that, in addition to carbonate formation, oxidation according to Equation 19.2 also takes place.

At higher temperatures free Ba will more readily diffuse from the coating to its surface and thus counteract the decrease of emission by surface oxidation. Conversely, at lower temperatures, where carbonates would be stable, their formation according to Equation 19.3 also proceeds at a slower rate. For oxygen poisoning the reaction rate is still considerable even at low temperatures. The corresponding curves are shown in Figure 19.8. Even at room temperature the work function of an activated cathode is much increased by exposure to oxygen (or air).

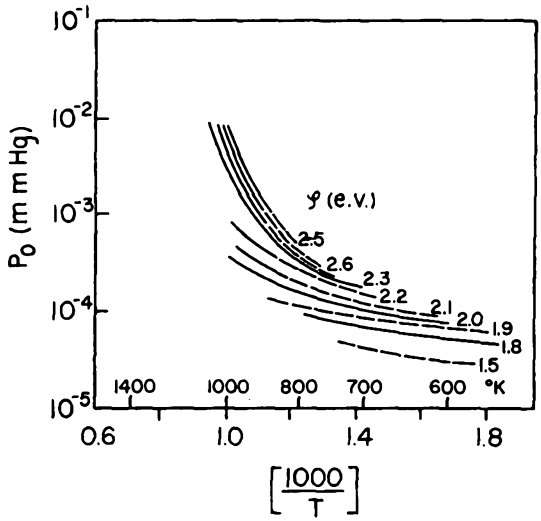

Fig. 19.8. Pressure-temperature diagram with curves of constant work function φ indicating degree of poisoning of oxide cathodes by oxygen after 10 minutes exposure. After Herrmann and Krieg.[48] *(Courtesy Verlag Johann Ambrosius Barth, Leipzig.)*

"Carbon-monoxide (CO) also decreases the emission from an oxide cathode, although to a lesser extent than CO_2. Re-activation is necessary after poisoning. The reactions may occur according to

$$M + CO \rightleftharpoons MO + C \tag{19.4}$$

or

$$MO + 2CO \rightleftharpoons MCO_3 + C \tag{19.5}$$

Again, the formation of carbonates has been shown to be responsible for the poisoning effect. Figure 19.9 gives the corresponding diagram. The steep rise of the curves at lower temperatures indicates a greater temperature dependence of the reaction velocity. Indeed, exposure of activated cathodes to CO at less than 500°K has hardly any effect on the emission.

"A good deal of work has been done by several investigators on the thermal decomposition of hydrocarbons, but few of the prevailing conditions apply to the study of oxide cathodes. It has been found that the temperature at which decomposition sets in is lowered by the presence of catalysts. Thermodynamic calculations by Schultze[50] have led to the result that the tendency toward decomposition can be expressed by the equilibrium constant of the equation, which describes the reaction if this constant is divided by the number of free carbon atoms. Figure 19.10 shows this relation where high ordinate values indicate a small tendency toward decomposi-

tion, and vice versa. Figure 19.11 gives the pressure-temperature diagrams together with the constant work-function curves determined by Herrmann and Krieg. The hatched region indicates the range of carbon deposition on the cathode as observed after 10-minutes reaction time. The degree of emission poisoning follows the sequence suggested by increasing tendency toward decomposition, as shown in Figure 19.9 (i.e., methane, propane, and benzol). It is to be expected that other hydrocarbons will fall in line. The mechanism of poisoning in the case of hydrocarbons is not a chemical reaction of their decomposition products (H_2 has been shown to have no adverse effect and carbide formation is most unlikely) but a deposition of free carbon

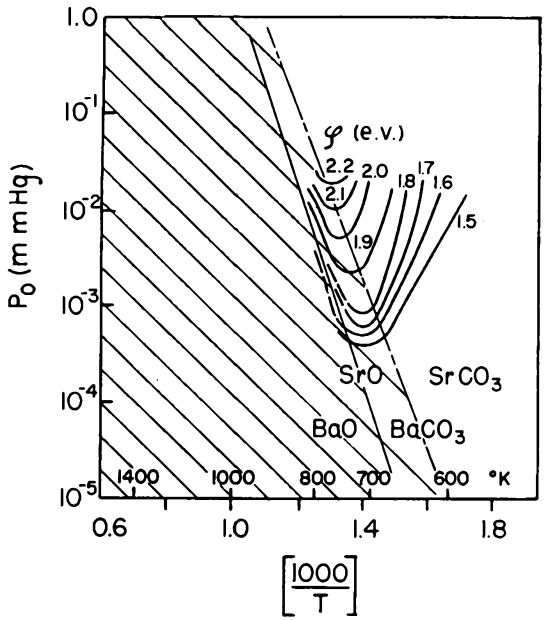

Fig. 19.9. Pressure-temperature diagram showing ranges where the oxides and carbonates of Ba and Sr are stable. Curves of constant work function indicate the degree of poisoning of oxide cathodes after 10 minutes exposure to CO. After Herrmann and Krieg.[48] (*Courtesy Verlag Johann Ambrosius Barth, Leipzig.*)

on the active centers of the coating. Repeated reactivation of poisoned cathodes was found to be possible.*

"As positive determinations of the end product of the various reactions cannot be made by either chemical or x-ray methods, further light was shed on the course of the reactions by observing the change in gas pressure within the tube during 10 minutes after gas or vapor had been admitted to an initial pressure P_0. The results are shown in Figure 19.12. Oxygen poisoning thus leads to a marked decrease in pressure over the entire range of temperature. CO_2 likewise shows a large pressure drop at low temperatures but none at high temperatures where BaO is stable and no increase would be expected from the reaction $Ba + CO_2 \rightarrow BaO + CO$. For the less active CO the decrease in pressure is slow and goes through a maximum which corresponds

* Hannay et al.[51] report the activation of oxide cathodes by exposing them to methane at a pressure of 10–25 microns for 5–10 minutes at 1320°K. No visible deposits of carbon are formed.

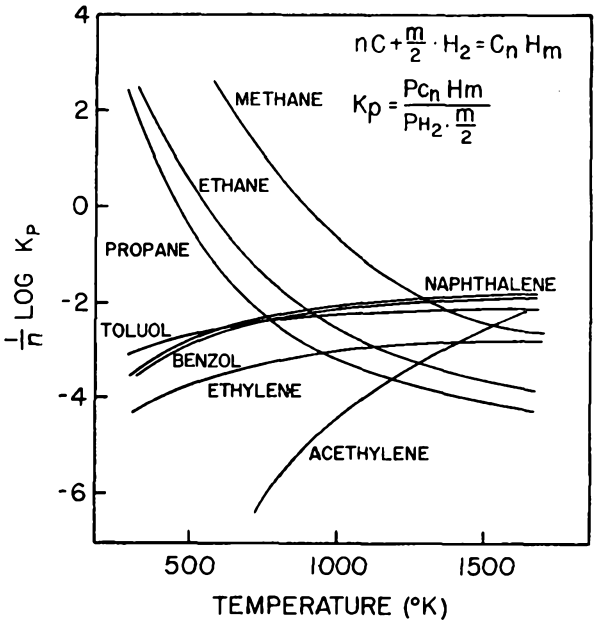

Fig. 19.10. Graphs showing the tendency towards decomposition of simple carbons as a function of temperature (°K). High ordinate values indicate low decomposition probability. After G. R. Schultze[50] according to Herrmann and Krieg.[48] (*Courtesy Verlag Johann Ambrosius Barth, Leipzig.*)

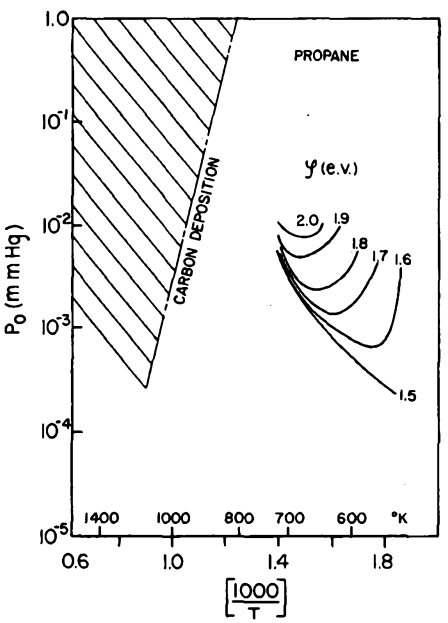

Fig. 19.11. Pressure-temperature diagrams and curves of equal work function indicating the degree of poisoning of oxide cathodes after 10-minute exposure to (a) methane; (b) propane; (c) benzol. Onset of carbon deposition on the cathode is indicated by the hatched region. After Herrmann and Krieg.[48] (*Courtesy Verlag Johann Ambrosius Barth, Leipzig.*)

to the temperature range of maximum poisoning. All hydrocarbons bring about an increase in pressure and the temperature at which a sharp rise sets in is an indication of the decomposition temperature. Figure 19.13 finally shows pressure temperature curves for constant work functions $\varphi = 2$ e.v. after 10-minute exposure for all gases and vapors investigated. To account for the rapidly decreasing pressure during oxygen poisoning, curves for constant oxygen pressure are also indicated which emphasize the even more severe poisoning in this case."

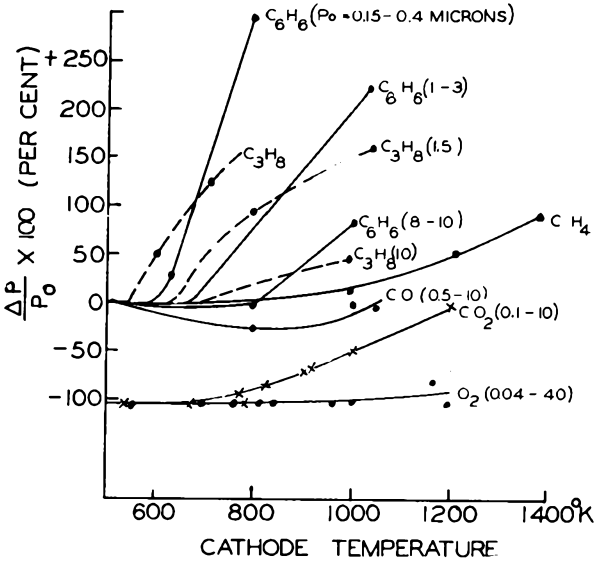

Fig. 19.12. Relative change in gas pressure during 10-minute exposure of oxide cathodes to various gases and vapors, which were admitted at initial pressure P_0 as a function of cathode temperature. After Herrmann and Krieg.[48] (*Courtesy Verlag Johann Ambrosius Barth, Leipzig.*)

A very extensive study, entitled "Fundamental Research on Raw Materials Used for Electron Emissivity on Indirectly Heated Cathodes," has been carried out from 1947 to 1950 by Nottingham, Cardell, and Levy.* During this work the ASTM standard diode was first used, but a purified diode and refined test methods developed when it became apparent that the results of the ASTM survey (see Chapter 11) were not sufficiently consistent. Great care had to be taken to prevent the presence of impurities in all the components used or to prevent their migration to the cathode under study before the influence of small additives to cathode core or coating could be accurately appraised. Processing techniques were rigorously controlled and carried out by trained operators in an independent laboratory. It would, of course, lead us too far afield to attempt even a summary of this investigation, especially as the reports are available from the contracting agency. Some interesting correlation

* Contract N7onr-389, Task Order NR-074-251. Work was carried out at the Department of Physics, M.I.T. and Raytheon Mfg. Co., Newton, Mass.

was established between pulsed and continuous emission which, under the conditions of test, gave a linear relationship with a slope of 0.45 when pulse emission in amperes at 885°K was plotted as ordinate against d.c. emission at 605°K in microamperes as abscissa. Studies on interface resistance were carried out at M.I.T. by J. F. Waymouth, Jr.,[52] who

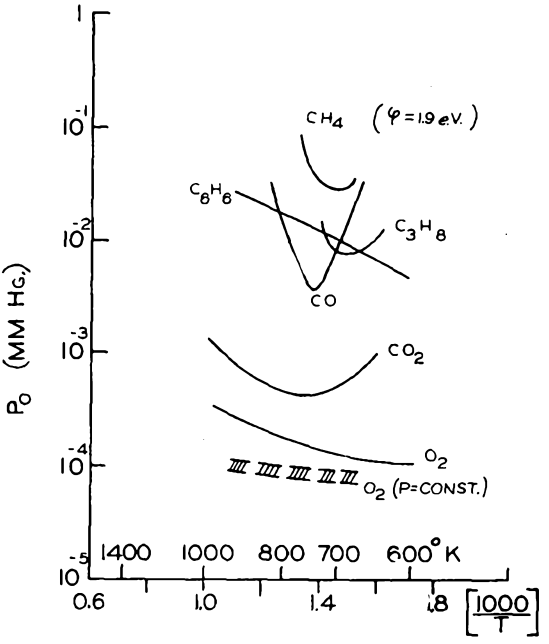

Fig. 19.13. Pressure-temperature diagrams with curves of constant work function equal to 2 e.v. indicating degree of poisoning of oxide cathodes after 10-minute exposure to various gases and vapors, as a function of cathode temperature. After Herrmann and Krieg.[48] (*Courtesy Verlag Johann Ambrosius Barth, Leipzig.*)

established the presence of barium-ortho-silicate (Ba_2SiO_4) in all tubes investigated, regardless of the life-test history. The cathode sleeves consisted of 699 active nickel, while all other metallic parts of the diodes were made from 499 nickel alloy. (See Chapter 11.) When these tubes were life tested while a current was being drawn from the cathode, an interface resistance developed after 4000 hours life was noticeable in only 1 tube out of 20. In contrast, the other tubes aged without current load developed very appreciable interface resistance and less than 50 per cent of the tubes gave 2000 hours life before the interface resistance had developed. The interface resistances ranged from 40 ohms to about 1000 ohms. A mechanism is suggested by Waymouth which explains the observed effects.

The most suitable coating composition for oxide cathodes has recently been redetermined by Widell and Hellar.[53] A good many conflicting

reports have been published on this question in recent years, and it must be remembered that different composition ratios may give optimum service for special applications. It was found that solid solutions of the earth-alkali oxides, containing 70-molar per cent SrO and 30-molar per cent BaO, gave the maximum electron emission when subject to pulses of 3-microsecond duration at a pulse repetition rate of 500 per second. No measurable decay was noticed during pulses of 10-microsecond duration.

For 3-component oxides Elizabeth Grey[54] reports a maximum pulsed emission of about 8 amp/cm^2, measured at 1000°K, for a molecular composition BaO:SrO:CaO equal to the ratios 47:43:10. The emission falls away sharply from the maximum with any variation of composition greater than 2 per cent. The optimum composition found from a study of about 100 varying compositions agrees well with the results obtained by Violet and Riethmueller. (See Chapter 11.)

Experimenters in the laboratory, who are confronted with the problem of making an electron tube with an oxide-coated cathode for the first time, will no doubt have many questions in regard to details of processing procedures and material supply. It is suggested that they procure a copy of the pamphlet entitled "Proposed Method of Test for Relative Thermionic Emissive Properties of Materials Used in Electron Tubes" from the American Society of Testing Materials.[55]*

* 1916 Race St., Philadelphia 3, Pa.

REFERENCES

1. Herring, C., and Nichols, M. H., "Thermionic Emission," *Rev. Mod. Phys.*, **21**, 185–270 (1949).
2. Eisenstein, A. S., "Oxide-Coated Cathodes," Advances in Electronics, Vol. 1, 1–64. New York, Academic Press, Inc., 1948.
3. Herrmann, G., and Wagener, S., "Die Oxydkathode," 2 Volumes, Leipzig Johann Ambrosius Barth., 1942–43.
4. Biguenet, C., "Les Cathodes Chaudes. Théorie et Pratique," Paris (1947). Editions de la revue d'optique théorique et instrumentale.
5. Michaelson, H. B., "Work Functions of the Elements," *J., Appl. Phys.*, **21**, 536–540 (1950).

5a. Danforth, W. E., "Elements of Thermionics," *Proc. Inst. Radio Eng.*, **39**, 485–499 (1951).

6. Reimann, A. L., "The Evaporation of Atoms, Ions, and Electrons from Tungsten," *Phil. Mag.*, **25**, 834–848 (1938).

6a. Langmuir, D. B., and Malter, L., "The Rate of Evaporation of Tantalum," *Phys. Rev.* **55**, 743–747 (1939).

7. Jones, H. A., Langmuir, I., and Mackay, G. M. J., "The Rates of Evaporation and the Vapor Pressures of Tungsten, Molybdenum, Platinum, Nickel, Iron, Copper, and Silver," *Phys. Rev.*, **30**, 201–214 (1927).
8. Claasen, A., and Veenemans, C. F., "Vapor Pressure of Earth-Alkali Oxides as a Function of Temperature" (In German), *Z. f. Phys.*, **80**, 342–351 (1933).
9. Van Liempt, J. A. M., "The Vapor Pressure of Barium" (In German), *Rec. Trav. Chim. Pays-Bas*, **55**, 468–470 1936.

10. Ditchburn, R. W., and Gilmour, J. C., "The Vapor Pressures of Monatomic Vapors," *Rev. Mod. Phys.*, **13**, 310-327 (1941).
11. Law, R. R., "Vapor-Pressure Data for Various Substances," *Rev. Sci. Inst.*, **19**, 920-922 (1948).
12. Jones, H. A., and Langmuir, I., "The Characteristics of Tungsten Filaments as Functions of Temperature," *G. E. Rev.*, **30**, 310-319, 354-361, 408-412 (1927).
12a. Bas-Taymaz, E., "On the Life of an Incandescent Tungsten Helix and the Rate of Evaporation of Tungsten in High Vacuum" (In German), *Zs. f. Ang. Phys.*, **2**, 374-376 (1950)
12b. Zwikker, C., "Properties of Tungsten at High Temperatures," Diss. Amsterdam 1925.
13. Espersen, G. A., "Fine Wires in the Electron-Tube Industry," *Proc. I.R.E.*, **36**, 116W-120W (1946).
14. Dailey, H. J., "Designing Thoriated Tungsten Filaments," *Electronics*, 107-109 (Jan. 1948).
15. Ivey, H. F., and Shackelford, C. L. (Westinghouse Electric Corp., Bloomfield, N.J.), "Convenient Methods for Thermionic Emission Calculations," Presented. at Symposium on Thermionics, Div. of Electron Physics, Amer. Phys. Soc, New York (Feb. 1, 1950); *Tele Tech.*, **10**, 42-43, 68 (1951).
16. Atlee, Z. J., "Thoriated Tungsten Filaments in Rectifiers," *El. Eng.* **68**, 863 (1949).
17. Horsting, C. W., "Carbide Structures in Carburized Thoriated Tungsten Filaments," *J. Appl. Phys.*, **18**, 95-102 (1947).
18. Pomerantz, M. A., "Thorium Oxide Cathodes," *Report* 517, Bartol Research Foundation. NDRC Div. (Oct. 31, 1945).
19. Prater, C. D., and Danforth, W. E., "The Fabrication of Sinthor Cathodes," Bartol Research Foundation, NDRC Contract OEMsr-358, Bureau of Ships Contract NObsr-34141 (June 15, 1946).
20. The Bartol Foundation Cathode Research Group, "The Fabrication and Performance of Sinthor Cathodes," Bureau of Ships Contract NObsr-34141 (June 1, 1947).
21. Keighton, W. B., "Thoria, Its Properties and Analysis," Bartol Research Foundation, Bureau of Ships Contract NObsr-34141 (June 1, 1947).
22. Keighton, W. B., "Properties of Thoria Ceramics: Influence of Particle Size and Thoria Treatment." *Progress Report*, Bartol Research Foundation, Bureau of Ships Contract NObsr-34141 (May 1, 1948).
23. Dean, H. M., "Thoria Particle Size by Sedimentation," *ibid.*
24. Weinreich, O. A., "Activation Phenomena of Thoria Cathodes," *Progress Report*, Bartol Research Foundation, Bureau of Ships Contract NObsr-34141 (Nov. 15, 1948).
25. Danforth, W. E., and Morgan, F. H., "Electrical Resistance of ThO_2," *Phys. Rev.*, **79**, 142-144 (1950).
26. Weinreich, O. A., "Emissivity Changes of Thoria Cathodes," *J. Appl. Phys.*, **21**, 1272-1275 (1950).
27. Mesnard, G., and Uzan, R., "On the Optical Emissivity of Thorium Oxide" (In French), *LeVide*, **28/29**, 844-852 (1950).
28. Danforth, W. E., "Abstract of Summary of Bartol Cathode Work," *J. Franklin Inst.*, **248**, 449 (1949).
29. Haddad, R. E., Goldwater, D. L., and Morgan, F. H., "Abstract of Zirconium Carbide as a Thermionic Emitter," *J. Franklin Inst.*, **248**, 449 (1949).
29a. Goldwater, D. L., and Haddad, R. E., "Certain Refractory Compounds as Thermionic Emitters," *Jour. Appl. Phys.*, **22**, 70-73 (1951).

30. Fan, H. Y., "Thermionic Emission from Sintered Cathode of Thoria and Tungsten Mixture," *J. Appl. Phys.*, **20**, 682–690 (1949).
31. Bush, O. B., Vandegrift, R. B., and Hanley, T. E., "The Use of Titanium and Zirconium Nitrides as a Conducting Element in Thoria Cathodes," *J. Appl. Phys.*, **20**, 295 (1949).
32. Espersen, G. A., "Thermionic Emitting Properties of Thoria-Rhenium," *J. Appl. Phys.*, **21**, 261 (1950).
33. Stone, A. M., "Oxide-Coated Cathodes in Great Britain," *Tech. Rep't.*, OANAR-5-48, Office of Naval Research, London Branch (1948).
34. Danforth, W. E., and Haddad, T. A., "Radiation Transfer Considerations in the Heating of a Cathode Sleeve," *J. Franklin Inst.*, **250**, 135–145 (1950).
35. Danforth, W. E., "Radiation Heating of a Plane Parallel Slab by a Parallel Semi-Infinite Heater," *Ibid.*, 146–150 (1950).
36. Mesnard, G., and Uzan, R., "Preparation of Thoria Cathodes by Cataphoresis" (In French), *LeVide*, **26**, 769–776 (1950).
37. Mesnard, G., "On Electrode Polarization in Electrophoresis and Electrolysis of Thorium Oxide and Thorium Nitrate" (In French), *LeVide*, **28/29**, 866–869 (1950).
38. Weinreich, O. A., "Some New Experiments on Thorium Oxide Cathodes" (In French), *Rev. Gén. d'Electr.*, **54**, 243–256 (1945).
39. Hanley, T. E., "Spectral Emissivity and Electron Emission Constants of Thoria Cathodes," *J. Appl. Phys.*, **19**, 583–589 (1948).
40. Lafferty, J. M., "Boride Cathodes," *Phys. Rev.*, **79**, 1012 (1950); also, *J. Appl. Phys.*, **22**, 299–309 (1951).
41. Hull, A. W., "A New Type of Thermionic Cathode," *Phys. Rev.*, **53**, 936 (1938).
42. Espe, W., and Evers, F., "Glow Cathode," *U.S. Patent 1,954,474* (Apr. 10, 1934).
43. Woeckel, and Sparmann, "Telefunken-Thorium Kathode," *Ger. Patent Appl.*, (May 23, 1940) PB 8660.
44. Fisk, J. B., Hagstrum, H. D., and Hartman, P. L., "The Magnetron as a Generator of Centimeter Waves," *Bell System Tech. J.*, **25**, 167–348 (1945).
45. Lemmens, H. J., Jansen, M. J., and Loosjes, R., "A New Thermionic Cathode for Heavy Loads," *Philips Tech. Rev.*, **11**, 341–350 (1950).
46. Biguenet, C., "Photo-Adsorption of a Thin Film of Barium"(In French), *LeVide*, **28/29**, 831–836 (1950).
47. Moore, G. E., and Allison, H. W., "Thermionic Emission of Thin Films of Alkaline-Earth Oxide Deposited by Evaporation," *Phys. Rev.*, **77**, 246–257 (1950).
48. Herrmann, G., and Krieg, O., "The Influence of Gases and Vapors on the Emission of Oxide Cathodes" (In German), *Ann. d. Phys.*, **4**, 441–464 (1949).
49. Espe, W., and Knoll, M., "Werkstoffkunde der Hochvakuumtechnik," 241, Berlin, J. Springer, 1936.
50. Schultze, G. R., "Thermodynamic Equilibrium of Hydrocarbon Reactions Applied to Their Decomposition" (2) (in German), *Z. Angew. Chem.*, **49**, 17, 268 (1936).
51. Hannay, N. B., MacNair, D., and White, A. H., "Semi-conducting Properties in Oxide Cathodes," *Jour. Appl. Phys.*, **20**, 669–681 (1949).
52. Waymouth, J. F., Jr., "Determination of Oxide-coated Cathodes under Low-Duty-Factor Operation," *Appl. Phys.*, **22**, 80–86 (1951).
53. Widell, E. G., and Hellar, R. A., "Effect of Coating Composition of Oxide-Coated Cathodes on Electron Emission," *J. Appl. Phys.*, **21**, 1115–1118 (1950).
54. Grey, L., Elizabeth, "Pulsed Emission from the BaO-SIO-CaO System," *Nature*, **167**, 522 (Mar. 31, 1951).
55. See Reference 26a in Chapter 11.

Author Index

The numbers after the name indicate the pages on which the names appear either in full or by reference number. At the end of each chapter all references are listed in the sequence in which they appear in the text. These reference numbers, together with the chapter in which they appear, are listed below after the letter R. Example: Acker, J. T., 246, 255 R 11:25 i. e., in Chapter 11 Mr. Acker appears as reference 25 on pages 246 and 255.

Subject Index